BNL-107682-2015

RIKEN/RBRC Workshop

Theory and Modeling for the Beam Energy Scan: From Exploration to Discovery

February 26-27, 2015

Proceedings of RIKEN BNL Research Center Workshop

Volume 121

RBRC

RIKEN BNL Research Center

DISCLAIMER

Preface to the Series

The RIKEN BNL Research Center (RBRC) was established in 1997 at Brookhaven National Laboratory.* RBRC is funded by "Rikagaku Kenkyosho" (RIKEN, The Institute of Physical and Chemical Research) in Japan and the United States Department of Energy's Office of Science.

A Memorandum of Understanding between RIKEN and BNL, initiated in 1997, has been renewed in 2002, 2007 and 2012.

RBRC is dedicated to the study of strong interactions, including spin physics, lattice QCD and relativistic heavy ion physics through the nurturing of new generations of young physicists. The RBRC founding Director T.D. Lee and the second Director N. P. Samios conceived and implemented this vision, which has been maintained and further developed down to the present day.

The RBRC research program has theory, lattice gauge computing and high-energy experimental nuclear physics components. Recently, an astrophysics/cosmology component has been added. The RBRC Theory, Computing and Experimental Groups presently comprise 48 researchers. Positions include full-time RBRC Fellows, half-time joint RHIC Physics Fellows and full-time postdoctoral Research Associates. The RHIC Physics Fellows hold joint appointments with RHIC and other institutions, where they have tenure track positions. To date, RBRC has over 101 graduates (Fellows and Research Associates) of whom approximately 67 have already attained tenure at major research institutions worldwide.

In 2001 a RIKEN Spin Program (RSP) was initiated at RBRC. The research staff comprises joint appointments in theory and experiment between RBRC and RIKEN, including RSP Researchers, RSP Research Associates and Young Researchers. They are mentored by senior RBRC Scientists. A number of RIKEN junior Research Associates and Visiting Scientists also contribute to the program.

In support of the lattice gauge program at RBRC and elsewhere, a series of high-performance computers has been designed and built by researchers from Columbia University, IBM, BNL, RBRC and University of Edinburgh, with the U.S. DOE Office of Science providing infrastructure support at BNL. To date, the steps in this program have been: QCDSP (0.6 TFlops, 1998-2006), which was awarded the Gordon Bell Prize for price performance in 1998; QCDOC (10 TFlops, 2005-2012); QCDCQ (600 TFlops, 2011-present). Recent $K^\circ \rightarrow \pi\pi$ results were awarded the Ken Wilson Prize in 2012.

A very important activity of RBRC is its active Workshop series on Strong Interaction Physics, with each workshop focused on a specific physics problem. A list of proceedings of all past Workshops can be found on the RBRC website (http://www.bnl.gov/riken/proceedings.php). The talks from many of the recent workshops can be accessed from the link at the top of the Proceedings page. To date, about 119 Workshops have taken place; the full proceedings of most of the workshops from 2005 – 2014 are available at this link.

S. H. Aronson, Director
March 2015

* Work Performed under the auspices of U.S.D.O.E. Contract No. DE-SC0012704

Introduction

The Relativistic Heavy Ion Collider (RHIC) at Brookhaven National Laboratory has concluded phase I of its Beam Energy Scan (BES) program. The goal of the RHIC BES program is to explore the phase diagram of strongly interacting matter at high baryonic densities and search for the QCD critical point by performing systematic scans at lower beam energies. Results from the RHIC BES I program are intriguing. There indeed seem to be several signals suggesting a softening of the equation of state, which may result from a first-order transition, as well as possible indications of a critical point. In light of these intriguing results, several accelerator and detector upgrades have been planned to conduct the phase II of the RHIC BES during the period 2017-2020. The goal of the RHIC BES II is discovery of the QCD critical point by performing high luminosity scans within the interesting beam energy range revealed through explorations at RHIC BES I.

Past experience has proven that even qualitative understanding of the physics encoded within the RHIC experimental data requires substantial theoretical input based on QCD calculations as well as detailed, quantitative modeling of the medium created at the RHIC. However, the coordinated theoretical and modeling efforts necessary for comprehensive understanding of the RHIC BES data is presently lacking.

The purpose of this workshop was to gather a small group of expert theorists, phenomenologists and experimentalists to identify the necessary theoretical and modeling developments required for RHIC BES, to delineate a clear path towards extracting concrete physics utilizing the RHIC BES data, and to kick-start collaborations among theorists, phenomenologists and experimentalists to ensure that the necessary theoretical and modeling developments can be achieved before the start of the RHIC BES II experimental program.

Contents

Presentations

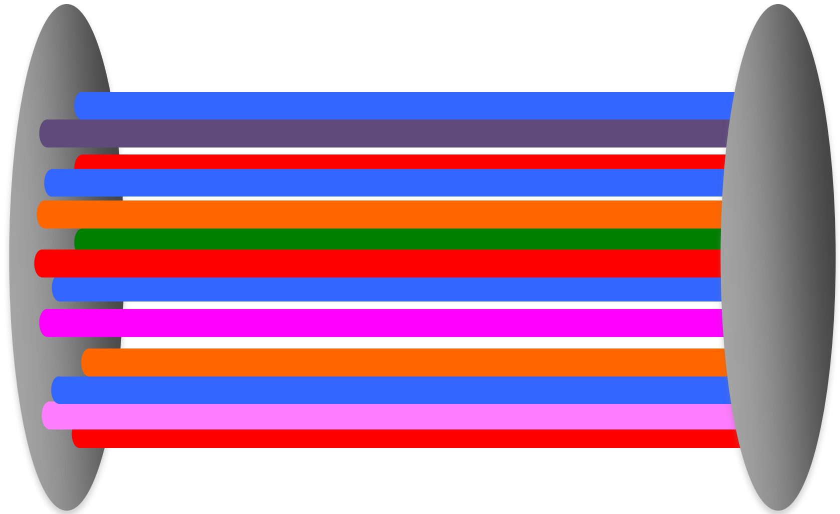

Dynamical modeling of the chiral magnetic effect in heavy-ion collisions
[arXiv:1412.0311]

Yuji Hirono [Stony Brook Univ.]

Collaborators: T. Hirano[Sophia U], D. E. Kharzeev [SBU/BNL]

Anomalous transport in heavy-ion collisions?

$$\boxed{\boldsymbol{j} = \frac{e^2\mu_5}{2\pi^2}\boldsymbol{B} \qquad \boldsymbol{j}_5 = \frac{e^2\mu}{2\pi^2}\boldsymbol{B}}$$

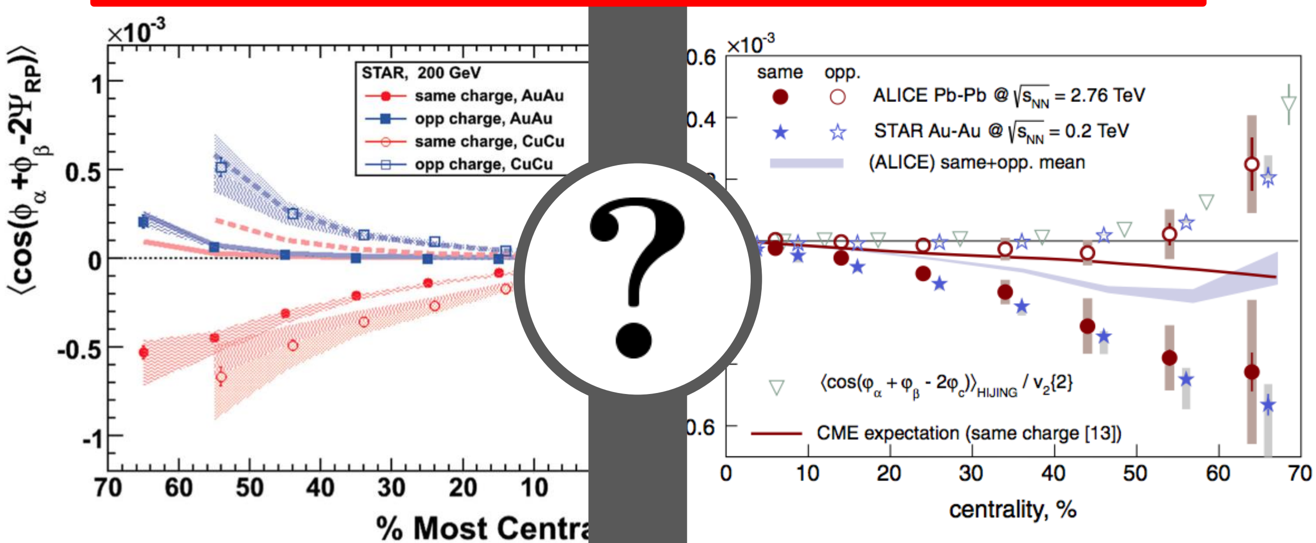

[STAR, PRL2009, PRC2010]

[ALICE, PRL2013]

$$\boxed{\langle \cos(\phi_1^\alpha + \phi_2^\beta - 2\Psi_{\mathrm{RP}}) \rangle}$$

Anomalous transport in heavy-ion collisions?

$$\boldsymbol{j} = \frac{e^2 \mu_5}{2\pi^2} \boldsymbol{B} \qquad \boldsymbol{j}_5 = \frac{e^2 \mu}{2\pi^2} \boldsymbol{B}$$

Outline

1. Physical meaning of obs.
2. EbE anomalous hydro
3. Results

$$\langle \cos(\phi_1^\alpha + \phi_2^\beta - 2\Psi_{\mathrm{RP}}) \rangle$$

Charge dependent correlations [STAR]

$$\boxed{\langle \cos(\phi_1^\alpha + \phi_2^\beta - 2\Psi_{\mathrm{RP}}) \rangle}$$

$$\alpha, \beta \in \{+, -\}$$

$$\langle \cos(\phi_1^+ + \phi_2^+ - 2\Psi_{\mathrm{RP}}) \rangle$$

$$= \langle \cos(\phi_1^+ - \Psi_{\mathrm{RP}}) \cos(\phi_2^+ - \Psi_{\mathrm{RP}}) \rangle - \langle \sin(\phi_1^+ - \Psi_{\mathrm{RP}}) \sin(\phi_2^+ - \Psi_{\mathrm{RP}}) \rangle$$

$$= \langle \left(v_1^+\right)^2 \rangle - \langle \left(a_1^+\right)^2 \rangle$$

Charge dependent correlations [STAR]

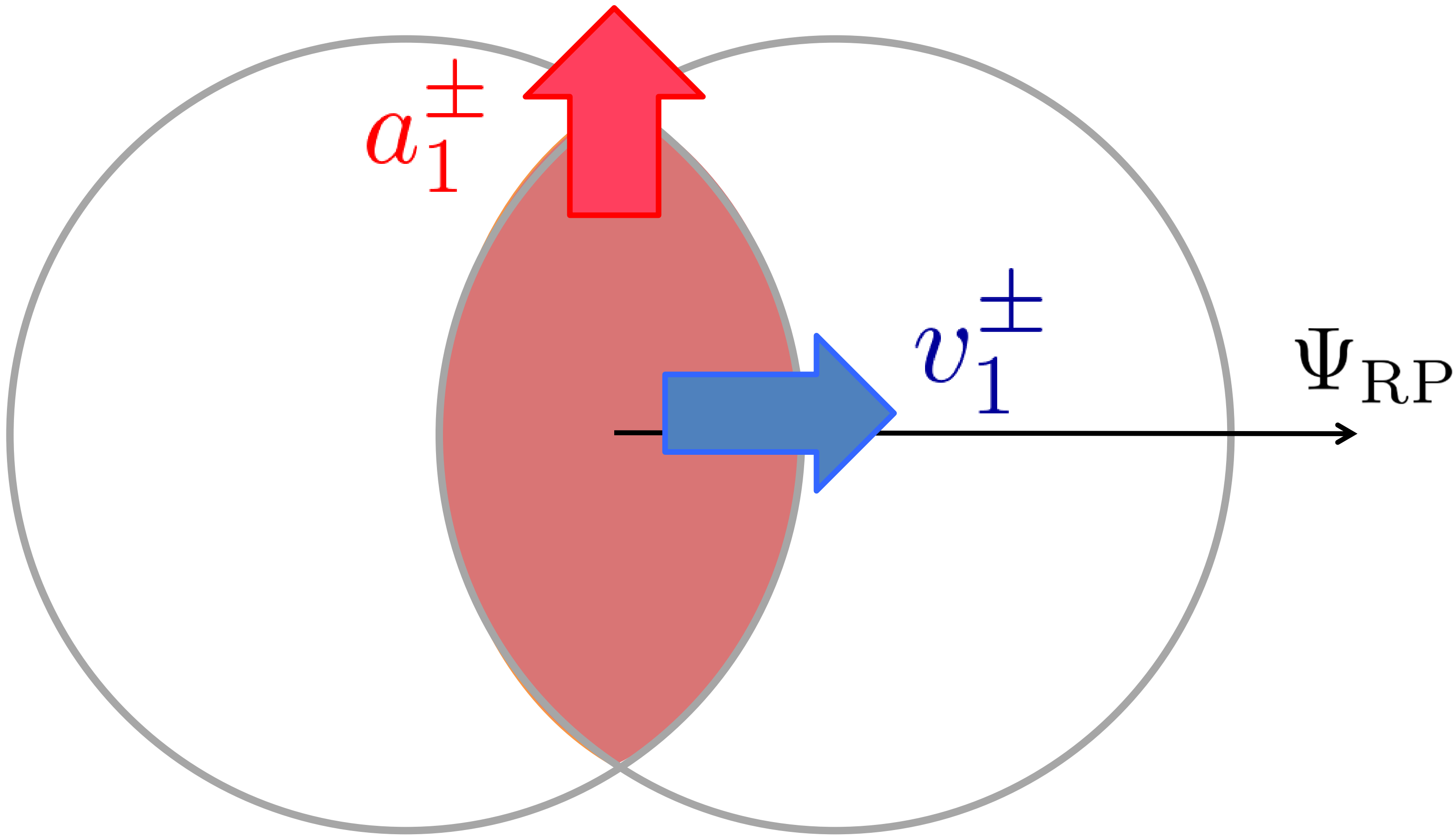

$$\langle \cos(\phi_1^+ + \phi_2^+ - 2\Psi_{\mathrm{RP}}) \rangle = \langle (v_1^+)^2 \rangle - \langle (a_1^+)^2 \rangle$$

Charge dependent correlations [STAR]

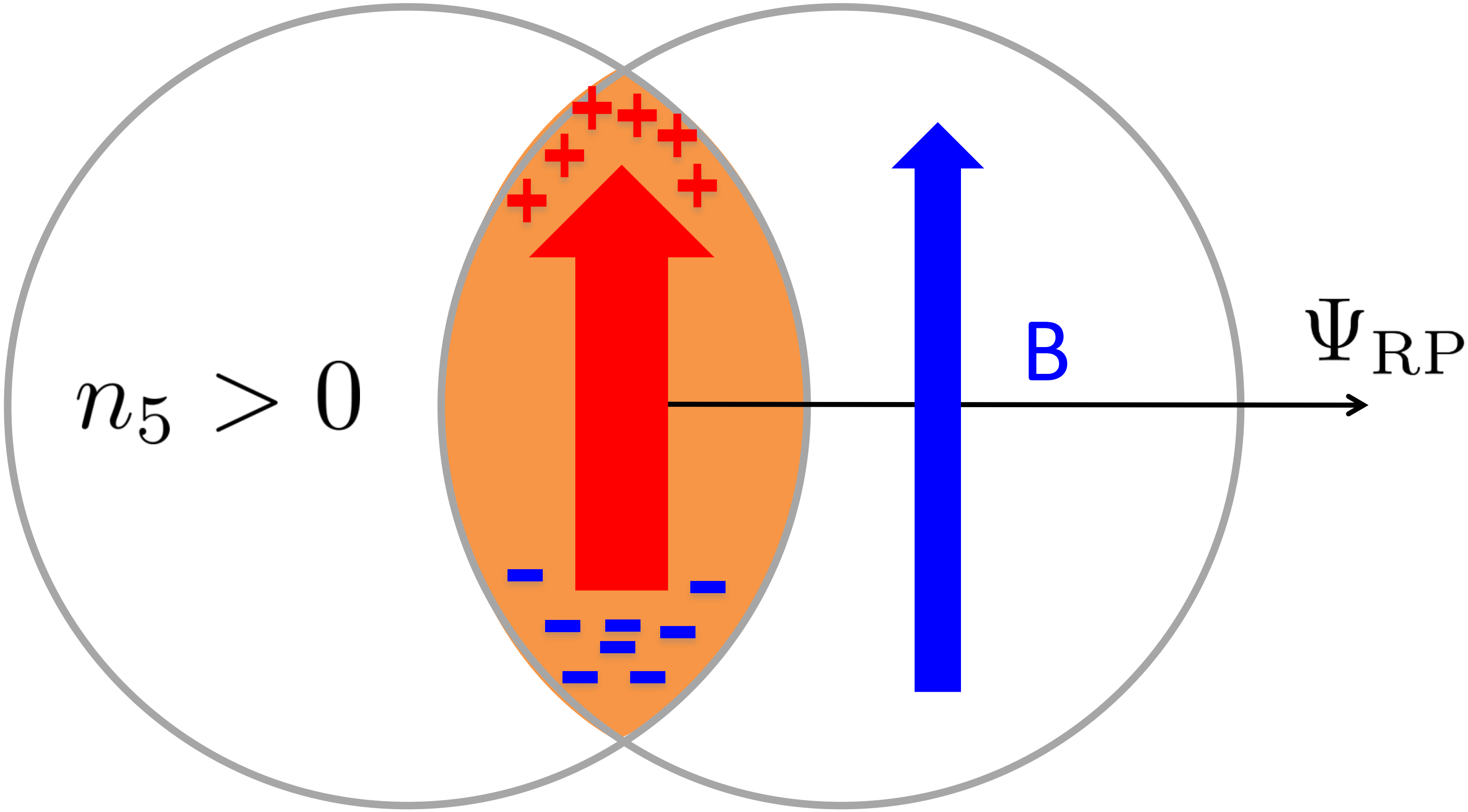

$$a_1^+ > 0 \quad a_1^- < 0$$

Charge dependent correlations [STAR]

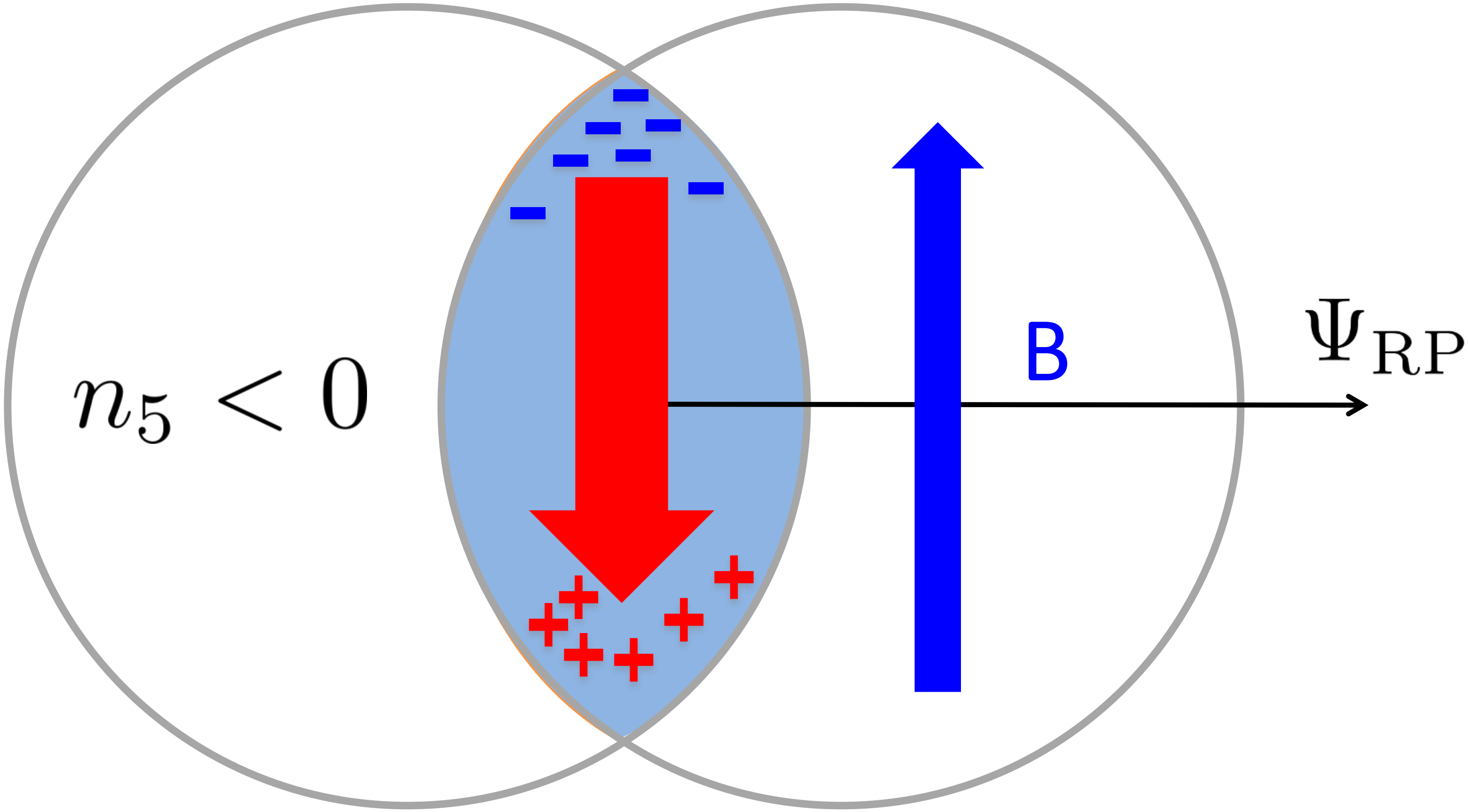

$a_1^+ < 0 \quad a_1^- > 0$

Charge dependent correlations [STAR]

$$\langle a_1^+ \rangle = \langle a_1^- \rangle = 0$$

$$\langle (a_1^+)^2 \rangle = \langle (a_1^-)^2 \rangle > 0$$

$$\langle a_1^+ a_1^- \rangle < 0$$

Charge dependent correlations [STAR]

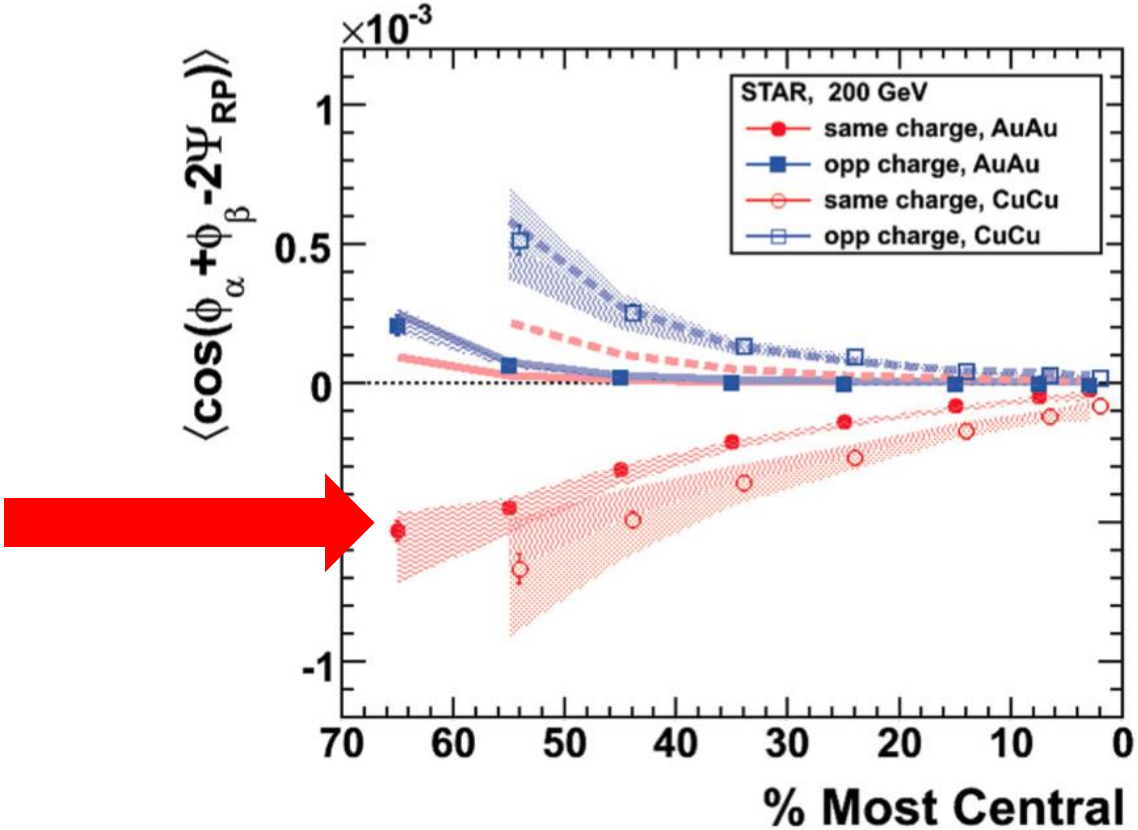

$$\langle \cos(\phi_1^+ + \phi_2^+ - 2\Psi_{\mathrm{RP}}) \rangle = \langle (v_1^+)^2 \rangle - \langle (a_1^+)^2 \rangle$$

Anomalous transport in heavy-ion collisions?

$$\boldsymbol{j} = \frac{e^2 \mu_5}{2\pi^2} \boldsymbol{B} \qquad \boldsymbol{j}_5 = \frac{e^2 \mu}{2\pi^2} \boldsymbol{B}$$

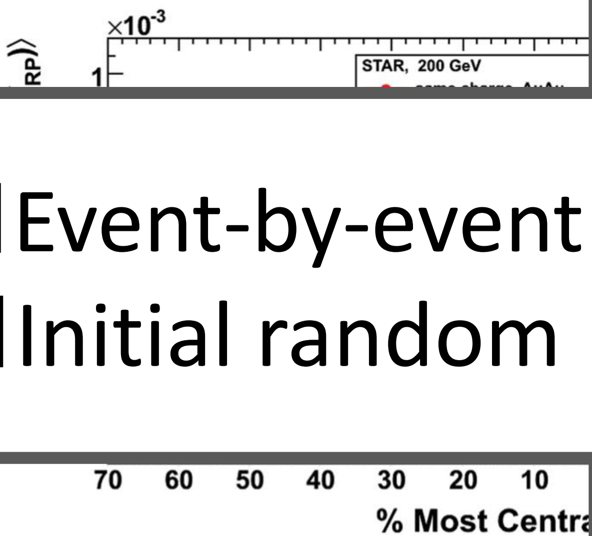

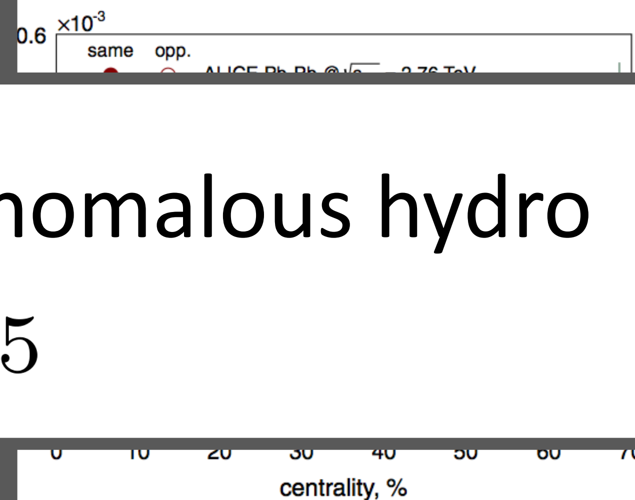

☐ Event-by-event anomalous hydro
☐ Initial random n_5

[STAR, PRL2009, PRC2010]

[ALICE, PRL2013]

$$\langle \cos(\phi_1^\alpha + \phi_2^\beta - 2\Psi_{\mathrm{RP}}) \rangle$$

Event-by-event anomalous hydrodynamic model

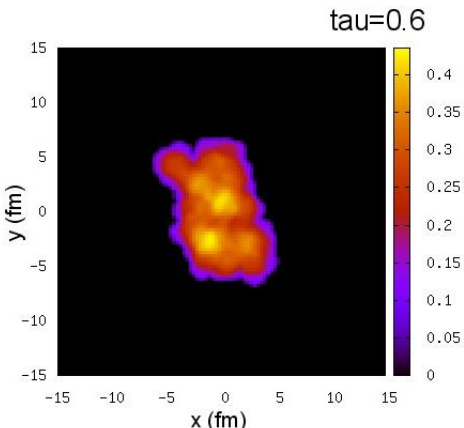

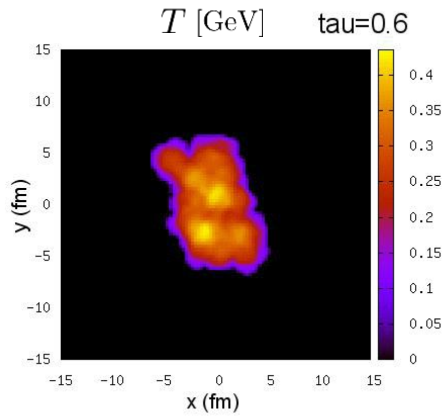

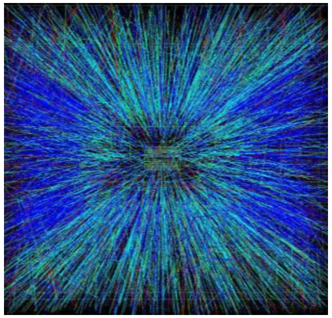

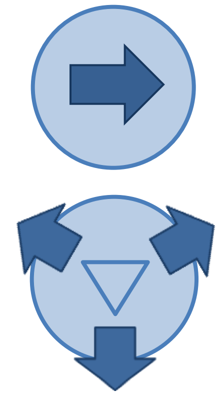

t

Initial state

Anomalous
hydro evolution

Freeze-out

Correlations

An initial cond.

Particle data
for 1 event

Anomalous hydrodynamics equations

- Non-dissipative anomalous fluid in 3+1D
  - no viscosity/Ohmic conductivity
- Background electromagnetic fields

$$\partial_\mu T^{\mu\nu} = \boxed{F^{\nu\rho} j_\rho}$$

$$\partial_\mu j^\mu = 0 \qquad \partial_\mu j_5^\mu = \boxed{C E_\mu B^\mu}$$

$$C = \frac{N_\mathrm{c} N_\mathrm{f}}{2\pi^2}$$

Anomalous hydrodynamics equations

- Constitutive equations

$$j^\mu = nu^\mu + \boxed{\kappa_B B^\mu} \qquad j_5^\mu = n_5 u^\mu + \boxed{\xi_B B^\mu}$$

CME CSE

$$e\kappa_B = C\mu_5 \left(1 - \frac{\mu n}{e+p}\right) \quad e\xi_B = C\mu \left(1 - \frac{\mu_5 n_5}{e+p}\right)$$

[Son & Surowka (2009)]
[Kalaydzhyan & Kirsch (2011)]

- Equation of state - conformal
  - massless quarks & gluons

$$p\left(T, \boxed{\mu, \mu_5}\right) = \frac{g_{\mathrm{qgp}}\pi^2}{90} T^4 + \frac{N_c N_f}{6}\left(\mu^2 + \mu_5^2\right) T^2 + \frac{N_c N_f}{12\pi^2}\left(\mu^4 + 6\mu^2\mu_5^2 + \mu_5^4\right)$$

MC Sampling of particles

Isothermal hypersurface

$$T_{\rm fo} = 160\ \mathrm{MeV}$$

$$dN = \int \frac{d^3p}{E} \frac{p_\mu d\sigma^\mu}{e^{\beta(p\cdot u - \mu)} \mp_{\rm BF} 1}$$

K. Murase
[U-Tokyo]

Can be written as 1D integral!
[PPNP70, 108[arxiv:1204.5814]]

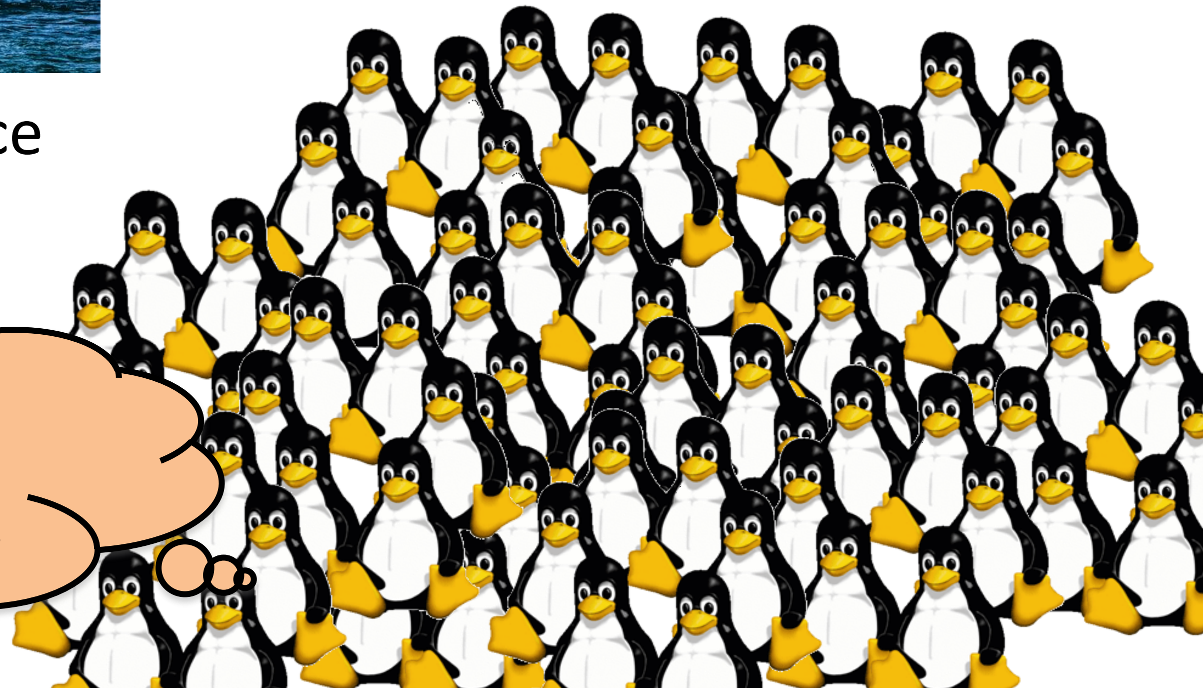

Linux cluster at Sophia Univ.
- 128 cores
- A few days per 100k events

Anomalous transport in heavy-ion collisions?

$$\boldsymbol{j} = \frac{e^2 \mu_5}{2\pi^2} \boldsymbol{B} \qquad \boldsymbol{j}_5 = \frac{e^2 \mu}{2\pi^2} \boldsymbol{B}$$

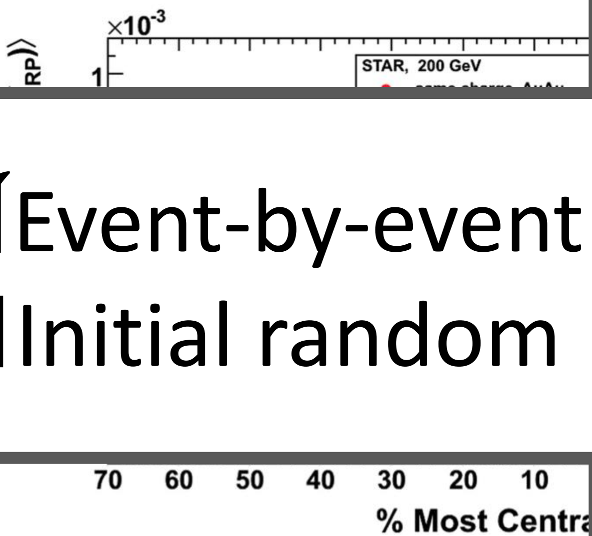

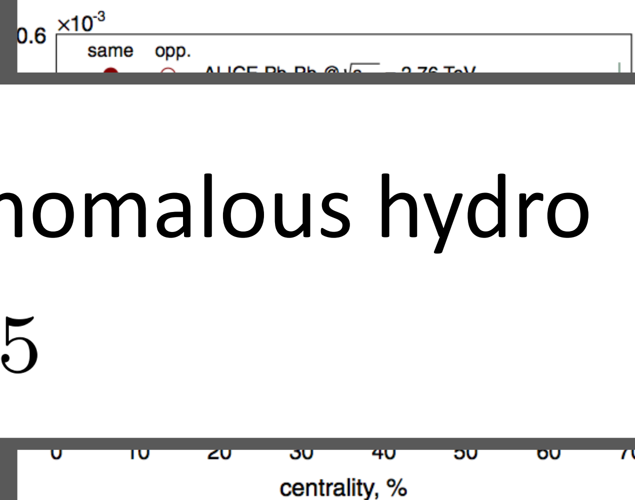

☑ Event-by-event anomalous hydro

☐ Initial random n_5

[STAR, PRL2009, PRC2010]

[ALICE, PRL2013]

$$\langle \cos(\phi_1^\alpha + \phi_2^\beta - 2\Psi_{\mathrm{RP}}) \rangle$$

Sources of axial charges

- Color flux tubes **Spatially random**
- Electromagnetic field $\boldsymbol{E} \cdot \boldsymbol{B}$ **Random** **&** **Coherent**
- QCD sphalerons **Diffusive** **&** **fluctuation**

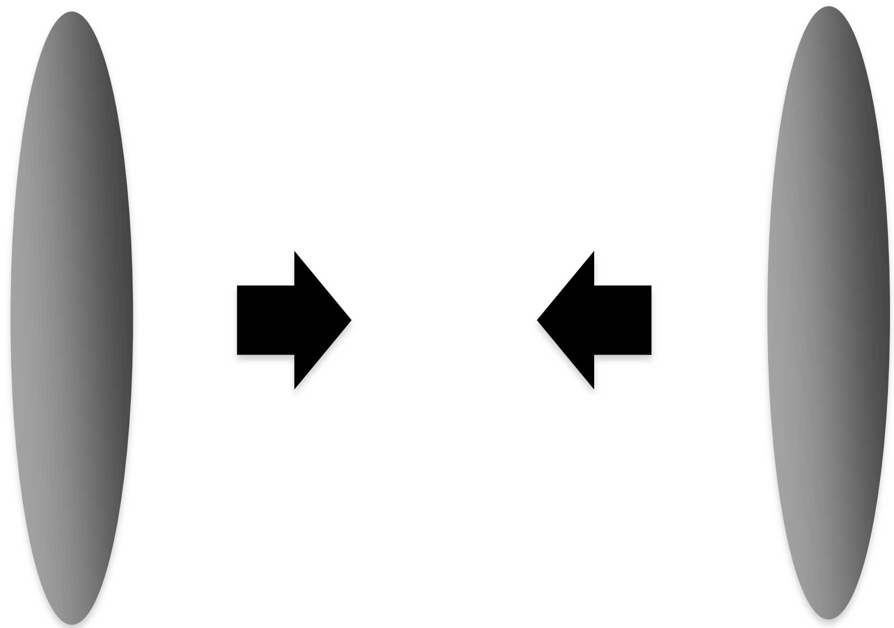

$$\partial_\mu j_5^\mu = \frac{g^2}{16\pi^2}\boldsymbol{E}^a \cdot \boldsymbol{B}^a$$

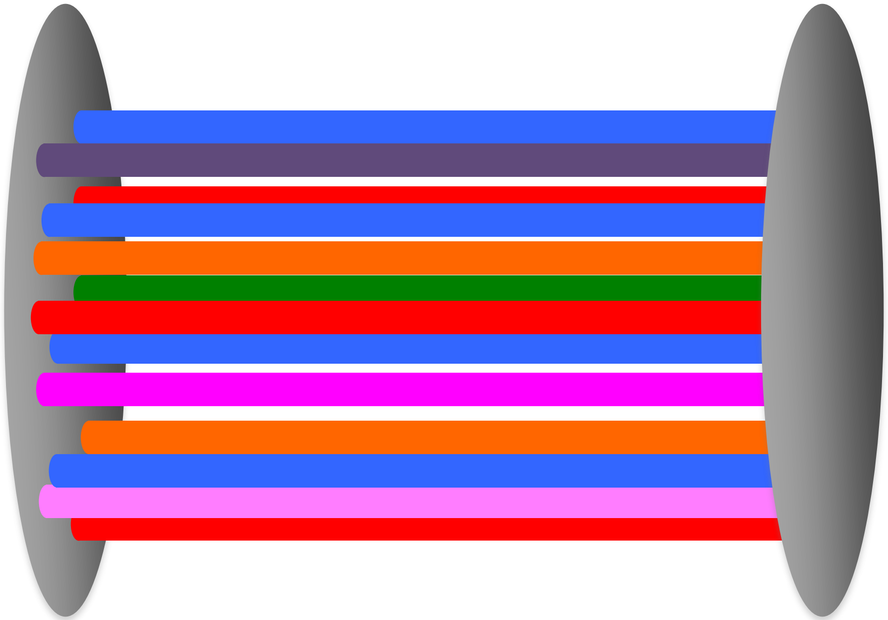

$$\partial_\mu j_5^\mu = \frac{g^2}{16\pi^2} \boldsymbol{E}^a \cdot \boldsymbol{B}^a$$

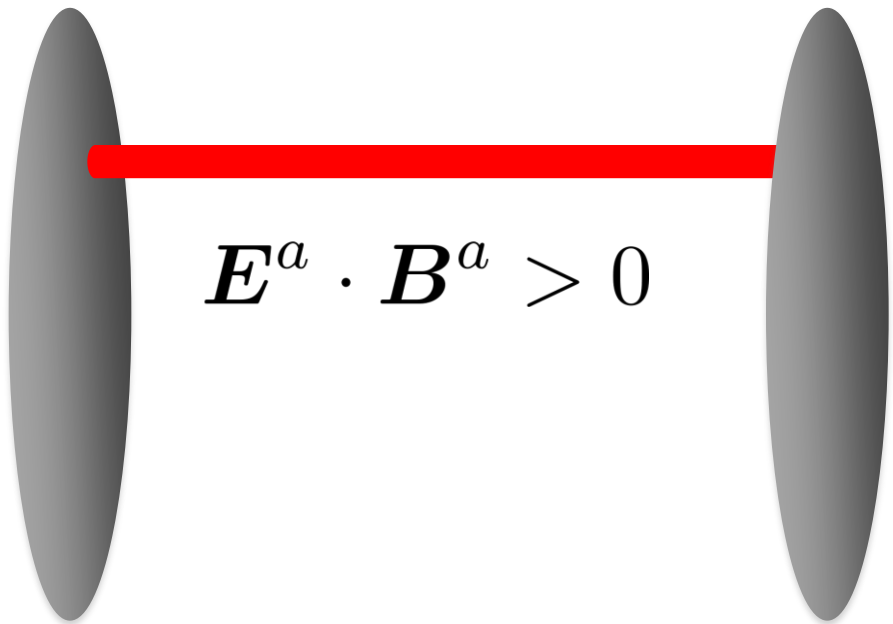

$$\boldsymbol{E}^a \cdot \boldsymbol{B}^a > 0$$

$$\partial_\mu j_5^\mu = \frac{g^2}{16\pi^2} \boldsymbol{E}^a \cdot \boldsymbol{B}^a$$

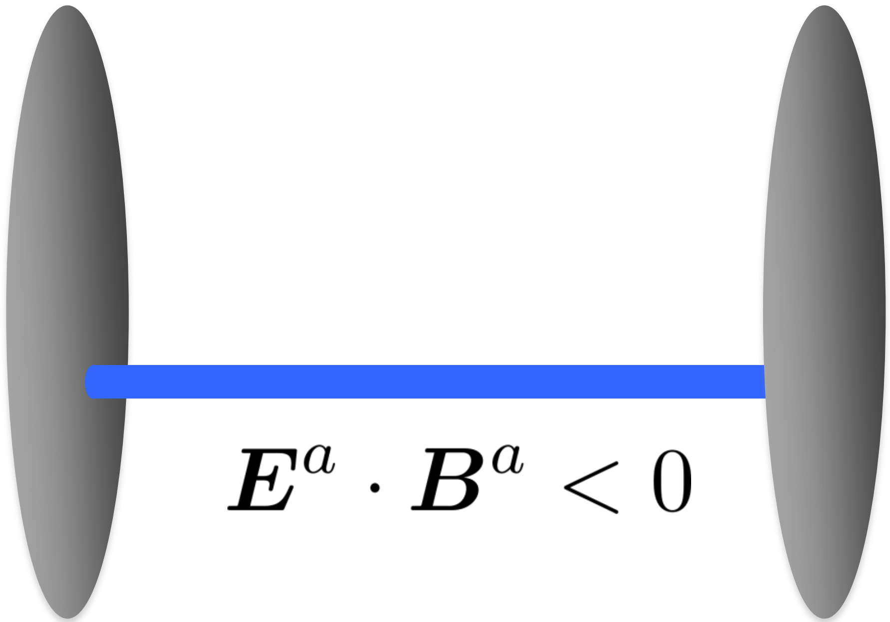

Axial charges from color flux tubes

$N_{\mathrm{part}}^{\mathrm{A(B)}}(\boldsymbol{x}_{\mathrm{T}})$: # of 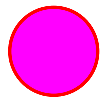 (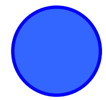) $N_{\mathrm{coll}}(\boldsymbol{x}_{\mathrm{T}})$: # of pairs 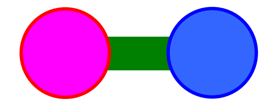

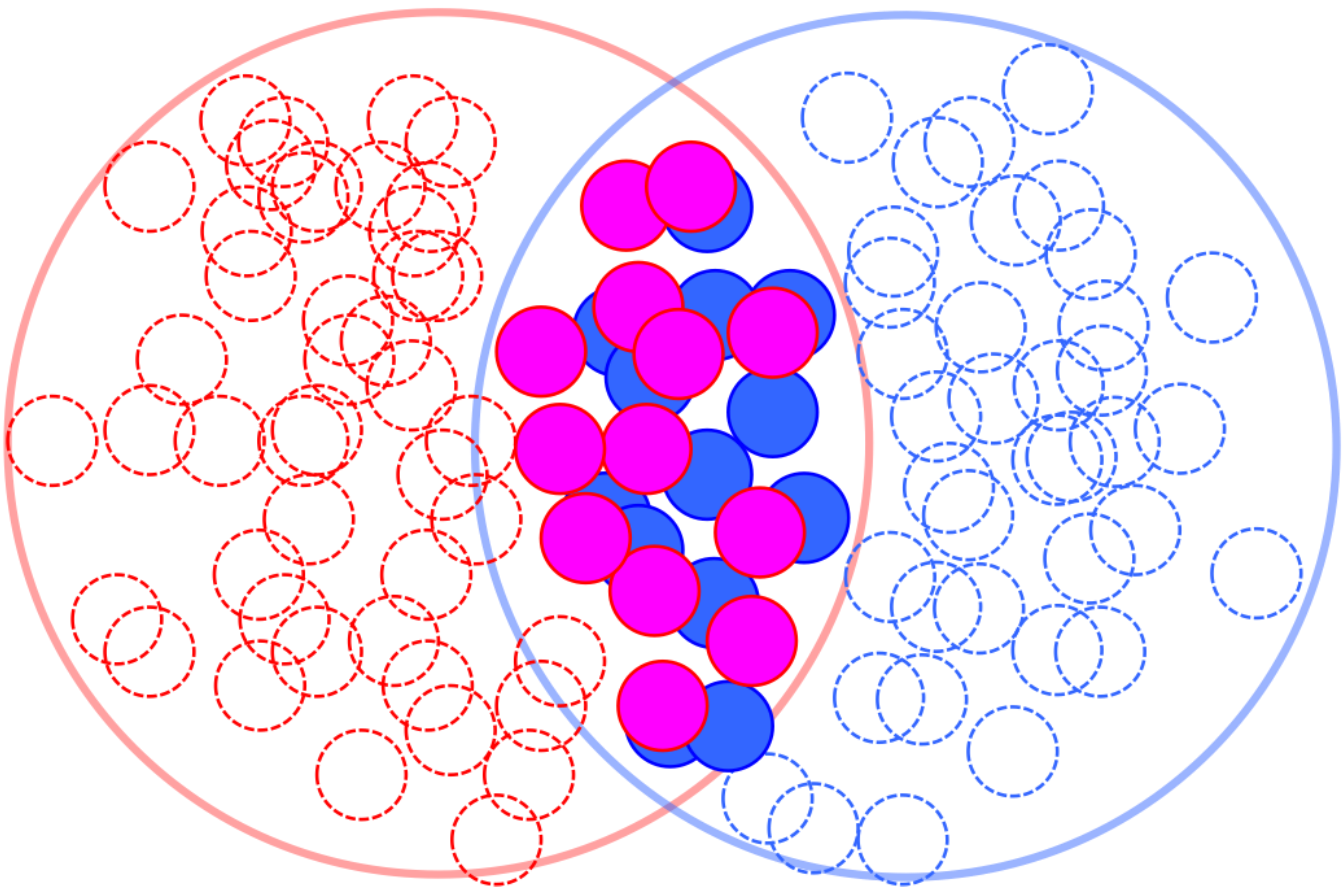

Axial charges from color flux tubes

$$s(\boldsymbol{x}_{\mathrm{T}}, \eta_s) = A f(\eta_s) \left[\frac{1-\alpha}{2} \frac{d^2 N_{\mathrm{part}}}{dx_{\mathrm{T}}^2} + \alpha \frac{d^2 N_{\mathrm{coll}}}{dx_{\mathrm{T}}^2} \right]$$

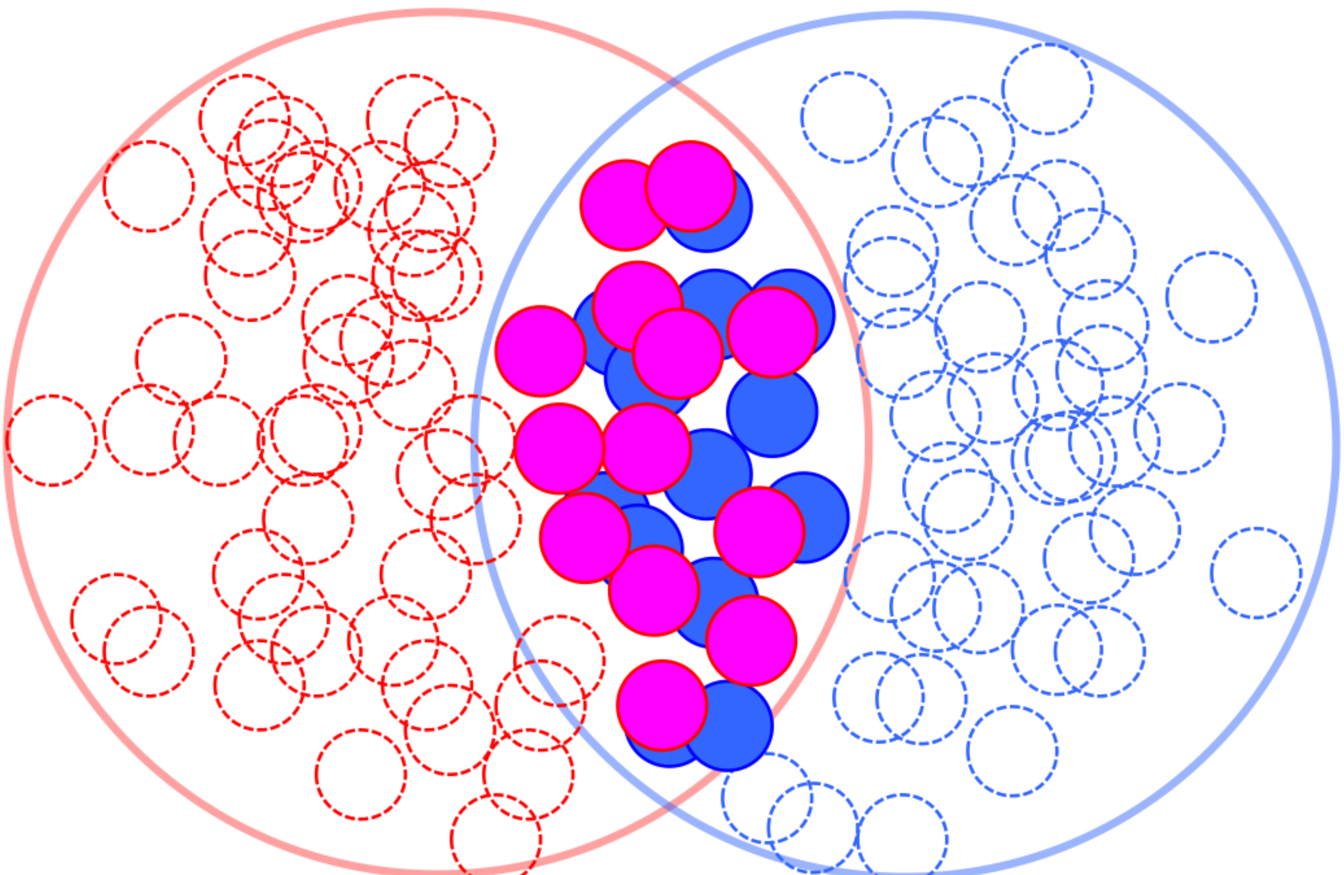

Axial charges from color flux tubes

$$X_j \in \{+1, -1\}$$

Sign of $\boldsymbol{E}^a \cdot \boldsymbol{B}^a$

$$\mu_5(\boldsymbol{x}_\mathrm{T}) = C_{\mu_5} \sum_{j=1}^{N_\mathrm{coll}(\boldsymbol{x}_\mathrm{T})} X_j$$

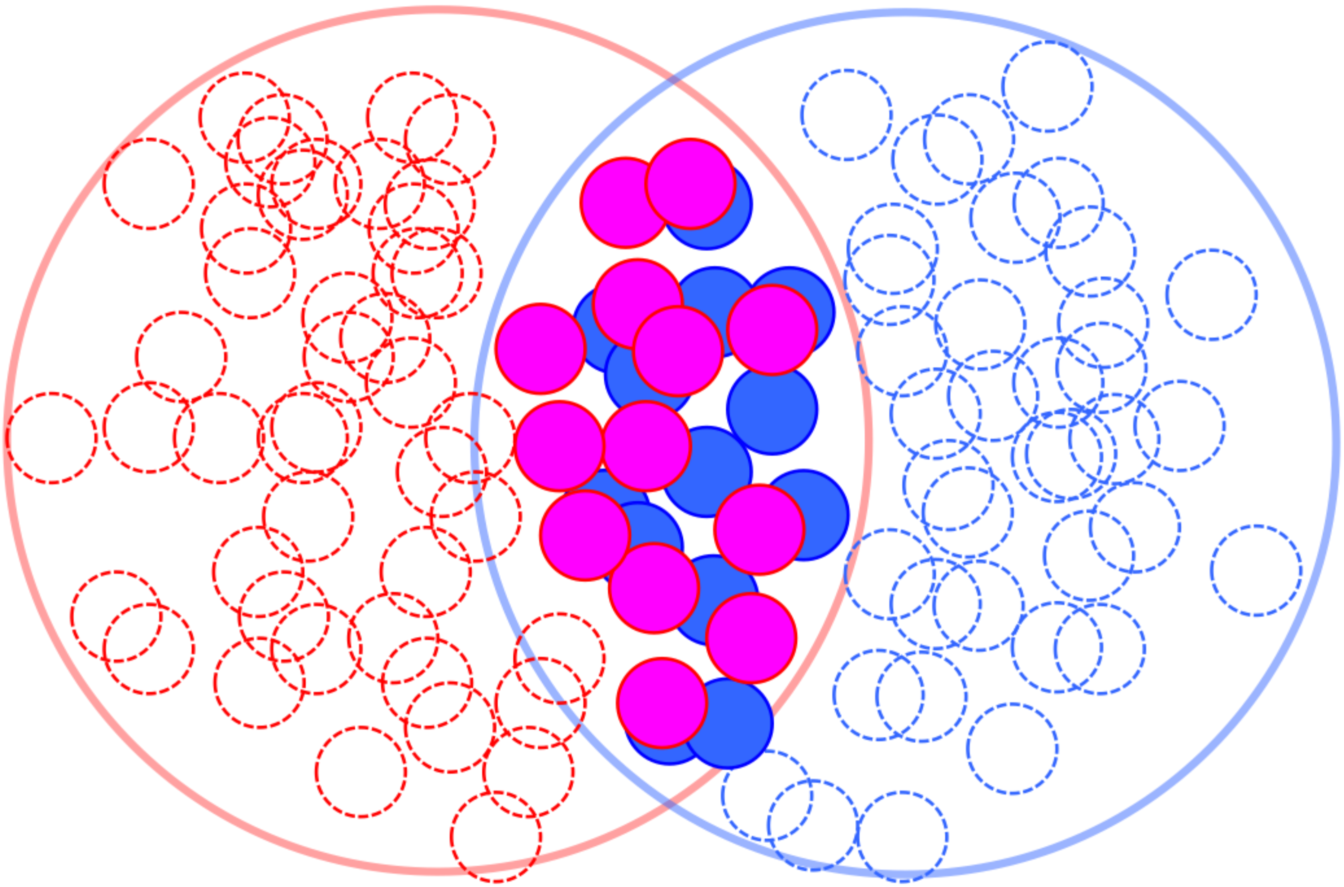

Axial charges from color flux tubes

$$X_j \in \{+1, -1\}$$

Sign of $\boldsymbol{E}^a \cdot \boldsymbol{B}^a$

$$\mu_5(\boldsymbol{x}_\mathrm{T}) = C_{\mu_5} \sum_{j=1}^{N_\mathrm{coll}(\boldsymbol{x}_\mathrm{T})} X_j$$

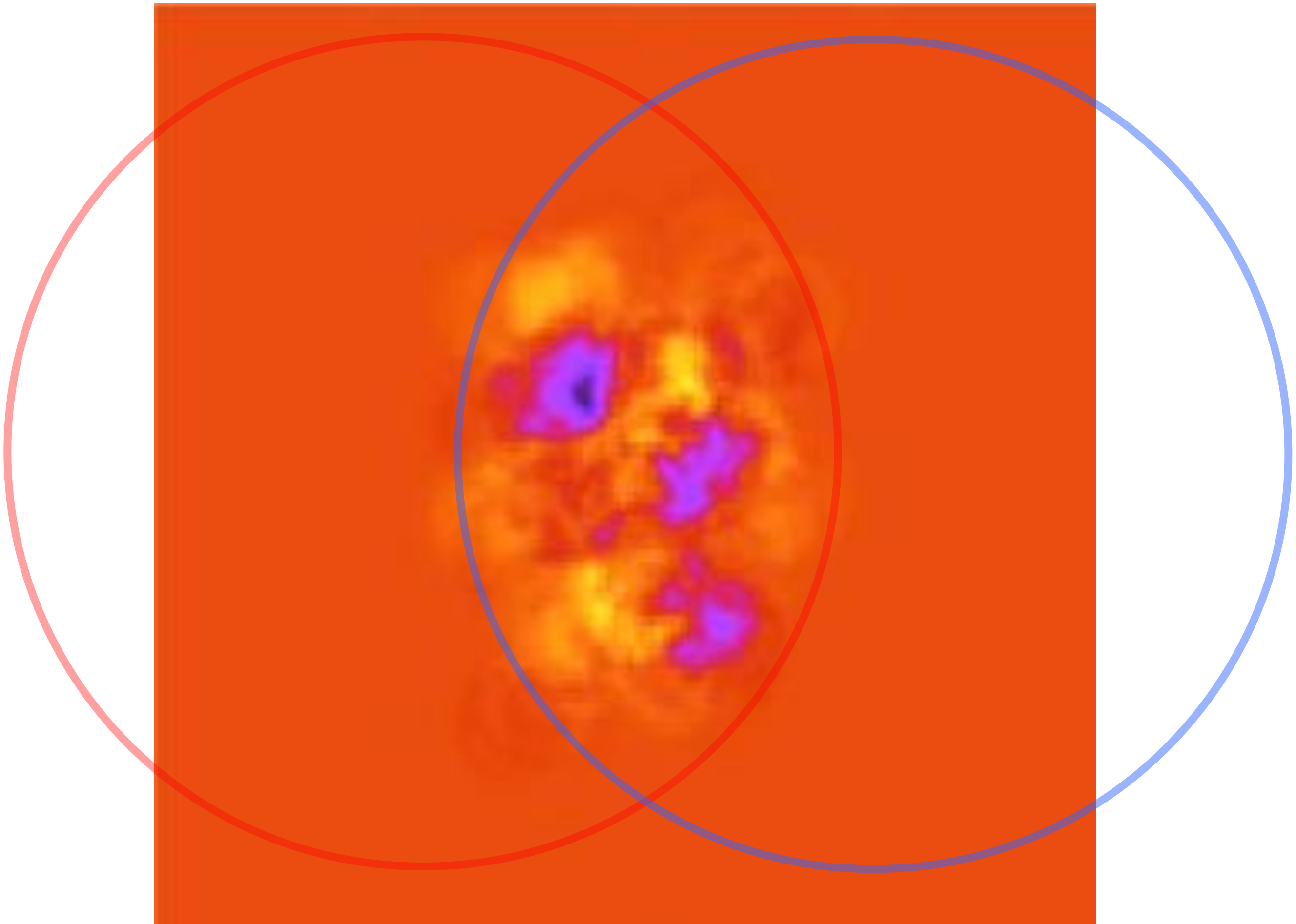

C_{μ_5} estimated by anomaly equation

$$\boxed{\partial_\mu j_5^\mu = \frac{g^2 N_\mathrm{f}}{32\pi^2} G^a_{\mu\nu} \tilde{G}^{a,\mu\nu}}$$

$$n_5(t_\mathrm{in}) \sim \frac{g^2 N_\mathrm{f}}{32\pi^2} G^a_{\mu\nu} \tilde{G}^{a,\mu\nu} \times t_\mathrm{in}$$

$$t_\mathrm{in} \sim 0.6\ [\mathrm{fm}] \qquad g G^a_{\mu\nu} \sim 1\ [\mathrm{GeV}^2]$$

$$\boxed{n_5(t_\mathrm{in}) \sim (0.3\ [\mathrm{GeV}])^3}$$

$$\Rightarrow C_{\mu_5} = 0.1\ [\mathrm{GeV}]$$

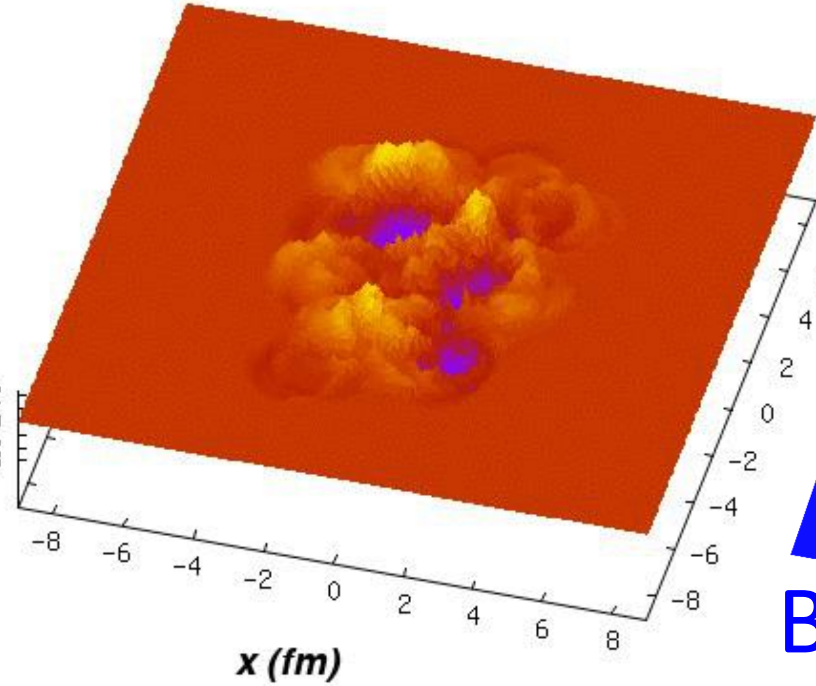

μ_5 [GeV]

B

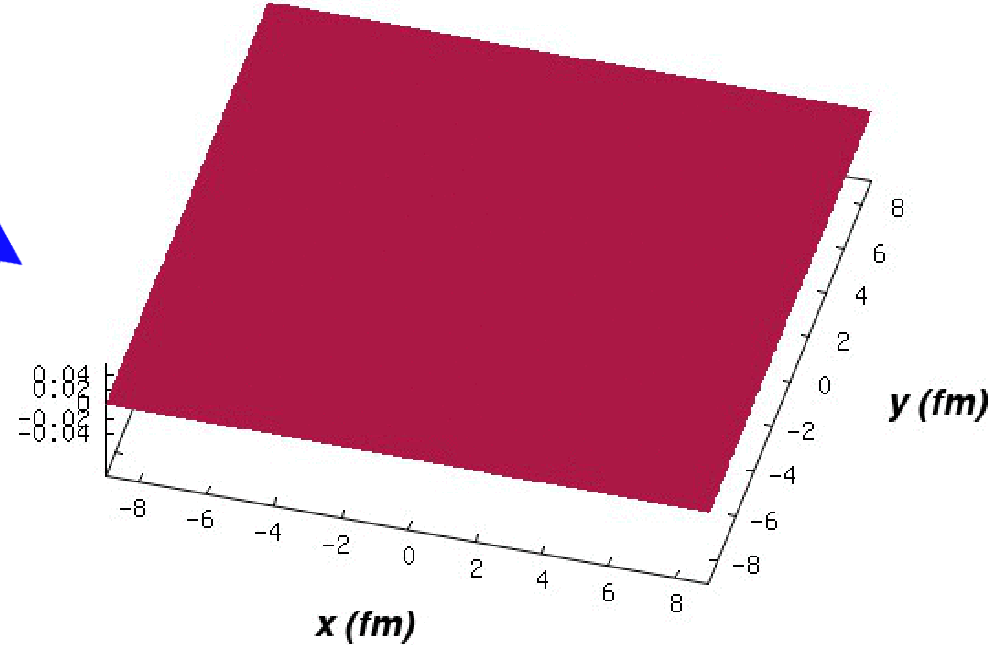

μ [GeV]

- RHIC energy
- b=7.2fm(20-30%)
- $eB_{\max} \simeq (2m_\pi)^2$
- $\tau_B = 3$ [fm]
- $C_{\mu_5} = 0.1$ [GeV]

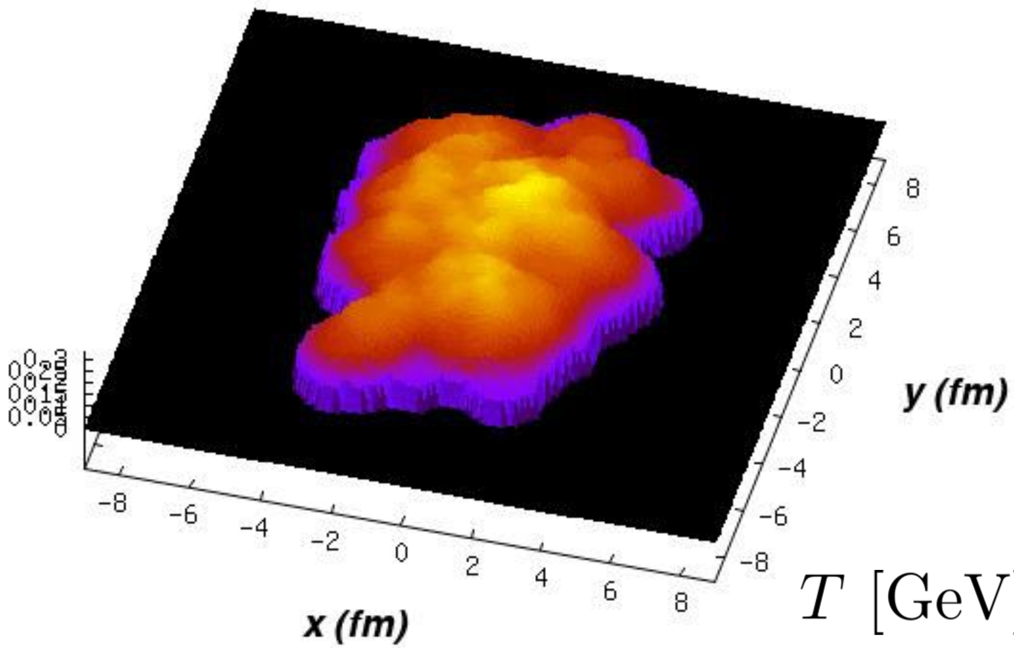

T [GeV]

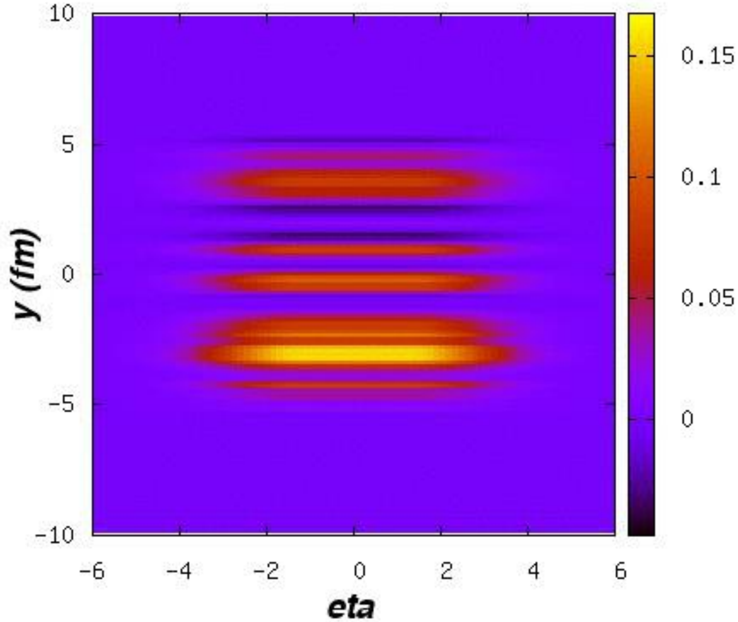

μ_5 [GeV]

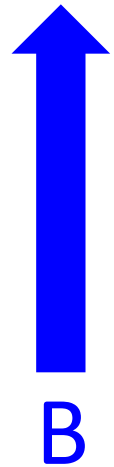

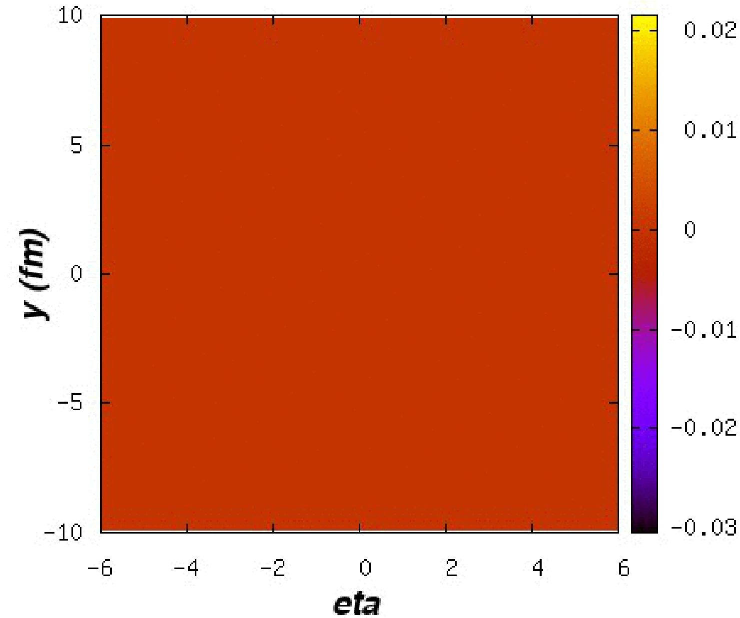

μ [GeV]

- RHIC energy
- b=7.2fm(20-30%)
- $e\boldsymbol{B}_{\mathrm{max}} \simeq (2m_\pi)^2$
- $\tau_B = 3$ [fm]
- $C_{\mu_5} = 0.1$ [GeV]

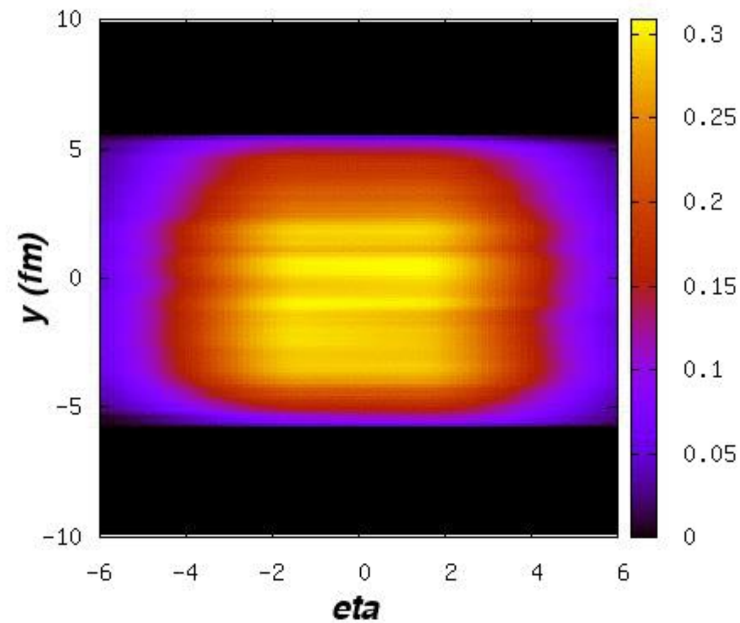

T [GeV]

Anomalous transport in heavy-ion collisions?

$$\boldsymbol{j} = \frac{e^2 \mu_5}{2\pi^2} \boldsymbol{B} \qquad \boldsymbol{j}_5 = \frac{e^2 \mu}{2\pi^2} \boldsymbol{B}$$

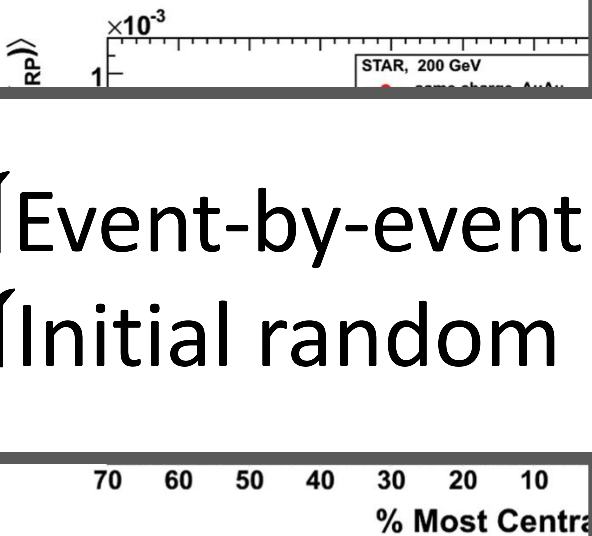

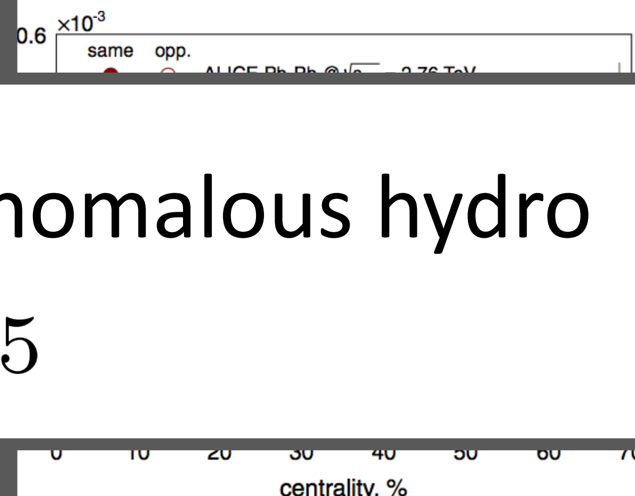

☑Event-by-event anomalous hydro

☑Initial random n_5

[STAR, PRL2009, PRC2010]

[ALICE, PRL2013]

$$\langle \cos(\phi_1^\alpha + \phi_2^\beta - 2\Psi_{\mathrm{RP}}) \rangle$$

Correlations

same-charge

$$\Delta\phi_i^\alpha \equiv \phi_i^\alpha - \Psi_{\mathrm{RP}}$$

$$\langle (v_1^\alpha)^2 \rangle \equiv \left\langle \frac{1}{{}_{M_\alpha}\mathrm{P}_2} \sum_{<i,j>\in S_\alpha} \cos\Delta\phi_i^\alpha \cos\Delta\phi_j^\alpha \right\rangle$$

$$\langle (a_1^\alpha)^2 \rangle \equiv \left\langle \frac{1}{{}_{M_\alpha}\mathrm{P}_2} \sum_{<i,j>\in S_\alpha} \sin\Delta\phi_i^\alpha \sin\Delta\phi_j^\alpha \right\rangle$$

opposite-charge

$$\left\langle v_1^\alpha v_1^\beta \right\rangle \equiv \left\langle \frac{1}{M_\alpha M_\beta} \sum_{i\in S_\alpha, j\in S_\beta} \cos\Delta\phi_i^\alpha \cos\Delta\phi_j^\beta \right\rangle$$

$$\left\langle a_1^\alpha a_1^\beta \right\rangle \equiv \left\langle \frac{1}{M_\alpha M_\beta} \sum_{i\in S_\alpha, j\in S_\beta} \sin\Delta\phi_i^\alpha \sin\Delta\phi_j^\beta \right\rangle$$

Correlations: $\langle (v_1^-)^2 \rangle$, $\langle (a_1^-)^2 \rangle$

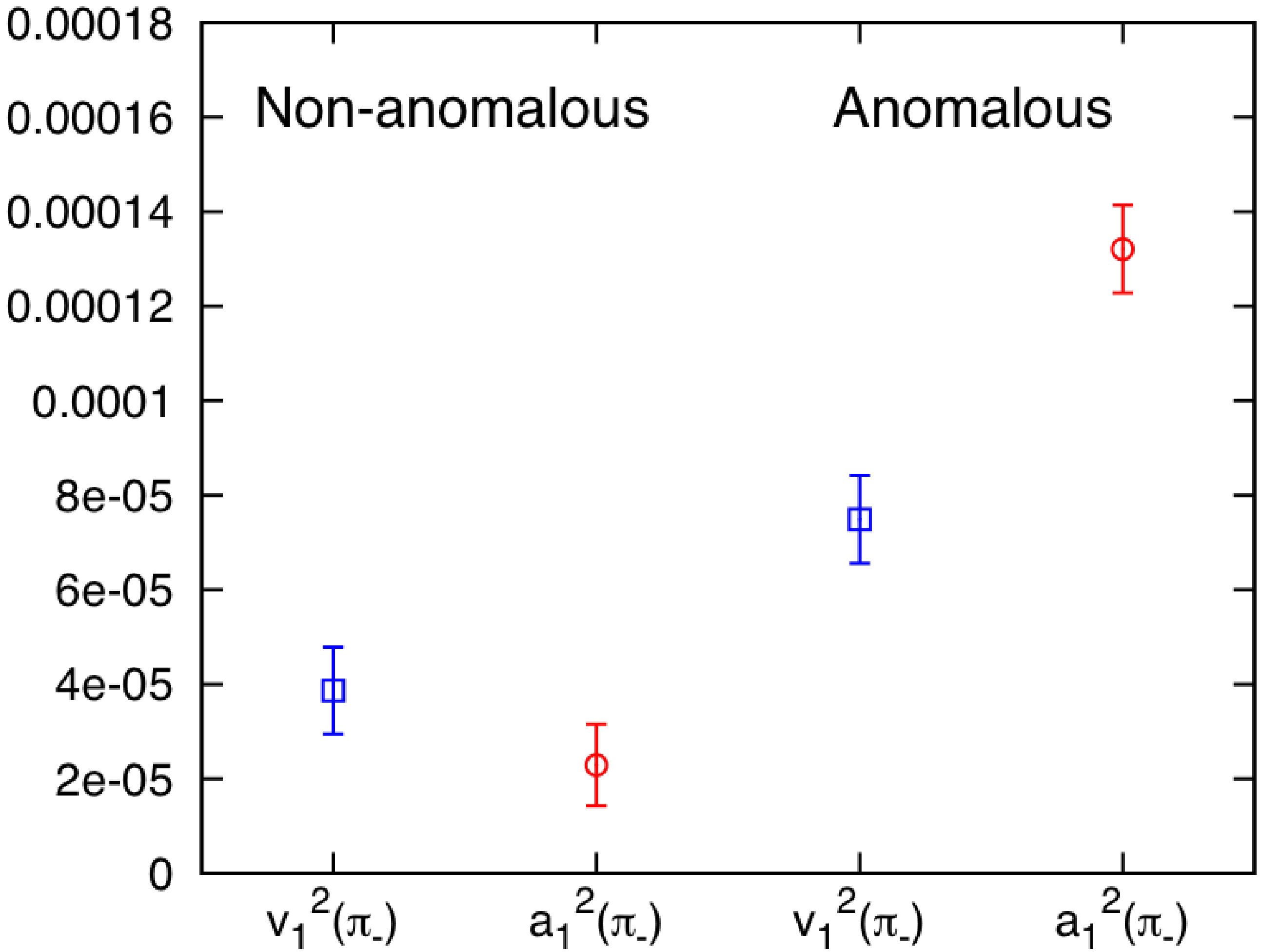

- b=7.2(20-30%)
- RHIC energy
- 100k events
- $eB_{\max} \simeq (3m_\pi)^2$

$$\langle \cos(\phi_1^- + \phi_2^- - 2\Psi_{RP}) \rangle = \langle (v_1^-)^2 \rangle - \langle (a_1^-)^2 \rangle$$

Why v_1 fluctuation also become larger?

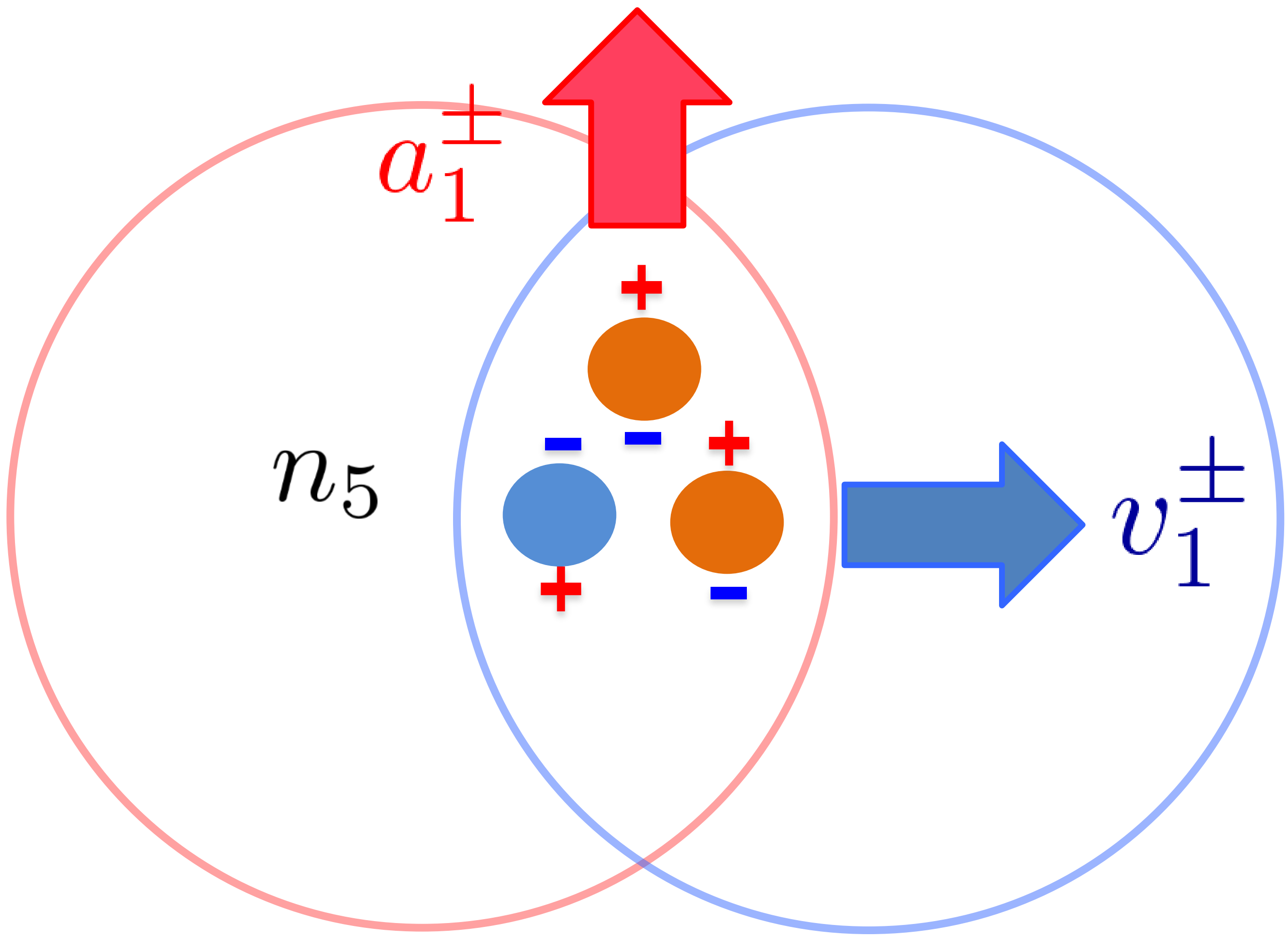

Correlations: $\langle v_1^+ v_1^- \rangle$, $\langle a_1^+ a_1^- \rangle$

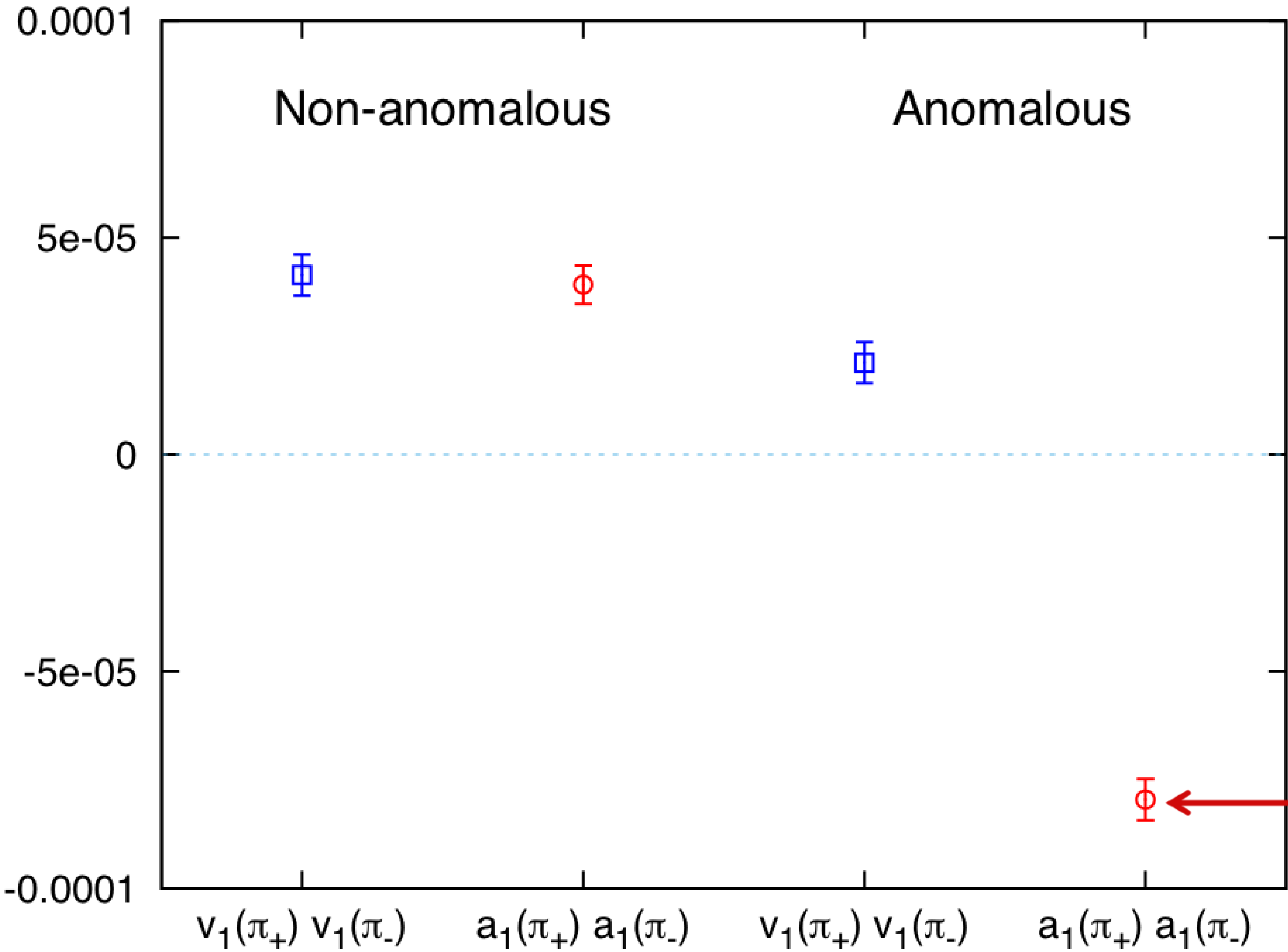

- b=7.2(20-30%)
- RHIC energy
- 100k events
- $eB_{\max} \simeq (3m_\pi)^2$

Anti-correlation btw. a_1^+ & a_1^-

$\langle\cos(\phi_1^\alpha + \phi_2^\beta - 2\Psi_{\mathrm{RP}})\rangle$ (same) vs centrality

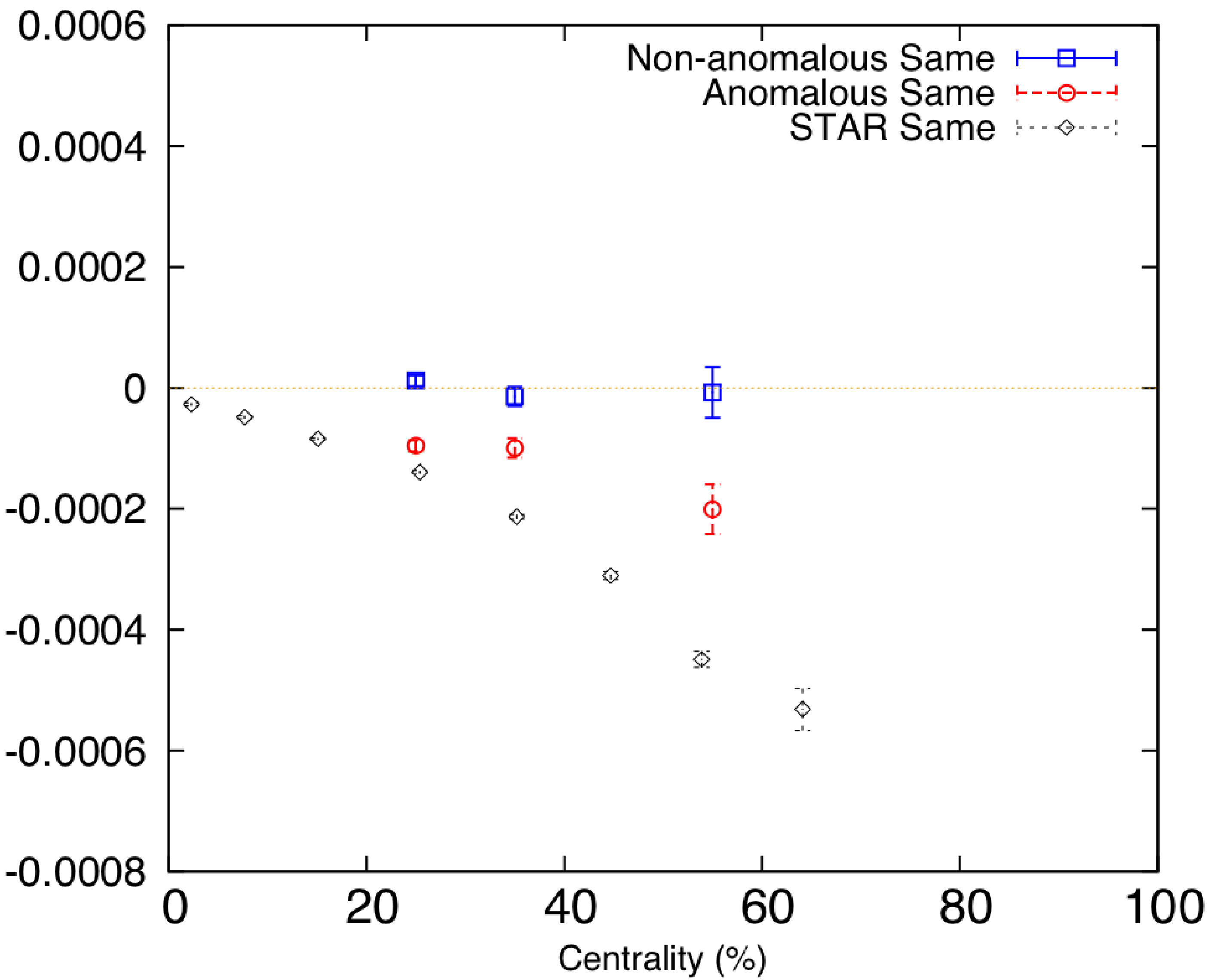

$\langle\cos(\phi_1^\alpha + \phi_2^\beta - 2\Psi_{\mathrm{RP}})\rangle$ (opposite) vs centrality

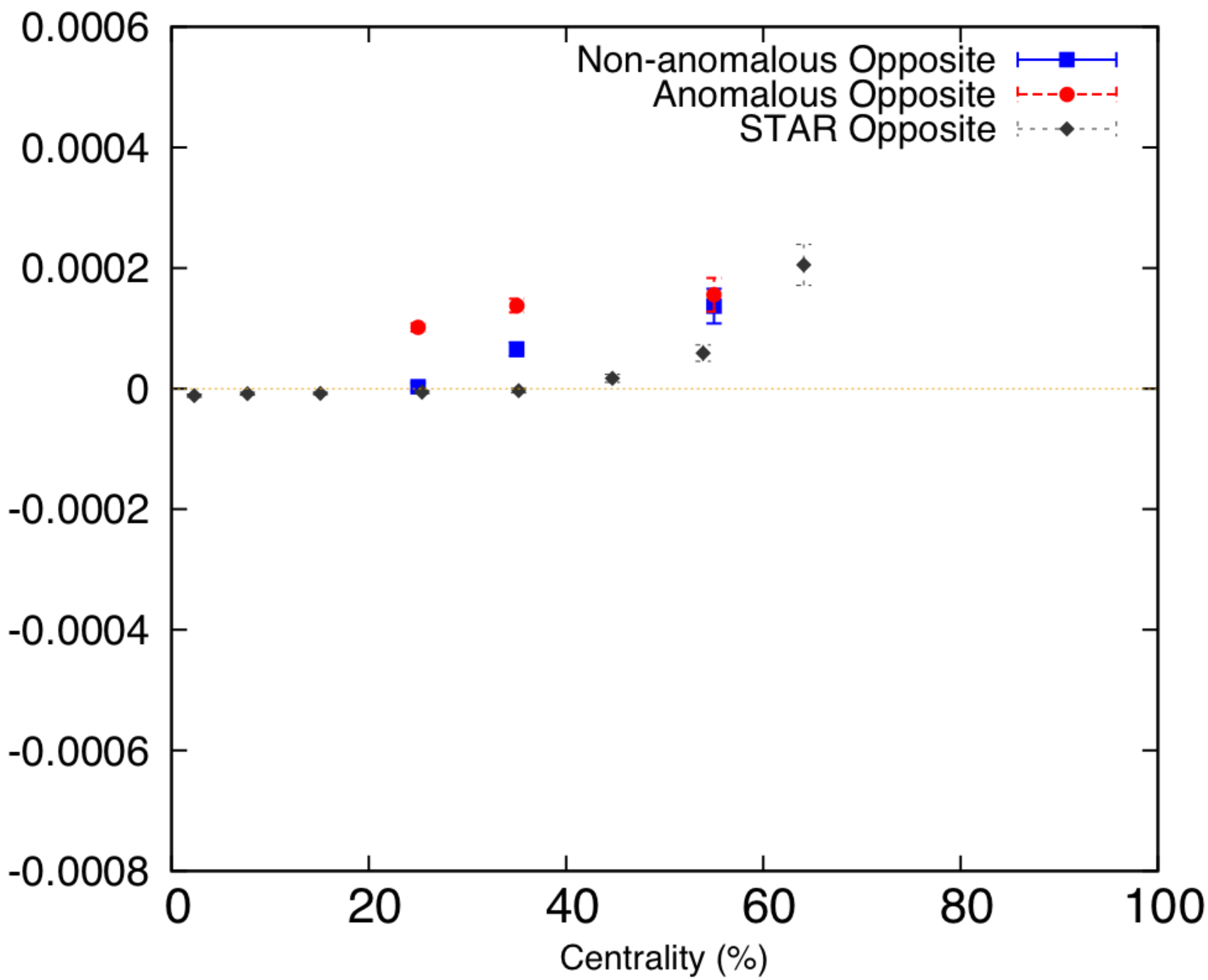

Background effects

- Transverse momentum conservation [S. Pratt, S. Schlichting, S. Gavin, PRC(2011)]
  [A. Bzdak, V. Koch, J. Liao, PRC(2011)]
- Local charge conservation [S. Schlichting and S. Pratt, PRC(2011)]
  [Y. Hori, S. Schlichting, et al [1208.0603]]
- Cluster particle correlations [F. Wang, PRC(2010)]

In our current simulations,
multi-particle correlations are not imposed

$$E\frac{d^3N}{dp^3}(\boldsymbol{p}) = \int \frac{p^\mu d\sigma_\mu}{e^{\beta(p\cdot u-\mu)} \mp_{\mathrm{BF}} 1}$$

Cooper-Frye formula → single-particle distributions

Anomalous transport in heavy-ion collisions?

Outlook

- pt & eta dependence / parameter dependence (√s, tau_B, …)
- Back reaction/Dissipations/CVE/realistic EOS/…
- Better experimental observables

☑Event-by-event anomalous hydro

☑Initial random n_5

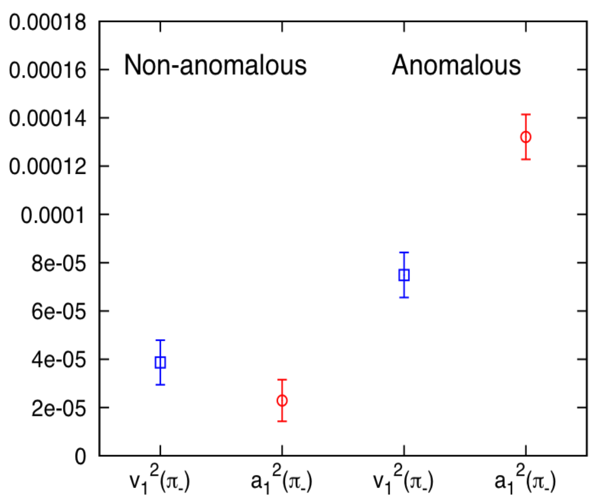

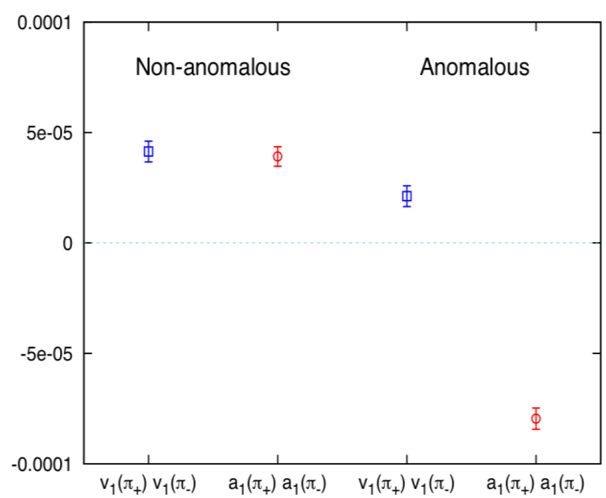

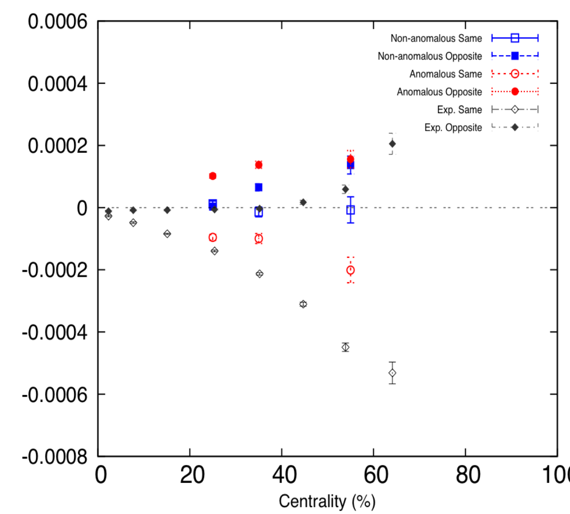

Possible improvements

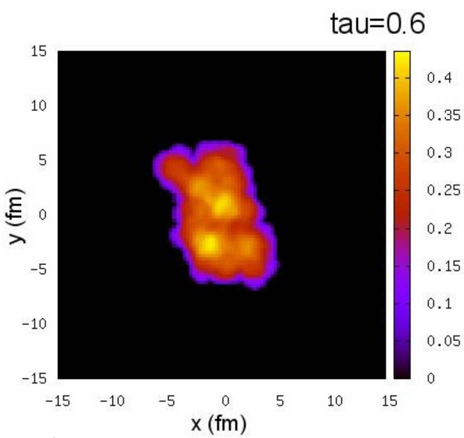

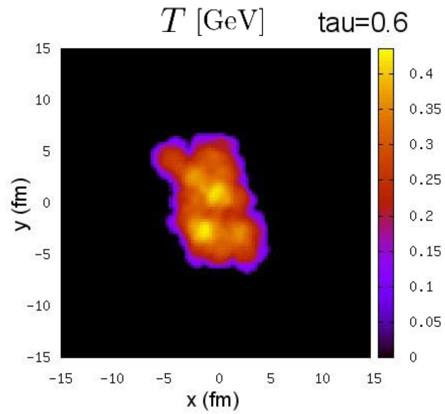

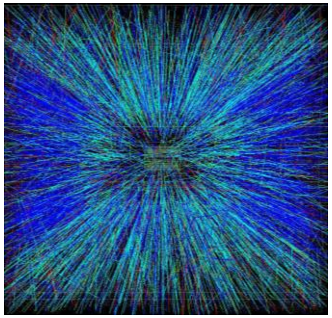

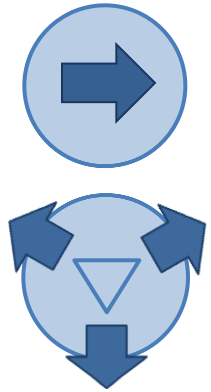

t

Initial state

Anomalous
hydro evolution

Freeze-out

Correlations

- n5 profile
  based on CGC
- Charge separation
  in glasma

- More realistic EOS
  with mu & mu5 dep.
- Chiral vortical effect
- Backreaction to EM field
- Dissipational effects
  - viscosity
  - conductivity

- Multi-particle corr.

- Differential analysis
  - eta, pt
- Parameter dep.
  - Cmu5, B, √s
- New obs. insensitive
  to background

Backup slides

Background magnetic fields

$$B_y(\tau, \eta_s, \boldsymbol{x}_\perp) = B_0 \frac{b}{2R} \exp\left[-\frac{x^2}{\sigma_x^2} - \frac{y^2}{\sigma_y^2} - \frac{\eta^2}{\sigma_{\eta_s}^2} - \frac{\tau}{\tau_{\mathrm{B}}}\right]$$

$$B_y(\tau_{\mathrm{in}}, 0, \boldsymbol{0}) \sim (3m_\pi)^2$$

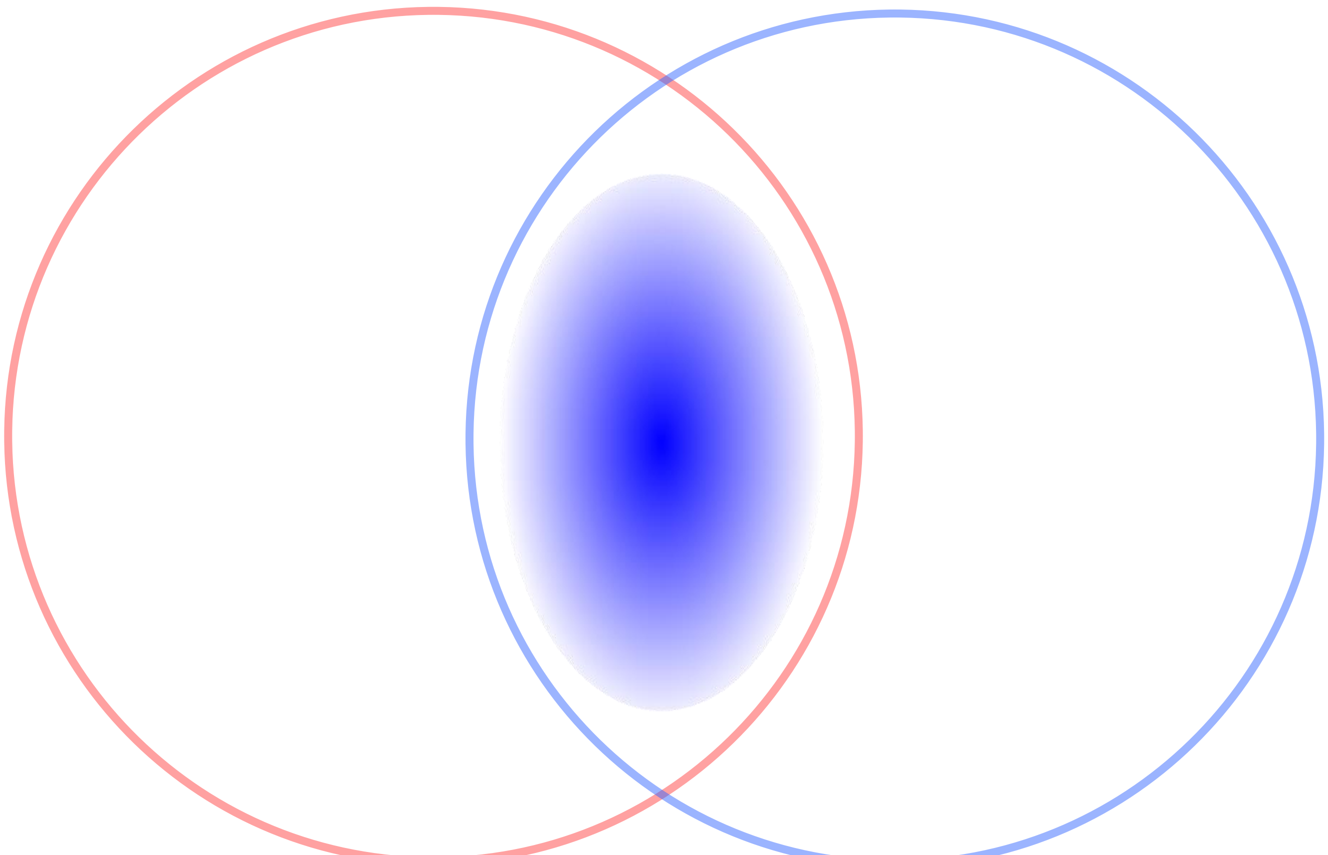

$\langle\cos(\phi_1^\alpha + \phi_2^\beta - 2\Psi_{\rm RP})\rangle$ vs centrality

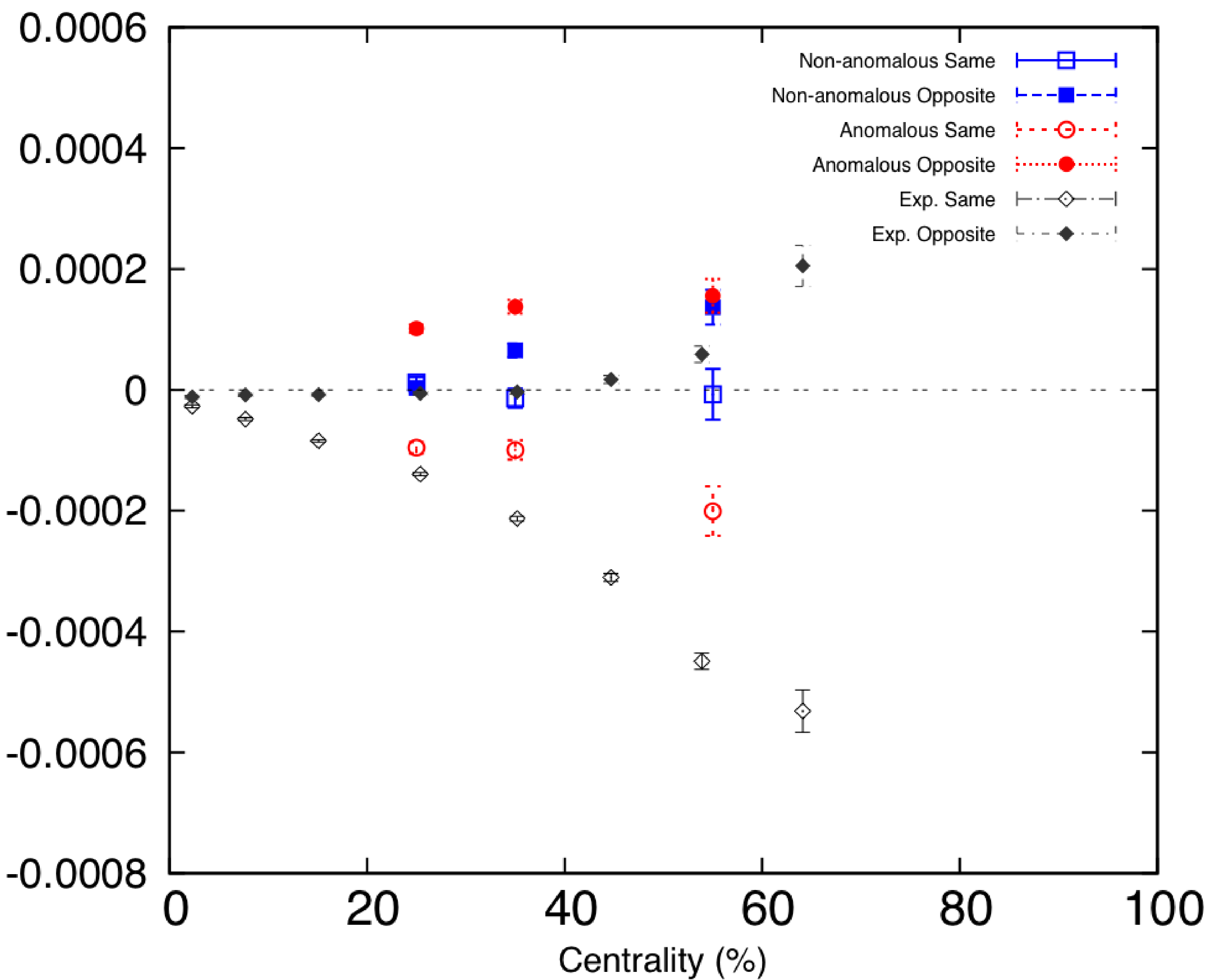

Electromagnetic fields

$$B_y(\tau, \eta_s, \boldsymbol{x}_\perp) = B_0 \frac{b}{2R} \exp\left[-\frac{x^2}{\sigma_x^2} - \frac{y^2}{\sigma_y^2} - \frac{\eta^2}{\sigma_{\eta_s}^2} - \frac{\tau}{\tau_{\mathrm{B}}} \right]$$

$$E_y(\tau, \eta_s, \boldsymbol{x}_\perp) = \frac{y}{y_0} \times E_0 \frac{b}{2R} \exp\left[-\frac{x^2}{\sigma_x^2} - \frac{y^2}{\sigma_y^2} - \frac{\tau}{\tau_{\mathrm{E}}} - \frac{\eta^2}{\sigma_{\eta_s}^2} \right]$$

$$\sigma_x = 0.8 \left(R - \frac{b}{2} \right) \quad \sigma_y = 0.8 \sqrt{R^2 - \left(\frac{b}{2} \right)^2} \quad \sigma_\eta = \sqrt{2}$$

Harmonics v_n

- Azimuthal angle distribution of observed particles

$$\frac{dN}{d\phi} = \bar{N}\left[1 + \sum_{n=1}^{\infty} 2 v_n \cos n(\phi - \Psi_n)\right]$$

- Represents the shape the flow

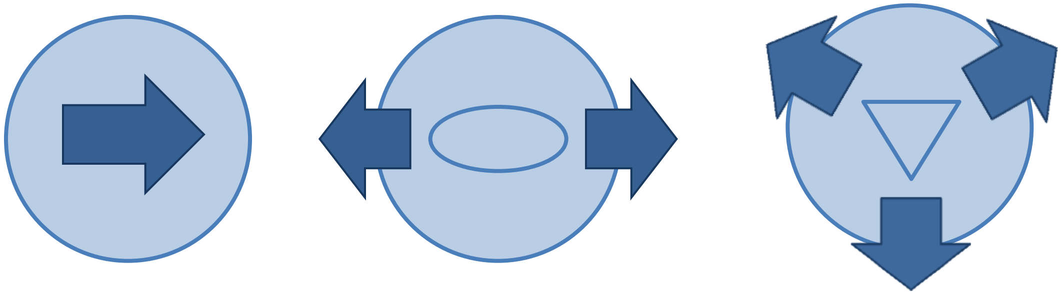

v_1 "directed"

v_2 "elliptic"

v_3 "triangle"

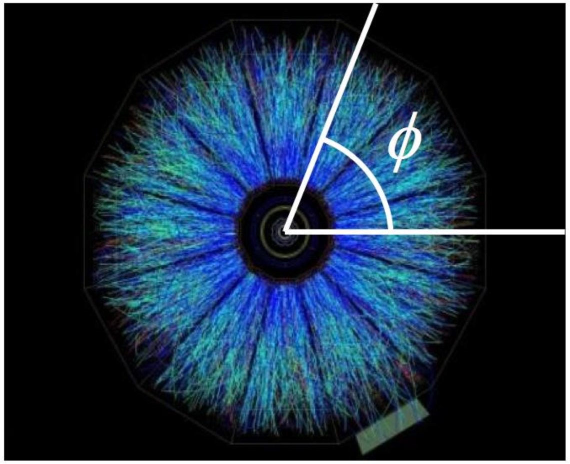

Charge dependent correlations [STAR]

$$\boxed{\langle \cos(\phi_1^{\alpha} + \phi_2^{\beta} - 2\Psi_{\mathrm{RP}}) \rangle}$$

$$\alpha, \beta \in \{+, -\}$$

$$\langle (v_1^+)^2 \rangle \equiv \left\langle \frac{1}{{}_M\mathrm{P}_2} \sum_{<i,j>} \cos(\phi_i^+ - \Psi_{\mathrm{RP}}) \cos(\phi_j^+ - \Psi_{\mathrm{RP}}) \right\rangle$$

$$\langle (a_1^+)^2 \rangle \equiv \left\langle \frac{1}{{}_M\mathrm{P}_2} \sum_{<i,j>} \sin(\phi_i^+ - \Psi_{\mathrm{RP}}) \sin(\phi_j^+ - \Psi_{\mathrm{RP}}) \right\rangle$$

MC-Glauber initial condition

$$\frac{d^2 N_{\mathrm{part}}}{dx_{\mathrm{T}}^2}(\eta_{\mathrm{s}}, \boldsymbol{x}_{\mathrm{T}}) = \theta(y_{\mathrm{beam}} - \eta_{\mathrm{s}}) \left[\frac{y_{\mathrm{beam}} + \eta_{\mathrm{s}}}{y_{\mathrm{beam}}} \frac{d^2 N_{\mathrm{part}}^{\mathrm{A}}}{dx_{\mathrm{T}}^2} + \frac{y_{\mathrm{beam}} - \eta_{\mathrm{s}}}{y_{\mathrm{beam}}} \frac{d^2 N_{\mathrm{part}}^{\mathrm{B}}}{dx_{\mathrm{T}}^2} \right]$$

$$s(\boldsymbol{x}_{\mathrm{T}}, \eta_{\mathrm{s}}) = C f(\eta_{\mathrm{s}}) \left[\frac{1-\alpha}{2} \frac{d^2 N_{\mathrm{part}}}{dx_{\mathrm{T}}^2} + \alpha \frac{d^2 N_{\mathrm{coll}}}{dx_{\mathrm{T}}^2} \right]$$

$$f(\eta_{\mathrm{s}}) = \exp\left[-\theta(|\eta_{\mathrm{s}}| - \Delta\eta_{\mathrm{s}}) \frac{(|\eta_{\mathrm{s}}| - \Delta\eta_{\mathrm{s}})^2}{\sigma_\eta^2} \right]$$

Beam energy scan
using a viscous hydro+cascade model

Iurii KARPENKO

Frankfurt Institute for Advanced Studies/
Bogolyubov Institute for Theoretical Physics

Theory and Modeling for the Beam Energy Scan, February 26-27, 2015

IK, Huovinen, Petersen, Bleicher, `arXiv:1502.01978`

Introduction: heavy ion collision in pictures

https://www.jyu.fi/fysiikka/tutkimus/suurenergia/urhic/anim1.gif/image_view_fullscreen

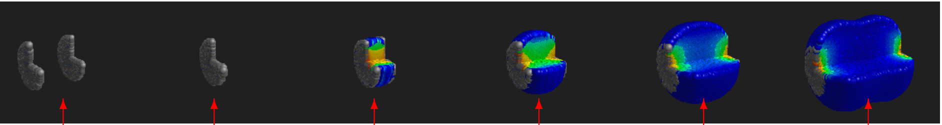

incoming nuclei　　dense medium (QGP)　　phase transition

initial stage of the reaction　　expansion　　hadrons

Hybrid model: initial state + hydrodynamic phase + hadronic cascade

thermalization　　particlization

This study's motivation: apply a hybrid for RHIC BES, FAIR/NICA

to understand whether fluid is created at lower energies,
find its transport properties (η/s,...) and constrain its EoS.

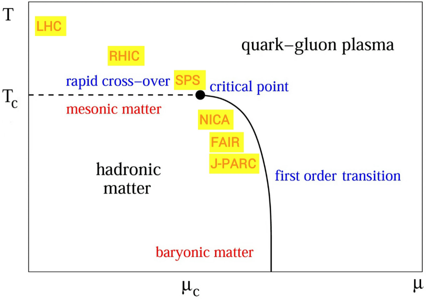

For Beam energy scan, we need a more elaborate model (vs. full RHIC):

1. 3D (non-boost-invariant) fluctuating initial state
   - CGC picture does not work as good as at full RHIC!
2. Baryon and electric charge densities
   - obtained from an initial state model
   - propagated in hydro phase and included in EoS
   - taken into account in particlization procedure

The model

Initial (pre-thermal) phase

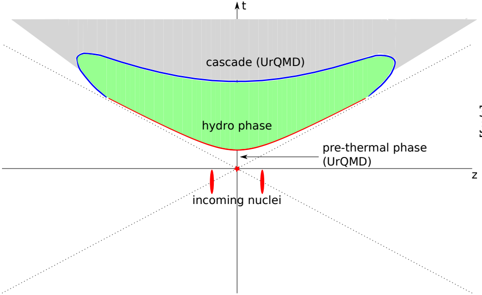

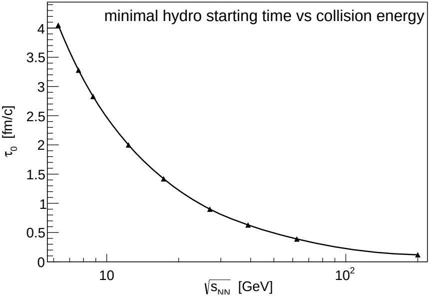

Pre-thermal phase: UrQMD cascade [1],
which involves PYTHIA for $\sqrt{s} \gtrsim 10$ GeV scatterings

The scatterings are allowed until $\tau = \sqrt{t^2 - z^2} = \tau_0$ (red curve), $\tau_0 = \frac{2R}{\gamma v_z}$

[1] M. Bleicher et al., J.Phys. G25 (1999) 1859-1896. `http://urqmd.org/`

“Thermalization”

At $\tau = \tau_0$ we deposit the energy/momentum P^α, baryon and electric charge N^0 of every particle into fluid cells:

$$\Delta P^\alpha_{ijk} = P^\alpha \cdot C \cdot \exp\left(-(\Delta x_i^2 + \Delta y_j^2)/R_\perp^2 - \Delta\eta_k^2 \gamma_\eta^2 \tau_0^2 / R_\eta^2\right)$$
$$\Delta N^0_{ijk} = N^0 \cdot C \cdot \exp\left(-(\Delta x_i^2 + \Delta y_j^2)/R_\perp^2 - \Delta\eta_k^2 \gamma_\eta^2 \tau_0^2 / R_\eta^2\right)$$

Some typical initial energy density profiles in the transverse plane:

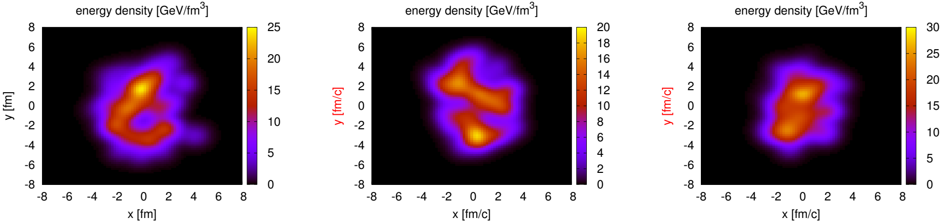

Hydrodynamic phase

The hydrodynamic equations: local energy-momentum and charge conservation

$$\partial_{;\nu} T^{\mu\nu} = \partial_\nu T^{\mu\nu} + \Gamma^\mu_{\nu\lambda} T^{\nu\lambda} + \Gamma^\nu_{\nu\lambda} T^{\mu\lambda} = 0, \quad \partial_{;\nu} N^\nu = 0 \tag{1}$$

where (we choose Landau definition of velocity)

$$T^{\mu\nu} = \varepsilon u^\mu u^\nu - (p + \Pi)(g^{\mu\nu} - u^\mu u^\nu) + \pi^{\mu\nu} \tag{2}$$

Evolutionary equations for shear/bulk, coming from **Israel-Stewart** formalism:

$$< u^\gamma \partial_{;\gamma} \pi^{\mu\nu} > = -\frac{\pi^{\mu\nu} - \pi^{\mu\nu}_{\text{NS}}}{\tau_\pi} - \frac{4}{3} \pi^{\mu\nu} \partial_{;\gamma} u^\gamma \tag{3a}$$

* Bulk viscosity $\zeta = 0$, charge diffusion=0

`vHLLE` code: IK, Huovinen, Bleicher, Comput. Phys. Commun. 185 (2014), 3016
`http://cpc.cs.qub.ac.uk/summaries/AETZ_v1_0.html`

Equations of state for hydrodynamic phase

- Chiral model
  - coupled to Polyakov loop to include the deconfinement phase transition
  - good agreement with lattice QCD data at $\mu_B = 0$, also applicable at finite baryon densities
  - (current version) has crossover type PT between hadron and quark-gluon phase at all μ_B
- Hadron resonance gas + Bag Model (a.k.a. `EoS Q`)
  - hadron resonance gas made of u, d quarks including repulsive meanfield
  - the phases matched via Maxwell construction, resulting in 1^{st} order PT

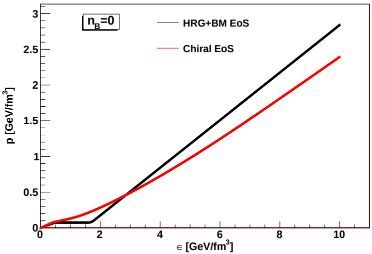

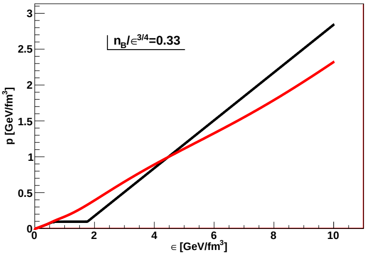

refs: J. Steinheimer, S. Schramm and H. Stocker, J. Phys. G 38, 035001 (2011); P.F. Kolb, J. Sollfrank, and U. Heinz, Phys.Rev. C 62, 054909 (2000).

Fluid→particle transition and hadronic phase

$\varepsilon = \varepsilon_{sw} = 0.5$ GeV/fm^3 (blue curve), when the system is in hadronic phase:
$\{T^{0\mu}, N_b^0, N_q^0\}$ of hadron-resonance gas = $\{T^{0\mu}, N_b^0, N_q^0\}$ of fluid

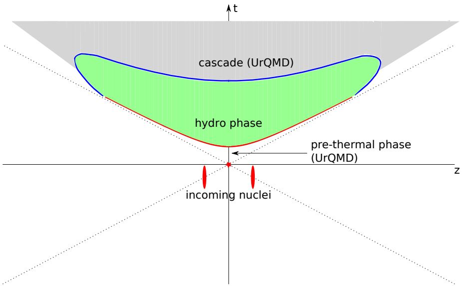

▷ Momentum distribution from Landau/Cooper-Frye prescription:

$$p^0 \frac{d^3 n_i}{d^3 p} = \int \left(f_{\text{l.eq.}}(x,p) + \delta f(x,p) \right) p^\mu d\sigma_\mu$$

▷ Cornelius subroutine* is used to compute $\Delta\sigma_i$ on transition hypersurface.

▷ Hadron gas phase: UrQMD cascade is employed after particlization surface.

*Huovinen and Petersen, *Eur.Phys.J.* A **48** (2012), 171

Results 1

From the first round of simulations: fixed η/s, Chiral EoS

The rest of the parameters are fixed to their reasonable values:

$R_\perp = R_\eta = 1$ fm,
$\tau_0 = \max\left\{\frac{2R}{\gamma v_z}, 1\,\mathrm{fm/c}\right\}$
$\varepsilon_{\mathrm{sw}} = 0.5$ GeV/fm^3

Results: $E_{\text{lab}} = 40$ A GeV Pb-Pb (SPS)

$\sqrt{s_{NN}} = 8.8$ GeV, 0-5% central collisions ($b = 0 \ldots 3.4$ fm)   (Chiral EoS only)

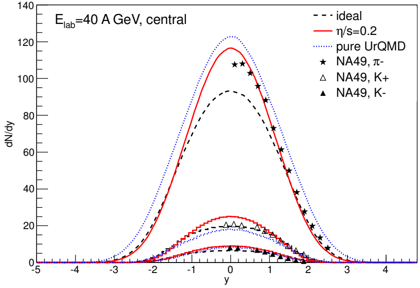

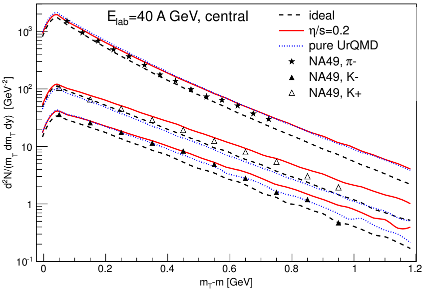

- viscous entropy production
- viscosity causes stronger transverse expansion

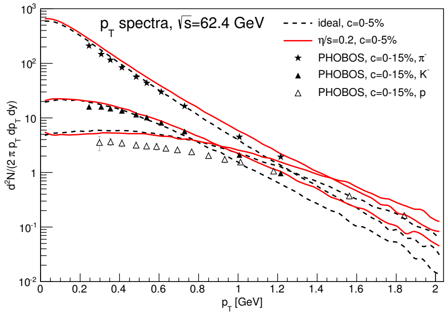

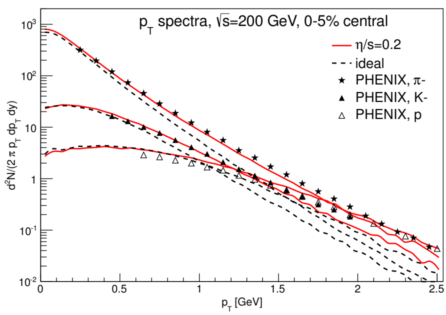

$dN/d\eta$+p_T from existing RHIC data ($\sqrt{s_{NN}} = 19.6, 62.4, 200$ GeV Au-Au)

Fine tuning is required for every energy individually to reproduce $dN/d\eta$ and v_2 (see next slide).

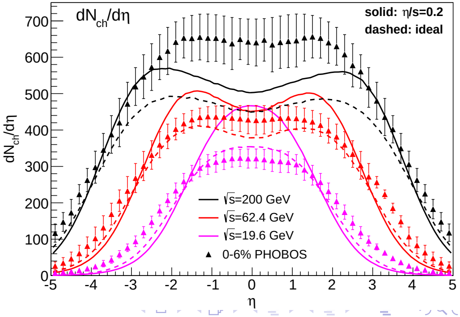

v_2 and v_3 at $\sqrt{s_{NN}} = 7.7 \ldots 200$ GeV Au-Au

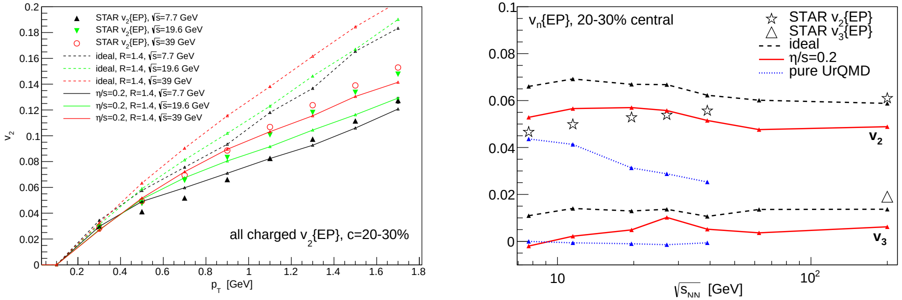

- shear viscosity suppresses the elliptic flow (as expected)
- the suppression is too small for $\sqrt{s} < 30$ GeV and too large otherwise
- triangular flow is similarly suppressed

Results 2:

parameter adjustment to the data in BES region using Chiral EoS

!!! Observables in the model strongly depend on the details of the initial state for hydrodynamic expansion, because the hydro phase is shorter compared to full RHIC/LHC energies

Parameter dependence

Response of the observables:

- T_{eff} from $\frac{dN}{m_T dm_T dy} = C \exp\left(-\frac{m_T}{T_{\mathrm{eff}}}\right)$ fit
- dN/dy in $|y < 0.2|$
- p_T integrated elliptic flow $v_2\{\mathrm{EP}\}$

to the change of every individual parameter with respect to its default value.

Defaults: $\eta/s = 0$, $R_\perp = R_\eta = 1$ fm, $\varepsilon_{\mathrm{crit}} = 0.5$ GeV/fm^3.

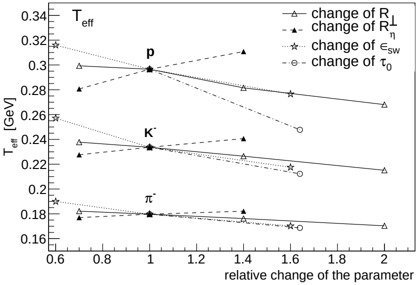

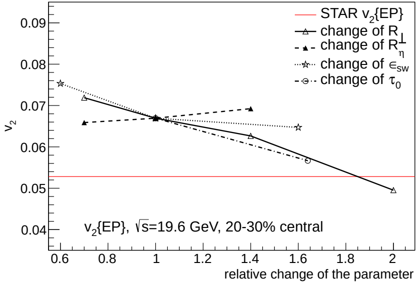

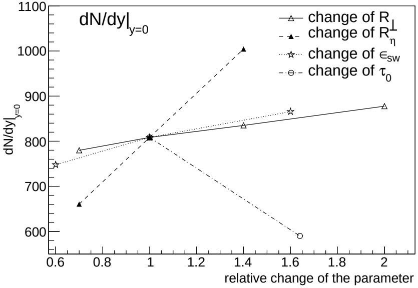

par. $\uparrow$	$R_\perp$	R_z	η/s	τ_0	$\varepsilon_{\rm crit}$
$T_{\rm eff}$	$\downarrow$	$\uparrow$	$\uparrow$	$\downarrow$	$\downarrow$
dN/dy	$\uparrow$	$\uparrow$	$\uparrow$	$\downarrow$	$\uparrow$
v_2	$\downarrow$	$\uparrow$	$\downarrow$	$\downarrow$	$\downarrow$

$\Downarrow$ visual adjustment to experimental data

Energy dependent model parameters:

$\sqrt{s}$ [GeV]	τ_0 [fm/c]	$R_\perp$ [fm]	R_z [fm]	η/s
7.7/8.8	3.2/2.83	1.4	0.5	0.2
11.5	2.1	1.4	0.5	0.2
19.6/17.3	1.22/1.42	1.4	0.5	0.15
27	1.0	1.2	0.5	0.12
39	0.9	1.0	0.7	0.08
62.4	0.7	1.0	0.7	0.08
200	0.4	1.0	1.0	0.08

As a result...

40 + 158 A GeV PbPb SPS ($\sqrt{s} = 8.8$ and 17.3 GeV)

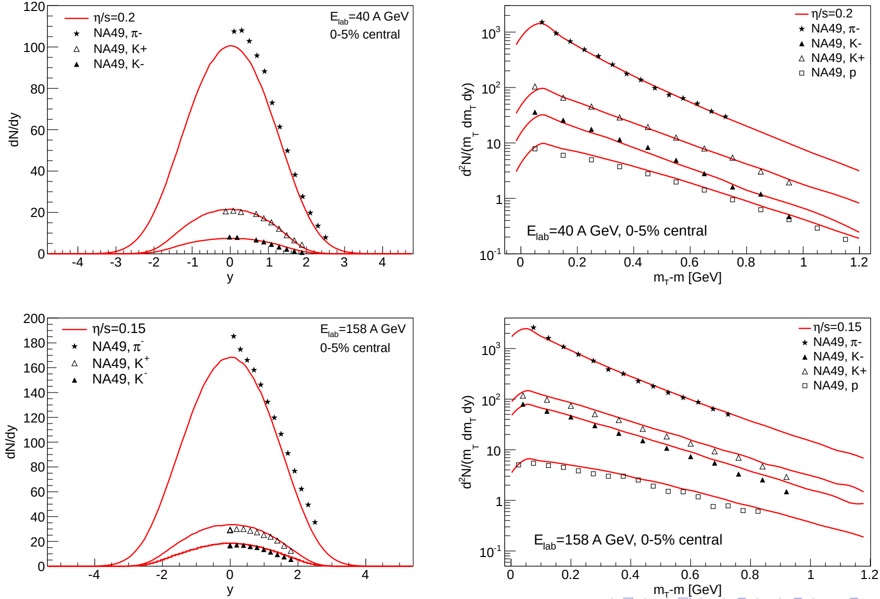

RHIC BES + top RHIC

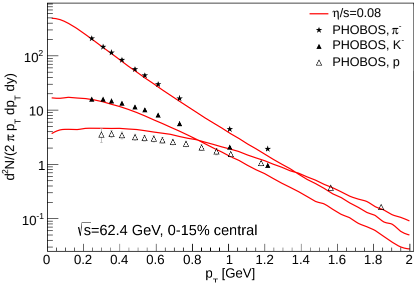

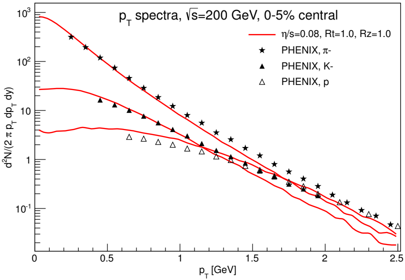

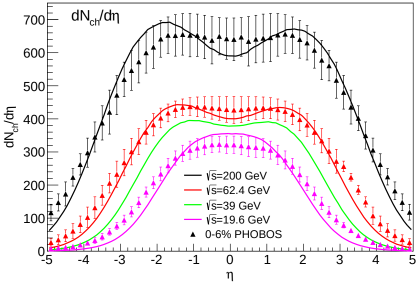

Elliptic and triangular flows at RHIC BES + top RHIC

v_2, v_3 vs collision energy

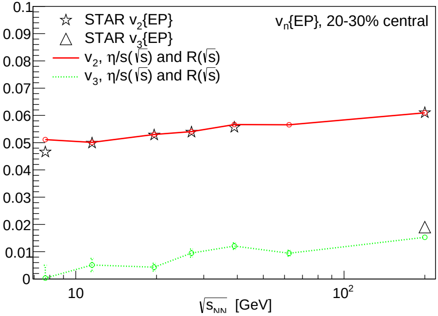

v_2, v_3 vs centrality

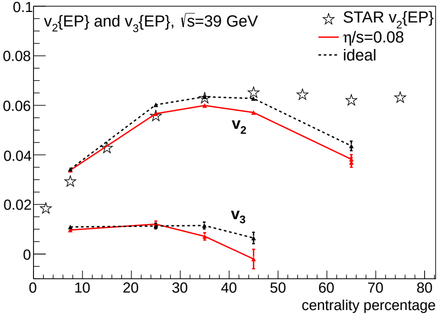

v_3: prediction!

Peripheral events: the system is too small compared to the smearing radius, which results in decreased initial eccentricity ε_2.

The Horn and the Step

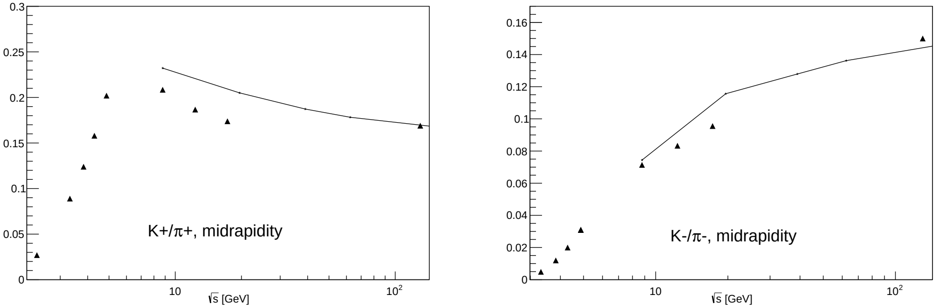

An outcome of the adjustment to the data

Effective (constant) η/s in hydrodynamic phase

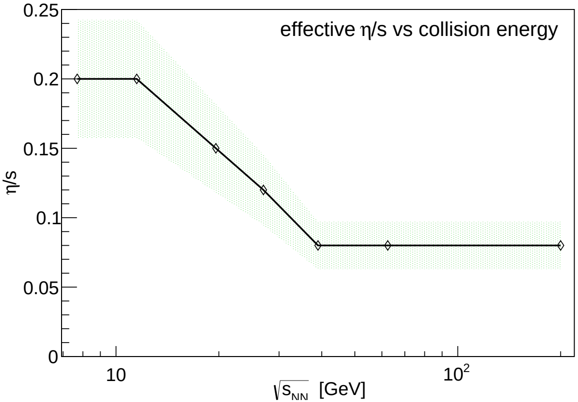

Green (error) band: estimated assuming that the parameters are varied such that v_2 stays the same and the inverse slope of p_T spectrum of protons changes within 5%.

! This is no actual error bar. That would require a proper χ^2 fitting of the model parameters (and enormous amount of CPU time).

Another prediction: femtoscopy

HBT(interferometry) measurements

The only tool for space-time measurements at the scales of 10^{-15}m, 10^{-23}s

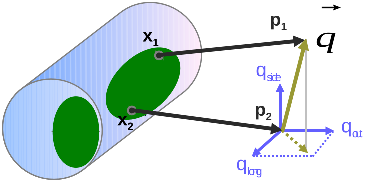

$$\vec{q} = \vec{p}_2 - \vec{p}_1$$

$$\vec{k} = \frac{1}{2}(\vec{p}_1 + \vec{p}_2)$$

$$C(p_1, p_2) = \frac{P(p_1, p_2)}{P(p_1)P(p_2)} = \frac{\text{real event pairs}}{\text{mixed event pairs}}$$

Gaussian approximation of CFs ($q \to 0$):

$$C(\vec{k}, \vec{q}) = 1 + \lambda(k) e^{-q_{out}^2 R_{out}^2 - q_{side}^2 R_{side}^2 - q_{long}^2 R_{long}^2}$$

$R_{out}, R_{side}, R_{long}$ (HBT radii) correspond to *homogeneity lengths*, which reflect the space-time scales of emission process

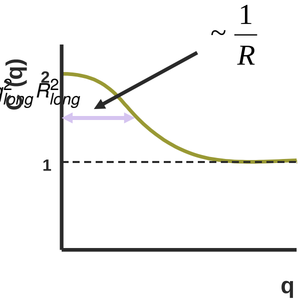

In an event generator, BE/FD two-particle amplitude (anti)symmetrization must be introduced

Femtoscopic radii from azimuthally integrated analysis

$\pi^-\pi^-$ pairs, $\langle k_T \rangle = 0.22$ GeV. Experimental data from STAR: arXiv:1403.4972

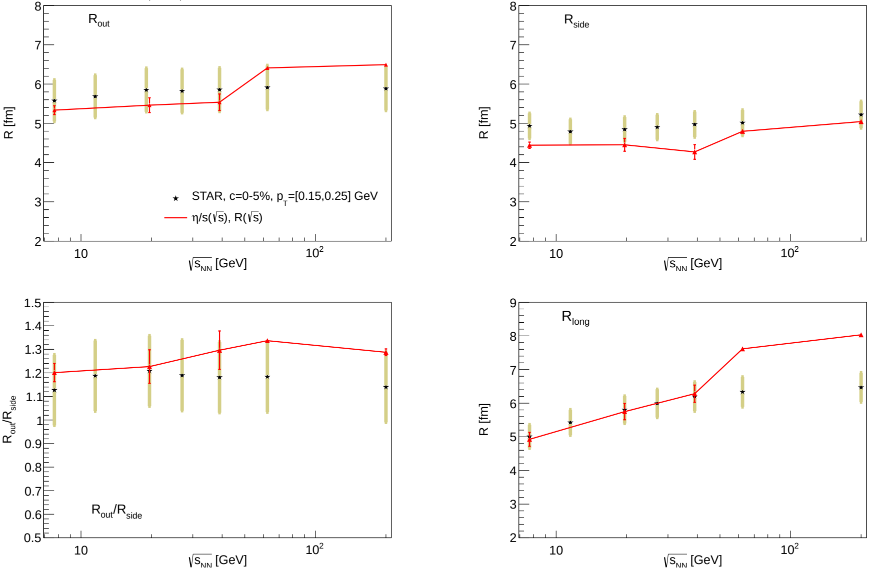

Theoretical error bars come from uncertainties in Gaussian fitting procedure

m_T dependence of R_{long}

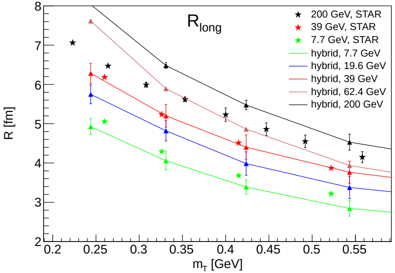

At higher energies, R_{long} at low-p_T overestimates the data

$\sqrt{s_{\mathrm{NN}}}$ dependence of the intercept parameter of the CF

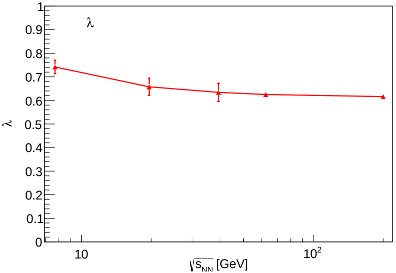

Larger fraction of resonances produced at high energies, which lowers λ for pion pairs.

Addition to the Results 1:

EoS dependence

From the first round of simulations: fixed η/s,

$$R_\perp = R_\eta = 1\ \text{fm},$$
$$\tau_0 = \max\left\{\frac{2R}{\gamma v_z}, 1\,\mathrm{fm/c}\right\}$$
$$\varepsilon_{\mathrm{sw}} = 0.5\ \text{GeV/fm}^3$$

Effects of the `EoS Q` compared to Chiral EoS?

Yes: hydro phase in average lasts longer with `EoS Q`

Plots: τ distribution of hadrons sampled at the transition surface (left) and τ of last interactions (right)

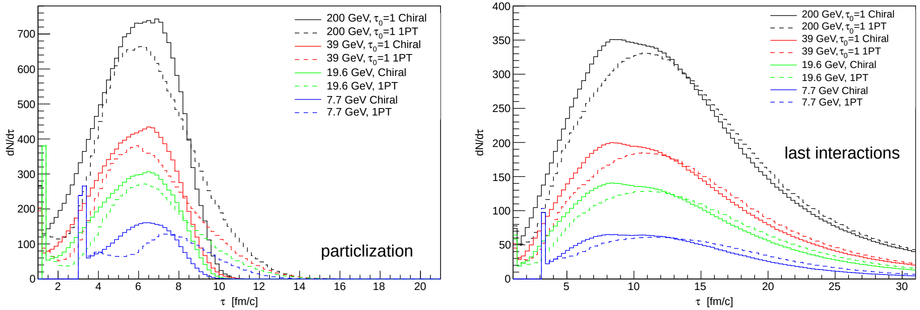

Can we see it in femtoscopy (HBT), or any other observables?

Femtoscopic radii: ideal hydro/Chiral EoS, ideal hydro/EoS Q, visc.hydro/Chiral EoS

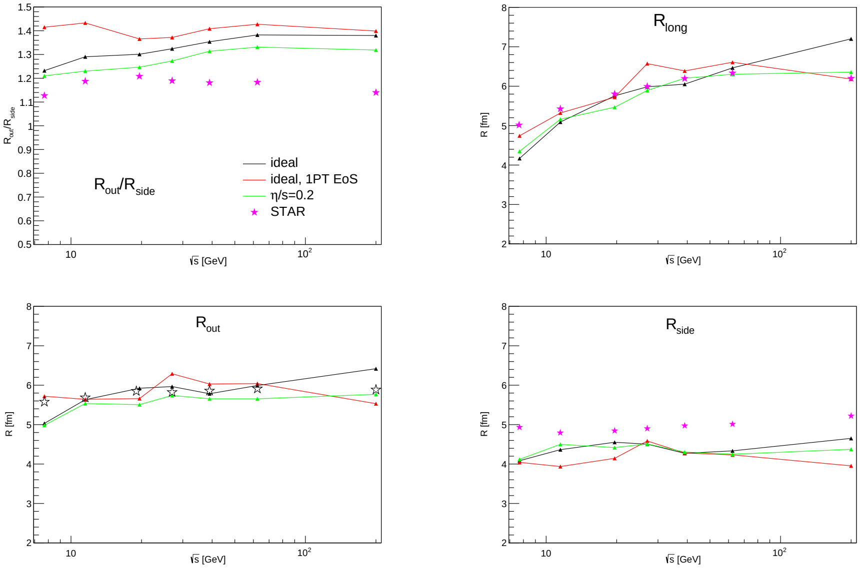

Previous results for EoS dependence of HBT in hybrid UrQMD, see Q. Li et al., Phys.Lett.B674:111,2009

EoS dependence of the elliptic flow

ideal hydro/Chiral EoS, ideal hydro/EoS Q, visc.hydro/Chiral EoS, pure UrQMD

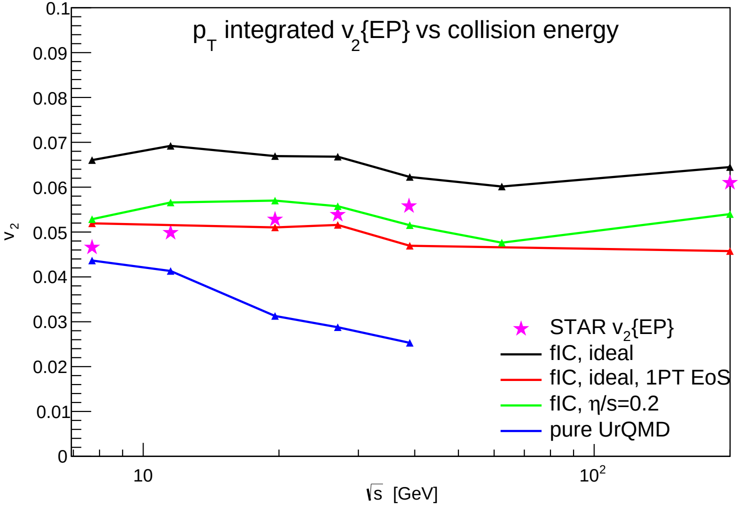

Summary

3+1D EbE viscous hydro + UrQMD model:

- pre-termal stage: UrQMD
- 3+1D viscous hydrodynamics
- EoS at finite μ_B: Chiral model, `EoS Q`

Conclusions:

- Model applied for $\sqrt{s_{NN}} = 7.7 \ldots 200$ GeV A+A collisions.
- A fit to experimental data suggests $\eta/s = 0.2 \to 0.08$ when $\sqrt{s} = 7.7 \to 200$ GeV,
  modulo initial state (UrQMD) and EoS (Chiral model) used.
- This hints for μ_B dependent η/s or $\eta/(\varepsilon + p)$ being appropriate quantity.
- More experimental data and much more parameter space exploration is needed to extract η/s and other model parameters less ambiguously.

Work in progress.

Thank you for your attention!

Lattice QCD and the search for the critical point

Frithjof Karsch

Brookhaven National Laboratory & Bielefeld University

OUTLINE

– the QCD critical point
– EoS at non-zero baryon chemical potential
– cumulant ratios of conserved charge fluctuations
– freeze-out conditions from QCD
– power of Taylor expansions

Exploring the QCD phase diagram

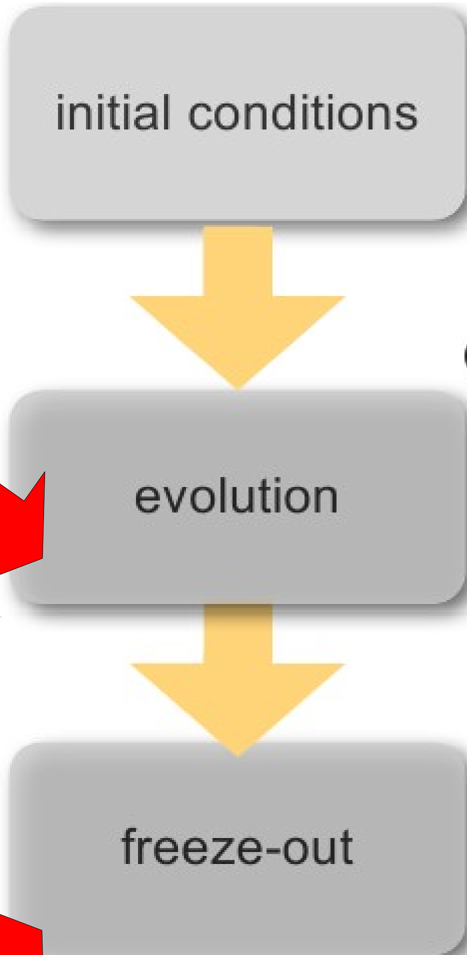

controlled by the **QCD equation of state**, T_c

expectation:
freeze-out close to QCD transition line

PBMetalPLB2004

observable consequences:
freeze-out pattern of mesons and baryons, controlled by T_f, μ_B, μ_S

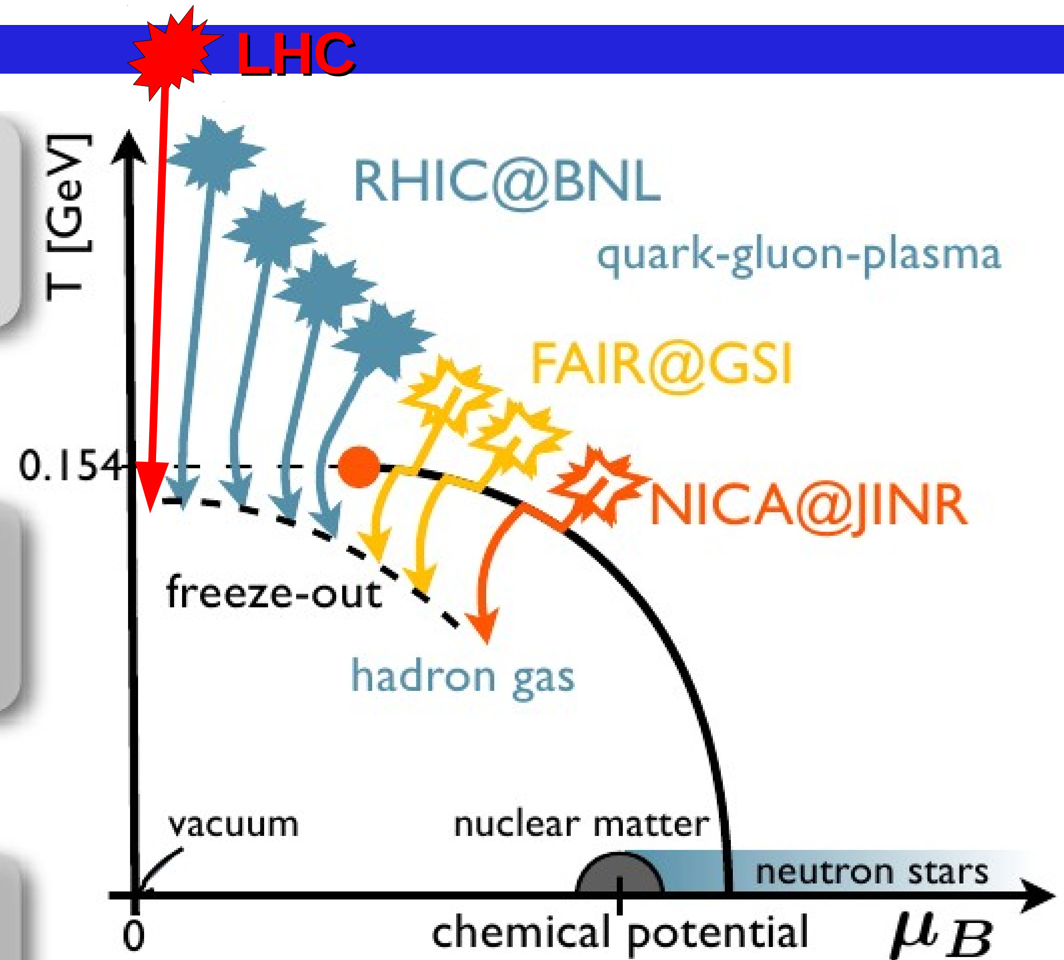

– LHC: establish contact with the QCD PHASE transition

– RHIC: locate/provide evidence for the QCD critical point

Exploring the QCD phase diagram

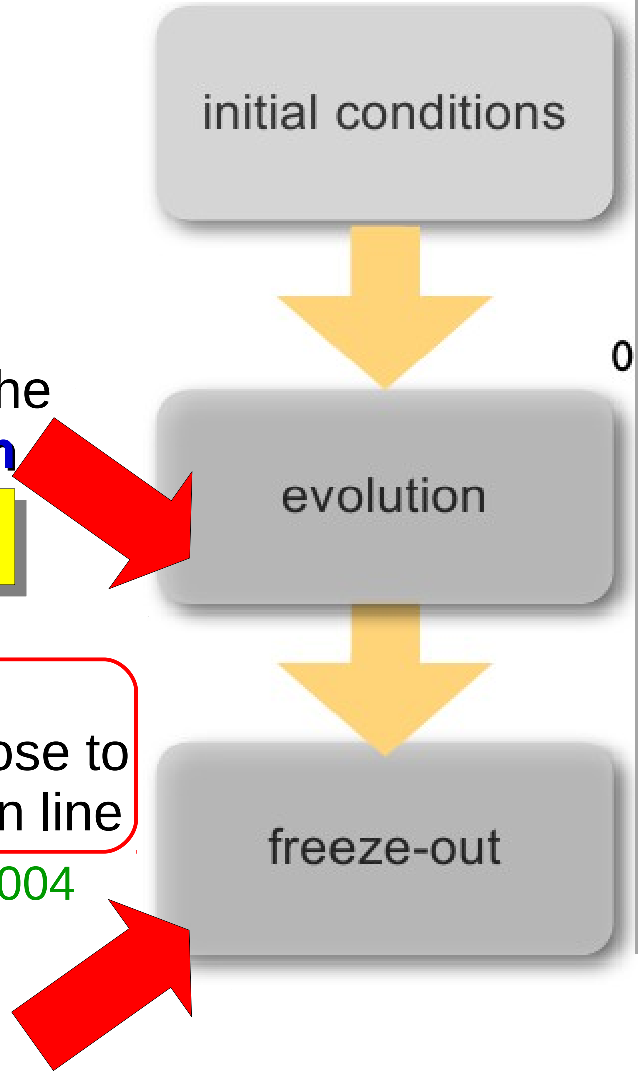

controlled by the **QCD equation of state**, T_c

expectation: **freeze-out** close to QCD transition line

PBMetalPLB2004

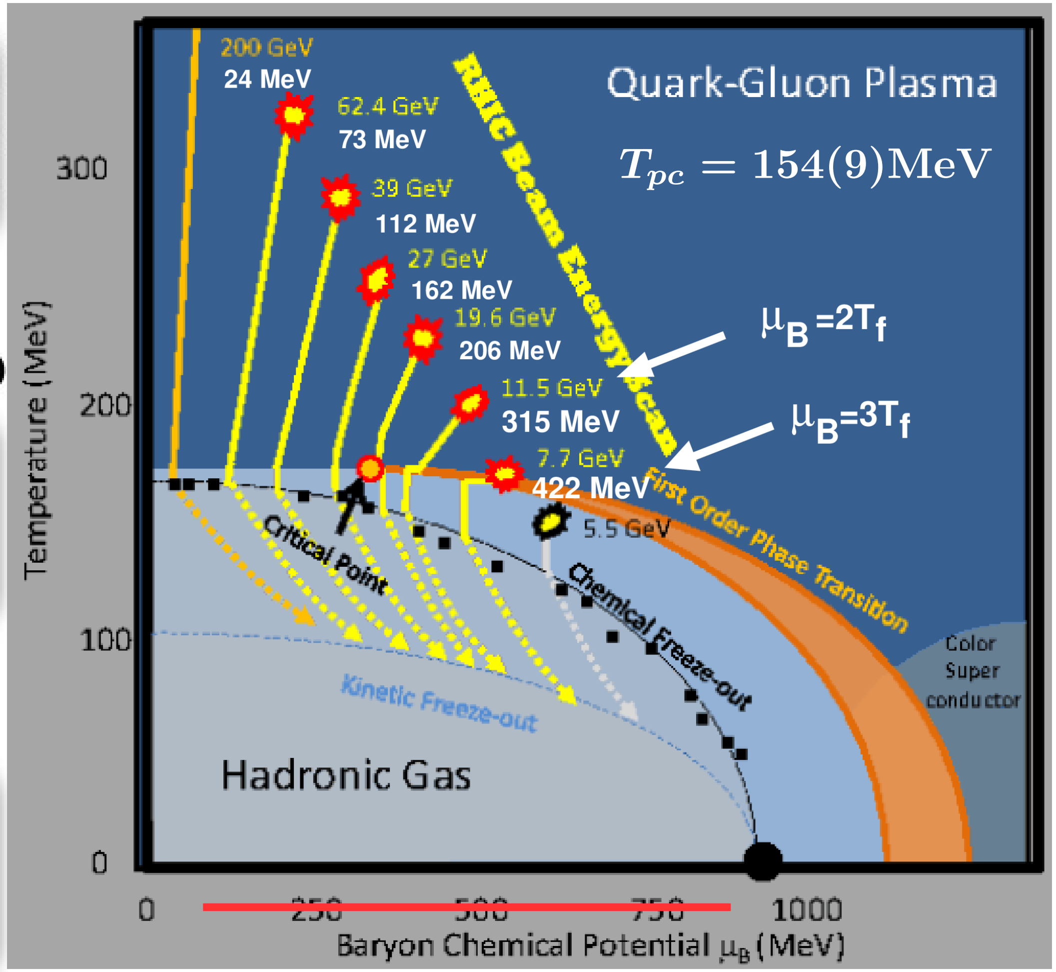

observable consequences:
freeze-out pattern of mesons and baryons, controlled by T_f, μ_B, μ_S

– LHC: establish contact with the QCD PHASE transition

– RHIC: locate/provide evidence for the QCD critical point

Exploring the QCD phase diagram

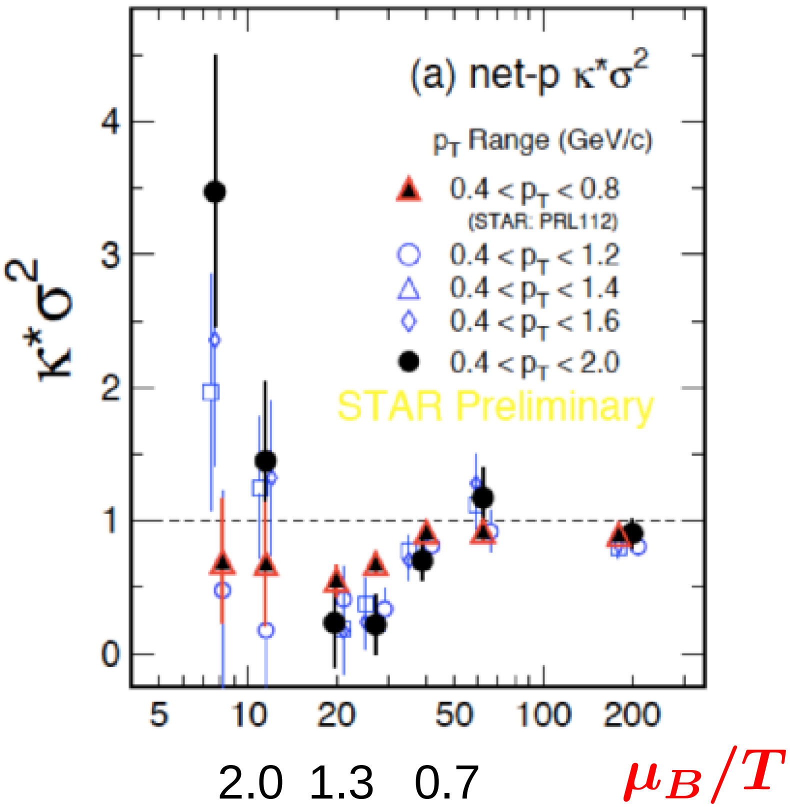

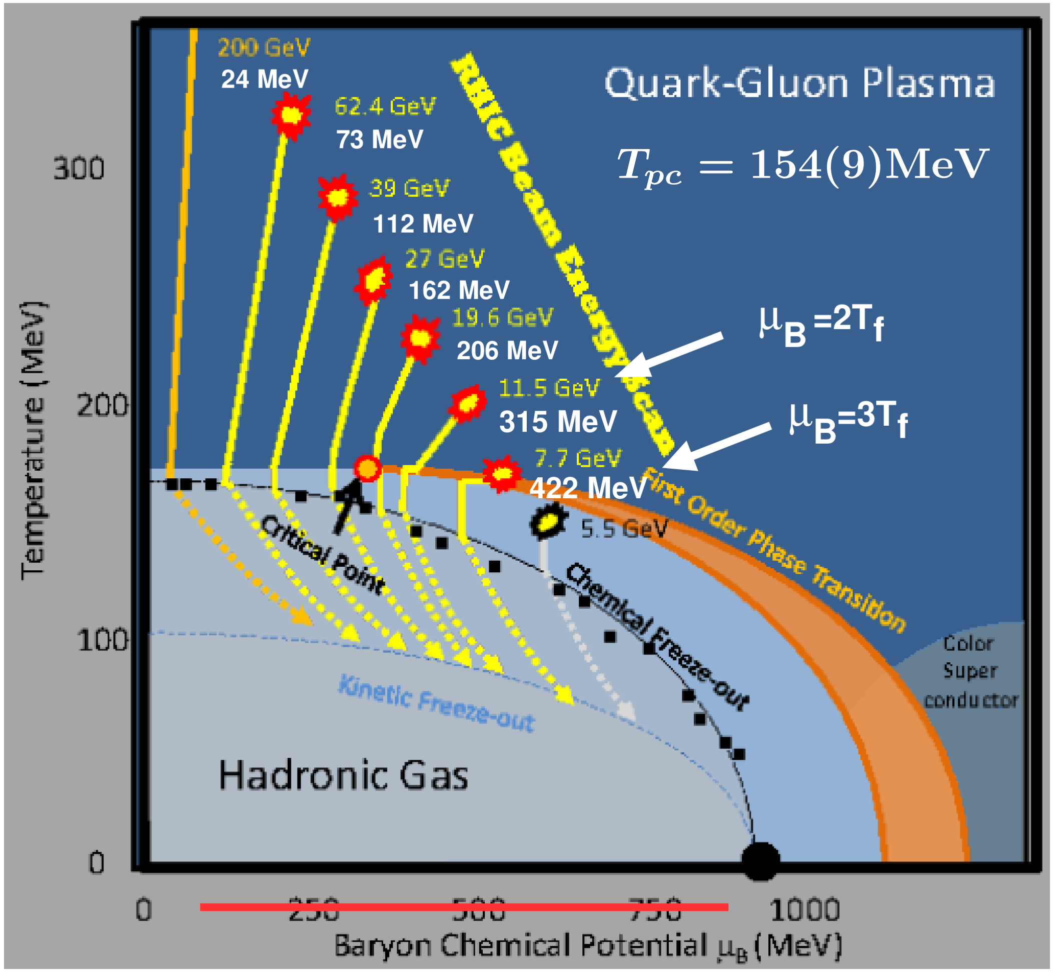

observable consequences:

conserved charge fluctuation

controlled by $\boxed{T_f, \mu_B, \mu_S}$

Exploring the QCD phase diagram

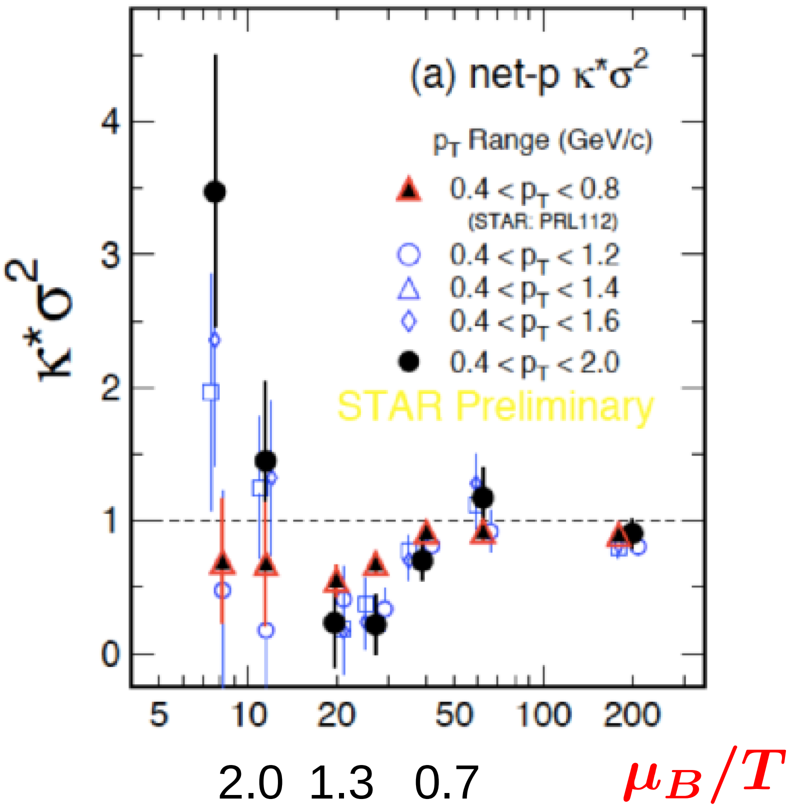

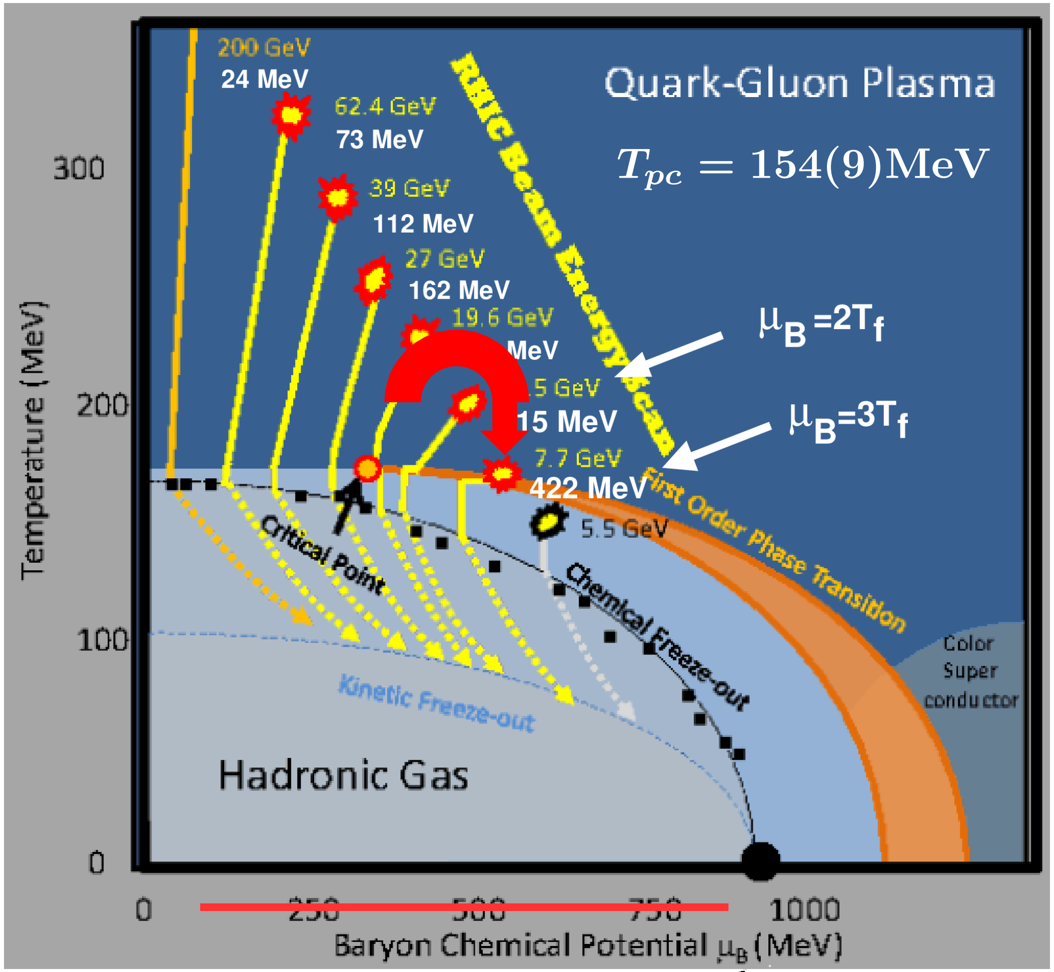

observable consequences:

conserved charge fluctuation

controlled by $\boxed{T_f, \mu_B, \mu_S}$

Where is the critical point?

LGT attempts to find the critical point

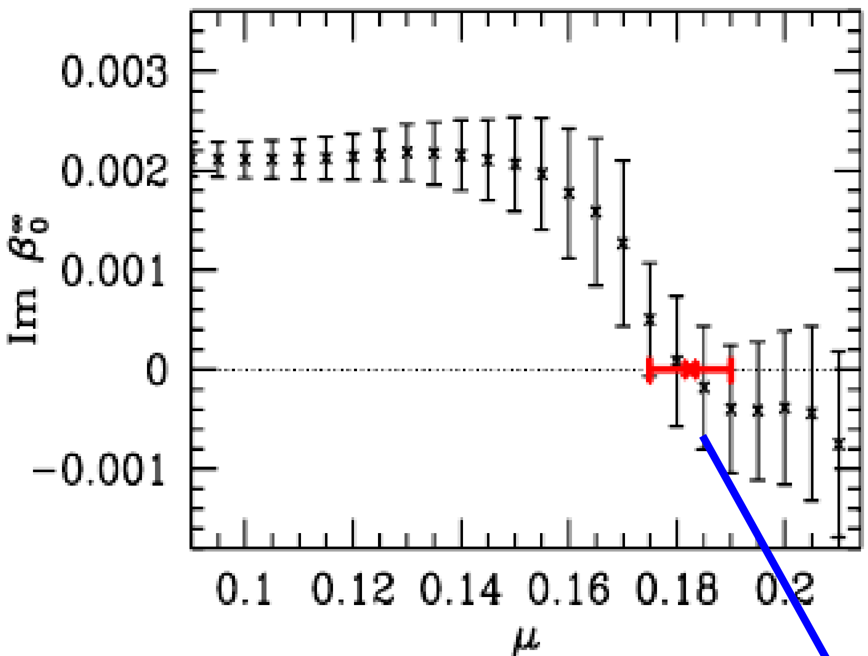

Z. Fodor, S. Katz. 2001, 2004

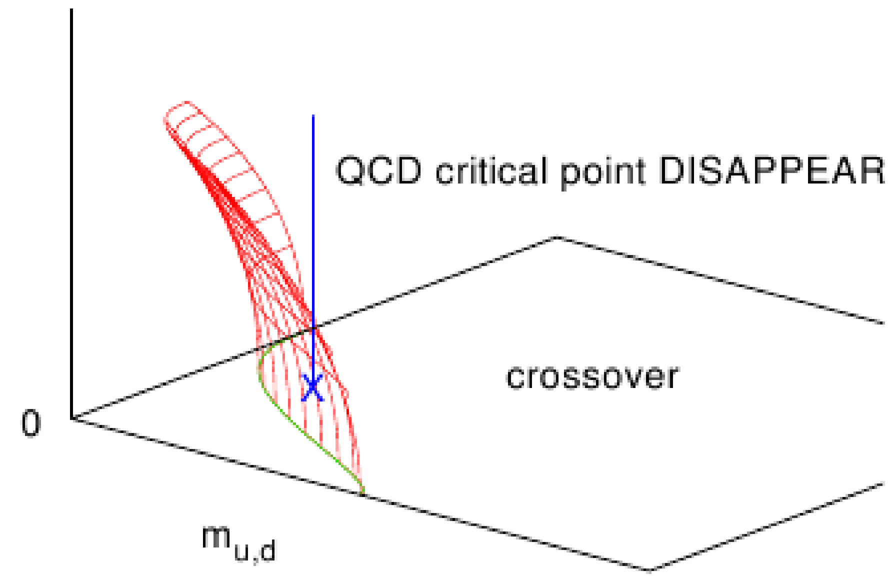

P. deForcrand, O. Philipsen, 2002

these calculations were possible because
(I) the lattices were coarse,
(II) the discretization schemes were crude

critical point or breakdown of the reweighting approach (loosing the overlap) ?

S. Ejiri, PRD69, 094506 (2004)

since 10 years no progress along this line

Taylor expansion of the pressure and critical point

$$\frac{P}{T^4} = \sum_{n=0}^{\infty} \frac{1}{n!} \chi_n^B(T) \left(\frac{\mu_B}{T}\right)^n$$

for simplicity : $\mu_Q = \mu_S = 0$

estimator for the radius of convergence:

$$\left(\frac{\mu_B}{T}\right)^{\chi}_{crit,n} \equiv r_n^{\chi} = \sqrt{\left|\frac{n(n-1)\chi_n^B}{\chi_{n+2}^B}\right|}$$

– radius of convergence corresponds to a critical point only, iff

$$\chi_n > 0 \text{ for all } n \geq n_0$$

forces P/T^4 and $\chi_n^B(T,\mu_B)$ to be monotonically growing with μ_B/T

at T_{CP} : $\kappa_B \sigma_B^2 = \dfrac{\chi_4^B(T,\mu_B)}{\chi_2^B(T,\mu_B)} > 1$

if not:

– radius of convergence does not determine the critical point

– Taylor expansion can not be used close to the critical point

Chiral model and negative χ^B_4/χ^B_2:

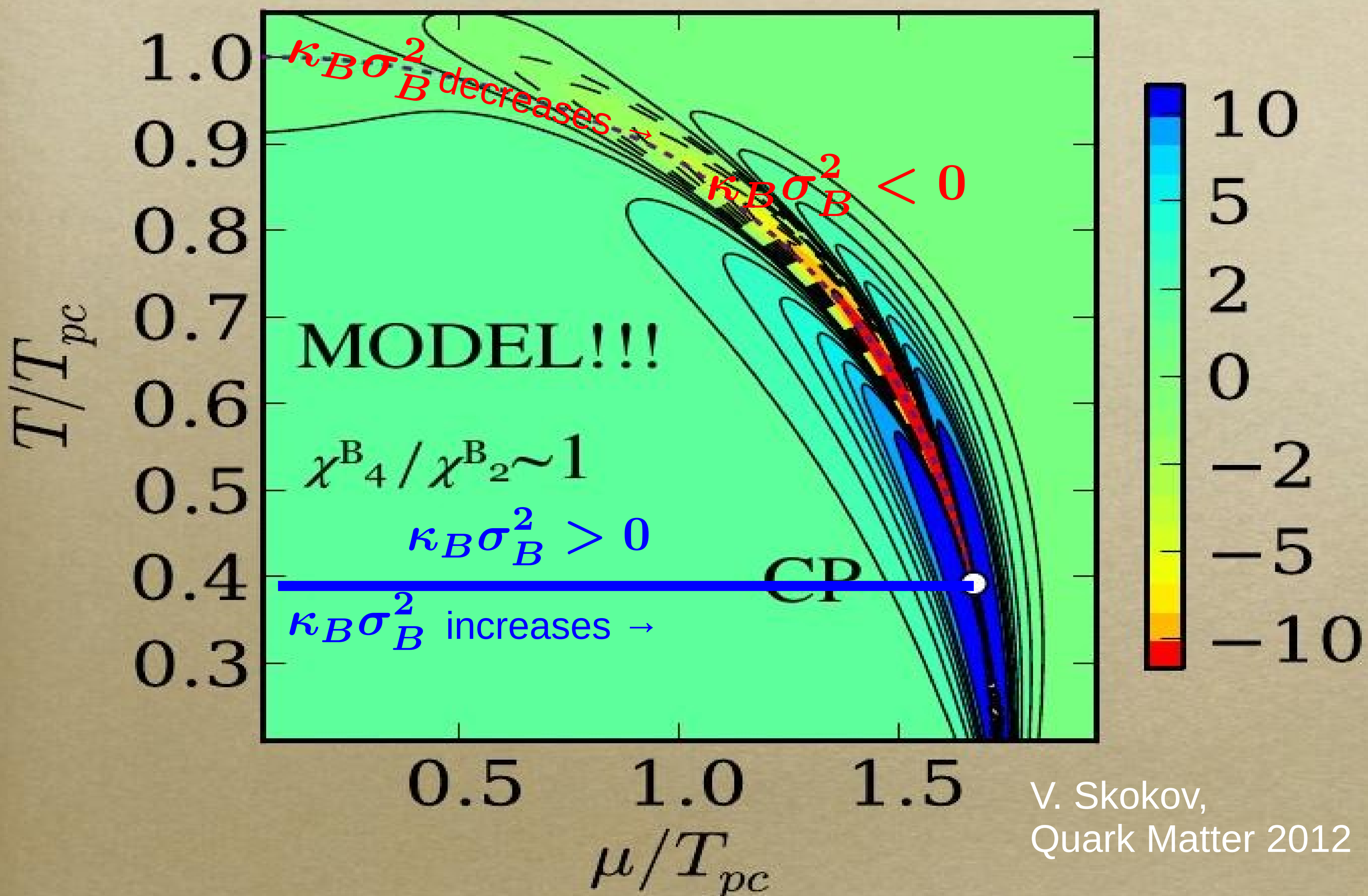

V. Skokov, Quark Matter 2012

Estimates of the radius of convergence

a challenging prediction from susceptibility series for standard staggered fermions:

$$\left(\frac{\mu_B}{T}\right)^{\chi}_{crit,n} \equiv r_n^{\chi} = \sqrt{\left|\frac{n(n-1)\chi_n^B}{\chi_{n+2}^B}\right|}$$

suggests large deviations from HRG in the hadronic phase

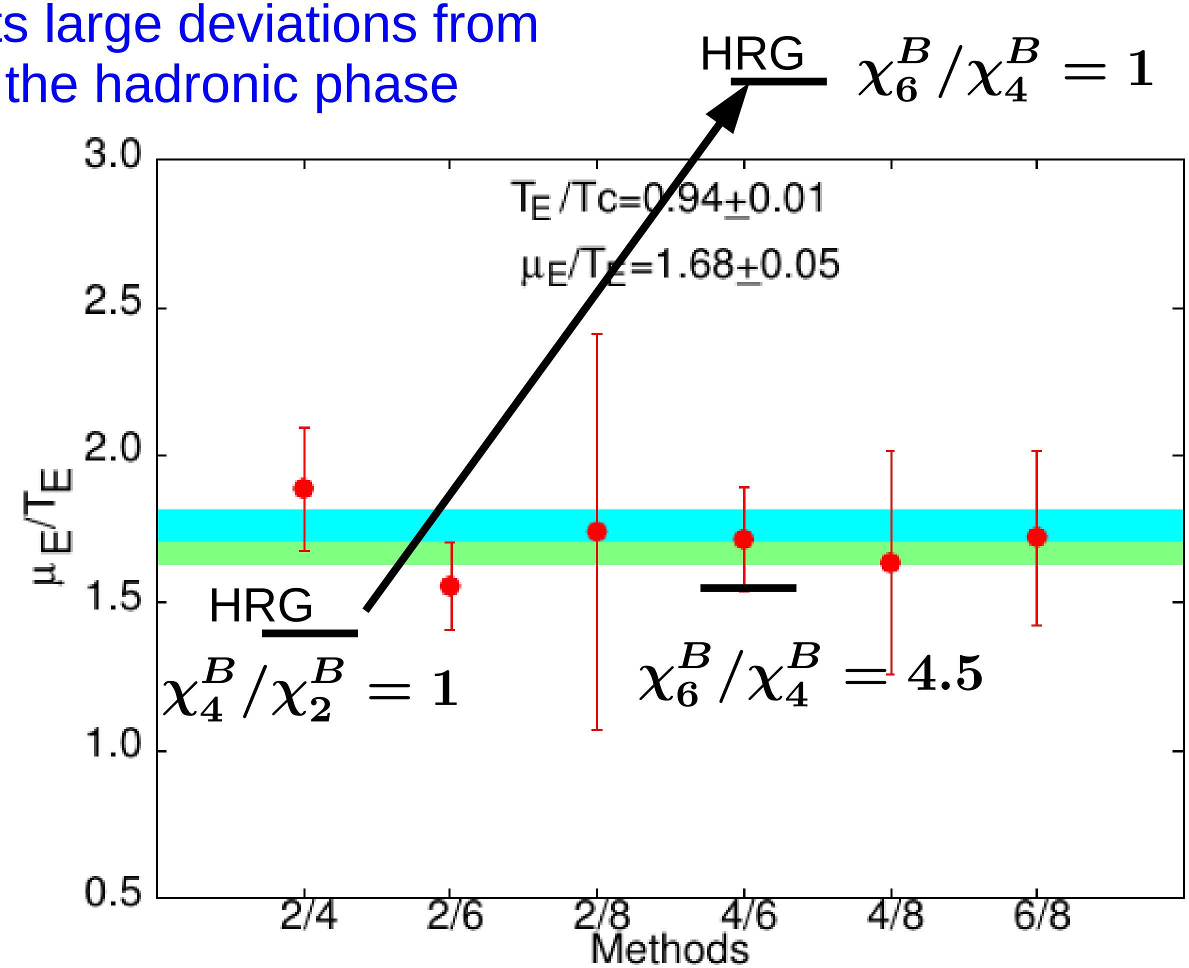

huge deviations from HRG in 6[th] order cumulants!

S. Datta et al., PoS Lattice2013 (2014) 202

suggests a critical point for $\mu_B/T < 2$

at present, we cannot rule it out!

BNL-Bielefeld-CCNU

Taylor expansion of the EoS and critical point

$$\frac{p}{T^4} = \frac{1}{VT^3} \ln Z(V,T,\mu_B,\mu_S,\mu_Q)$$
$$= \sum_{i,j,k} \frac{1}{i!j!k!} \chi_{ijk}^{BQS} \left(\frac{\mu_B}{T}\right)^i \left(\frac{\mu_Q}{T}\right)^j \left(\frac{\mu_S}{T}\right)^k$$

generalized susceptibilities: $\chi_{ijk}^{BQS} = \left.\frac{\partial^{i+j+k} p/T^4}{\partial\hat{\mu}_B^i \partial\hat{\mu}_Q^j \partial\hat{\mu}_S^k}\right|_{\mu=0}$

– valid up to radius of convergence: μ_c (critical point?)

Some 4th and 6th order cumulants

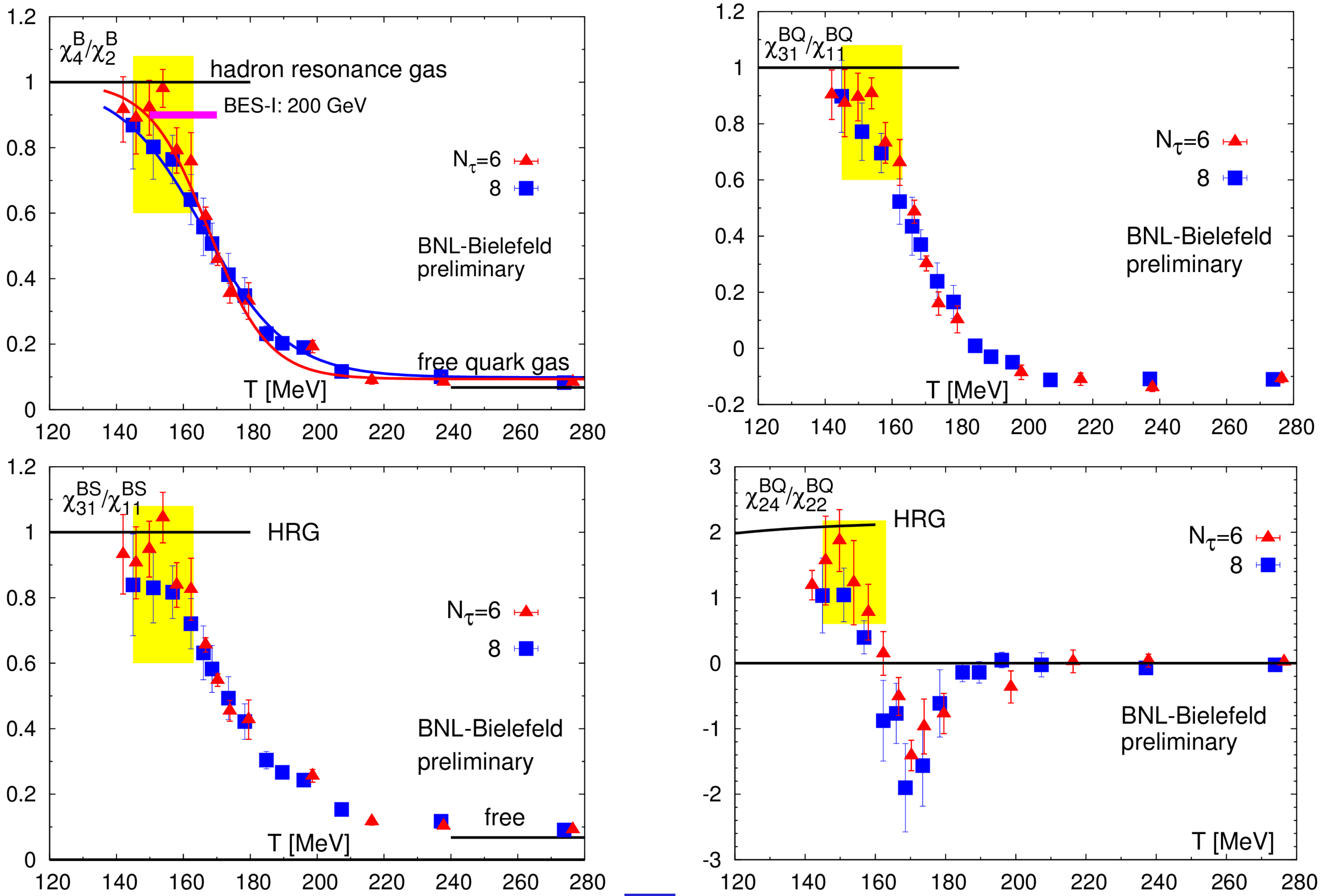

Some 4th and 6th order cumulants

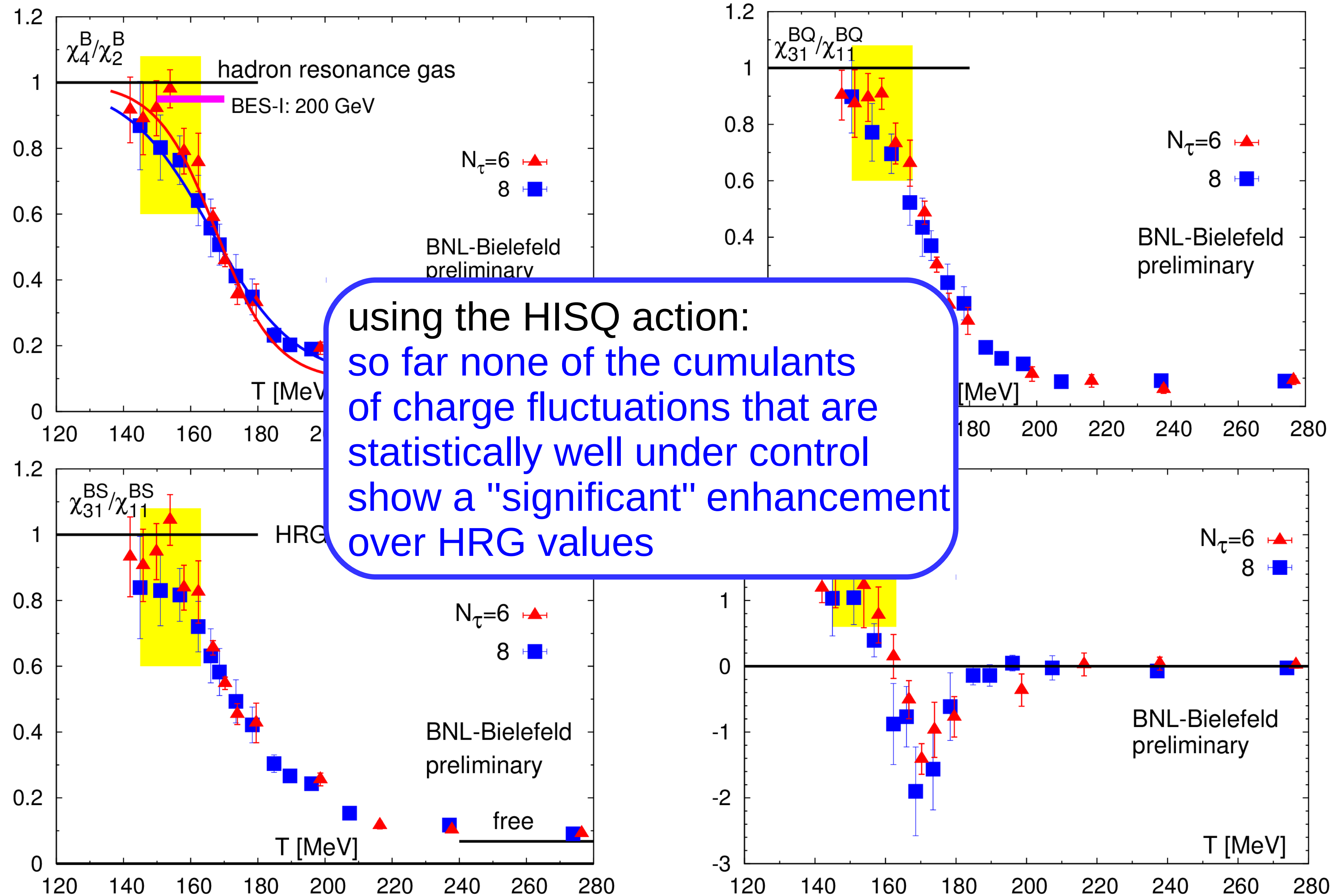

using the HISQ action:

so far none of the cumulants of charge fluctuations that are statistically well under control show a "significant" enhancement over HRG values

Equation of state of (2+1)-flavor QCD: $\mu_B/T > 0$

$$\frac{P}{T^4} = \sum_{i,j,k=0}^{\infty} \frac{1}{i!j!k!} \chi_{i,j,k}^{BQS}(T) \left(\frac{\mu_B}{T}\right)^i \left(\frac{\mu_Q}{T}\right)^j \left(\frac{\mu_S}{T}\right)^k$$

the simplest case: $\mu_S = \mu_Q = 0$

$$\frac{P(T,\mu_B)}{T^4} = \frac{P(T,0)}{T^4} + \frac{\chi_2^B(T)}{2} \left(\frac{\mu_B}{T}\right)^2 + \frac{\chi_4^B(T)}{24} \left(\frac{\mu_B}{T}\right)^4 + \mathcal{O}((\mu_B/T)^6)$$

Equation of state of (2+1)-flavor QCD: $\mu_B/T > 0$

$$\frac{P}{T^4} = \sum_{i,j,k=0}^{\infty} \frac{1}{i!j!k!} \chi_{i,j,k}^{BQS}(T) \left(\frac{\mu_B}{T}\right)^i \left(\frac{\mu_Q}{T}\right)^j \left(\frac{\mu_S}{T}\right)^k$$

the simplest case: $\mu_S = \mu_Q = 0$

$$\frac{P(T,\mu_B)}{T^4} = \frac{P(T,0)}{T^4} + \frac{\chi_2^B(T)}{2}\left(\frac{\mu_B}{T}\right)^2 + \frac{\chi_4^B(T)}{24}\left(\frac{\mu_B}{T}\right)^4 + \mathcal{O}((\mu_B/T)^6)$$

An $\mathcal{O}((\mu_B/T)^4)$ expansion is exact in a QGP up to $\mathcal{O}(g^2)$

How good is an $\mathcal{O}((\mu_B/T)^4)$ expansion in a HRG?

– deviation is less than 3% at $\mu_B/T = 2$

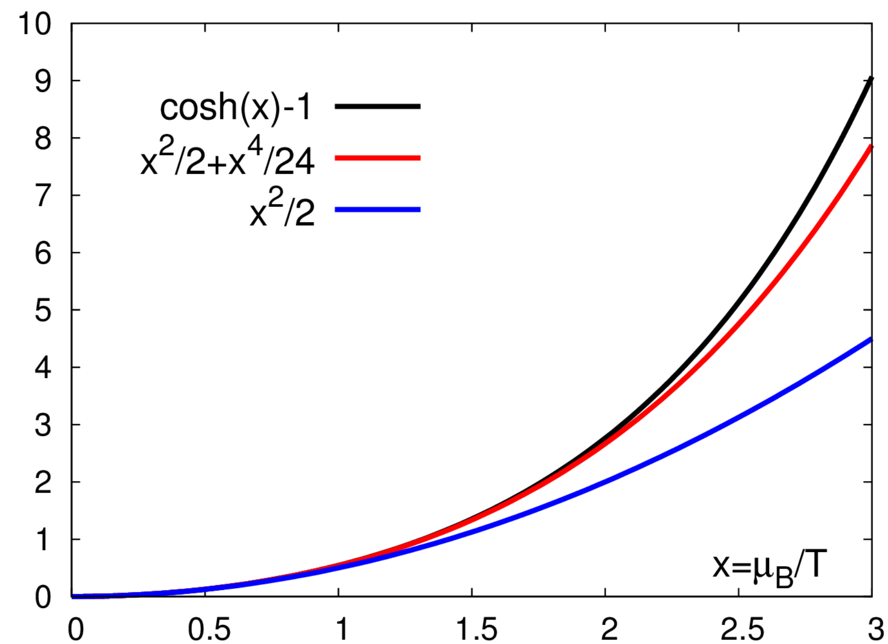

Equation of state of (2+1)-flavor QCD: $\mu_B/T > 0$

$$\frac{P}{T^4} = \sum_{i,j,k=0}^{\infty} \frac{1}{i!j!k!} \chi_{i,j,k}^{BQS}(T) \left(\frac{\mu_B}{T}\right)^i \left(\frac{\mu_Q}{T}\right)^j \left(\frac{\mu_S}{T}\right)^k$$

the simplest case: $\mu_S = \mu_Q = 0$

$$\frac{P(T,\mu_B)}{T^4} = \frac{P(T,0)}{T^4} + \frac{\chi_2^B(T)}{2}\left(\frac{\mu_B}{T}\right)^2 + \frac{\chi_4^B(T)}{24}\left(\frac{\mu_B}{T}\right)^4 + \mathcal{O}((\mu_B/T)^6)$$

An $\mathcal{O}((\mu_B/T)^4)$ expansion is exact in a QGP up to $\mathcal{O}(g^2)$

How good is an $\mathcal{O}((\mu_B/T)^4)$ expansion in a HRG?

– an $\mathcal{O}((\mu_B/T)^6)$ expansion is almost perfect up to $\mu_B/T = 3$

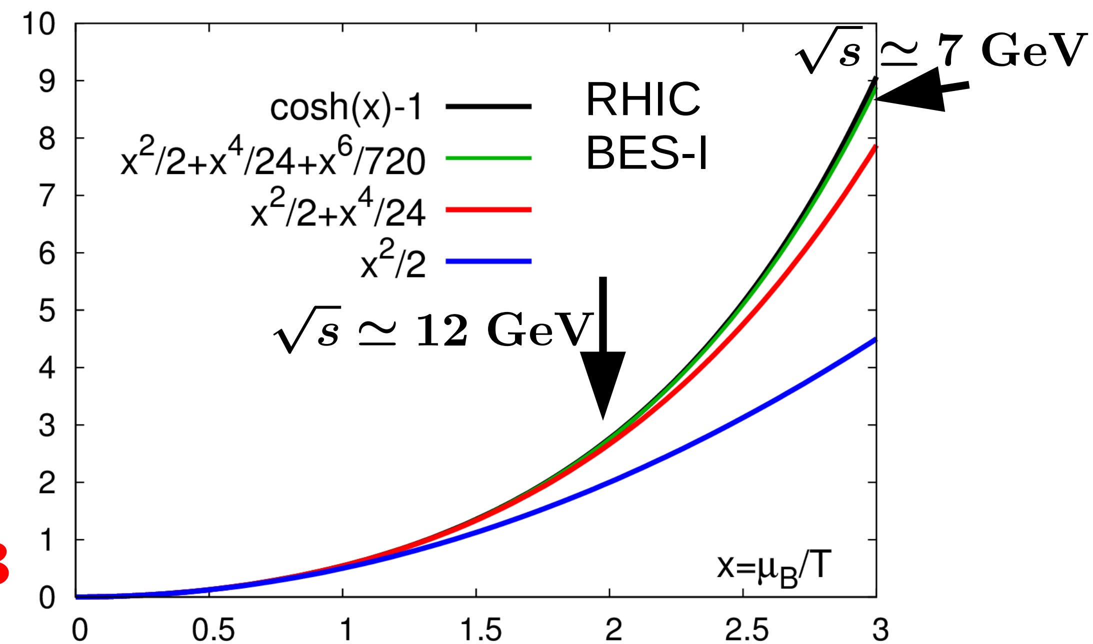

Equation of state of (2+1)-flavor QCD

pressure, **entropy** & **energy** density

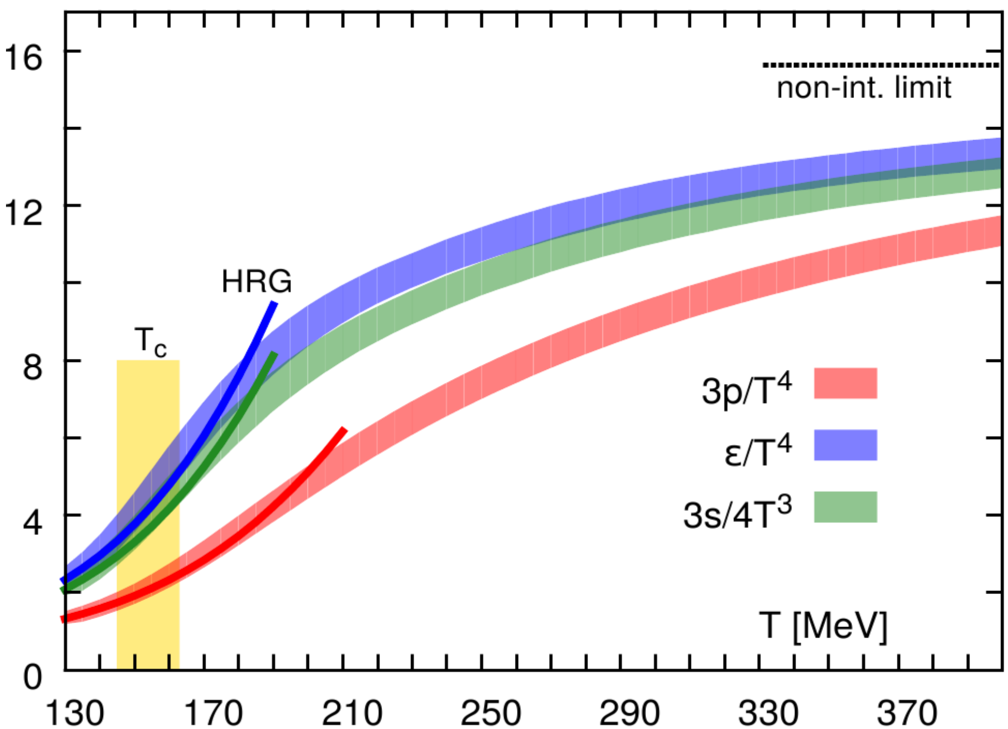

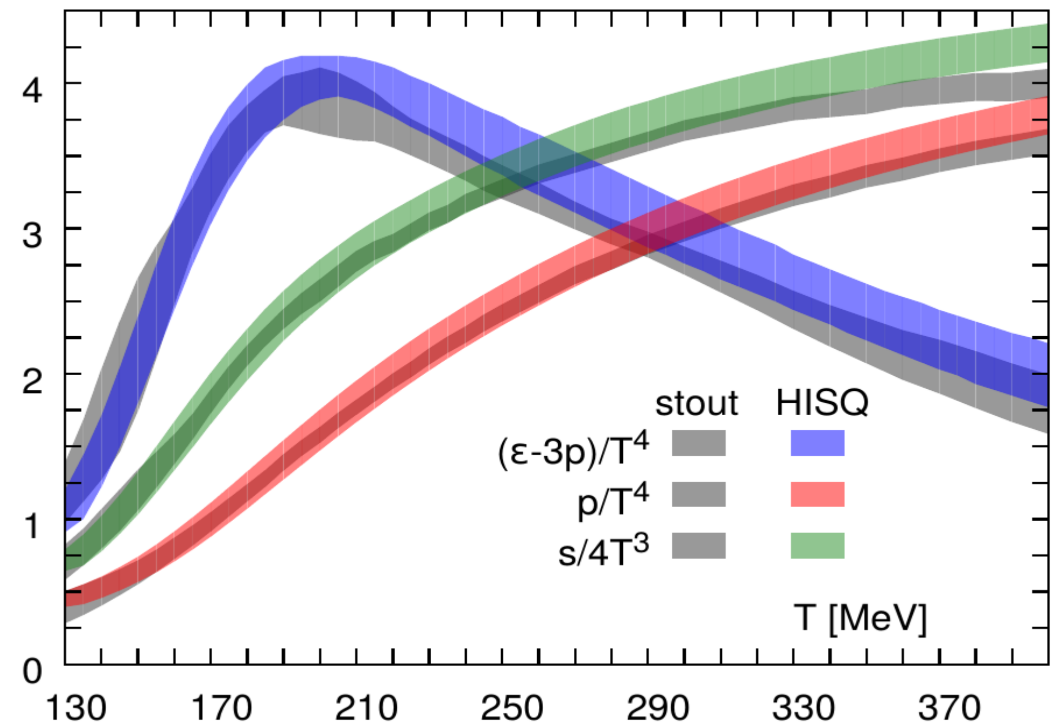

A. Bazavov et al. (hotQCD) ,
Phys. Rev. D90 (2014) 094503

– improves over earlier hotQCD calculations:
A. Bazavov et al., Phys. Rev. D80, 014504 (2009)

– consistent with results from Budapest-Wuppertal (stout): S. Borsanyi et al., PL B730, 99 (2014)

– up to the crossover region the QCD EoS agrees quite well with hadron resonance gas (HRG) model calculations; **However**, QCD results are systematically above HRG

Crossover transition parameters

PDG: Particle Data Group hadron spectrum
QM: Quark model hadron spectrum

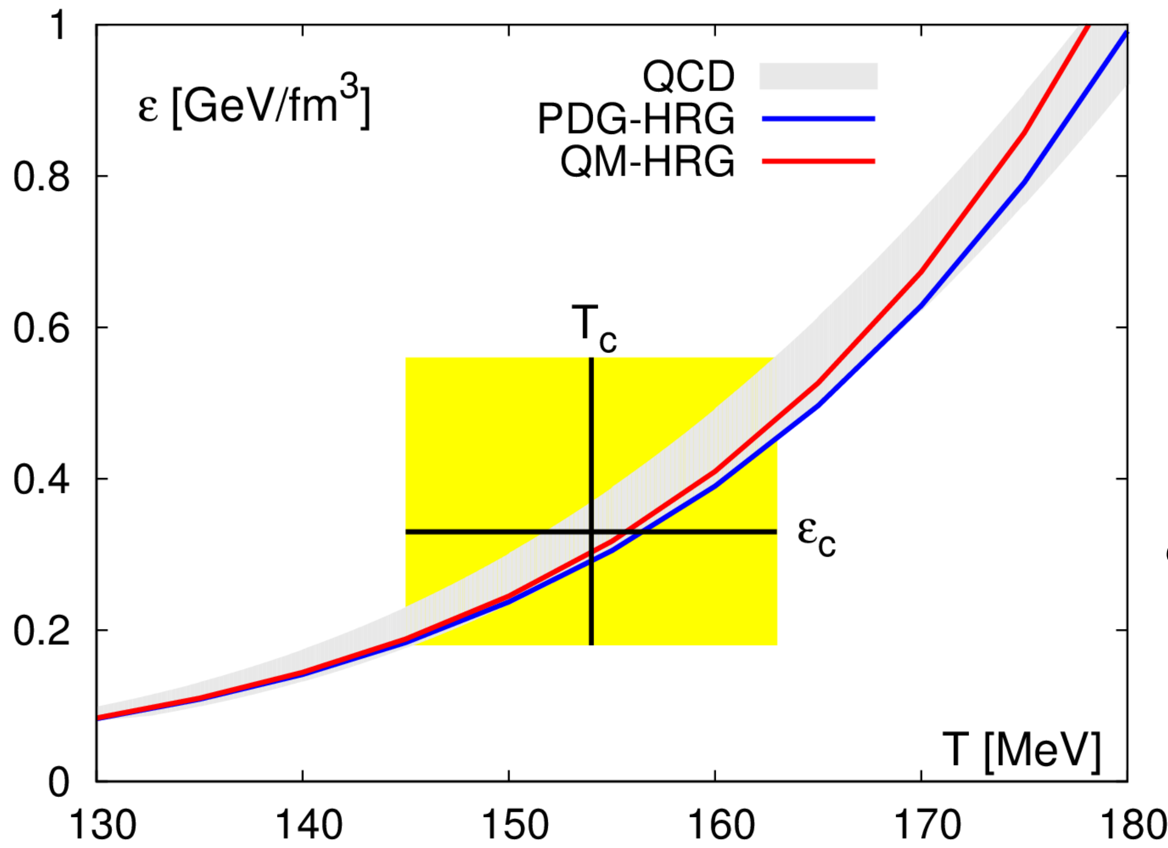

$$T_c = (154 \pm 9)\ \mathrm{MeV}$$

$$\epsilon_c = (0.34 \pm 0.16)\mathrm{GeV/fm^3}$$

compare with:

$$\epsilon^{\mathrm{nucl.\ mat.}} \simeq 150\ \mathrm{MeV/fm^3}$$

$$\epsilon^{\mathrm{nucleon}} \simeq 450\ \mathrm{MeV/fm^3}$$

A. Bazavov et al. (hotQCD) ,
Phys. Rev. D90 (2014) 094503

Equation of state of (2+1)-flavor QCD: $\mu_B/T > 0$

$$\frac{P}{T^4} = \sum_{i,j,k=0}^{\infty} \frac{1}{i!j!k!} \chi_{i,j,k}^{BQS}(T) \left(\frac{\mu_B}{T}\right)^i \left(\frac{\mu_Q}{T}\right)^j \left(\frac{\mu_S}{T}\right)^k$$

the simplest case: $\mu_S = \mu_Q = 0$

$$\frac{\Delta(T,\mu_B)}{T^4} = \frac{P(T,\mu_B) - P(T,0)}{T^4} = \frac{\chi_2^B}{2}\left(\frac{\mu_B}{T}\right)^2 \left(1 + \frac{1}{12}\frac{\chi_4^B}{\chi_2^B}\left(\frac{\mu_B}{T}\right)^2\right)$$

variance of net-baryon
number distribution

kurtosis*variance

$\kappa_B \sigma_B^2$

Equation of state of (2+1)-flavor QCD: $\mu_B/T > 0$

$$\frac{\Delta(T,\mu_B)}{T^4} = \frac{P(T,\mu_B) - P(T,0)}{T^4} = \frac{\chi_2^B}{2}\left(\frac{\mu_B}{T}\right)^2 \left(1 + \frac{1}{12}\frac{\chi_4^B}{\chi_2^B}\left(\frac{\mu_B}{T}\right)^2\right)$$

variance of net-baryon number distribution

kurtosis*variance

$\kappa_B \sigma_B^2$

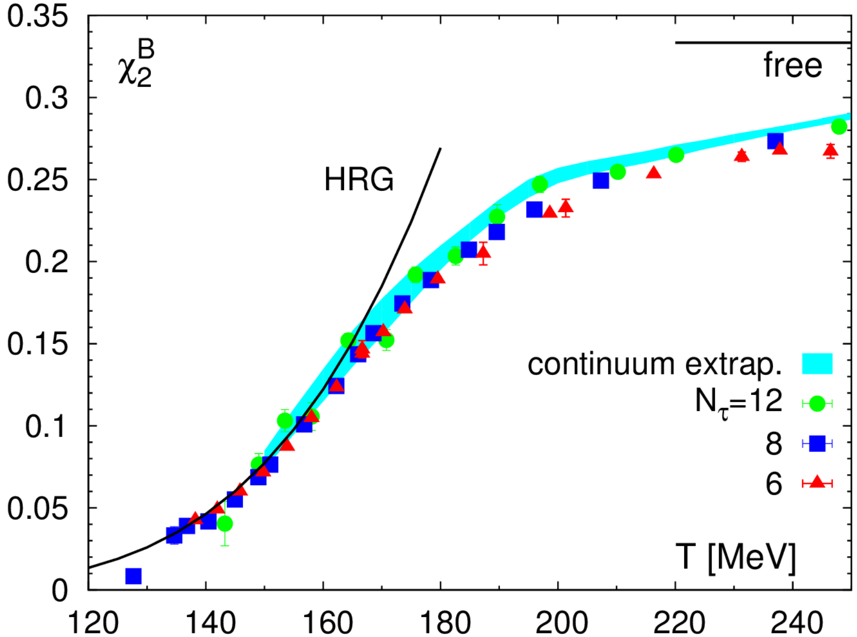

leading order correction agrees well with HRG in crossover region

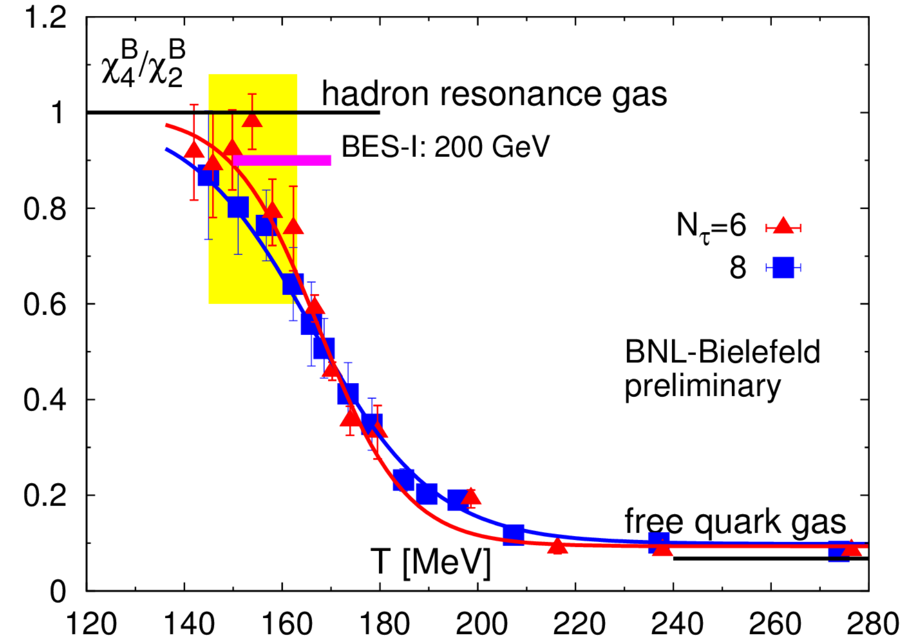

~20% deviations from HRG in crossover region

Equation of state of (2+1)-flavor QCD: $\mu_B/T > 0$

$$\frac{\Delta(T,\mu_B)}{T^4} = \frac{P(T,\mu_B)-P(T,0)}{T^4} = \frac{\chi_2^B}{2}\left(\frac{\mu_B}{T}\right)^2 \left(1+\frac{1}{12}\frac{\chi_4^B}{\chi_2^B}\left(\frac{\mu_B}{T}\right)^2\right)$$

estimating the $\mathcal{O}((\mu_B/T)^6)$ correction: $\sim \frac{1}{720}\frac{\chi_6^B}{\chi_2^B}\left(\frac{\mu_B}{T}\right)^6$

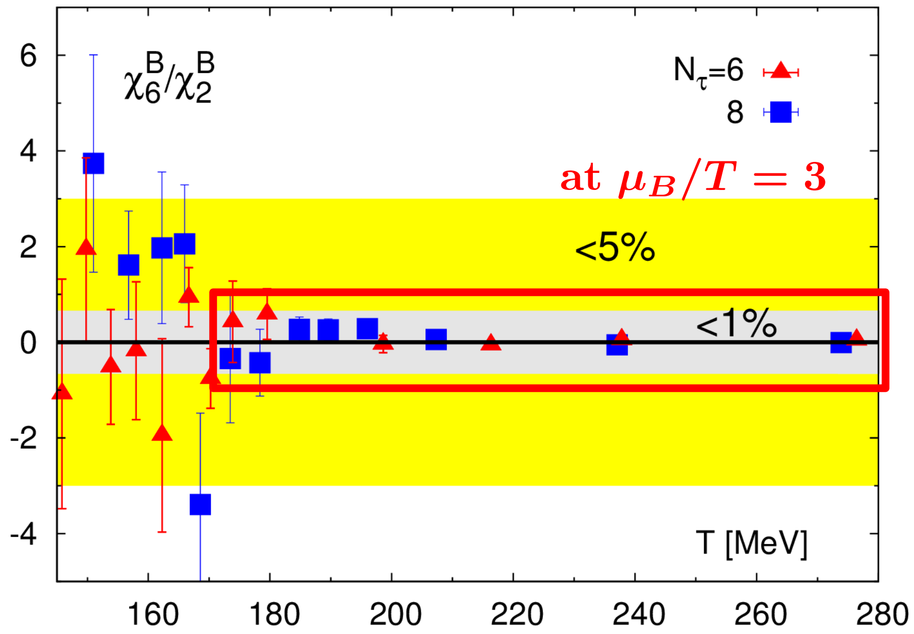

bands: magnitude of 6th order contribution relative to total of 0th, 2nd and 4th order

for $\mu_B/T \le 2$:

$\mathcal{O}((\mu_B/T)^6)$ corrections to P/T^4

contribute less than 1% for T>170 MeV

Equation of state of (2+1)-flavor QCD: $\mu_B/T > 0$

$$\frac{\Delta(T,\mu_B)}{T^4} = \frac{P(T,\mu_B)-P(T,0)}{T^4} = \frac{\chi_2^B}{2}\left(\frac{\mu_B}{T}\right)^2\left(1+\frac{1}{12}\frac{\chi_4^B}{\chi_2^B}\left(\frac{\mu_B}{T}\right)^2\right)$$

estimating the $\mathcal{O}((\mu_B/T)^6)$ correction: $\sim \frac{1}{720}\frac{\chi_6^B}{\chi_2^B}\left(\frac{\mu_B}{T}\right)^6$

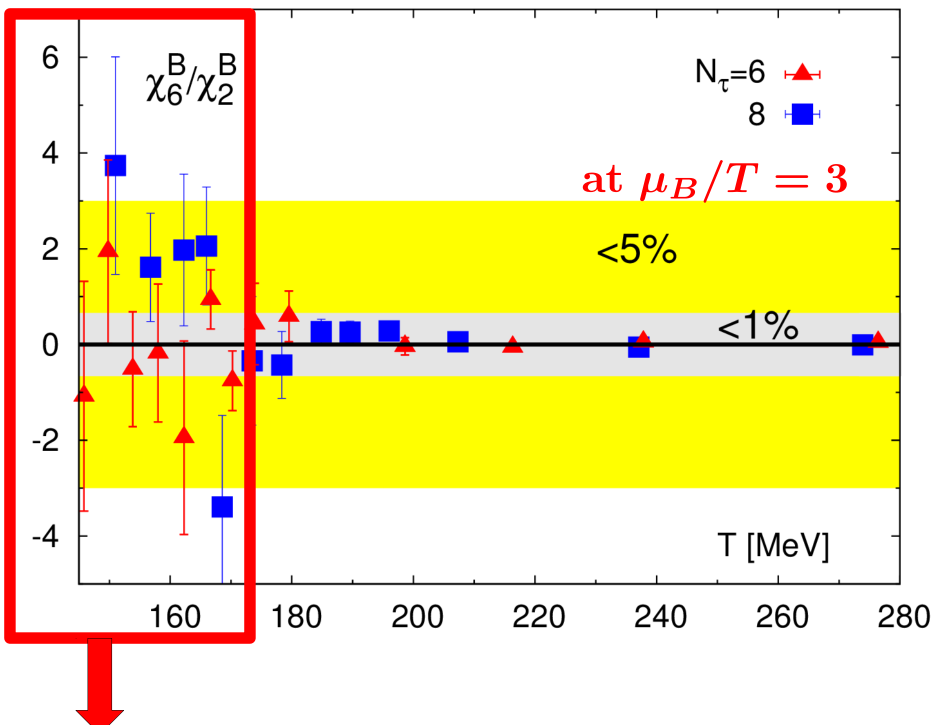

bands: magnitude of 6th order contribution relative to total of 0th, 2nd and 4th order

for $\mu_B/T \leq 2$:

$\mathcal{O}((\mu_B/T)^6)$ corrections to P/T^4

contribute less than 1% for T>170 MeV and less than ~ 5% for 150 MeV < T < 170 MeV

crucial: control 6th order cumulants in and below the crossover region

Equation of state of (2+1)-flavor QCD: $\mu_B/T > 0$

$$\frac{\Delta(T,\mu_B)}{T^4} = \frac{P(T,\mu_B) - P(T,0)}{T^4} = \frac{\chi_2^B}{2}\left(\frac{\mu_B}{T}\right)^2 \left(1 + \frac{1}{12}\frac{\chi_4^B}{\chi_2^B}\left(\frac{\mu_B}{T}\right)^2\right)$$

estimating the $\mathcal{O}((\mu_B/T)^6)$ correction: $\sim \frac{1}{720}\frac{\chi_6^B}{\chi_2^B}\left(\frac{\mu_B}{T}\right)^6$

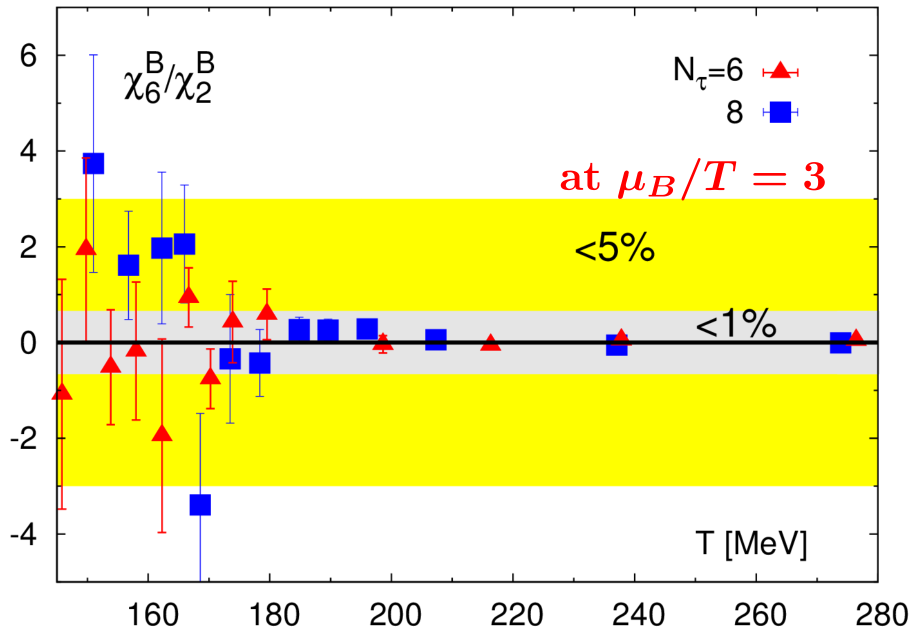

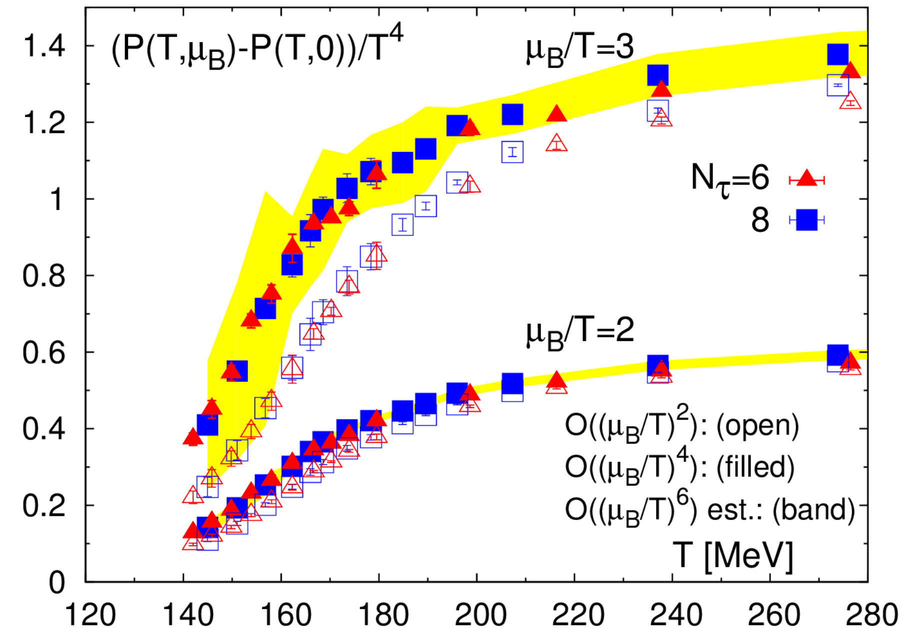

The EoS is well controlled for $\mu_B/T \leq 2$

Lines of constant thermodynamics and freeze-out

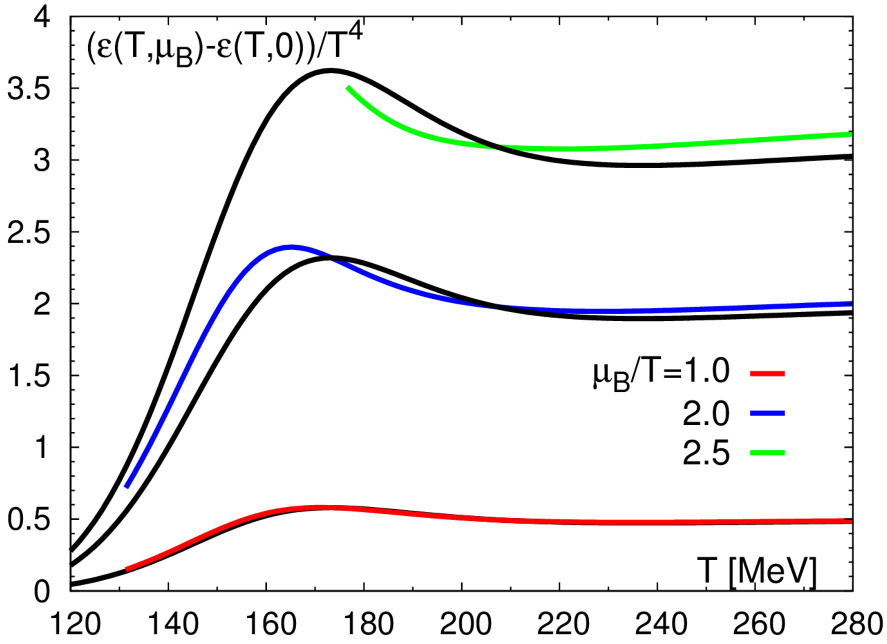

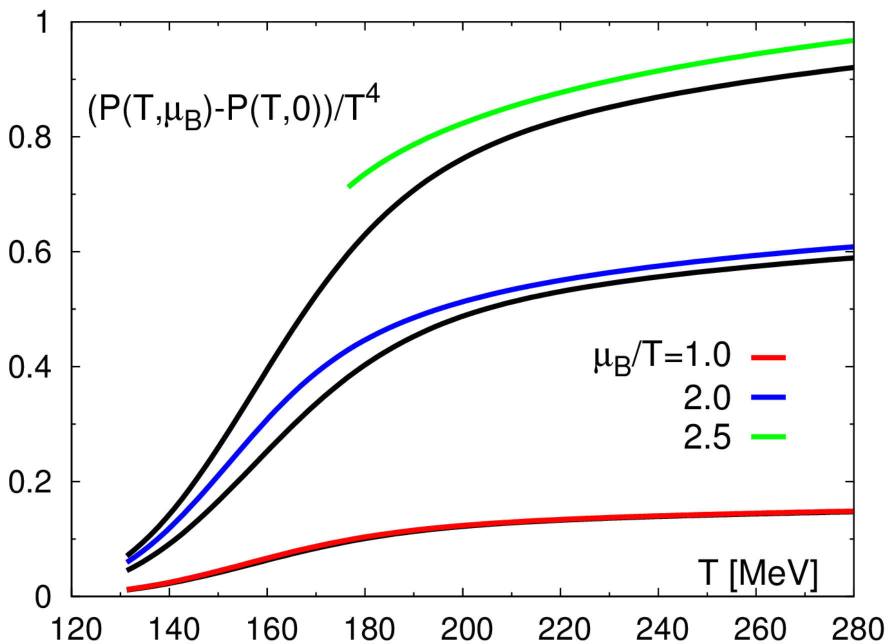

black lines: $\mathcal{O}(\mu_B^2)$

colored lines: $\mathcal{O}(\mu_B^4)$

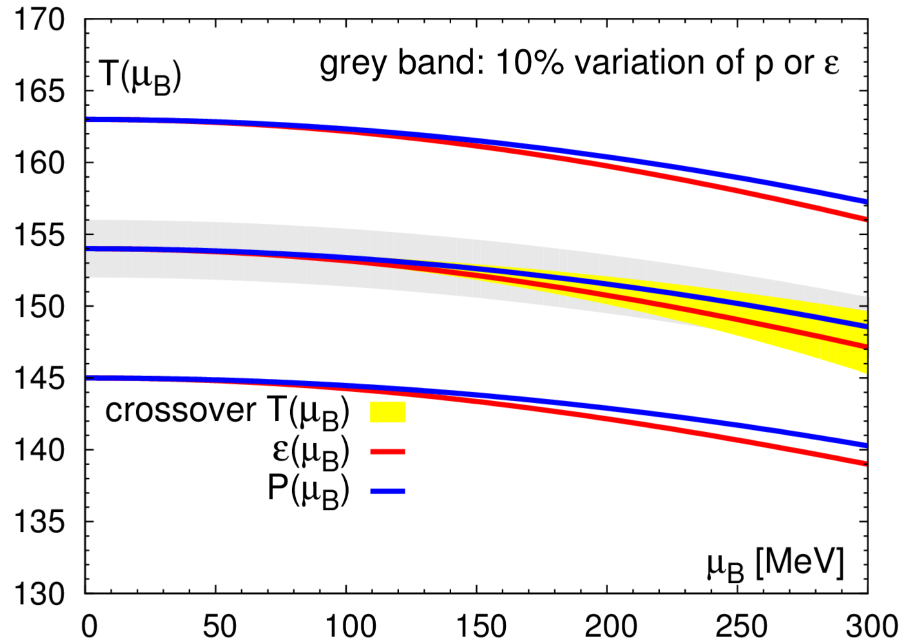

$\mathcal{O}(\mu_B^4)$ is shown only when the estimated $\mathcal{O}(\mu_B^6)$ contribution is smaller than 5%

Lines of constant thermodynamics and freeze-out

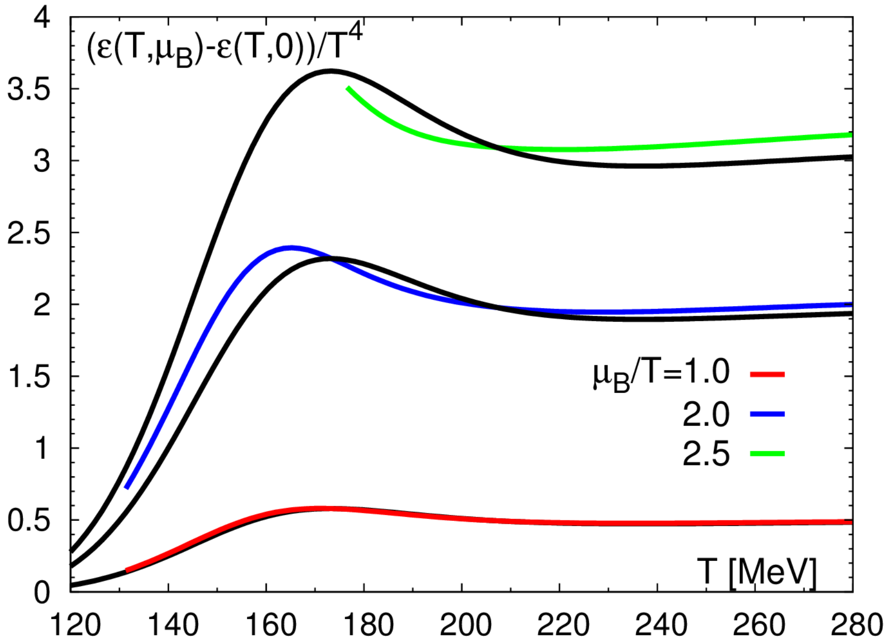

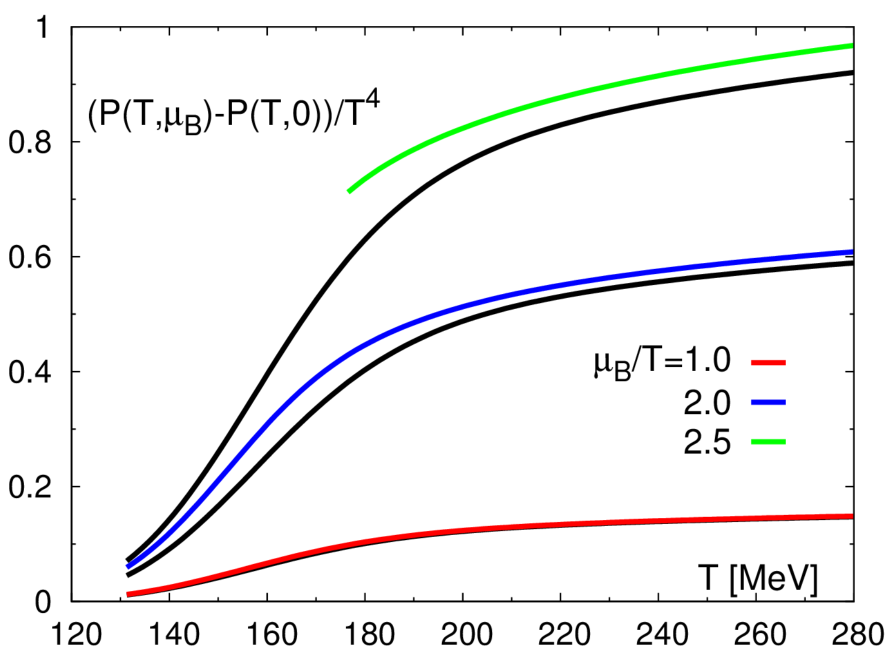

black lines: $\mathcal{O}(\mu_B^2)$

colored lines: $\mathcal{O}(\mu_B^4)$

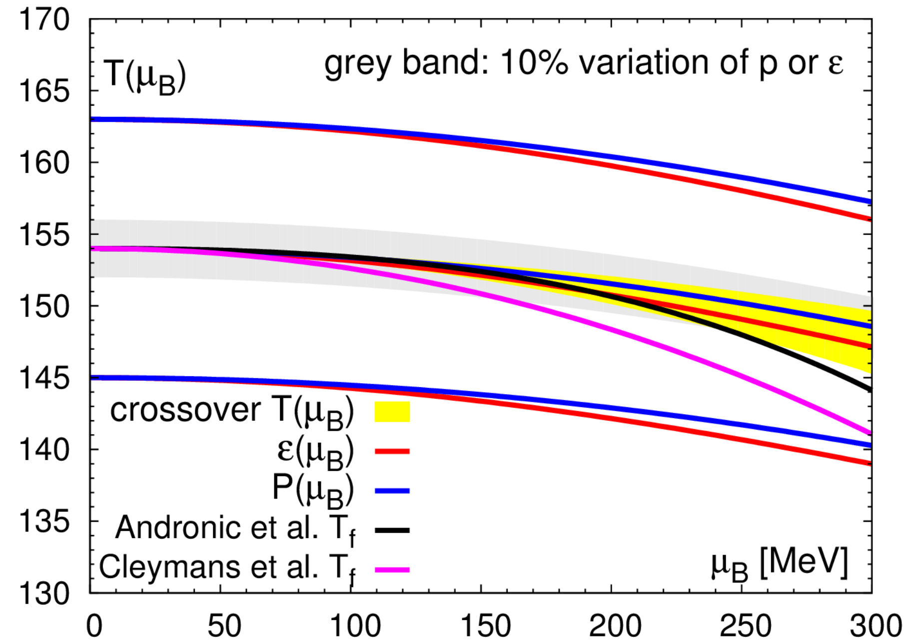

energy density and pressure decrease on the commonly used phenomenological freeze-out curves, but stay approximately constant on the crossover line for

$$\mu_B/T \lesssim 2$$

Conserved charge fluctuations and freeze-out

$$\frac{\Delta(T,\mu_B)}{T^4} = \frac{P(T,\mu_B)-P(T,0)}{T^4} = \frac{\chi_2^B}{2}\left(\frac{\mu_B}{T}\right)^2\left(1+\frac{1}{12}\frac{\chi_4^B}{\chi_2^B}\left(\frac{\mu_B}{T}\right)^2\right)$$

kurtosis*variance

$$(\kappa_B\sigma_B^2)_{\mu_B/T=0}$$

controls also leading terms in several ratios of conserved charge fluctuations

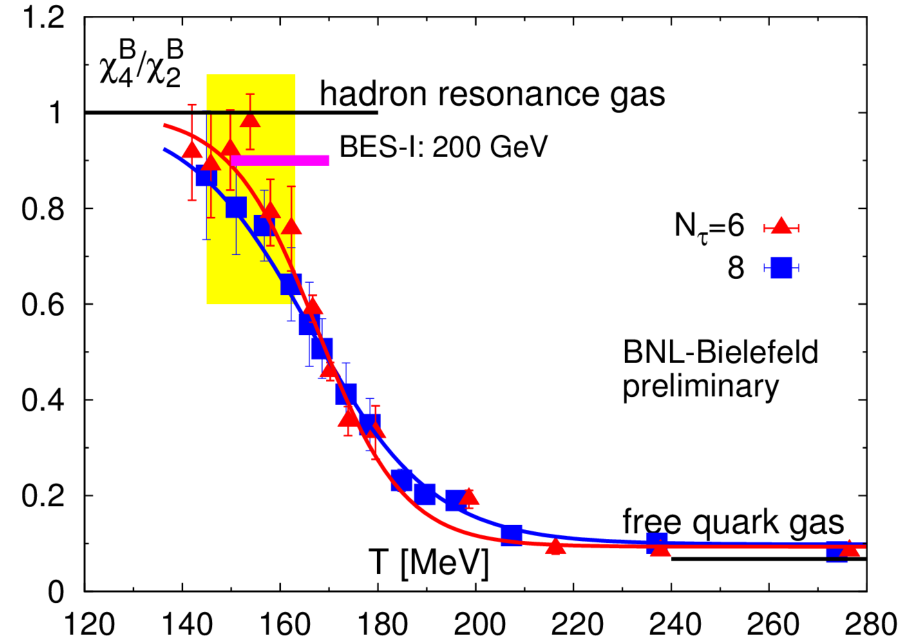

Conserved charge fluctuations and freeze-out

$$\frac{\Delta(T,\mu_B)}{T^4} = \frac{P(T,\mu_B)-P(T,0)}{T^4} = \frac{\chi_2^B}{2}\left(\frac{\mu_B}{T}\right)^2\left(1+\frac{1}{12}\frac{\chi_4^B}{\chi_2^B}\left(\frac{\mu_B}{T}\right)^2\right)$$

$$\frac{M_B}{\sigma_B^2} = \frac{\mu_B}{T} + \mathcal{O}(\mu_B^3)$$

$$S_B\sigma_B = \frac{\mu_B}{T}\frac{\chi_4^B}{\chi_2^B} + \mathcal{O}(\mu_B^3)$$

$$\boxed{S_B\sigma_B = \frac{M_B}{\sigma_B^2}\frac{\chi_4^B}{\chi_2^B} + \mathcal{O}(\mu_B^3)}$$

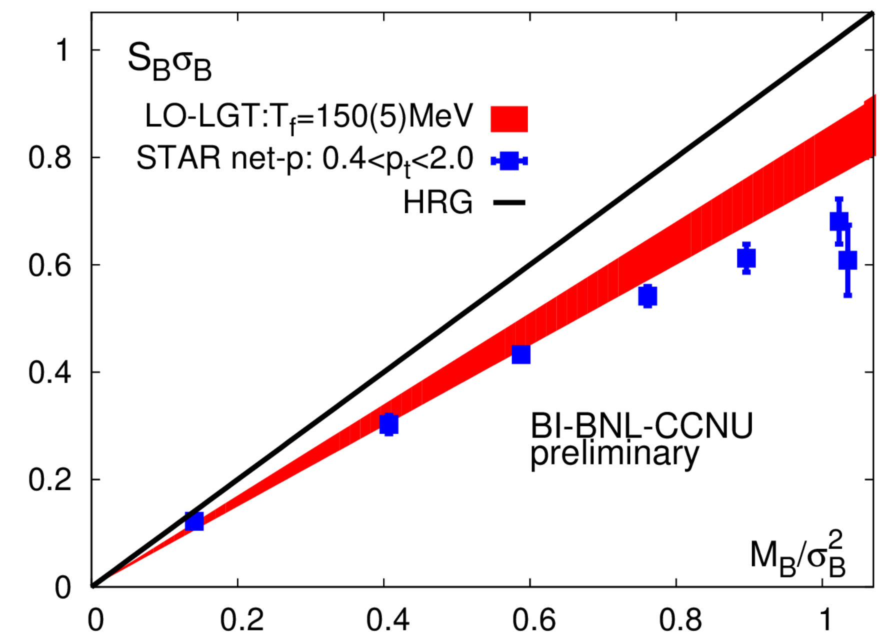

warning: net-proton $\neq$ net-baryon

M.Kitazawa et al, PR C86 (2012) 024904

A.Bzdak et al., PR C87 (2013) 014901

Conserved charge fluctuations and freeze-out

$$\frac{\Delta(T,\mu_B)}{T^4} = \frac{P(T,\mu_B)-P(T,0)}{T^4} = \frac{\chi_2^B}{2}\left(\frac{\mu_B}{T}\right)^2\left(1+\frac{1}{12}\frac{\chi_4^B}{\chi_2^B}\left(\frac{\mu_B}{T}\right)^2\right)$$

$$\boxed{S_B\sigma_B = \frac{M_B}{\sigma_B^2}\frac{\chi_4^B}{\chi_2^B} + \mathcal{O}(\mu_B^3)}$$

fit: $S_P\sigma_P = 0.79(2)\dfrac{M_P}{\sigma_P^2} - 0.15(3)\left(\dfrac{M_P}{\sigma_P^2}\right)^3$

warning:
net-proton $\neq$ net-baryon

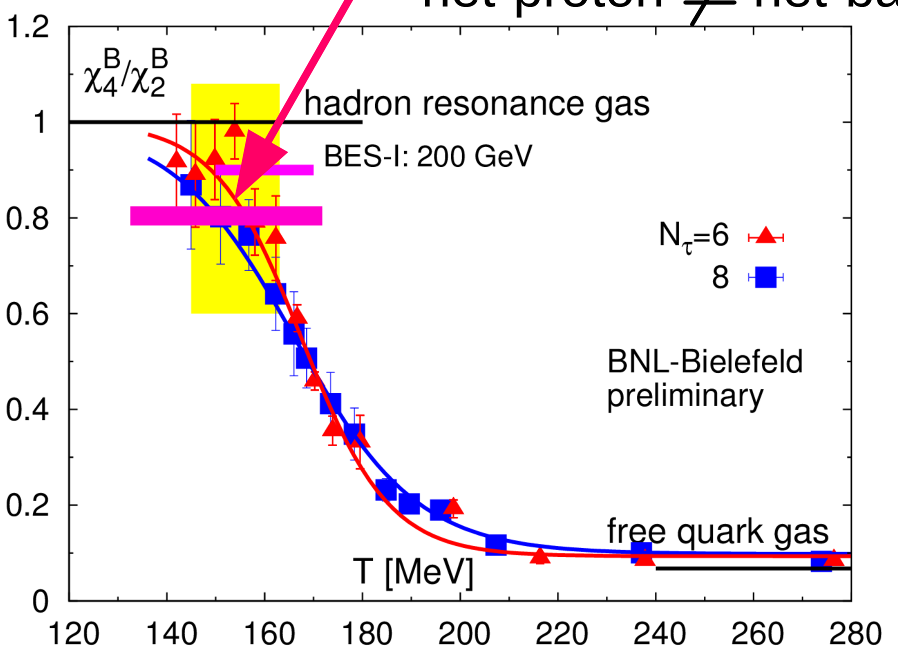

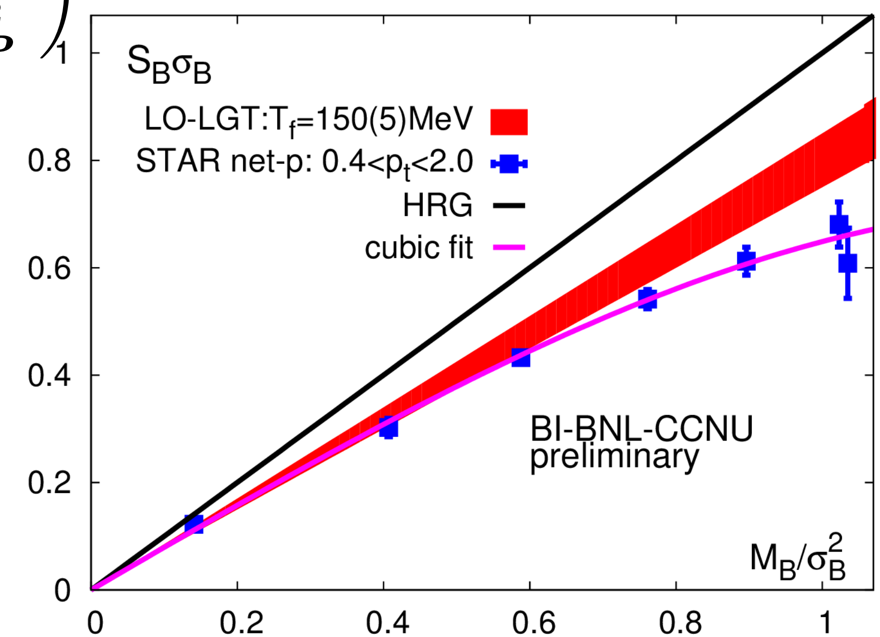

warning: net-proton $\neq$ net-baryon

M.Kitazawa et al, PR C86 (2012) 024904
A.Bzdak et al., PR C87 (2013) 014901

Conserved charge fluctuations and freeze-out

Next order: depends on 6[th] order cumulants and requires knowledge on the parametrization of the freeze-out curve, eg.

$$T_f(\mu_B) = T_f(0)\left(1 - \kappa_f \left(\frac{\mu_B}{T}\right)^2\right)$$

ratio of cumulants on "a line" in the (T, μ_B) plane

$$\frac{M_B}{\sigma_B^2} = \frac{\mu_B}{T} \frac{1 + \frac{1}{6}\frac{\chi_4^B}{\chi_2^B}\left(\frac{\mu_B}{T}\right)^2}{1 + \frac{1}{2}\frac{\chi_4^B}{\chi_2^B}\left(\frac{\mu_B}{T}\right)^2}$$

$$S_B\sigma_B = \frac{\mu_B}{T}\frac{\chi_4^B}{\chi_2^B}\frac{1 + \frac{1}{6}\frac{\chi_6^B}{\chi_4^B}\left(\frac{\mu_B}{T}\right)^2}{1 + \frac{1}{2}\frac{\chi_4^B}{\chi_2^B}\left(\frac{\mu_B}{T}\right)^2}$$

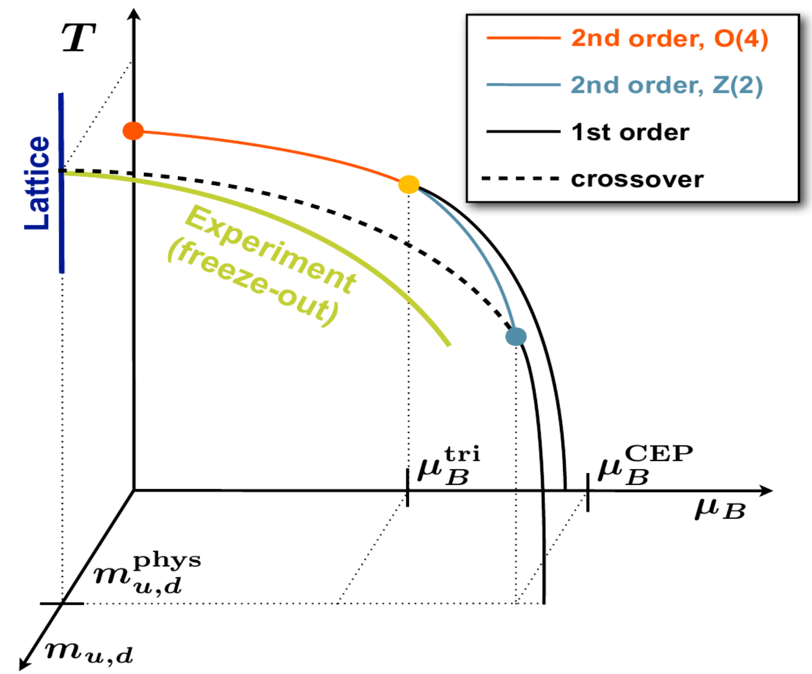

$$\equiv \left(\frac{\chi_4^B}{\chi_2^B}\right)_{T_f(0)} - \kappa_f T_f(0)\left(\frac{\chi_4^B}{\chi_2^B}\right)'\left(\frac{\mu_B}{T}\right)^2$$

Freeze-out parameter from conserved charge fluctuations

cumulant ratios of electric charge fluctuations

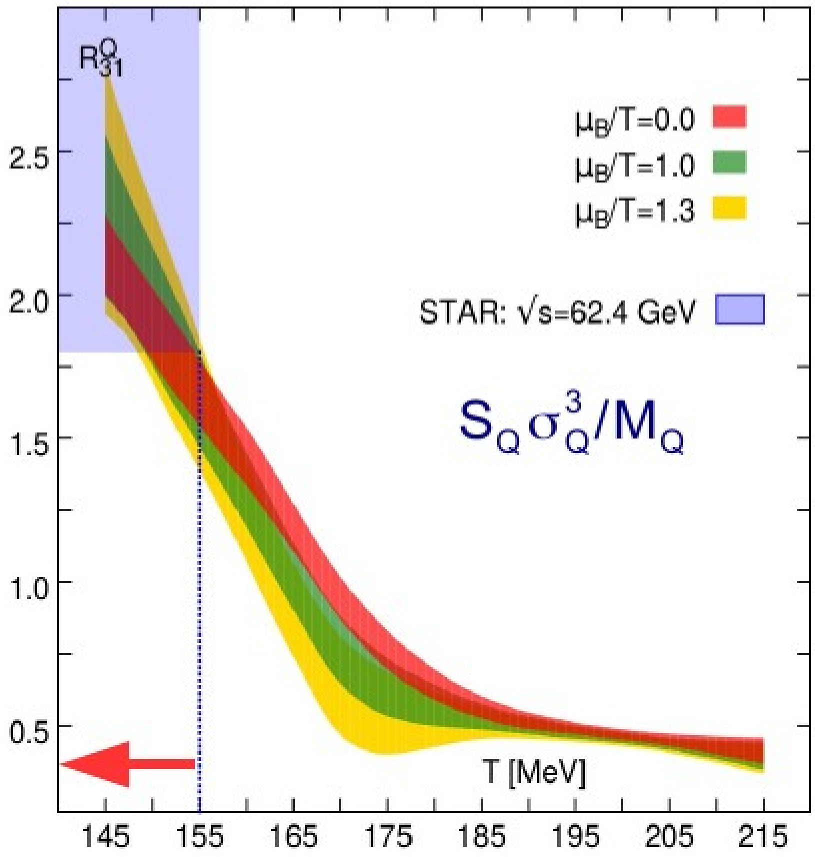

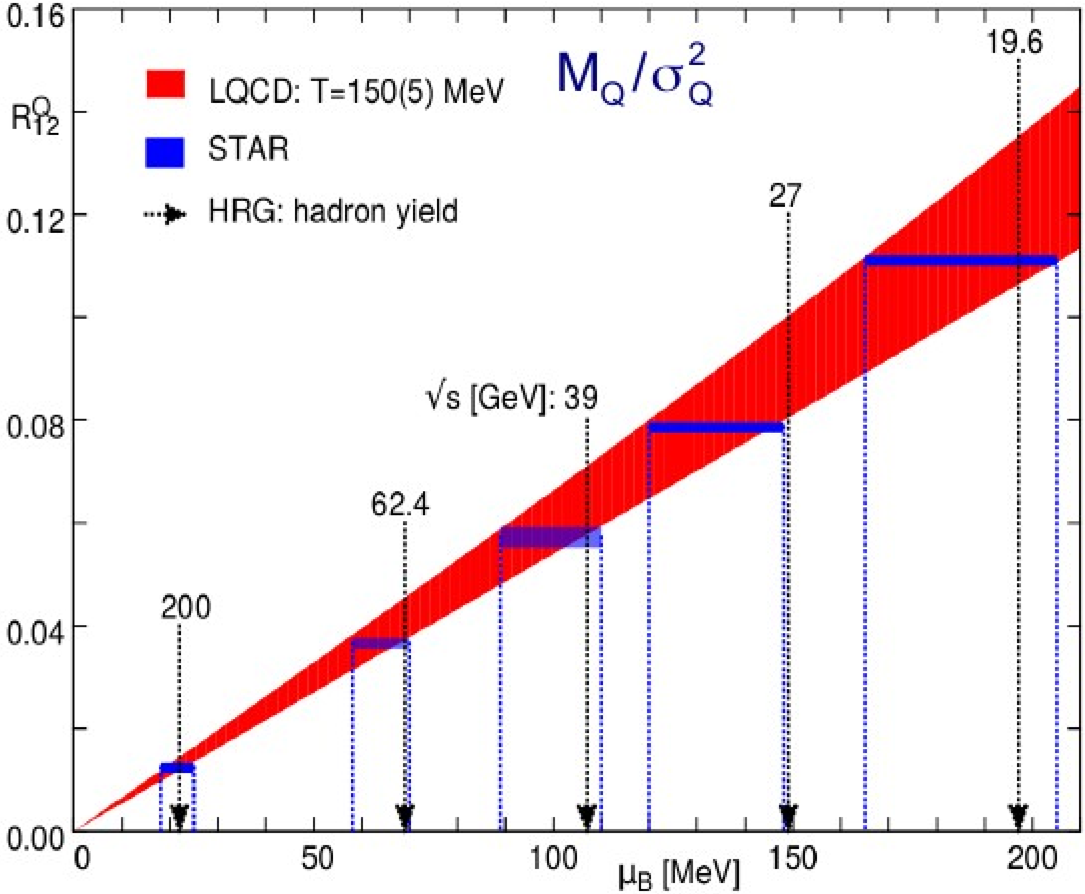

constraints freeze-out temperature

$$T_f \simeq (150 \pm 5)\ \mathrm{MeV}$$

determines freeze-out chemical potential

BI-BNL, PRL 109, 192302 (2012)
S. Mukherjee, M. Wagner, PoS CPOD2013 (2013) 039

Strangeness vs. baryon chemical potential

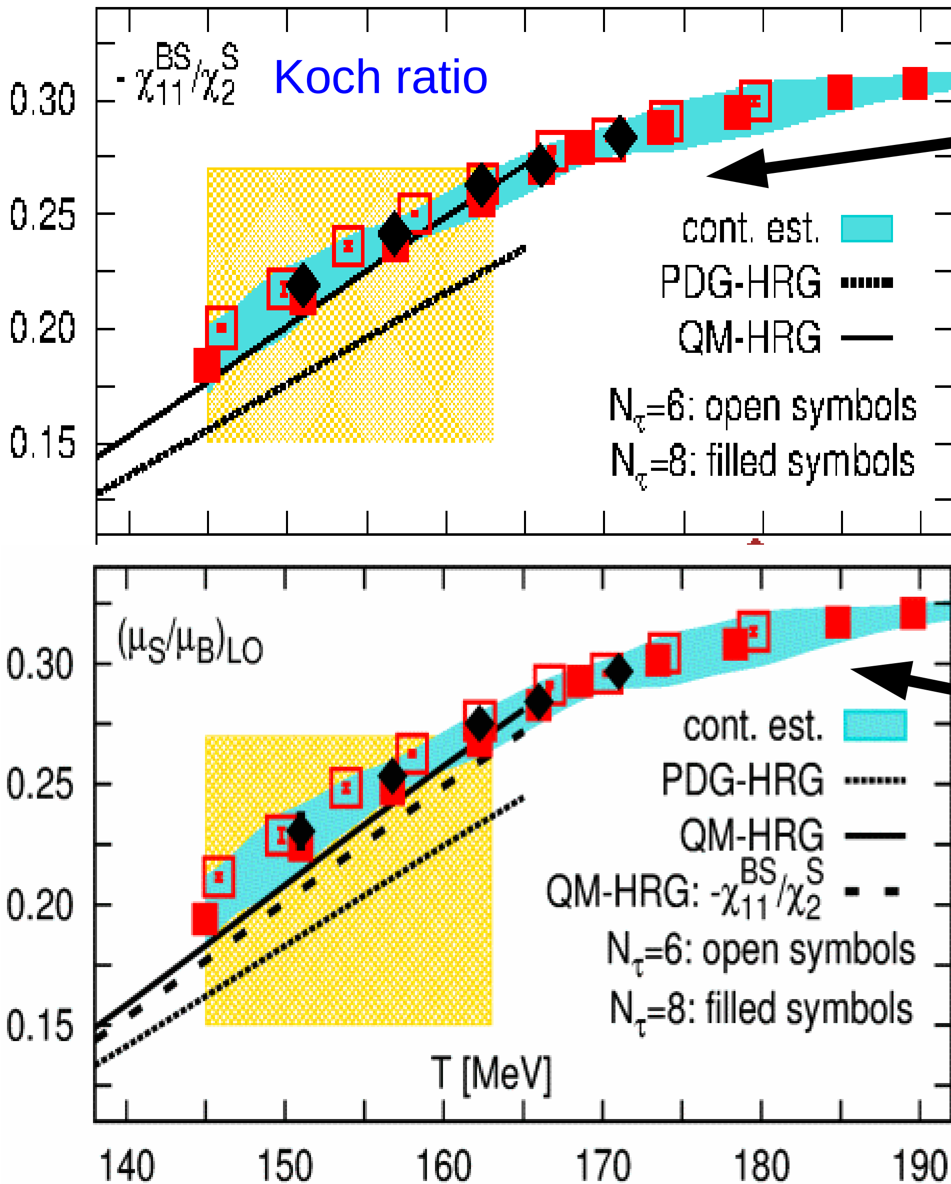

A. Bazavov et al., PRL 113, 072001 (2014), arXiv:1404.6511

enhanced
strangeness-baryon correlation over strangeness fluctuations

strangeness neutrality
enforces relation between chemical potentials

$$\langle n_S \rangle = 0$$
$$= \chi_2^S \hat{\mu}_S^2 + \chi_{11}^{BS} \hat{\mu}_S \hat{\mu}_B + \mathcal{O}(\mu^4)$$

$$\boxed{\frac{\mu_S}{\mu_B} = -\frac{\chi_{11}^{BS}}{\chi_2^S} + \mathcal{O}(\mu^2)}$$

HRG provides good guidance for thermal conditions at freeze-out. However,

HRG is not QCD

we need/want a self-consistent determination of freeze-out parameters based on QCD

Kurtosis*variance on the freeze-out line

$$\kappa_B\sigma_B^2 = \frac{\chi_4^B}{\chi_2^B}\,\frac{1+\frac{1}{2}\frac{\chi_6^B}{\chi_4^B}\left(\frac{\mu_B}{T}\right)^2}{1+\frac{1}{2}\frac{\chi_4^B}{\chi_2^B}\left(\frac{\mu_B}{T}\right)^2} \simeq \frac{\chi_4^B}{\chi_2^B}\left(1-\frac{1}{2}\left(\frac{\chi_4^B}{\chi_2^B}-\frac{\chi_6^B}{\chi_4^B}\right)\left(\frac{\mu_B}{T}\right)^2\right)$$

$\frac{\chi_6^B}{\chi_4^B}$ changes sign in crossover region

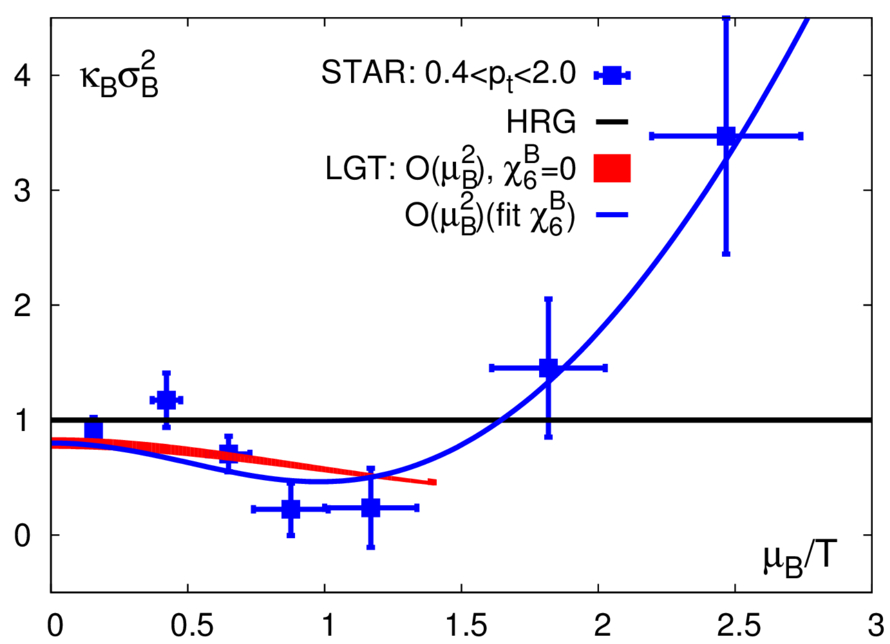

ansatz: $\frac{\chi_6^B}{\chi_4^B} = a_6 + b_6\left(\frac{\mu_B}{T}\right)^2$

consistent treatment requires knowledge of T-dependence of

$$\frac{\chi_4^B}{\chi_2^B}\,,\ \frac{\chi_6^B}{\chi_4^B}$$

on the freeze-out line

To do list

What is needed to understand equilibrium properties of conserved charge fluctuations on the freeze-out line?

– accurate lattice QCD results on 6th (and 8th) order cumulants of conserved charge fluctuations

– self-consistent determination of freeze-out parameters within QCD: $T_f(\mu_B),\ \mu_B,\ [\mu_S(\mu_B),\ \mu_Q(\mu_B)]$

– Quantify influence of finite-V, acceptance, p $\neq$ B etc. in close interaction with experiment and HI-phenomenology

What can be done about "locating the critical point"?

– use 6th (and 8th) order cumulants to put bounds on its location

– keep working on new simulation techniques

By-product: EoS in the entire parameter range accessible to the RHIC BES-II

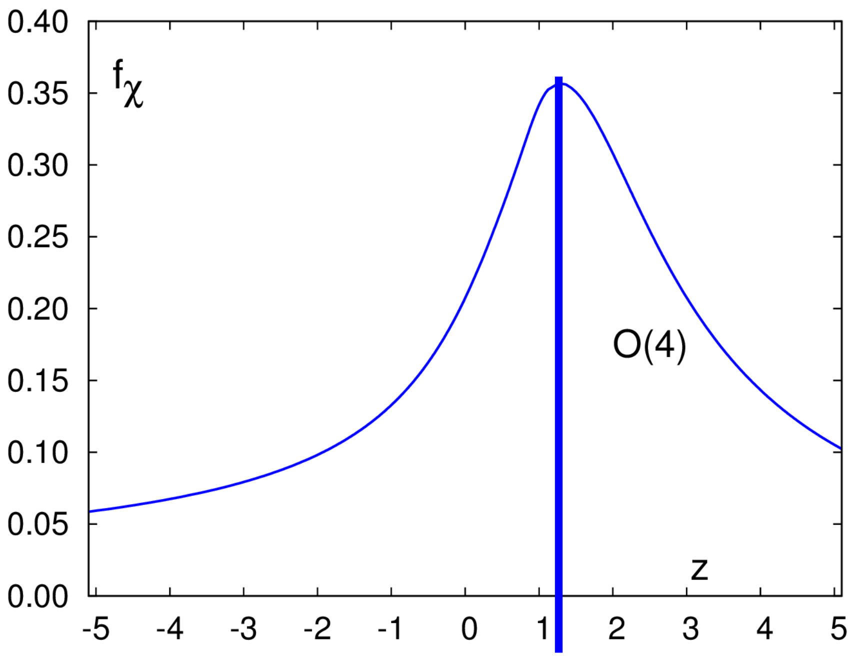

$$z_p = 1.33(5)$$

The peak in the scaling function that determines the location of the chiral crossover transition as seen by the chiral susceptibility is at (almost) the same temperature, at which the 6th order quark number susceptibility has its minimum – if contributions from regular terms are small!!

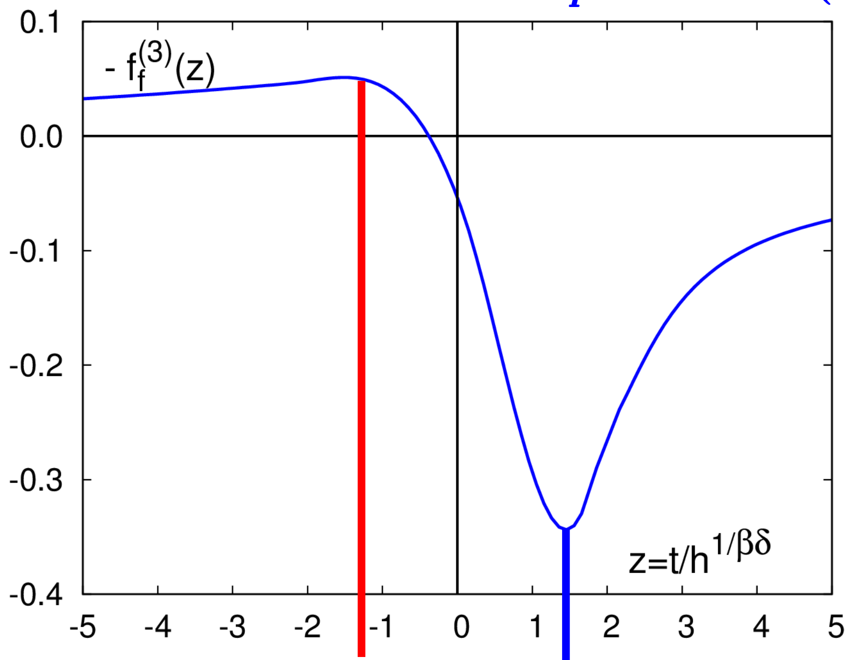

$$z_- \simeq -1.50 \qquad z_+ \simeq 1.48$$

6-th order net "up-ness" fluctuations

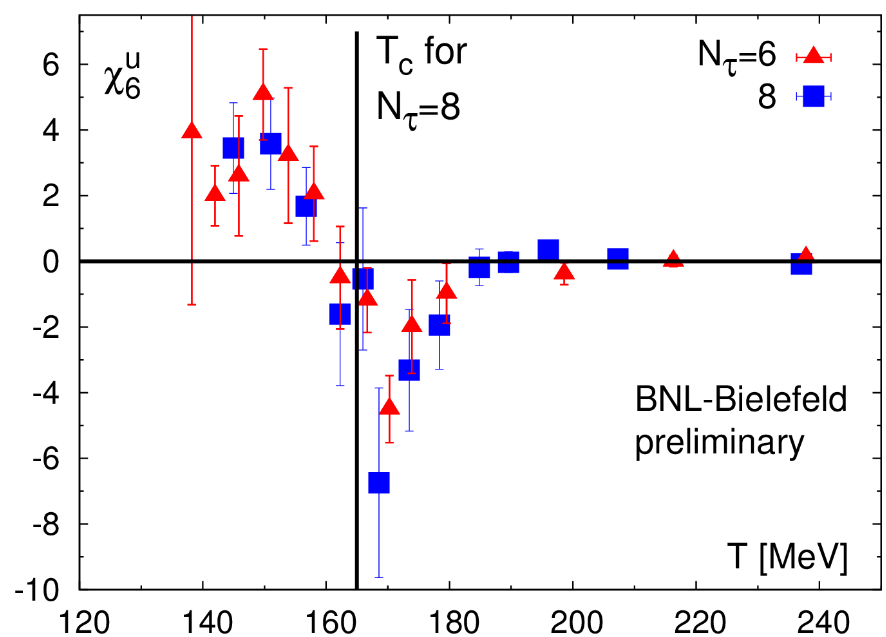

qualitatively as expected

Chiral Transition at small μ_B/T

- close to the chiral limit thermodynamics in the vicinity of the QCD transition(s) is controlled by a universal O(4) scaling function

singular — regular

$$\frac{p}{T^4} = \frac{1}{VT^3}\ln Z(V,T,\vec{\mu}) = -h_0\, h^{1+1/\delta} f_f(t/h^{1/\beta\delta}) - f_r(V,T,\vec{\mu})$$

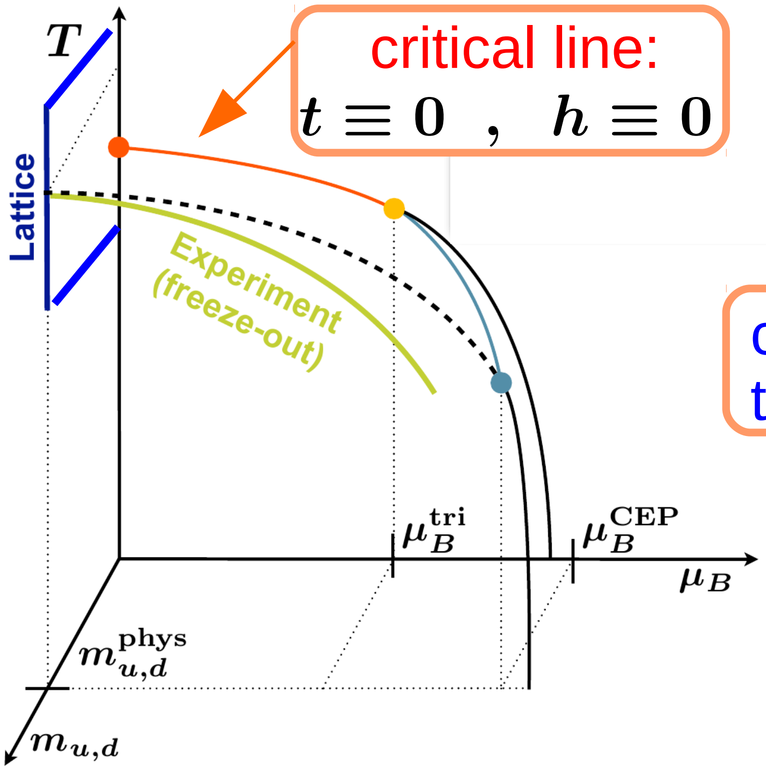

critical line: $t \equiv 0 \;\;,\;\; h \equiv 0$

$$t \sim \frac{T-T_c}{T_c} + \kappa_q \left(\frac{\mu_q}{T}\right)^2 \;\;,\;\; h \sim \frac{m_q}{T_c}$$

controls curvature of the critical line

suppressing dependence on strange quark chemical potential

$$\chi_n^q = \frac{\partial^n P/T^4}{\partial(\mu_q/T)^n} \sim \kappa_q^n f_f^{(n)}(t/h^{1/\beta\delta})$$

O(4) Scaling in QCD: Curvature of the critical line

$$M_b \equiv \frac{m_s\langle\bar\psi\psi\rangle}{T^4} = h^{1/\delta} f_G(z)$$

$$\frac{\chi_{m,q}}{T} = \frac{\partial^2\langle\bar\psi\psi\rangle/T^3}{\partial(\mu_q/T)^2}$$

$$= \frac{2\kappa_q T}{t_0 m_s} h^{(\beta-1)/\delta\beta} f'_G(z)$$

$$\boxed{\kappa_B = \kappa_q/9 = 0.0066(7)}$$

scaling function of order parameter

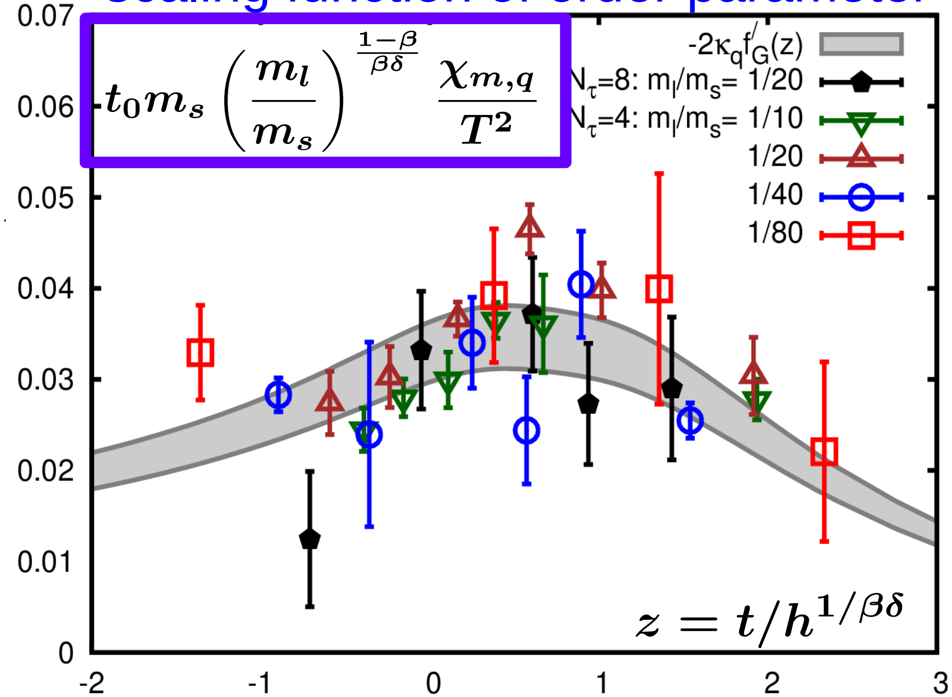

p4-action: $N_\tau = 4$

Bielefeld-BNL, Phys. Rev. D83, 014504 (2011)

O(4) Scaling in QCD: Curvature of the critical line

summary of current values
for the curvature term:

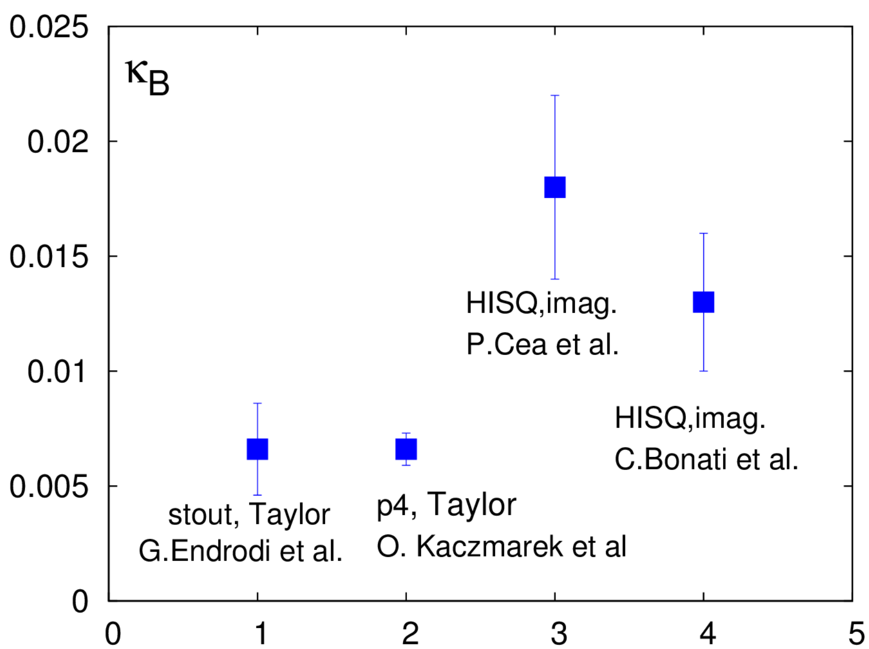

$$0.006 \lesssim \kappa_B \lesssim 0.018$$

scaling function of order parameter

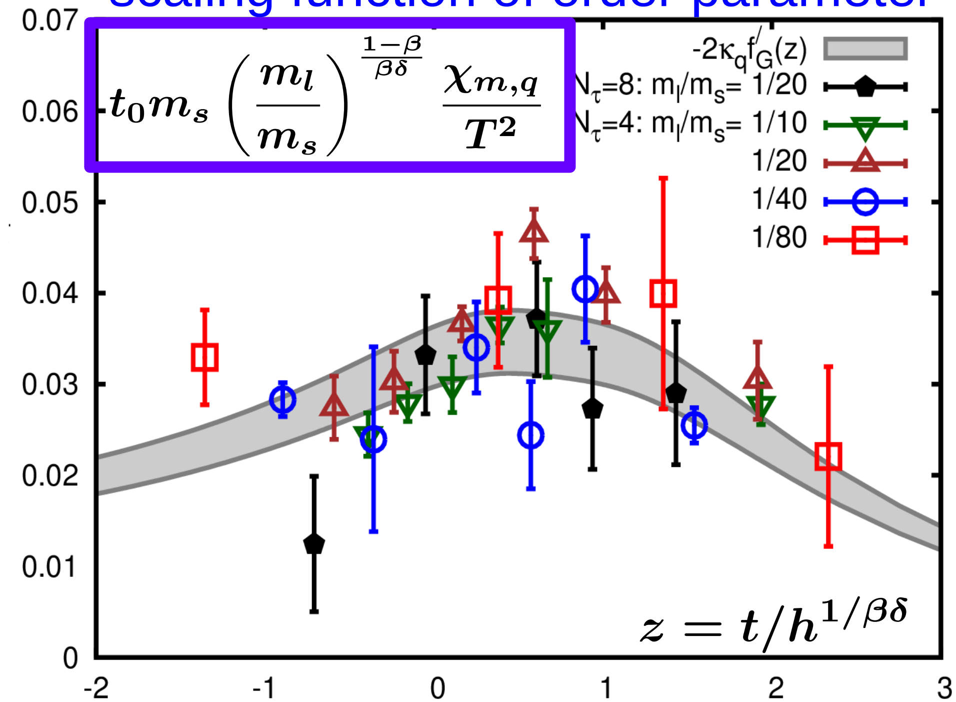

p4-action: $N_\tau = 4$

Bielefeld-BNL, Phys. Rev. D83, 014504 (2011)

→ the crossover temperature changes by (4-12) MeV

for $0 \leq \mu_B/T \leq 2$

or $15\ \mathrm{GeV} < \sqrt{s} < \infty$

Critical Point searches

lattice QCD

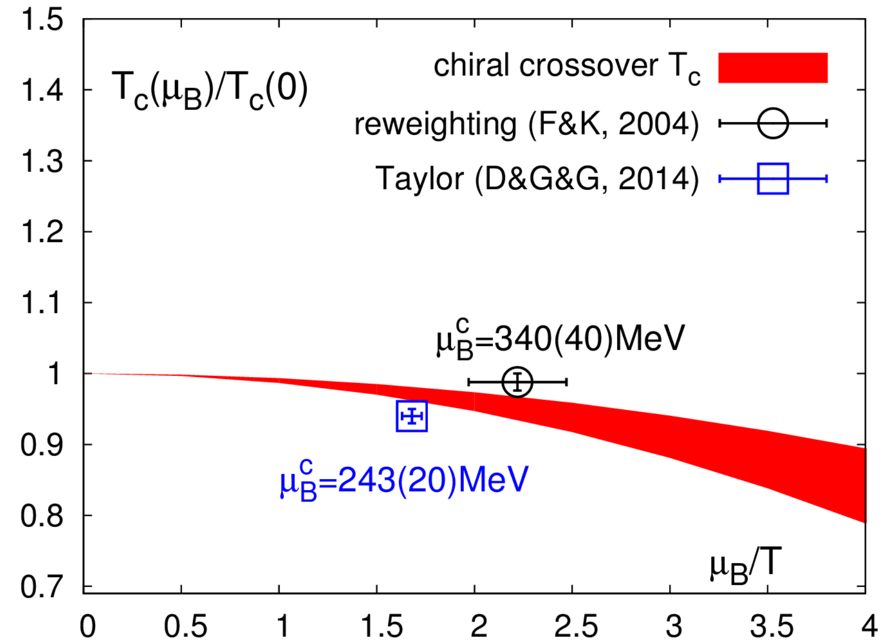

reweighting:
Z. Fodor, S. Katz,
JHEP 04, 204 (2004)

Taylor expansion:
S. Datta, R.V. Gavai, S. Gupta,
PoS Lattice 2013 (2014) 202

Observation of the critical end point in the phase diagram for hot and dense nuclear matter

Roy A. Lacey
Stony Brook University

arXiv:1411.7931

Outline

- ***Introduction***
  - ✓ *Phase Diagram*
- ***Search strategy for the CEP***
  - ✓ *Guiding principles*
- ***A probe***
  - ✓ *Femtoscopic susceptibility*
- ***Analysis Details***
  - ✓ *Finite-Size-Scaling*
  - ✓ *Dynamic Finite-Size-Scaling*
- ***Summary***
  - ✓ ***Epilogue***

The QCD Phase Diagram

A central goal of the worldwide program in relativistic heavy ion collisions, is to chart the QCD phase diagram

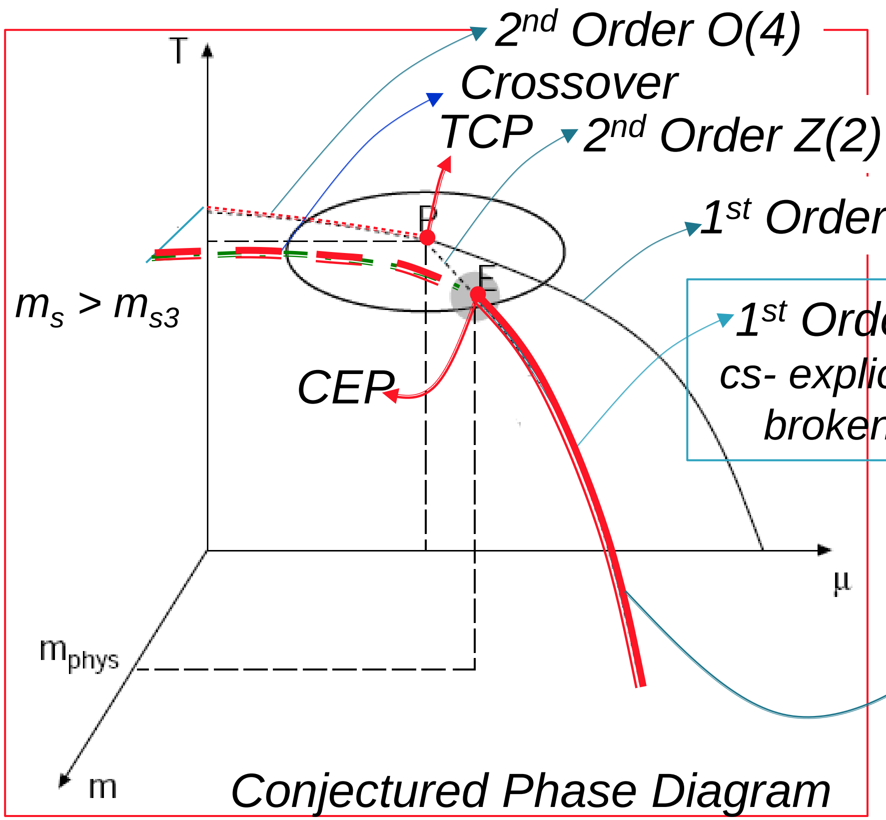

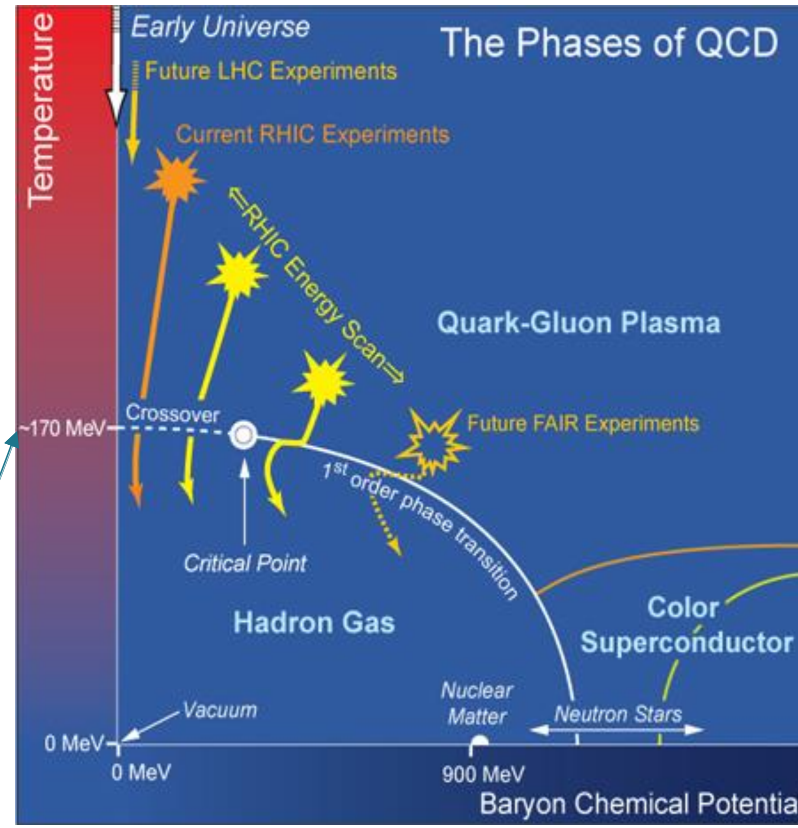

The QCD Phase Diagram

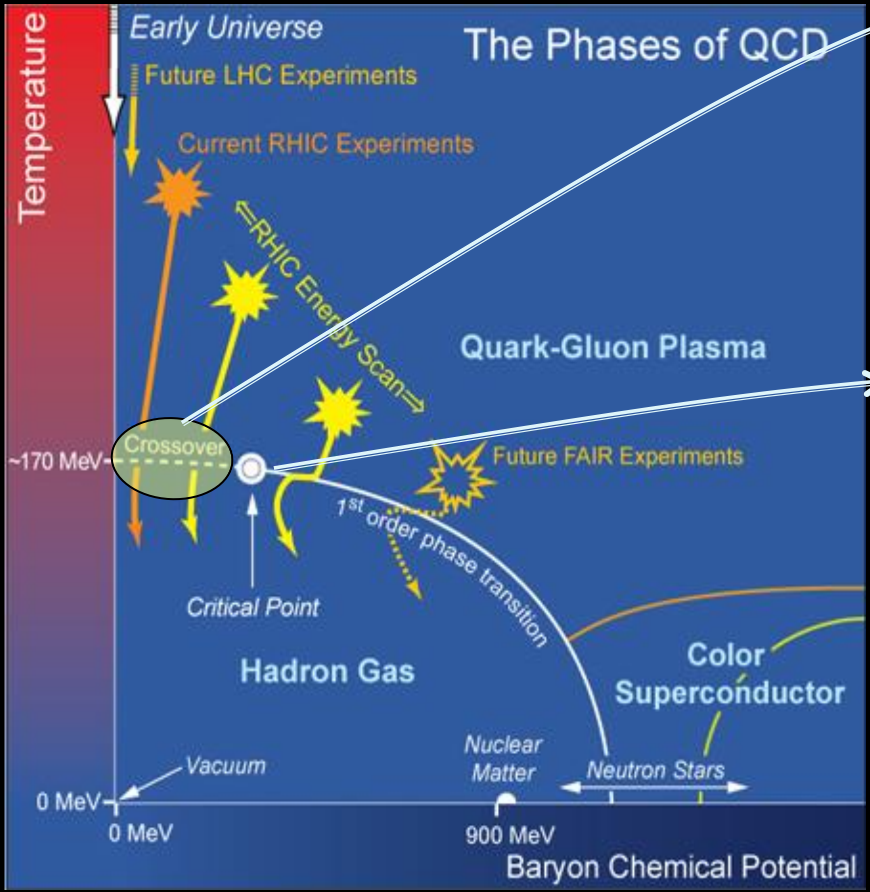

Known knowns

Spectacular achievement:

- *Validation of the crossover transition leading to the QGP*
- *Initial estimates for the transport properties of the QGP*

Known unknowns

- Location of the critical End point (CEP)?
  - ✓ Order of the phase transition?
  - ✓ Value of the critical exponents?
- Location of phase coexistence regions?
- Detailed properties of each phase?

All are fundamental to charting the phase diagram

*(New) measurements, analysis techniques and theory efforts which probe a broad range of the **(T, μ_B)-plane,** are essential to fully unravel the unknowns!*

Theoretical Guidance

Theoretical Consensus

"Static" Universality class for the CEP

- *3D-Ising*

Dynamic Universality class for the CEP

- *Model H*

CEP Location Estimates

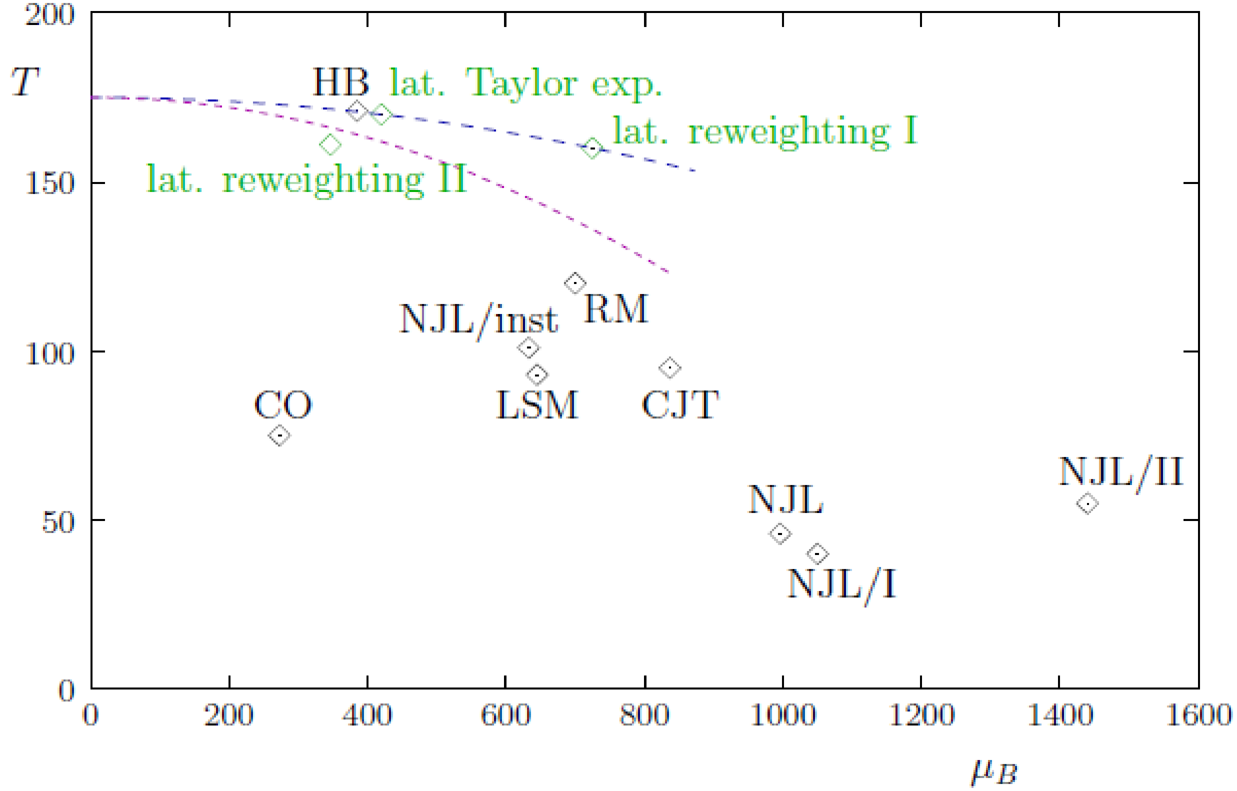

No theoretical convergence on CEP location to date

→ Experimental question/opportunity?

Ongoing studies in search of the CEP

- Systematic study of various probes as a function of $\sqrt{s}$:
  - Collapse of directed flow – v_1
  - Critical fluctuations
  - Emission Source radii ⟸ ***Focus of this talk***
  - Viscous coefficients for flow
  - …
  - …

These are all guided by a central search strategy

Anatomy of search strategy

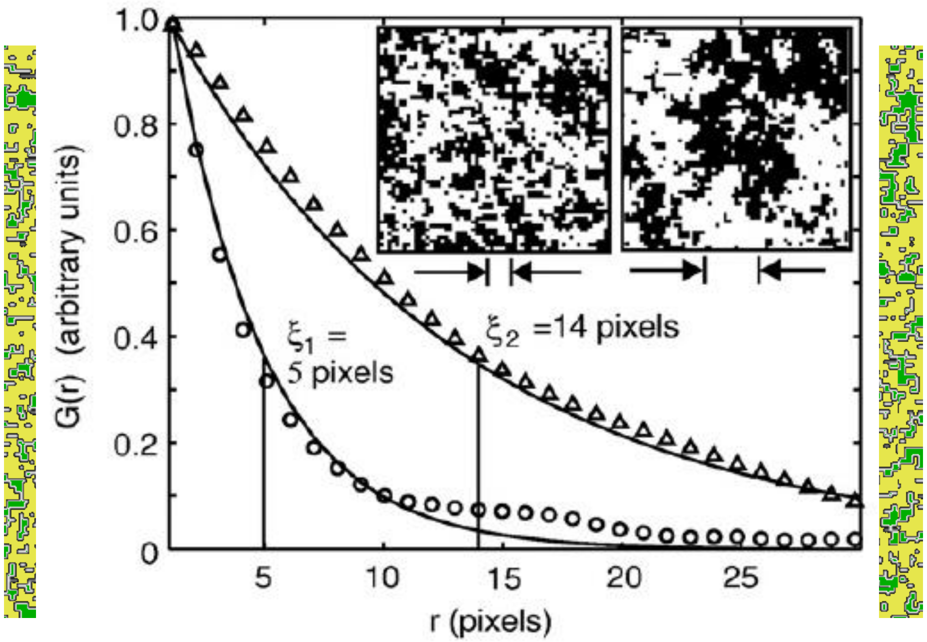

Approaching the critical point of a 2nd order phase transitions

- ***Search for "critical fluctuations" in HIC***

Stephanov, Rajagopal, Shuryak PRL.81, 4816 (98)

- The correlation length diverges
  - ✓ Renders microscopic details (largely) irrelevant
- This leads to universal power laws and scaling functions for static and dynamic properties

Ising model

Magnetization	$M \sim \lvert T - T_c \rvert^{\beta}$
Mag. Sucep.	$\chi_M \sim \lvert T - T_c \rvert^{-\gamma}$
Heat Cap.	$C_V = \frac{1}{V}\frac{d\langle E\rangle}{dT} \sim \lvert T - T_c \rvert^{-\alpha}$
Corr. Length	$\xi \sim \lvert T - T_c \rvert^{-\nu}$

The critical end point is characterized by several (power law) divergences

Anatomy of search strategy

H_2O

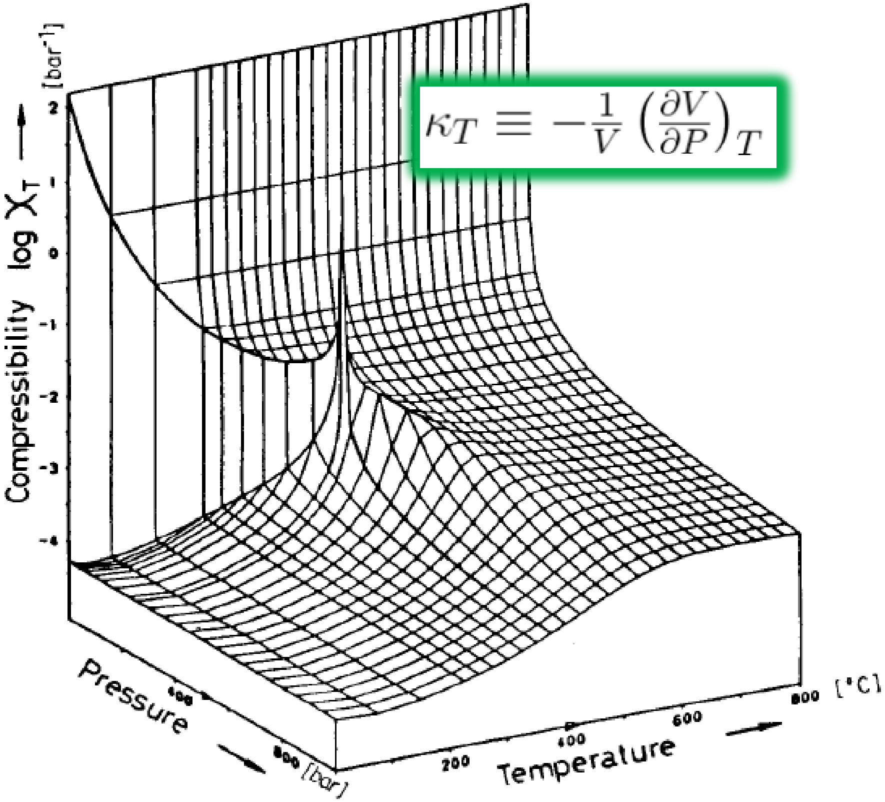

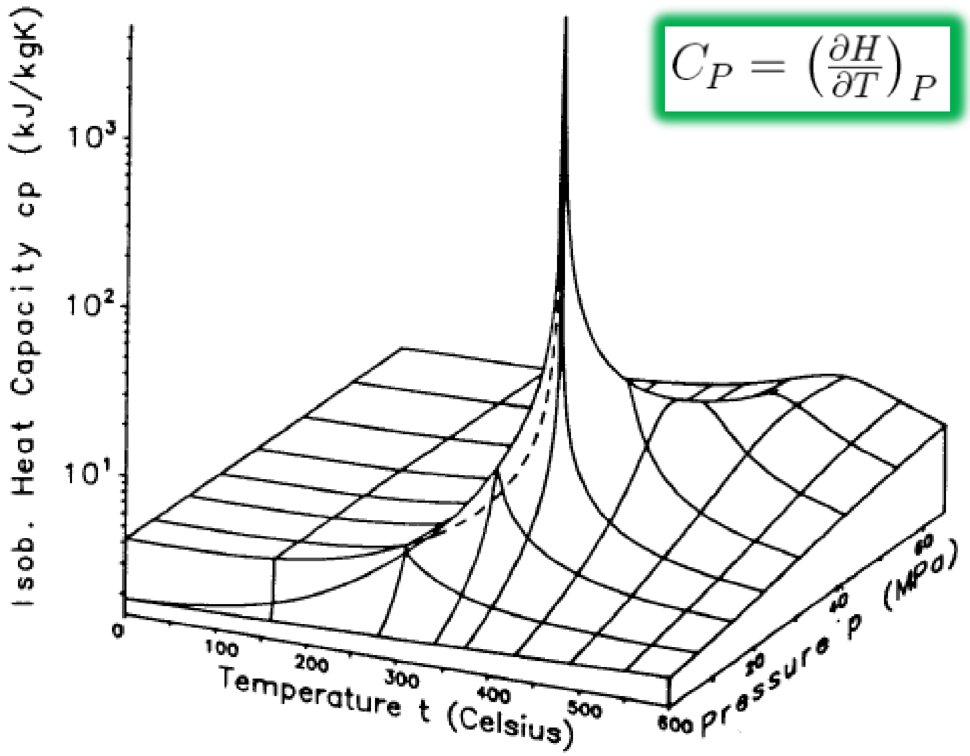

The critical end point is characterized by several (power law) divergent signatures

For HIC we can use beam energy scans to vary μ_B & *T to search for non-monotonic patterns in a susceptibility*

Search Strategy

Exploit the RHIC-LHC beam energy lever arm

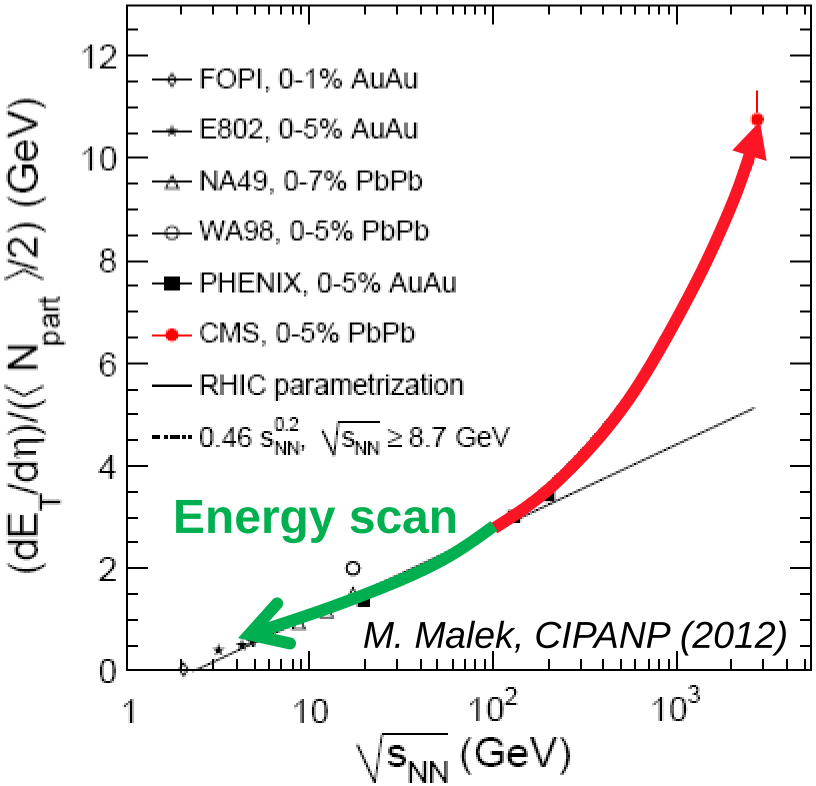

(μ_B, *T*) at chemical freeze-out

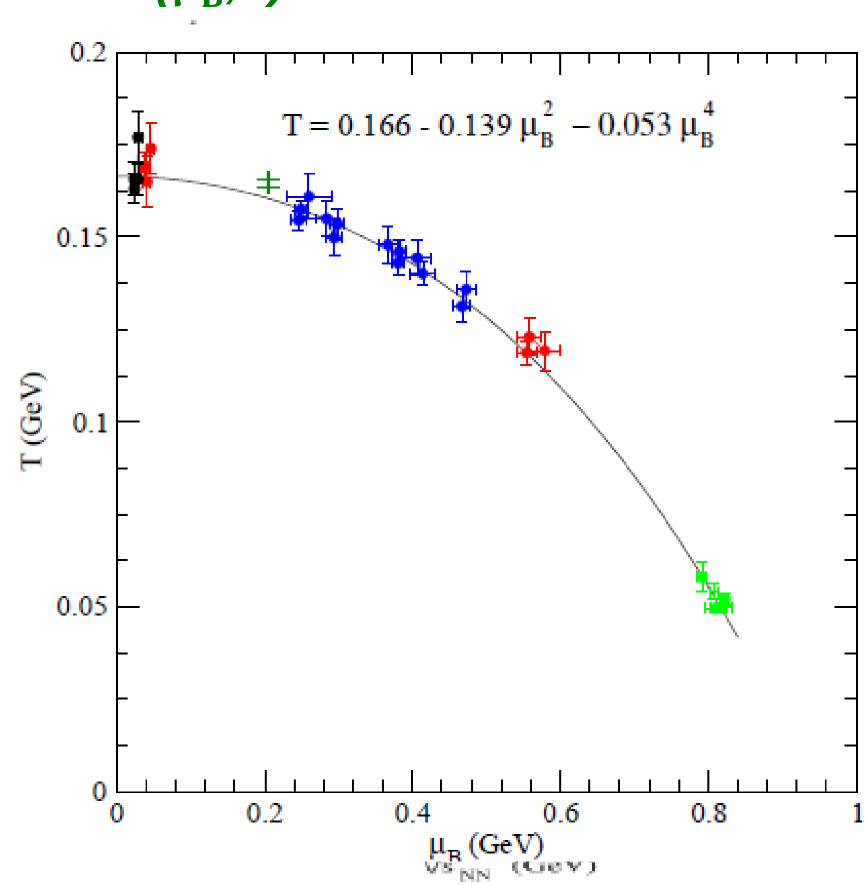

- ➢ ***LHC → access to high T and small μ_B***
- ➢ ***RHIC → access to different systems and a broad domain of the (μ_B,T)-plane***

$RHIC_{BES}$ to LHC → ~360 $\sqrt{s_{NN}}$ increase

$\sqrt{s_{NN}}$ is a good proxy for (T, μ_B) combinations!

Challenge → identification of a robust signal

Interferometry as a susceptibility probe

3D Koonin Pratt Eqn.

$$R(\vec{q}) = C(\vec{q}) - 1 = 4\pi \int dr r^2 K_0(\vec{q},\vec{r}) S(\vec{r}) \quad (1)$$

Correlation function

Encodes FSI

Source function (Distribution of pair separations)

Alias (HBT)
Hanbury Brown & Twist

Two-particle correlation function

$$C(\mathbf{q}) = \frac{dN_2 / d\mathbf{p}_1 d\mathbf{p}_2}{(dN_1 / d\mathbf{p}_1)(dN_1 / d\mathbf{p}_2)}$$

S. Afanasiev et al. (PHENIX) PRL 100 (2008) 232301

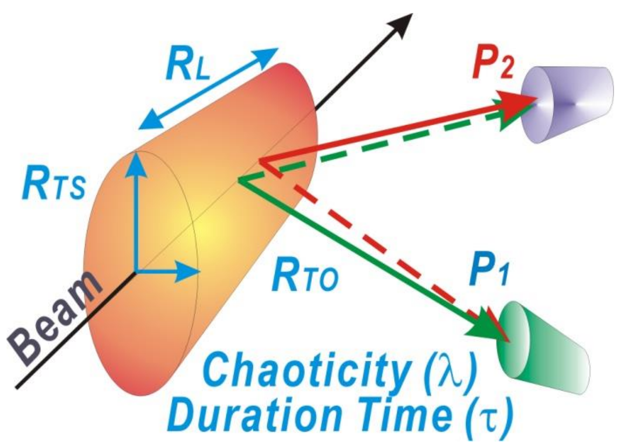

Inversion of this integral equation ➔ Source Function

$$c_s^2 = \frac{1}{\rho \kappa_S}$$

In the vicinity of a phase transition or the CEP, the divergence of the compressibility leads to anomalies in the expansion dynamics

→ BES measurements of the space-time extent provides a good probe for the (T,μ_B) dependence of the susceptibility

Interferometry Probe

Hung, Shuryak, PRL. 75,4003 (95)
Chapman, Scotto, Heinz, PRL.74.4400 (95)

Makhlin, Sinyukov, ZPC.39.69 (88)

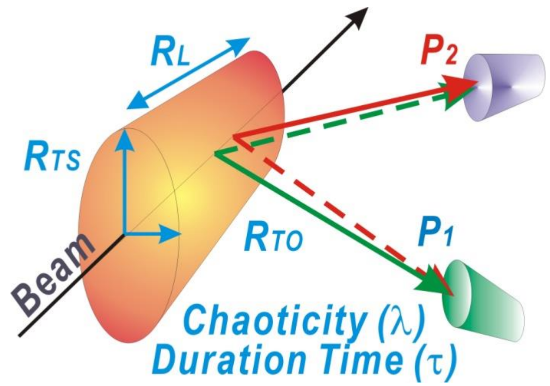

$$R^2_{side} = \frac{R^2_{geo}}{1+\frac{m_T}{T}\beta_T^2}$$

$$R^2_{out} = \frac{R^2_{geo}}{1+\frac{m_T}{T}\beta_T^2} + \beta_T^2(\Delta\tau)^2$$

$$c_s^2 = \frac{1}{\rho\kappa_S}$$

$$R^2_{long} \approx \frac{T}{m_T}\tau^2$$

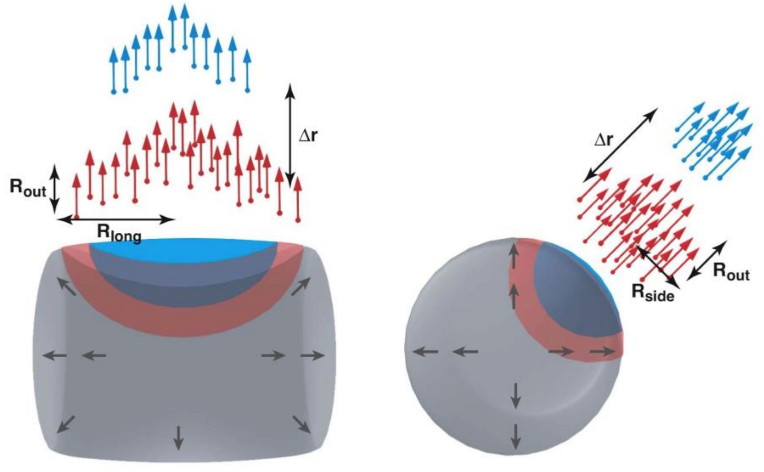

(R^2_{out}-R^2_{side}) sensitive to the susceptibility

Specific non-monotonic patterns expected as a function of $\sqrt{s_{NN}}$
- **A maximum for (R^2_{out} - R^2_{side})**
- ***A minimum for* (R_{side} - R_i)/R_{long}**

Interferometry Probe

Dirk Rischke and Miklos Gyulassy
Nucl.Phys.A608:479-512,1996

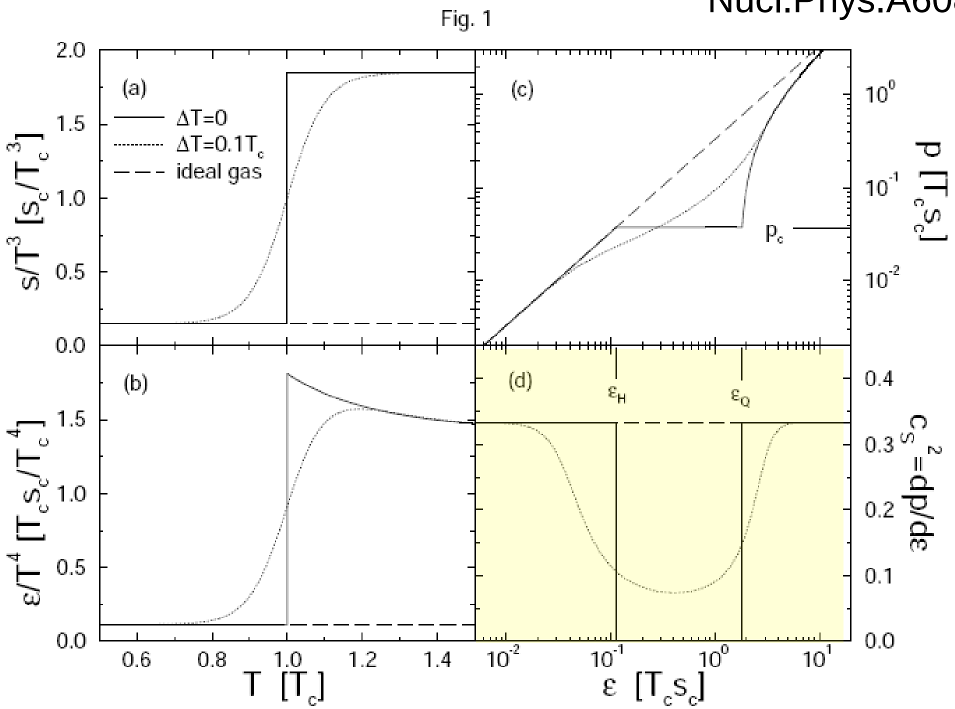

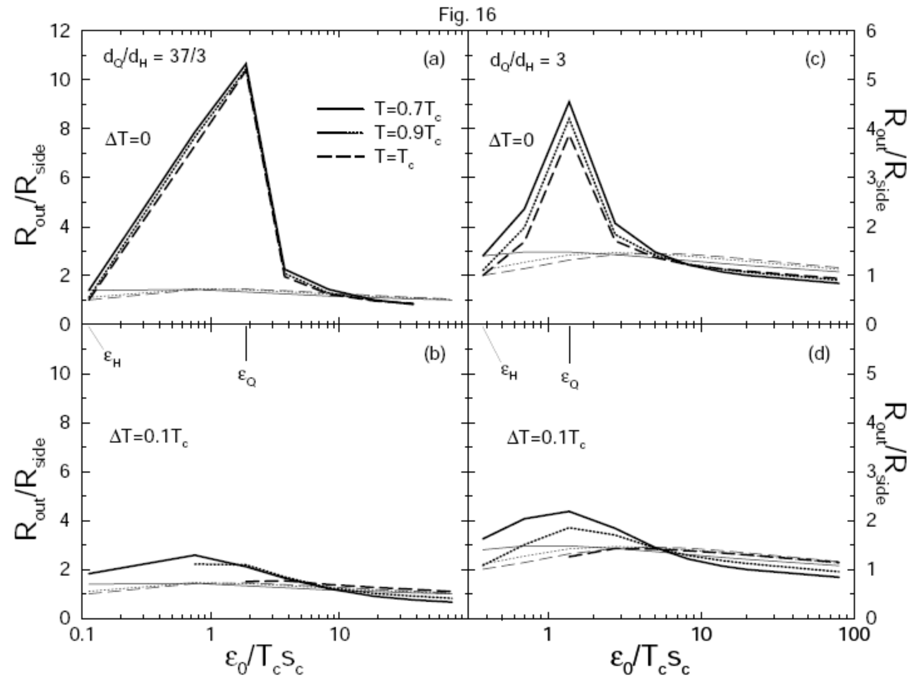

In the vicinity of a phase transition or the CEP, the sound speed is expected to soften considerably.

$$c_s^2 = \frac{1}{\rho \kappa_S}$$

The divergence of the compressibility leads to anomalies in the expansion dynamics

→ *Enhanced emission duration* and non-monotonic excitation function for R^2_{out} - R^2_{side}

Interferometry signal

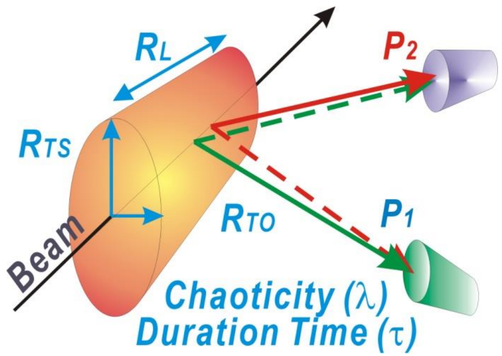

$$C(\mathbf{q}) = \frac{dN_2 / d\mathbf{p}_1 d\mathbf{p}_2}{(dN_1 / d\mathbf{p}_1)(dN_1 / d\mathbf{p}_2)}$$

Adare et. al. (PHENIX)
arXiv:1410.2559

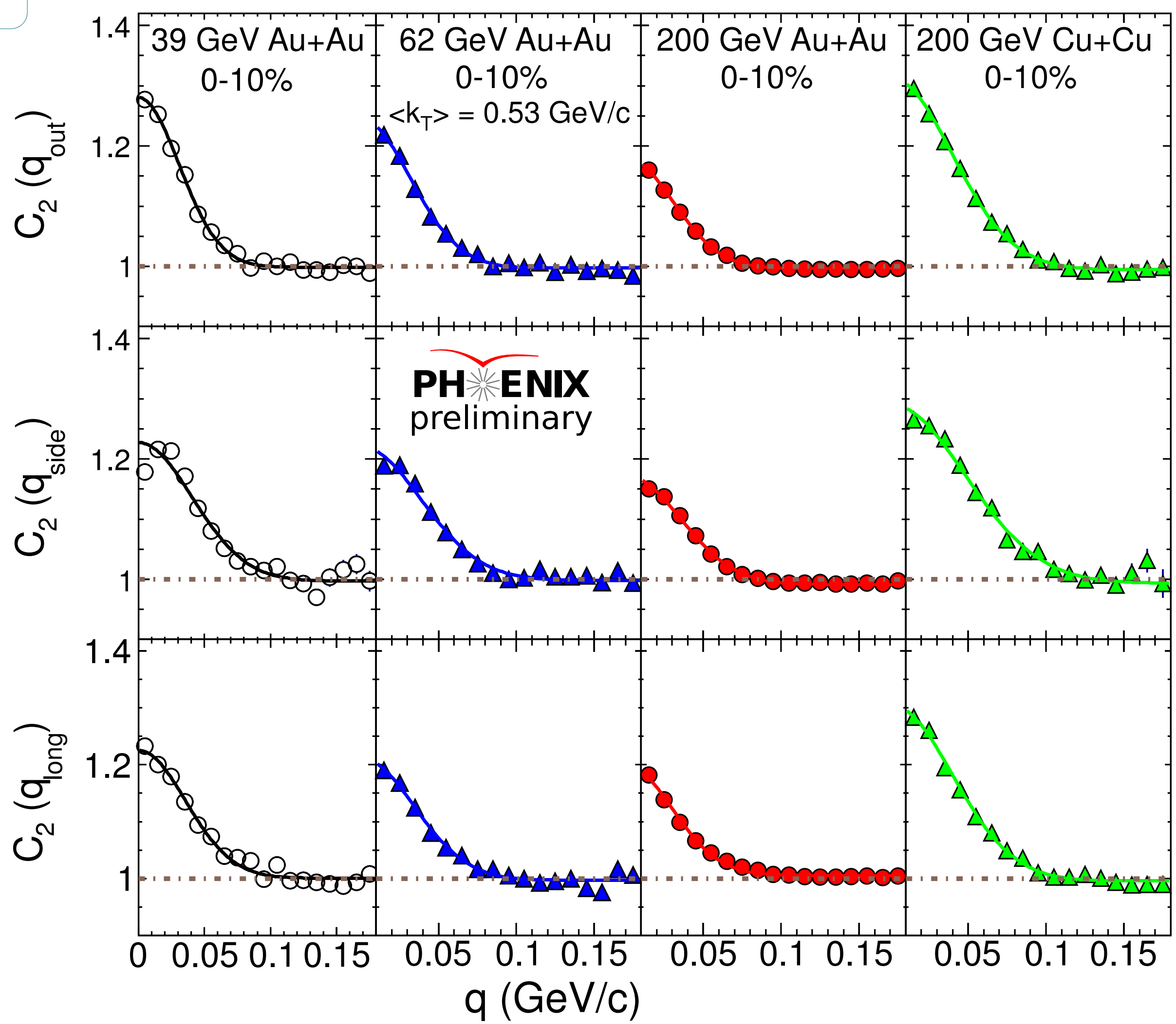

$$C_2(\mathbf{q}) = N[(\lambda(1 + G(\mathbf{q})))F_c + (1-\lambda)],$$

$$G(\mathbf{q}) \cong \exp(-R_{\rm side}^2 q_{\rm side}^2 - R_{\rm out}^2 q_{\rm out}^2 - R_{\rm long}^2 q_{\rm long}^2)$$

HBT Measurements

These data are used to search for non-monotonic patterns as a function of $\sqrt{s_{NN}}$

ALICE -PoS**WPCF2011**

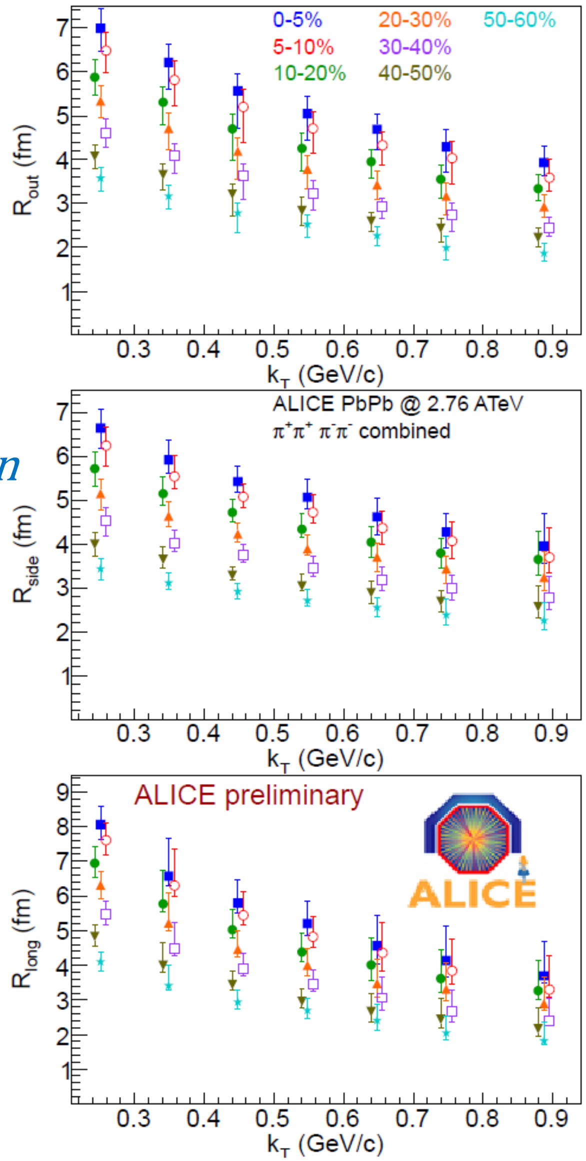

STAR - 1403.4972

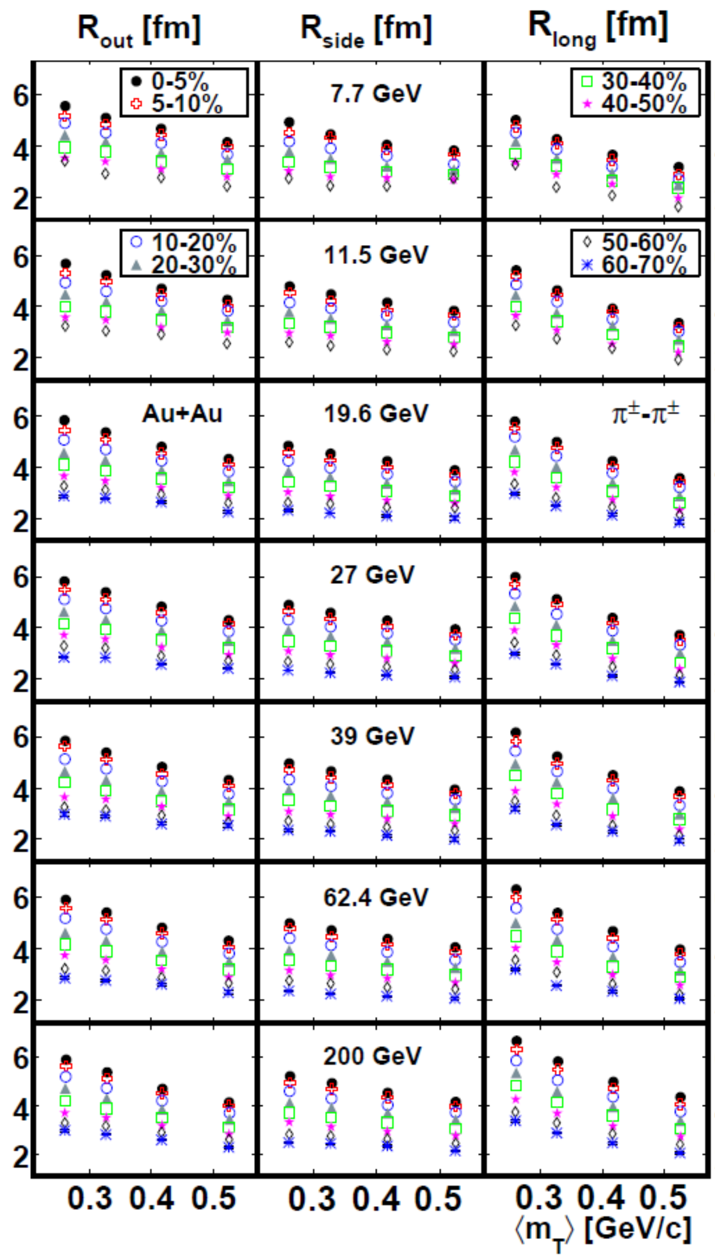

Exquisite data set for study of the HBT excitation function!

$\sqrt{s_{NN}}$ dependence of interferometry signal

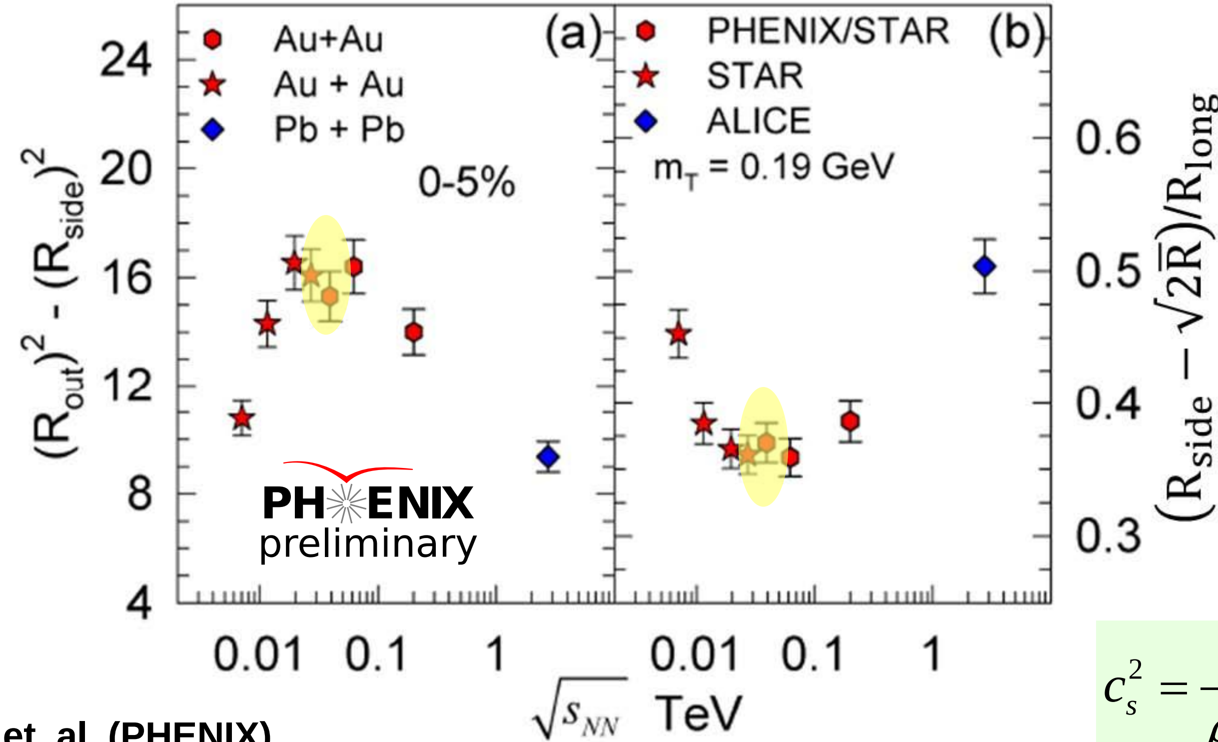

$R_{long} \propto \tau$

$\left(R_{out}^2 - R_{side}^2\right) \propto \Delta\tau^2$

$\left(R_{side} - R_i\right) / R_{long} \propto u$

$R_i = \sqrt{2}\bar{R}$

$c_s^2 = \frac{1}{\rho\kappa_S}$

Adare et. al. (PHENIX)
arXiv:1410.2559

These characteristic non-monotonic patterns signal a suggestive change in the reaction dynamics → Deconfinement Phase transition? CEP?

How to pinpoint the onset of the Deconfinement Phase transition? and the CEP?
→ Study explicit finite-size effects

Finite size scaling and the Crossover Transition

Finite size scaling played an essential role for identification of the crossover transition!

Y. Aoki, et. Al.,Nature , 443, 675(2006).

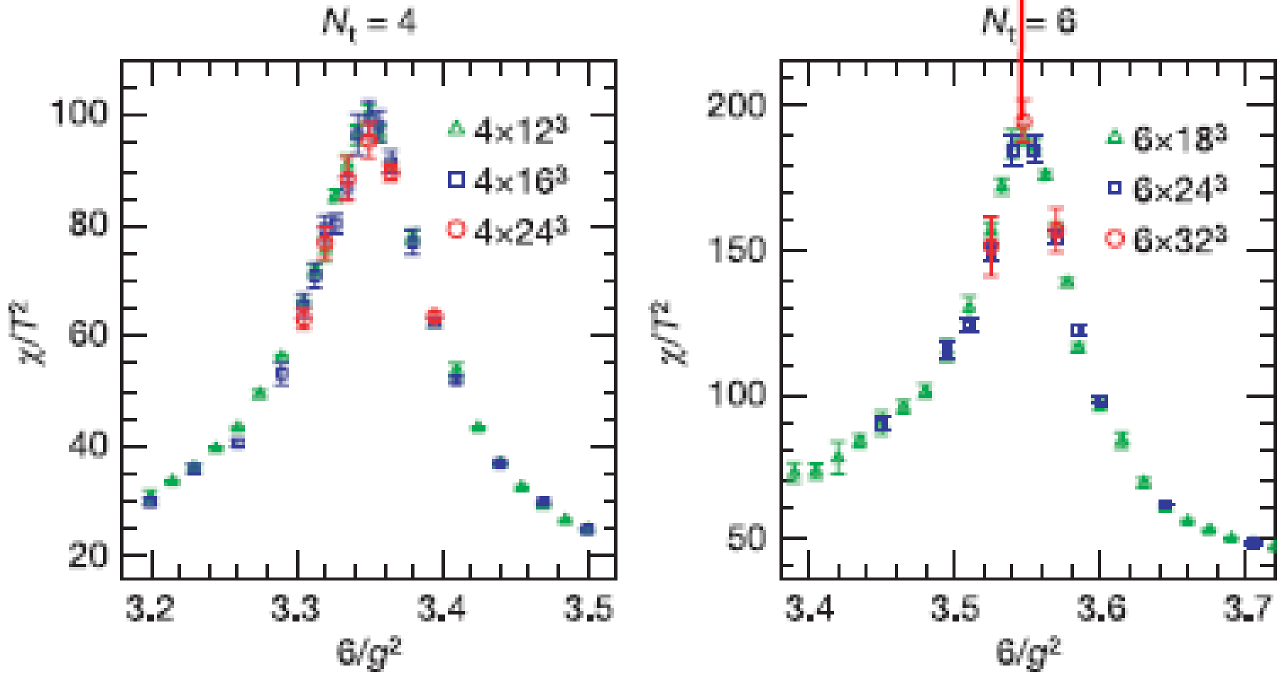

Reminder

Crossover: size independent.

1st-order: finite-size scaling function, and scaling exponent is determined by spatial dimension (integer).

2nd-order: finite-size scaling function $\chi(T,L) = L^{\gamma/\nu} P_\chi(tL^{1/\nu})$

Influence of finite size on the CEP

$$C_P = \left(\frac{\partial H}{\partial T}\right)_P$$

$$\boxed{C_P = \frac{1}{k_B T^2} < (E+PV)^2 > - < E+PV >^2}$$

from partition function

$$\kappa_T \equiv -\frac{1}{V}\left(\frac{\partial V}{\partial P}\right)_T$$

$$V k_B T \kappa_T = \left\langle V^2 \right\rangle - \left\langle V \right\rangle^2$$

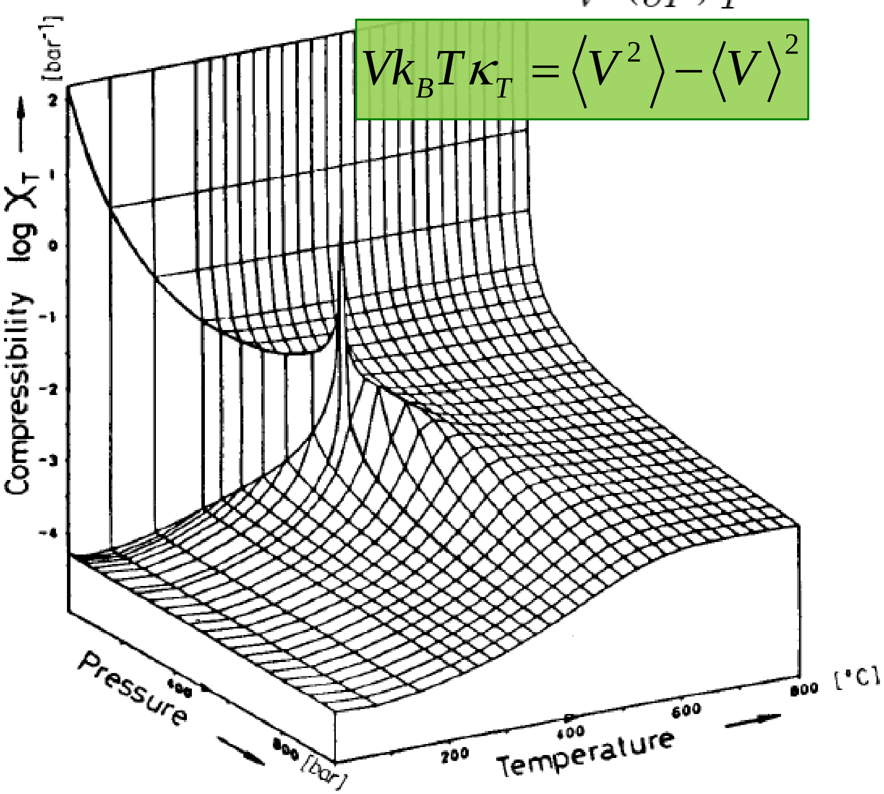

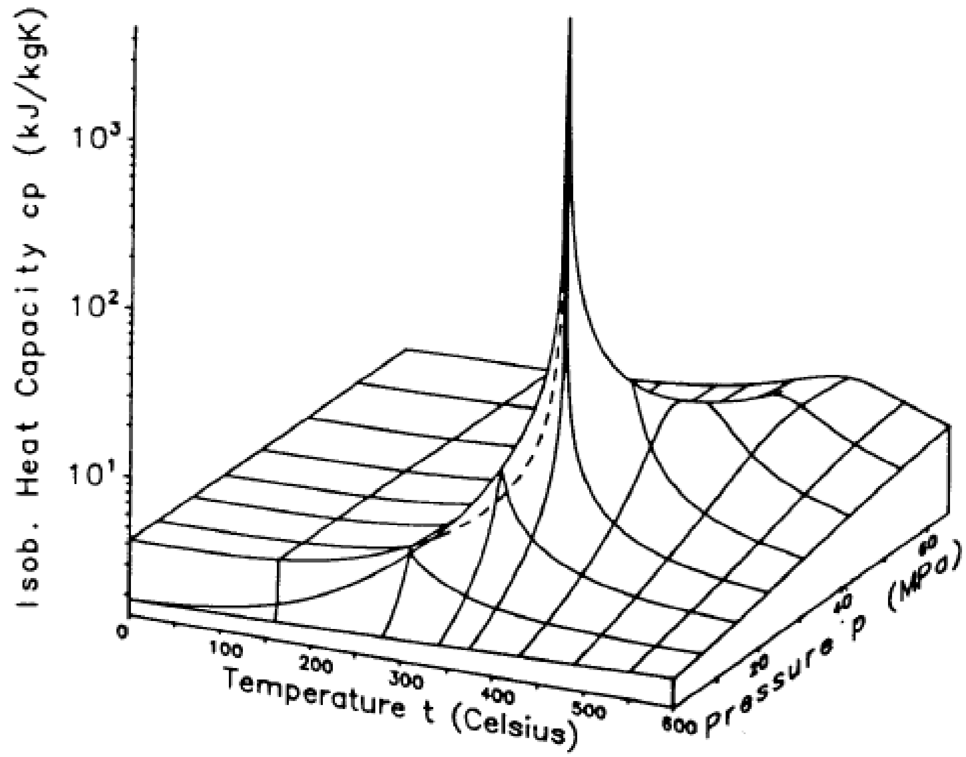

→ Divergences are modulated by the effects of finite-size

The curse of Finite-Size effects

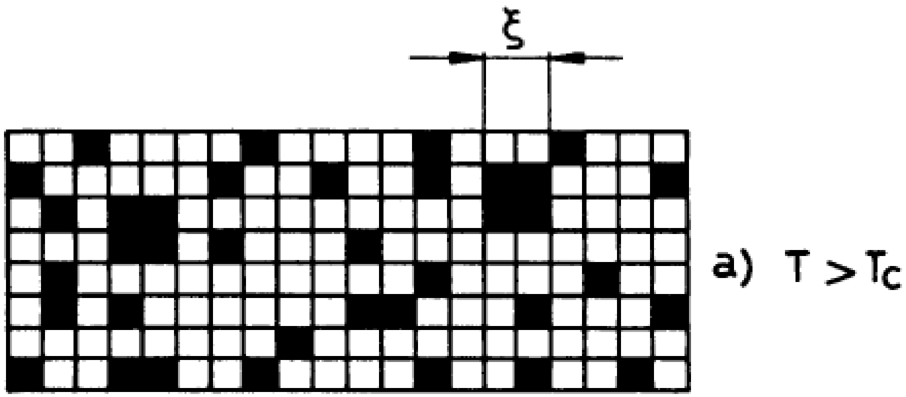

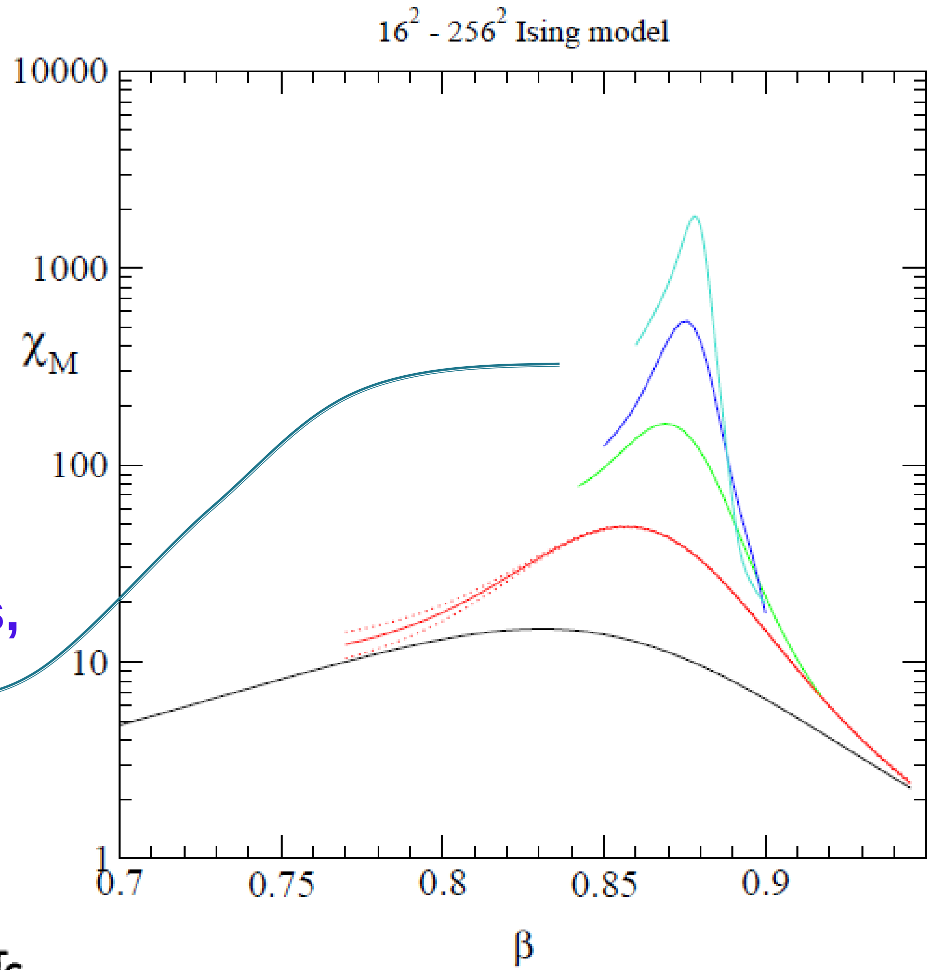

(note change in peak heights, positions & widths)

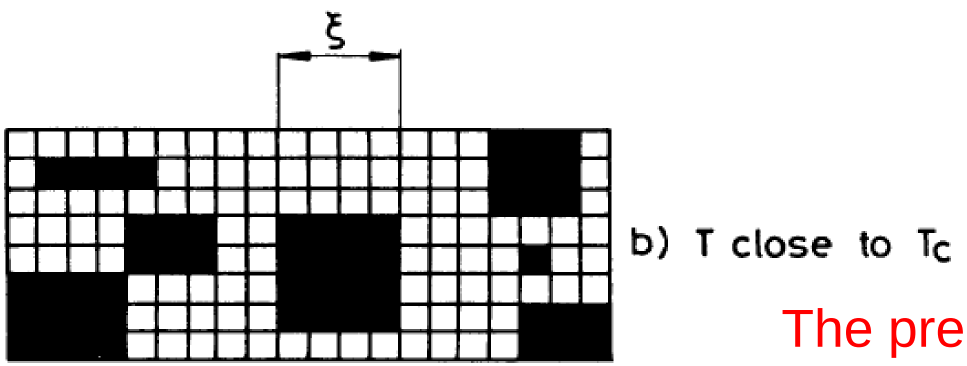

The precise location of the critical end point is influenced by Finite-size effects

→ Only a pseudo-critical point is observed → shifted from the genuine CEP

The curse of Finite-Size effects

E. Fraga et. al.
J. Phys.G 38:085101, 2011

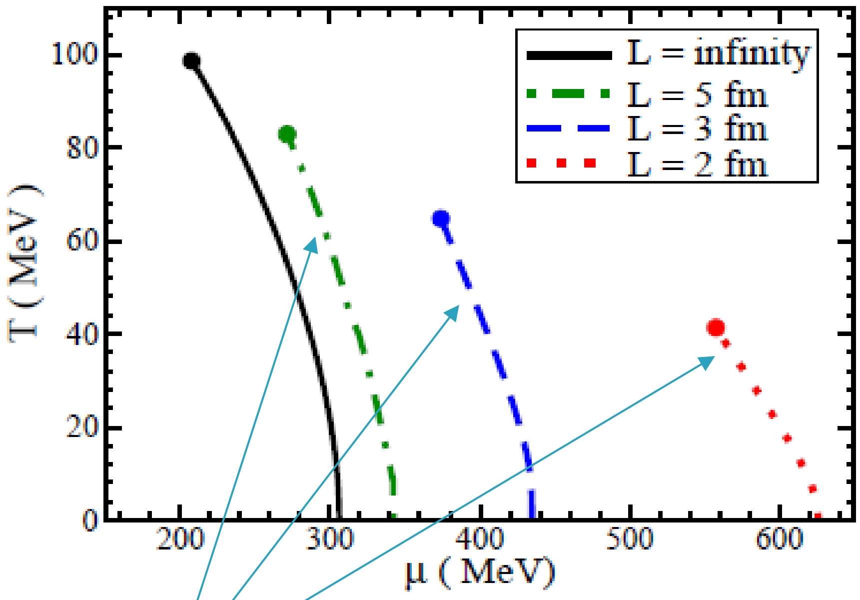

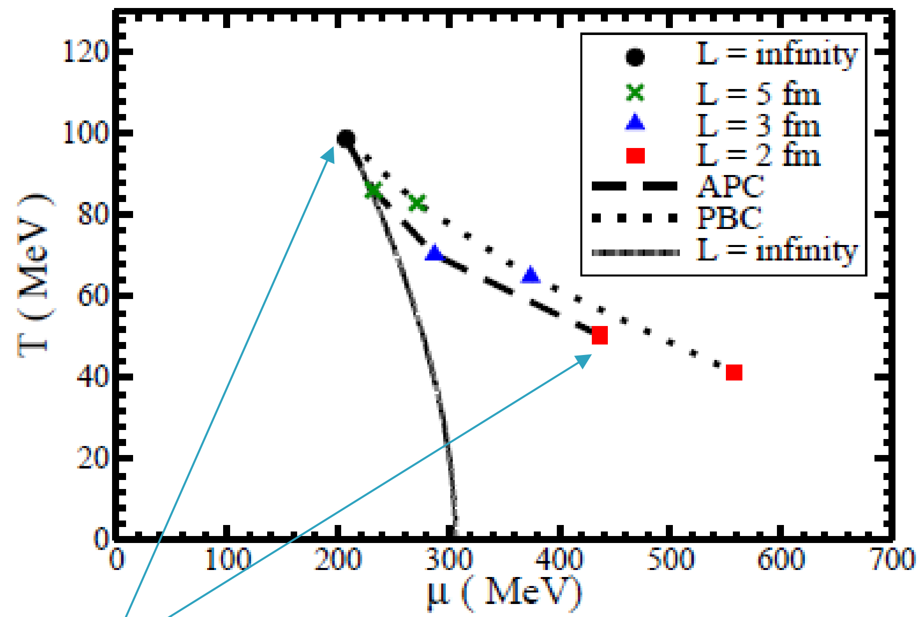

Displacement of pseudo-first-order transition lines and CEP due to finite-size

Finite-size shifts both the pseudo-critical endpoint and the transition line

→ *Even flawless measurements **Can** **Not** give the precise location of the CEP in finite-size systems*

The Blessings of Finite-Size

$$\chi_T^{\max}(V) \sim L^{\gamma/\nu},$$
$$\delta T(V) \sim L^{-\frac{1}{\nu}},$$
$$\tau_T(V) \sim T^{\mathrm{cep}}(V) - T^{\mathrm{cep}}(\infty) \sim L^{-\frac{1}{\nu}},$$

$$c(T,L) = L^{g/n} P_c(tL^{1/n}) \qquad t = \frac{T - T_c}{T_c}$$

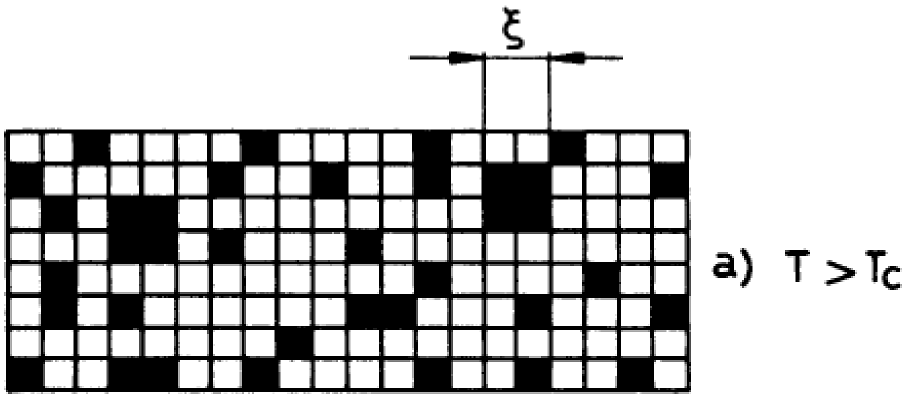

(note change in peak heights, positions & widths)

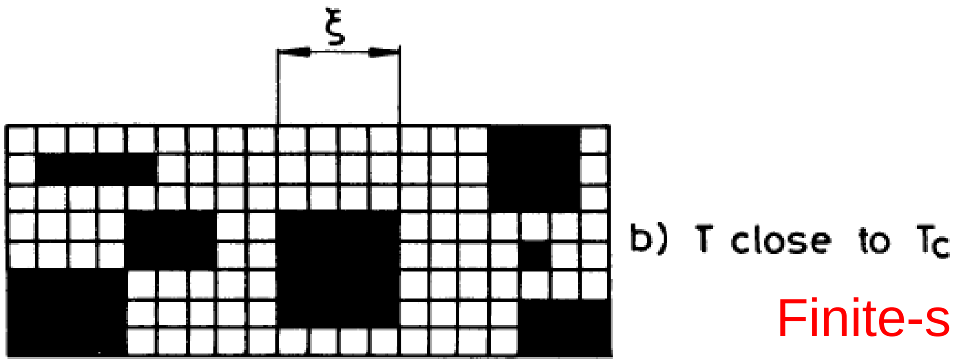

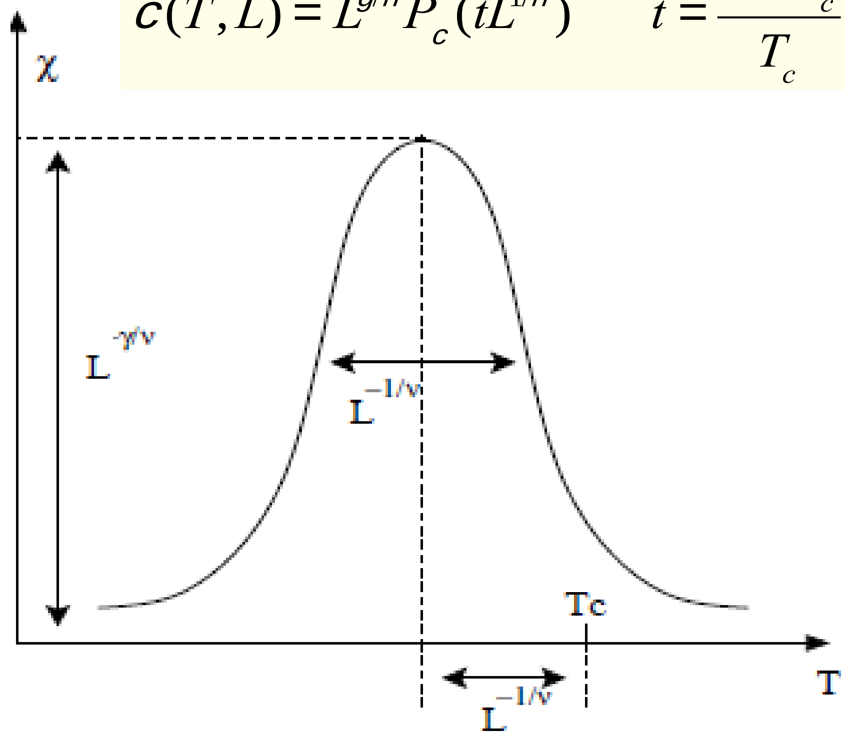

Finite-size effects are specific → allow access to CEP location and the critical exponents

→ **L scales the volume**

The blessings of Finite-Size Scaling

$$\chi_T^{\max}(V) \sim L^{\gamma/\nu},$$
$$\delta T(V) \sim L^{-\frac{1}{\nu}},$$
$$\tau_T(V) \sim T^{\text{cep}}(V) - T^{\text{cep}}(\infty) \sim L^{-\frac{1}{\nu}},$$

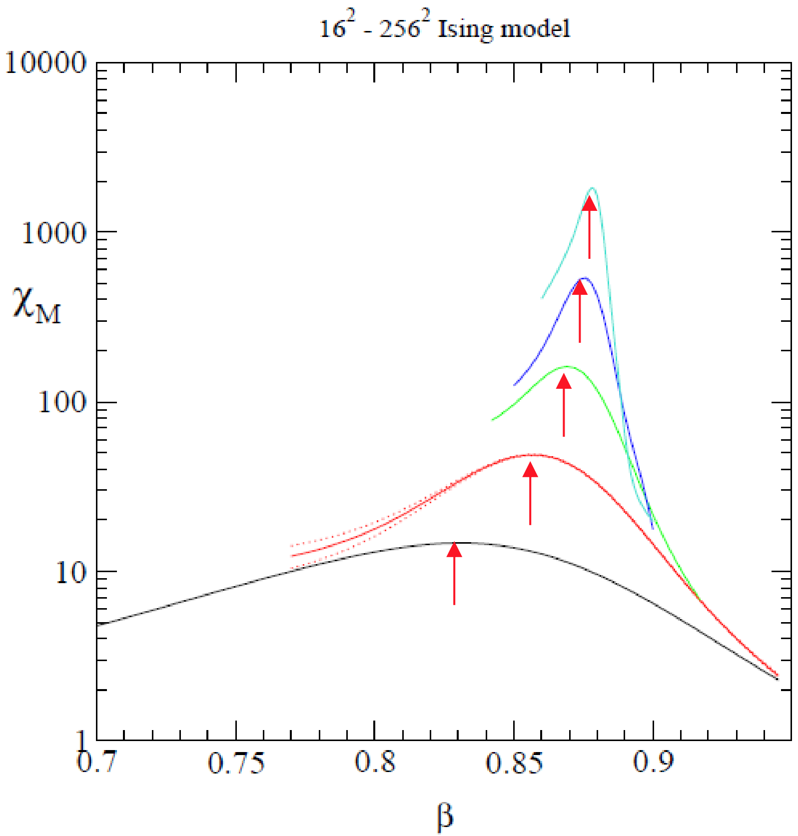

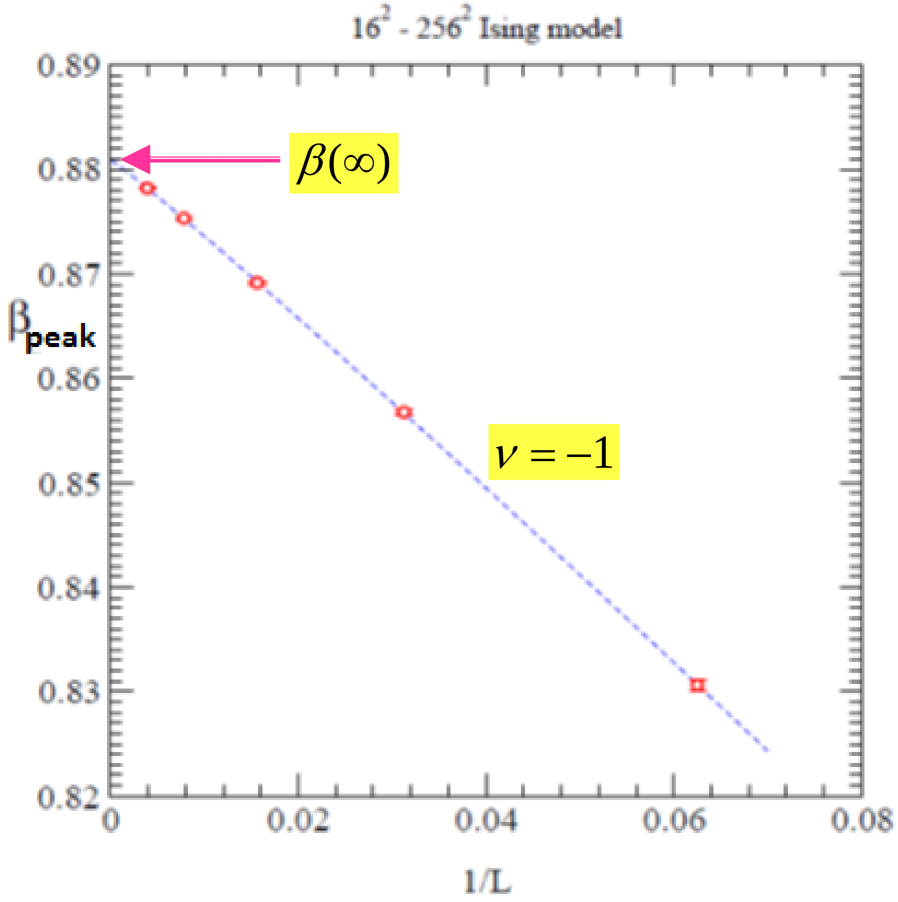

Finite-Size Scaling can be used to extract the location of the deconfinement transition and the critical exponents

The blessings of Finite-Size Scaling

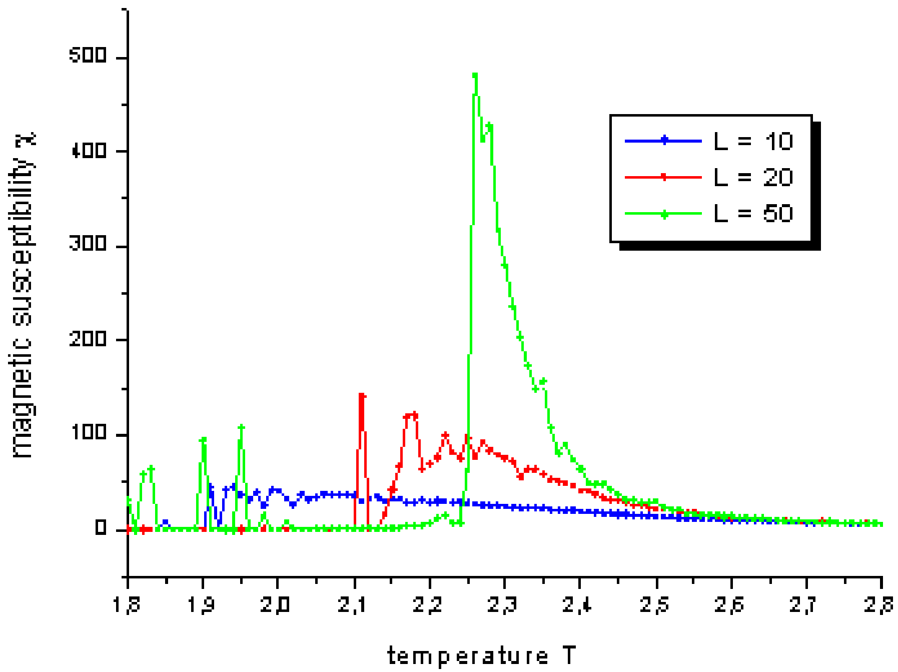

$$\chi_T^{\max}(V) \sim L^{\gamma/\nu},$$
$$\delta T(V) \sim L^{-\frac{1}{\nu}},$$
$$\tau_T(V) \sim T^{\rm cep}(V) - T^{\rm cep}(\infty) \sim L^{-\frac{1}{\nu}},$$

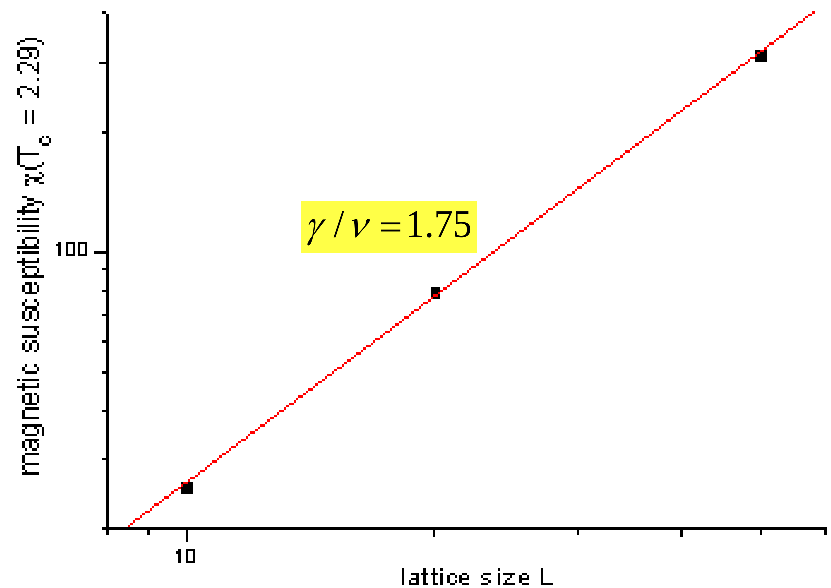

Finite-Size Scaling can be used to extract the location of the deconfinement transition and the critical exponents

Critical exponents reflect the universality class and the order of the phase transition

The blessings of Finite-Size Scaling

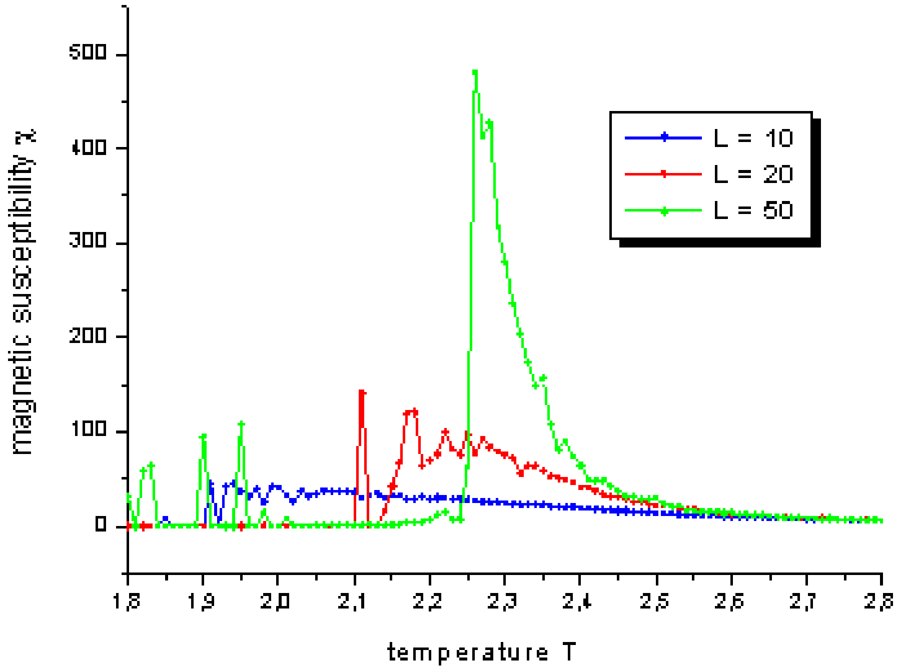

$$L^{-\gamma/\nu} \times \chi \;\; \text{vs.} \;\; \mathrm{L}^{1/\nu} \times t_T$$
$$t_T = (T - T^{\mathrm{cep}}) / T^{\mathrm{cep}}$$

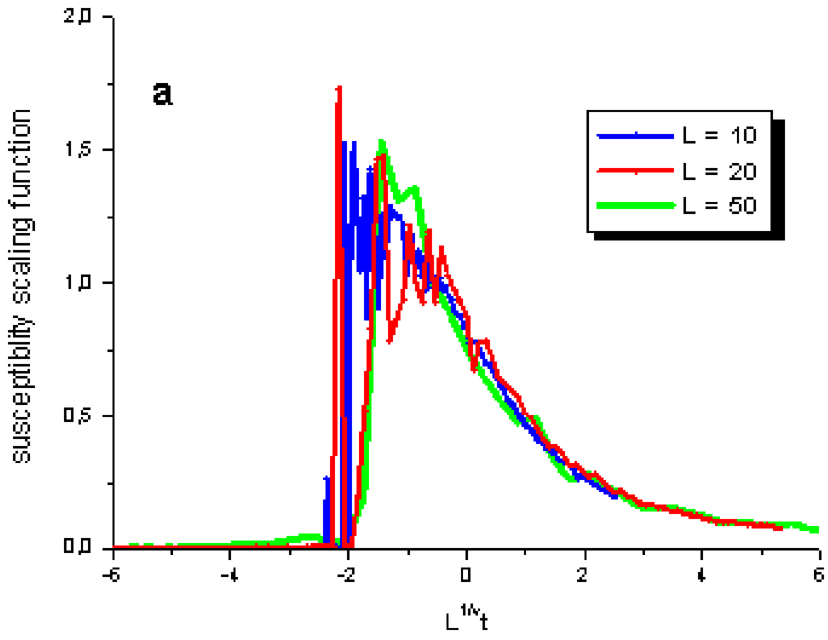

Cross Check

Extracted critical exponents and CEP values should lead to data collapse onto a single curve

Essential Message

Search for & utilize finite-size scaling!

Size dependence of HBT excitation functions

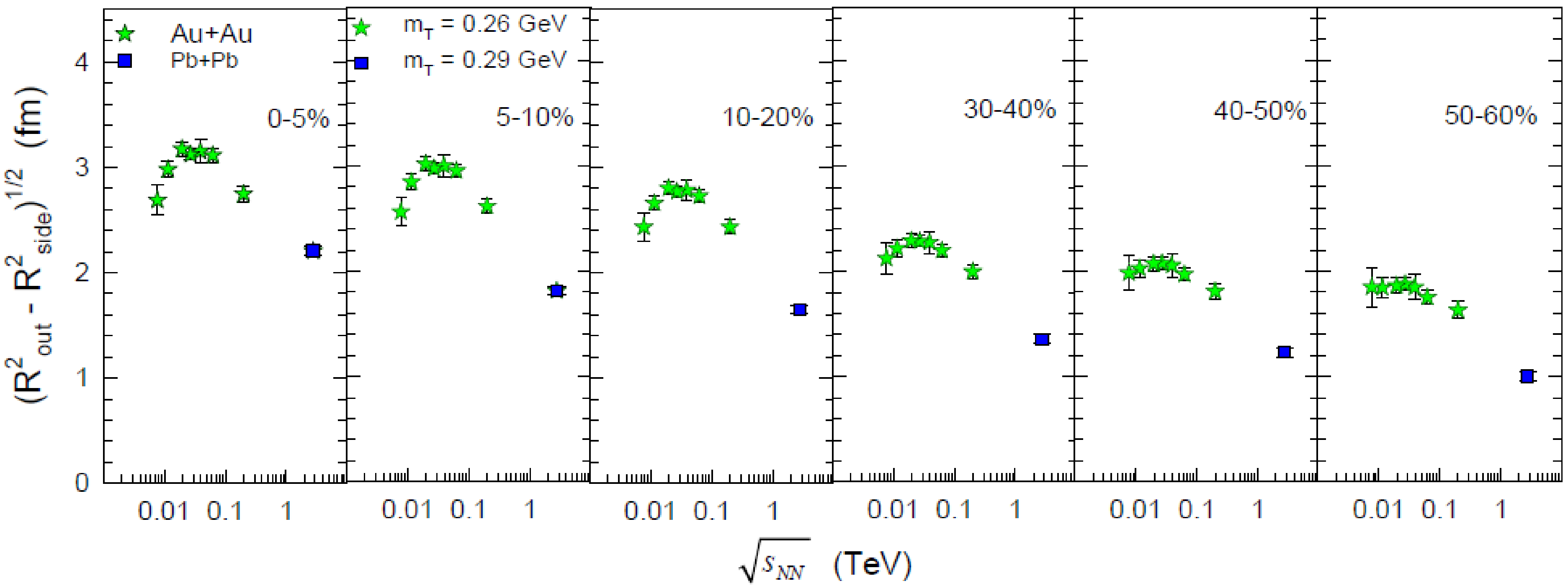

I. Max values decrease with decrease in system size
II. Peaks shift with decreasing system size
III. Widths increase with decreasing system size

These characteristic patterns signal the effects of finite-size

Size dependence of the excitation functions

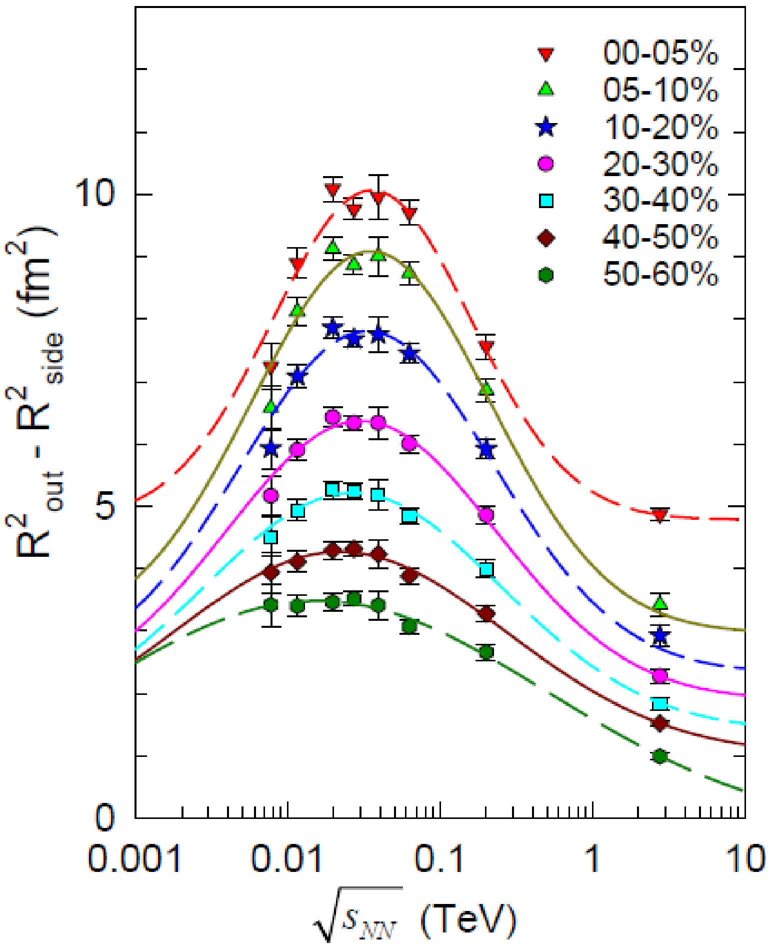

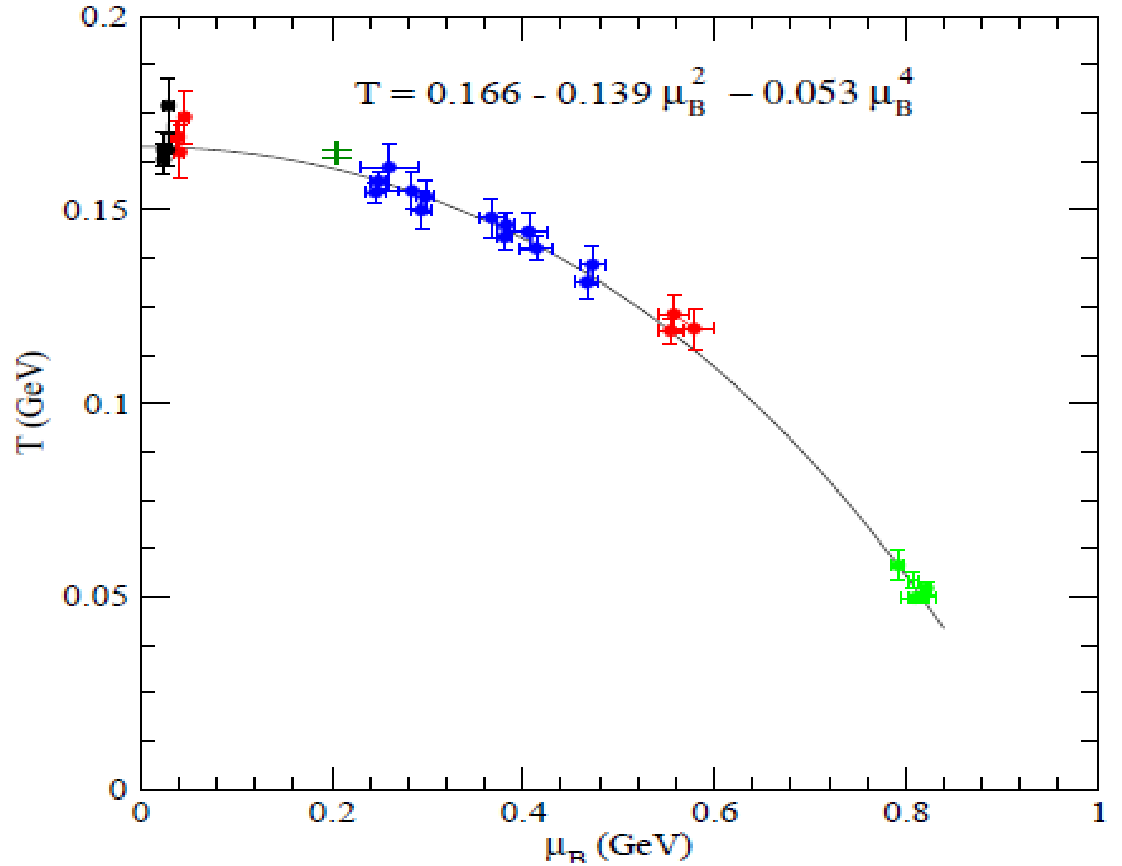

II. Parameterize distance to the CEP by $\sqrt{s_{NN}}$

$$\tau_s = \left(\sqrt{s} - \sqrt{s_{CEP}}\right)/\sqrt{s_{CEP}}$$

characteristic patterns signal the effects of finite-size

→ Perform Finite-Size Scaling analysis with characteristic initial transverse size $\bar{R}$

Initial Geometric Transverse Size

Geometry

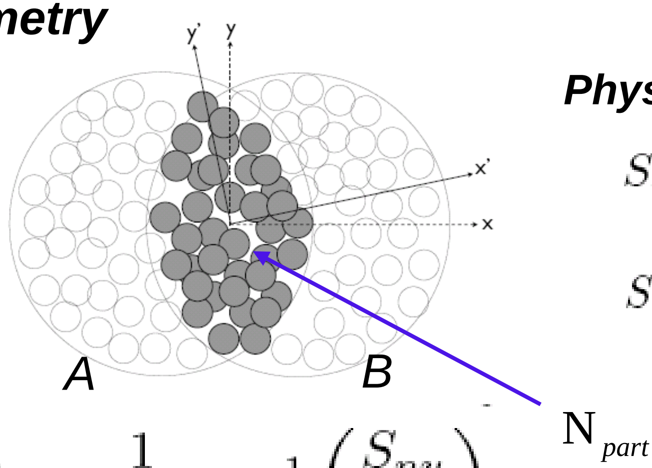

Phys. Rev. C 81, 061901(R) (2010)

$$S_{nx} \equiv S_n \cos(n\Psi_n^*) = \int d\mathbf{r}_\perp \rho_s(\mathbf{r}_\perp)\omega(\mathbf{r}_\perp)\cos(n\phi)$$

$$S_{ny} \equiv S_n \sin(n\Psi_n^*) = \int d\mathbf{r}_\perp \rho_s(\mathbf{r}_\perp)\omega(\mathbf{r}_\perp)\sin(n\phi),$$

$$\Psi_n^* = \frac{1}{n}\tan^{-1}\left(\frac{S_{ny}}{S_{nx}}\right)$$

$$\varepsilon_n = \left\langle \cos n\left(\phi - \psi_n^*\right)\right\rangle$$

$$\boxed{\frac{1}{\bar{R}} = \sqrt{\left(\frac{1}{\sigma_x^2} + \frac{1}{\sigma_y^2}\right)}}$$

arXiv:1203.3605

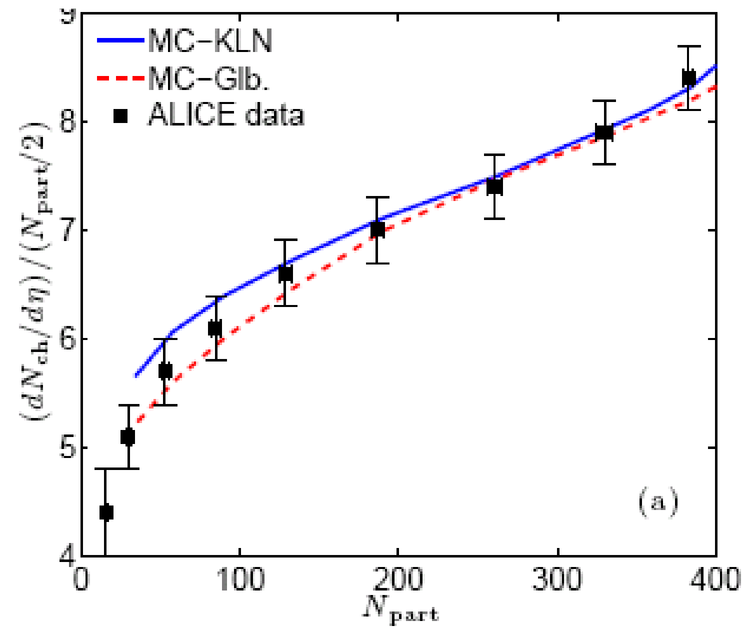

σ_x & σ_y → RMS widths of density distribution

- ***Geometric fluctuations included***
- ***Geometric quantities constrained by multiplicity density.***

Acoustic Scaling of HBT Radii

$$R_{out}, R_{side}, R_{long} \propto \bar{R}$$

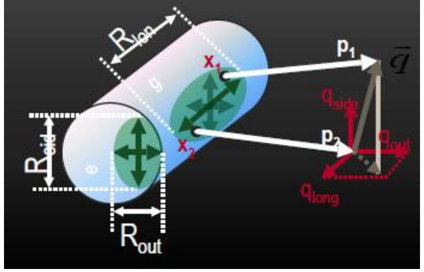

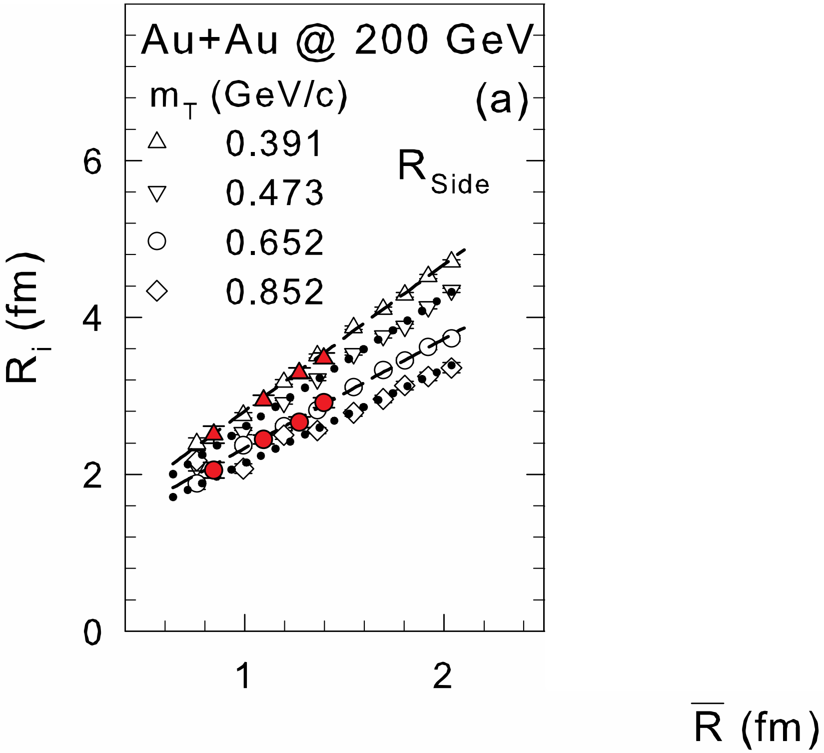

- $\bar{R}$ ***and m$_T$ scaling of the full RHIC and LHC data sets***
- ***The centrality and m$_T$ dependent data scale to a single curve for each radii.***
- $R_{out}, R_{side}, R_{long} \propto \bar{R}$

Finite – Size Scaling Analysis

(only two exponents are independent)

$$\chi_T^{\max}(V) \sim L^{\gamma/\nu},$$
$$\delta T(V) \sim L^{-\frac{1}{\nu}},$$
$$\tau_T(V) \sim T^{\rm cep}(V) - T^{\rm cep}(\infty) \sim L^{-\frac{1}{\nu}},$$

$$\boxed{\begin{aligned}(R^2_{\rm out} - R^2_{\rm side})^{\max} &\propto \bar{R}^{\gamma/\nu},\\ \sqrt{s_{NN}}(V) &= \sqrt{s_{NN}}(\infty) - k \times \bar{R}^{-\frac{1}{\nu}},\end{aligned}}$$

Note that $\left(\mu_B^f, T^f\right)$ *is not strongly dependent on V*

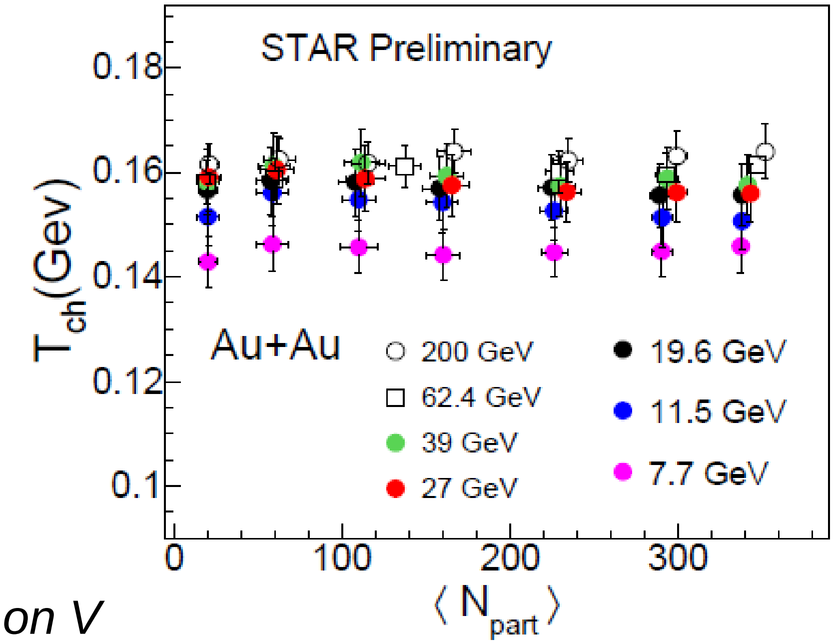

- ✓ ***Locate*** (T, μ_B) ***position of deconfinement transition and extract critical exponents***
- ✓ ***Determine Universality Class***
- ✓ ***Determine order of the phase transition to identify CEP***

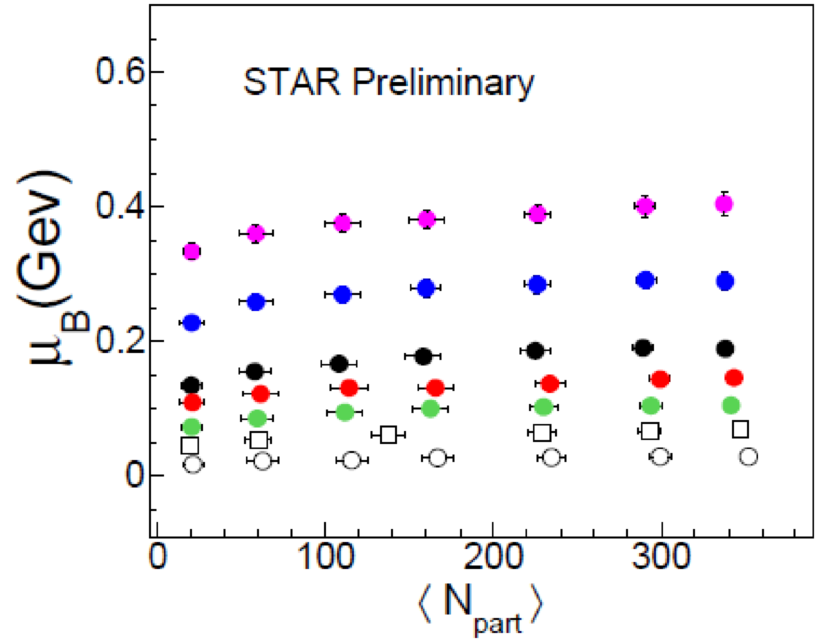

Finite – Size Scaling

$$(R_{\rm out}^2 - R_{\rm side}^2)^{\rm max} \propto \bar{R}^{\gamma/\nu},$$

$$\sqrt{s_{NN}}(V) = \sqrt{s_{NN}}(\infty) - k \times \bar{R}^{-\frac{1}{\nu}},$$

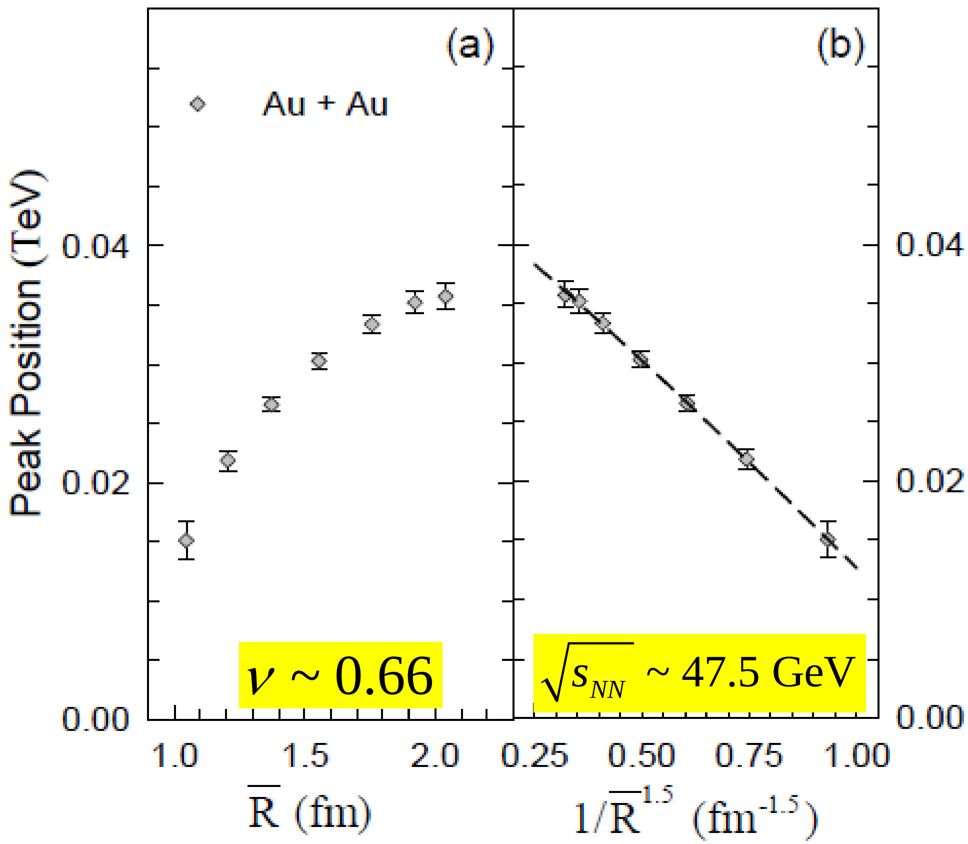

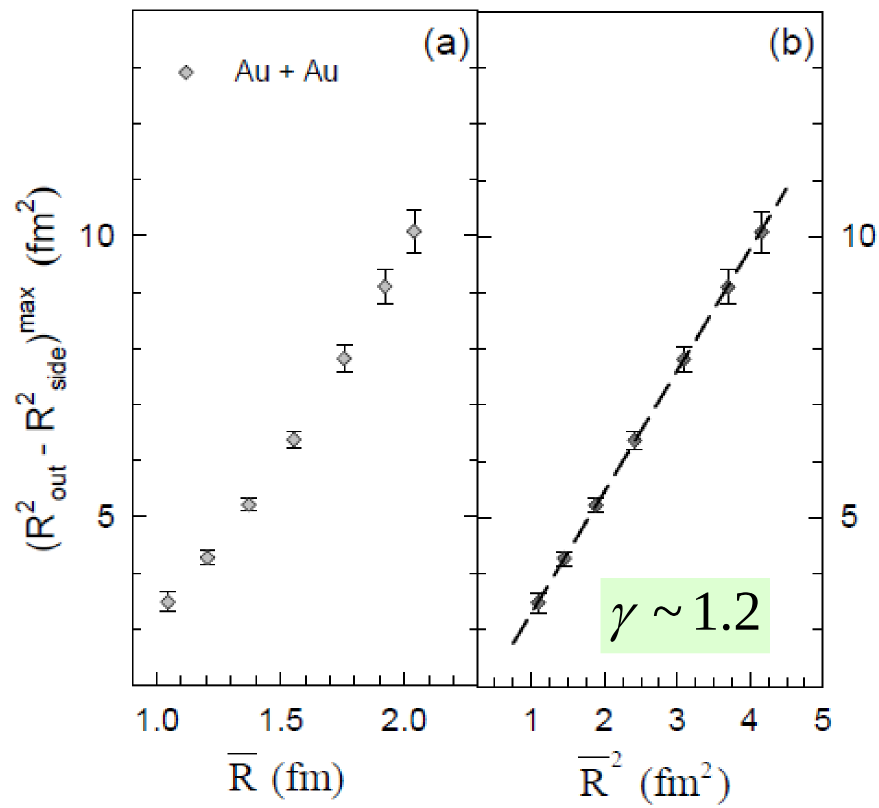

Similar result from analysis of the widths

Finite-Size Scaling gives

- ***Critical exponents compatible with 3D Ising model universality class***
- ***2nd order phase transition for CEP***

$T^{cep} \approx 165$ MeV, $\mu_B^{cep} \approx 95$ MeV

(Chemical freeze-out systematics)

Closurer test for FSS

- ***2nd order phase transition***
- ***3D Ising Model Universality class for CEP***

$\nu \sim 0.66$ $\gamma \sim 1.2$

T^{cep} □ 165 MeV, μ_B^{cep} □ 95 MeV

Finite-Size Scaling validation

$$\bar{R}^{-\gamma/\nu} \times (R^2_{\rm out} - R^2_{\rm side}) \text{ vs. } \bar{R}^{1/\nu} \times t_T,$$
$$\bar{R}^{-\gamma/\nu} \times (R^2_{\rm out} - R^2_{\rm side}) \text{ vs. } \bar{R}^{1/\nu} \times t_{\mu_B},$$
$$t_T = (T - T^{\rm cep})/T^{\rm cep}$$
$$t_{\mu_B} = (\mu_B - \mu_B^{\rm cep})/\mu_B^{\rm cep}$$

Finite-Size Scaling validated

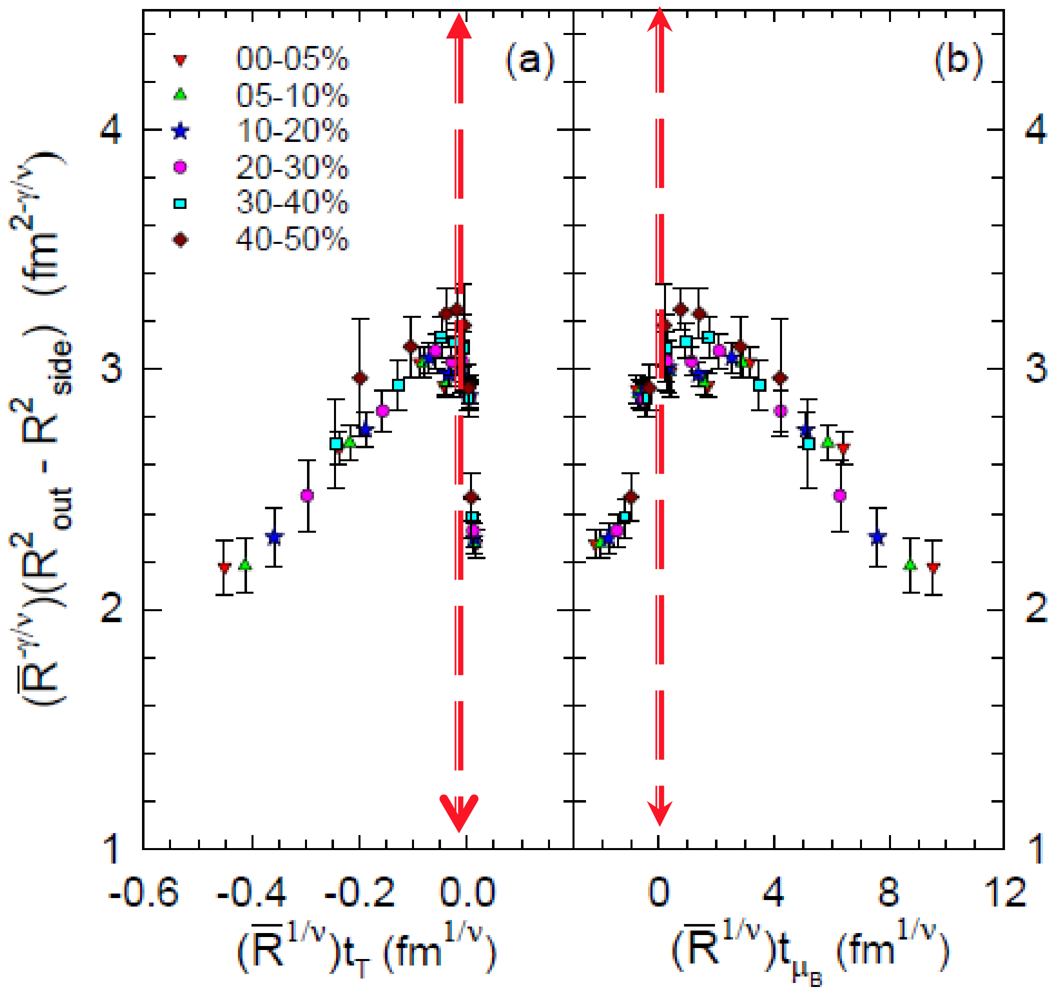

*****A further confirmation of the location of the CEP*****

FAQ

What about finite time effects?

$$\xi \sim \tau^{1/z}$$

Finite – time Scaling

➢ ***2^{nd} order phase transition With critical exponents***

$\nu \sim 0.66$ $\gamma \sim 1.2$

T^{cep} □ 165 MeV, μ_B^{cep} □ 95 MeV

$\xi \sim \tau^{1/z}$

At time τ when T is near T_c

DFSS ansatz

$$\chi\left(L,T,\tau\right) = L^{\gamma/\nu} f\left(L^{1/\nu} t_T, \tau L^{-z}\right)$$

For $T = T_c$

$$\chi\left(L,T_c,\tau\right) = L^{\gamma/\nu} f\left(\tau L^{-z}\right)$$

$R_{long} \propto \tau$

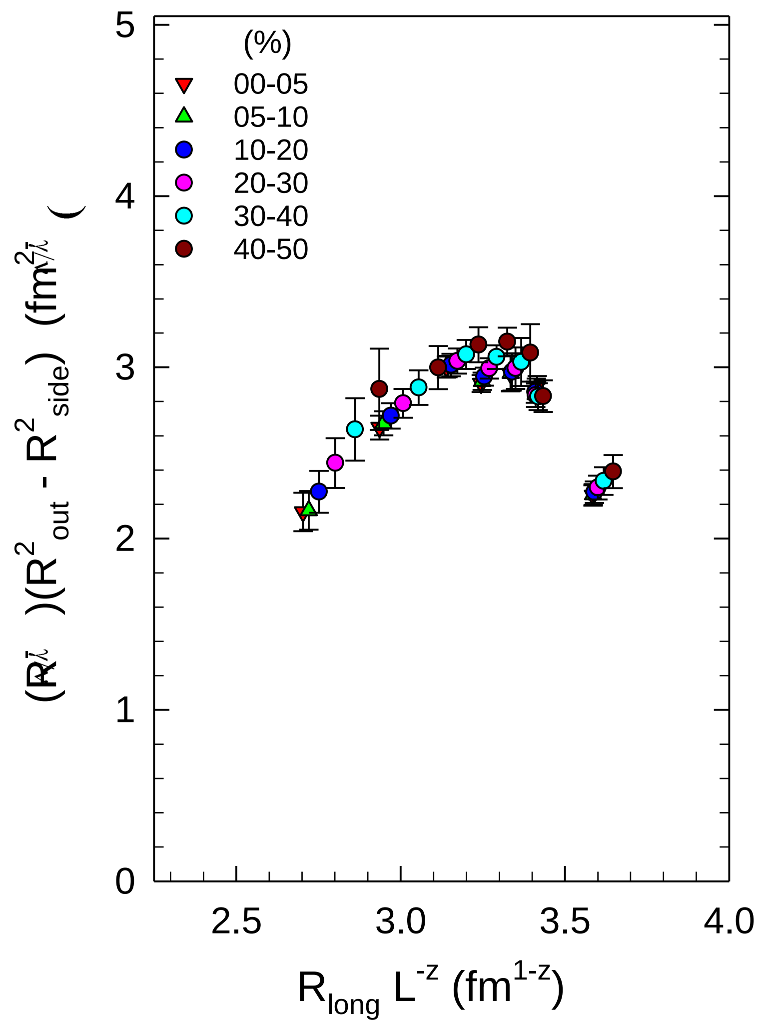

*****A first estimate of the dynamic critical exponent*****

Epilogue

- *Strong experimental indication for the CEP and its location*

Finite-Size Analysis with $(R^2_{out}\text{-}R^2_{side})$

- ***2^{nd} order phase transition***
- ***3D Ising Model Universality class for CEP***

$\nu \sim 0.66$

$\gamma \sim 1.2$

$T^{cep} \sim 165\ \text{MeV},\ \mu_B^{cep} \sim 95\ \text{MeV}$

✓ *Landmark validated*
✓ *Crossover validated*
✓ *Deconfinement Validated*
✓ *$m_s > m_{s3}$*
✓ *Other implications!*

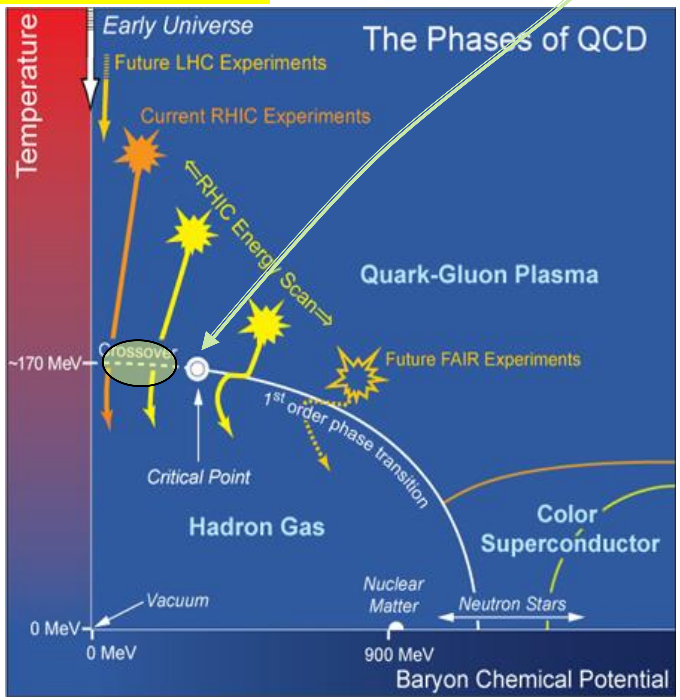

Additional Data from RHIC (BES-II) together with mature and sophisticated theoretical modeling still required!

Lots of work still to be done to fully chart the QCD phase diagram!!

End

Experimental Overview of RHIC BES

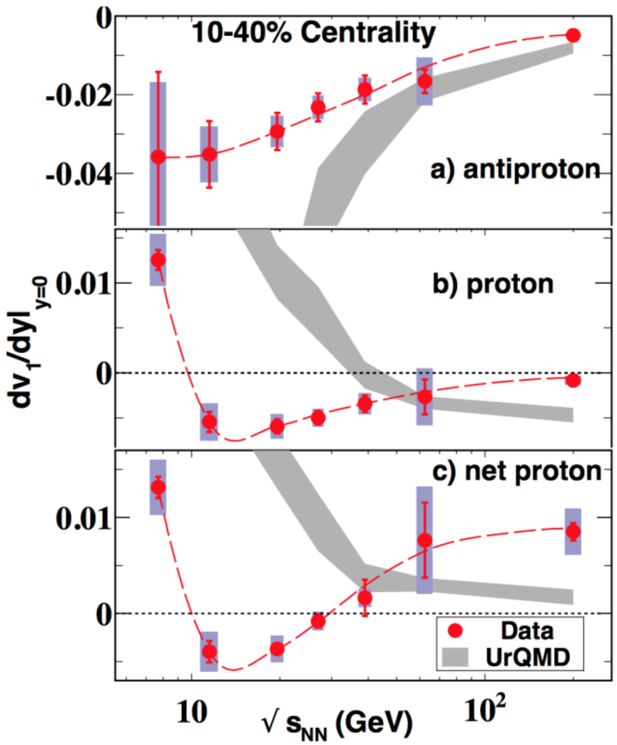

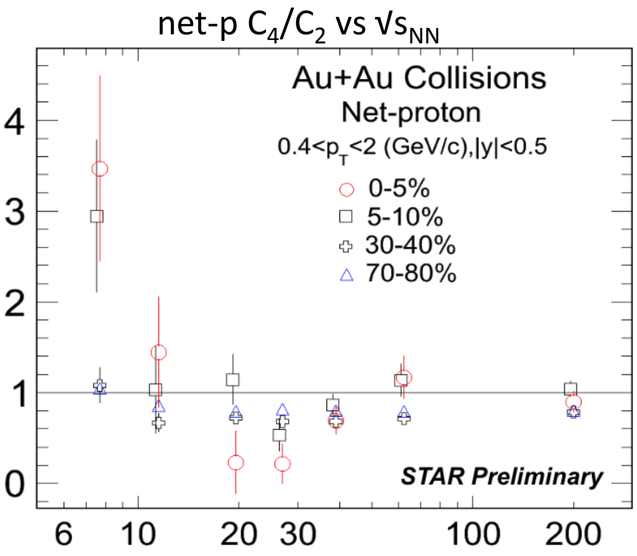

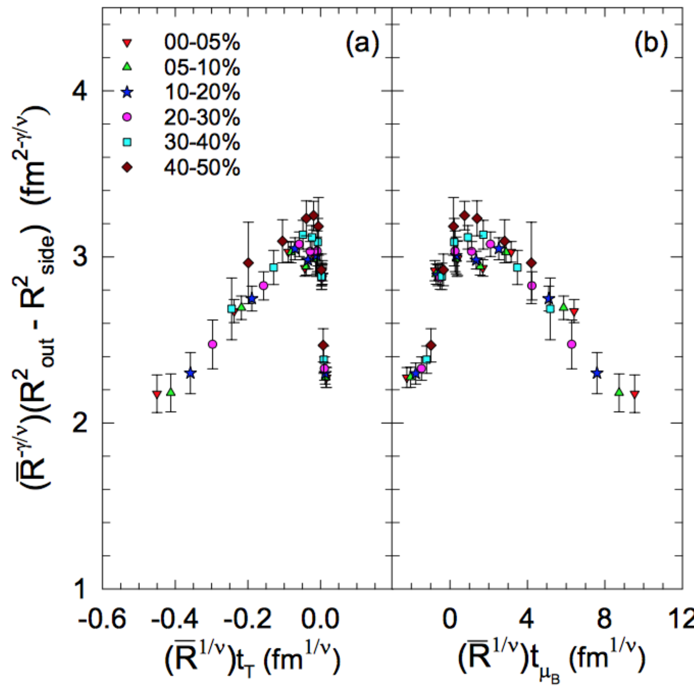

BNL-Bi-CCNU: Phys. Rev. Lett. 113 (2014) 072001

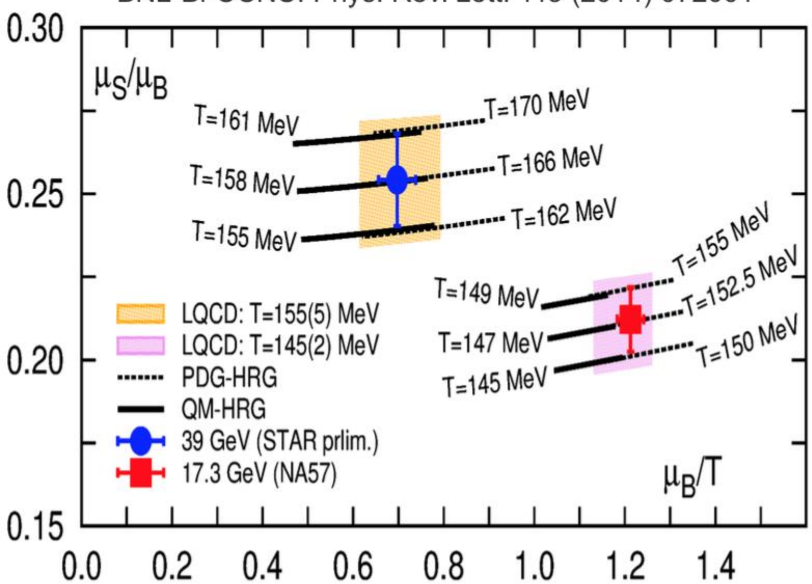

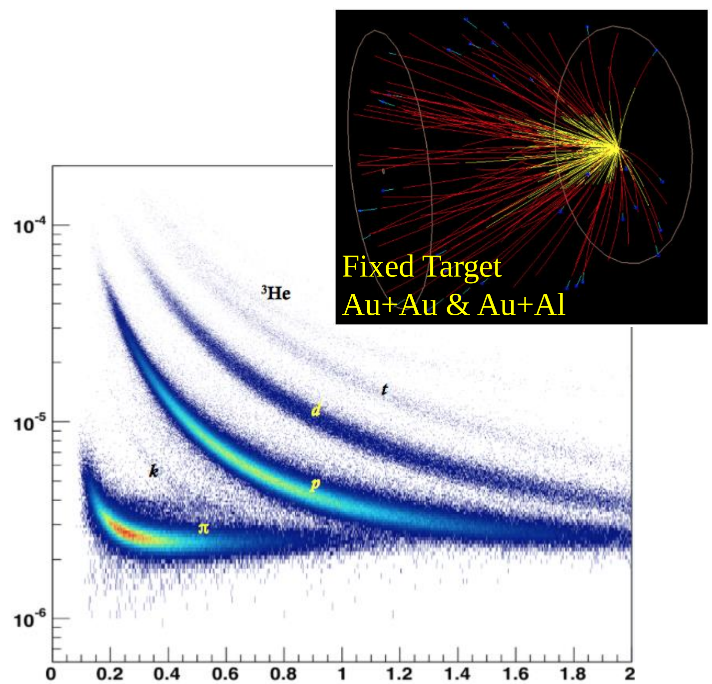

Experimental Overview of RHIC BES

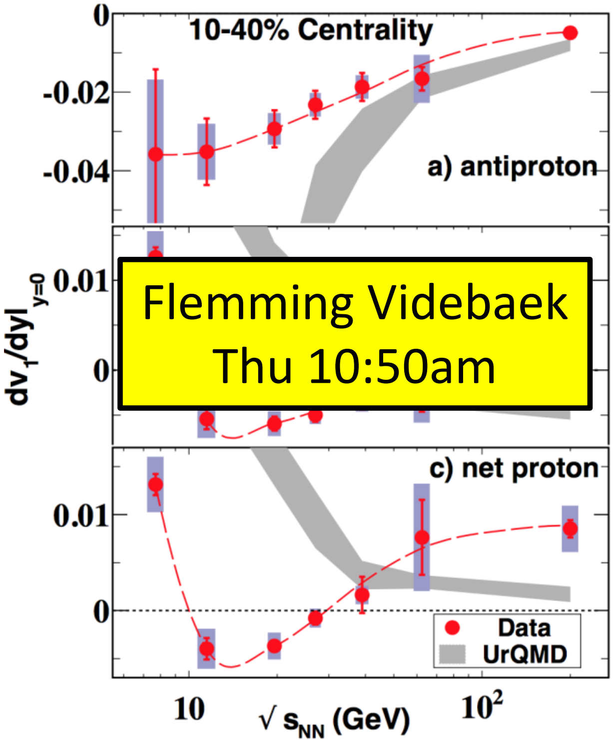

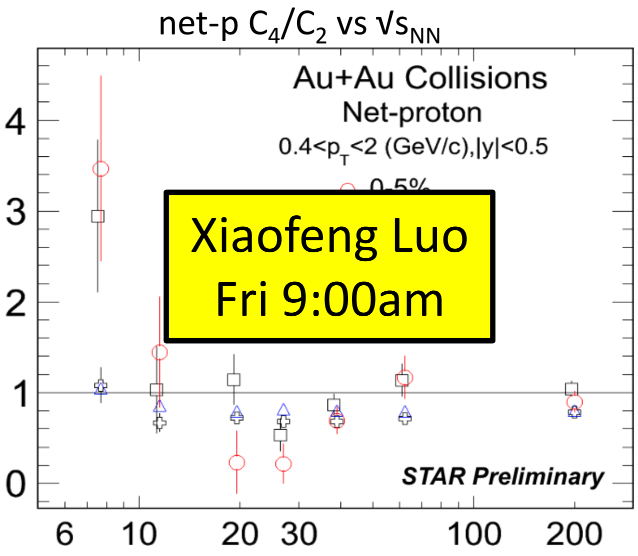

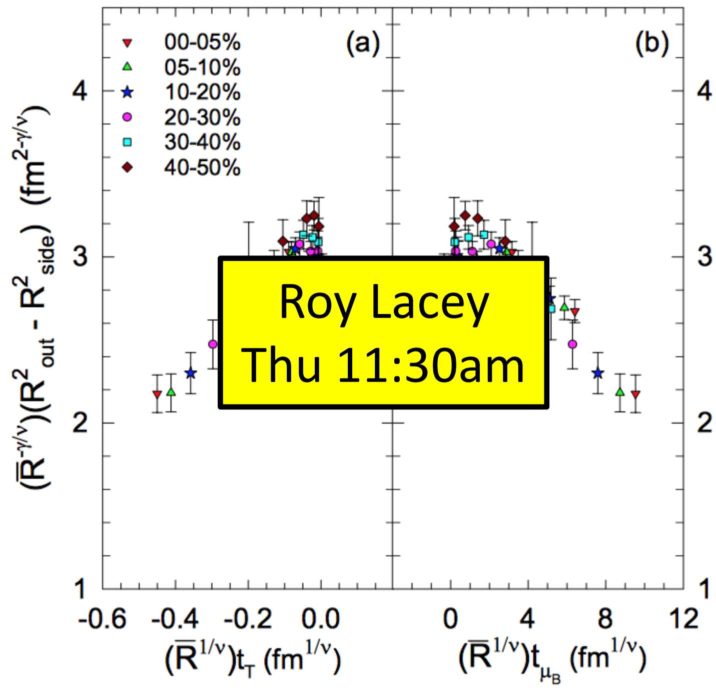

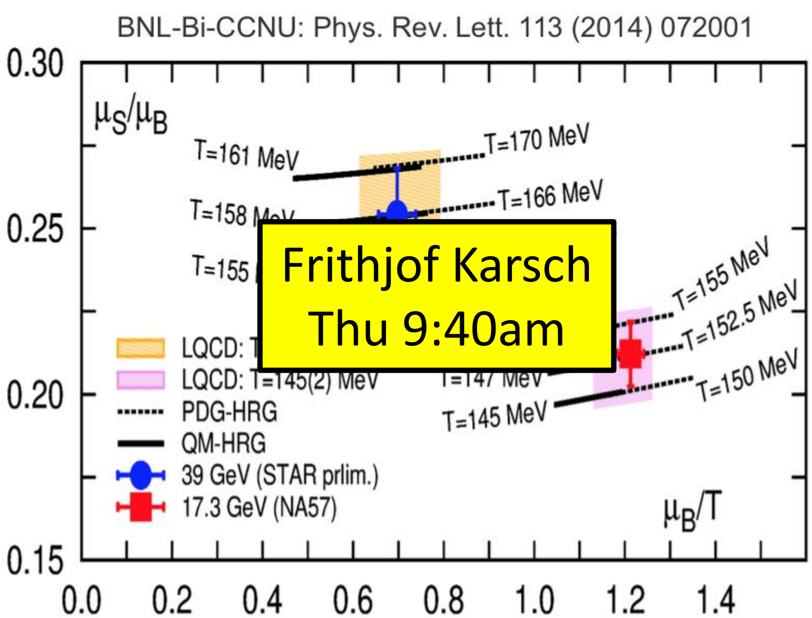

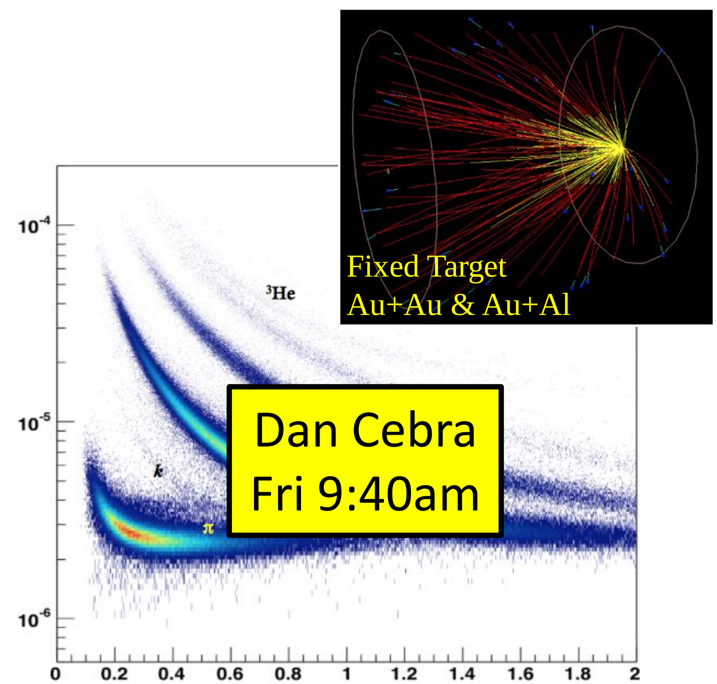

Multiplicity Cumulants & Correlations

W.J. Llope
Wayne State University

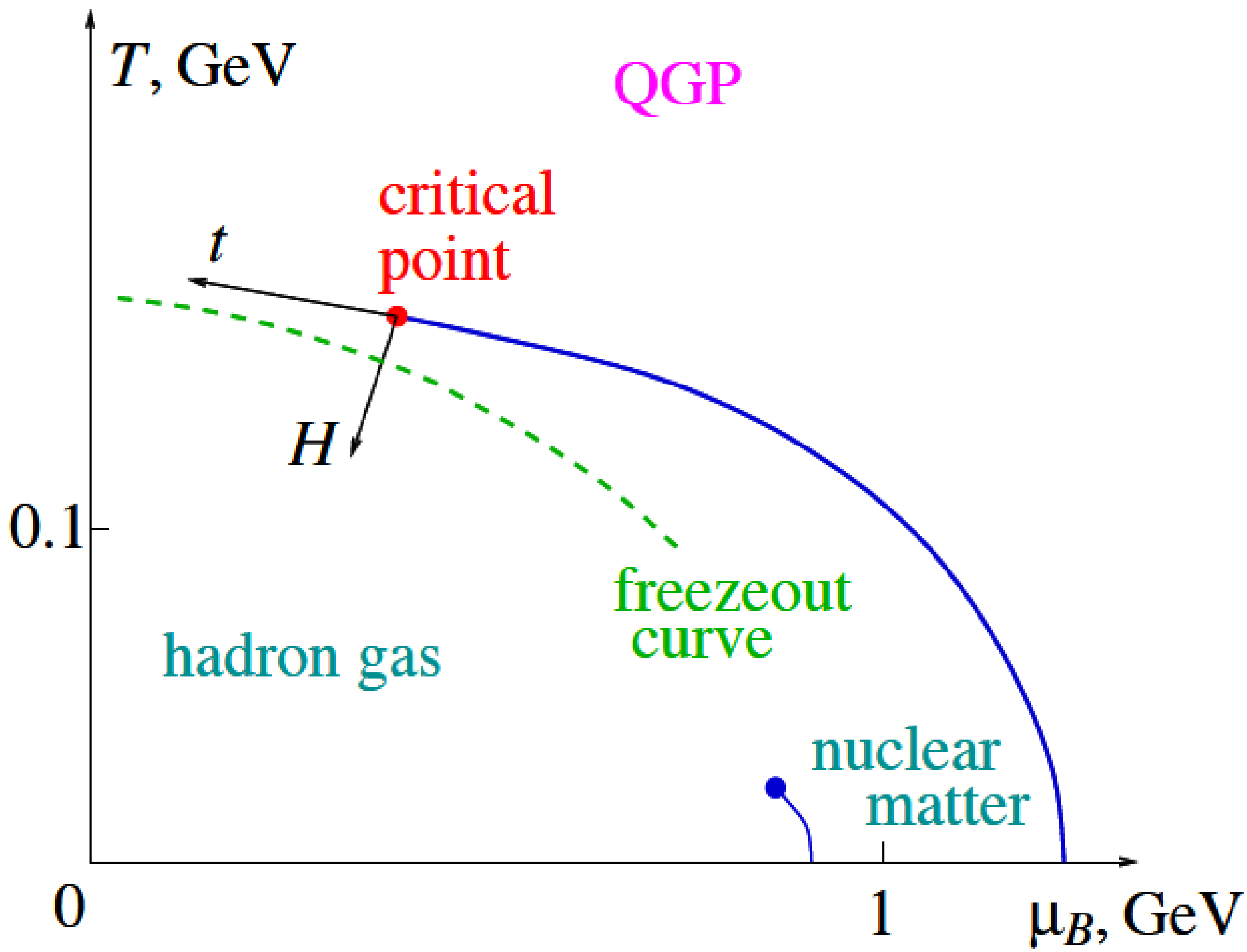

A cartoon of the Phase Diagram (experimentalist's view)

Top beam energy at RHIC: crossover transition from QGP to HG.

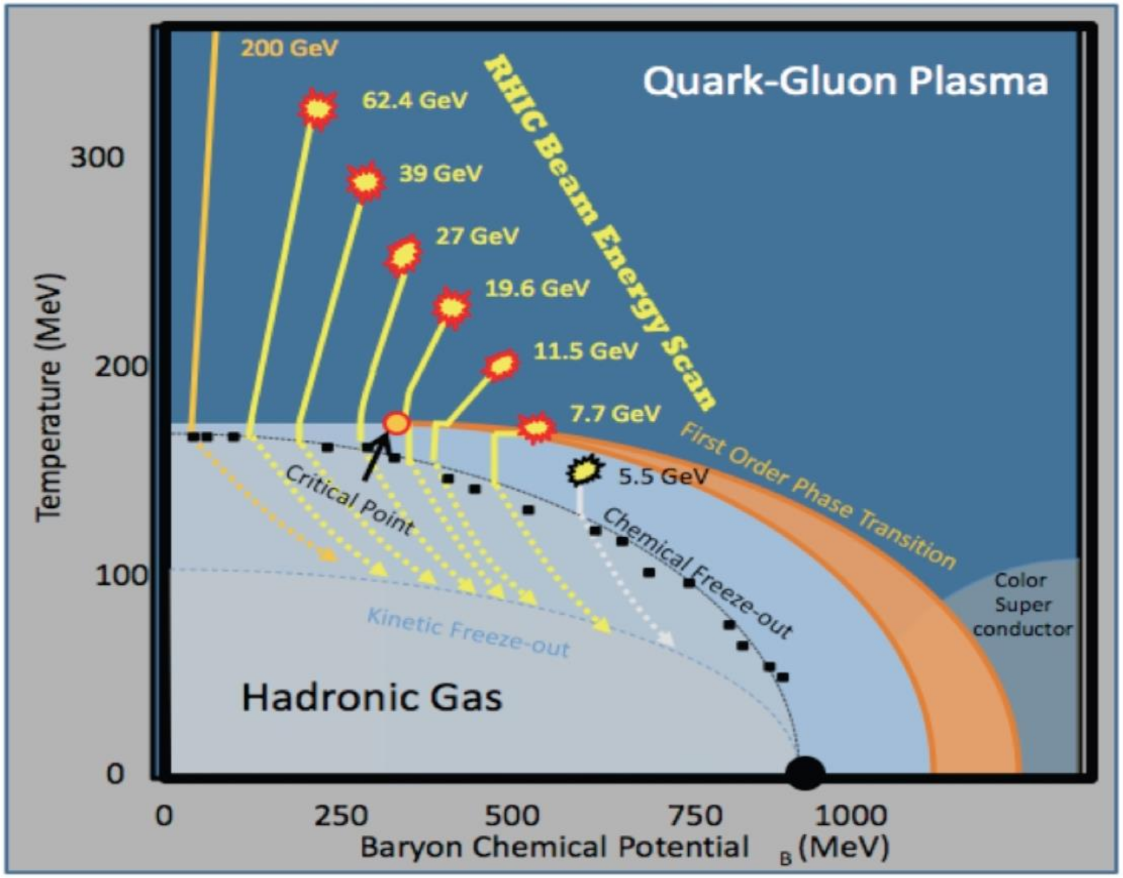

STAR BES data sets from RHIC Runs 10 and 11 (2010-2011)

$\sqrt{s_{NN}}$ (GeV)	MB Events in 10^6
7.7	4.3
11.5	11.7
19.6	35.8
27	70.4
39	130.4
62.4	67.3

200 GeV	>1B events	2010,11
14.5 GeV	~15M evts	2014
"BES-II"	10× BES-I	2018,19

Decreasing the beam energy increases the baryochemical potential

Systematic study of the data as a function of the beam energy allows a "scan" in streaks across the phase diagram...

How can multiplicity cumulants help us here?

Experimentally: The average values of specific powers of deviates give cumulants & cumulant ratios (or moments and moments products)....

No. of particles in a single event...

Average No. of particles in all "similar" events...

$$\delta x \equiv x - \langle x \rangle$$

C_2 $$\kappa_{2x} \equiv \langle\langle x^2 \rangle\rangle \equiv \langle (\delta x)^2 \rangle$$

C_3 $$\kappa_{3x} \equiv \langle\langle x^3 \rangle\rangle \equiv \langle (\delta x)^3 \rangle$$

C_4 $$\kappa_{4x} \equiv \langle\langle x^4 \rangle\rangle \equiv \langle (\delta x)^4 \rangle - 3 \langle (\delta x)^2 \rangle^2$$

$$\text{skewness} = \frac{\kappa_3}{\kappa_2^{3/2}}, \quad \text{kurtosis} = \frac{\kappa_4}{\kappa_2^2}$$

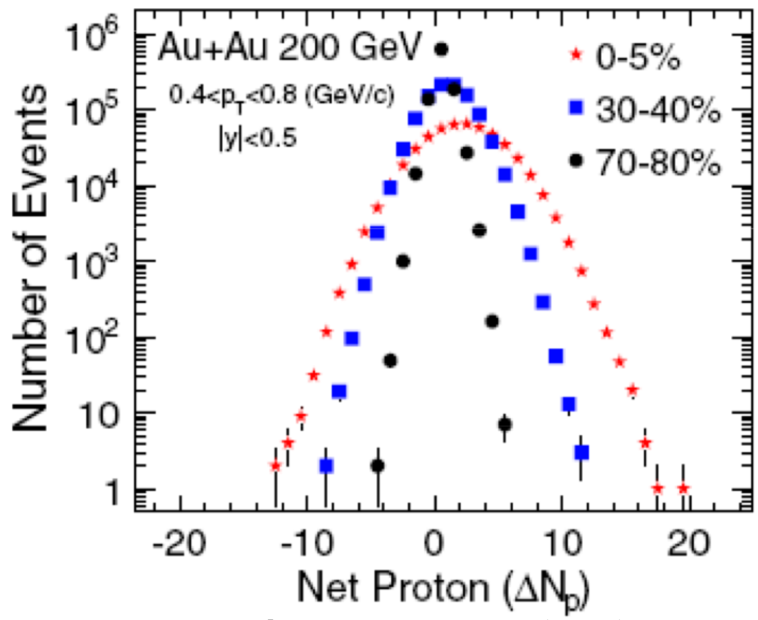

STAR, Phys. Rev. Lett. 105 (2010) 022302

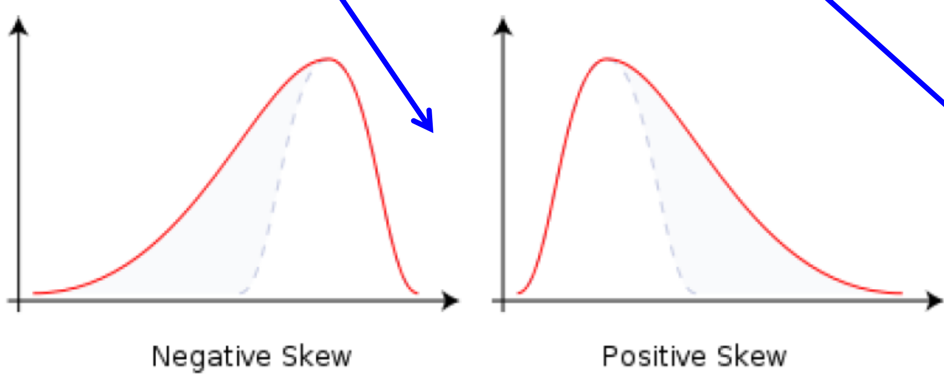

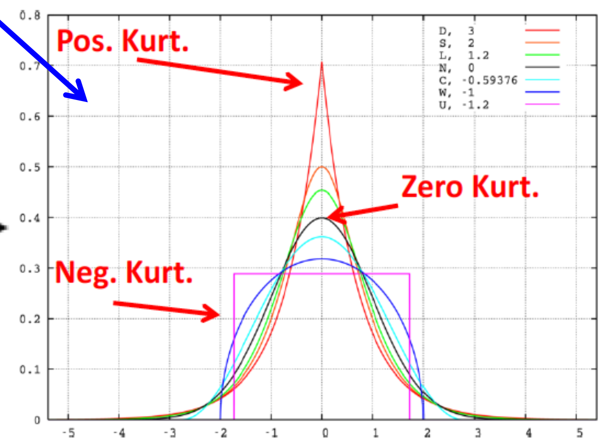

Cumulants

@ some $\sqrt{s_{NN}}$ and
in some centrality class

Yield Ratios
Y(i)/Y(j), where i,j
are different particles

$\xrightarrow{\text{SHM}}$

(μ_B,T)
Location on P.D.

Selected Spectra and Ratios

TPC & TOF
π, K, p spectra
$\sqrt{s_{NN}}$ =39 GeV

|y|<0.1

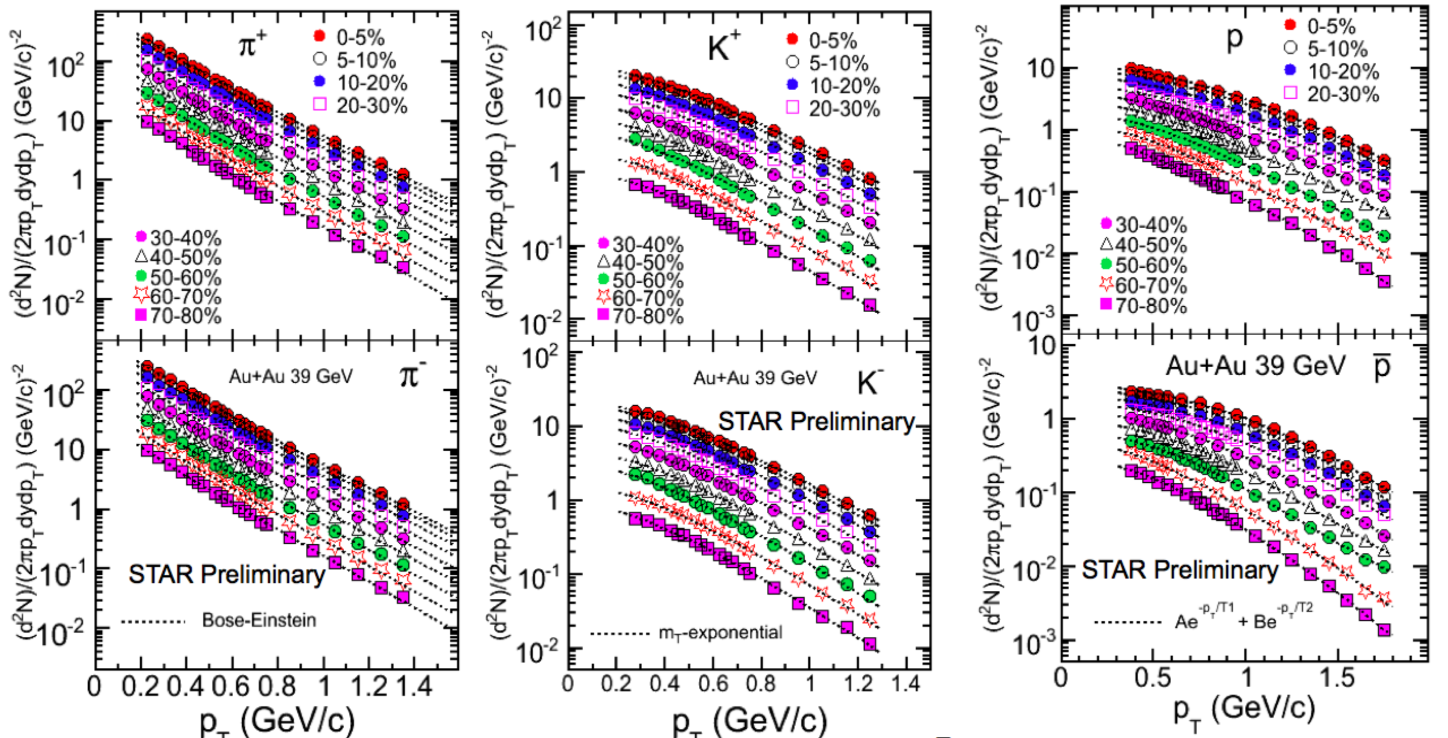

p̄ and p spectra not feed-down corrected

Ratios of integrated yields

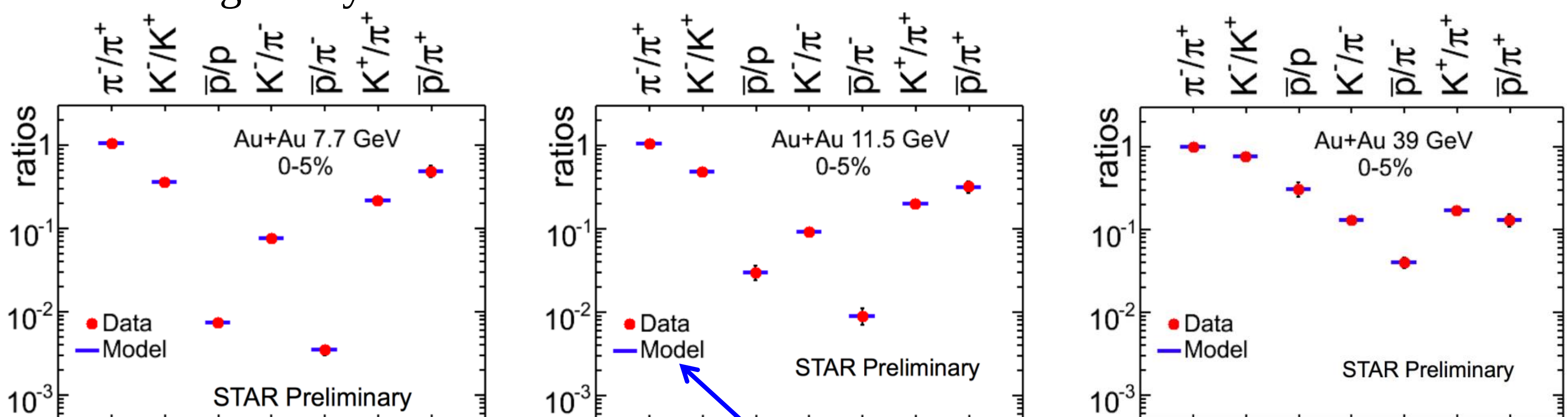

model described on next slide... (~2 parameters)

Statistical-Thermal Model (*e.g.* THERMUS) Computer Physics Communications **180**, 84 (2009)

$$N_i^{GC} = \frac{g_i V}{2\pi^2} \sum_{k=1}^{\infty} (\mp 1)^{k+1} \frac{m_i^2 T}{k} K_2\left(\frac{k m_i}{T}\right) e^{\beta k \mu_i} = \sum_{k=1}^{\infty} z_i^k e^{\beta k \mu_i}$$

Free Parameters: T, μ

β = 1/T
-1 (fermions), +1 (bosons)
Z = partition function
V = volume
m = mass
K_2 = Bessel function
g = degeneracy
- Grand Canonical ensemble

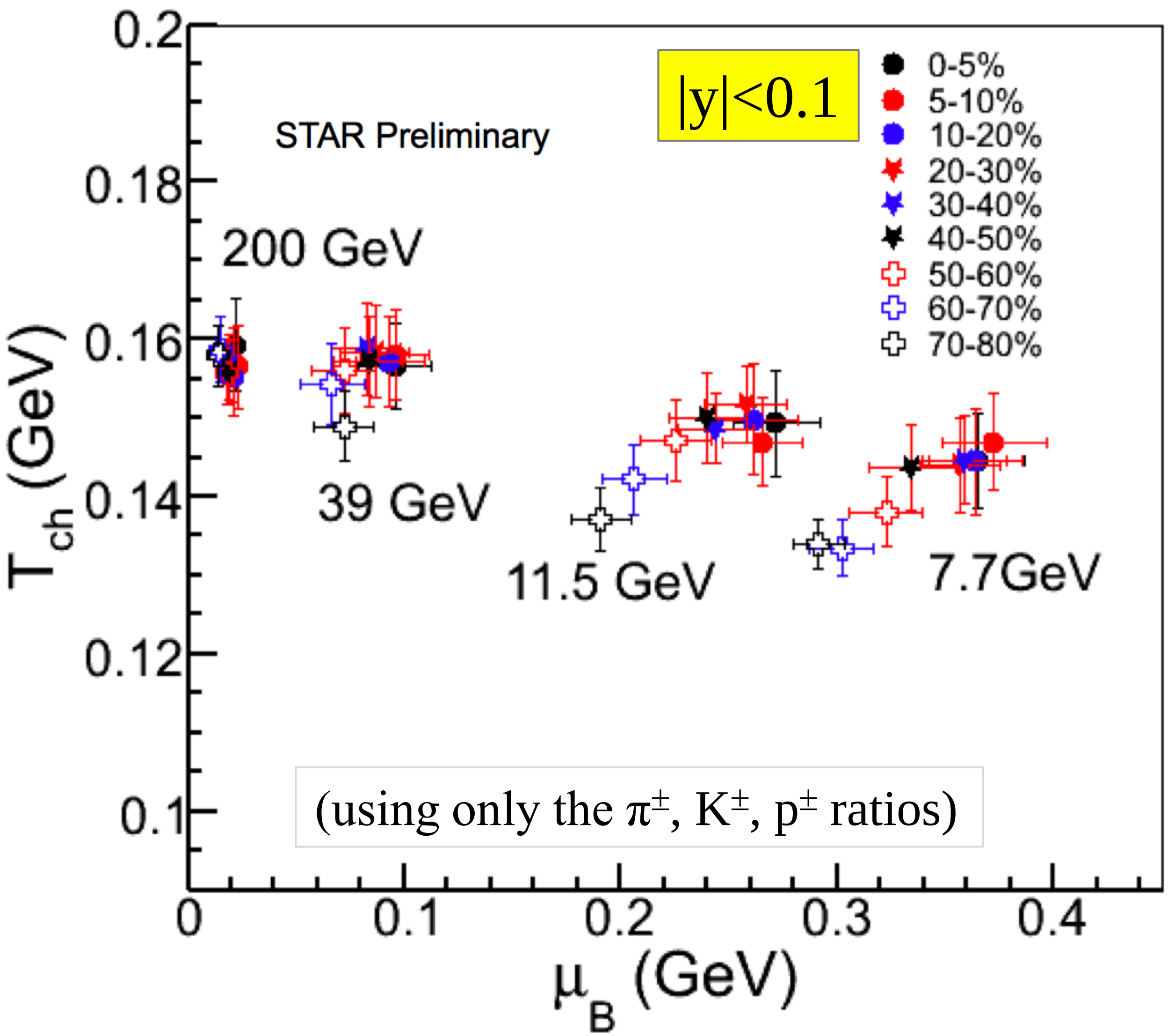

…(μ_B,T) values depend on $\sqrt{s_{NN}}$ *and* centrality…

…also depend on GCE, SCE, μCE…

no correlations

Cumulants

@ some $\sqrt{s_{NN}}$ and
in some centrality class

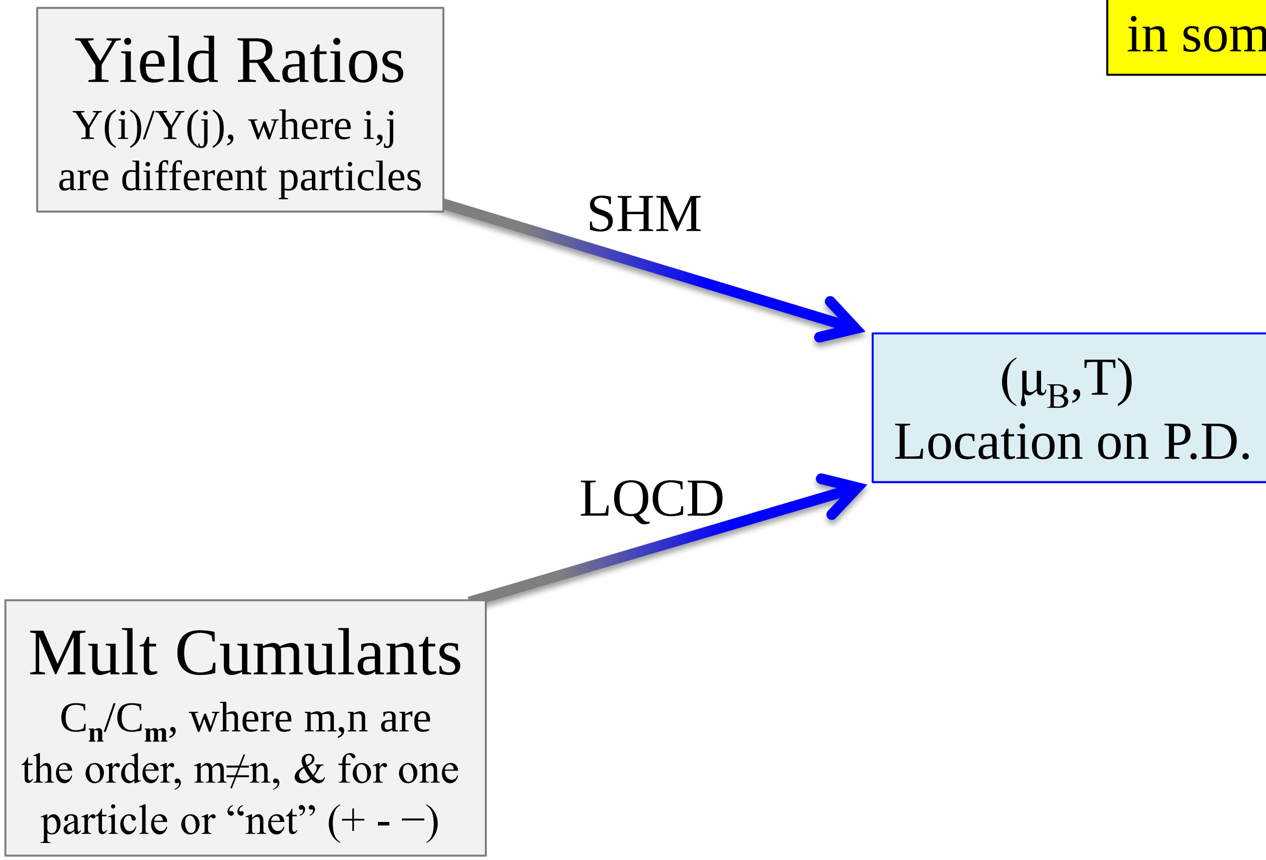

Coming back full circle again…

We have results on the net-p and net-q multiplicity distribution cumulants.

Use ratios of multiplicity cumulants, $R_{xy} = C_x/C_y$. plus Lattice QCD to infer (μ_B, T)

A. Bazavov, *et al.* (BNL-Bielefeld), Phys. Rev. Lett., **109**, 192302 (2012)

S. Borsányi, *et al.* (Wuppertal-Budapest), Phys. Rev. Lett., **111**, 062005 (2013)

Frithjof Karsch, University of Houston Colloquium, Sept. 24, 2013

Determination of T and μ_B from cumulant ratios

– in thermal equilibrium any two ratios of cumulants should allow to fix temperature and baryon chemical potential ♥

$$R^X_{n,m} = \frac{\chi^X_{n,\mu}}{\chi^X_{m,\mu}} \,, \quad X = B,\ Q,\ S$$

NLO Taylor expansion

– ratios with n+m even or odd show different sensitivity to T and μ_B

$$R^X_{12} \equiv \frac{M_X}{\sigma^2_X} = \frac{\mu_B}{T}\left(R^{X,1}_{12} + R^{X,3}_{12}\left(\frac{\mu_B}{T}\right)^2 + \mathcal{O}(\mu_B^4)\right) ,$$

$$R^X_{31} \equiv \frac{S_X \sigma^3_X}{M_X} = R^{X,0}_{31} + R^{X,2}_{31}\left(\frac{\mu_B}{T}\right)^2 + \mathcal{O}(\mu_B^4) ,$$

$M_X \sim \chi^X_1$: mean

$\sigma^2_X \sim \chi^X_2$: variance

$S_X \sim \chi^X_3/(\chi^X_2)^{3/2}$: skewness

♥ if fluctuations are sensitive to equilibrium physics at a unique (T, μ_B) pair

S. Mukherjee @ **Workshop on Beam Energy Scan II**
BES - II 2014
September 27-29, 2014

Charge fluctuations, LQCD and freeze-out in HIC

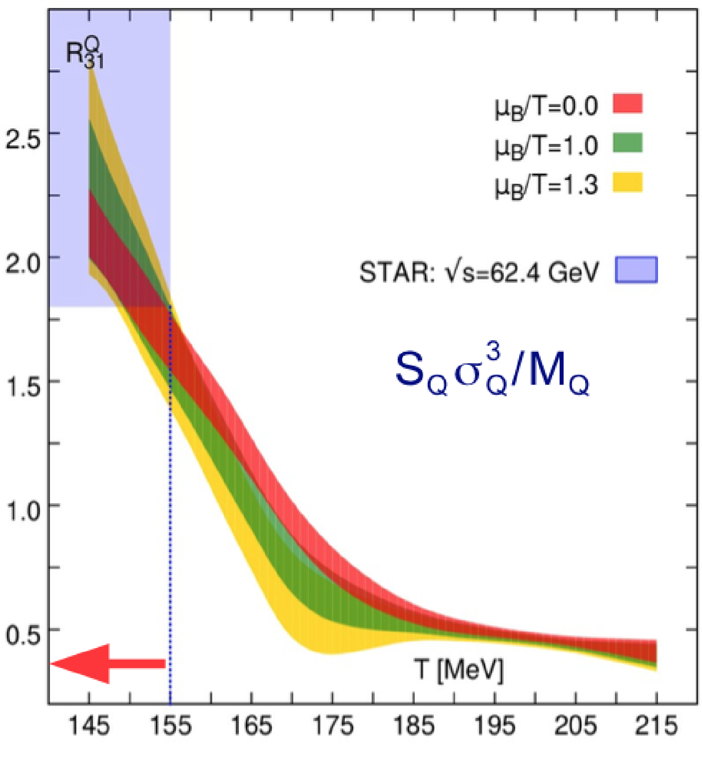

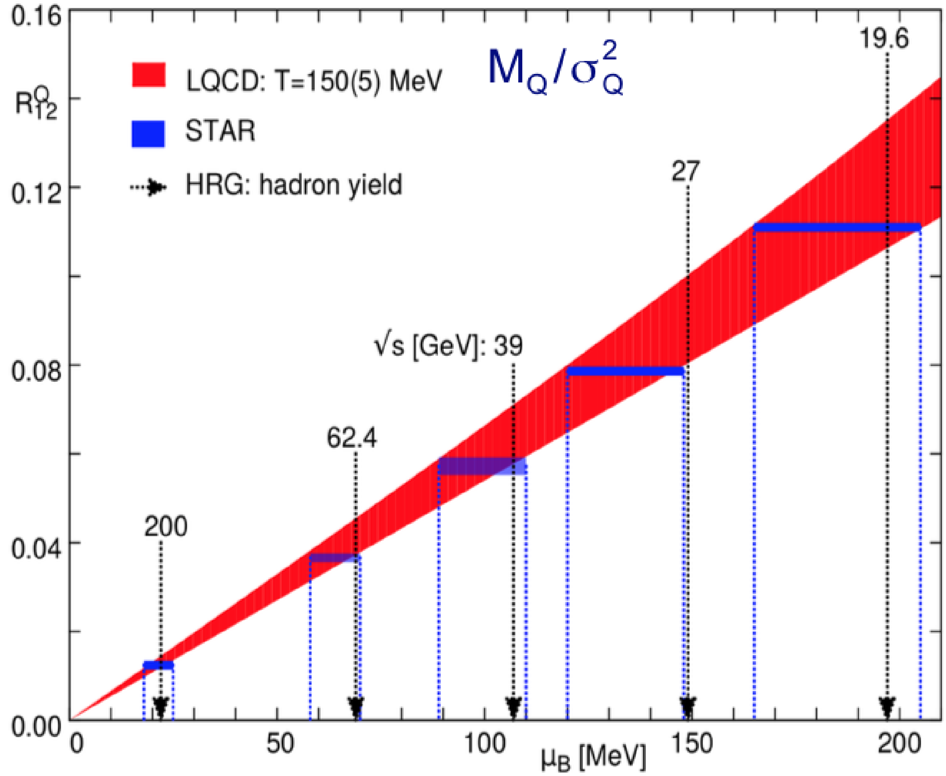

thermometer: T^f

baryometer: μ_B^f

$T^f \leqslant 155$ MeV

STAR: Phys.Rev.Lett. 113 (2014) 092301

BNL-Bi: Phys. Rev. Lett. 109, 192302 (2012)

SM: PoS CPOD2013, 039 (2013) 8

W-B: Phys. Rev. Lett. 113 (2014) 052301

need more precise measurements from BES-II

“Keyhole acceptance” (V. Koch’s term) drives cumulants to Poisson

RIKEN BNL Research Center Workshop on Fluctuations, Correlations and RHIC Low Energy Runs , October 3-5, 2011
http://quark.phy.bnl.gov/~htding/fcrworkshop/Koch.pdf

X. Luo, QM2014

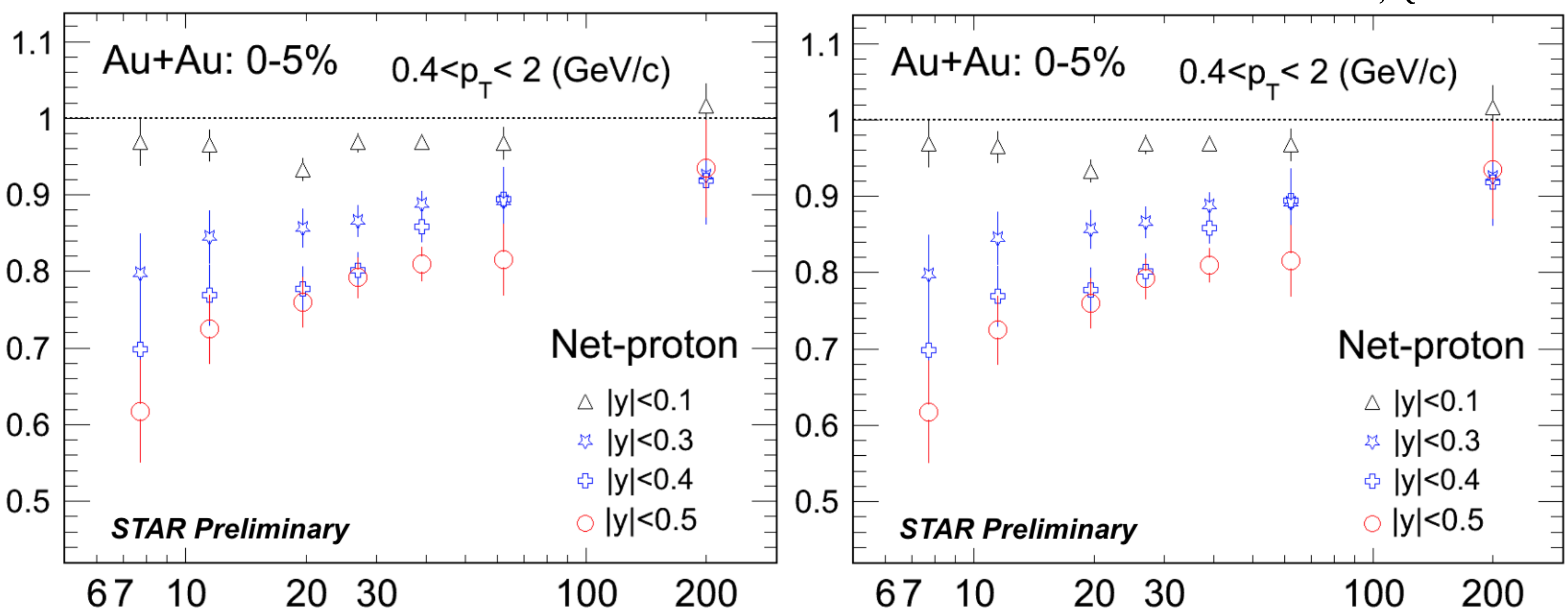

Such rapidity dependence would seem to bear on interpretation of comparisons of measured net-p cumulant ratios to LQCD to extract (μ_B,T)

Systematic study of rapidity window dependence of cumulant ratios needed

M. Kitazawa, BES-II workshop at LBNL
http://besii2014.lbl.gov/Program/bes-ii-talk-files/05%201409Berkeley_fluc.pdf

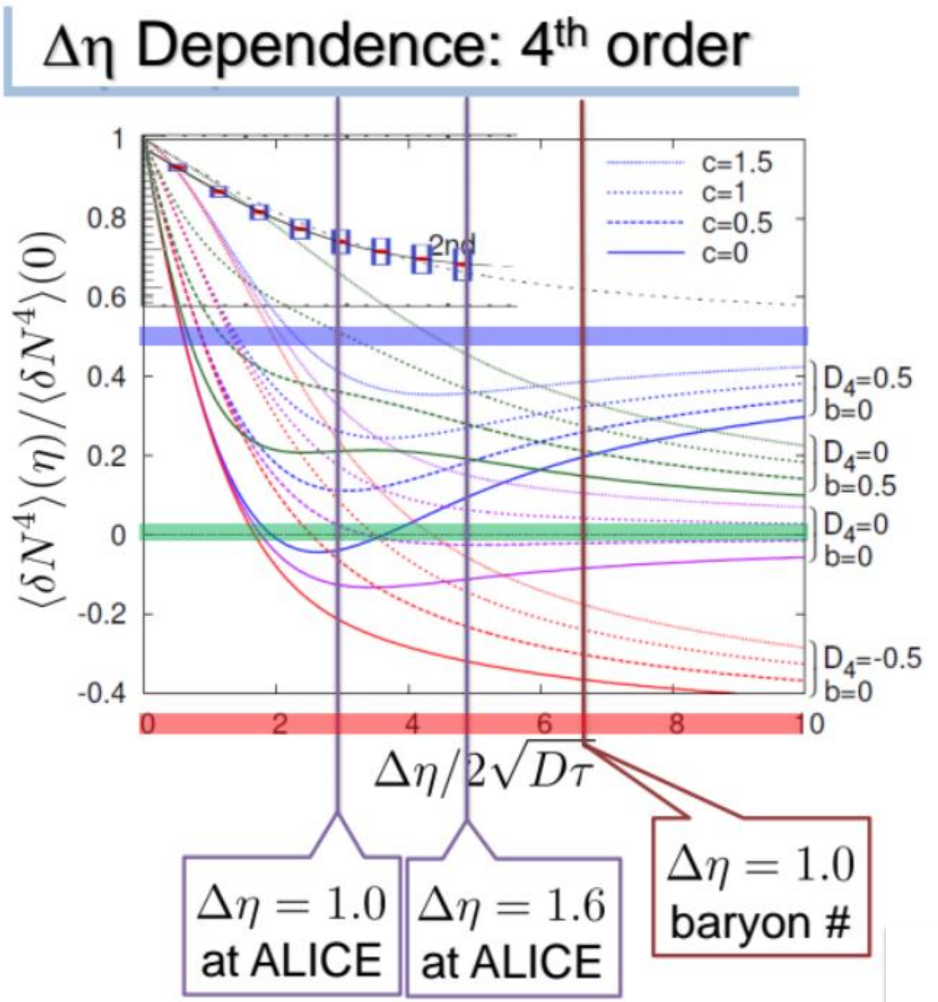

At present, Δy or Δη dependence for |y| or |η| < ~0.5 is easy...

Centrality:
net-p: use π & K multiplicity
net-q: use $q^{\pm}$ multiplicity 0.5<|η|<1.0
net-K: use $q^{\pm}$ multiplicity 0.5<|η|<1.0

I've explored alternate techniques
- BEMC ΣE (not well calibrated)
- BBC or ZDC (best at high $\sqrt{s_{NN}}$)

BES-II: Use EPD? opens up TPC...

Cumulants

@ some $\sqrt{s_{NN}}$ and
in some centrality class

Yield Ratios

Y(i)/Y(j), where i,j
are different particles

SHM

(μ_B,T)
Location on P.D.

LQCD

Mult Cumulants

C_n/C_m, where m,n are
the order, m≠n, & for one
particle or "net" (+ - −)

NLSM

ξ > ~1fm
Critical behavior?

An experimental avenue to finding a possible Critical Point

So how could we find a Critical Point if it exists?

Assume that it's going to have the same basic features of other CPs

divergence of the susceptibilities, χ… *e.g.* magnetism transitions 0801.4256v2

divergence of the correlation lengths, ξ *e.g.* critical opalescence

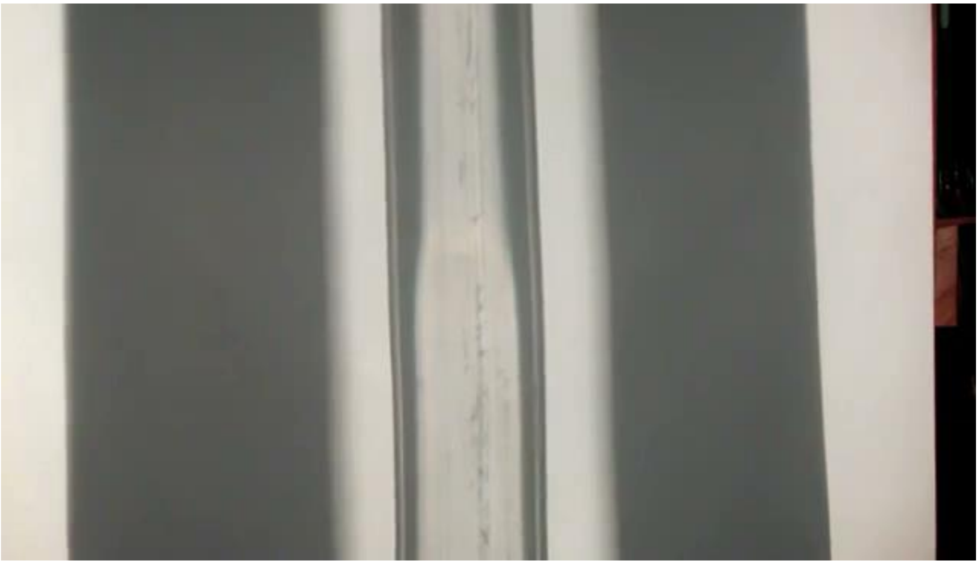

Brown University Undergraduate Physics Demonstration

liquid SF_6 at 37atm heated to ~43.9 C and then cooled

CO$_2$ near the liquid-gas transition

$T > T_C$ $T \sim T_C$ $T < T_C$

T. Andrews. Phil. Trans. Royal Soc., 159:575, 1869

M. Smoluchowski, *Annalen der Physik, 25 (1908) 205 - 226*

A. Einstein, *Annalen der Physik, 33 (1910) 1275-1298*

In the Nonlinear Sigma Model, the cumulants of the occupation numbers (integral=multiplicity) are also related to ξ

the higher the order of the moment, the stronger the dependence on ξ

M. Stephanov arXiv:0809.3450v1

$$\kappa_2 = \langle \sigma_0^2 \rangle = \frac{T}{V}\,\xi^2\,; \qquad \kappa_3 = \langle \sigma_0^3 \rangle = \frac{2\lambda_3 T}{V}\,\xi^6\,;$$

$$\kappa_4 = \langle \sigma_0^4 \rangle_c \equiv \langle \sigma_0^4 \rangle - \langle \sigma_0^2 \rangle^2 = \frac{6T}{V}\left[2(\lambda_3\xi)^2 - \lambda_4\right]\xi^8$$

"signal" of CP is then nonmonotic behavior of cumulants (ratios) *vs.* $\sqrt{s_{NN}}$

Cumulants

@ some $\sqrt{s_{NN}}$ and
in some centrality class

Yield Ratios
Y(i)/Y(j), where i,j
are different particles

SHM

(μ_B,T)
Location on P.D.

LQCD

Mult Cumulants
C_n/C_m, where m,n are
the order, m≠n, & for one
particle or "net" (+ - −)

NLSM

"Correlations" @ the core here
R_{12} depends on C_2
ξ is the correlation length
Dependence on $\Delta\eta$?

ξ > ~1fm
Critical behavior?

M.A. Stephanov, J. Phys.: Conf. Ser. **27**, 144 (2005)

In the vicinity of the critical point, the static (equal time) correlation function develops a divergent correlation length:

$$\langle \bar\psi\psi(\boldsymbol{x})\bar\psi\psi(\boldsymbol{0})\rangle_c \sim \begin{cases} \dfrac{1}{|\boldsymbol{x}|^{1+\eta}}, & |\boldsymbol{x}| \ll \xi; \\ e^{-|\boldsymbol{x}|/\xi}, & |\boldsymbol{x}| \gg \xi; \end{cases}$$

Promising experimental observables could be obtained starting from the two-particle correlator:
$$\langle \Delta n^\alpha_{\boldsymbol{p}} \Delta n^\beta_{\boldsymbol{k}} \rangle = \langle n^\alpha_{\boldsymbol{p}} n^\beta_{\boldsymbol{k}} \rangle - \langle n^\alpha_{\boldsymbol{p}} \rangle \langle n^\beta_{\boldsymbol{k}} \rangle$$

Cumulative measures: electric charge or baryon number fluctuations

sum over momenta p and k of all particles in the acceptance and weight each particle with its charge

$$\Delta Q = \sum_{\boldsymbol{p},\alpha} q^\alpha \Delta n^\alpha_{\boldsymbol{p}}; \quad \text{thus} \quad \langle (\Delta Q)^2 \rangle = \sum_{\boldsymbol{p},\alpha} \sum_{\boldsymbol{k},\beta} q^\alpha q^\beta \langle \Delta n^\alpha_{\boldsymbol{p}} \Delta n^\beta_{\boldsymbol{k}} \rangle$$

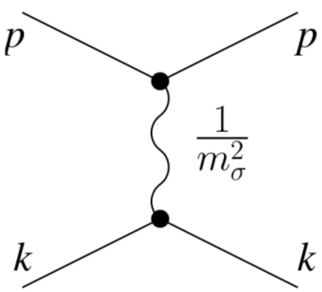

singular contribution to the correlator $\langle \Delta n_{\boldsymbol{p}} \Delta n_{\boldsymbol{k}} \rangle$ "variance" measures $\sim \xi^2$

absolute strength of the singularity depends on the coupling of the critical mode σ to the corresponding hadron, which is difficult to estimate

3- and 4-particle correlations:
(stronger ξ-dependence)

M.A. Stephanov, PRL **102**, 032301 (2009)
C. Athanasiou et al., **PRD** 82, 074008 (2010)
M.A. Stephanov, PRL **107**, 052301 (2011)

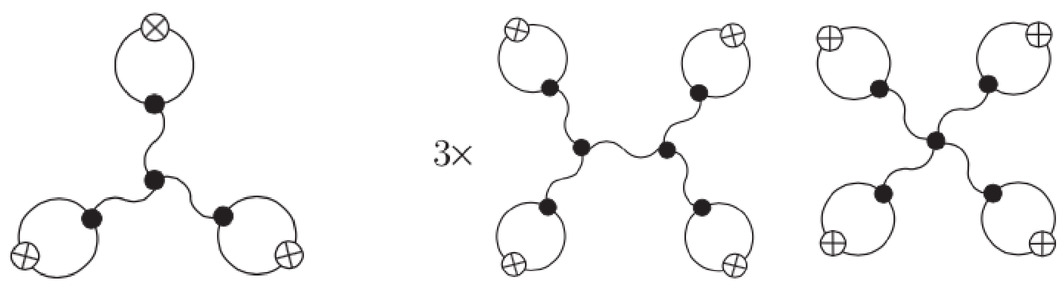

J. Nagle, last talk at QM2012

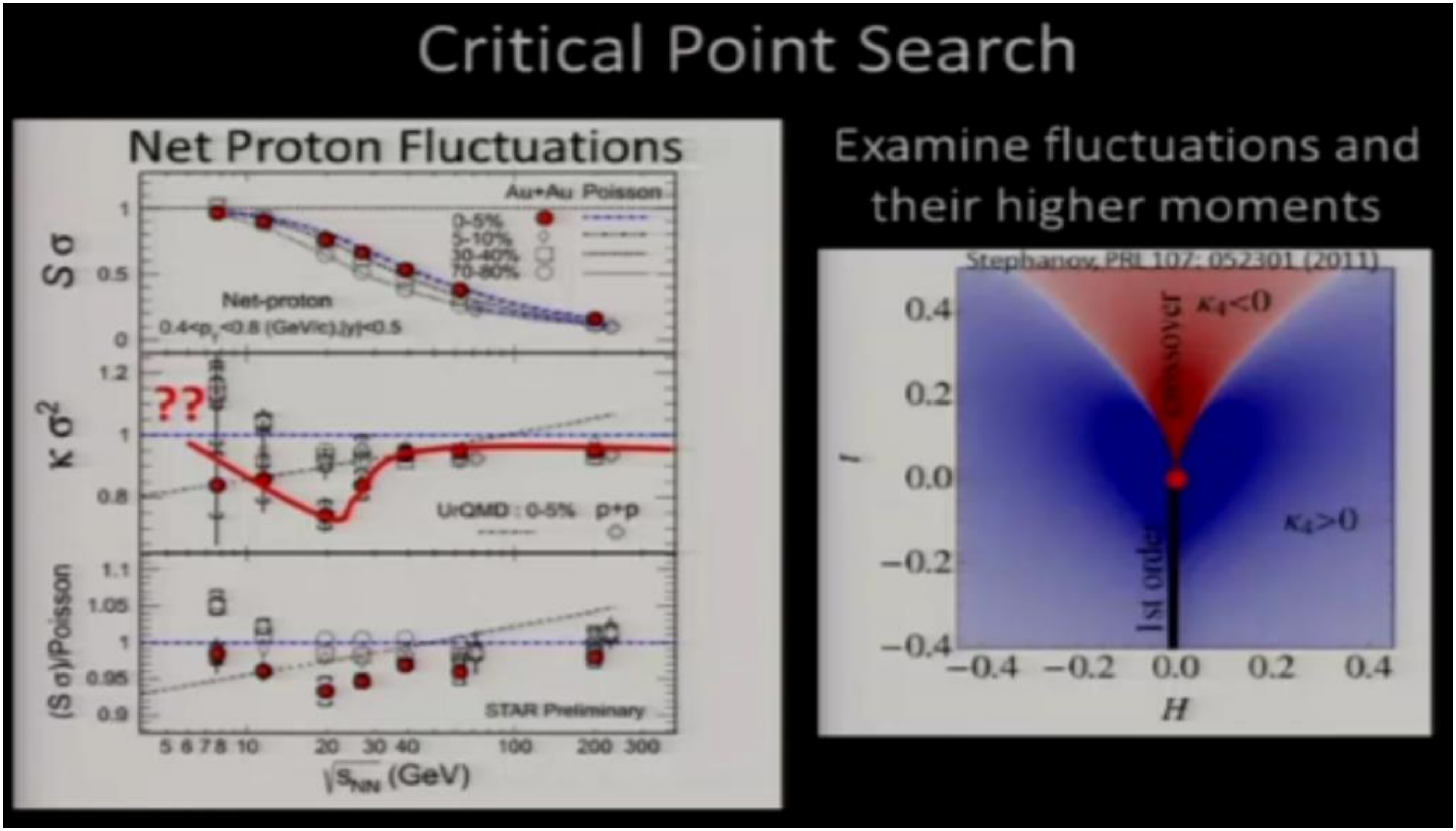

Kurtosis < Poisson for $\sqrt{s_{NN}}$ just above CP?
M.A. Stephanov, Phys. Rev. Lett. 107, 052301 (2011)

J. Nagle, last talk at QM2012

C. Athanasiou et al., **PRD** 82, 074008 (2010)
M.A. Stephanov, PRL **107**, 052301 (2011)

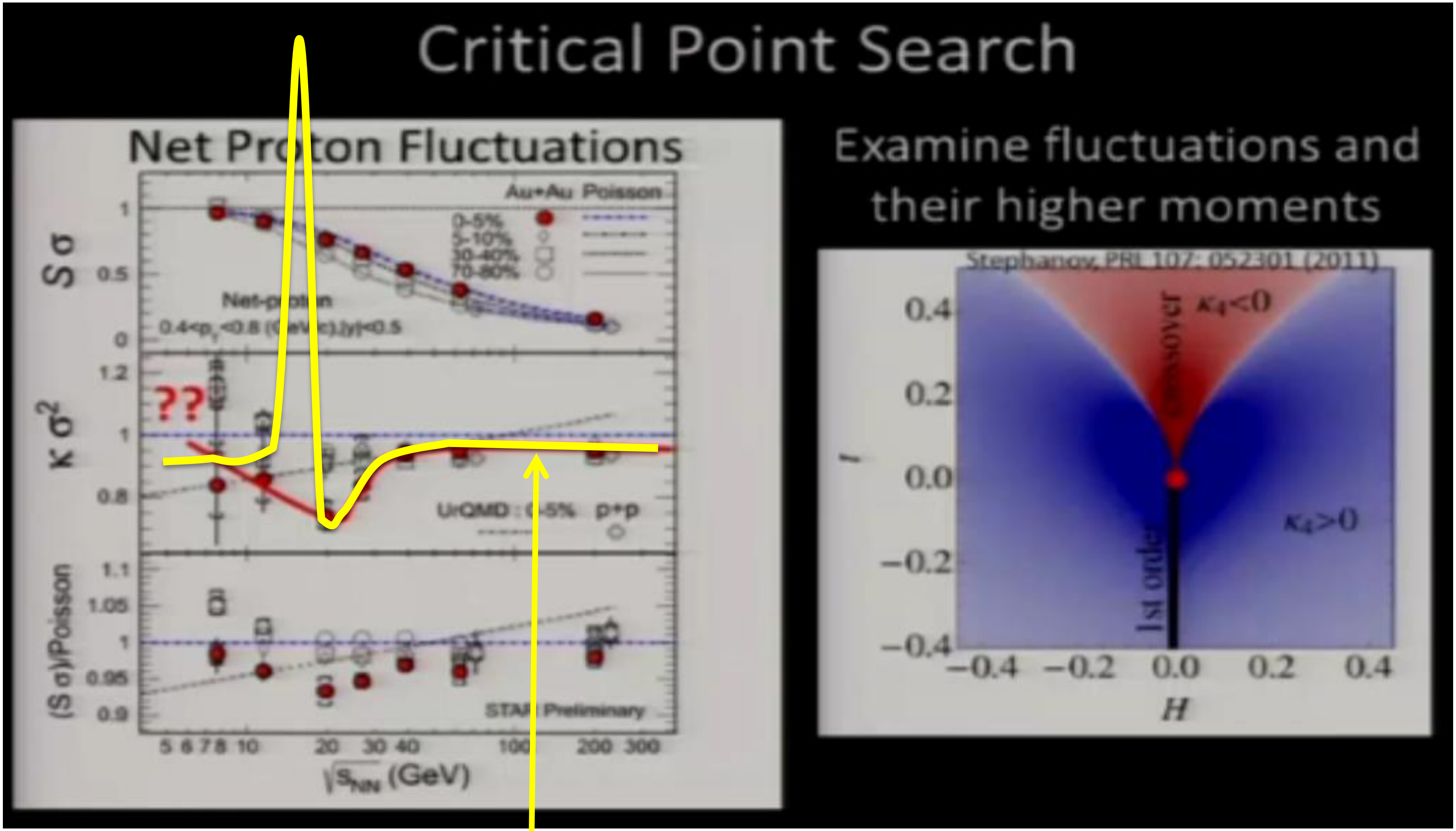

…what the NLSM would expect for a CP at $\sqrt{s_{NN}}$~15 GeV
(14.5 GeV data collected in Run 14… Production just finished!)

"independent production" involves either sampling from pos and neg multiplicity distributions, or Independent Random Value (IRV) cumulant arithmetic:

given two IRVs: $C_k net = C_k pos + (-1)^k \times C_k neg$ (for all k)

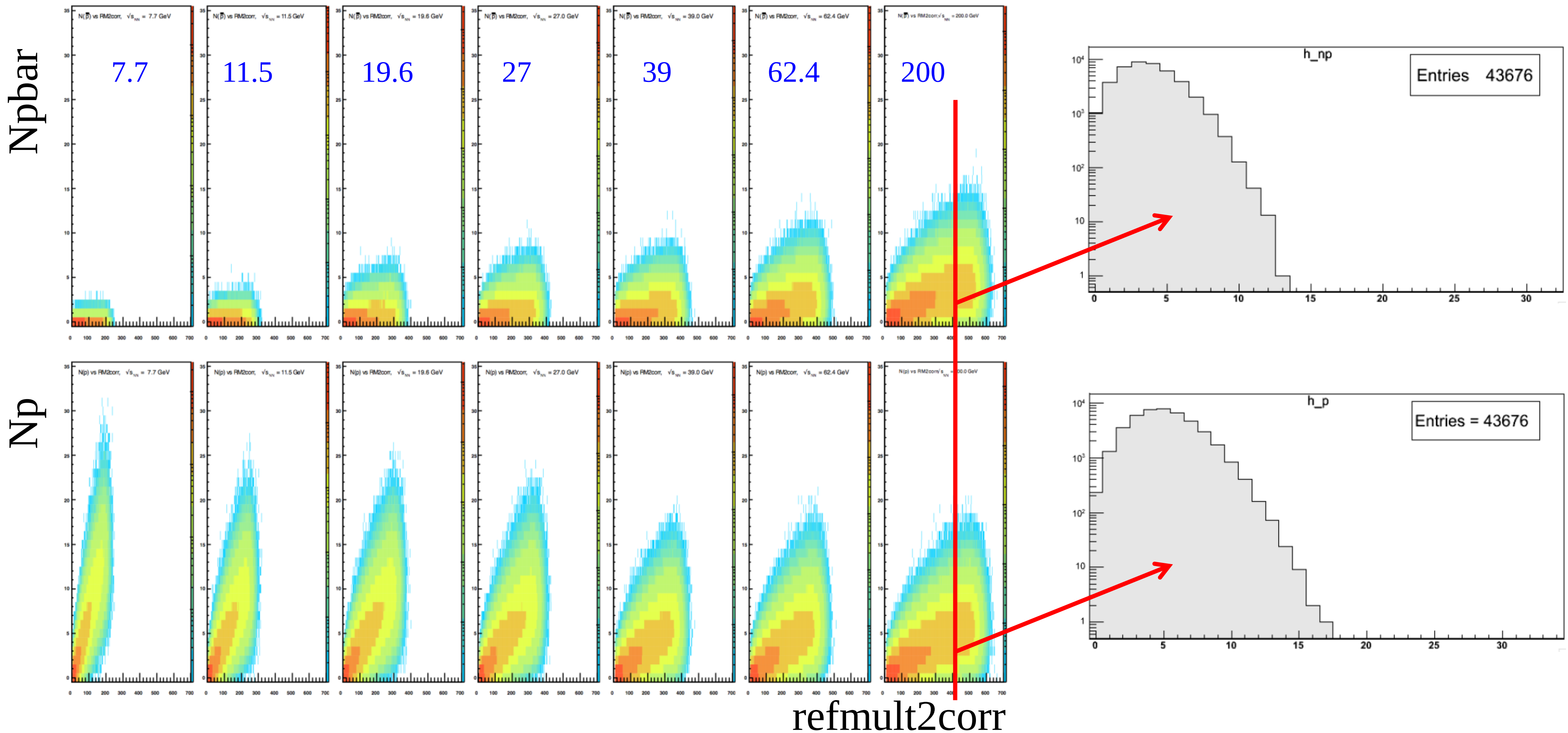

Destroys all intra-event correlations between Npos and Nneg, reproduces singles distributions, & has the same statistical certainty as the data by construction…

see also G. Torrieri *et al.*, J. Phys. G, **37**, 094016 (2010)

Corrected net-p $S\sigma$ and $K\sigma^2$ vs $\sqrt{s_{NN}}$ for 0-5% and 70-80% centrality

W.J. Llope for the STAR Collaboration, APS-DNP Fall Meeting, Newport News, Virginia, October 25, 2013.

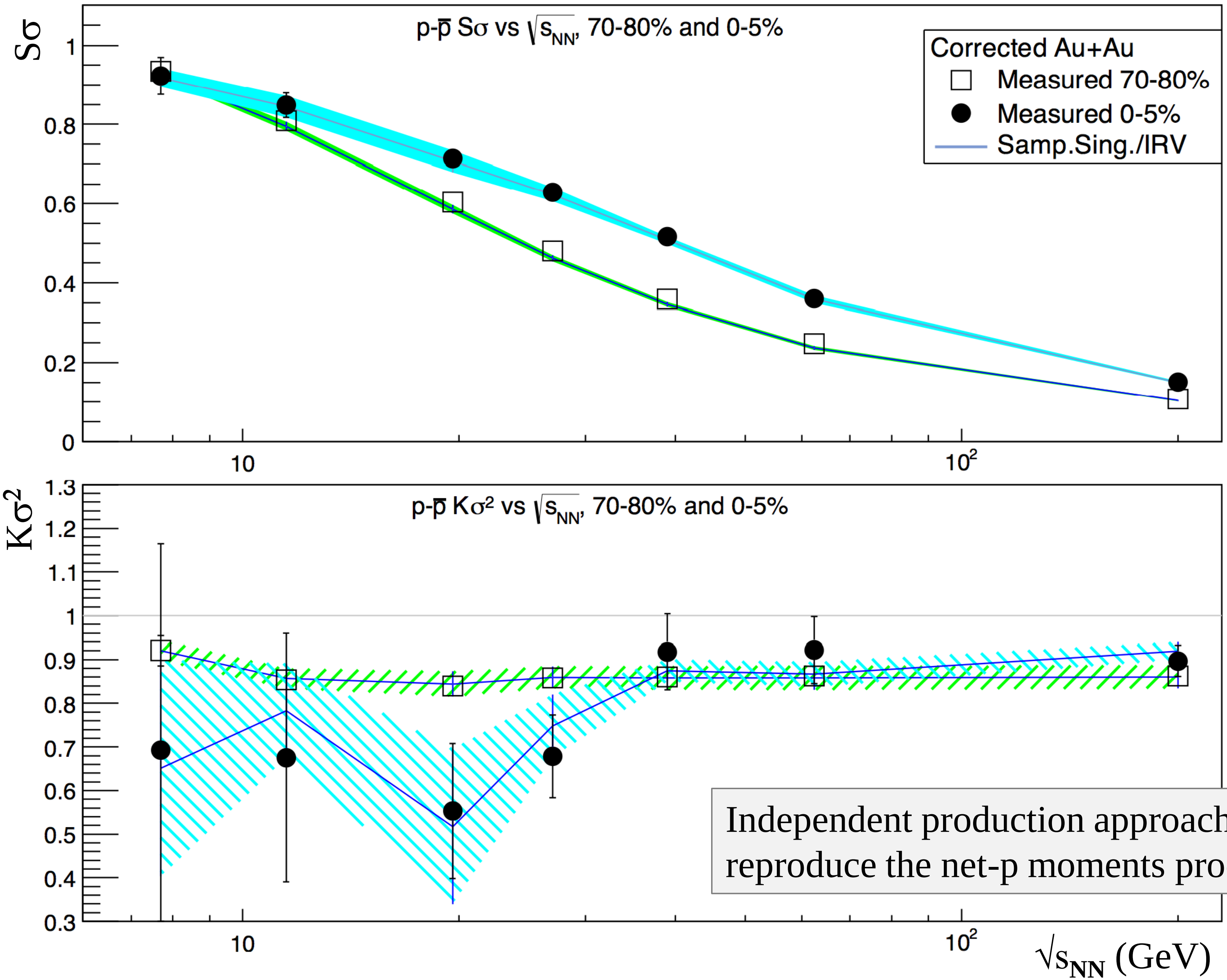

Independent production approaches reproduce the net-p moments products

Efficiency-corrected net-p $K\sigma^2$ vs centrality by $\sqrt{s_{NN}}$

W.J. Llope for the STAR Collaboration, APS-DNP Fall Meeting, Newport News, Virginia, October 25, 2013.

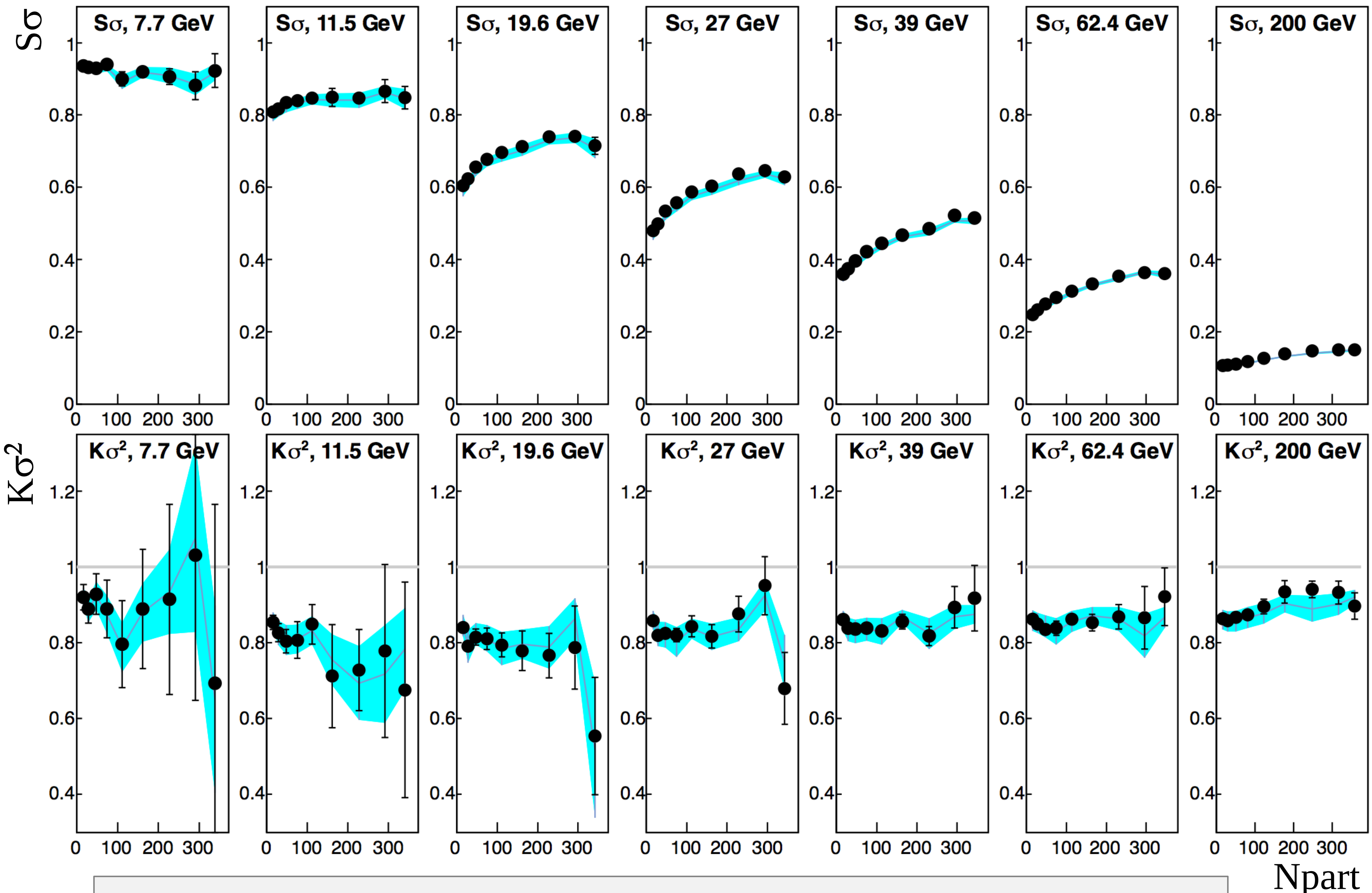

IRV and sampled singles approaches (cyan) quantitatively reproduce the net-proton moments products at all beam energies and centralities…

W.J. Llope for the STAR Collaboration, APS-DNP Fall Meeting, Newport News, Virginia, October 25, 2013.

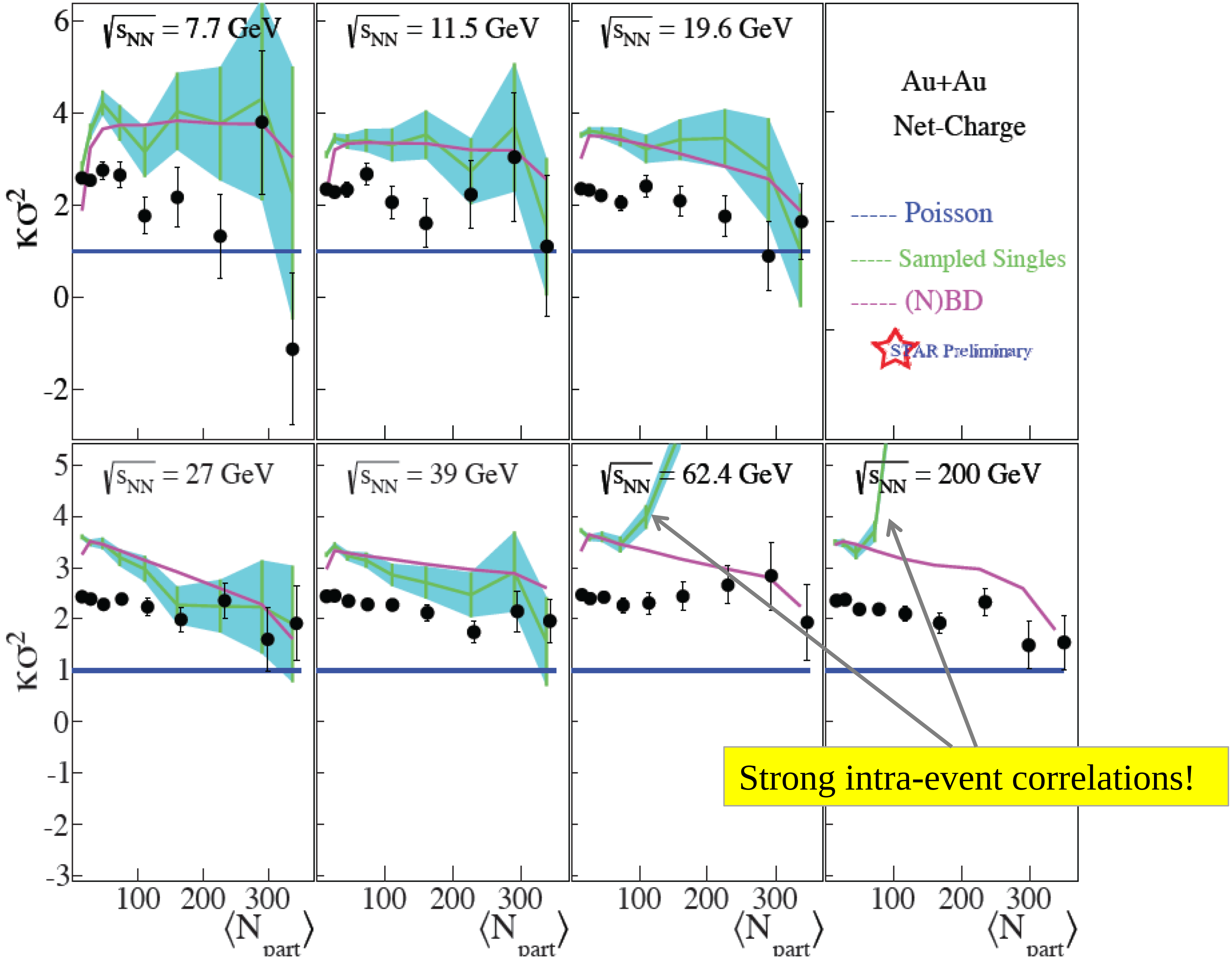

What can we learn about the shape of the net-p C4/C2 ?

STAR net-p PRL
January 23, 2014

L. Adamczyk, et al., [STAR Collaboration], Phys. Rev. Lett. 112 (2014) 032302.

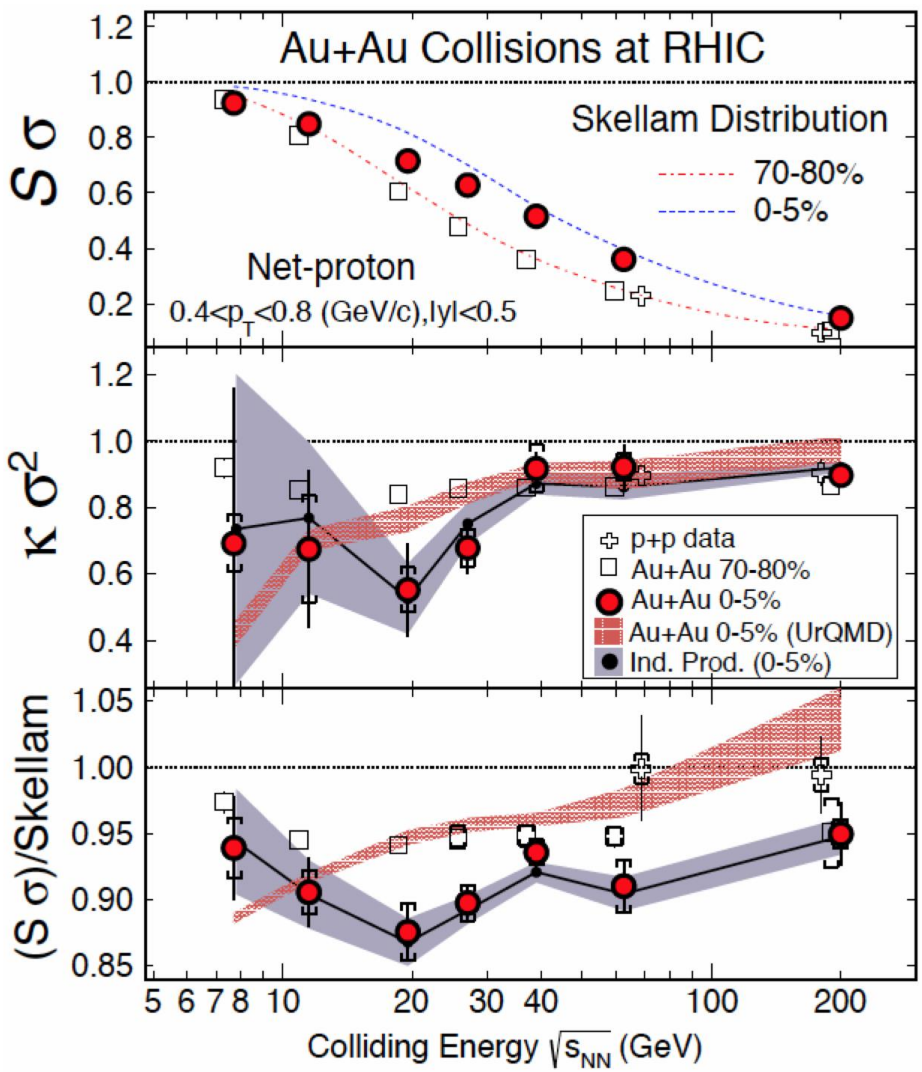

What can we learn about the shape of the net-p C4/C2 ?

STAR net-p PRL
January 23, 2014

L. Adamczyk, et al., [STAR Collaboration], Phys. Rev. Lett. 112 (2014) 032302.

STAR White Paper on BES-I
June 1, 2014

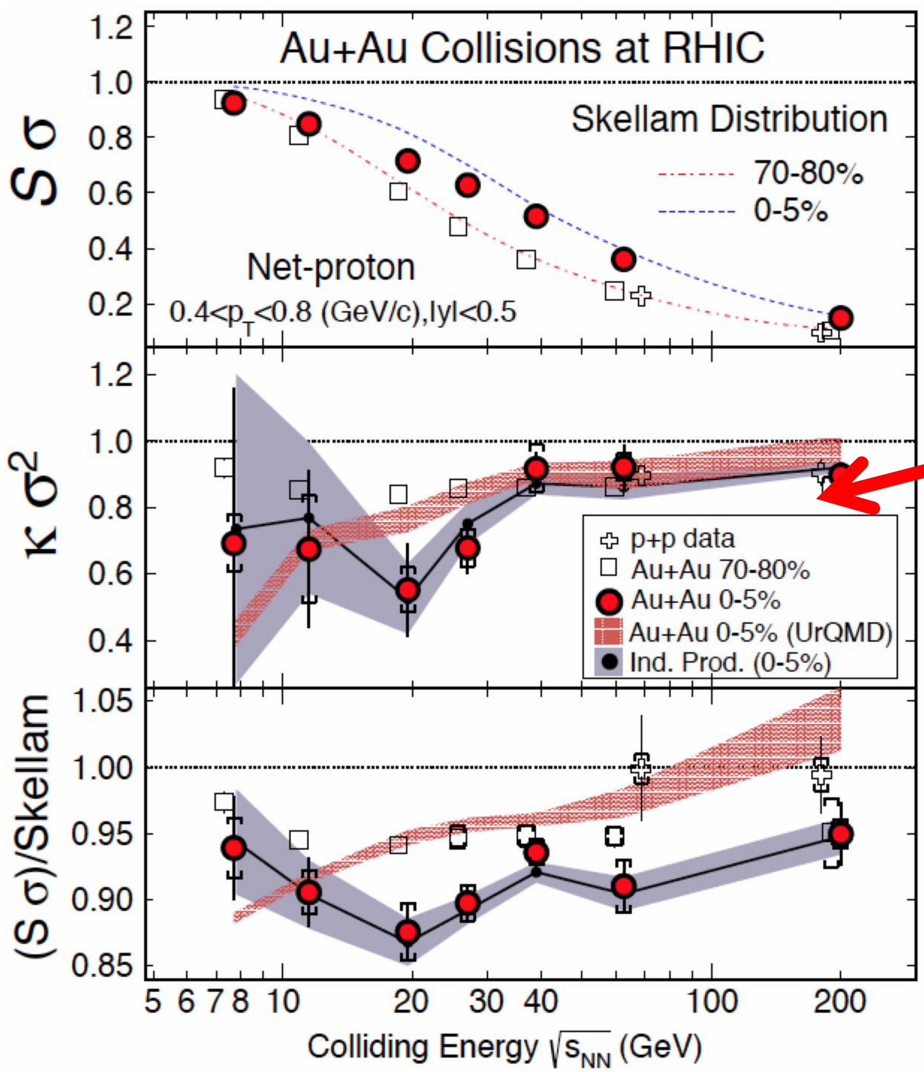

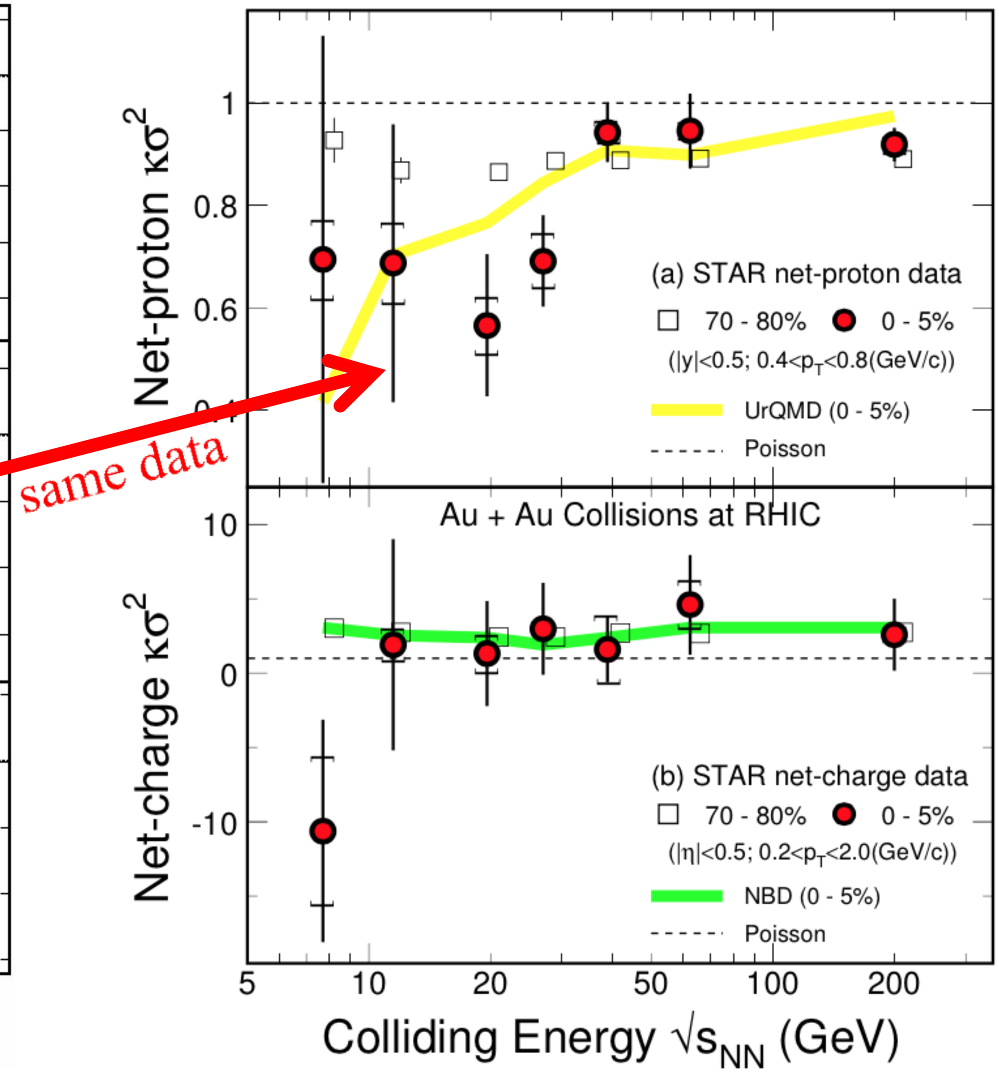

Independent Production exactly reproduces the measured net-proton cumulant ratios…
(within the statistical certainties possible with the presently available event totals)

…indicates that intra-event correlations between p and pbar multiplicities are not strong enough to be seen in presently available multiplicity cumulant ratios

Note, I did *not* say:
this means there are no correlations between Np and Npbar in these data
nor did I say:
this is a baseline for a CP search, hence no CP signal in these data

Nparticle vs Nantiparticle

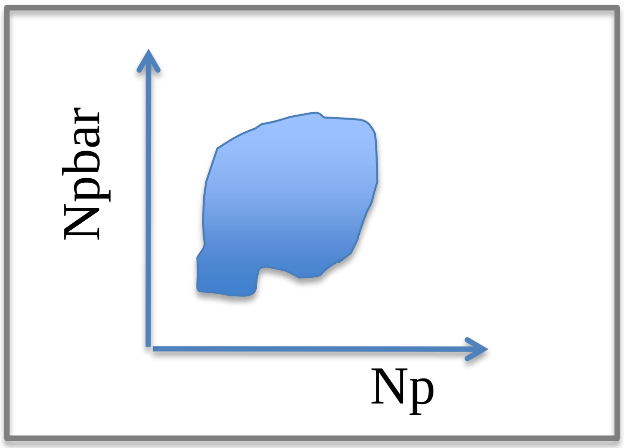

vs.

4 baryons

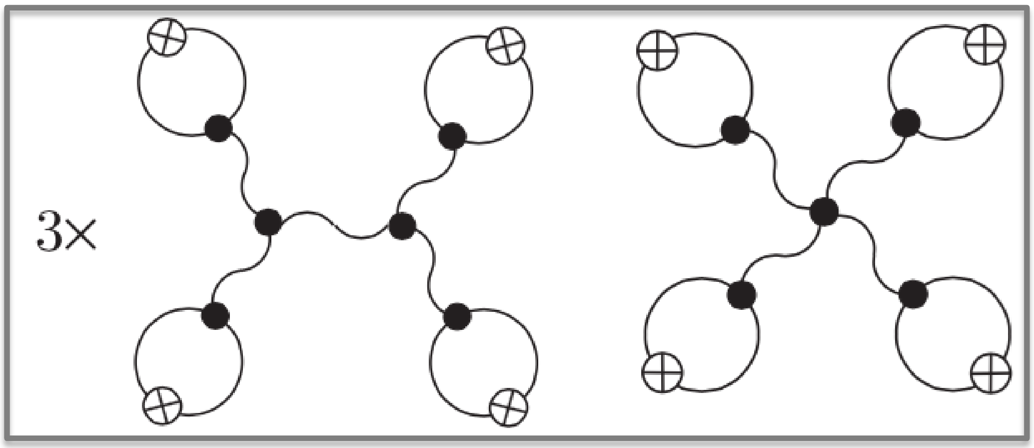

"independent production" approaches reproduce the net-proton C_3/C_2 and C_4/C_2…
Involves either sampling from pos and neg multiplicity distributions,
or IRV cumulant arithmetic: $C_k\text{net} = C_k\text{pos} + (-1)^k \times C_k\text{neg}$ (holds for all k)

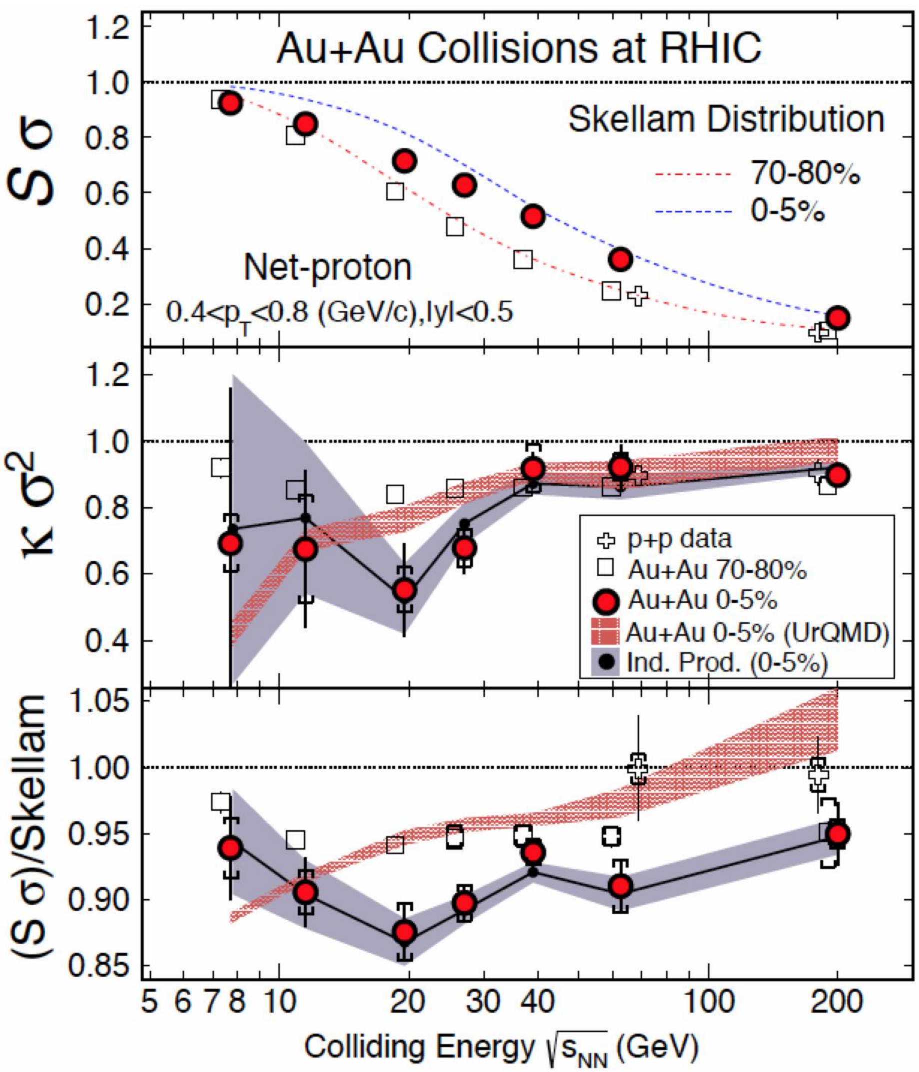

Complaints were, generally…

1. "no pbars at $\sqrt{s_{NN}}$ < 39 GeV!"
2. "there *must* be correlations at high $\sqrt{s_{NN}}$!"
   baryon number transport at low $\sqrt{s_{NN}}$
   baryon-pair production at high $\sqrt{s_{NN}}$

P.K. Netrakanti *et al.*, arXiv:1405.4617 [hep-ph]

Coming up:
Where does "the dip" come from then?
Why are these cumulant ratios not seeing any correlations?

Further exploring the moments products by deconstructing them…

The net-proton moments products can be understood using the p and pbar multiplicity distributions separately…

Intra-event correlations of N_p and N_{pbar} do not measurably affect the net-p moments products

That is…

$K\sigma^2$(net-p)

$= C_4\text{(net-p)}/C_2\text{(net-p)}$

$= [C_4(p)+C_4(\text{pbar})] / [C_2(p)+C_2(\text{pbar})]$

Four quantities there.

Are the experimental values of $K\sigma^2$(net-p) driven by all four quantities equally?
Or does one of these dominate?

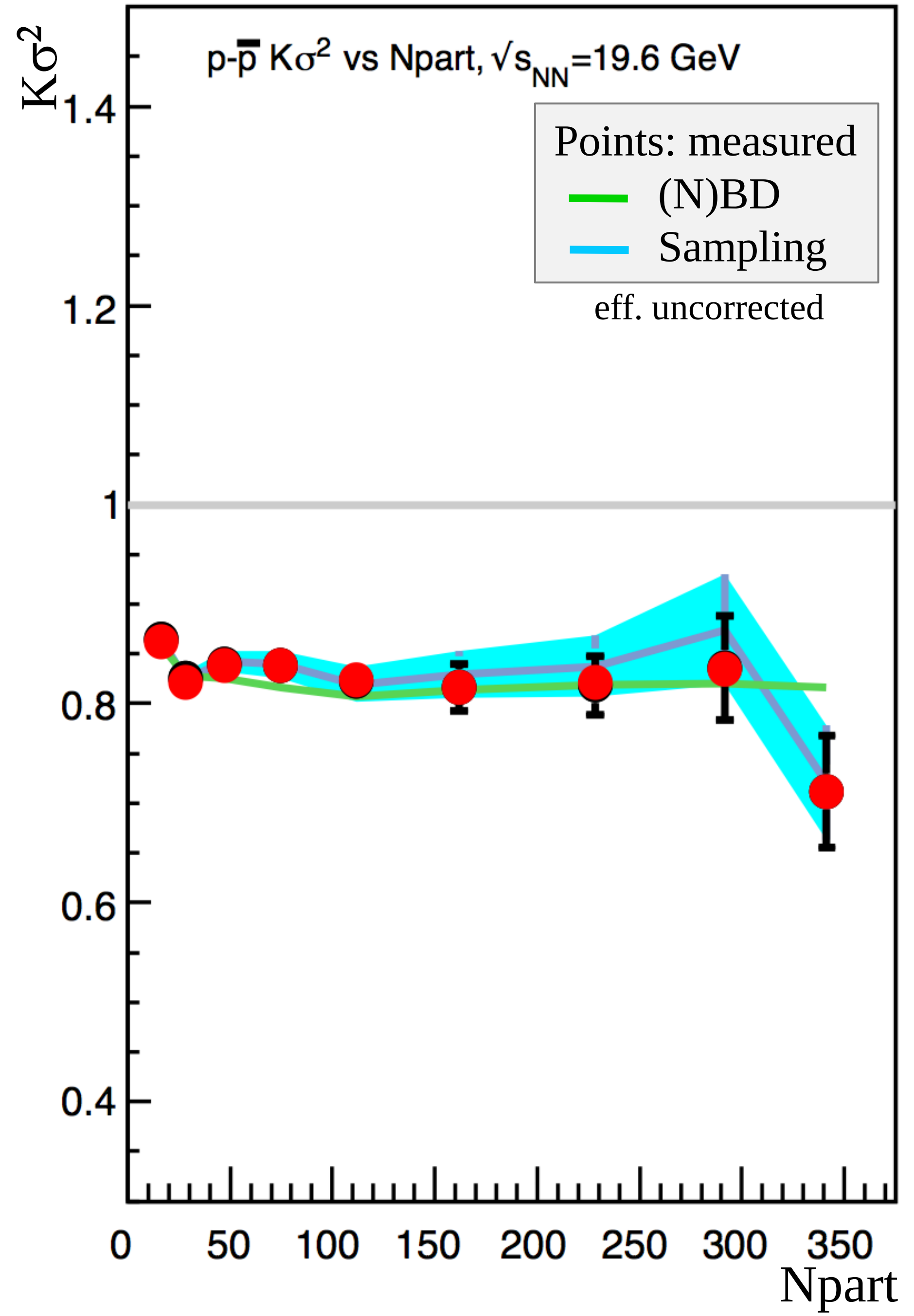

Charge-separated uncorrected $K\sigma^2$ *vs.* centrality by $\sqrt{s_{NN}}$

W.J. Llope for the STAR Collaboration, APS-DNP Fall Meeting, Newport News, Virginia, October 25, 2013.

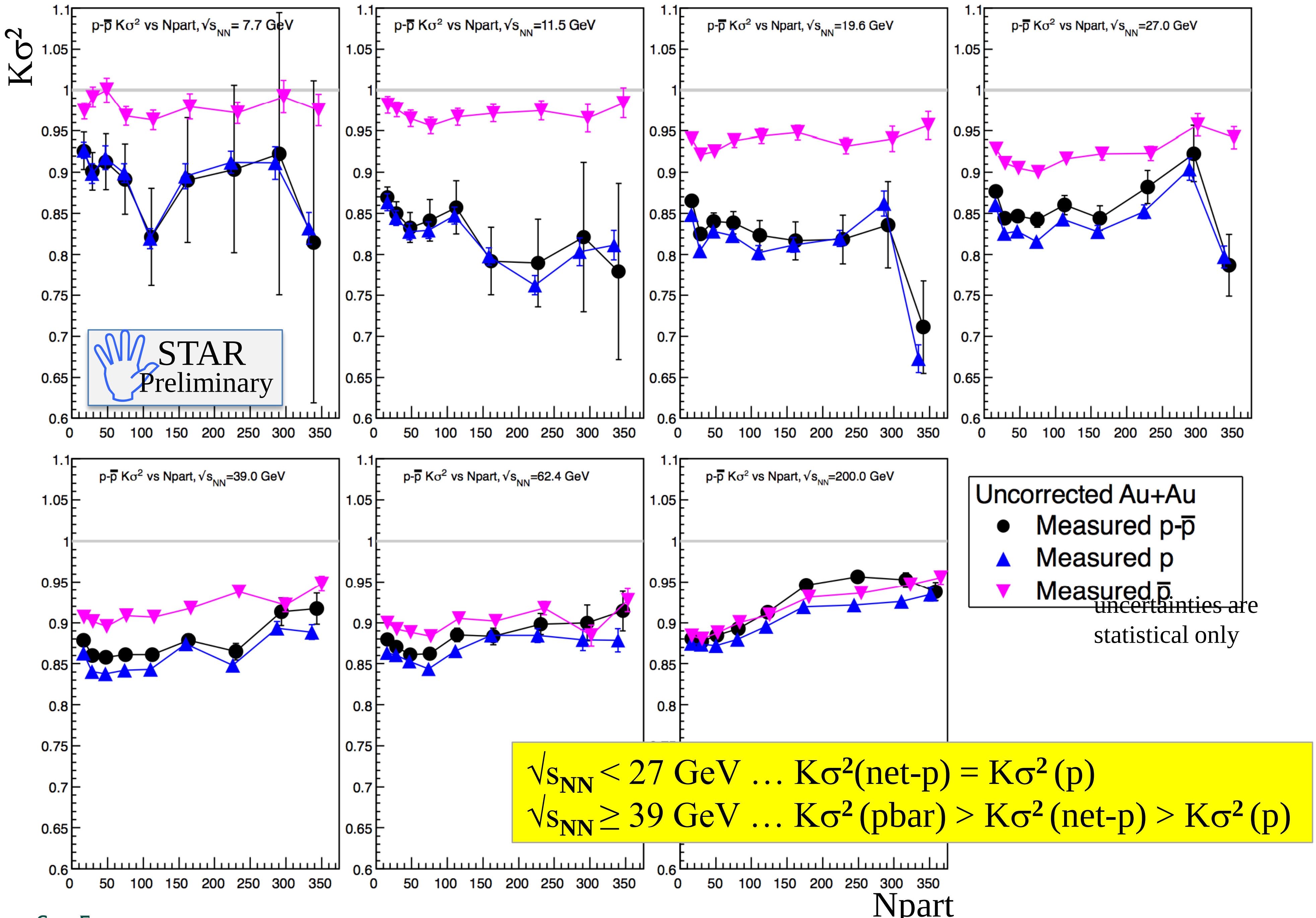

$\sqrt{s_{NN}} < 27$ GeV … $K\sigma^2$(net-p) = $K\sigma^2$ (p)
$\sqrt{s_{NN}} \geq 39$ GeV … $K\sigma^2$ (pbar) > $K\sigma^2$ (net-p) > $K\sigma^2$ (p)

Uncorrected net-proton C_2 (variance) *vs.* centrality by $\sqrt{s_{NN}}$

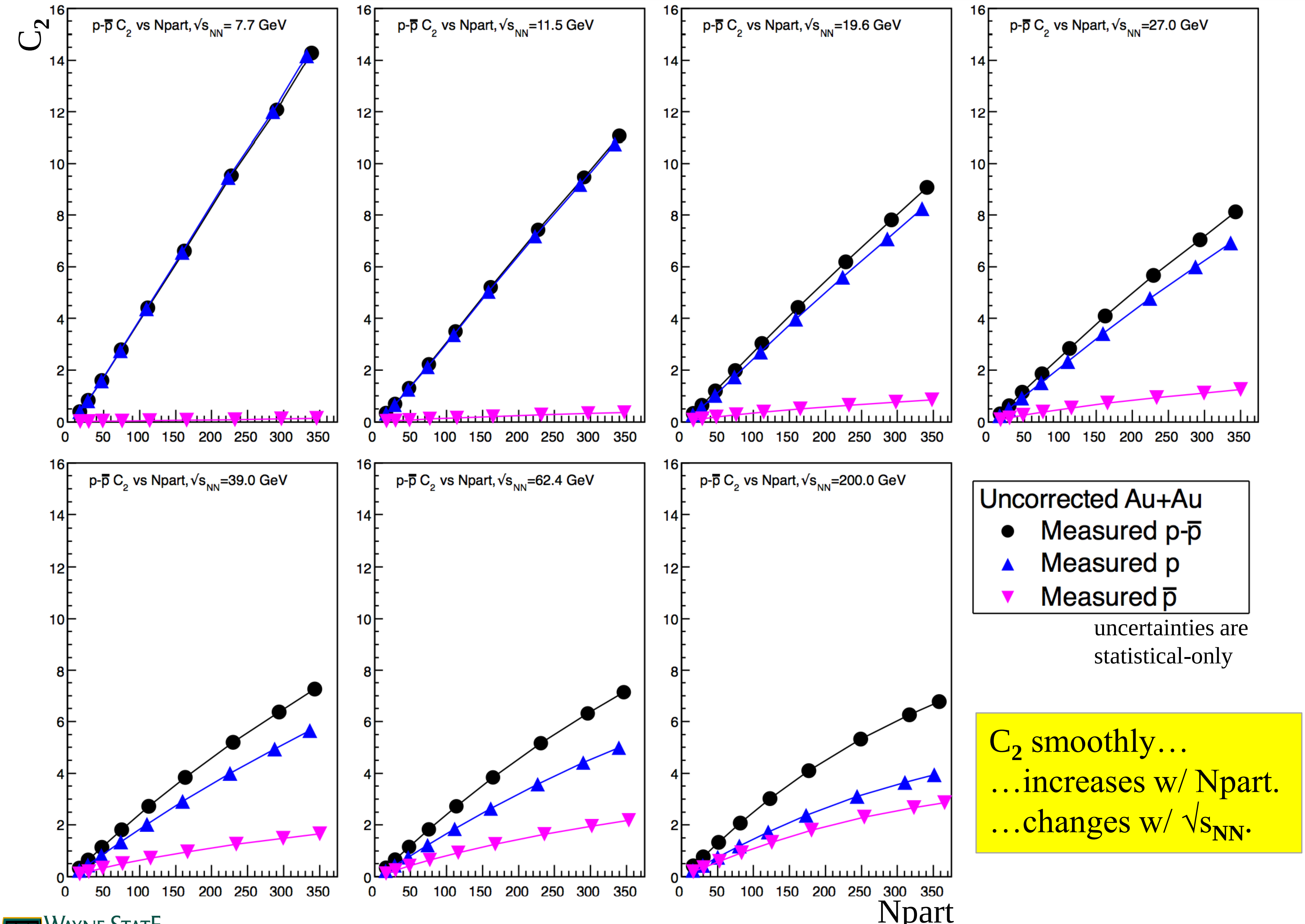

uncertainties are statistical-only

C_2 smoothly…
…increases w/ Npart.
…changes w/ $\sqrt{s_{NN}}$.

Uncorrected net-proton C_4 *vs.* centrality by $\sqrt{s_{NN}}$

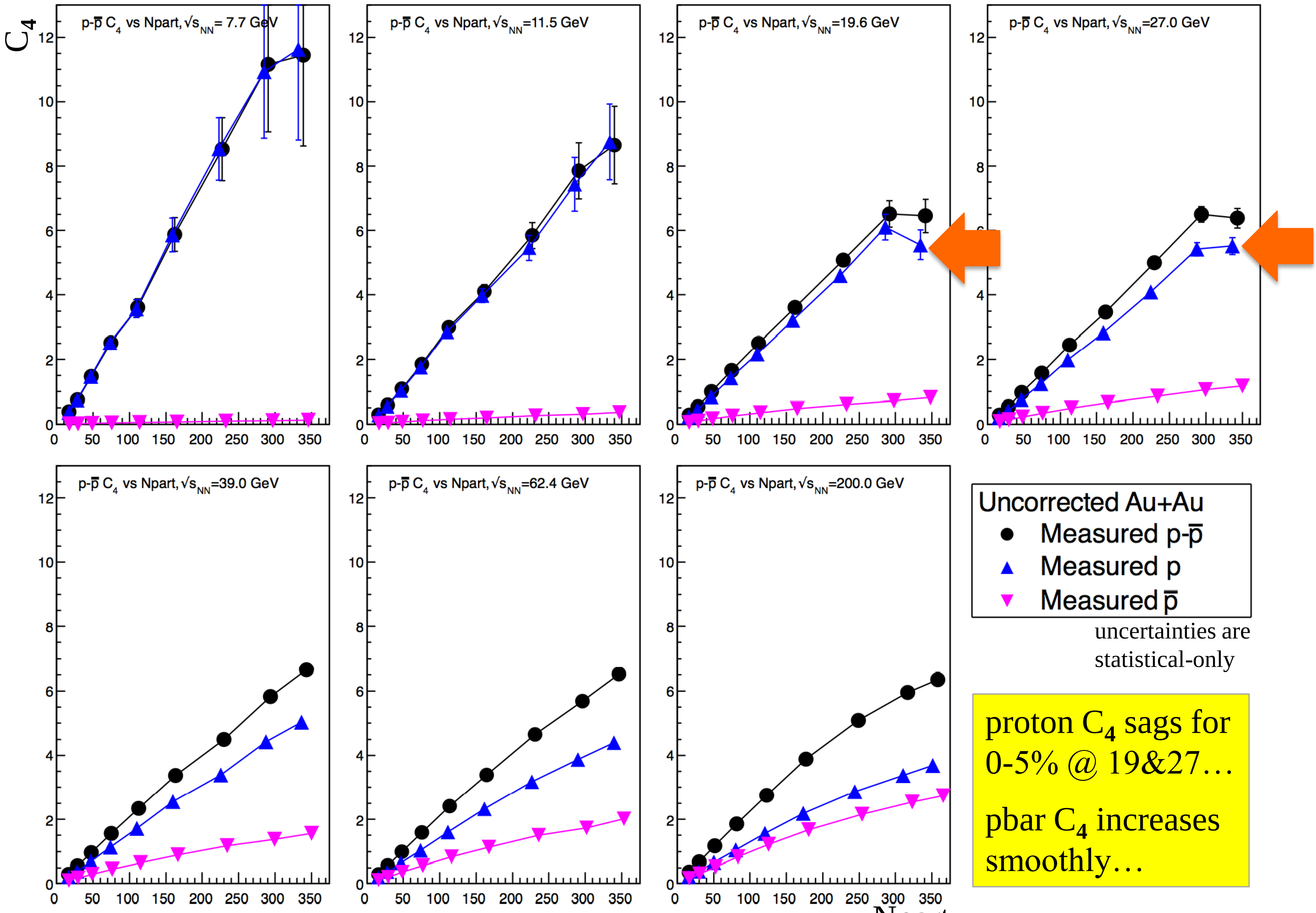

uncertainties are statistical-only

proton C_4 sags for 0-5% @ 19&27…

pbar C_4 increases smoothly…

Uncorrected net-proton C_4 *vs.* centrality by $\sqrt{s_{NN}}$

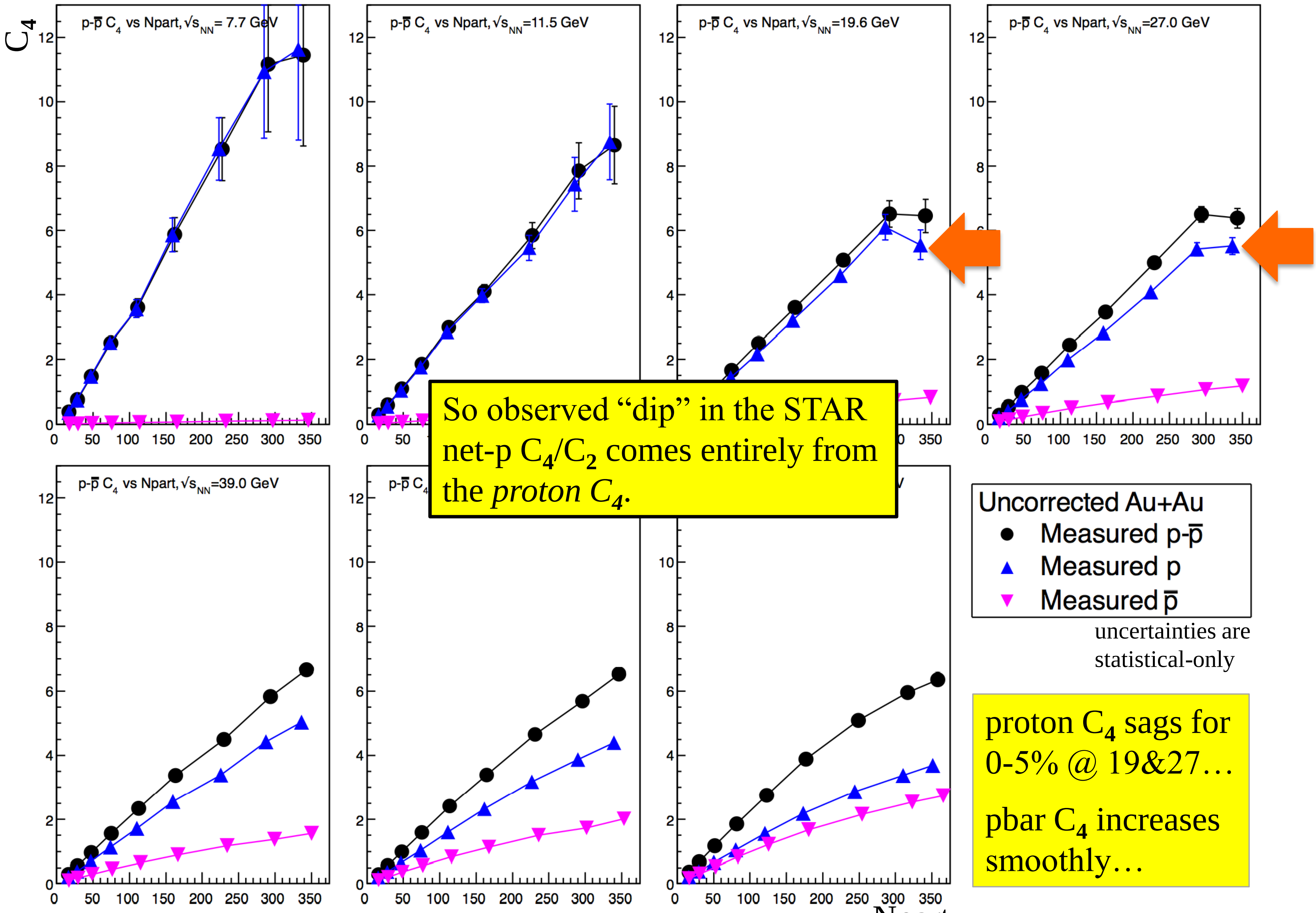

So observed "dip" in the STAR net-p C_4/C_2 comes entirely from the *proton C_4*.

uncertainties are statistical-only

proton C_4 sags for 0-5% @ 19&27…

pbar C_4 increases smoothly…

Kronecker δ's describe Poisson fluctuations (ξ-independent)
Last term describes contribution from critical contributions

Proton/Pion Mixed Cumulant:

$$\begin{aligned}\omega_{ipj\pi} &= \delta_{i,0} + \delta_{j,0} + \frac{\tilde{\lambda}'_r\,(r-1)!}{T^{r/2}}\,\frac{\alpha_p^i}{n_p^{i/r}}\,\frac{\alpha_\pi^j}{n_\pi^{j/r}}\,\xi^{\frac{5}{2}r-3} \quad (2.19)\\ &= \delta_{i,0} + \delta_{j,0} + \omega_{ipj\pi}^{\text{prefactor}}\left(\frac{n_p}{n_0}\right)^{i-\frac{i}{r}}\left(\frac{\xi}{\xi_{\max}}\right)^{\frac{5}{2}r-3},\end{aligned}$$

Net-Proton/Pion Mixed Cumulant:

$$\omega_{i(p-\bar{p})j\pi} = \delta_{i,0} + \delta_{j,0} + \omega_{i(p-\bar{p})j\pi}^{\text{prefactor}}\left(\frac{n_{p-\bar{p}}}{n_0}\right)^{i-\frac{i}{r}} \times\left(\frac{n_{p-\bar{p}}}{n_p+n_{\bar{p}}}\right)^{\frac{i}{r}}\left(\frac{\xi}{\xi_{\max}}\right)^{\frac{5}{2}r-3},$$

Which is more sensitive (for i≠0 and any j): $\omega_{ipj\pi}$ or $\omega_{i(p\text{-}pbar)j\pi}$?

At any value of the correlation length, ξ, the n_p-dependence that enters into the expressions ω_{4p} and $\omega_{4(p\text{-}pbar)}$ is: at $\sqrt{s_{NN}}$ = 200, 62, 19, 7.7 respectively

$$\left(\frac{n_p}{n_0}\right)^3 = 0.34,\ 0.77,\ 4.9,\ 31$$

$$\left(\frac{n_{p-\bar{p}}}{n_0}\right)^3\left(\frac{n_{p-\bar{p}}}{n_p+n_{\bar{p}}}\right) = 0.00072,\ 0.064,\ 3.4,\ 30.$$

Since n(net-p) < n(p) & n(p+pbar), proton normalized cumulant, ω_{ip}, is more sensitive to critical fluctuations than the net-proton normalized cumulant, $\omega_{i(p\text{-}pbar)}$

At assumed μ_B^C = 400 MeV and benchmark values of the couplings g_p and g_π, then
ω_{4p} is the most sensitive to critical fluctuations.
However if μ_B^C << 400 MeV and/or g_p/g_π is smaller than expected, then
$\omega_{4\pi}$ is the most sensitive to critical fluctuations.

Athanasiou, Rajagopal, & Stephanov, **PRD** 82, 074008 (2010)

TABLE I: Parameter dependence of the contribution of critical fluctuations to various particle multiplicity cumulant ratios. We have subtracted the Poisson contribution from each cumulant before taking the ratio. The table shows the power at which the parameters enter in each case. We only considered cases with $r \equiv i+j = 2, 3, 4$. We defined $2\tilde{\lambda}_3^2 - \tilde{\lambda}_4 \equiv \tilde{\lambda}_4'$.

ratio	V	$n_p(\mu_B)$	g_p	g_π	$\tilde{\lambda}_3$	$\tilde{\lambda}_4'$	ξ
N_π	1	-	-	-	-	-	-
N_p	1	1	-	-	-	-	-
$\kappa_{ipj\pi}$	1	i	i	j	$\delta_{r,3}$	$\delta_{r,4}$	$\frac{5}{2}r-3$
$\omega_{ipj\pi}$	-	$i-\frac{i}{r}$	i	j	$\delta_{r,3}$	$\delta_{r,4}$	$\frac{5}{2}r-3$
$\kappa_{ipj\pi}N_\pi^{i-1}/N_p^i$	-	-	i	j	$\delta_{r,3}$	$\delta_{r,4}$	$\frac{5}{2}r-3$
$\kappa_{2p2\pi}N_\pi/\kappa_{4\pi}\kappa_{2p}$	-	-	-	-2	-	-	-2
$\kappa_{4p}N_\pi^2/\kappa_{4\pi}\kappa_{2p}^2$	-	-	-	-4	-	-	-4
$\kappa_{2p2\pi}N_p^2/\kappa_{4p}N_\pi^2$	-	-	-2	2	-	-	-
$\kappa_{3p1\pi}N_p/\kappa_{4p}N_\pi$	-	-	-1	1	-	-	-
$\kappa_{3p}N_p^{3/2}/\kappa_{2p}^{9/4}N_\pi^{1/4}$	-	-	$-3/2$	-	1	-	-
$\kappa_{2p}\kappa_{4p}/\kappa_{3p}^2$	-	-	-	-	-2	1	-
$\kappa_{3p}\kappa_{2\pi}^{3/2}/\kappa_{3\pi}\kappa_{2p}^{3/2}$	-	-	-	-	-	-	-
$\kappa_{4p}\kappa_{2\pi}^2/\kappa_{4\pi}\kappa_{2p}^2$	-	-	-	-	-	-	-
$\kappa_{4p}^3\kappa_{3\pi}^4/\kappa_{4\pi}^3\kappa_{3p}^4$	-	-	-	-	-	-	-
$\kappa_{2p2\pi}^2/\kappa_{4\pi}\kappa_{4p}$	-	-	-	-	-	-	-
$\kappa_{2p1\pi}^3/\kappa_{3p}^2\kappa_{3\pi}$	-	-	-	-	-	-	-

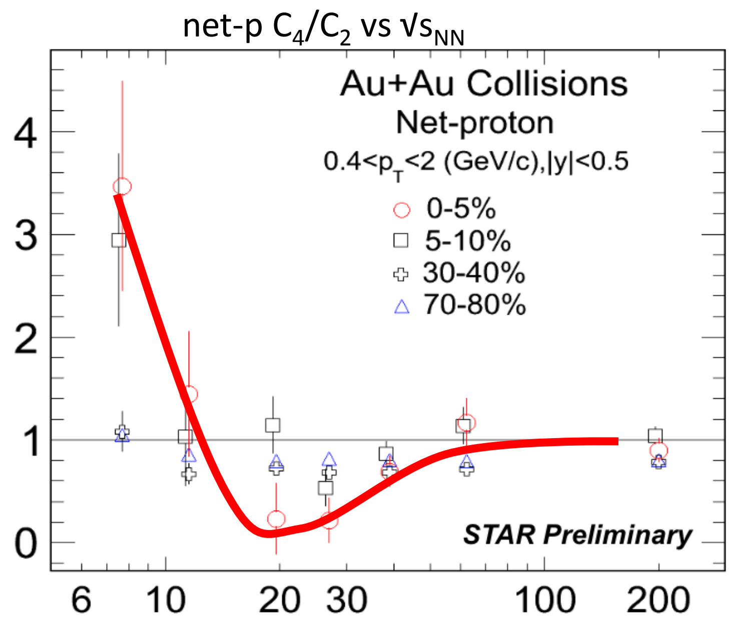

Apparently, C_4/C_2 is exceeding the poisson baseline near and below ~12 GeV.

Are these are critical fluctuations?

Are these 5 mixed cumulant ratios consistent with Poisson?

Minimum multiplicity and systematics

Net-proton "dip" appears to result entirely from proton C4
Consistent with NLSM expectations...

Another aspect:
multiplicities of POI need to be large enough to allow multi-particle correlations

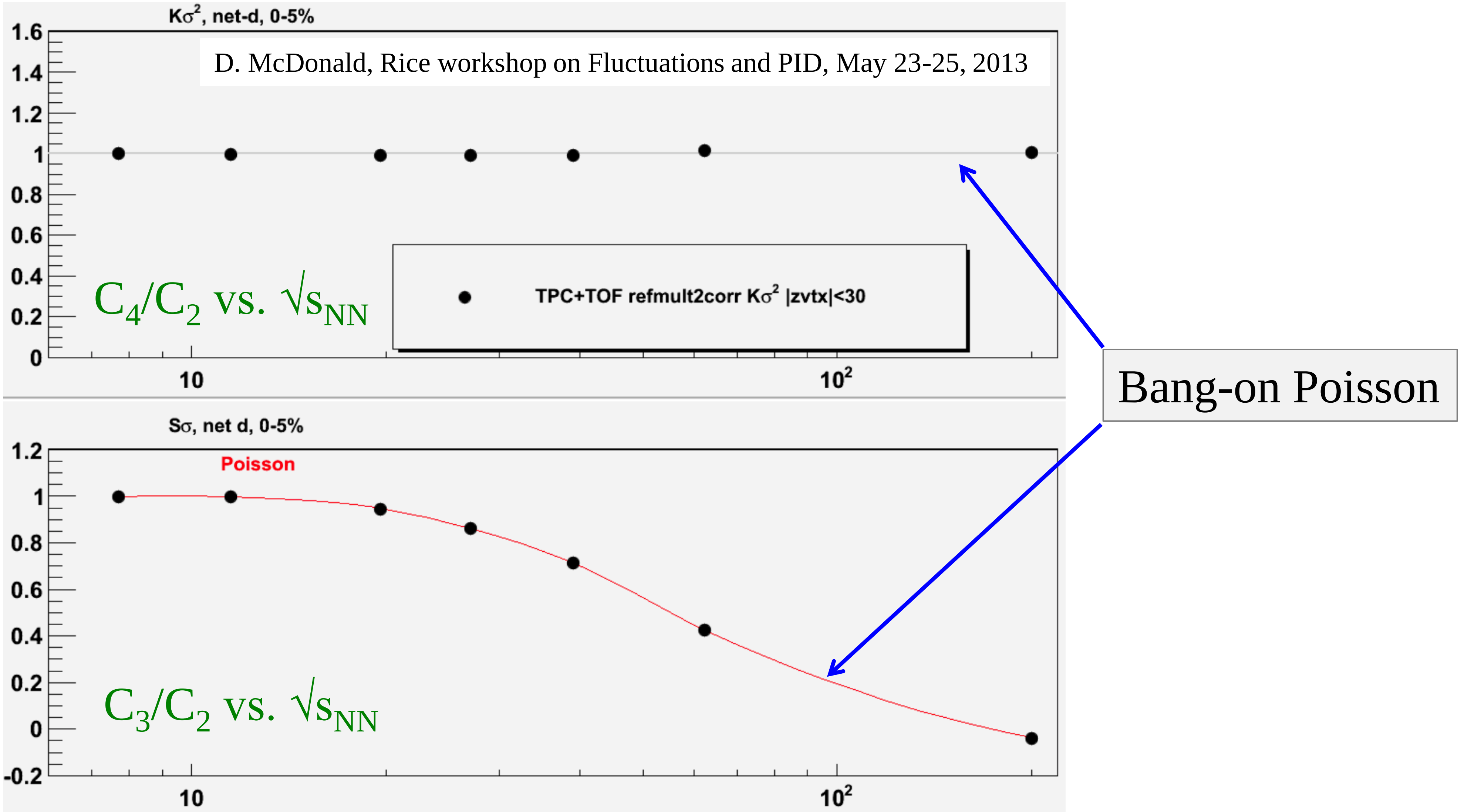

Sensitivity to correlations of Np and Npbar -- Clinical study

Now, let's do a "clinical" study of cumulants ratios with controlled correlations in multiplicity distributions that are realistic compared to experiment.

Consider the following 2D correlation plot....
think X=Nneg, Y=Npos (or vice versa)

The 1D projections are called the "marginals"

The shape of the 2D density of points in the plot of Prob(X,Y) is sensitive to the correlations of X and Y.
"contingency table"

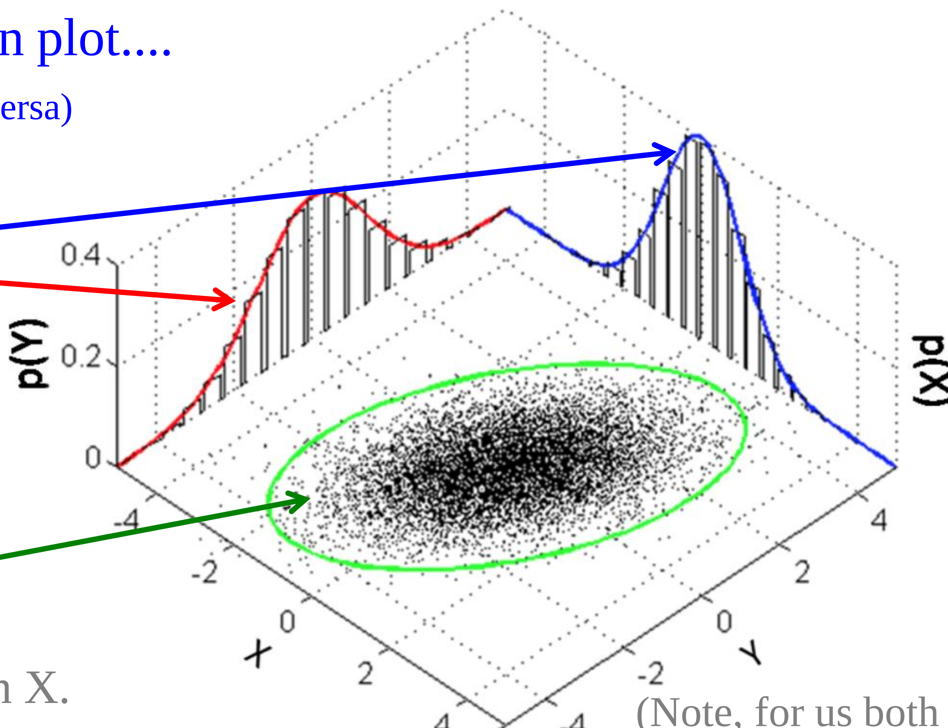

Here, Y is positively correlated with X. An increase in X tends to increase Y.

(Note, for us both marginals are actually non-negative)

1. Take parameters of marginals (p and pbar multiplicity distributions) from data…
2. Generate 2D prob. distribution of controlled strength but leaving marginals unchanged…
3. Look at dependence of cumulants and cumulants ratios *vs.* correlation strength…

Fixed marginals with controlled correlations…

Kocherlakota, S. and Kocherlakota, K. (1992) *Bivariate Discrete Distributions*. New York: Dekker.
Johnson, N., Kotz, S. and Balakrishnan, N. (1997) *Discrete Multivariate Distributions*. New York: Wiley.
D. Karlis & I. Ntzoufras, *The Statistician* (2003) 52, Part 3, pp. 381–393

Poissonian marginals:

Given random variables X_κ, κ=1,2,3, which follow independent Poisson distributions with parameters $\lambda_\kappa > 0$.
Then the random variables $X=X_1+X_3$ and $Y=X_2+X_3$ jointly follow a bivariate Poisson distribution, BP(λ_1, λ_2, λ_3), with the joint probability function with λ_3 as a measure of the correlation strength

$$P_{X,Y}(x,y) = P(X=x, Y=y)$$
$$= \exp\{-(\lambda_1+\lambda_2+\lambda_3)\}\frac{\lambda_1^x}{x!}\frac{\lambda_2^y}{y!}\sum_{k=0}^{\min(x,y)}\binom{x}{k}\binom{y}{k}k!\left(\frac{\lambda_3}{\lambda_1\lambda_2}\right)^k$$

A. Biswas & J.-S. Hwang, Statistics and Probability Letters, **60** (2002) 231-240

Binomial marginals:

Marginals: $C_1^{\,i} = p_i n_i$

$C_2^{\,i} = (1\text{-}p_i)\, p_i\, n_i$

where i=x,y (*a.k.a.* pos and neg)

Controlled correlation parameter here is α…

Here we propose a model by assuming $n_2 \geqslant n_1$. The other case can be similarly dealt with. In this present paper we propose the following probability model:

$$\Pr(Y_1=y_1, Y_2=y_2) = \binom{n_1}{y_1} p_1^{y_1}(1-p_1)^{n_1-y_1} \times f(y_2|y_1), \tag{1.1}$$

where

$$f(y_2|y_1) = (1+\alpha)^{-n_1}\sum_{(j_1,j_2,j_3)\in S}\binom{y_1}{j_1}\binom{n_1-y_1}{j_2}\binom{n_2-n_1}{j_3}\{p_2+\alpha(p_2-p_1)+\alpha\}^{j_1}$$
$$\times\{1-p_2-\alpha(p_2-p_1)\}^{y_1-j_1}\{p_2+\alpha(p_2-p_1)\}^{j_2}$$
$$\times\{1-p_2-\alpha(p_2-p_1)+\alpha\}^{n_1-y_1-j_2}p_2^{j_3}(1-p_2)^{n_2-n_1-j_3}, \tag{1.2}$$

with $S=\{(j_1,j_2,j_3): j_1+j_2+j_3=y_2; j_1=0,1,\ldots,y_1; j_2=0,1,\ldots,n_1-y_1; j_3=0,1,\ldots,n_2-n_1\}$. Although the model is complicated in its expression, it can be derived from a simple conditioning mechanism. From the discussions of Section 2, it will follow that for model (1.1) and (1.2), marginally Y_1 and Y_2 are simple binomials, and they have a correlation coefficient

$$\rho = \sqrt{\frac{m}{M}}\left(\frac{\alpha}{1+\alpha}\right)\sqrt{\frac{p_1(1-p_1)}{p_2(1-p_2)}}, \tag{1.3}$$

where $m=\min(n_1,n_2)$ and $M=\max(n_1,n_2)$.

Clinical approach

Fix the marginals to be Poisson or Binomial, take the pos and neg C_1 (and C_2) parameters of these distributions from experimentally measured distributions

Then vary a parameter in a numerical prescription from anticorrelation to no correlation to correlation but without changing the marginals!

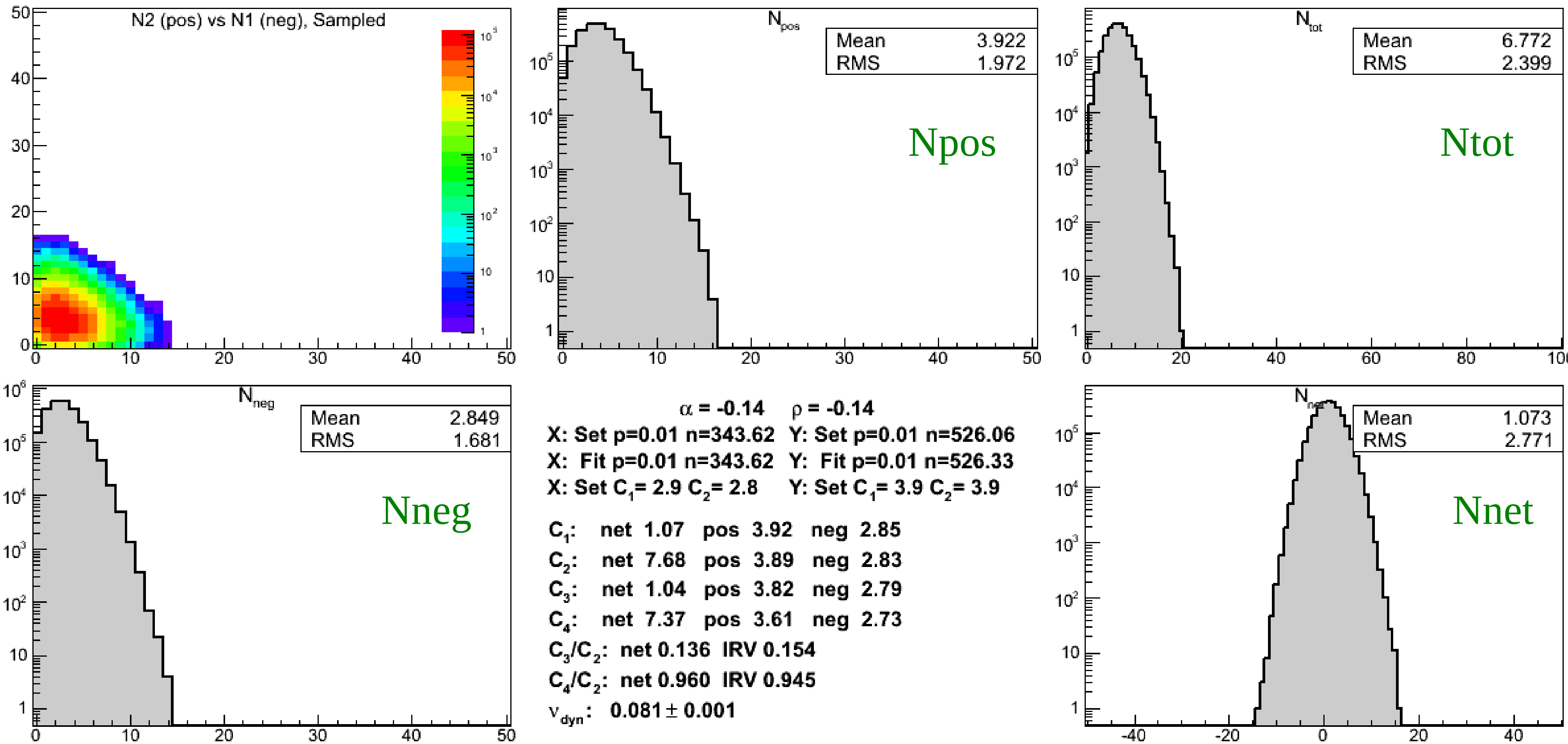

Poisson marginals, C_1pos and C_1neg from net-p, 0-5%, 200 GeV

Let's get quantitative!

x-axis in all frames is ρ
(controlled correlation parameter)
Black: net mult, controlled correlation
Gray: net mult, sampled singles/IRV

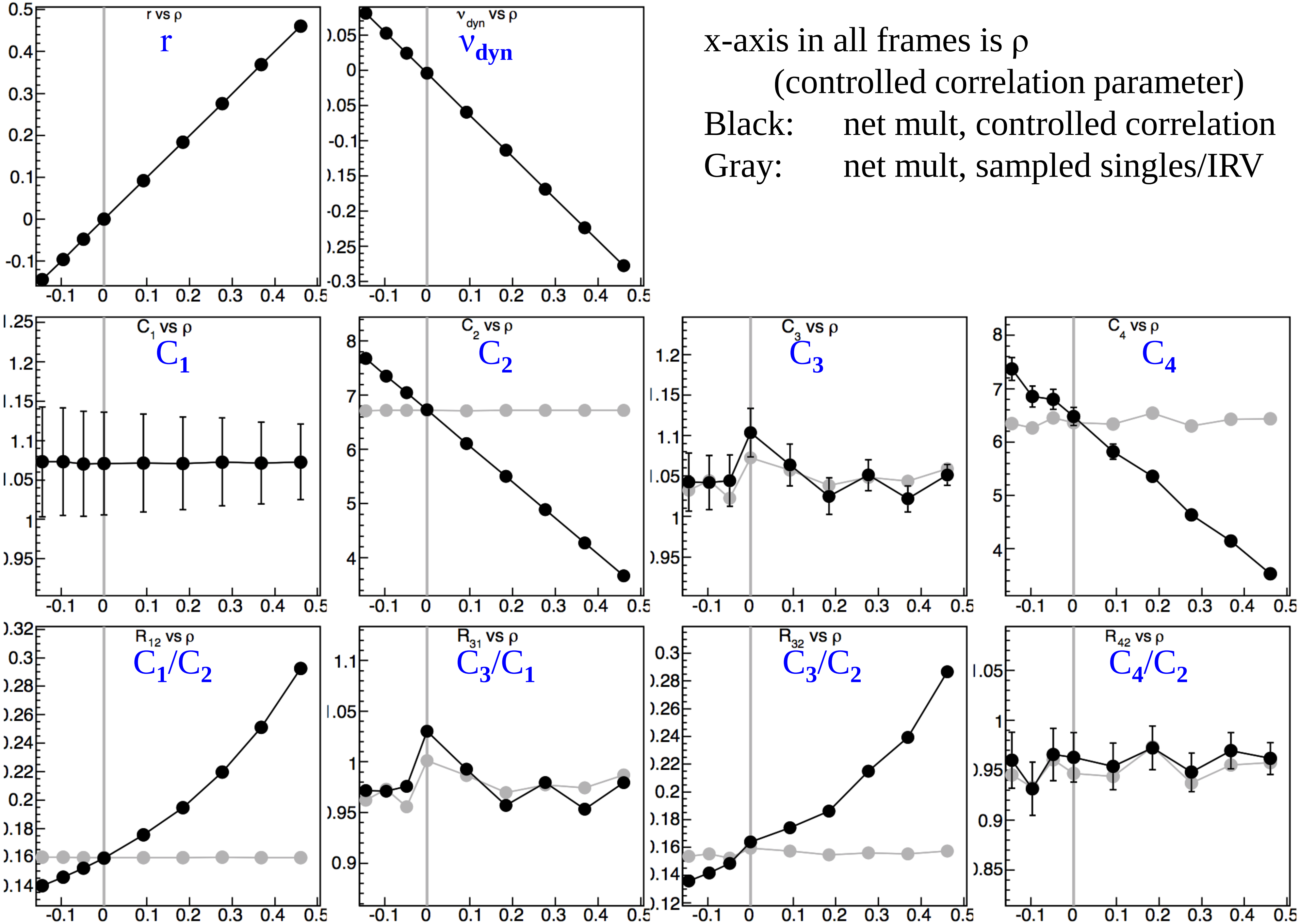

Let's get quantitative!

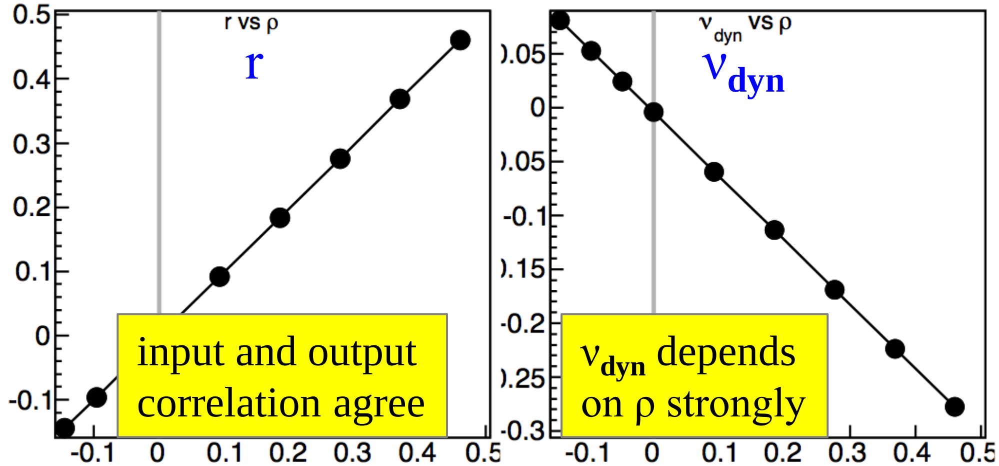

x-axis in all frames is ρ
(controlled correlation parameter)

Black: net mult, controlled correlation

Gray: net mult, sampled singles/IRV

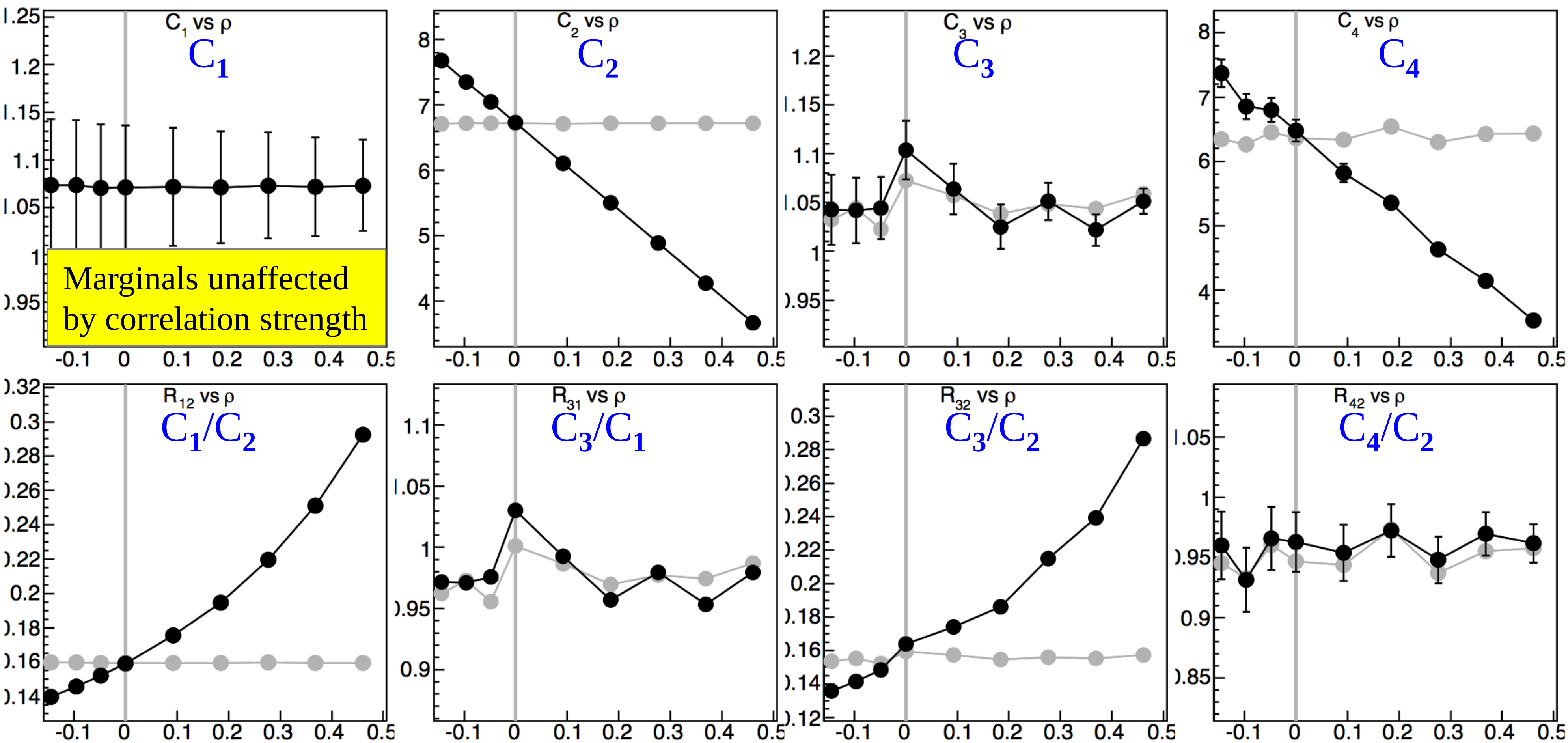

Let's get quantitative!

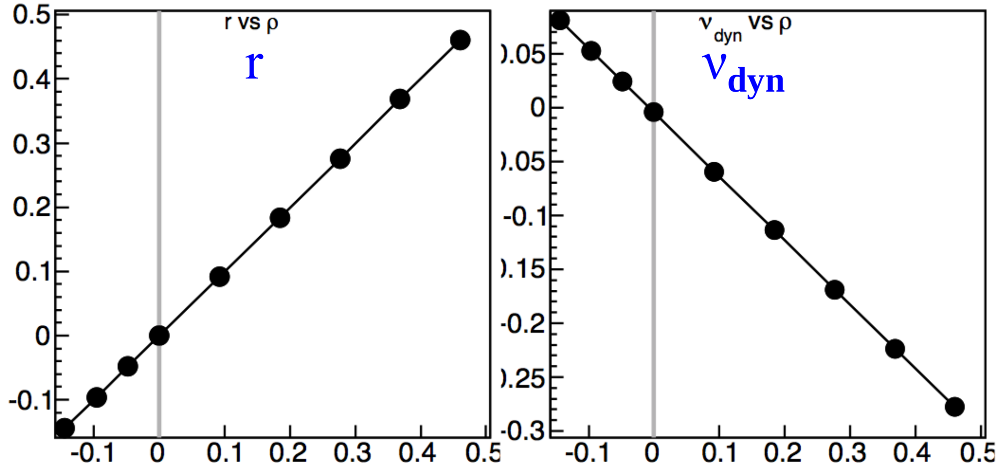

x-axis in all frames is ρ
(controlled correlation parameter)
Black: net mult, controlled correlation
Gray: net mult, sampled singles/IRV

Black and gray must agree when ρ=0 (and they do)

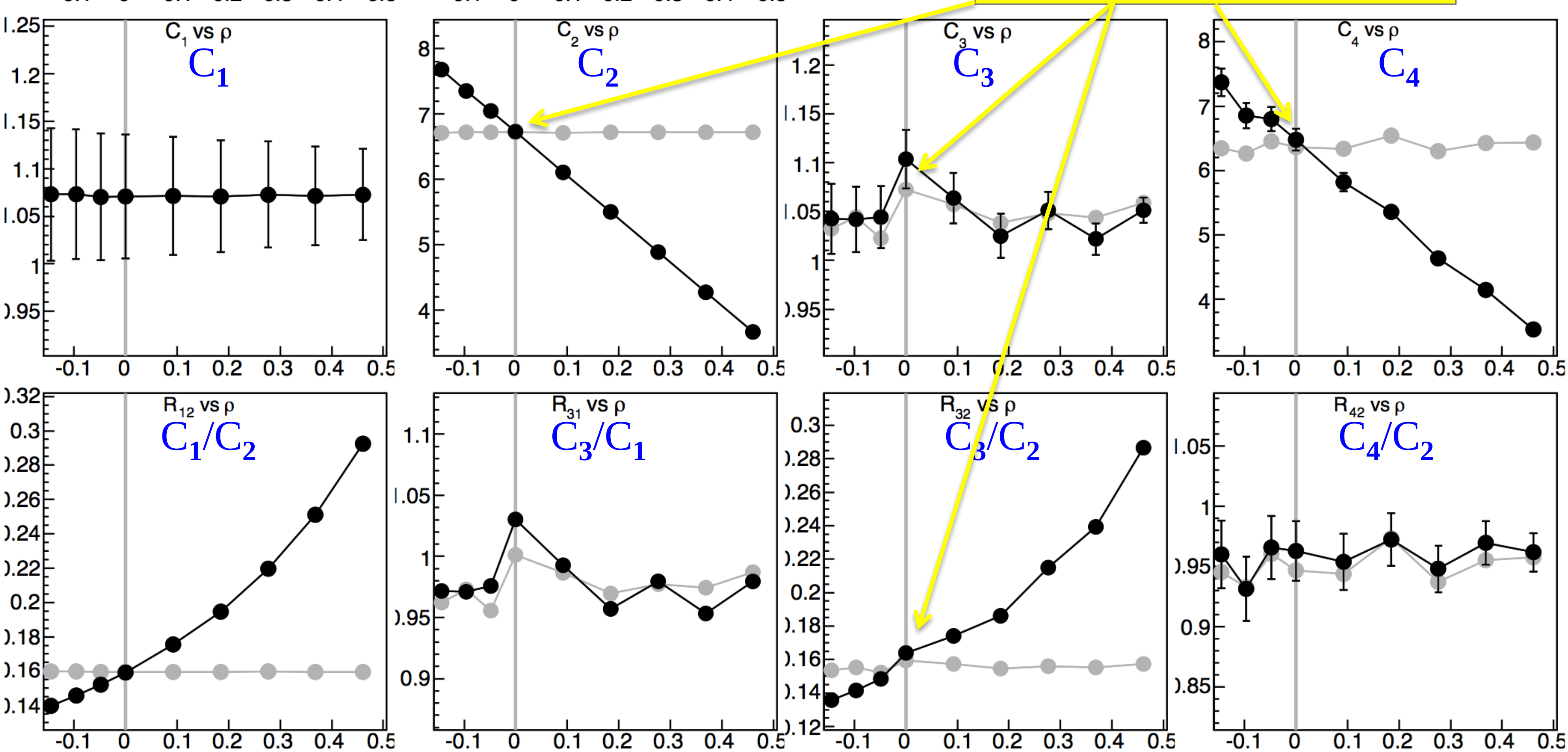

Let's get quantitative!

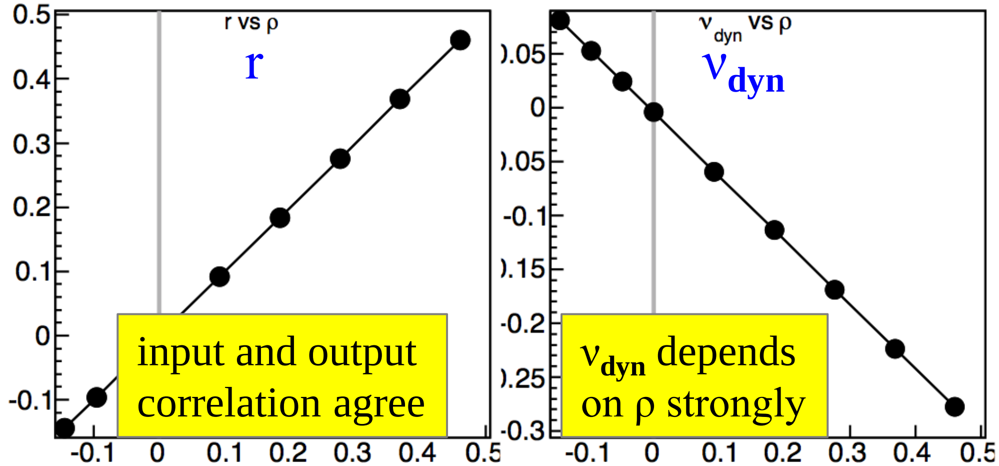

x-axis in all frames is ρ
(controlled correlation parameter)

Black: net mult, controlled correlation

Gray: net mult, sampled singles/IRV

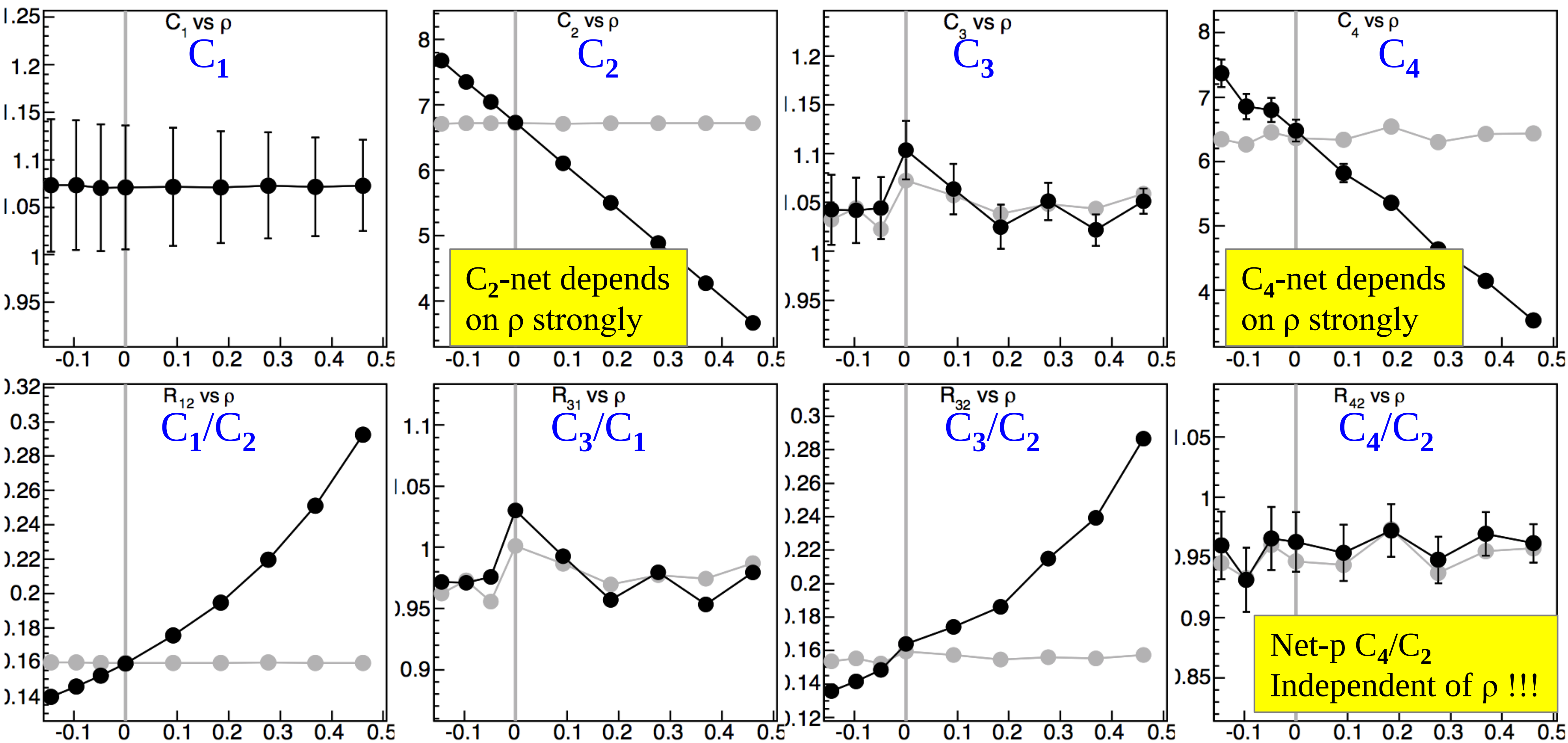

Now let's do the same thing at 11.5 GeV

marginals for net-p 0-5% at 11.5 GeV

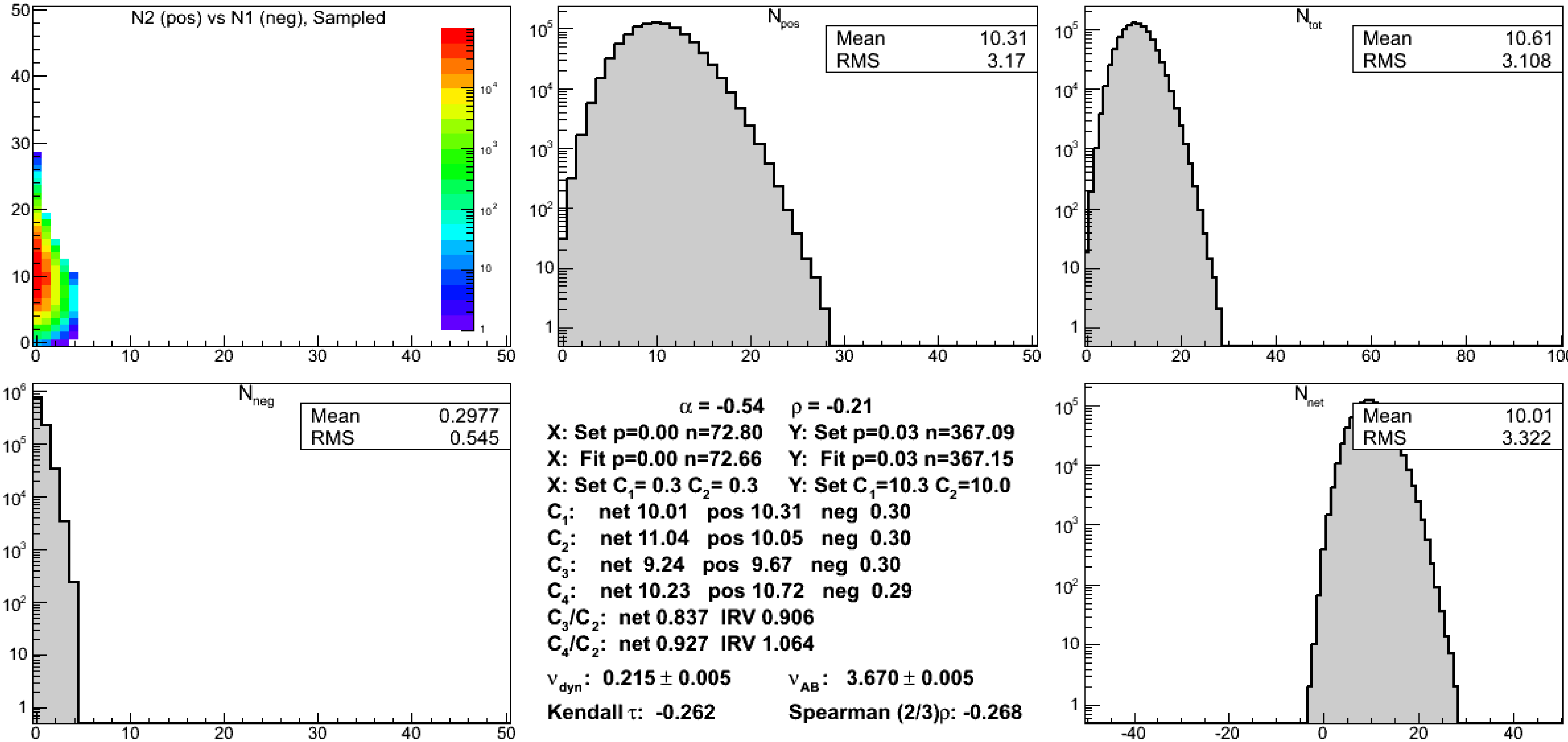

absolutely measurable intra-event correlations in C_2 and C_4 & the various correlation indices.

This is *not* about C_1neg (pbar) being so small there can't be any effect from correlations, it's about C_2neg being large enough to see the possible intra-event correlations… And it is!

Fine-tuning the experimental control of μ_B?

We tacitly assume that a tight (0-5%) centrality cut at a given beam energy tightly constrains the events on the phase diagram…

If this is not true, then the experimental signal could be buried by events that are not near enough to the critical point to result in the expected enhancements to the moments products.

What is the *variance* of μ_B in such samples of events?

This question was studied by coupling URQMD and THERMUS.

- URQMD 3.3p1, default parameters, six centrality bins
  - save identified particle multiplicities in 1fm/c time-steps
- run Thermus for each time-step in each event, GCE

$\sqrt{s_{NN}}$	$\langle\mu_B\rangle$*
7.7	421
11.5	316
19.6	206
27	156
39	112
62.4	73
200	24

* Cleymans *et al.* PRC **73**, 034905 (2006)

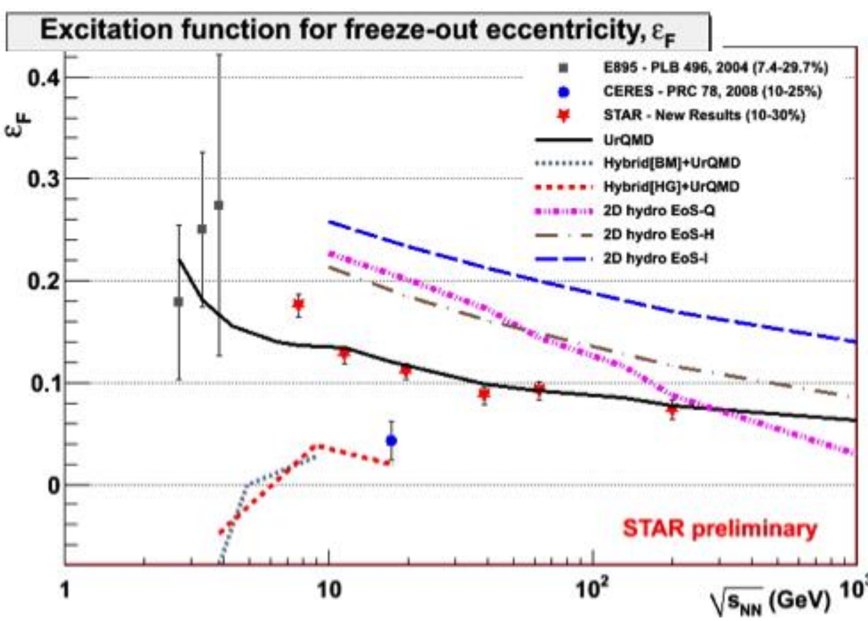

M. Lisa, Workshop On Fluctuations, Correlations and RHIC LE Runs, BNL, Oct 2011

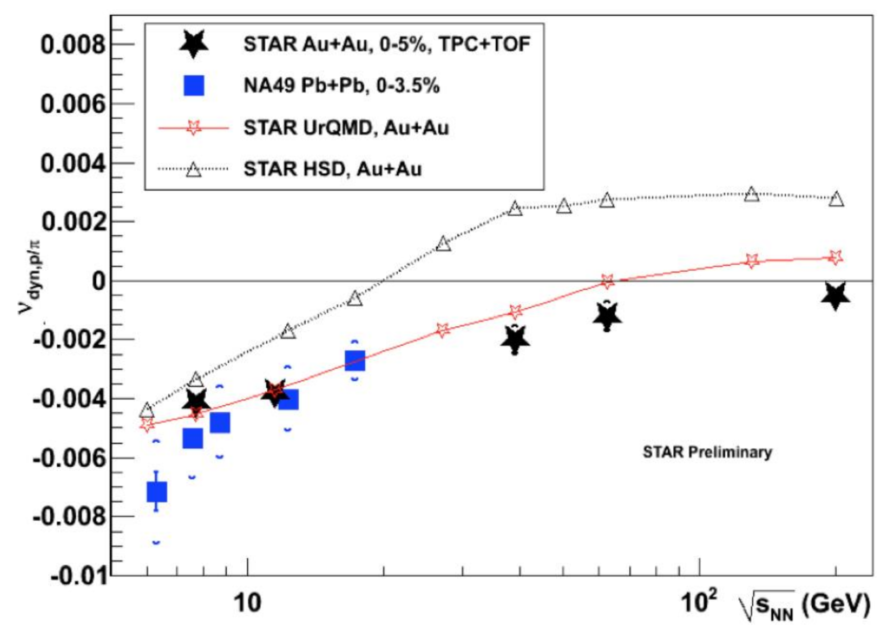

T. Tarnowsky for STAR, QM2011

Example Fits of a single event *vs.* time, 19.6 GeV, 0-5%

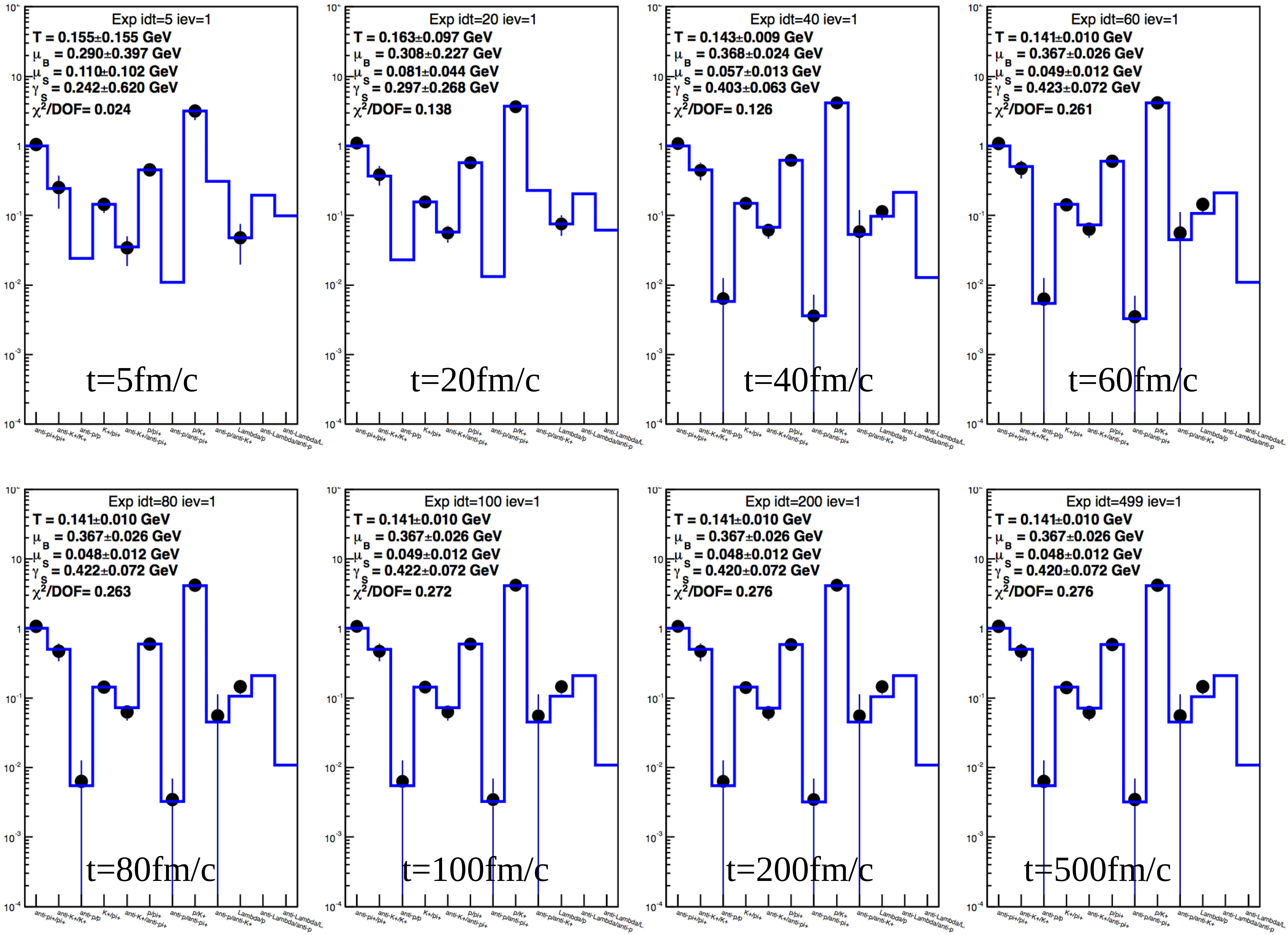

Example Fits of a single event *vs* time, 200 GeV, 0-5%

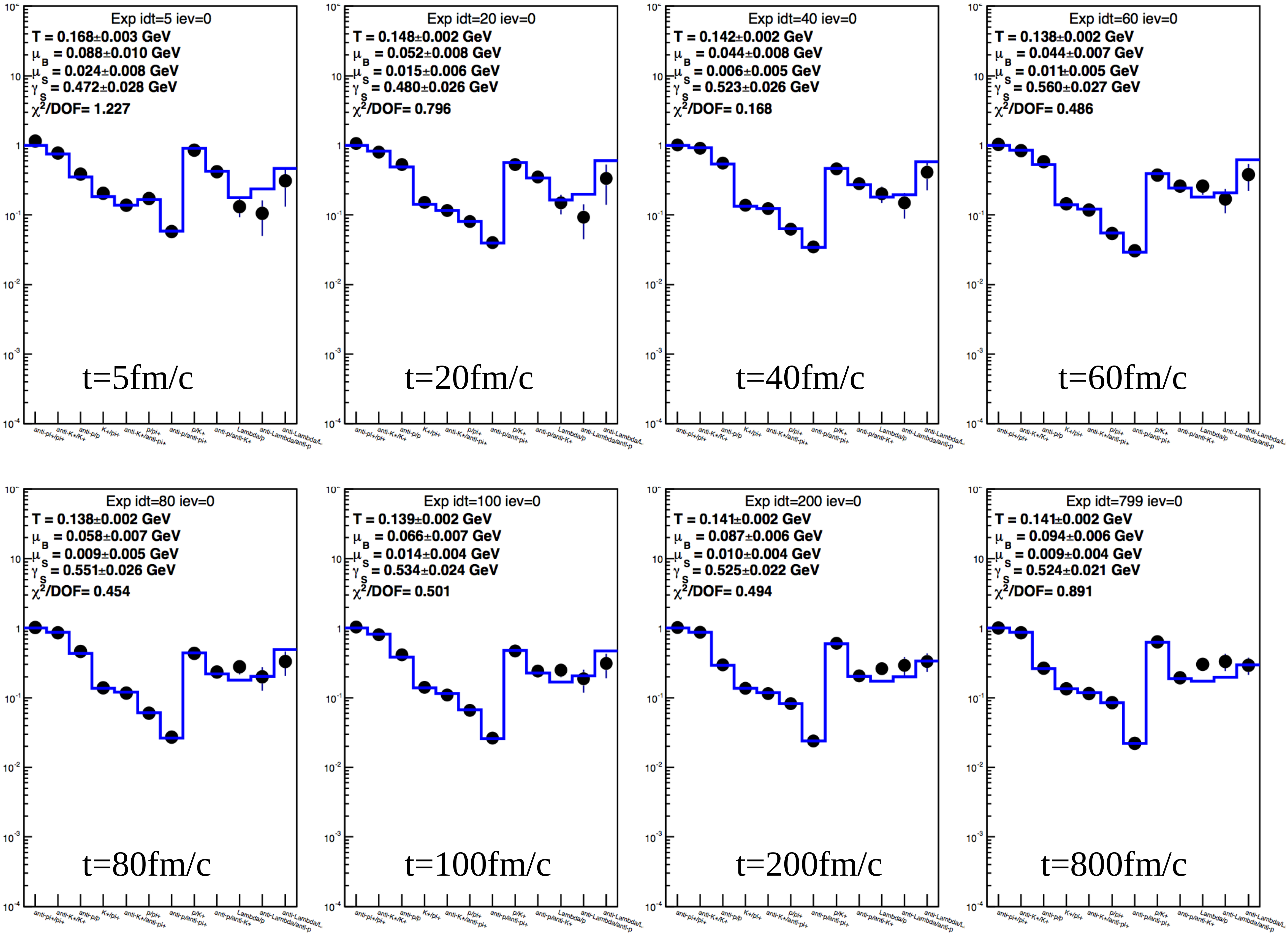

Example time dependence of the ratios, 200 GeV, 0-5%

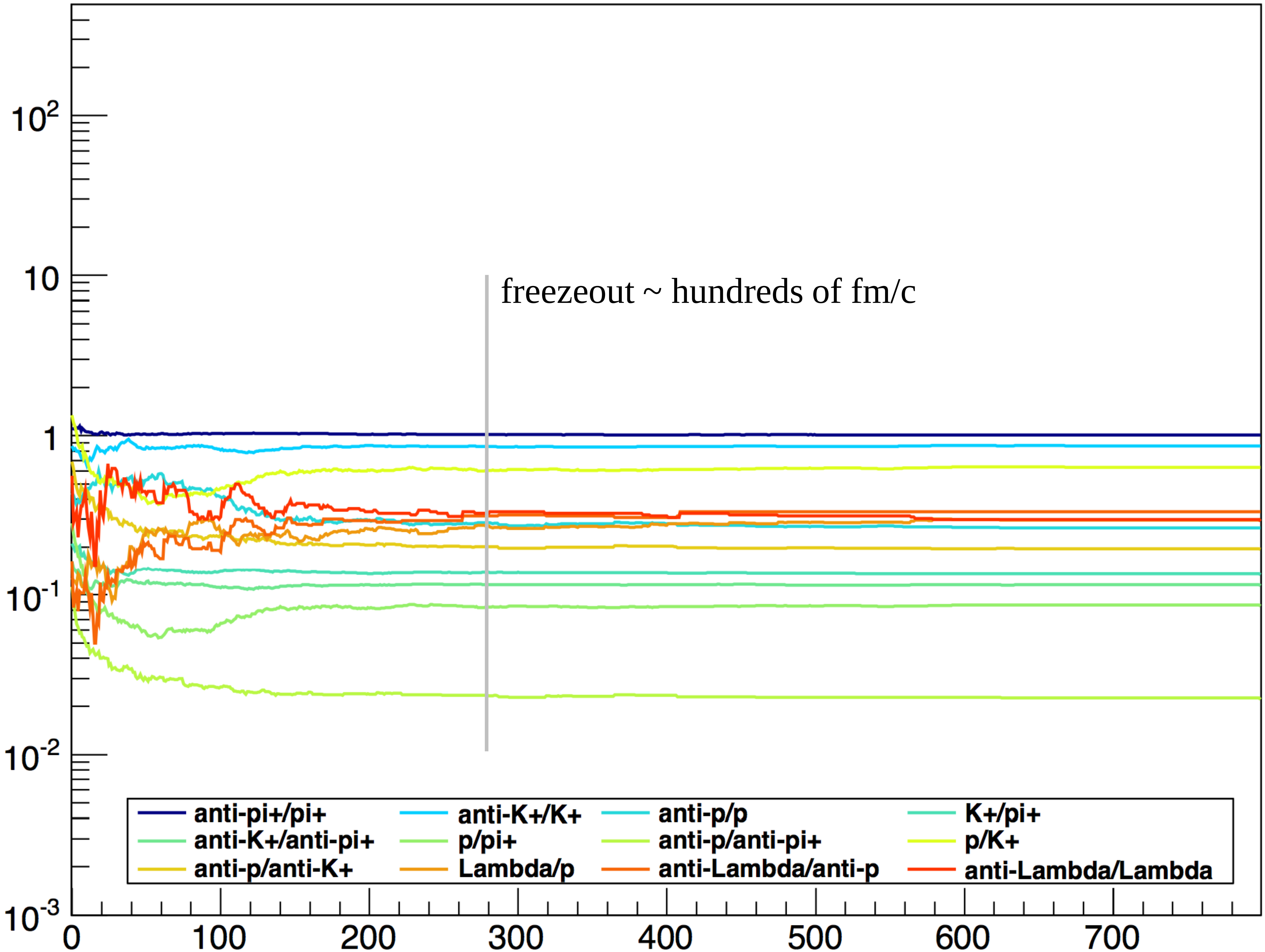

Fit Examples, UrQMD by root-s and centrality

60-80% 40-60% 20-40% 10-20% 5-10% 0-5%

7.7

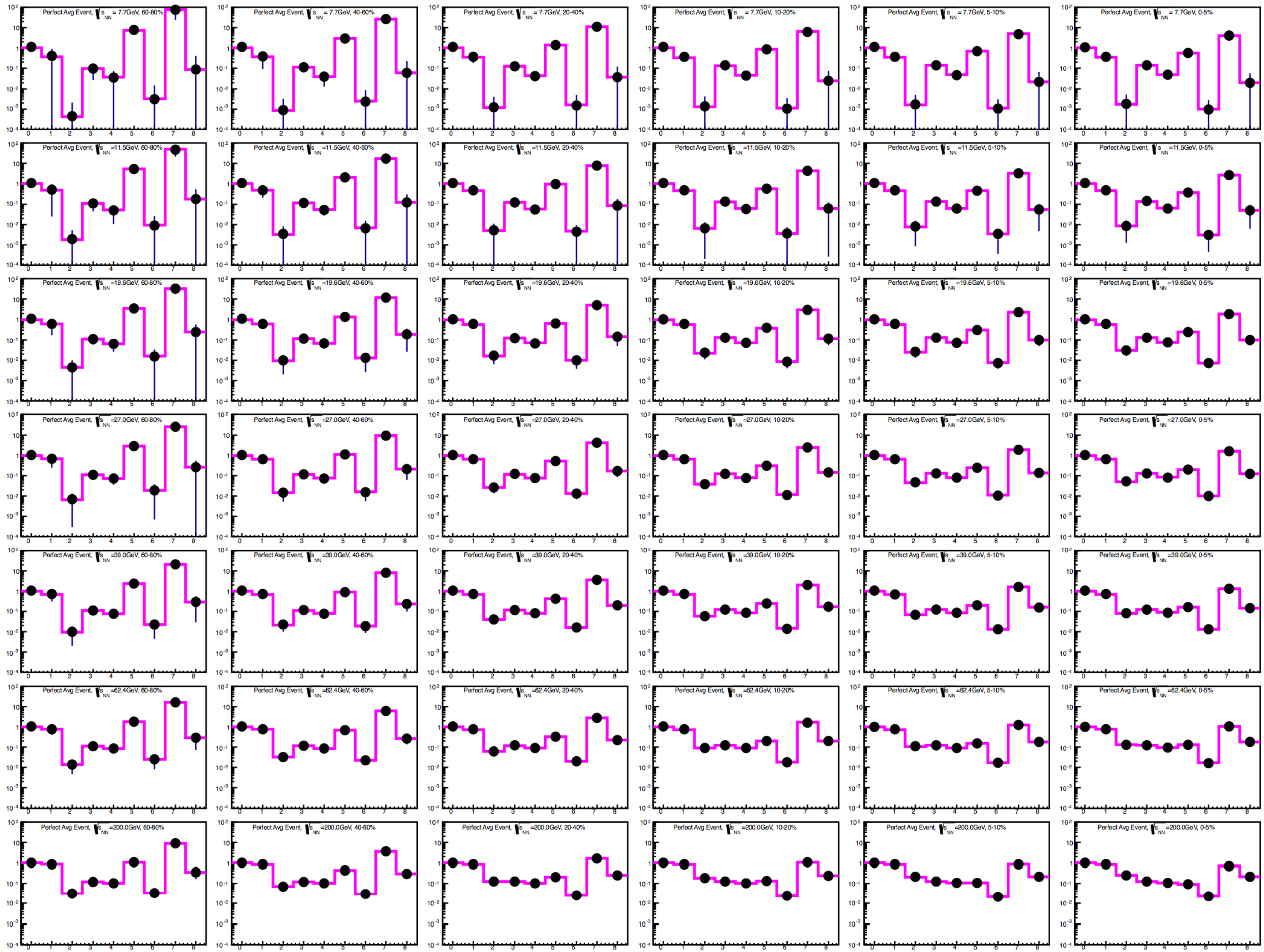

200

μ_B distributions at freeze-out, 0-5% and 5-10% central

Run UrQMD to 500-800 fm/c in each of thousands of events, plot Probability(μ_B) by $\sqrt{s_{NN}}$

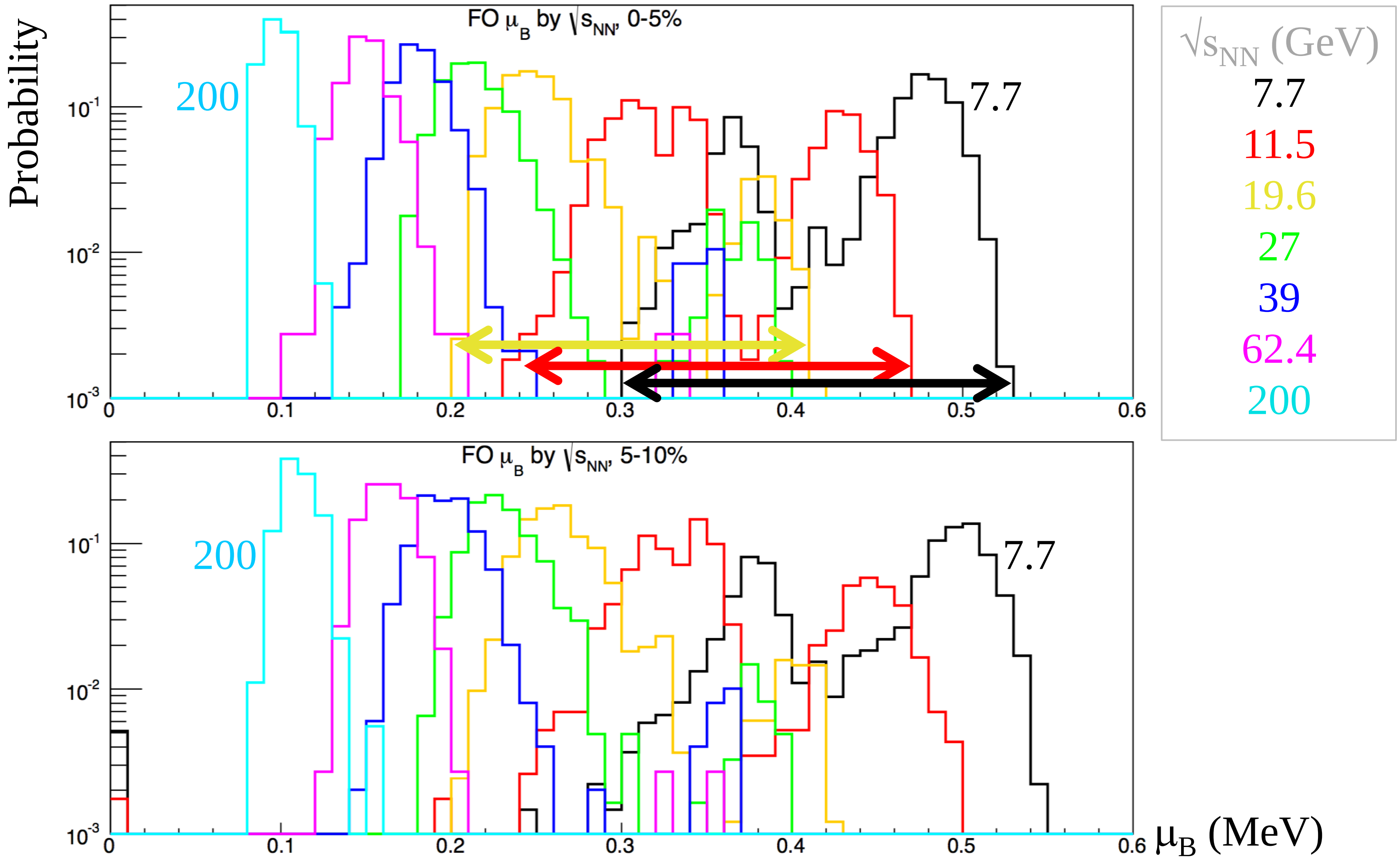

For the μ_B range of interest (μ_B>~200MeV), the μ_B distributions are ~200 MeV wide!
Compare to expected μ_B-width of critical enhancement of $\Delta(\mu_B)$~50-100 MeV…

C. Athansiou *et al.*, PRD **82**, 074008 (2010), R. Gavai & S. Gupta, PRD **78**, 114503 (2008)

Use event-by-event values of pbar/p to constrain event-by-event values of μ_B

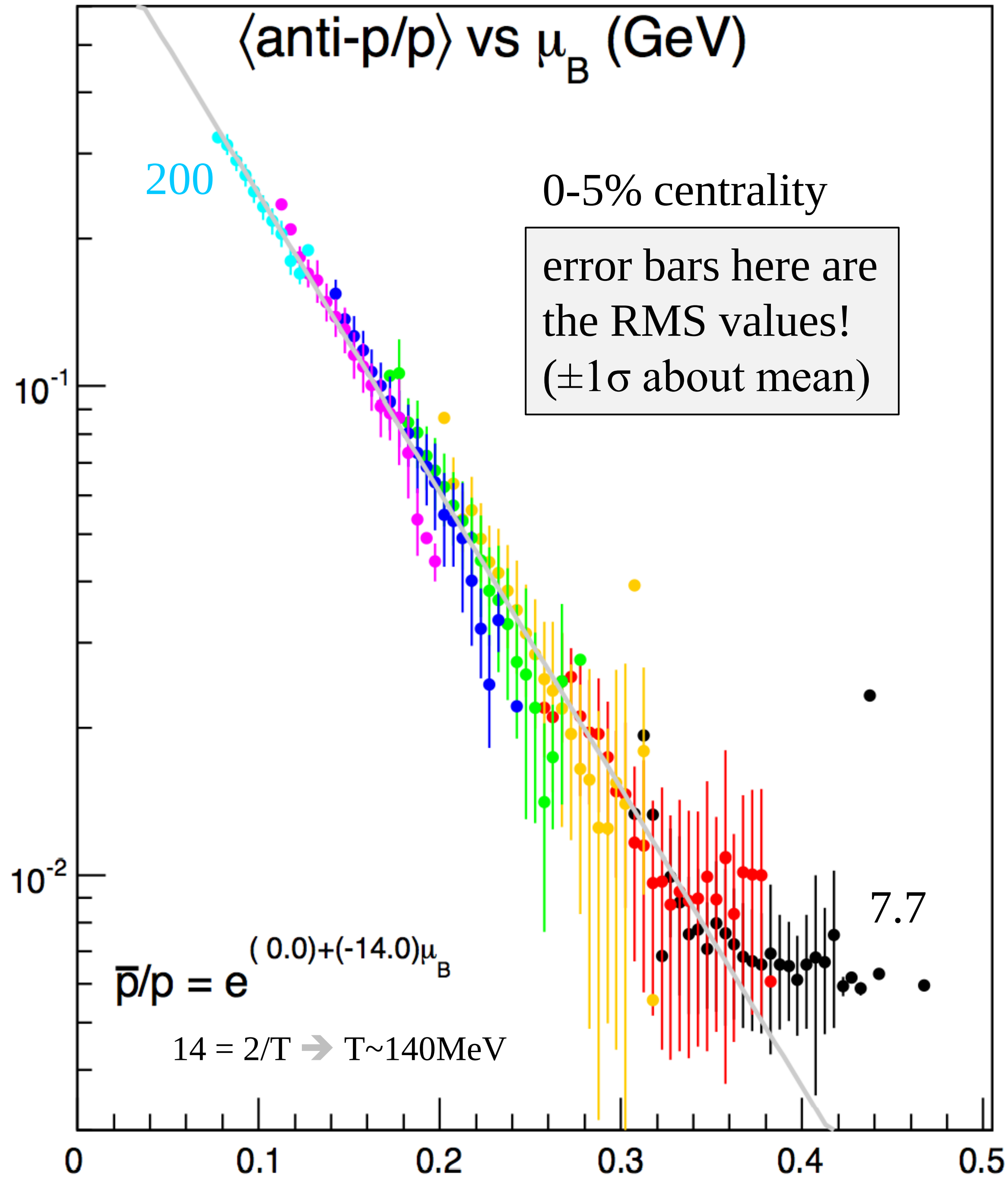

Use event-by-event pbar/p ratio to gate the moments analyses!

$$\text{pbar/p} = \exp(-2\mu_B/T)$$

Temperature is a weak function of centrality and $\sqrt{s_{NN}}$

S. Das for STAR, QM2012

➔ Direct relationship between pbar/p and apparent μ_B values event-by-event!

Significant overlap in μ_B distributions from different root-s values even in 0-5% central collisions

trend also holds for less central events w/ non-zero pbar and p multiplicities

Use event-by-event values of pbar/p to constrain event-by-event values of μ_B

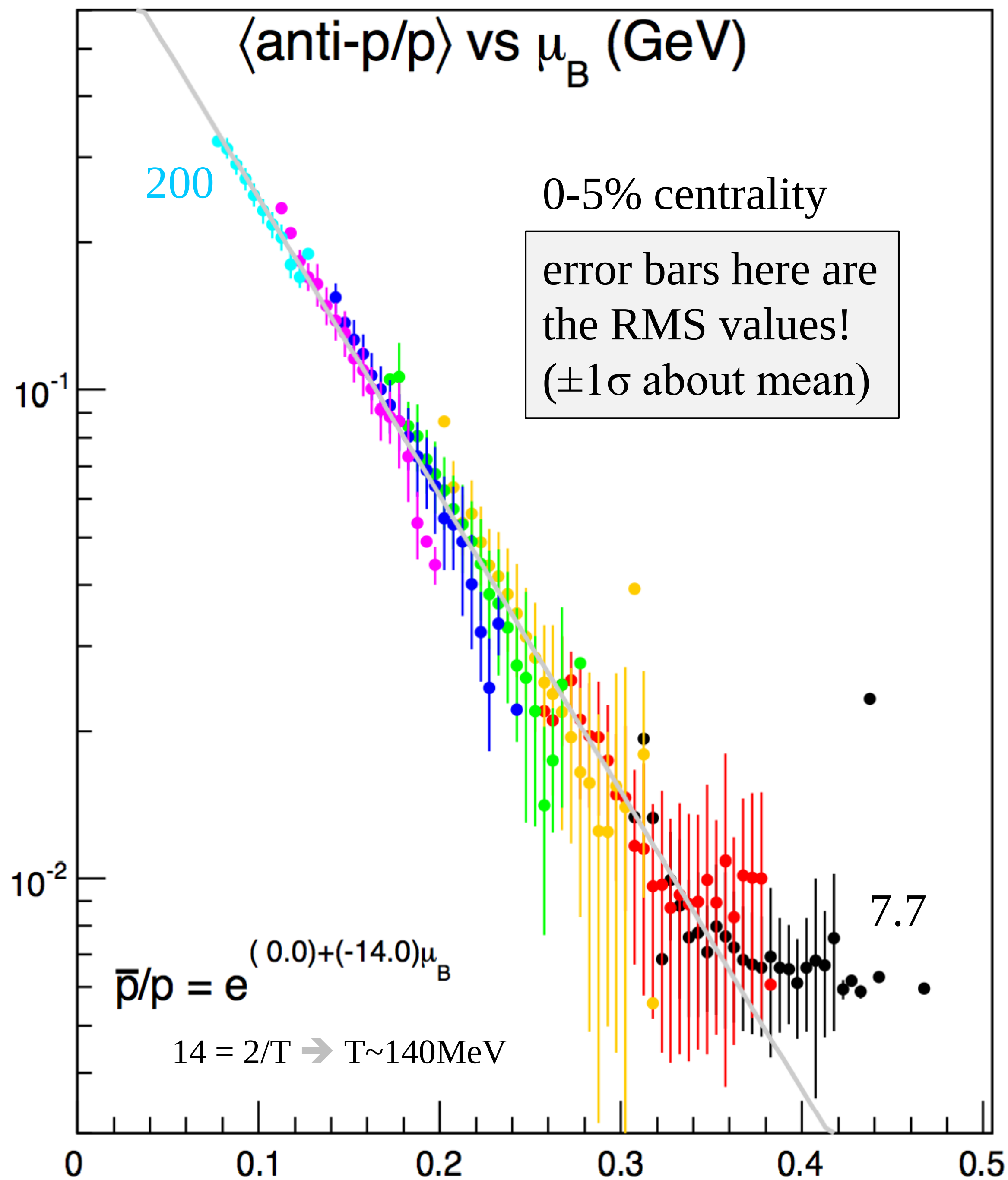

Bin	$\bar{p}/p$ ratio	μ_B (GeV)
1	0.020-0.029	0.279-0.252
2	0.029-0.043	0.252-0.225
3	0.043-0.063	0.225-0.197
4	0.063-0.093	0.197-0.170
5	0.093-0.136	0.170-0.142
6	0.136-0.200	0.142-0.115
7	0.200-0.294	0.115-0.088
8	0.294-0.431	0.088-0.060
9	0.431-0.632	0.060-0.033
10	0.632-0.928	0.033-0.005
11	0.928-1.363	0.005-$^{-}$0.022

Net-K C_4/C_2 gated on pbar/p

D. McDonald, Ph.D. Thesis, Rice University (2013)

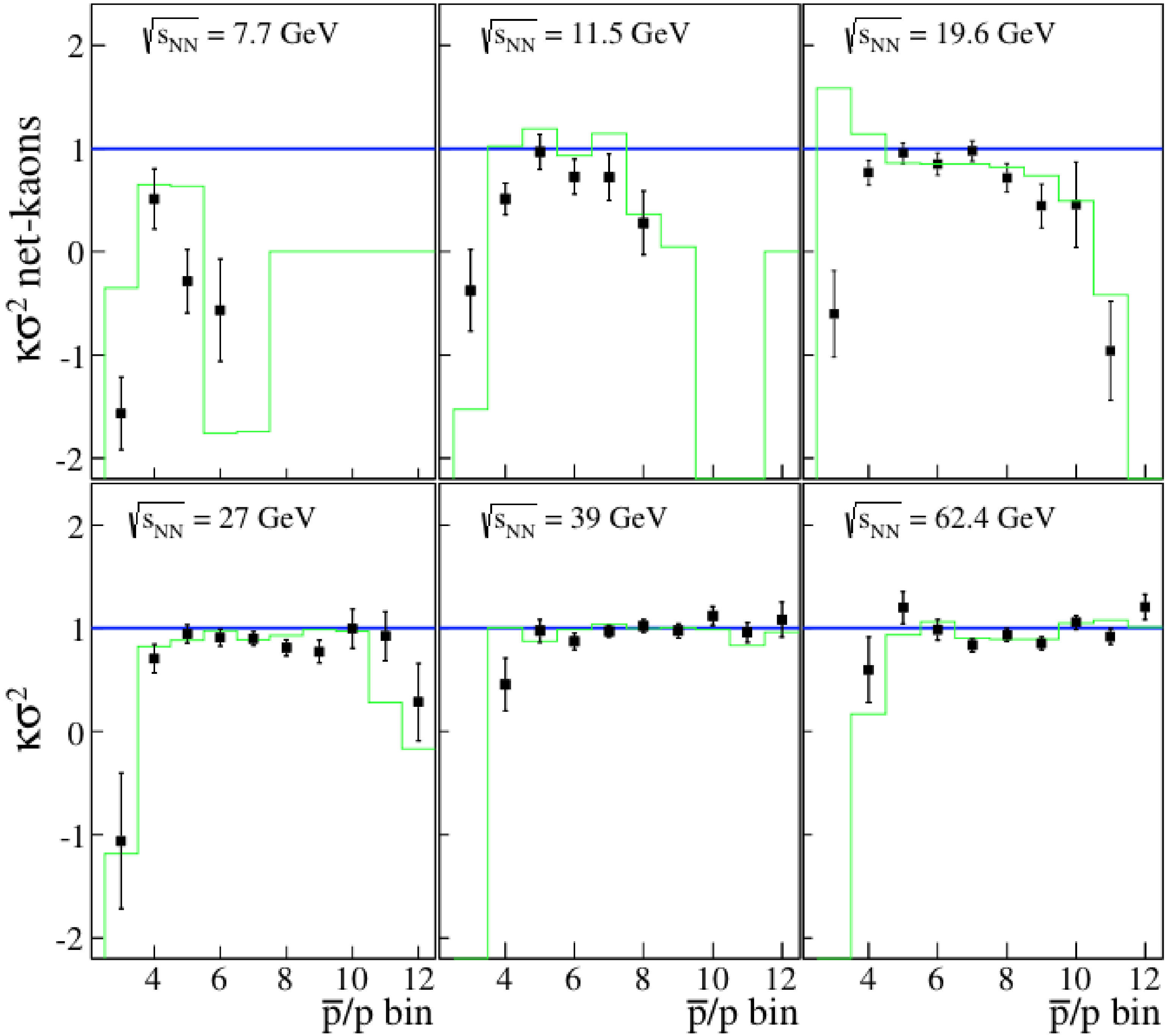

Summary

IRV cumulant arithmetic (or “sampled singles”) imply:

at most weak intra-event correlations of Np and Npbar, within the present uncertainties…

strong intra-event correlations for Npos and Nneg for ~central data at 62.4 and 200 GeV

“Clinical study” (fixed Poisson or Binomial marginals from data, controlled correlations)

…Relative insensitivity of C_4/C_2 to Np and Npbar intra-event correlations…

…Even cumulants strongly depend on such correlations, odd cumulants do not.

Implications for cumulants+LQCD to extract (μ_B,T)? Dependence on rapidity window?

…C_2 and C_4 still depend strongly on intra-event correlations even when C_1neg (pbar) ~ 0…

As long as the variance is large enough to fill several bins, correlations are visible!

Intra-event correlations of Np and Npbar are not the correlations we are looking for though!

“independent production” is not a baseline for critical behavior,

but does focus the attention on the 4th cumulant of the protons alone.

Proton-only C_4 for CEP search? ...Net-p cumulant ratios for comparisons to LQCD & (μ_B,T)?

Need to revisit measurement of all possible pure and mixed p and π cumulants…

Simulations suggest gating on μ_B event-by-event via pbar/p may be possible…

should have improved resolution on this in BES-II

BACKUP SLIDES

Comparison of (N)BD to uncorrected net-proton C_4 *vs.* centrality by $\sqrt{s_{NN}}$

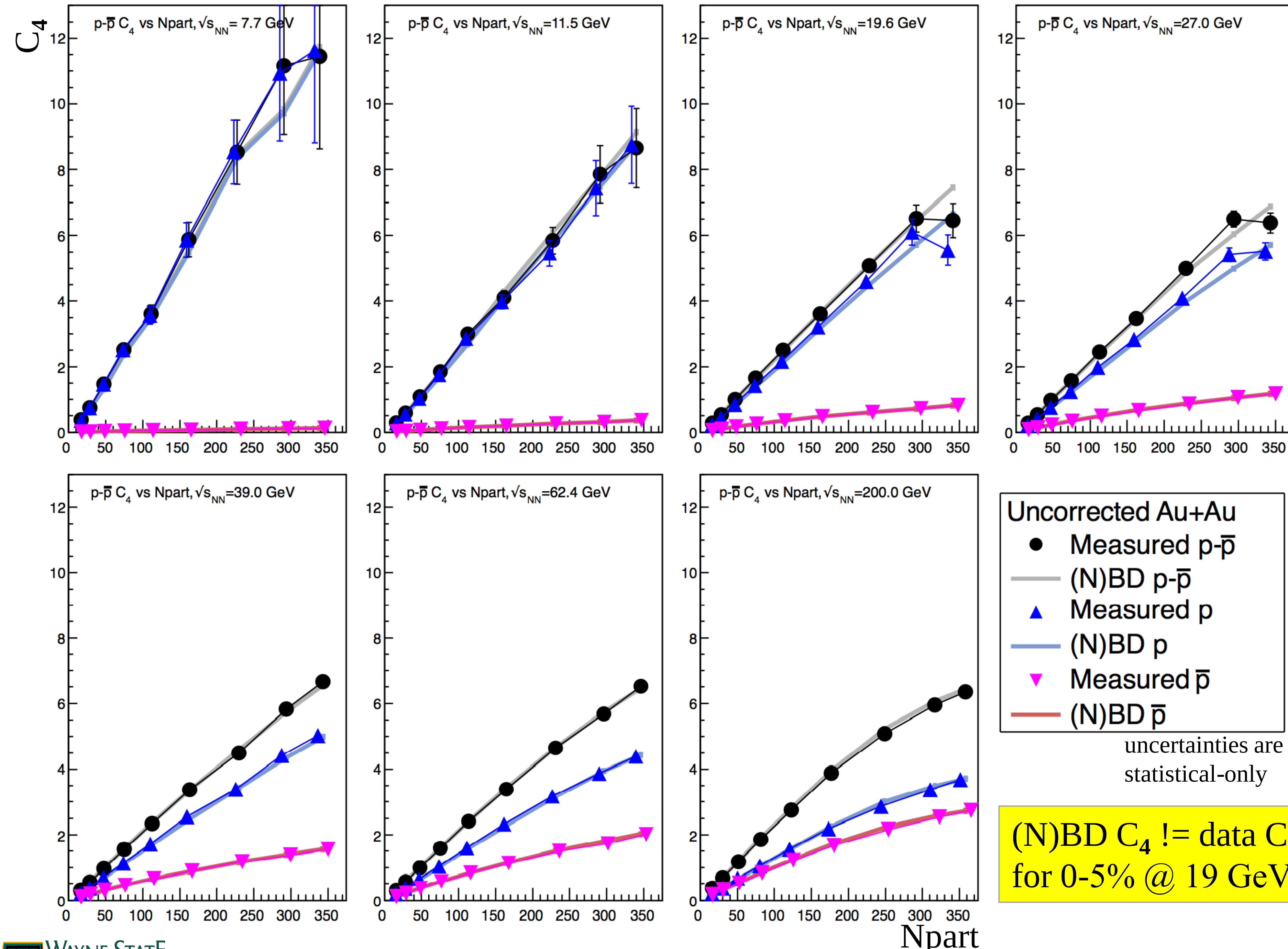

uncertainties are statistical-only

(N)BD C_4 != data C4 for 0-5% @ 19 GeV…

C_1 (mean) *vs.* centrality by $\sqrt{s_{NN}}$

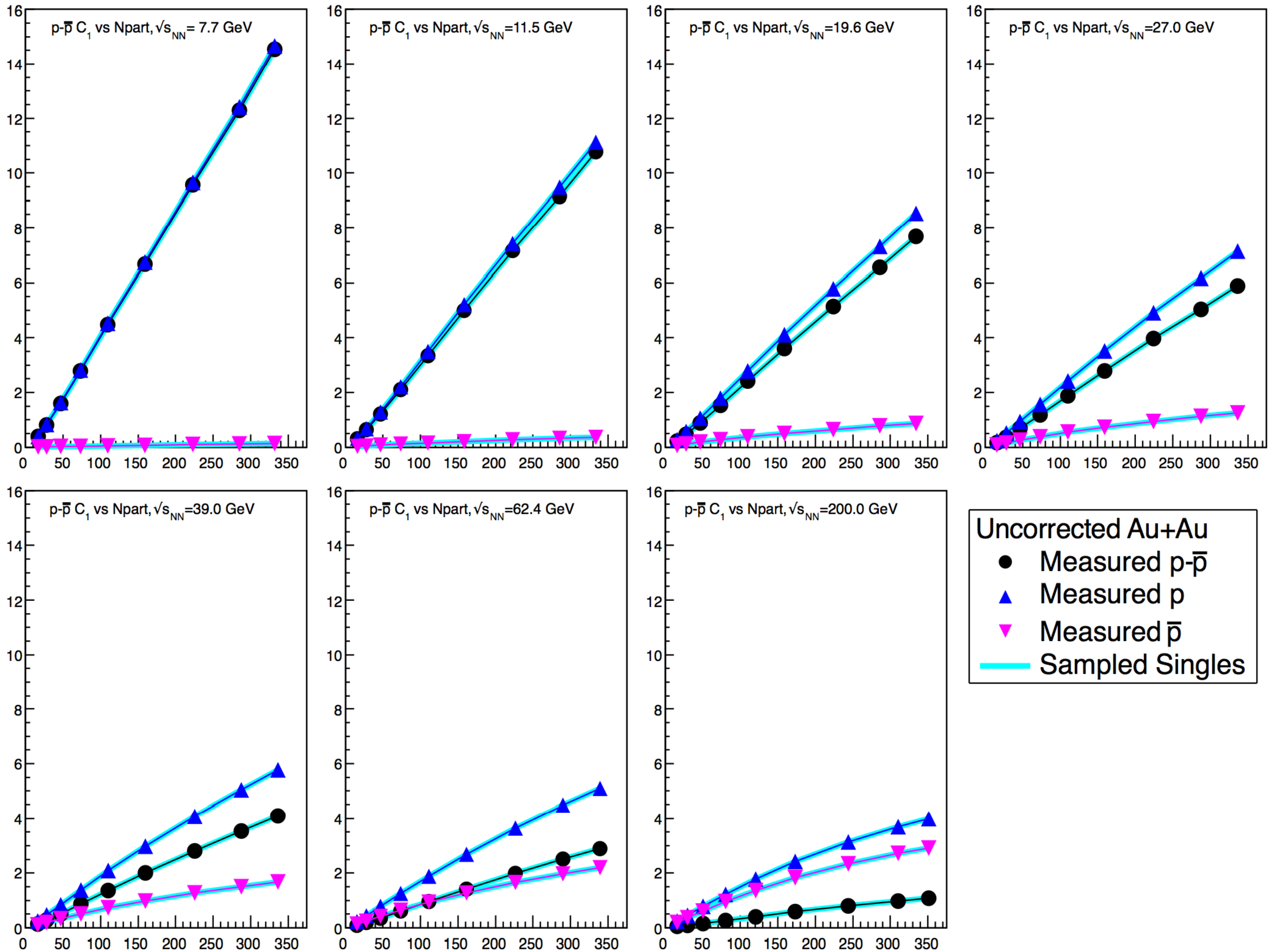

C_3 *vs.* centrality by $\sqrt{s_{NN}}$

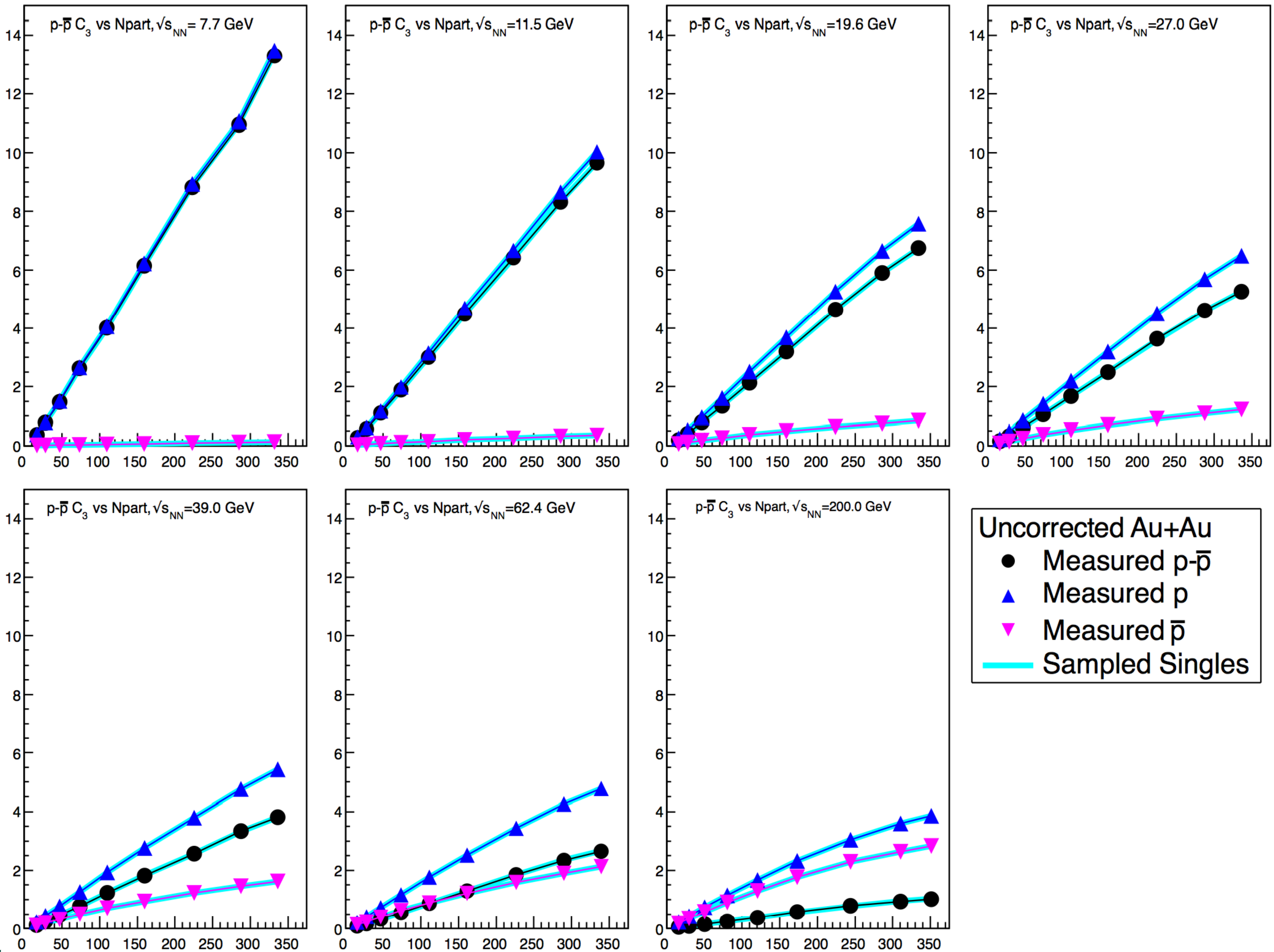

Quantifying the strength of correlations from the 2D distributions

Define an observable based on the 2D plot, or contingency table, that summarizes the degree of correlation between X and Y into a single value.

Statisticians call such an observable an “index”.

1. Pearson product-moment correlation coefficient, r...

$$r = \frac{\sum_{i=1}^{n}(X_i - \bar{X})(Y_i - \bar{Y})}{\sqrt{\sum_{i=1}^{n}(X_i - \bar{X})^2}\sqrt{\sum_{i=1}^{n}(Y_i - \bar{Y})^2}}$$

r<0 anticorrelation

r=0 no correlation

r>0 correlation

$$r = \frac{Cov(X,Y)}{\sigma_X \sigma_Y}$$

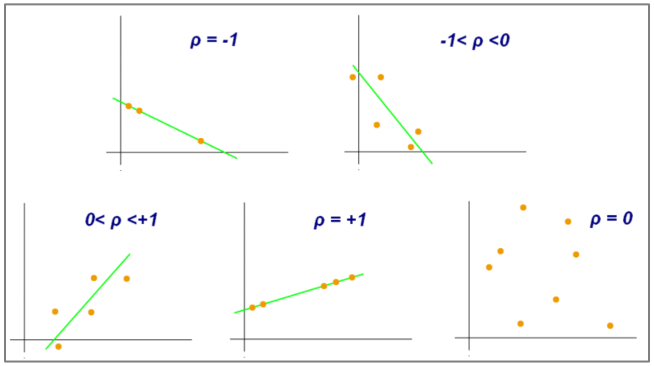

gives the strength of *linear correlations* between X and Y.
ρ = 0 does **not** imply independence!

2. $$\nu_{\mathrm{dyn,AB}} = \frac{\langle N_A(N_A-1)\rangle}{\langle N_A\rangle^2} + \frac{\langle N_B(N_B-1)\rangle}{\langle N_B\rangle^2} - 2\frac{\langle N_A N_B\rangle}{\langle N_A\rangle\langle N_B\rangle}$$

A=pos, B=neg

S. A. Volshin, Proceedings of INPC 2001 , 591 (2001), arXiv:0109006 [nucl-ex];
C. Pruneau, S. Gavin, and S. Voloshin, Phys. Rev. C66, 044904 (2002)

$\nu_{dyn}>0$ anticorrelation

$\nu_{dyn}=0$ uncorrelated (and Poisson marginals, by construction)

$\nu_{dyn}<0$ correlation

Alternatively, use Koch/Jeon form and calculate Poisson or (N)BD baseline directly

$$\nu_{AB} := \left\langle \left(\frac{A}{\langle A\rangle} - \frac{B}{\langle B\rangle} \right)^2 \right\rangle = \frac{\langle A^2\rangle}{\langle A\rangle^2} + \frac{\langle B^2\rangle}{\langle B\rangle^2} - 2\frac{\langle AB\rangle}{\langle A\rangle\langle B\rangle}$$

Quantifying the strength of correlations from the 2D distributions

Kendall τ, Spearman ρ

Let (x_1, y_1), (x_2, y_2), …, (x_n, y_n) be a set of observations of the joint random variables X and Y respectively, such that all the values of (x_i) and (y_i) are unique. Any pair of observations (x_i, y_i) and (x_j, y_j) are said to be *concordant* if the ranks for both elements agree: that is, if both $x_i > x_j$ and $y_i > y_j$ or if both $x_i < x_j$ and $y_i < y_j$. They are said to be *discordant*, if $x_i > x_j$ and $y_i < y_j$ or if $x_i < x_j$ and $y_i > y_j$. If $x_i = x_j$ or $y_i = y_j$, the pair is neither concordant nor discordant.

The Kendall τ coefficient is defined as:

$$\tau = \frac{(\text{number of concordant pairs}) - (\text{number of discordant pairs})}{\frac{1}{2}n(n-1)}.$$ [3]

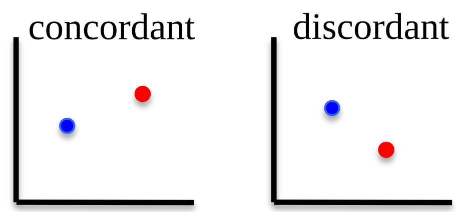

Spearman r is numerically similar in general. Uses triplets not pairs.

Distance Correlation

G. J. SZÉKELY1 AND M. L. RIZZO *The Annals of Applied Statistics* 2009, Vol. 3, No. 4, 1236–1265

Most complicated calculation by far, and very slow, but the "best" index for indicating the degree of correlation.

Pearson's correlation coefficient (-1 < r < 1)

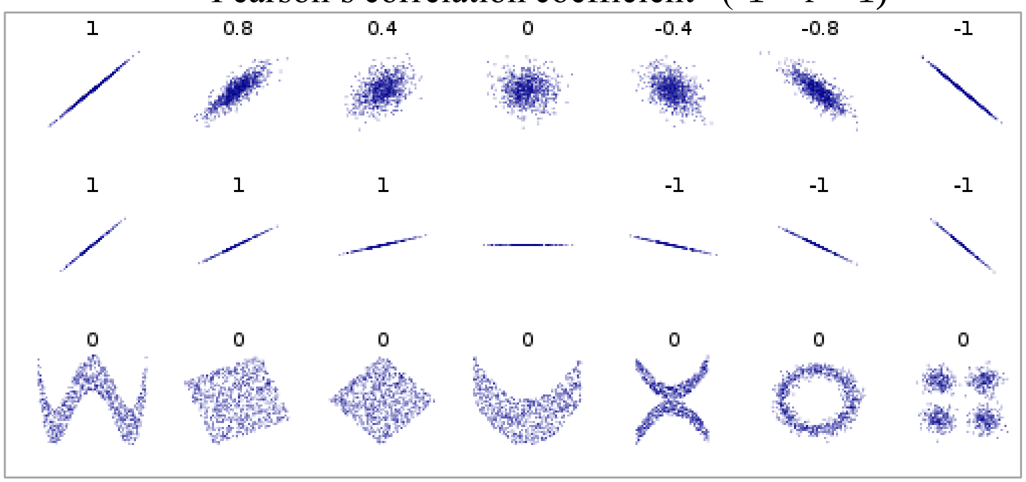

Distance correlation (0 < dCor < 1)

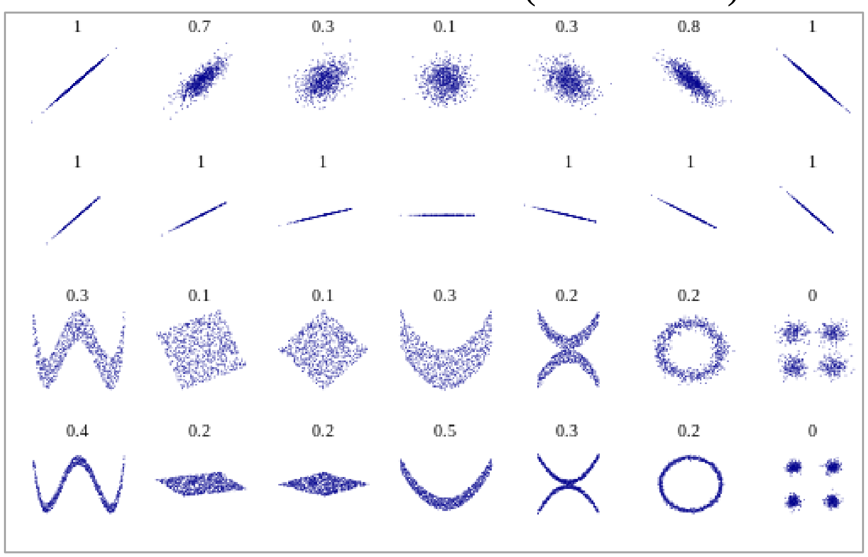

net-p Cumulant+LQCD *vs.* net-q Cumulant+LQCD *vs.* SHM

W.J. Llope, Bulk Correlations PWG Meeting, Nov. 27, 2013, http://wjllope.rice.edu/fluct/protected/bulkcorr_20131127.pdf

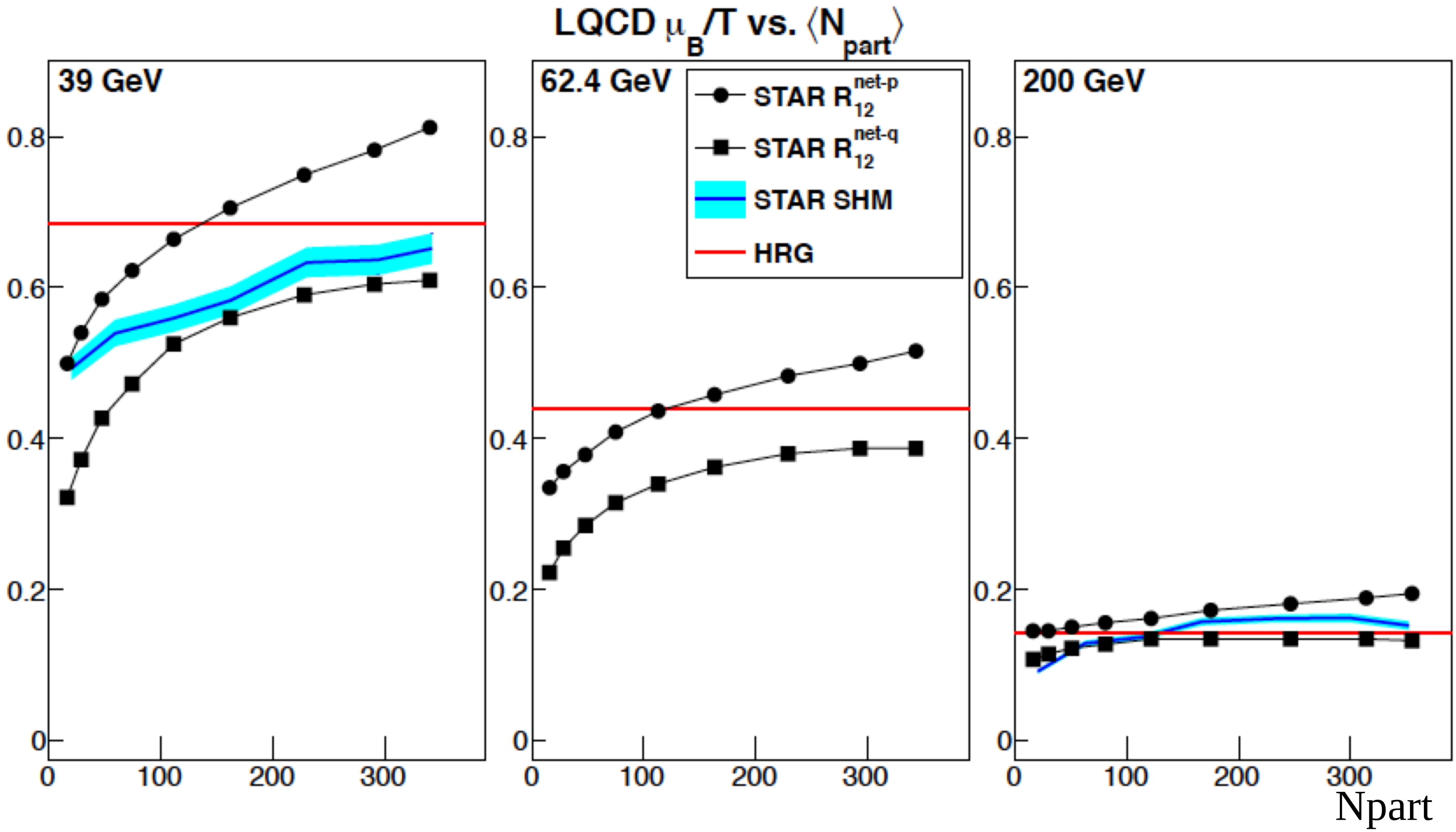

Cumulants+LQCD imply μ_B/T decreases as centrality decreases (similar to SHM w/ GCE)
μ_B/T from net-p and net-q diverge as $\sqrt{s_{NN}}$ decreases.
μ_B/T from net-p > μ_B/T from net-q
SHM results similar to the Cumulants+LQCD values (in between net-p & net-q)

μ_B/T from fluct net-p and net-q

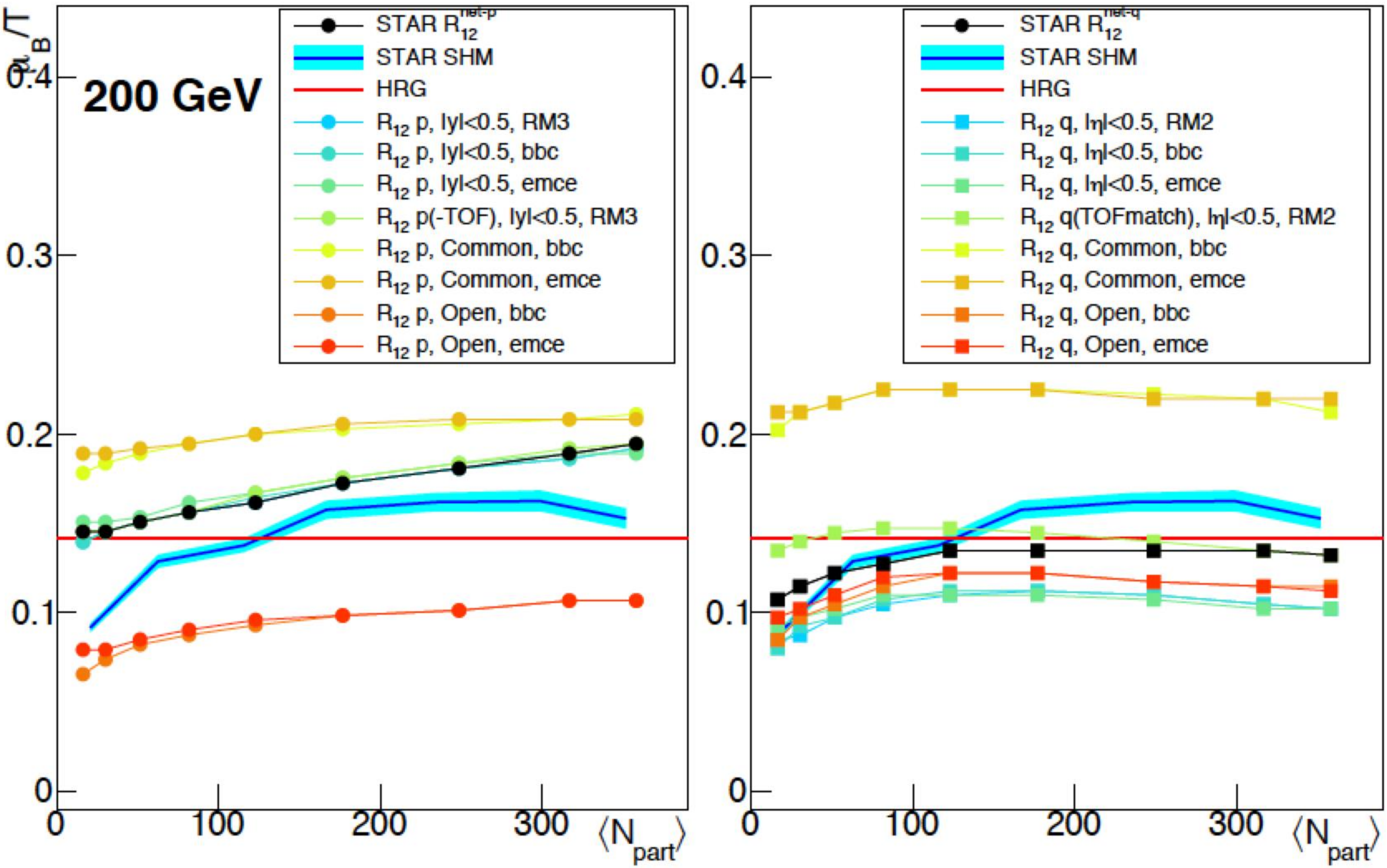

W.J. Llope, Bulk Correlations PWG Meeting, Nov. 27, 2013, http://wjllope.rice.edu/fluct/protected/bulkcorr_20131127.pdf
W.J. Llope, Bulk Correlations PWG Meeting, Feb. 11, 2014, http://wjllope.rice.edu/fluct/protected/bulkcorr_20140211.pdf

μ_B/T versus N_{part} from fluct net-p and net-q

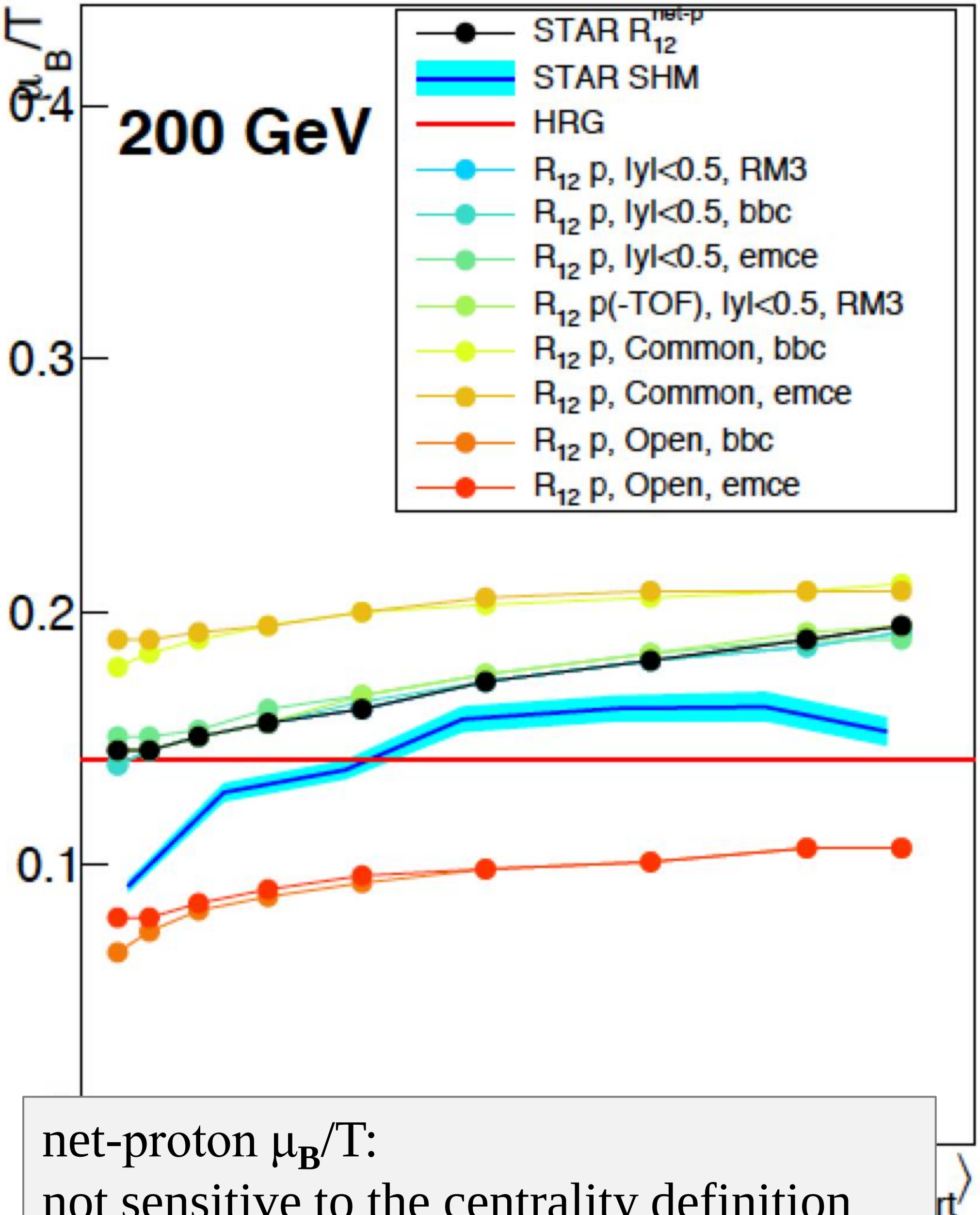

net-proton μ_B/T:
not sensitive to the centrality definition
very sensitive to the $\Delta(\eta,y)$ range allowed

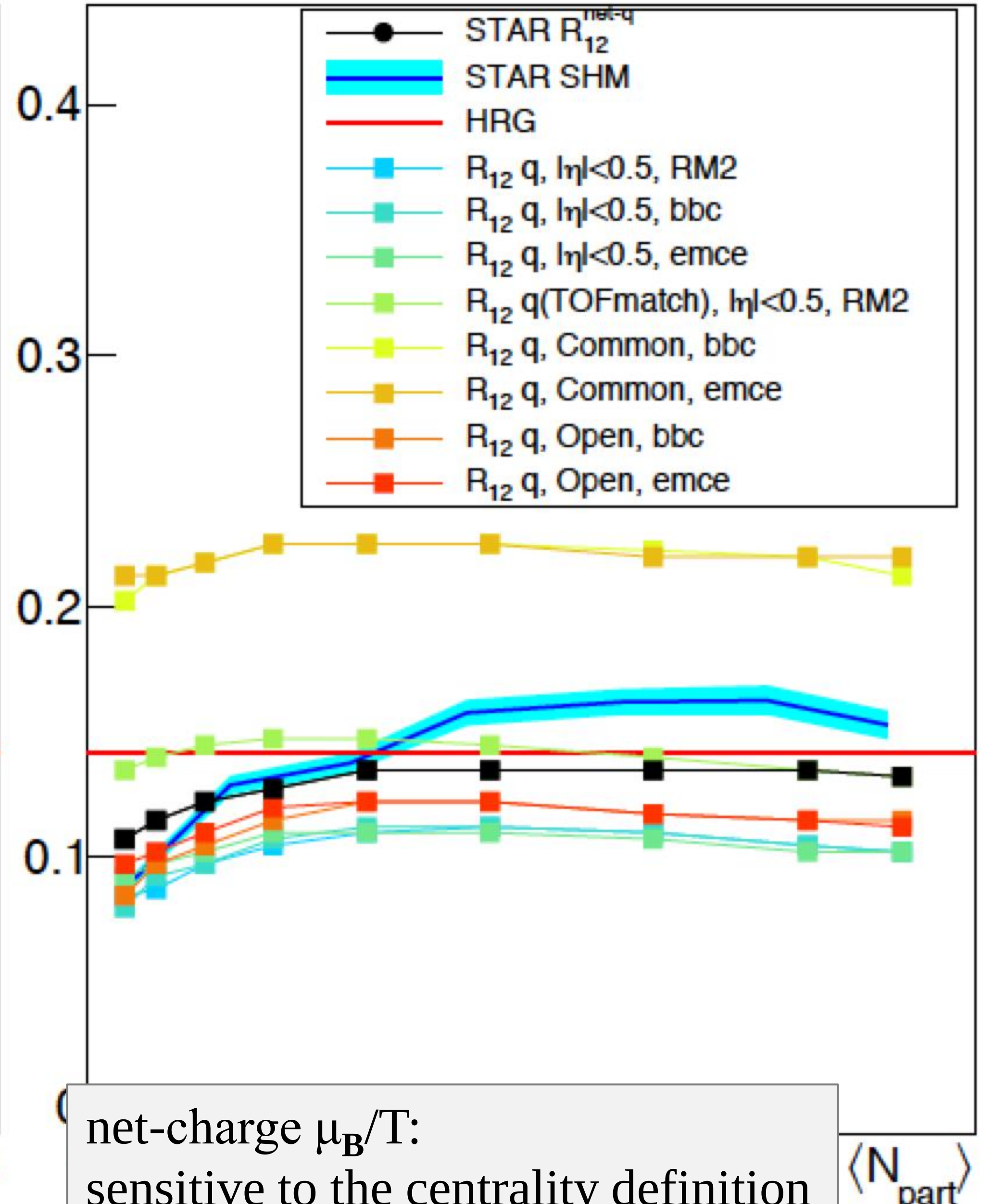

net-charge μ_B/T:
sensitive to the centrality definition
& the $\Delta(\eta,y)$ range allowed

Determining Average values of (μ_B,T) for given sample of events (@ centrality, $\sqrt{s_{NN}}$)…

A …Ratios of yields (C_1) of different particles + SHM (*e.g.* THERMUS)

B …Ratios of Cumulants (C_y/C_x) + LQCD (Taylor-expanded susceptibility ratios)

Looking for a critical point…

C …Critical opalescence > increasing correlation length > non-mononotic $\sqrt{s_{NN}}$ behavior of particle multiplicity cumulant ratios.

I've shown that the results from B depend on the (psuedo)rapidity range over which the cumulants are measured. Obvious A must also be sensitive to this choice.

Are (pseudo)rapidity-dependent correlations playing a role?

V. Koch, BNL Riken Fluctuations Workshop, BNL, 2011

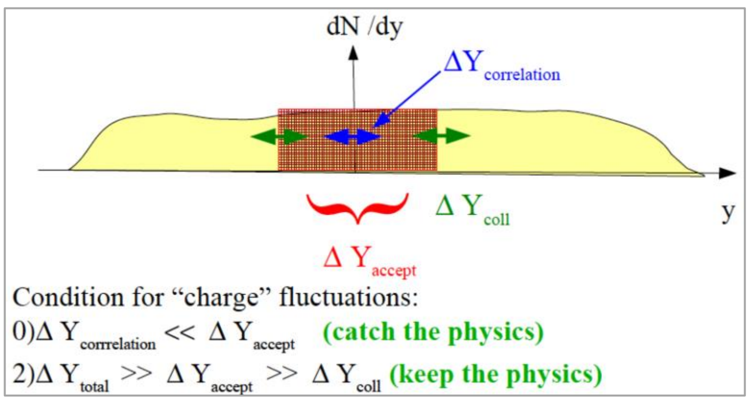

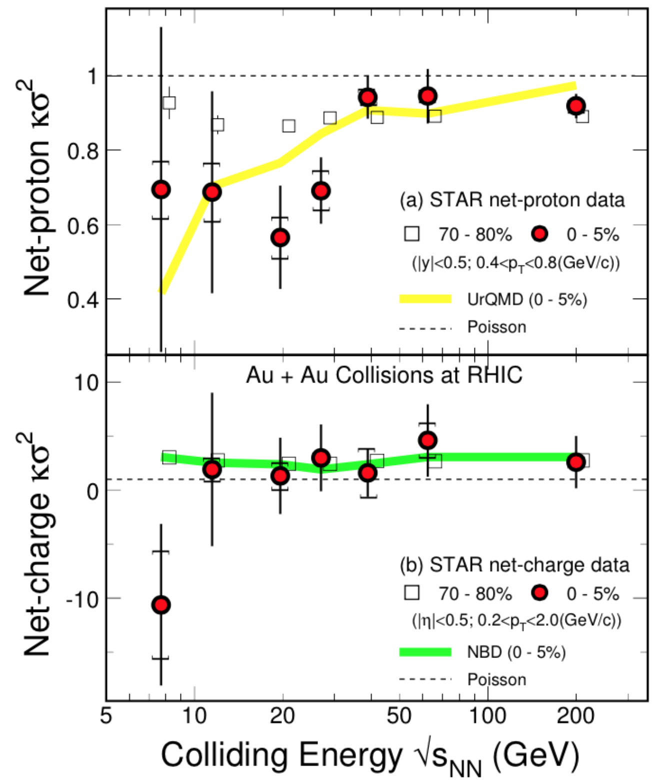

There is also a "dip" in the net-proton cumulant ratios (C_4/C_2=$K\sigma^2$) near ~19.6 GeV

Is this the dip from the NLSM, indicating critical fluctuations/correlations in the p and pbar multiplicities due to a CP?

Fluctuations of Conserved Quantities in High Energy Nuclear Collisions at RHIC

Xiaofeng Luo (罗晓峰)

Central China Normal University (CCNU)

Feb. 26-27, 2015

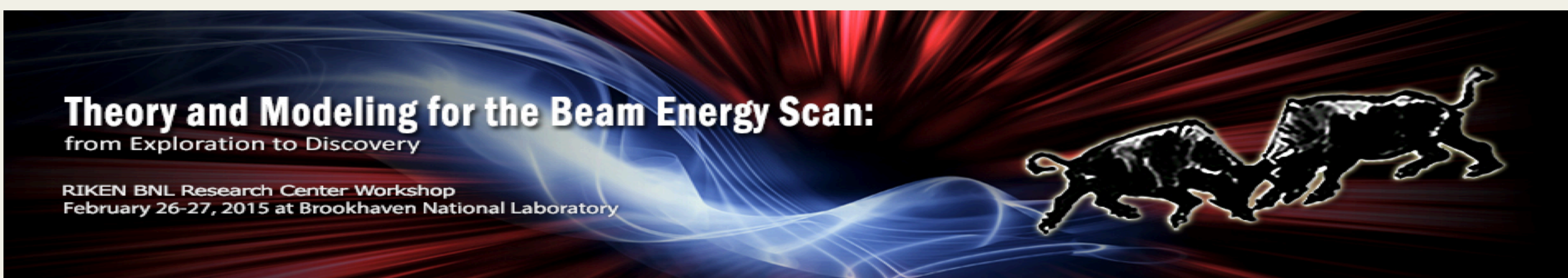

Outline

- Introduction
- Analysis Techniques
- Results for Net-proton and Net-charge.
- Summary and Outlook

QCD Phase Diagram (Conjectured)

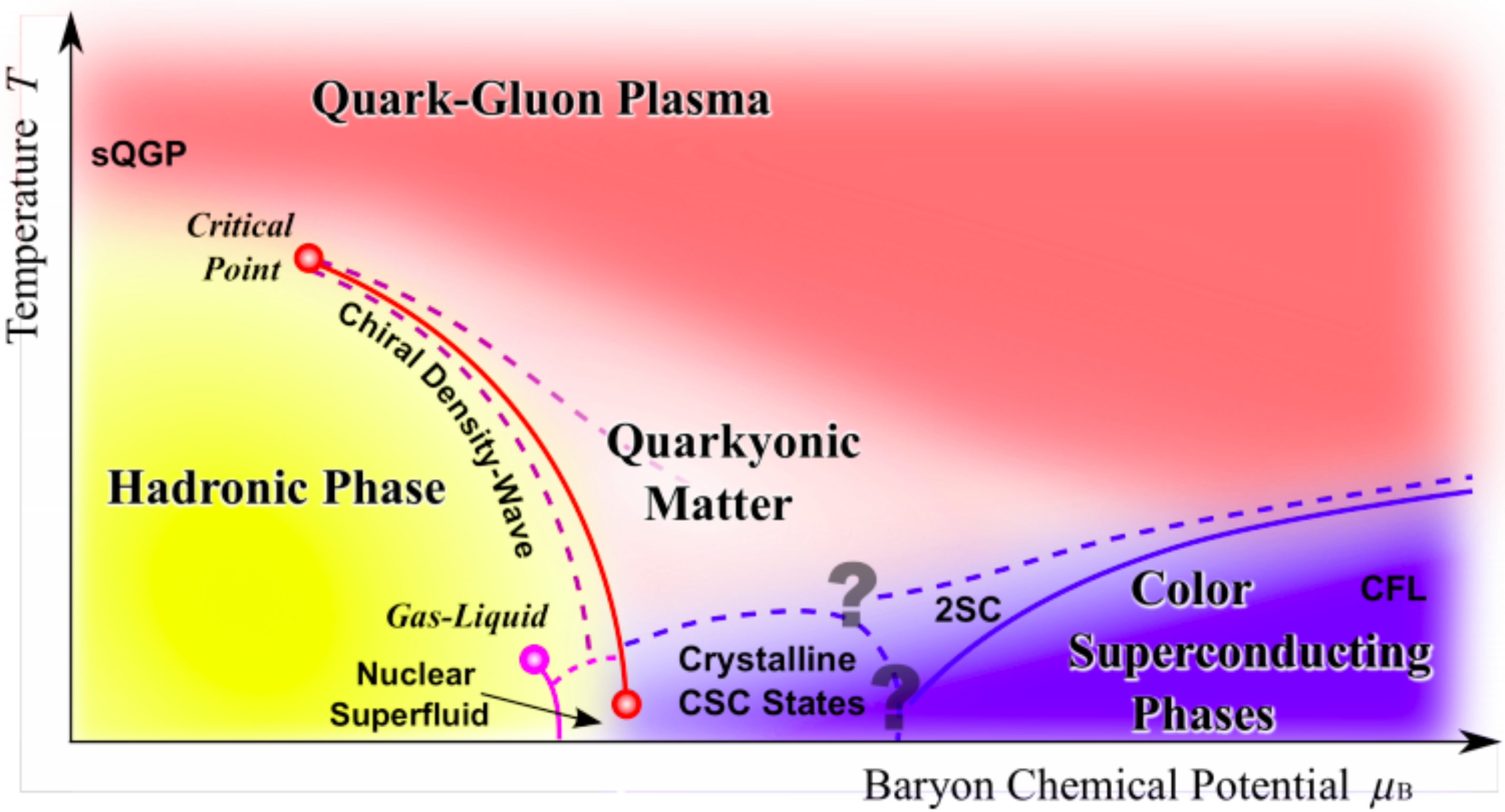

Hatsuda and Fukushima

Very rich phase structure in the QCD phase diagram.

Fluctuations of conserved quantities, such as net-baryon (B), net-charge (Q) and net-strangeness (S), can be used to probe the QCD phase transition and QCD critical point in heavy-ion collisions.

DSE:

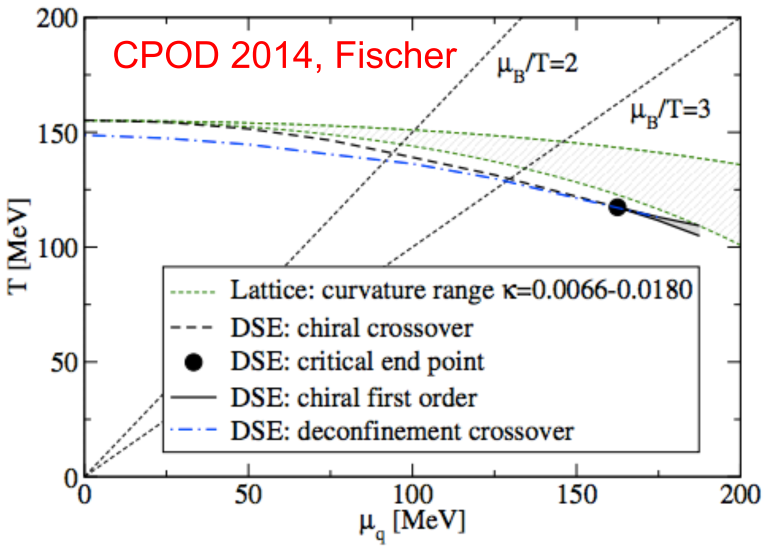

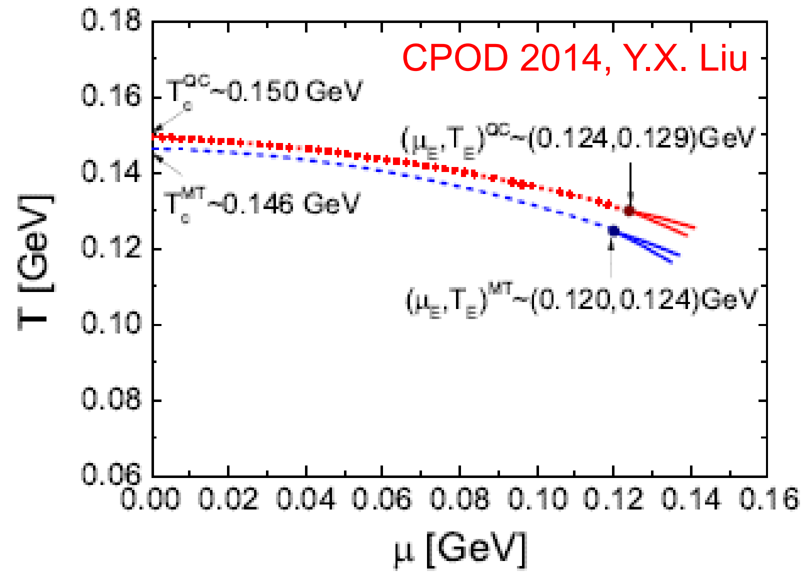

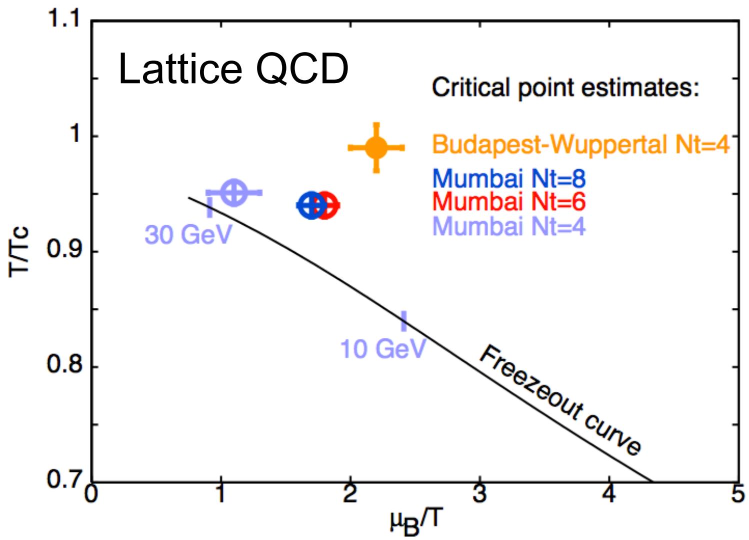

1) S. Datta, R. Gavai, S. Gupta, PoS (LATTICE 2013), 202.
$\mu^E_B/T^E \sim 1.7 \rightarrow \sqrt{s_{NN}} \sim 20$ GeV

2) Y. X. Liu, et al., PRD90, 076006 (2014).
$\mu^E_B/T^E \sim 2.88 \rightarrow \sqrt{s_{NN}} \sim 8$ GeV

3) C. S. Fischer et al., PRD90, 034022 (2014).
$\mu^E_B/T^E \sim 4.4 \rightarrow \sqrt{s_{NN}} \sim 6$ GeV

Different theoretical calculations give very different CP locations.

Higher Moments

Experimental Observables: Higher Moments of Conserved Quantities (q=B, Q, S).

1): **Sensitive to the correlation length (ξ):**

$$\left\langle (\delta N)^2 \right\rangle_c \approx \xi^2, \quad \left\langle (\delta N)^3 \right\rangle_c \approx \xi^{4.5}, \quad \left\langle (\delta N)^4 \right\rangle_c \approx \xi^7$$

2): **Direct comparison with calculations:**

$$S\sigma \approx \frac{\chi_q^3}{\chi_q^2}, \qquad \kappa\sigma^2 \approx \frac{\chi_q^4}{\chi_q^2}$$

χ_q^n

n^{th} order susceptibility for conserved quantity q.

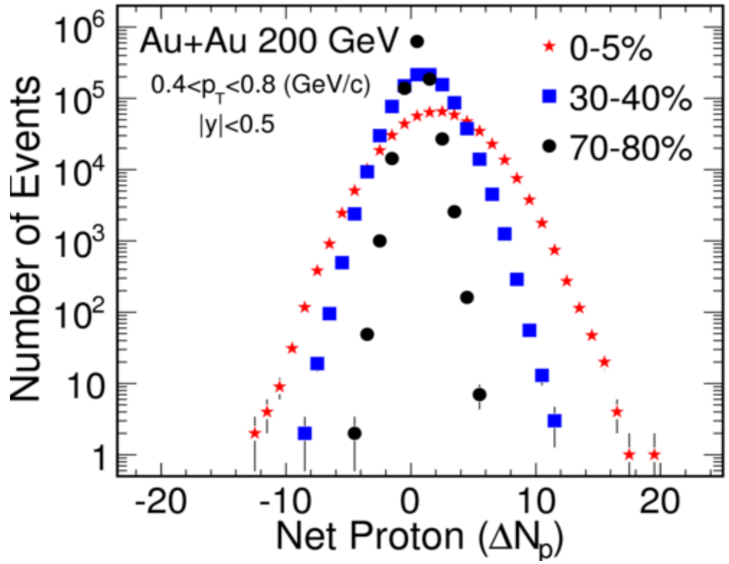

3): **Extract chemical freeze-out parameters.**

An independent/important test of thermal equilibrium in heavy-ion collisions.

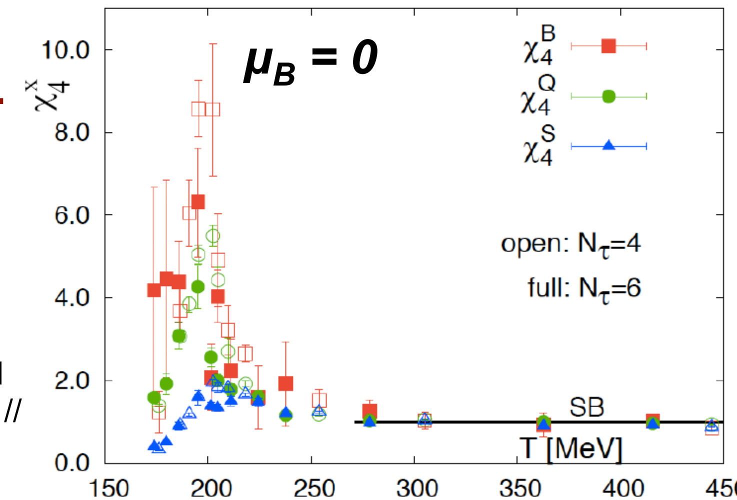

M. Cheng, et. al., PRD79, 074505 (2009).

References:

- STAR: *PRL105*, 22303(10); *PRL112*, 032302 (14). *PRL113*, 092301 (14).
- M. Stephanov: *PRL*102, 032301(09) // M. Akasawa, et al., *PRL103*,262301 (09).R.V. Gavai et al., *PLB696*, 459(11) // F. Karsch et al,*PLB695*,136(11) // S.Ejiri et al, *PLB633*, 275(06) , PBM et al., *PRC84*, 064911 (11).
- A. Bazavov et al., *PRL109*, 192302(12) // S. Borsanyi et al., *PRL111*, 062005(13) //S. Gupta, et al., *Science*, 332, 1525(12).

RHIC Beam Energy Scan–Phase I

In the first phase of the RHIC Beam Scan (BES), seven energies were surveyed in 2010 and 2011.

$\sqrt{s}$ (GeV)	Statistics(Millions) (0-80%)	Year	μ_B (MeV)	T (MeV)	μ_B /T
7.7	~3	2010	422	140	3.020
11.5	~6.6	2010	316	152	2.084
14.5	~10	2014	264	156	1.692
19.6	~15	2011	206	160	1.287
27	~32	2011	156	163	0.961
39	~86	2010	112	164	0.684
62.4	~45	2010	73	165	0.439
200	~238	2010	24	166	0.142

Chemical freeze-out μ_{B}, T : J. Cleymans et al., Phys. Rev. C 73, 034905 (2006).

The main goals of BES program:

- **Search for Onset of Deconfinement.**
- **Search for QCD critical point.**
- **Map the first order phase transition boundary.**

STAR Detector System

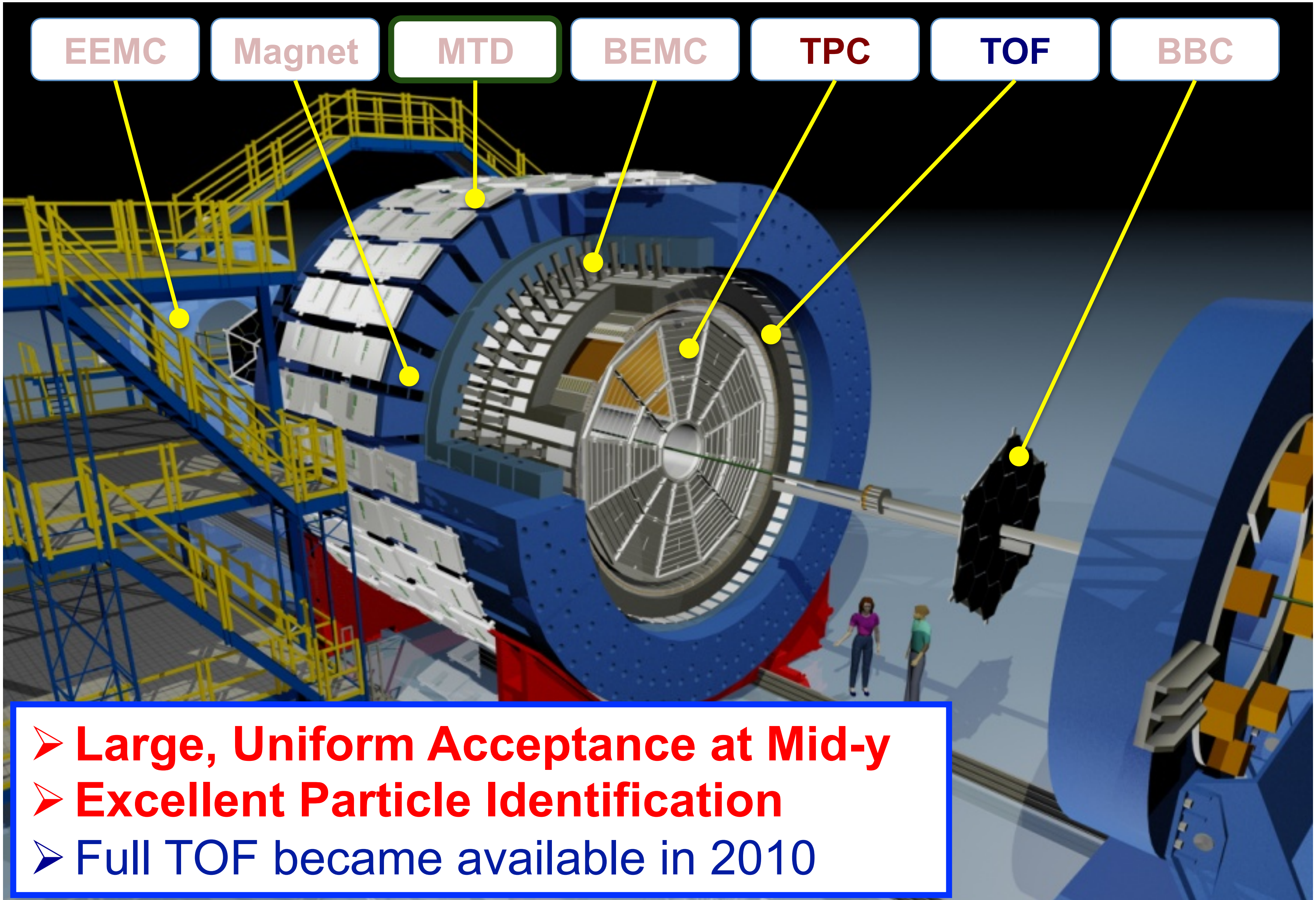

- **Large, Uniform Acceptance at Mid-y**
- **Excellent Particle Identification**
- Full TOF became available in 2010

Extend Phase Space Coverage with TOF

Published net-proton results: Only TPC used for proton/anti-proton PID. TOF PID can extend the phase space coverage. STAR, PRL 112, 032302 (2014).

TPC PID:

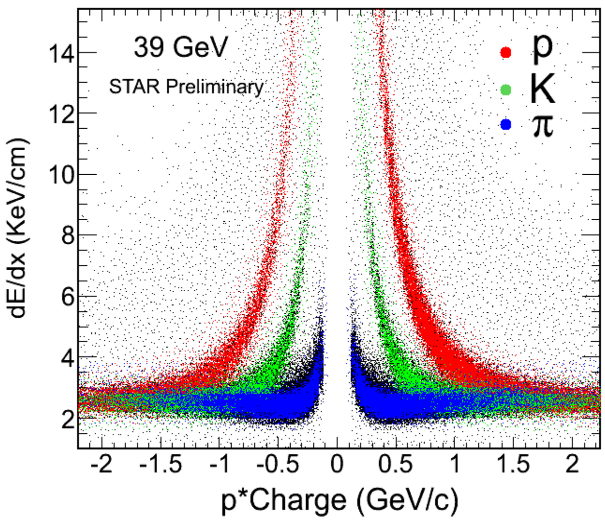

TOF PID:

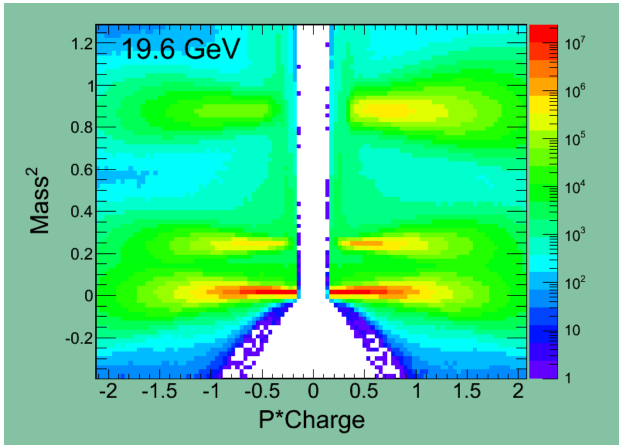

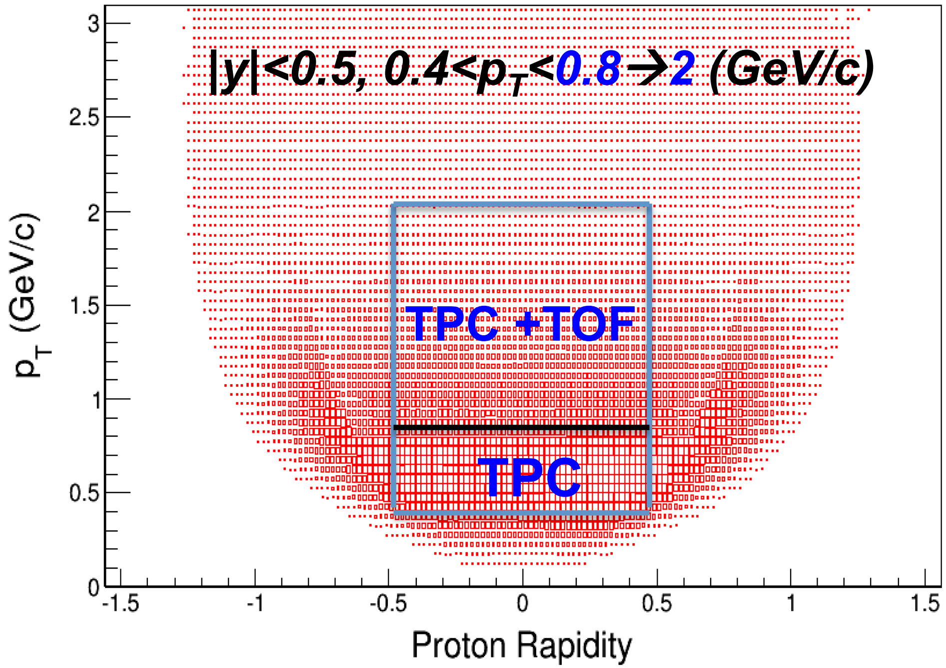

Doubled the accepted number of proton

1) Sufficiently large acceptance is important for fluctuation analysis and critical point search.

2) Need phase dependence efficiency correction, since eff. change dramatically between : TPC (ε_{TPC}~0.8) and TPC+TOF($\varepsilon_{TPC}*\varepsilon_{TOF}$~0.5).

Efficiencies for Protons and Anti-protons

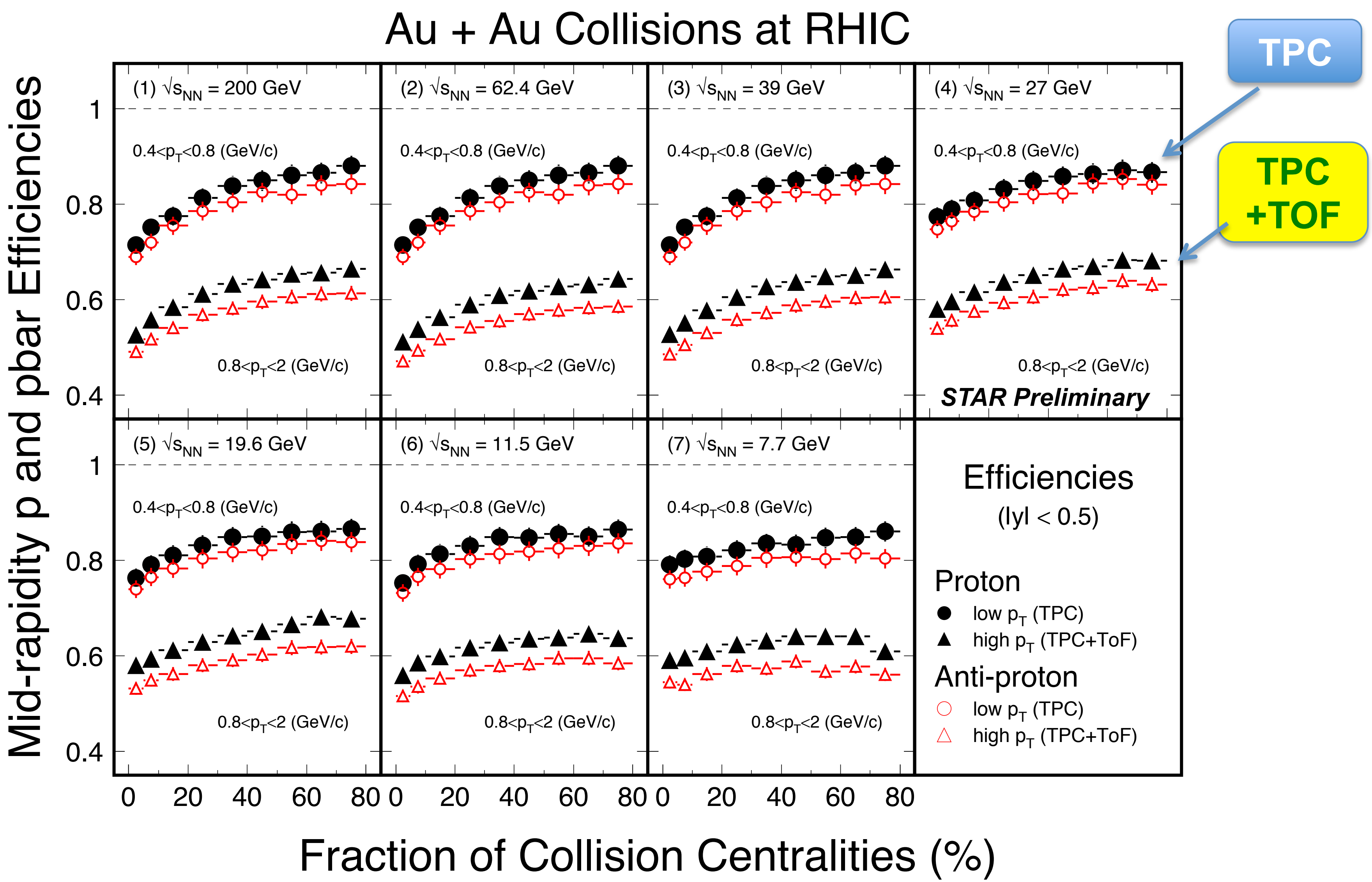

Efficiency Correlation and Error Estimation

We provide a unified description of efficiency correction and error estimation for higher moments analysis in heavy-ion collisions.

X. Luo, arXiv: 1410.3914

$$F_{r_1,r_2}(N_p, N_{\bar{p}}) = F_{r_1,r_2}(N_{p_1}+N_{p_2}, N_{\bar{p}_1}+N_{\bar{p}_2})$$
$$= \sum_{i_1=0}^{r_1}\sum_{i_2=0}^{r_2} s_1(r_1,i_1)s_1(r_2,i_2) < (N_{p_1}+N_{p_2})^{i_1}(N_{\bar{p}_1}+N_{\bar{p}_2})^{i_2} >$$
$$= \sum_{i_1=0}^{r_1}\sum_{i_2=0}^{r_2} s_1(r_1,i_1)s_1(r_2,i_2) < \sum_{s=0}^{i_1}\binom{i_1}{s} N_{p_1}^{i_1-s}N_{p_2}^{s}\sum_{t=0}^{i_2}\binom{i_2}{t} N_{\bar{p}_1}^{i_2-t}N_{\bar{p}_2}^{t} >$$
$$= \sum_{i_1=0}^{r_1}\sum_{i_2=0}^{r_2}\sum_{s=0}^{i_1}\sum_{t=0}^{i_2} s_1(r_1,i_1)s_1(r_2,i_2)\binom{i_1}{s}\binom{i_2}{t} < N_{p_1}^{i_1-s}N_{p_2}^{s}N_{\bar{p}_1}^{i_2-t}N_{\bar{p}_2}^{t} >$$
$$= \sum_{i_1=0}^{r_1}\sum_{i_2=0}^{r_2}\sum_{s=0}^{i_1}\sum_{t=0}^{i_2}\sum_{u=0}^{i_1-s}\sum_{v=0}^{s}\sum_{j=0}^{i_2-t}\sum_{k=0}^{t} s_1(r_1,i_1)s_1(r_2,i_2)\binom{i_1}{s}\binom{i_2}{t}$$
$$\times s_2(i_1-s,u)s_2(s,v)s_2(i_2-t,j)s_2(t,k) \times F_{u,v,j,k}(N_{p_1},N_{p_2},N_{\bar{p}_1},N_{\bar{p}_2})$$

Error Estimation: MC simulation

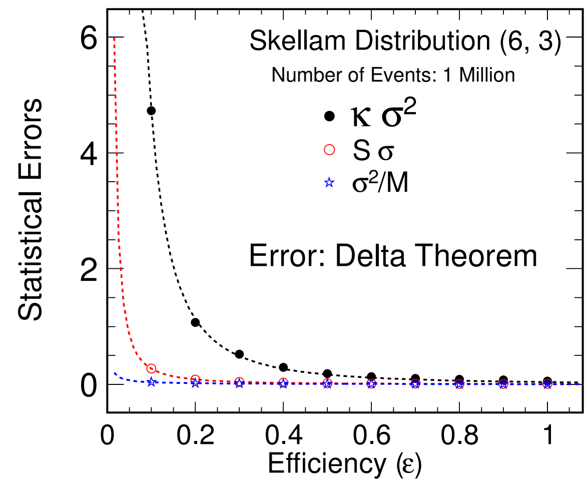

Fitting formula: $f(\varepsilon) = \frac{1}{\sqrt{n}}\frac{a}{\varepsilon^b}$

We can express the moments and cumulants in terms of the factorial moments, which can be easily efficiency corrected.

$$F_{u,v,j,k}(N_{p_1},N_{p_2},N_{\bar{p}_1},N_{\bar{p}_2}) = \frac{f_{u,v,j,k}(n_{p_1},n_{p_2},n_{\bar{p}_1},n_{\bar{p}_2})}{(\varepsilon_{p_1})^u(\varepsilon_{p_2})^v(\varepsilon_{\bar{p}_1})^j(\varepsilon_{\bar{p}_2})^k}$$

One can also see:
A. Bzdak and V. Koch,
PRC91,027901(2015),
PRC86，044904(2012).

For other analysis techniques, see: STAR, PRL112, 032302 (2014); PRL113, 092301 (2014).

AMPT model: Au+Au 39 GeV.

Set different efficiency for two p_T range. (0.4， 0.8) : 80%, (0.8， 2): 50% for p and pbar.

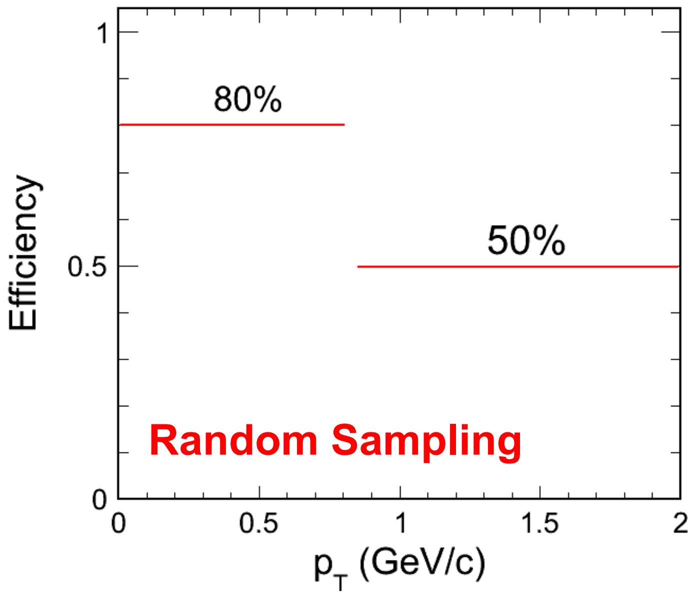

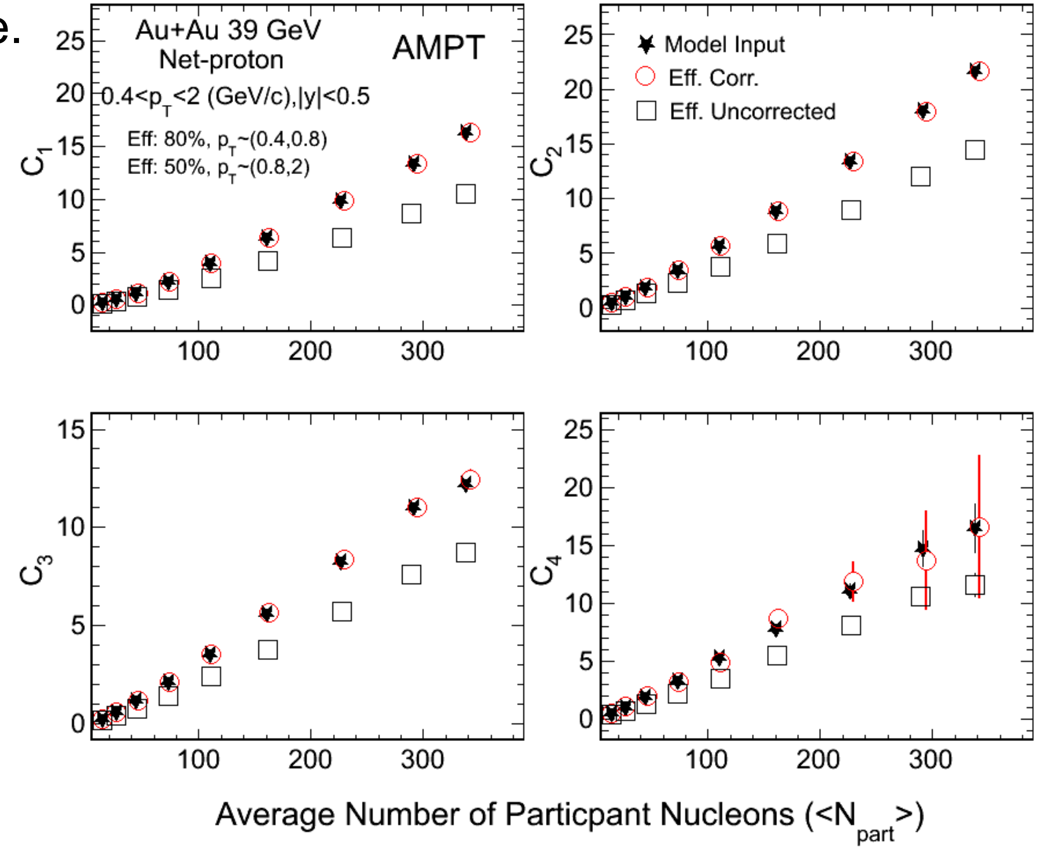

1. The eff. corrected results match the model inputs very well, which indicate the efficiency correction method works well.
2. The error estimation for eff. corrected results are based on the Delta theorem.

Results: Mean Net-p, p and pbar

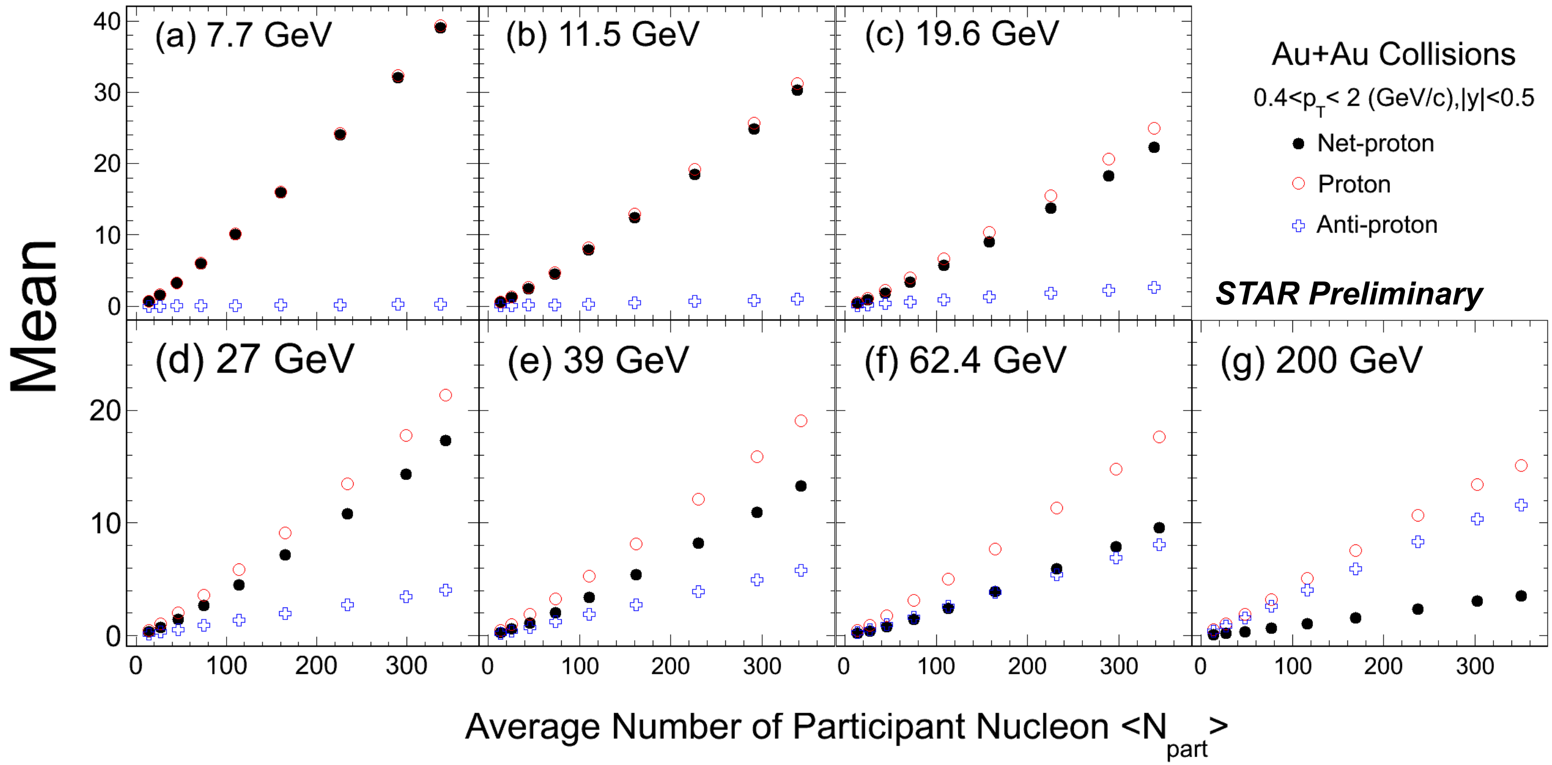

- Mean Net-proton, proton and anti-proton number increase with $\langle N_{part} \rangle$
- Net-proton number is dominated by protons at low energies and increases when energy decreases.
  (Interplay between baryon stopping and pair production)

Higher Order Cumulants for Net-p, p, pbar

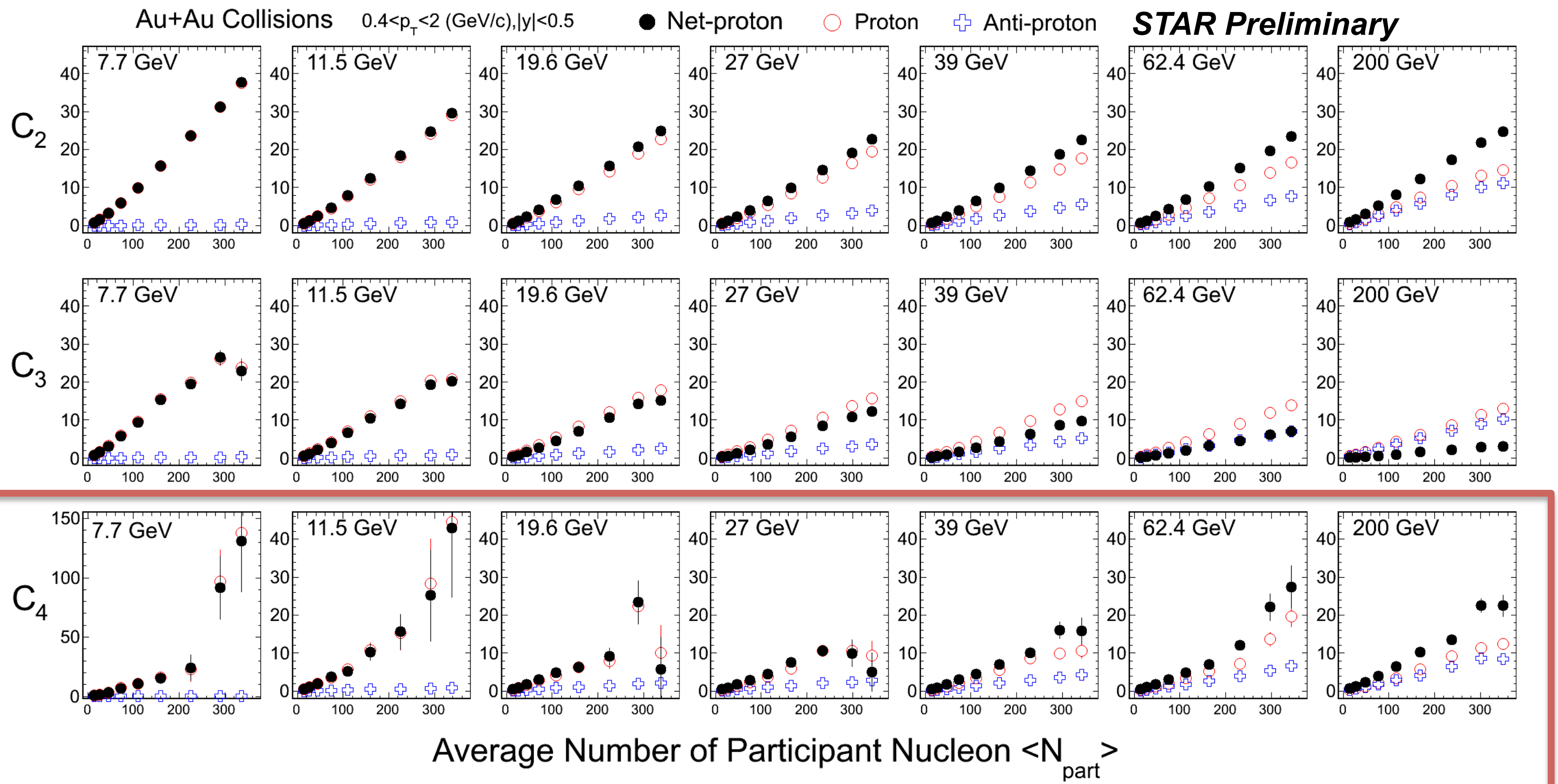

- In general, cumulants of Net-p, p and pbar are increasing with $\langle N_{part} \rangle$.
- The cumulants of net-proton distributions closely follow the proton cumulants when the colliding energy is decreasing.

Energy Dependence of Cumulants Ratios

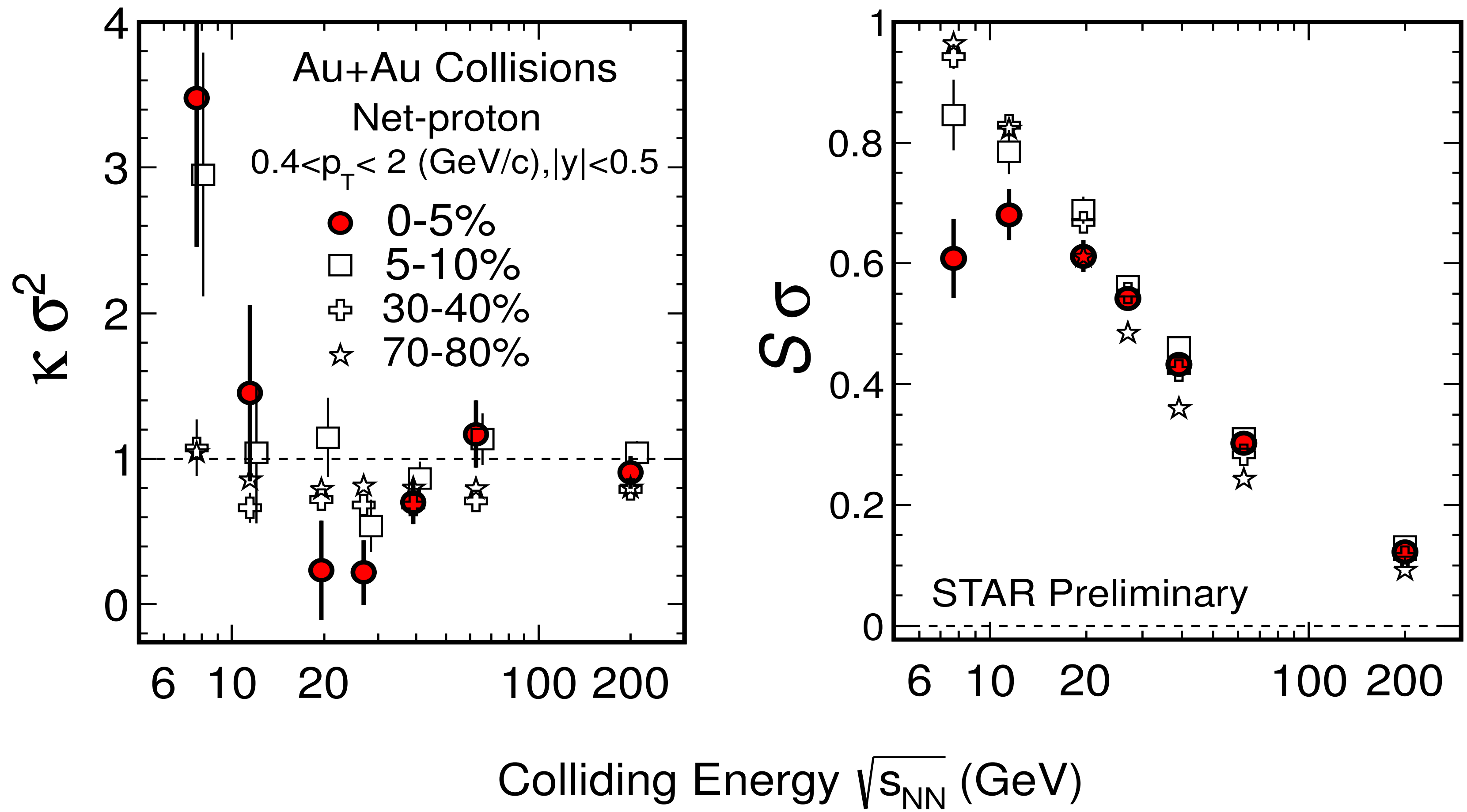

1) The most pronounced structure is observed at 0-5% centrality for $K\sigma^2$.
2) Error bars are statistical only. Systematic errors estimation underway. Dominant contributors: a) efficiency corrections b) PID;

Eff. Corrected and Eff. Uncorrected

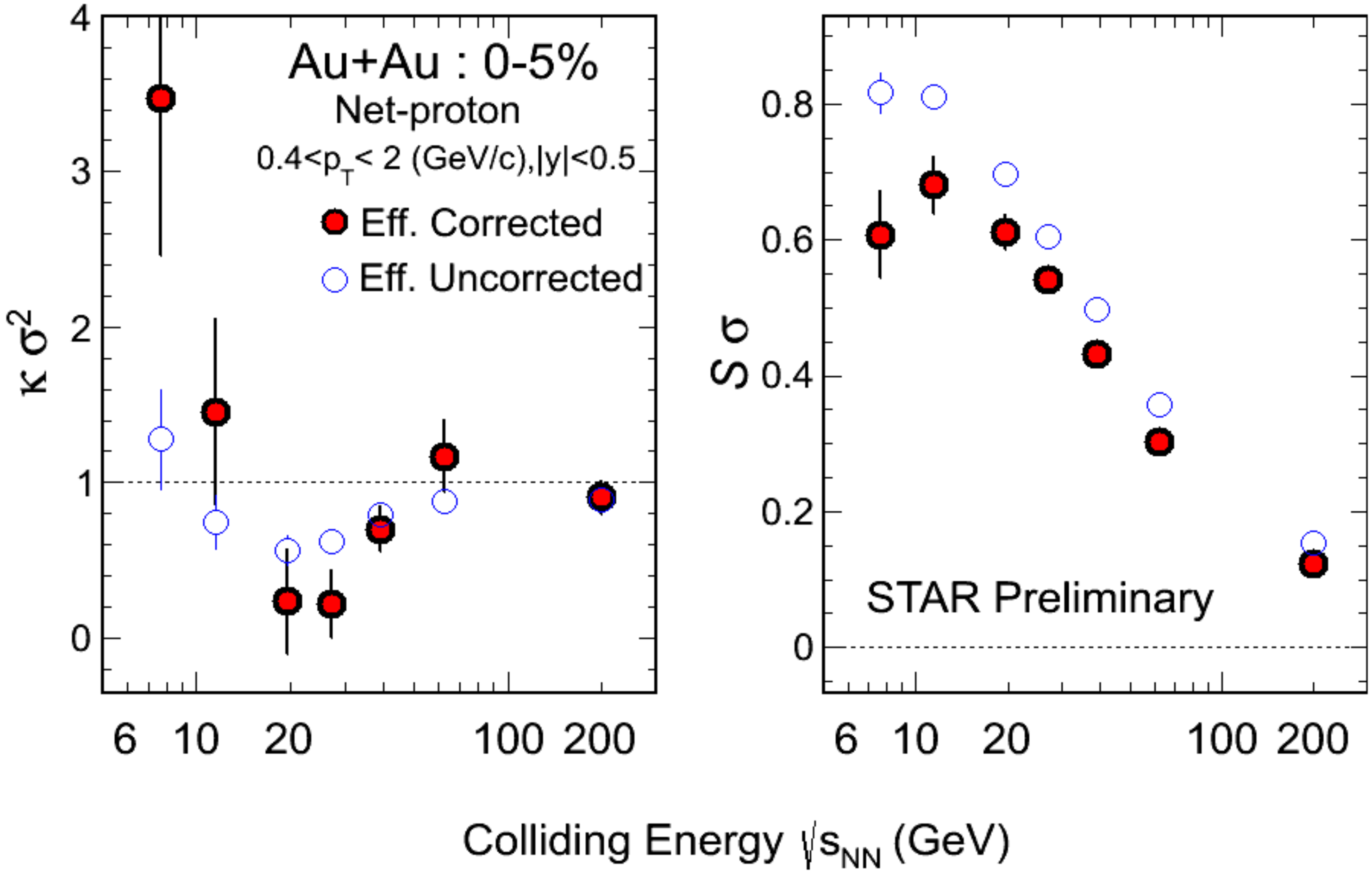

Efficiency corrections are important not only for the values in the higher moments analysis, but also the statistical errors. $error \propto O\left(\sigma^n / \varepsilon^\alpha\right)$

Cumulants vs. Baselines

Cumulants vs. Poisson

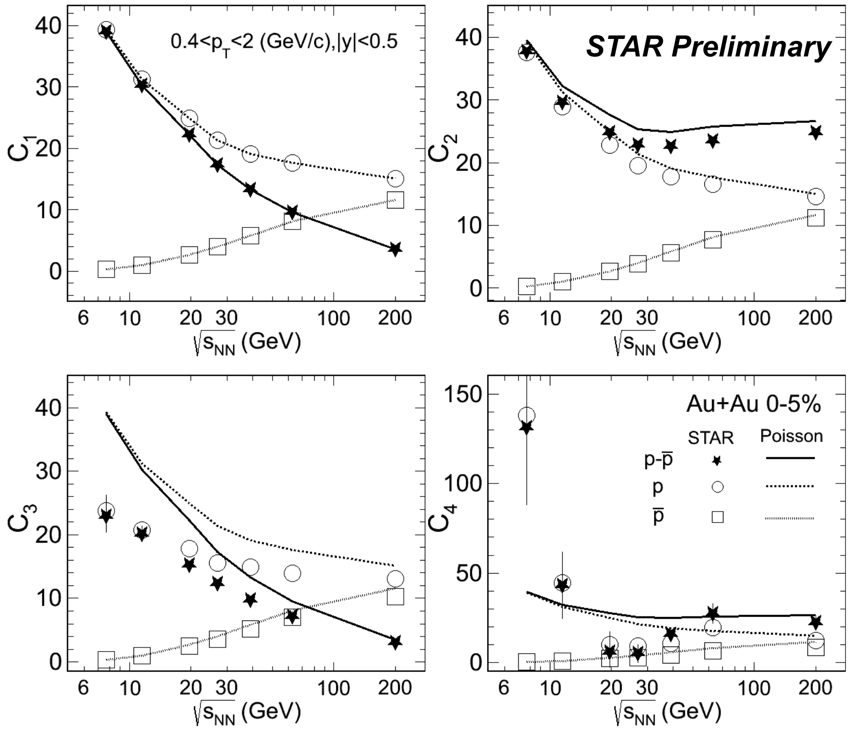

Cumulants vs. Binomial

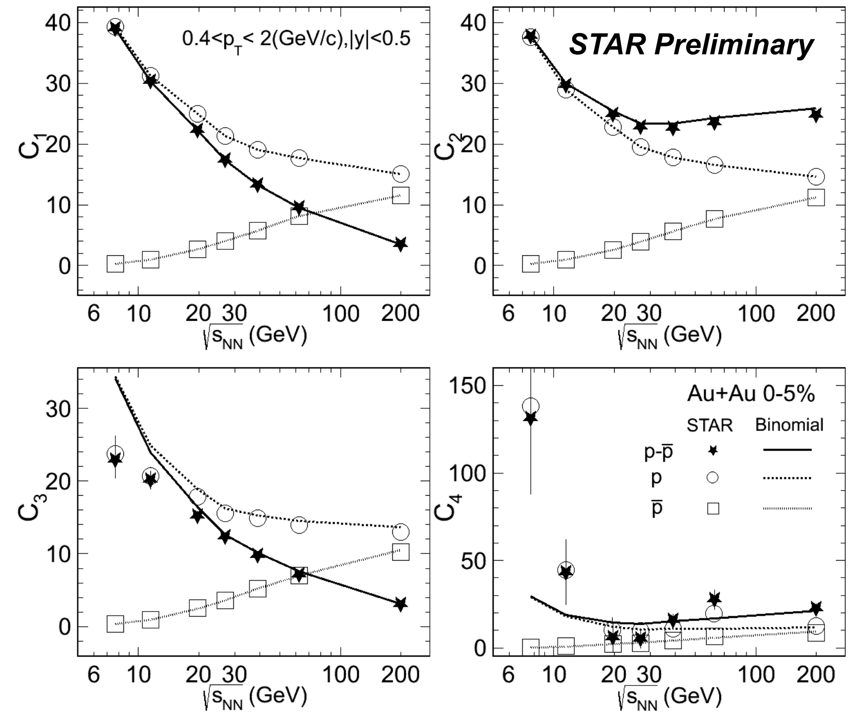

- The higher the order of cumulants the larger deviations from Poisson expectations for net-proton and proton.
- The binomial distribution (BD) better described the data than Poisson. But large deviations seen in C_3 and C_4 in central Au+Au collisions 7.7, 11.5, 19.6, 27 and 62.4 GeV.

Acceptance Study (I): p_T

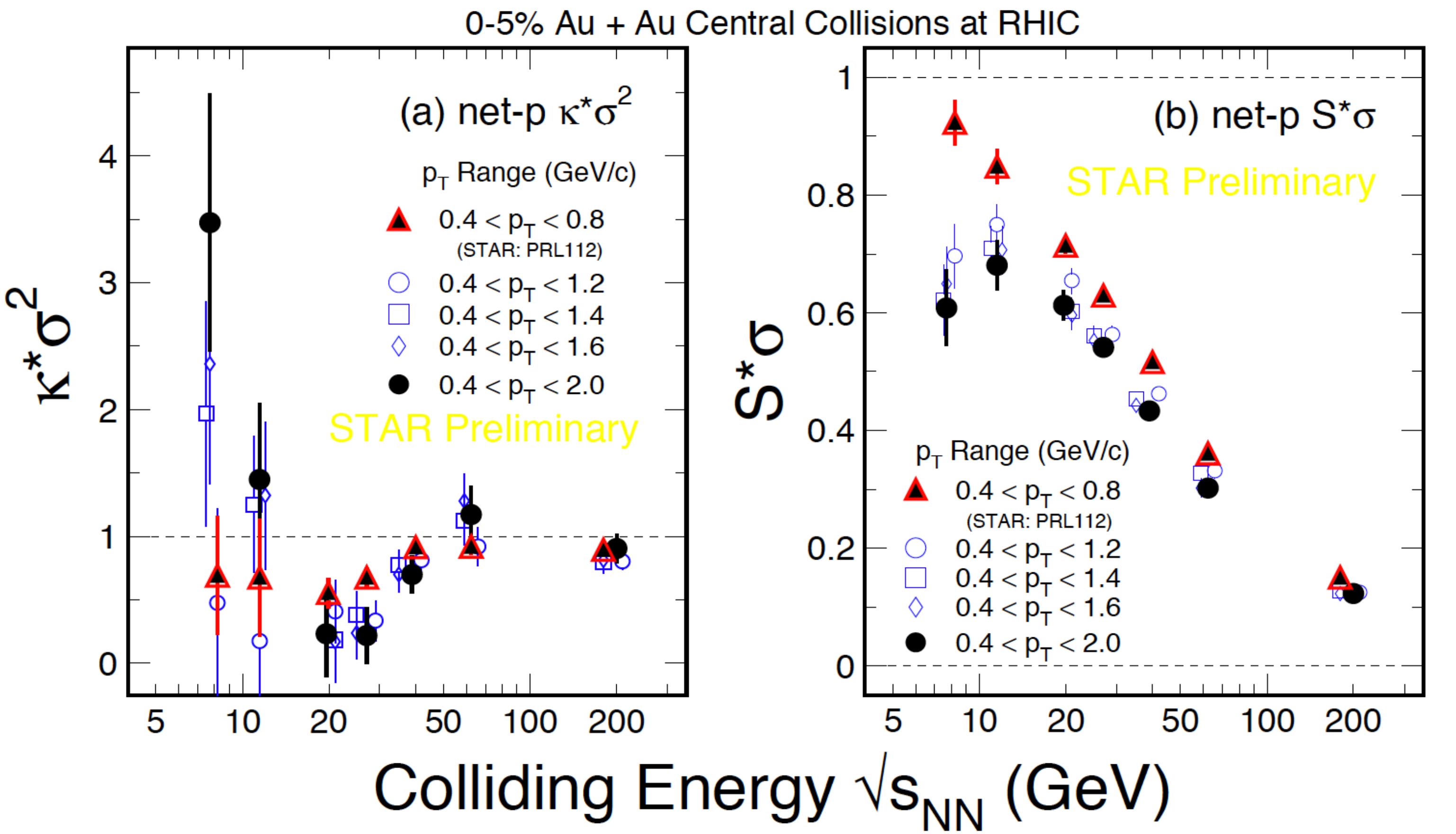

- K σ^2: the energy dependence tends to be more pronounced with wider p_T acceptance, relative to published results.
- S σ: the values are smaller for wider p_T acceptance.

Acceptance Study (II): Rapidity

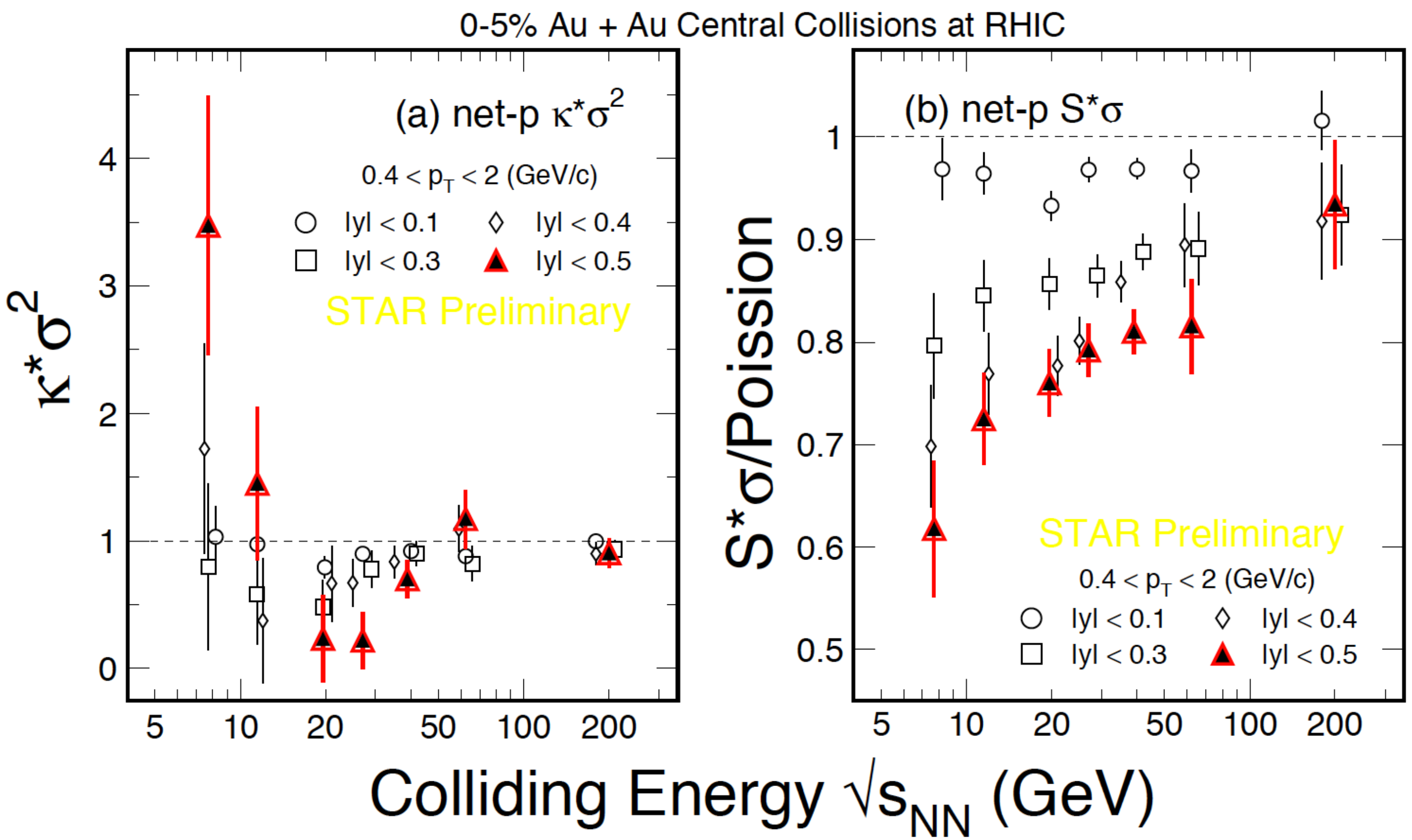

- The smaller the rapidity window the closer to the Poisson values.
- The acceptance needs to be large enough to capture the dynamical fluctuations. The related systematic errors should be carefully addressed.

Independent p, pbar Production Test

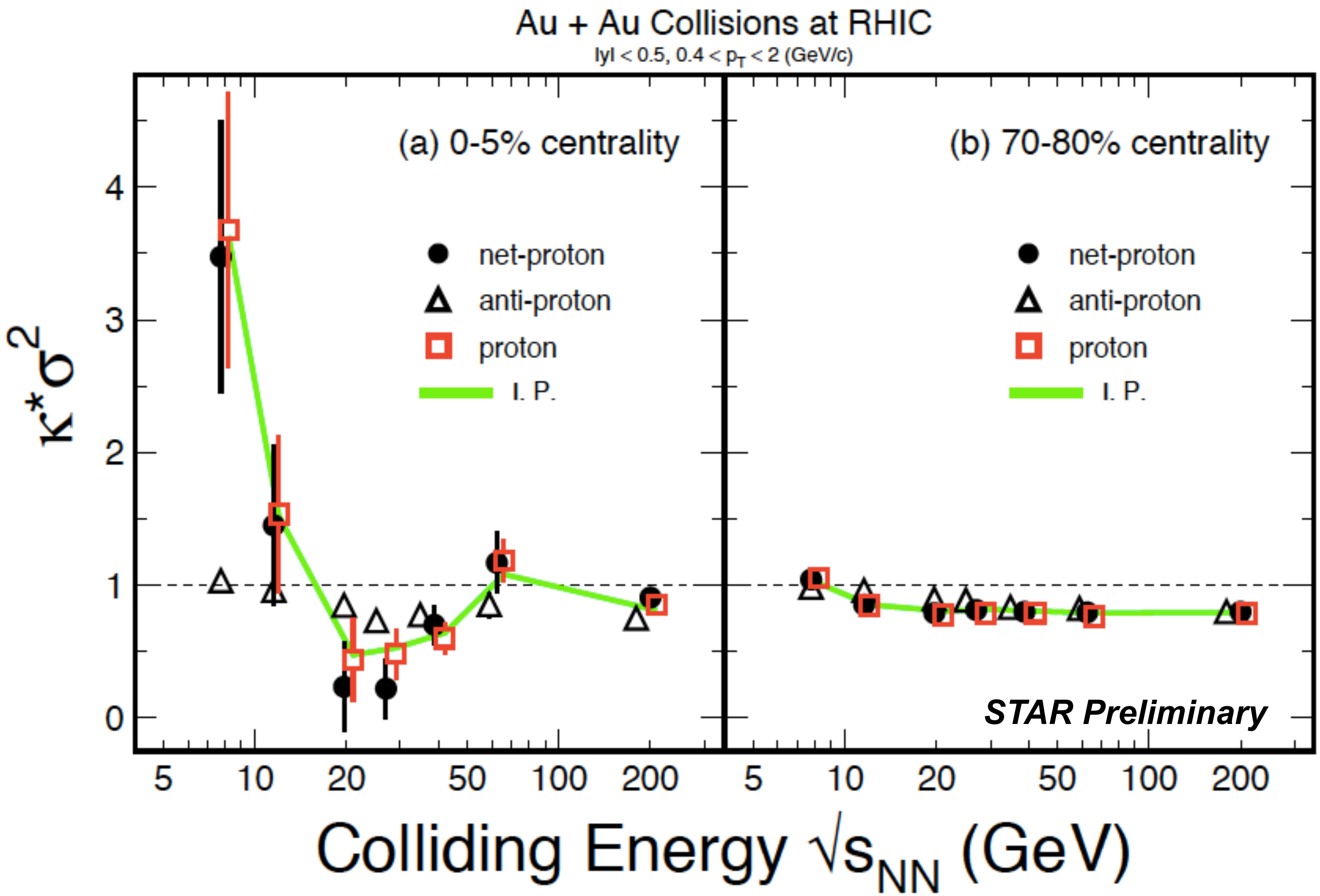

1) I.P. means de-correlation between protons and anti-protons.
2) I.P. closely traces proton and net-proton moments.
3) Anti-proton $\kappa*\sigma^2$ also show minimum around $\sqrt{s_{NN}}$ = 27 GeV .

Signature of CP：Theoretical Expectations

Misha Stephnov, CPOD 2014.

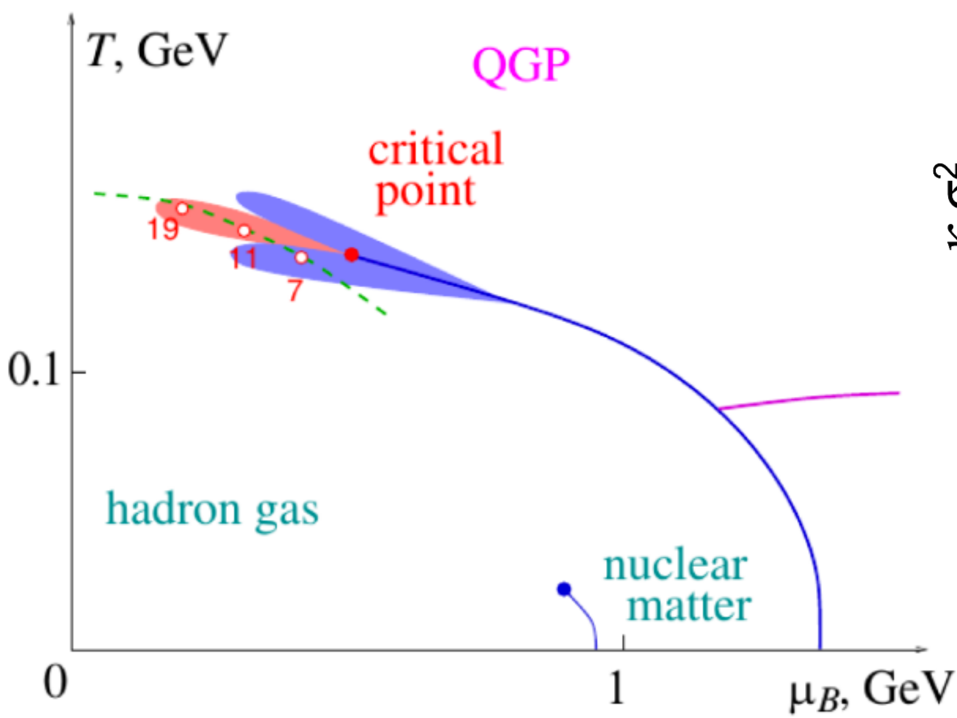

X. Luo, CPOD 2014

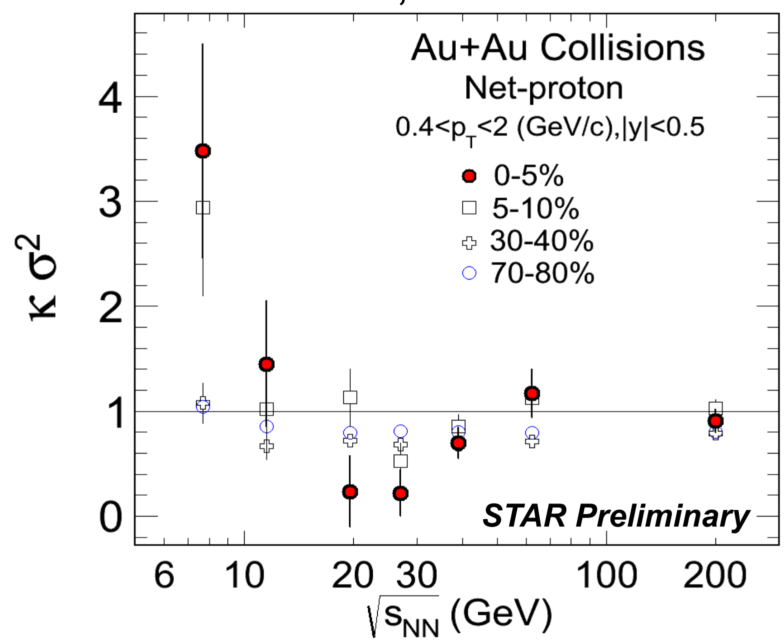

M.A. Stephanov, Phys. Rev. Lett. 107, 052301 (2011).
, J. Phys. G: 38, 124147 (2011).

$$\kappa_4 \sim N^4.$$

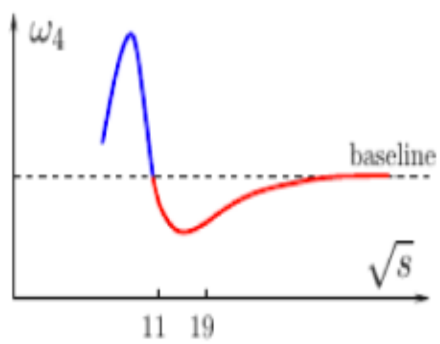

For Kurtosis, expecting a dip, then a significant increase with respect to the Poisson baseline near QCD Critical Point.

A similar calculation: J. Deng et al, arXiv: 1410.5454.

Discussion

1) To explore the QCD phase transition and CP of hot dense nuclear matter. The STAR experiment has carried out analysis for fluctuations of net-protons (proxy for net-B), net-kaons (proxy for net-S), and net-charge (Q).

2) To search for the CP, It is important to study contributions associated with heavy-ion collisions dynamics, such as finite size/time effects, volume fluctuations, resonance decay, hadronic scattering, conservation law effects, acceptance. Need proper modeling of the HIC.

3) To compare the experimental data with Lattice and/or HRG, one needs to know whether the system reach thermal equilibrium, GCE or CE?

Reference:

Experimental Data: STAR, PRL112, 032302 (2014). PRL113, 092301 (2014). PRL105, 022302 (2010).
HRG model studies: P. Garg, et al, PLB 726, 691 (2013). J. Fu, PLB722, 144 (2013). F. Karsch and K. Redlich , PLB695, 136 (2011). Marlene Nahrgang et al, arXiv: 1402.1238. P. Alba et al., arXiv:1403.4903
Transport model studies: X. Luo et al., JPG 40, 105104 (2013). N.R. Sahoo, et al., PRC 87, 044906 (2013).

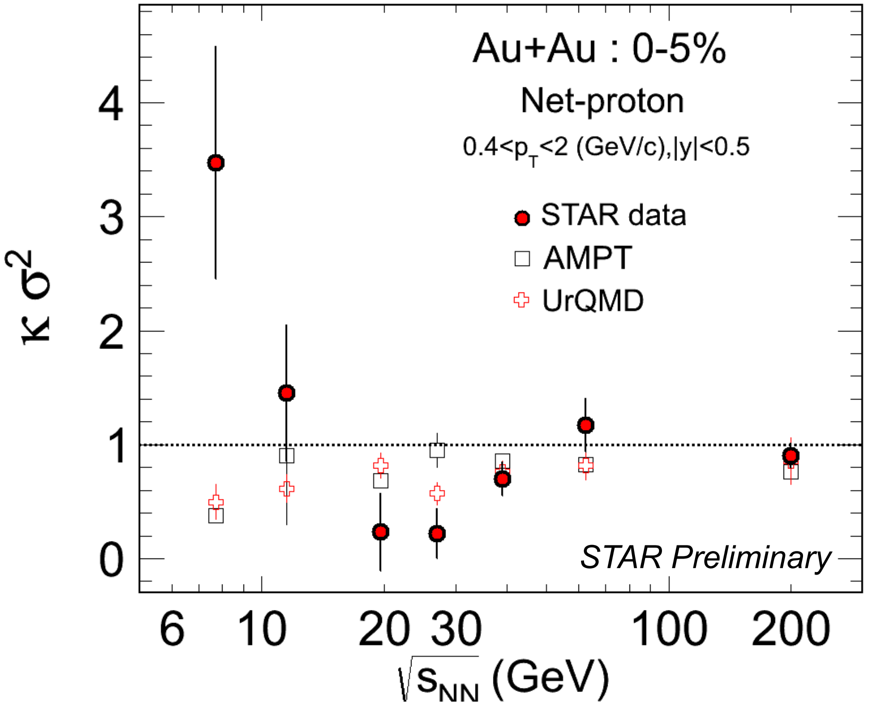

Rapidity Acceptance Study

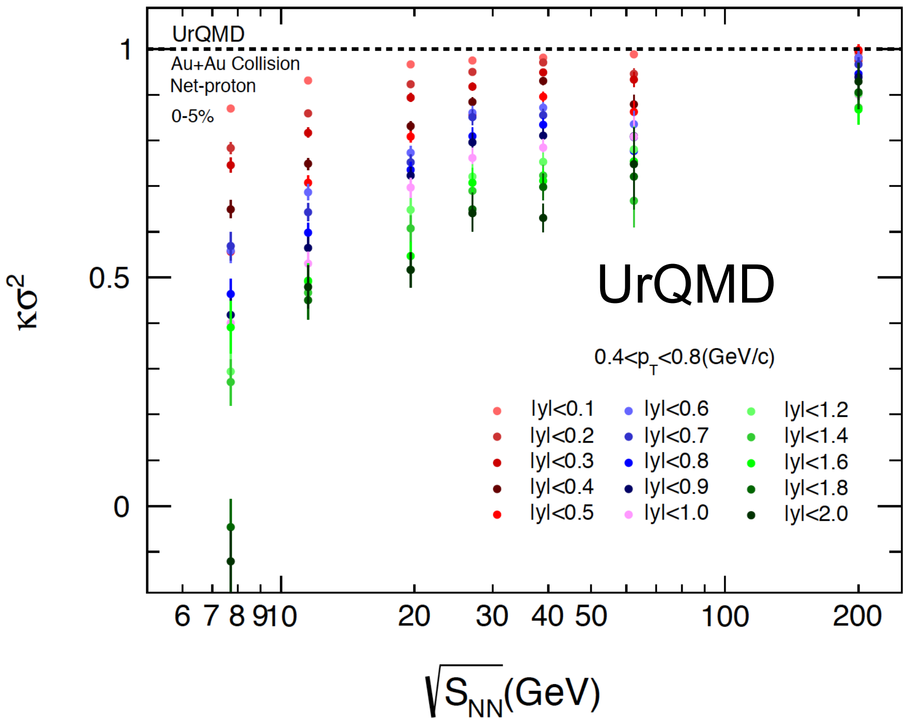

- The non-monotonic structure in the data cannot be reproduced by UrQMD and AMPT models.

- In UrQMD calculation, wider rapidity acceptance, larger suppression. Consistent with baryon number conservation effects.

Moments of Net-charge Distribution at RHIC

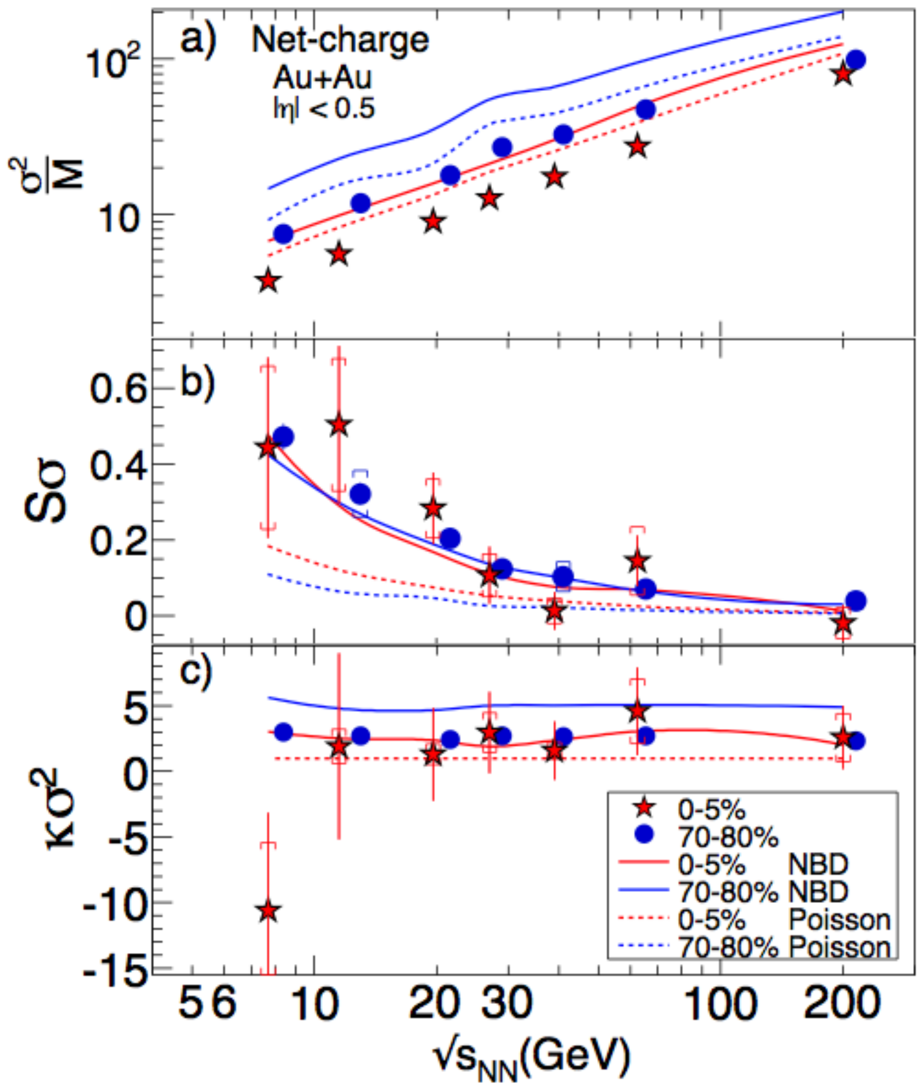

STAR results:
PRL**113** 092301 (2014).

- Within the current statistics, smooth energy dependence is observed for net-charge distributions.
- NBD has better description than Poisson for net-charges.
- Net-kaon analysis is ongoing.

$$error \propto O\left(\sigma^n / \varepsilon^\alpha\right)$$

σ (net-charge)>> σ (net-proton)

STAR Upgrades and BES Phase-II

- Fine energy scan at $\sqrt{s_{NN}}$ <~ 20 GeV
- Electron cooling will provide increased luminosity ~ 3-10 times
- STAR iTPC upgrade extends mid-rapidity coverage – beneficial to many crucial measurements.
- Forward Event Plane Detector (EPD)： Centrality and Event Plane Determination.

e-cooling

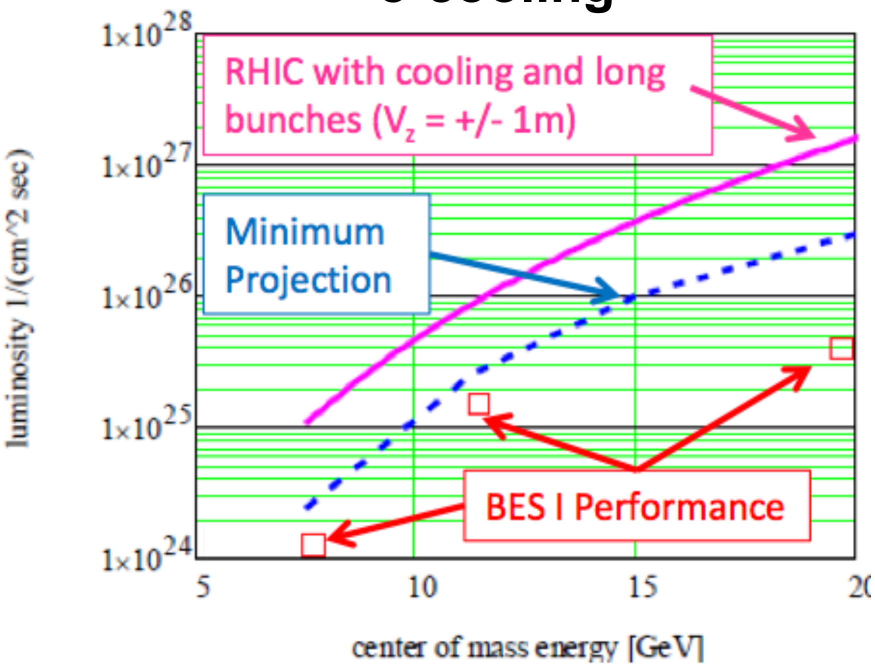

iTPC Upgrade

For moment analysis, iTPC upgrade will improve tracking efficiency and centrality resolution, EPD will provide centrality determination.

Summary and Outlook

- We present centrality and energy dependence of cumulants and their ratios for proton, antiproton and net-proton for the extended transverse momentum coverage [$|y|<0.5$, $0.4<p_T<2.0$ (GeV/c)] for Au+Au collisions at $\sqrt{s_{NN}}$ = 7.7,11.5, 19.6, 27, 39, 62.4 and 200 GeV.

- A unified description of efficiency correction and error estimation is applied to the moments of net-proton distributions.

- Significant impact of the kinematic cuts on higher moments of net-proton distributions observed. Evaluation of the systematic error is on going.

- Higher statistics are needed at low energies to explore the QCD phase structure: STAR upgrade and RHIC BES-II (from 2018). Fixed target experiment, CBM@FAIR.

Future CP Search in Exp. :

- **Higher Luminosity**
- **Higher Baryon Density**
- **Large Acceptance**

Thank you for your attention !!!

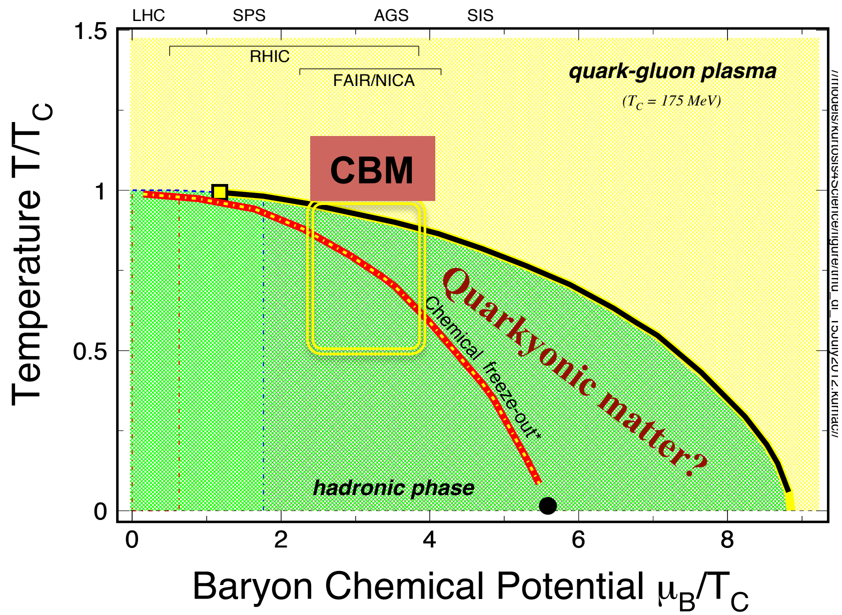

Exploring Phase Structure at High Baryon Density

（1） **QCD Critical Point**

（2） **Quarkyonic Phase/Phase Boundary**

Fixed Target Detector, CBM@FAIR

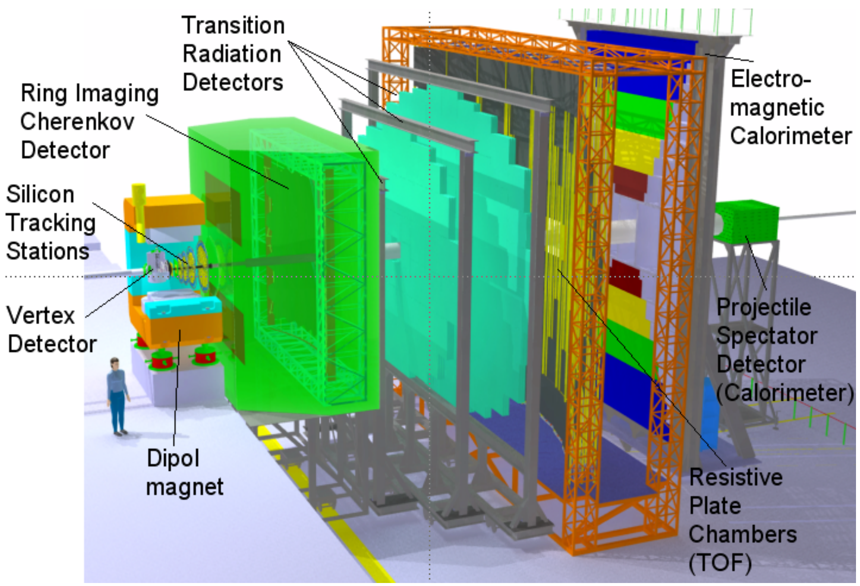

Center of Mass Energy $\sqrt{s_{NN}} \leqslant 8$ GeV per nucleon pair.

It allows us to explore the QCD phase structure at higher baryon density region with high precision !

Big Dipper Plot

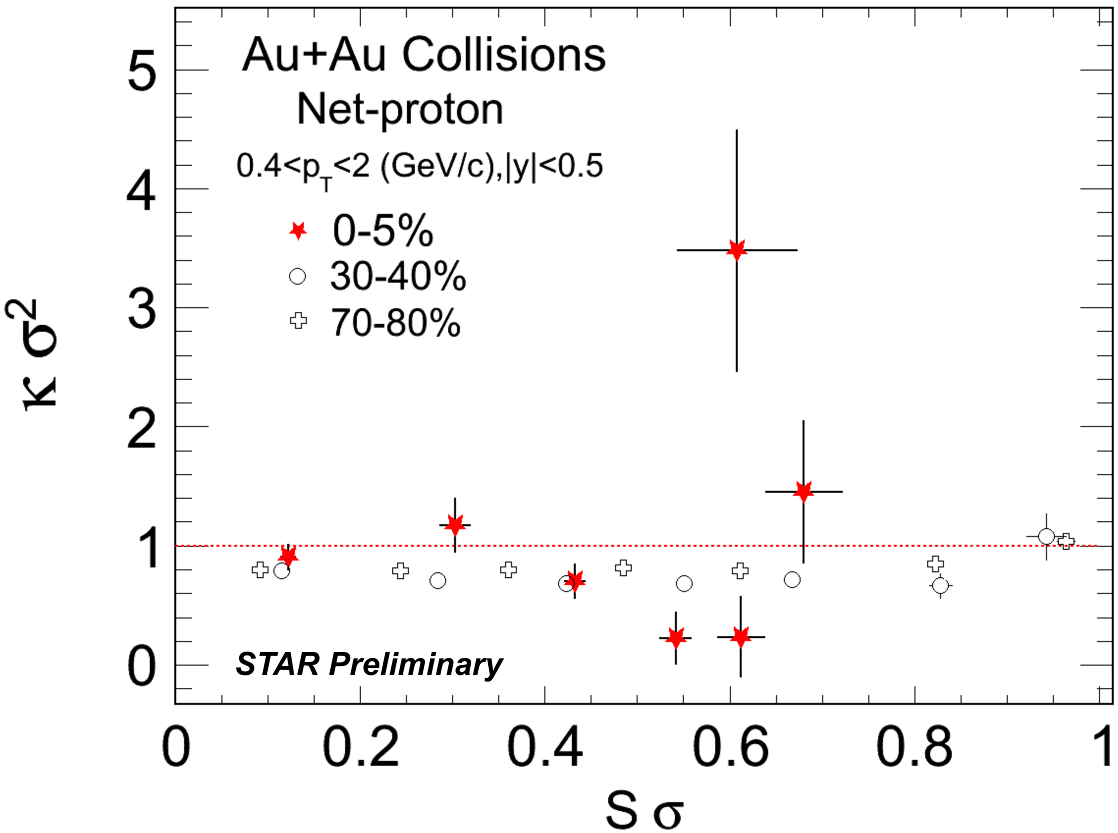

Taylor expansion in Lattice :

THERMO-meter :

$$\kappa\sigma^2 \sim \frac{\chi_B^4}{\chi_B^2}(T,0)$$

BARYO-meter :

$$S\sigma \sim \frac{\chi_B^3}{\chi_B^2}(T,\mu_B) \sim \tanh\left(\frac{\mu_B}{T}\right)$$

- A structure is observed for 0-5% most central data while it is flat for mid-central and peripheral collisions.
- Can be directly compared with theoretical calculations.

Baryon diffusion in heavy-ion collisions

Akihiko Monnai (RIKEN BNL Research Center)
In collaboration with: Björn Schenke (BNL)
G. Denicol, C. Shen, S. Jeon and C. Gale (McGill)

RIKEN BNL Center Workshop
"Theory and Modeling for the Beam Energy Scan: from Exploration to Discovery"
27th February 2015, BNL, NY, USA

Overview

1. Introduction
   - Collectivity in the era of beam energy scans
2. Dissipative hydrodynamics
   - Finite-density transport phenomena
   - Numerical analyses: Effects on baryon stopping
3. Towards full analyses of BES
   - (3+1)-D event-by-event analyses
4. Summary and outlook

AM, Phys. Rev. C 86, 014908 (2012)

B. Schenke and AM, in preparation

To collaborate with G. Denicol, C. Shen, S. Jeon and C. Gale (McGill)

Introduction

- Beam energy scans: exploration of QCD phase diagram in heavy-ion collisions

Big goals:

- Explicate the QGP properties at finite μ_B
- Search for a QCD critical point

Graphics by AM

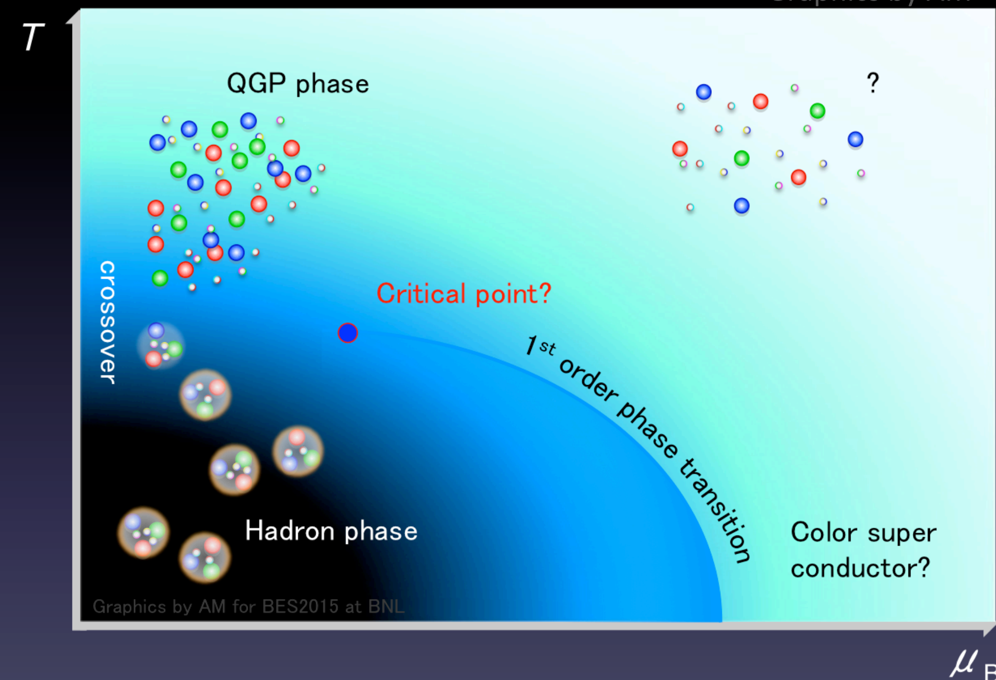

- Hydrodynamic approaches

The QGP at high energy is quantified as a relativistic fluid (2000)

We consider dissipative hydrodynamics at finite densities

Introduction

- Is hydrodynamics applicable?

STAR, arXiv:1206.5528

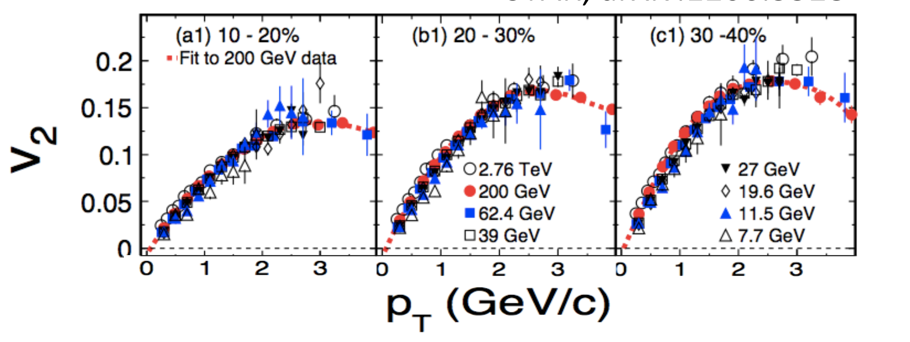

NA49 Col., PRC 68, 034903 (2003)

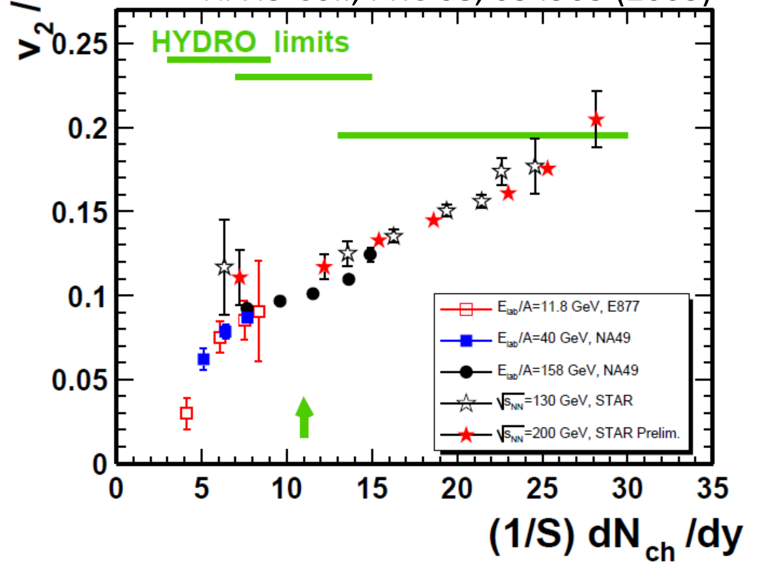

- Differential v_2 is large
- Integrated v_2 stays positive above $\sqrt{s_{NN}}$ ~ 3 GeV but is small

⇨ We will see, with off-equilibrium corrections, finite-density effects, state-of-art initial conditions and EoS

Introduction

- Schematic pictures of collision geometries

Graphics by AM

At high-energies

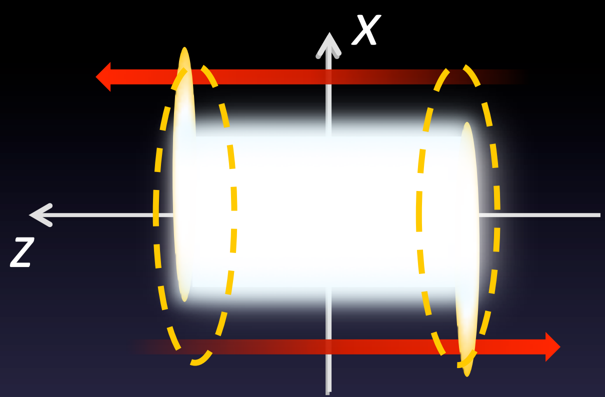

Net baryon at forward rapidity

At low-energies

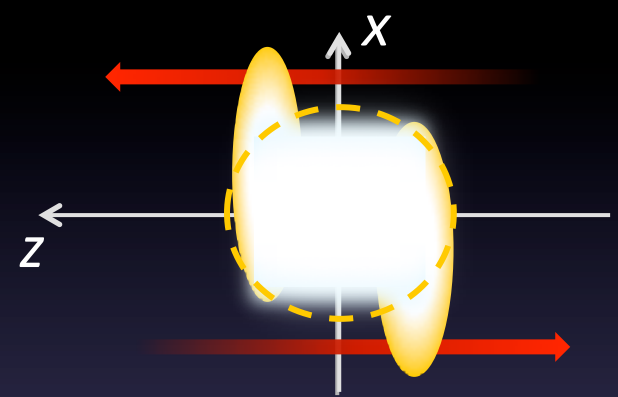

Net baryon at mid-rapidity

<u>Finite-density hydro is relevant in</u>

- Particle identification analyses (p/$\bar{\text{p}}$ ratio, etc.)
- Quantification of transport properties
- Bulk evolution for low energy collisions?

2. Dissipative hydrodynamics

Reference: AM, Phys. Rev. C 86, 014908 (2012)

Relativistic hydrodynamics

- Local thermalization; macroscopic variables are defined as fields

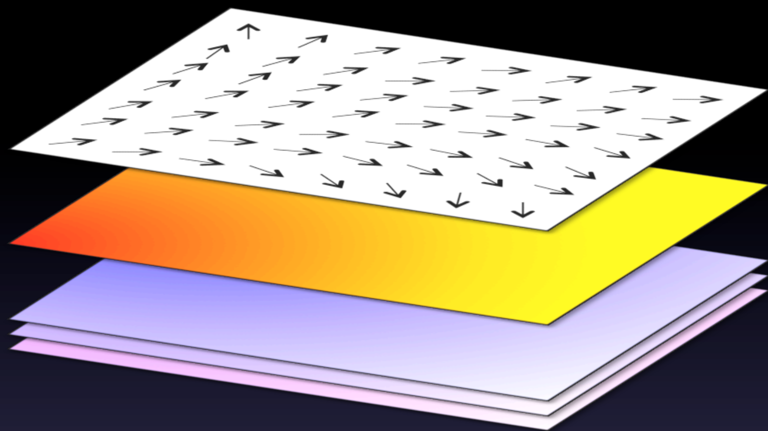

Flow $u^\mu(x)$ $\quad u^\mu u_\mu = 1$

Temperature $T(x)$

Chemical potentials $\mu_J(x)$

Gradient in the fields: thermodynamic force

Response to the gradients: transport coefficients (= 0 if ideal hydro)

- Energy-momentum tensor & conserved current are

$$T^{\mu\nu} = (e_0 + \delta e)u^\mu u^\nu - (P_0 + \Pi)\Delta^{\mu\nu} + 2W^{(\mu}u^{\nu)} + \pi^{\mu\nu}$$
$$N_J^\mu = (n_{J0} + \delta n_J)u^\mu + V_J^\mu$$

when decomposed with u^μ ; $\Delta^{\mu\nu} = g^{\mu\nu} - u^\mu u^\nu$

Thermodynamic quantities

- In local rest frame $u^\mu = (1,0,0,0)$

$$T^{\mu\nu} = T_0^{\mu\nu} + \delta T^{\mu\nu}$$

$$= \begin{pmatrix} e_0 & 0 & 0 & 0 \\ 0 & P_0 & 0 & 0 \\ 0 & 0 & P_0 & 0 \\ 0 & 0 & 0 & P_0 \end{pmatrix} + \begin{pmatrix} \delta e & W^x & W^y & W^z \\ W^x & \Pi + \pi^{xx} & \pi^{xy} & \pi^{xz} \\ W^y & \pi^{yx} & \Pi + \pi^{yy} & \pi^{yz} \\ W^z & \pi^{zx} & \pi^{yz} & \Pi + \pi^{zz} \end{pmatrix}$$

$$N_J^\mu = N_{J0}^\mu + \delta N_J^\mu \quad (J = 1,2,\ldots,N)$$

$$= \begin{pmatrix} n_{J0} \\ 0 \\ 0 \\ 0 \end{pmatrix} + \begin{pmatrix} \delta n_J \\ V_J^x \\ V_J^y \\ V_J^z \end{pmatrix}$$

2+*N* equilibrium quantities

Energy density: e_0

Hydrostatic pressure: P_0

J-th charge density: n_{J0}

10+4*N* dissipative currents

Energy density deviation: δe

Bulk pressure: Π

Energy current: W^μ

Shear stress tensor: $\pi^{\mu\nu}$

J-th charge density dev.: δn_J

J-th charge current: V_J^μ

Viscosity and diffusion

- Meaning of “dissipation” in fluids

Off-equilibrium processes at linear order

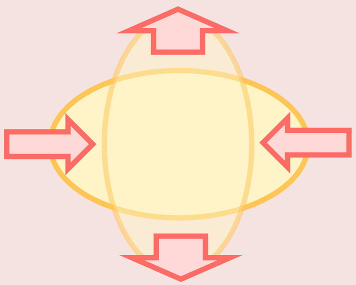

Shear viscosity
= response to
deformation

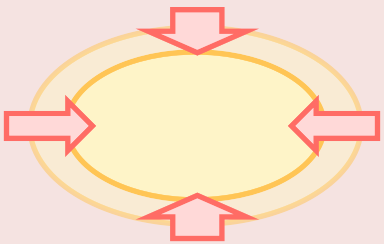

Bulk viscosity
= response to
expansion

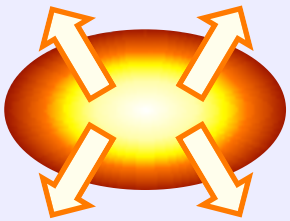

Energy dissipation
= response to
thermal gradient

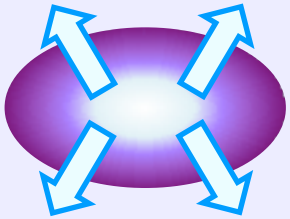

Charge diffusion
= response to
chemical gradients

viscosity

dissipation/diffusion

- Cross terms among thermodynamic forces are present (discussed later)
- 2^{nd} order corrections are required for hydrodynamic stability and causality

W. Israel, J. M. Stewart, Annals Phys 118, 341 (1979)
W.A. Hiscock, L. Lindblom, Phys. Rev. D 31, 725 (1985)

Dissipative hydrodynamics

- Relativistic hydrodynamic equations

Conservation laws $\partial_\mu T^{\mu\nu} = 0 \quad \partial_\mu N_B^\mu = 0$ +

$$D = u^\mu \partial_\mu$$
$$\nabla^\mu = \partial^\mu - u^\mu D$$

The law of increasing entropy -> Constitutive equations

$$\Pi = -\zeta \nabla_\mu u^\mu - \zeta_{\Pi\delta e} D\frac{1}{T} + \zeta_{\Pi\delta n_B} D\frac{\mu_B}{T} - \tau_\Pi D\Pi + \chi^a_{\Pi\Pi}\Pi D\frac{\mu_B}{T} + \chi^b_{\Pi\Pi}\Pi D\frac{1}{T} + \chi^c_{\Pi\Pi}\Pi\nabla_\mu u^\mu$$
$$+ \chi^a_{\Pi V} V_\mu \nabla^\mu \frac{\mu_K}{T} + \chi^b_{\Pi V} V_\mu \nabla^\mu \frac{1}{T} + \chi^c_{\Pi V} V_\mu D u^\mu + \chi^d_{\Pi V}\nabla^\mu V_\mu + \chi_{\Pi\pi}\pi_{\mu\nu}\nabla^{\langle\mu}u^{\nu\rangle}$$

$$V^\mu = \kappa_V \nabla^\mu \frac{\mu_B}{T} - \kappa_{VW}\left(\frac{1}{T}Du^\mu + \nabla^\mu \frac{1}{T}\right) - \tau_V \Delta^{\mu\nu} D V_\nu + \chi^a_{VV} V^\mu_K D\frac{\mu_B}{T} + \chi^b_{VV} V^\mu D\frac{1}{T}$$
$$+ \chi^c_{V_J V} V^\mu \nabla_\nu u^\nu + \chi^d_{VV} V^\nu_K \nabla_\nu u^\mu + \chi^e_{VV} V^\nu \nabla^\mu u_\nu + \chi^a_{V\pi}\pi^{\mu\nu}\nabla_\nu \frac{\mu_B}{T} + \chi^b_{V\pi}\pi^{\mu\nu}\nabla_\nu \frac{1}{T}$$
$$+ \chi^c_{V\pi}\pi^{\mu\nu} D u_\nu + \chi^d_{V\pi}\Delta^{\mu\nu}\nabla^\rho \pi_{\nu\rho} + \chi^a_{V\Pi}\Pi\nabla^\mu \frac{\mu_B}{T} + \chi^b_{V\Pi}\Pi\nabla^\mu \frac{1}{T} + \chi^c_{V\Pi}\Pi D u^\mu + \chi^d_{V\Pi}\nabla^\mu \Pi$$

$$\pi^{\mu\nu} = 2\eta\nabla^{\langle\mu}u^{\nu\rangle} - \tau_\pi D\pi^{\langle\mu\nu\rangle} + \chi_{\pi\Pi}\Pi\nabla^{\langle\mu}u^{\nu\rangle} + \chi^a_{\pi\pi}\pi^{\mu\nu} D\frac{\mu_B}{T} + \chi^b_{\pi\pi}\pi^{\mu\nu} D\frac{1}{T} + \chi^c_{\pi\pi}\pi^{\mu\nu}\nabla_\rho u^\rho$$
$$+ \chi^d_{\pi\pi}\pi^{\rho\langle\mu}\nabla_\rho u^{\nu\rangle} + \chi^{aJ}_{\pi V} V^{\langle\mu}\nabla^{\nu\rangle}\frac{\mu_B}{T} + \chi^b_{\pi V} V^{\langle\mu}\nabla^{\nu\rangle}\frac{1}{T} + \chi^c_{\pi V} V^{\langle\mu} D u^{\nu\rangle} + \chi^d_{\pi V}\nabla^{\langle\mu}V^{\nu\rangle}$$

Numerical analyses

- Baryon stopping

Plot: BRAHMS, PRL 93, 102301 (2004)

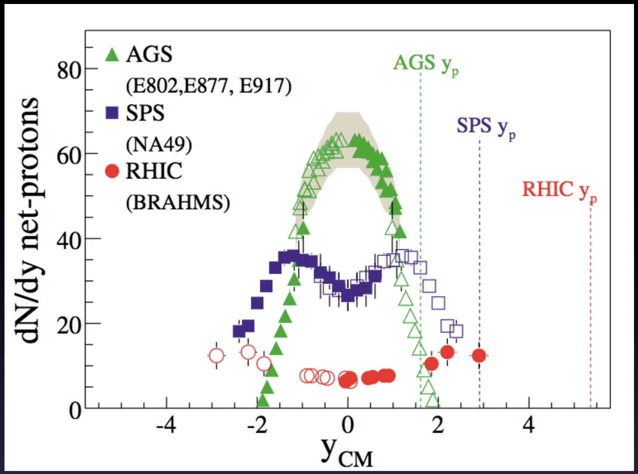

Baryon stopping can quantify kinetic energy available for QGP production

mean rapidity loss <δ*y*>
= rapidity of projectile nuclei y_b
– mean rapidity of net baryon <*y*>

- What we do:

▶ Estimate dissipative hydro evolution of net baryon rapidity distribution with viscosities and baryon diffusion

(1+1)-D expansion is considered because dependence on transverse geometry is small

PHOBOS, PRC 69, 034909 (2004)

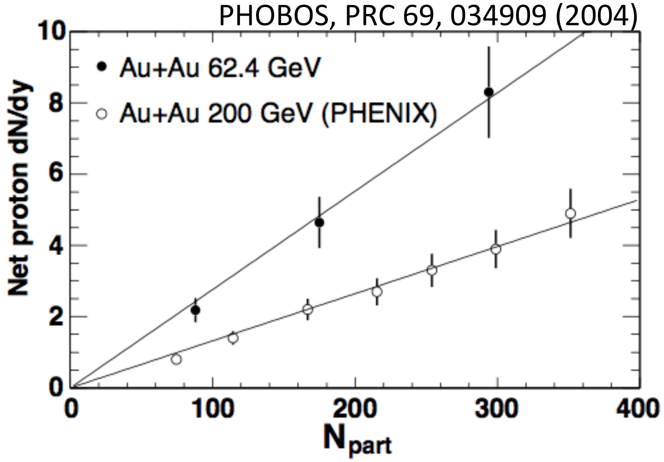

Simulation Setup

- Equation of state: Lattice QCD with Taylor expansion

$$\frac{P(T,\mu_B)}{T^4} = \frac{P(T,0)}{T^4} + \frac{\chi_B^{(2)}(T,0)}{2}\left(\frac{\mu_B}{T}\right)^2 + \mathcal{O}\left(\frac{\mu_B}{T}\right)^4$$

$P(T,0)$: Equation of state at vanishing μ_B — S. Borsanyi *et al.*, JHEP 1011, 077

$\chi_B^{(2)}(T,0)$: 2nd order baryon fluctuation — S. Borsanyi *et al.*, JHEP 1201, 138

- Transport coefficients: AdS/CFT + phenomenology

Shear viscosity: $\eta = s/4\pi$ — P. Kovtun *et al.*, PRL 94, 111601

Bulk viscosity: $\zeta = 5(\frac{1}{3} - c_s^2)\eta$ — A. Hosoya *et al.*, AP 154, 229

Baryon dissipation: $\kappa_V = \frac{c_V}{2\pi}(\frac{\partial \mu_B}{\partial n_B})_T^{-1}$ — M. Natsuume and T. Okamura, PRD 77, 066014

- Initial conditions: Color glass theory

Energy density: MC-KLN

Net baryon density: Valence quark dist.

H. J. Drescher and Y. Nara, PRC 75, 034905; 76, 041903
Y. Mehtar-Tani and G. Wolschin, PRL 102, 182301; PRC 80, 054905

Results

- Net baryon rapidity distribution at RHIC and LHC

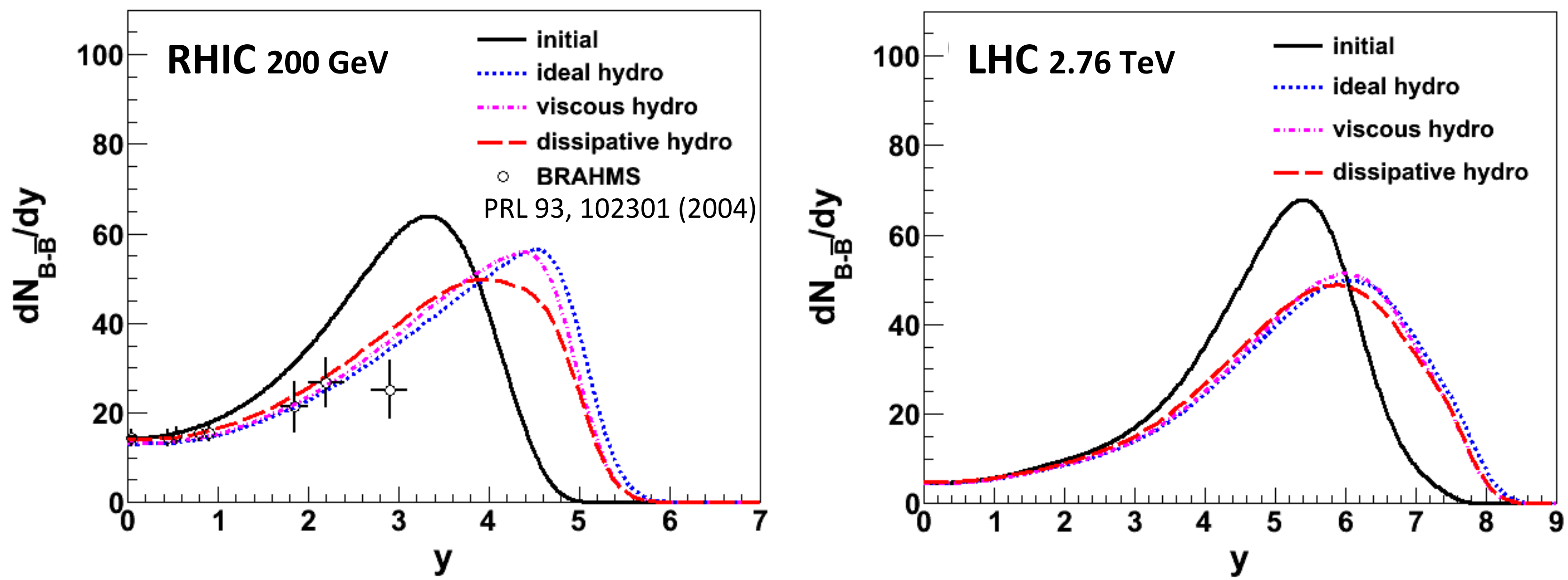

- Net baryon is carried to forward rapidity by convection
- Viscosities slow the longitudinal expansion
- Net baryon diffuses into mid-rapidity

Results

- Net baryon rapidity distribution at SPS and RHIC

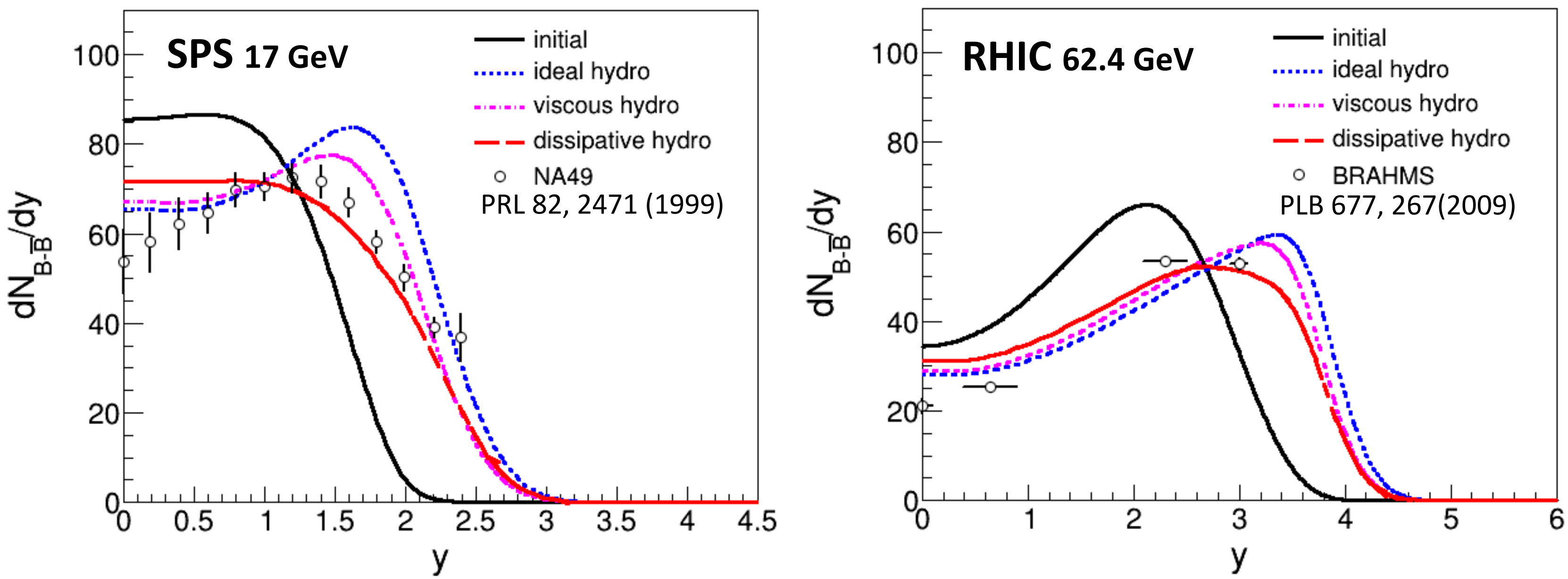

- Results can be comparable to data (not fine-tuned yet)
- Dissipative effect could be larger for lower energies

Note: CGC-based initial conditions (not best suitable at low energies)

Results

- Mean rapidity loss at RHIC

Mean rapidity loss $\langle \delta y \rangle = y_p - \langle y \rangle$

$$\langle y \rangle = \int_0^{y_p} y \frac{dN_{B-\bar{B}}(y)}{dy} dy \Big/ \int_0^{y_p} \frac{dN_{B-\bar{B}}(y)}{dy} dy$$

Initial loss (200GeV): $\langle \delta y \rangle = 2.67$

Ideal hydro: $\langle \delta y \rangle = 2.09$

Viscous hydro: $\langle \delta y \rangle = 2.16$

Dissipative hydro: $\langle \delta y \rangle = 2.26$

BRHAMS, PLB 677, 267 (2009) + Hydro results

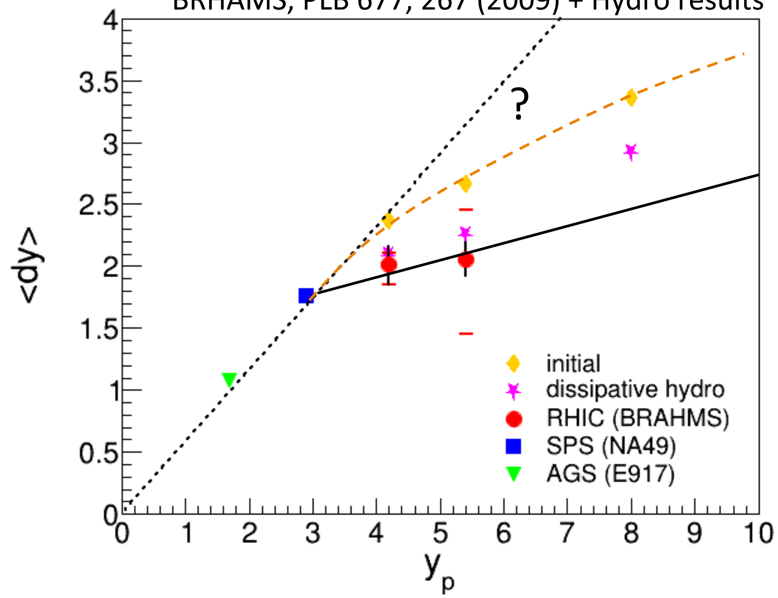

- The collision becomes effectively more transparent by hydrodynamic evolution

⇨ More kinetic energy is available for QGP production

Cross-coupling effects (1)

- Linear response theory and cross terms

Bulk pressure (w/o charges)

$$\Pi = \underbrace{-\zeta_{\Pi\Pi}\frac{1}{T}\nabla_\mu u^\mu}_{\text{Response to expansion}} \underbrace{- \zeta_{\Pi\delta e} D\frac{1}{T}}_{\text{Response to cooling}} = -\underbrace{\left(\frac{\zeta_{\Pi\Pi}}{T} + \frac{\zeta_{\Pi\delta e}}{T}c_s^2\right)}_{\text{bulk viscosity } \zeta}\nabla_\mu u^\mu$$

- Response to expansion itself can be as large as shear viscosity
- Cancelled by the cross term except for crossover where $c_s^2 \sim 0$

⇨ A reason for general smallness of bulk viscosity

Baryon dissipation current

$$V^\mu = \kappa_V \nabla^\mu \frac{\mu_B}{T} - \kappa_{VW}\left(\nabla^\mu \frac{1}{T} + \frac{1}{T} D u^\mu\right)$$

- Baryon dissipation can be induced by thermal gradient + acceleration

Results

- Thermo-diffusion effect (a.k.a. Soret effect)

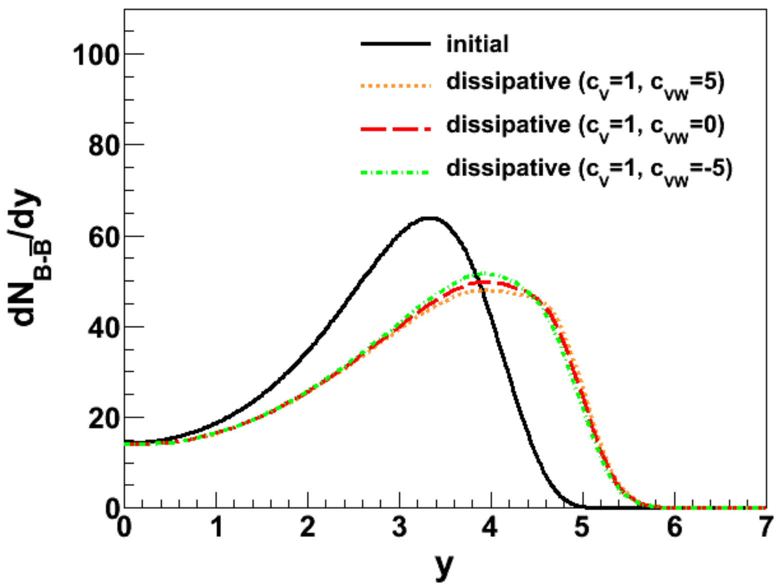

- Baryon dissipation can be induced by thermal gradients (and acceleration)

$$V^\mu = \kappa_V \nabla^\mu \frac{\mu_B}{T} - \kappa_{VW}\left(\nabla^\mu \frac{1}{T} + \frac{1}{T} D u^\mu\right)$$

at the linear order

- Cross coefficients can be negative if the coefficient matrix is positive definite

▪ The effect of cross coupling is likely to be small in high-energy collisions

because of the matter-antimatter symmetry

$V^\mu(\mu_B) = -V^\mu(-\mu_B)$ which leads to $\kappa_{VW}(\mu_B = 0) = 0$

Cross-coupling effects (2)

- Mixing of the currents at the 2nd order

System dependence

Hydrodynamic theory considers:
$\pi^{\mu\nu} \sim \Pi \sim V^{\mu}$

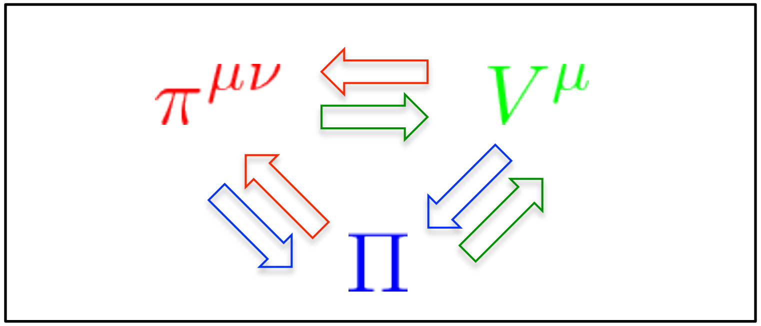

In high-energy nuclear collisions:
$\pi^{\mu\nu} > \Pi > V^{\mu}$

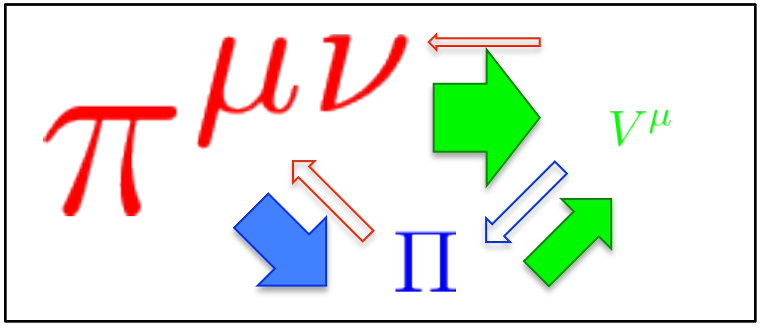

- Bulk-shear coupling term in bulk pressure
  Baryon-shear and baryon-bulk coupling terms in baryon dissipation
  have more impact than other 2nd order terms (numerically confirmed)
- Applicability of the expansion is dependent on the 2nd order transport coefficients

Summary so far

- Dissipative hydrodynamic model is developed and simulated in (1+1)D at finite baryon density
  - Net baryon distribution is widened in hydrodynamic evolution
    - ⇨ Transparency of the collision is effectively enhanced
    - ⇨ More kinetic energy may be available at QGP (and jet) production in early stages
  - The results can be sensitive to baryon diffusion coefficient
    - ⇨ Ambiguities remain in initial condition, but the distribution has important information
  - Hydrodynamic results for baryon stopping are comparable to the experimental data at lower energies

3. Towards full analyses of BES

B. Schenke and AM

To collaborate with G. Denicol, C. Shen, S. Jeon and C. Gale

Initial conditions

3D Monte-Carlo Glauber model

Net baryon distribution

Valence quark PDF for the rapidity distribution before collisions

⇨ A collision modifies the distribution via the kernel

S. Jeon and J. Kapusta, PRC 56, 468

$$Q(y-y_P, y_P-y_T, y-y_P) = \lambda \frac{\cosh(y-y_P)}{\sinh(y_P-y_T)} + (1-\lambda)\delta(y-y_P)$$

⇨ Keep sampling for all the parton-parton collisions

Entropy distribution

Entropy is deposited between the last collision pairs

A simple and straight-forward extension of 2D MC Glauber model

B. Schenke

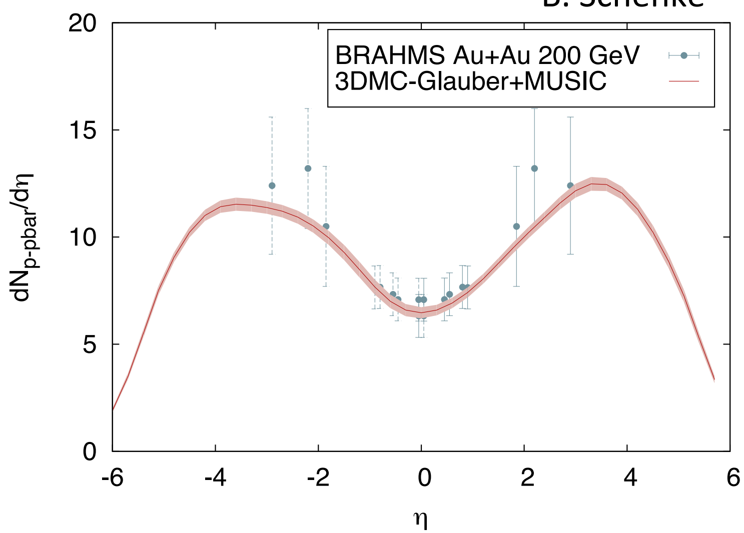

Equation of state

- Lattice QCD (Taylor expansion) + Hadron resonance gas

$$\frac{P}{T^4} = \frac{1}{2}\left[1 - \tanh\frac{T - T_c(\mu_B)}{\Delta T_c}\right]\frac{P_{\mathrm{HRS}}(T)}{T^4} + \frac{1}{2}\left[1 + \tanh\frac{T - T_c(\mu_B)}{\Delta T_c}\right]\frac{P_{\mathrm{lat}}(T_s)}{T_s^4}$$

where

$$T_c = 0.166 - c(0.139\mu_B^2 + 0.053\mu_B^4)$$
$$T_s = T + c[T_c(0) - T_c(\mu_B)]$$

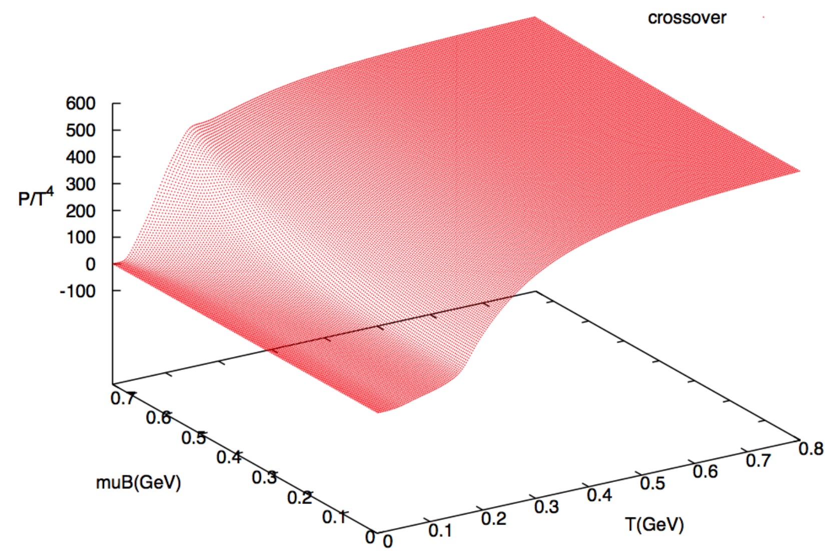

EoS of kinetic theory must match EoS for hydrodynamics at freeze-out (or energy-momentum/net baryon does not conserve)

u^μ, T, μ_B

Particle spectrum $$E_i \frac{dN_i}{d^3p} = \frac{g_i}{(2\pi)^3}\int_\Sigma p_i^\mu d\sigma_\mu f_i$$ Hydrodynamics

Hydrodynamic evolution

- 3+1 D event-by-event analyses (work in progress)

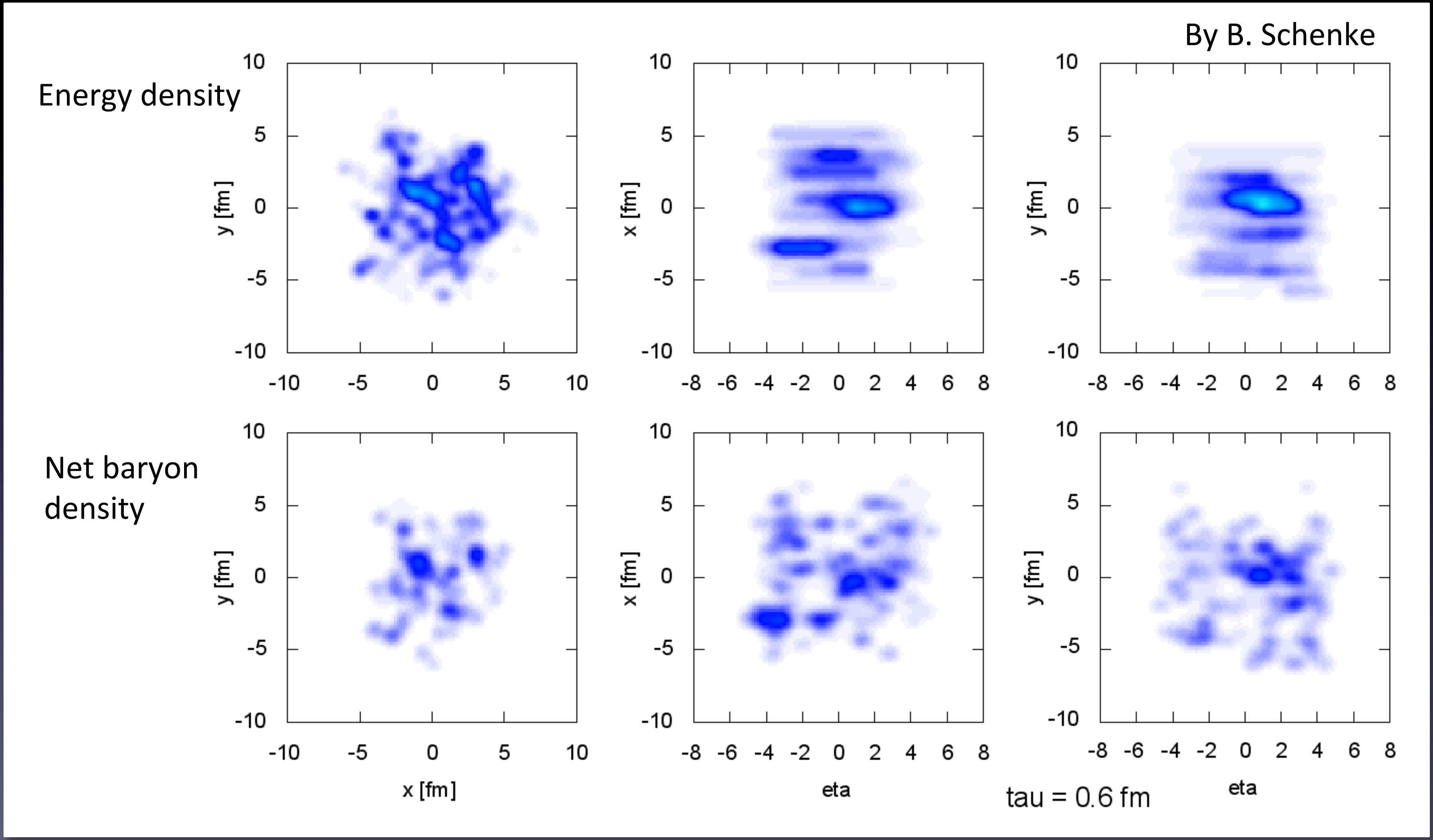

4. Summary and outlook

Summary and outlook

- (3+1)-D event-by-event hydrodynamic model at finite baryon density in preparation
  - Initial condition: 3D Monte-Carlo Glauber model
  - Equation of state: Lattice QCD with Taylor expansion method + Hadron resonance gas
  - Viscosity: shear viscosity + bulk viscosity
  - Baryon diffusion: *see next talk by Chun*

- Thank you for listening!

Fluid dynamics and fluctuations in the QCD phase diagram

Marlene Nahrgang

Duke University

RBRC Workshop, Theory and Modeling for the Beam Energy Scan

In collaboration with Christoph Herold (Suranaree University of Technology)

The goal...

... is to understand the phase structure and the phase diagram of QCD theoretically and experimentally.

Make the connection between QCD thermodynamics (LQCD) and heavy-ion collisions.

https://news.uic.edu/collider-reveals-sharp-change-from-quark-soup-to-atoms

From the theory side...

- Lattice QCD calculations:

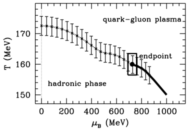

Wuppertal-Budapest (2002)

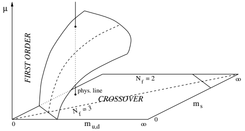

F. Karsch et al. (2004)

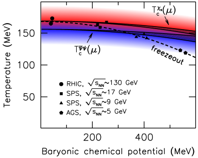

Wuppertal-Budapest (2011)

+ newer approaches to circumvent the sign problem!

- Functional methods of QCD:

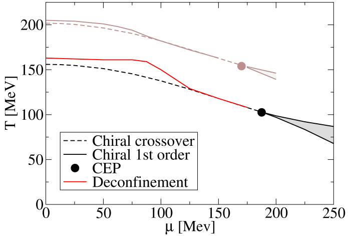

C. Fischer, J. Luecker, PLB**718** (2013)

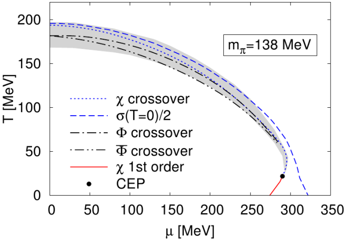

T. Herbst, J. Pawlowski, BJ. Schaefer PRD**88** (2013)

From the experimental side...

- One of the main goals of heavy-ion collisions is to understand the phase structure of hot and dense strongly interacting matter.

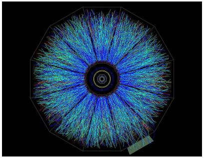

ALICE PHENIX FAIR SHINE NA61 NICA

- Can we experimentally produce a deconfined phase with colored degrees of freedom?
- What are the properties of this phase?
- What is the nature of the phase transition between deconfined and hadronic phase?

Dynamics of heavy-ion collisions

Systems created in heavy-ion collisions

- are short-lived,
- spatially small,
- inhomogeneous,
- and highly dynamical

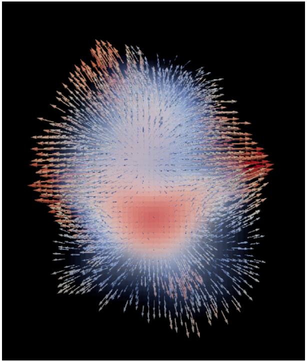

plot by H. Petersen, madai.us

Indications that we might still be able to learn about thermodynamic properties:

- success of fluid dynamics ($\Rightarrow$ local thermalization) with input from LQCD (EoS)
- success of statistical model and HRG analysis of particle yields and fluctuations

Dynamics of heavy-ion collisions

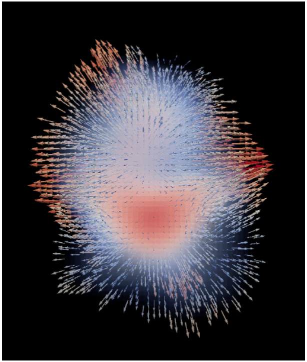

plot by H. Petersen, madai.us

Systems created in heavy-ion collisions

- are short-lived,
- spatially small,
- inhomogeneous,
- and highly dynamical

Indications that we might still be able to learn about thermodynamic properties:

- success of fluid dynamics ($\Rightarrow$ local thermalization) with input from LQCD (EoS)
- success of statistical model and HRG analysis of particle yields and fluctuations

Phase transitions in fluid dynamics

- Conceptually, studying phase transitions in fluid dynamics is really simple!
- $\Rightarrow$ Just need to know the equation of state and transport coefficients!

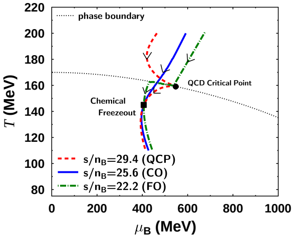

C. Nonaka, M. Asakawa PRC**71** (2005)

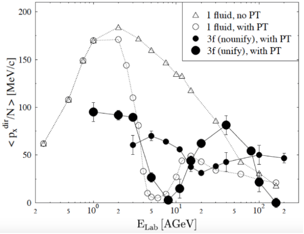

J. Brachmann et al. PRC**61** (2000)

-
-

Phase transitions in fluid dynamics

- Conceptually, studying phase transitions in fluid dynamics is really simple!
- $\Rightarrow$ Just need to know the equation of state and transport coefficients!

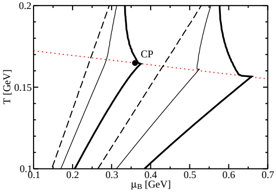

M. Bluhm, B. Kampfer CPOD 2006

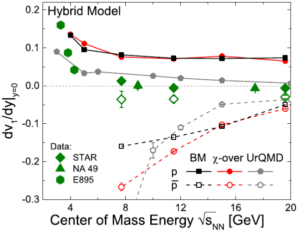

J. Steinheimer et al. PRC**89** (2014)

- No clear sensitivity on the equation of state in observables.
- BUT at the phase transition: fluctuations matter! Including fluctuations in fluid dynamics is more challenging...

Fluctuations at the phase transition

At a critical point

- correlation length of fluctuations of the order parameter diverges $\xi \to \infty$
- fluctuations of the order parameter diverge: $\langle \Delta\sigma^n \rangle \propto \xi^\alpha$ with higher powers of divergence for higher moments
- mean-field studies in Ginzburg-Landau theories, beyond mean-field: renormalization group
- relaxation time diverges $\Rightarrow$ critical slowing down!

$\Rightarrow$ fluctuations in equilibrated systems!

... and a first-order PT:

- at T_c coexistence of two stable thermodynamic phases
- metastable states above and below T_c $\Rightarrow$ supercooling and -heating
- nucleation and spinodal decomposition in nonequilibrium
- domain formation and large inhomogeneities

$\Rightarrow$ fluctuations in nonequilibrium!

... but also at the crossover:

- remnant of the $O(4)$ universality class in the chiral limit.

$\Rightarrow$ fluctuations in equilibrated systems!

Ref. by many people: M. Stephanov, E. Shuryak, K. Rajagopal, L. Csernai, J. Randrup, I. Mishustin, C. Sasaki, B. Friman, K. Redlich et al.

Nonequilibrium chiral fluid dynamics (NχFD)

IDEA: combine the dynamical propagation of fluctuations at the phase transition with fluid dynamical expansion!

(model-independent is nice, but in the end some real input is needed...)

- Langevin equation for the sigma field: damping and noise from the interaction with the quarks

$$\partial_\mu \partial^\mu \sigma + \frac{\delta U}{\delta \sigma} + g\rho_s + \eta \partial_t \sigma = \xi$$

- Phenomenological dynamics for the Polyakov-loop

$$\eta_\ell \partial_t \ell T^2 + \frac{\partial V_{\mathrm{eff}}}{\partial \ell} = \xi_\ell$$

- Fluid dynamical expansion of the quark fluid = heat bath, including energy-momentum exchange

$$\partial_\mu T^{\mu\nu}_{\mathrm{q}} = S^\nu = -\partial_\mu T^{\mu\nu}_\sigma \; , \quad \partial_\mu N^\mu_{\mathrm{q}} = 0$$

$\Rightarrow$ includes a stochastic source term!

MN, S. Leupold, I. Mishustin, C. Herold, M. Bleicher, PRC **84** (2011); PLB **711** (2012); JPG **40** (2013)
C. Herold, MN, I. Mishustin, M. Bleicher PRC **87** (2013); NPA**925** (2014), C. Herold, MN, Y. Yan, C. Kobdaj JPG **41** (2014)

Dynamical slowing down

Phenomenological equation:

$$\frac{\mathrm{d}}{\mathrm{d}t} m_\sigma(t) = -\Gamma[m_\sigma(t)](m_\sigma(t) - \frac{1}{\xi_{\mathrm{eq}}(t)})$$

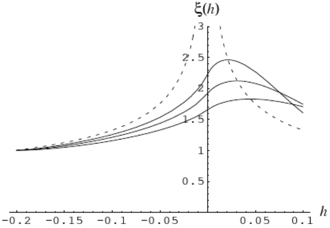

B. Berdnikov and K. Rajagopal, PRD **61** (2000))

Input from the dynamical universality class.

In NχFD:

$$\xi^2 = 1/m_\sigma^2 = (\frac{\mathrm{d}^2 V_{\mathrm{eff}}}{\mathrm{d}\sigma^2})^{-1}$$

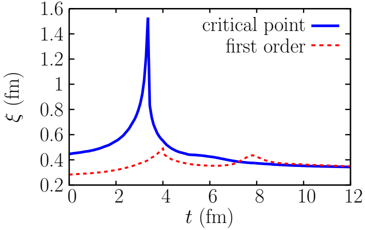

C. Herold, MN, I. Mishustin, M. Bleicher PRC **87** (2013)

Definition of ξ in inhomogeneous systems: involves averaging!

$\Rightarrow$ Similar magnitude of $\xi/\xi_0 \sim 1.5 - 2$!

Dynamics versus equilibration

- Fluctuations of the order parameter:

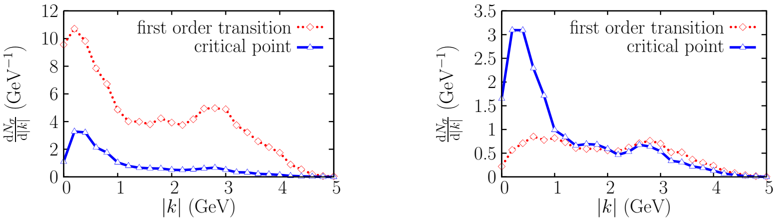

- Strong enhancement of the intensities for a first-order phase transition during the evolution.
- Strong enhancement of the intensities for a critical point scenario after equilibration.

C. Herold, MN, I. Mishustin, M. Bleicher PRC **87** (2013)

Trajectories and isentropes at finite μ_B

Isentropes in the PQM model

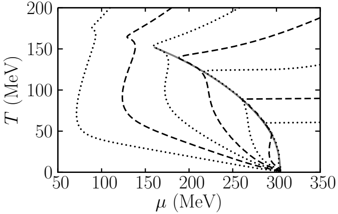

Fluid dynamical trajectories

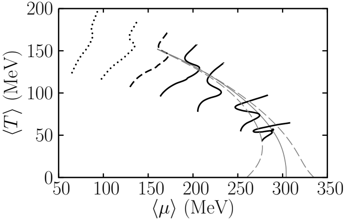

- Fluid dynamical trajectories similar to the isentropes in the crossover region.
- No significant features in the trajectories left of the critical point.
- Right of the critical point: trajectories differ from isentropes and the system spends significant time in the spinodal region! $\Rightarrow$ possibility of spinodal decomposition!

Bubble formation in net-baryon density

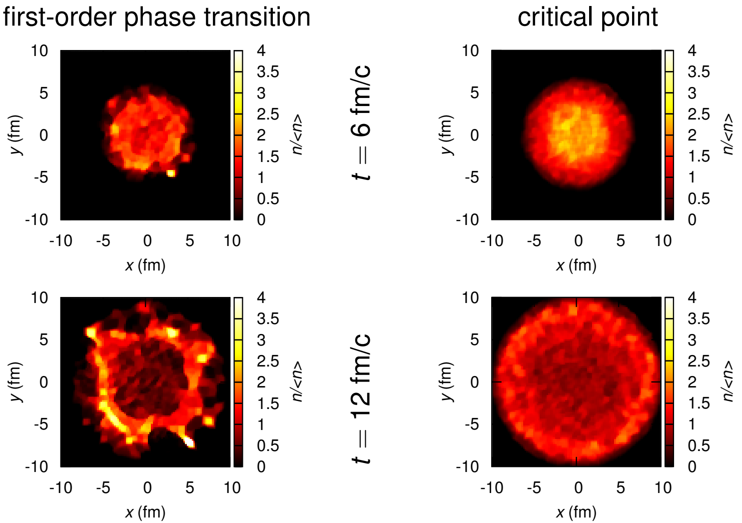

C. Herold, MN, I. Mishustin, M. Bleicher, arxiv:1304.5372

Bubble formation in net-baryon density

Fourier-decomposition of $n_B(x, y)$
$\rightarrow$ quantifies strong enhancement of first-order PT versus critical point/crossover.

not (yet) in momentum space!

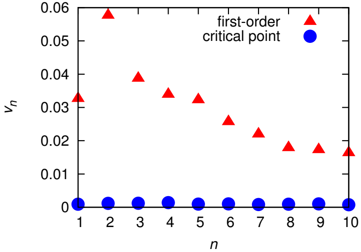

Can we expect experimental evidences for the first-order phase transition from bubble formation?

- Do the irregularities survive when a realistic hadronic phase is assumed?
- A strong pressure could transform the coordinate-space irregularities into momentum-space Fourier-coefficients of baryon-correlations $\Rightarrow$ enhanced higher flow harmonics at a first-order phase transition? Very eos dependent!

Comparison

- Nonequilibrium construction of the EoS from QGP and hadronic matter:

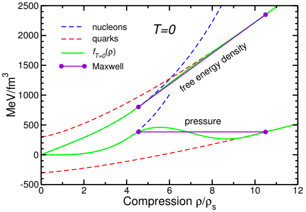

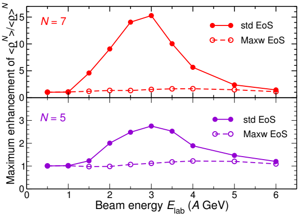

J. Steinheimer, J. Randrup, PRL **109** (2012), PRC **87** (2013)

- Significant amplification of **initial** density irregularities

With phase transition:

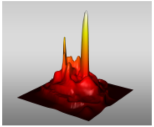

Without phase transition:

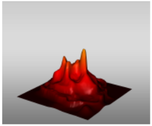

Density enhancement:

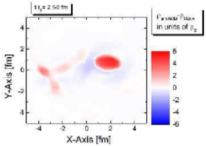

plot by V. Koch

- BUT: deterministic evolution of the system ⇒ No inhomogeneities for smooth initial conditions!

EoS: PQM versus QH

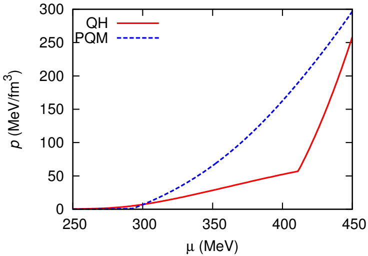

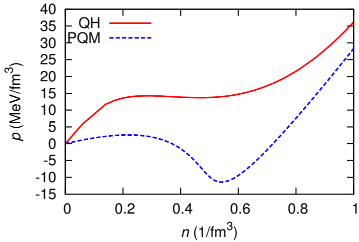

- Below μ_c, $p \approx 0$ in PQM, while it still decreases in HQ model and $p < 0$ can arise in PQM!
- Several eos lead to similar pressures at $\mu_B \approx 0$, but differ at large μ_B.
- With coexistence between dense quark matter and compressed nuclear matter (HQ-EoS) : $\partial p_c / \partial T < 0$
- From effective models, like PNJL, PQM etc.: $\partial p_c / \partial T > 0$

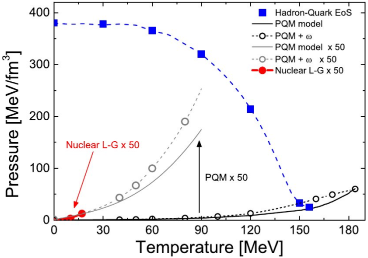

J. Steinheimer, J. Randrup, V. Koch PRC**89** (2014)

SU(3) chiral quark-hadron model

- Hadronic SU(3) non-linear sigma model including quark degrees of freedom

$$\mathcal{L} = \sum_i \bar{\psi}_i (i\gamma^\mu \partial_\mu - \gamma^0 g_{i\omega}\omega - M_i)\psi_i + 1/2(\partial_\mu \sigma)^2 - U(\sigma, \zeta, \omega) - \mathcal{U}(\ell)$$

and effective masses generated by

$$M_q = g_{q\sigma}\sigma + g_{q\zeta}\zeta + M_{0q} + g_{q\ell}(1-\ell)$$
$$M_B = g_{B\sigma}\sigma + g_{B\zeta}\zeta + M_{0B} + g_{qB}\ell^2$$

V. Dexheimer, S. Schramm, PRC**81** (2010); M. Hempel, V. Dexheimer, S. Schramm, I. Iosilevskiy PRC**88** (2013)

- hadrons are included as quasi-particle degrees of freedom
- yields a realistic structure of the phase diagram and phenomenologically acceptable results for saturated nuclear matter:

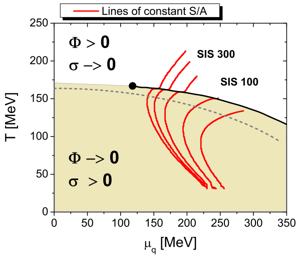

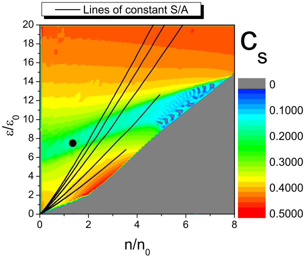

J. Steinheimer, V. Dexheimer, H. Petersen, M. Bleicher, S. Schramm, H. Stoecker, PRC**81** (2010)

PQM vs. QH model - stability of droplets

PQM EoS

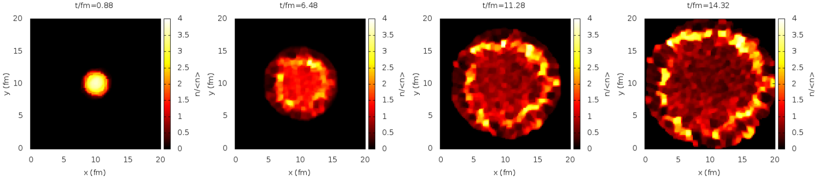

QH EoS

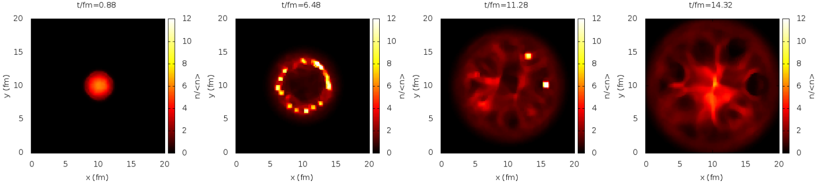

- Dynamical and stochastic droplet formation at the phase transition and subsequent decay in the hadronic phase.

PQM vs. QH model - moments of netbaryon density

Define normalized moments of the net-baryon density distribution as:

$$\langle n^N \rangle = \int \mathrm{d}^3 x n(x)^N P_n(x) \quad \text{with} \quad P_n(x) = \frac{n(x)}{\int \mathrm{d}^3 x n(x)}$$

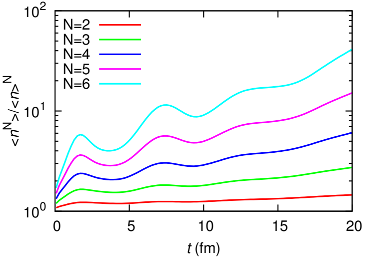

PQM EoS

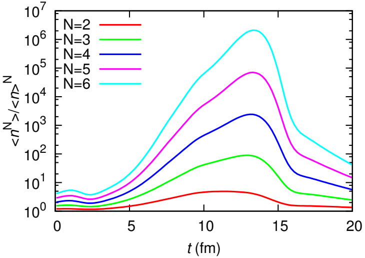

QH EoS

- Infinite increase in the PQM.
- Increase in the HQ model around the phase transition followed by a rapid decrease due to pressure in the hadronic phase!
- REMEMBER: We started with smooth initial conditions and all inhomogeneities are formed dynamically!

And the critical point?

- At $\mu_B \neq 0$ σ mixes with the net-baryon density n (and e and $\vec{m}$)
- In a Ginzburg-Landau formalism:

$$V(\sigma, n) = \int \mathrm{d}^3x (\sum_m (a_m \sigma^m + b_m n^m) + \sum_{m,l} c_{m,l} \sigma^m n^l) - h\sigma - jn$$

- $V(\sigma, n)$ has a flat direction in $(a\sigma, bn)$ direction
- Equations of motion (including symmetries in $V(\sigma, n)$):

$$\partial_t^2 \sigma = -\Gamma \delta V / \delta \sigma + \ldots$$

$$\partial_t n = \gamma \vec{\nabla}^2 \delta V / \delta n + \ldots$$

- two time scales (with $D \to 0$ at the critical point)

$$\omega_1 \propto -i\Gamma a$$

$$\omega_2 \propto -i\gamma D \vec{q}^2$$

- The diffusive mode becomes the critical mode in the long-time dynamics. These fluctuations need to be included at the critical point!

H. Fuji, M. Ohtani PRD**70** (2004); M. Stephanov, D. Son PRD**70** (2004)

Fluid dynamical fluctuations

- Already in equilibrium there are thermal fluctuations
- The fast processes, which lead to local equilibration also lead to noise!

Stochastic viscous fluid dynamics:

$$T^{\mu\nu} = T^{\mu\nu}_{\mathrm{eq}} + \Delta T^{\mu\nu}_{\mathrm{visc}} + \Xi^{\mu\nu} \qquad \text{with} \quad \langle \Xi^{\mu\nu} \rangle = 0$$
$$N^{\mu} = N^{\mu}_{\mathrm{eq}} + \Delta N^{\mu}_{\mathrm{visc}} + \mathrm{I}^{\mu} \qquad \text{with} \quad \langle \mathrm{I}^{\mu} \rangle = 0$$

The two formulations differ when one calculates correlation functions!

In linear response theory the retarded correlator

- $\langle T^{\mu\nu}(x) T^{\mu\nu}(x') \rangle$ gives the viscosities and
- $\langle N^{\mu}(x) N^{\mu}(x') \rangle$ the charge conductivities

via the dissipation-fluctuation theorem (Kubo-formula)!

When dissipation is included also fluctuations need to be included!

P. Kovtun, J.Phys. A**45** (2012); C. Chafin and T. Schäfer, PRA**87** (2013); P. Romatschke and R. E. Young, PRA**87** (2013);
K. Murase, T. Hirano, arXiv:1304.3243; C. Young et al. arxiv:1407.1077

Fluid dynamical fluctuations

- In second-order fluid dynamics the relaxation equations become (e.g. for $\pi^{\mu\nu}$):

$$u^\gamma \partial_\gamma \pi^{\mu\nu} = -\frac{\pi^{\mu\nu} - \pi^{\mu\nu}_{\rm NS}}{\tau_\pi} + I^{\mu\nu}_\pi + \xi^{\mu\nu}$$

- With the white noise approximation: $\langle \xi^{\mu\nu}_\pi \xi^{\alpha\beta}_\pi \rangle = 2T\eta\Delta^{\mu\nu\alpha\beta}\delta^{(4)}(x - x')$
- In a numerical treatment $\rightarrow$ discretization: $\langle \xi^2 \rangle \propto \frac{1}{\Delta V}$
- $\Rightarrow$ large fluctuations from cell to cell - can a fluid dynamical code handle this?

Example:
non-relativistic Navier-Stokes equations with fluctuations, one-dimensional, dilute gas, periodic boundary conditions

J. Bell, A. Garcia, S. Williams, PRE**76** (2007)

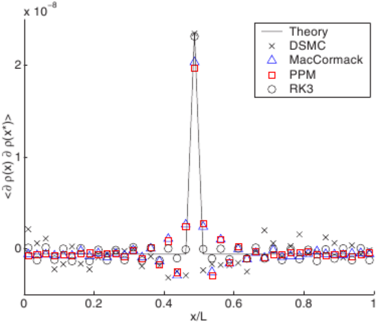

Summary

- Fluctuation data from heavy-ion collisions at finite μ_B can only be understood with dynamical models of the phase transition!
- In NχFD, effects like critical slowing down and droplet formation can be observed.
- PQM-like EoS do not include pressure in hadronic phase, droplets remain stable.
- In HQ-like EoS: droplets form dynamically at the phase transition, then decay.
- Next steps: particle production in NχFD and (net-baryon) fluid dynamical fluctuations.

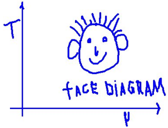

Challenges for the BES II

- Need good dynamical models.
- Need good input.
- Need good observables.
- Need good data.

Challenges for the BES II

- Need good dynamical models.
  Initial state, coupling to FD, propagation of fluctuations, coupling to hadrons, ...
- Need good input.
  Equation of state, phase transition dynamics, transport coefficients, ...
- Need good observables.
  Large scale simulations, sensitivity analysis, statistical tools, ...
- Need good data.
  Efficiency corrected, smaller error bars, 14.5 GeV, different particle species, ...

backup

Chiral model with dilatons

- Compare to a dilaton effective quark-meson model C. Sasaki, I. Mishustin PRC**85** (2012)

Susceptibilities along the spinodals:

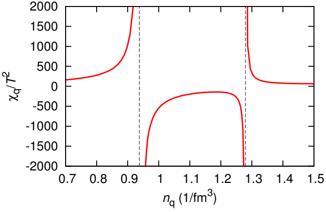

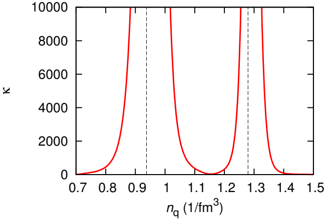

pressure vs density

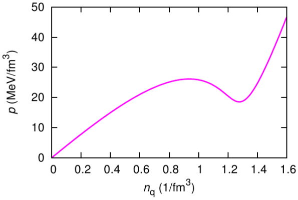

fluid dynamical trajectories

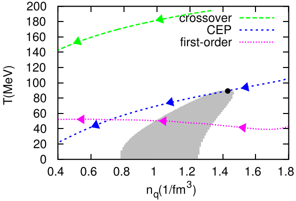

- Improvement over the PQM EoS!

Toward quantitative and rigorous conclusions from heavy ion collisions

Scott Pratt, Michigan State University

MADAI Collaboration

Models and Data Analysis Initiative

http://madai.us

Cyber-enabled Discovery and Innovation

MICHIGAN STATE UNIVERSITY

Duke UNIVERSITY

THE UNIVERSITY of NORTH CAROLINA at CHAPEL HILL

renci

1st MADAI Collaboration Meeting, SANDIA 2010

How this was done before (*v*2 and η/s)

Study single parameter vs. single observable

$$v_2 \equiv \langle \cos 2\phi \rangle$$

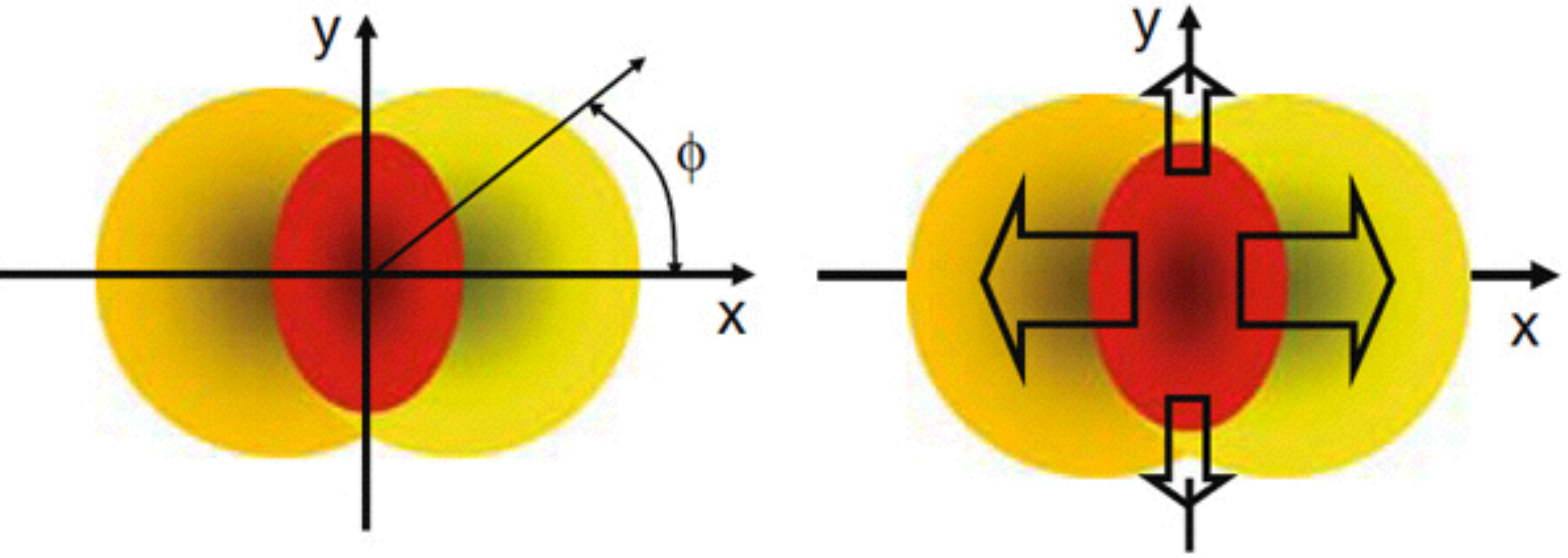

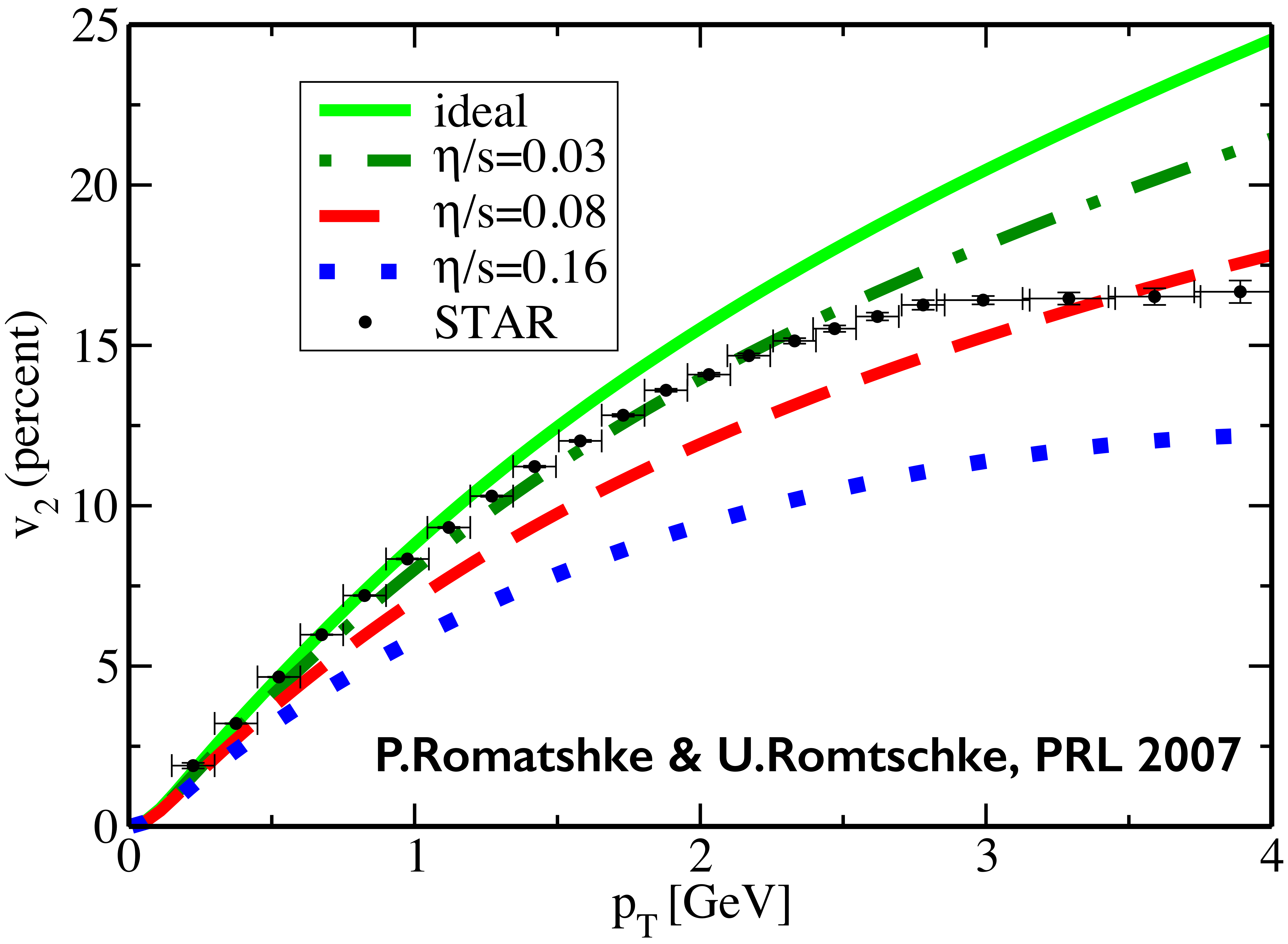

PROBLEM

v2 depends on ....

- viscosity
- saturation model
- pre-thermal flow
- Eq. of State
- T-dependence of η/s
- initial T_{xx}/T_{zz}
- . . . .

Correct Way (MCMC)

- Simultaneously vary *N* model parameters $\boldsymbol{x_i}$
- Perform random walk weight by likelihood

$$\mathcal{L}(\mathbf{x}|\mathbf{y}) \sim \exp\left\{ -\sum_a \frac{\left(y_a^{(\mathrm{model})}(\mathbf{x}) - y_a^{(\mathrm{exp})}\right)^2}{2\sigma_a^2} \right\}$$

- Use all observables $\boldsymbol{y_a}$
- Obtain representative sample of posterior

Difficult Because…

I. Too Many Model Runs
Requires running model $\sim 10^6$ times

II. Many Observables
Could be hundreds of plots,
each with dozens of points
Complicated Error Matrices

Model Emulators

1. **Run the model ~1000 times**
   Semi-random points (LHS sampling)

2. **Determine Principal Components**
   $(y_a - \langle y_a \rangle)/\sigma_a \to z_a$

3. **Emulate z_a (Interpolate) for MCMC**
   Gaussian Process…

$$\mathcal{L}(\mathbf{x}|\mathbf{y}) \sim \exp\left\{-\frac{1}{2}\sum_a (z_a^{(\text{emulator})}(\mathbf{x}) - z_a^{(\text{exp})})^2\right\}$$

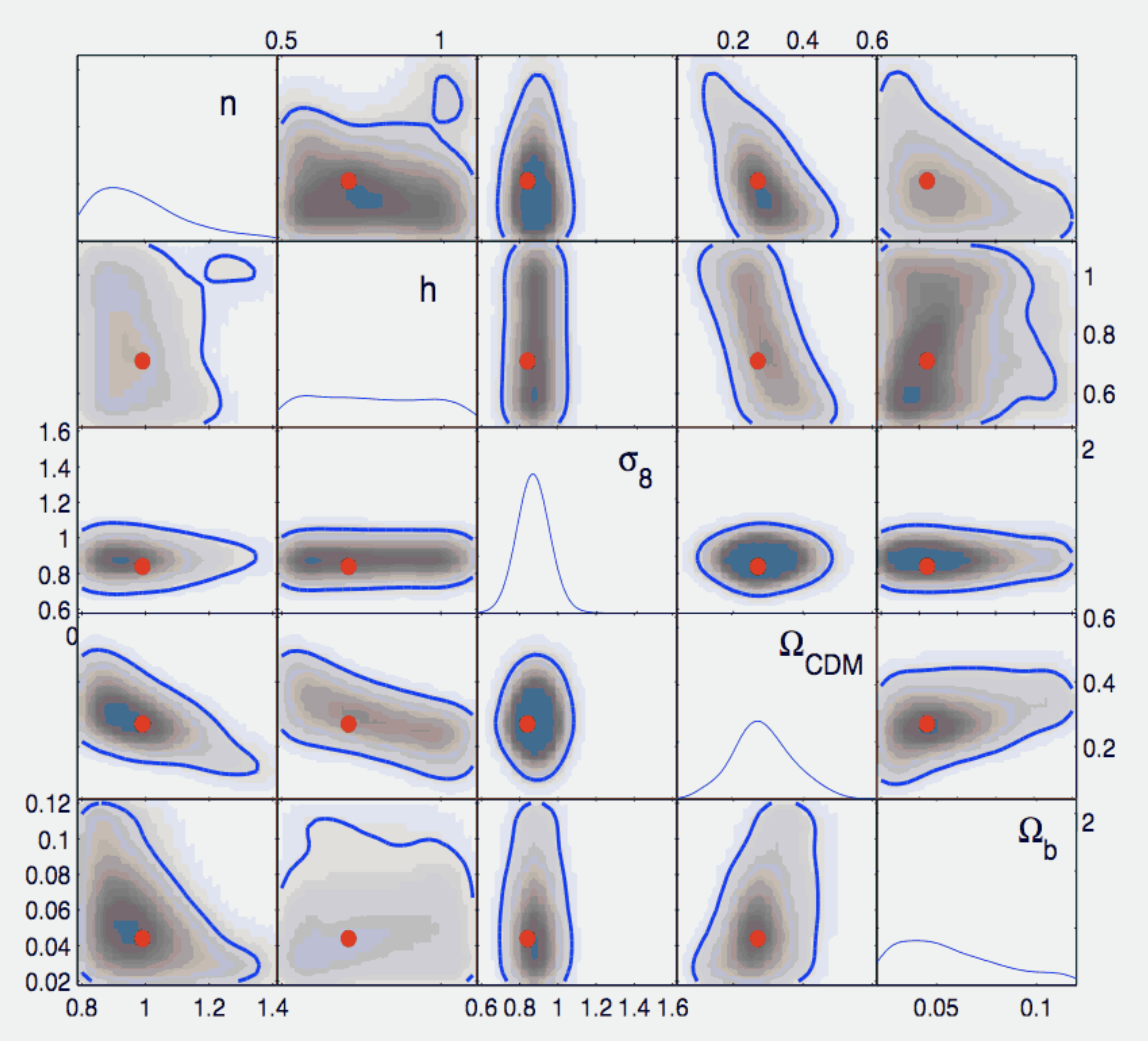

S. Habib, K. Heitman, D. Higdon, C. Nakhleh & B. Williams, PRD (2007)

Emulator Algorithms

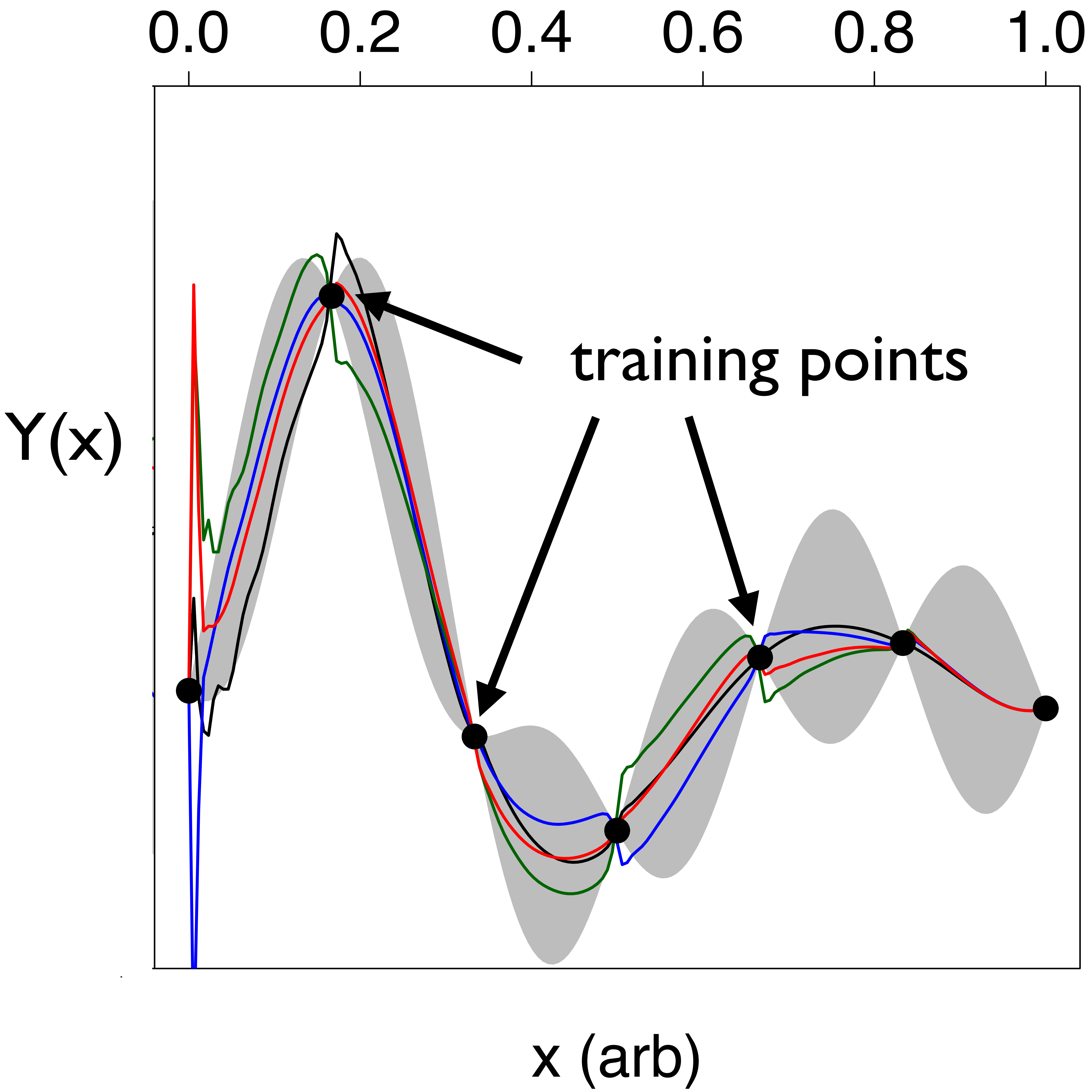

- Gaussian Process
  - Reproduces training points
  - Assumes localized Gaussian covariance
  - Must be trained, i.e. find “hyper parameters”
- Other methods also work

14 Parameters

- 5 for Initial Conditions at RHIC
- 5 for Initial Conditions at LHC
- 2 for Viscosity
- 2 for Eq. of State

30 Observables

- π, K, p Spectra
  $\langle p_t \rangle$, Yields
- Interferometric Source Sizes
- v_2 Weighted by p_t

Initial State Parameters

$$\epsilon(\tau = 0.8\text{fm}/c) = f_{\text{wn}}\epsilon_{\text{wn}} + (1 - f_{\text{wn}})\epsilon_{\text{cgc}},$$

$$\epsilon_{\text{wn}} = \epsilon_0 T_A \frac{\sigma_{\text{nn}}}{2\sigma_{\text{sat}}} \{1 - \exp(-\sigma_{\text{sat}} T_B)\} + (A \leftrightarrow B)$$

$$\epsilon_{\text{cgc}} = \epsilon_0 T_{\text{min}} \frac{\sigma_{\text{nn}}}{\sigma_{\text{sat}}} \{1 - \exp(-\sigma_{\text{sat}} T_{\text{max}})\}$$

$$T_{\text{min}} \equiv \frac{T_A T_B}{T_A + T_B},$$

$$T_{\text{max}} \equiv T_A + T_B,$$

$$u_\perp = \alpha\tau \frac{\partial T_{00}}{2T_{00}}$$

$$T_{zz} = \gamma P$$

5 parameters for RHIC, 5 for LHC

Equation of State and Viscosity

$$c_s^2(\epsilon) = c_s^2(\epsilon_h) + \left(\frac{1}{3} - c_s^2(\epsilon_h)\right) \frac{X_0 x + x^2}{X_0 x + x^2 + X'^2},$$

$$X_0 = X' R c_s(\epsilon)\sqrt{12},$$

$$x \equiv \ln \epsilon/\epsilon_h$$

$$\frac{\eta}{s} = \left.\frac{\eta}{s}\right|_{T=165} + \kappa \ln(T/165)$$

2 parameters for EoS, 2 for η/s

DATA Distillation

1. Experiments reduce PBs to 100s of plots

2. Choose which data to analyze
Does physics *factorize*?

3. Reduce plots to a few representative numbers, y_a

4. Transform to principal components

Checking the Distillation

Spectral information encapsulated by two numbers, dN/dy & $\langle p_t \rangle$

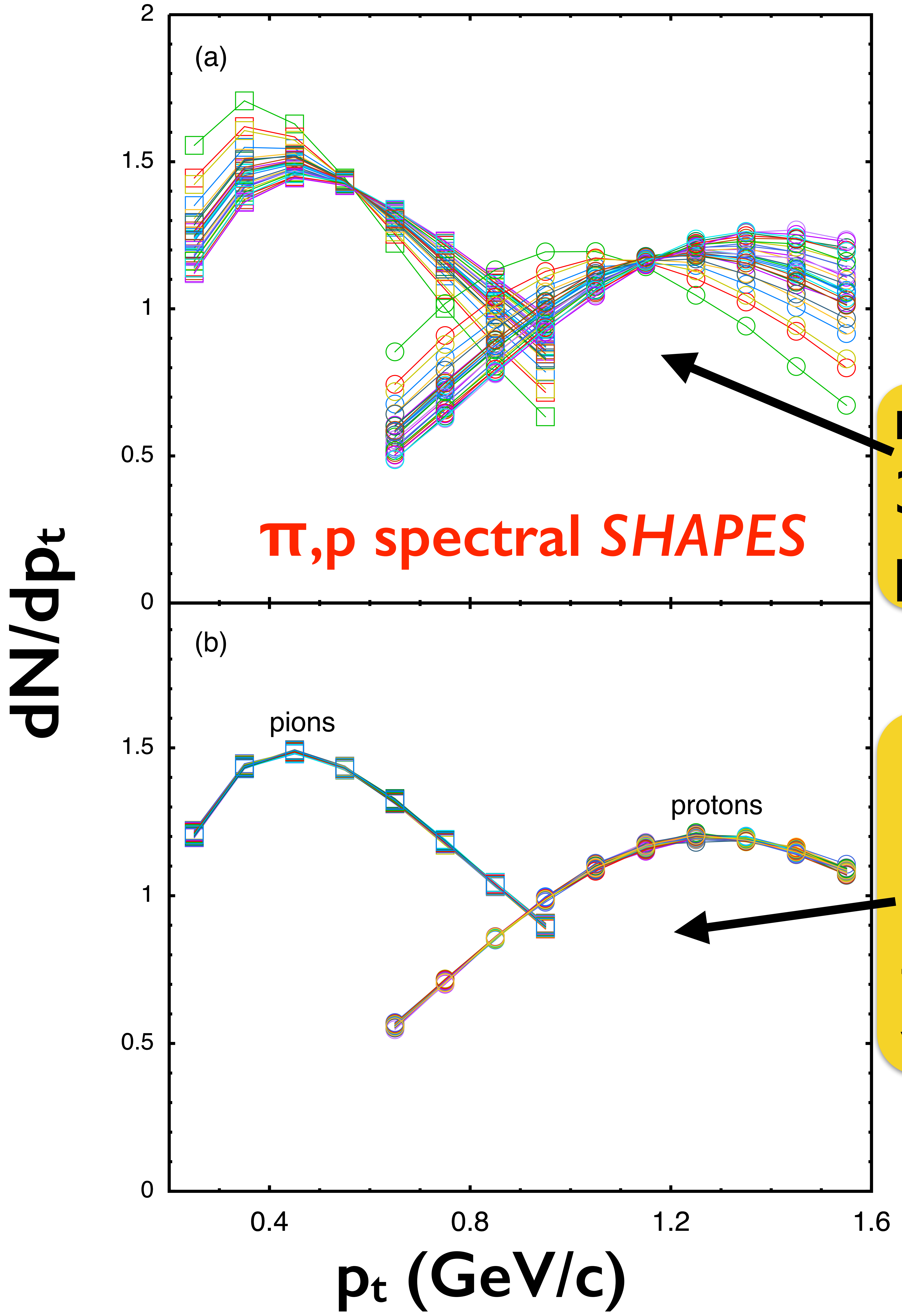

model spectra from 30 random points in parameter prior

74 pion spectra:
with $573 < \langle p_t \rangle_\pi < 575$ MeV

44 proton spectra:
with $1150 < \langle p_t \rangle_p < 1152$ MeV

Two Calculations

1. J.Novak, K. Novak, S.P., C.Coleman-Smith & R.Wolpert, ArXiv:1303.5769

RHIC Au+Au Data
6 parameters

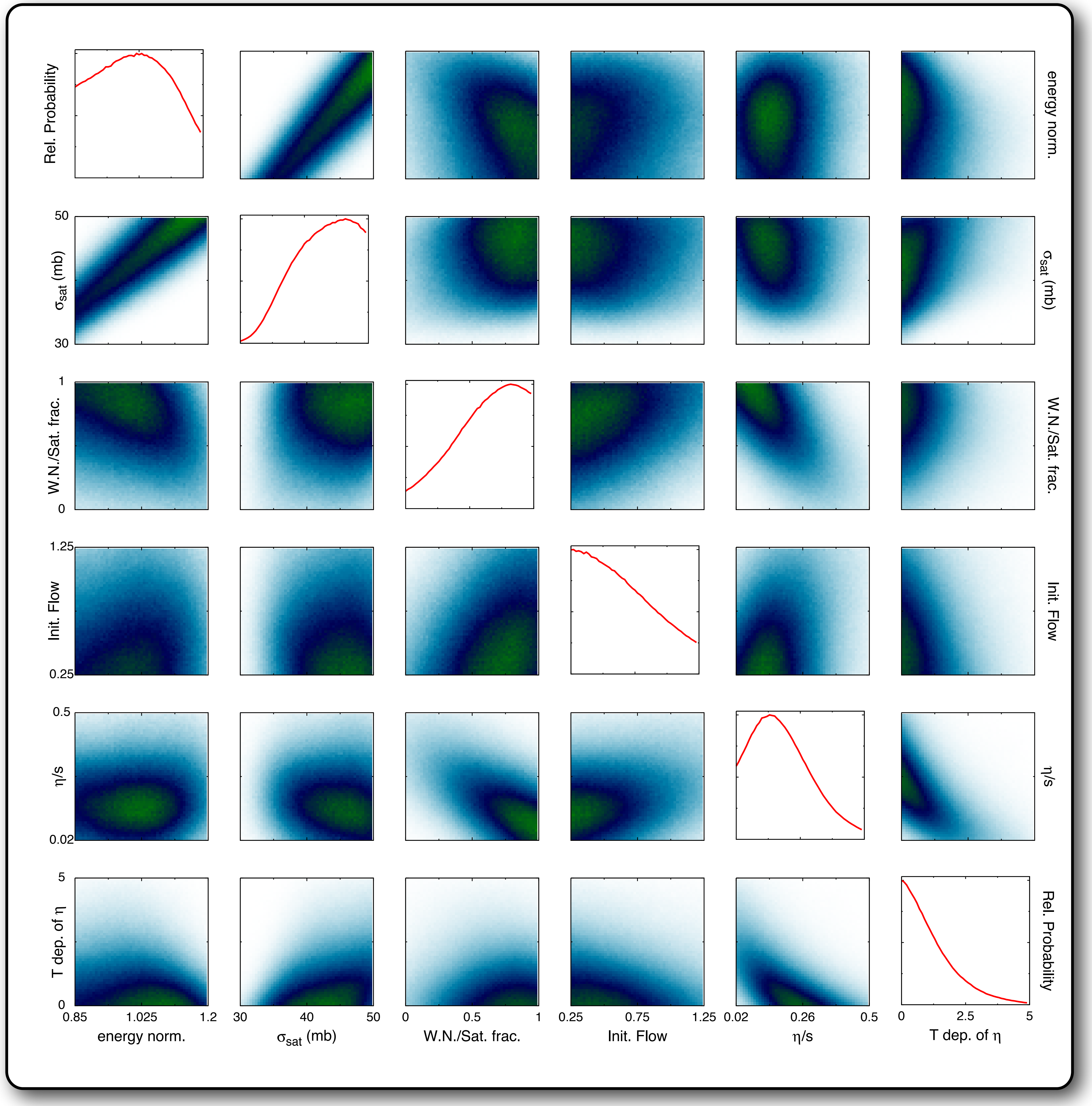

2. S.P., E.Sangaline, P.Sorensen & H.Wang, in progress

RHIC Au+Au and LHC Pb+Pb Data
14 parameters, include Eq. of State

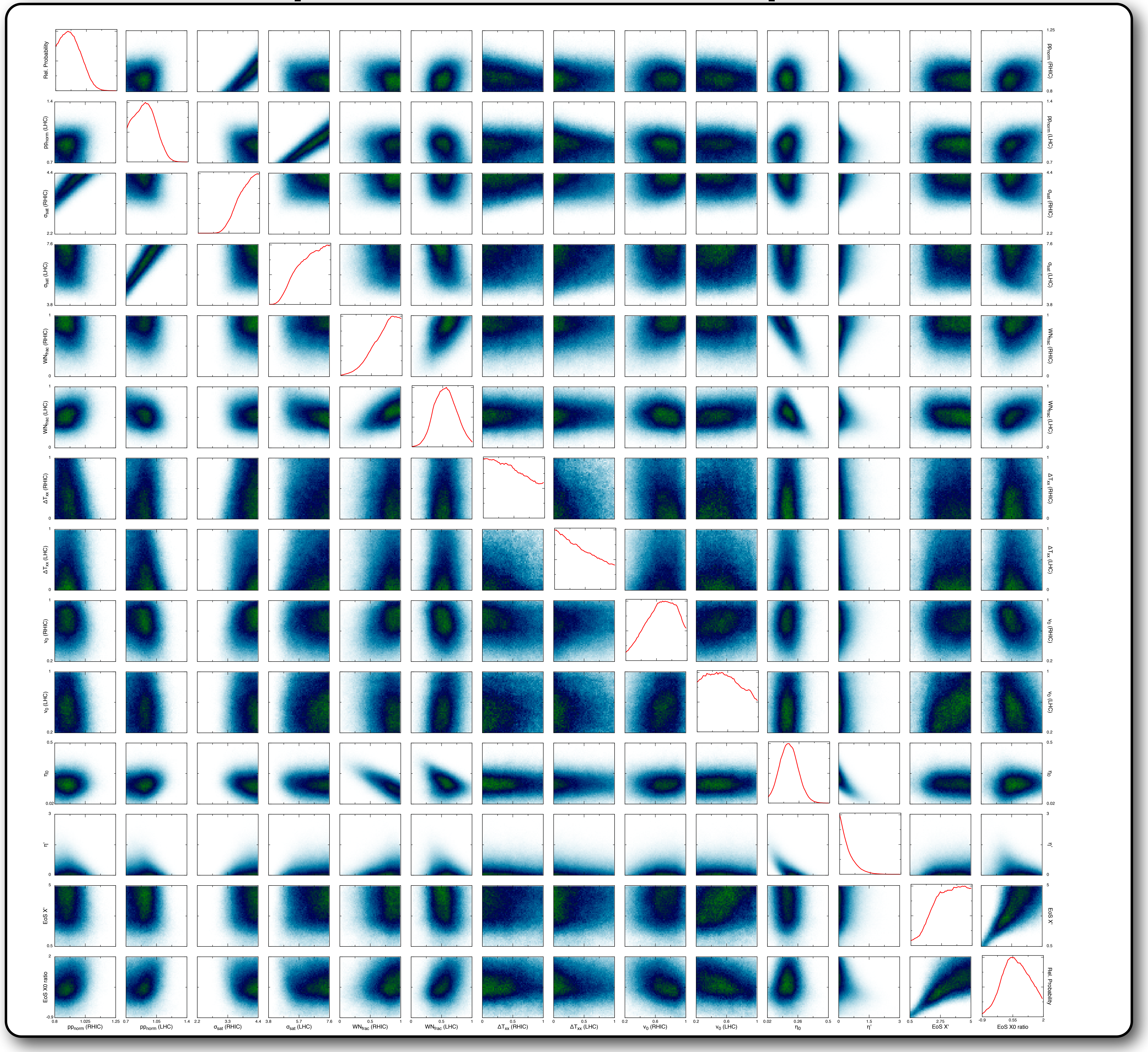

Sample Spectra from Prior and Posterior

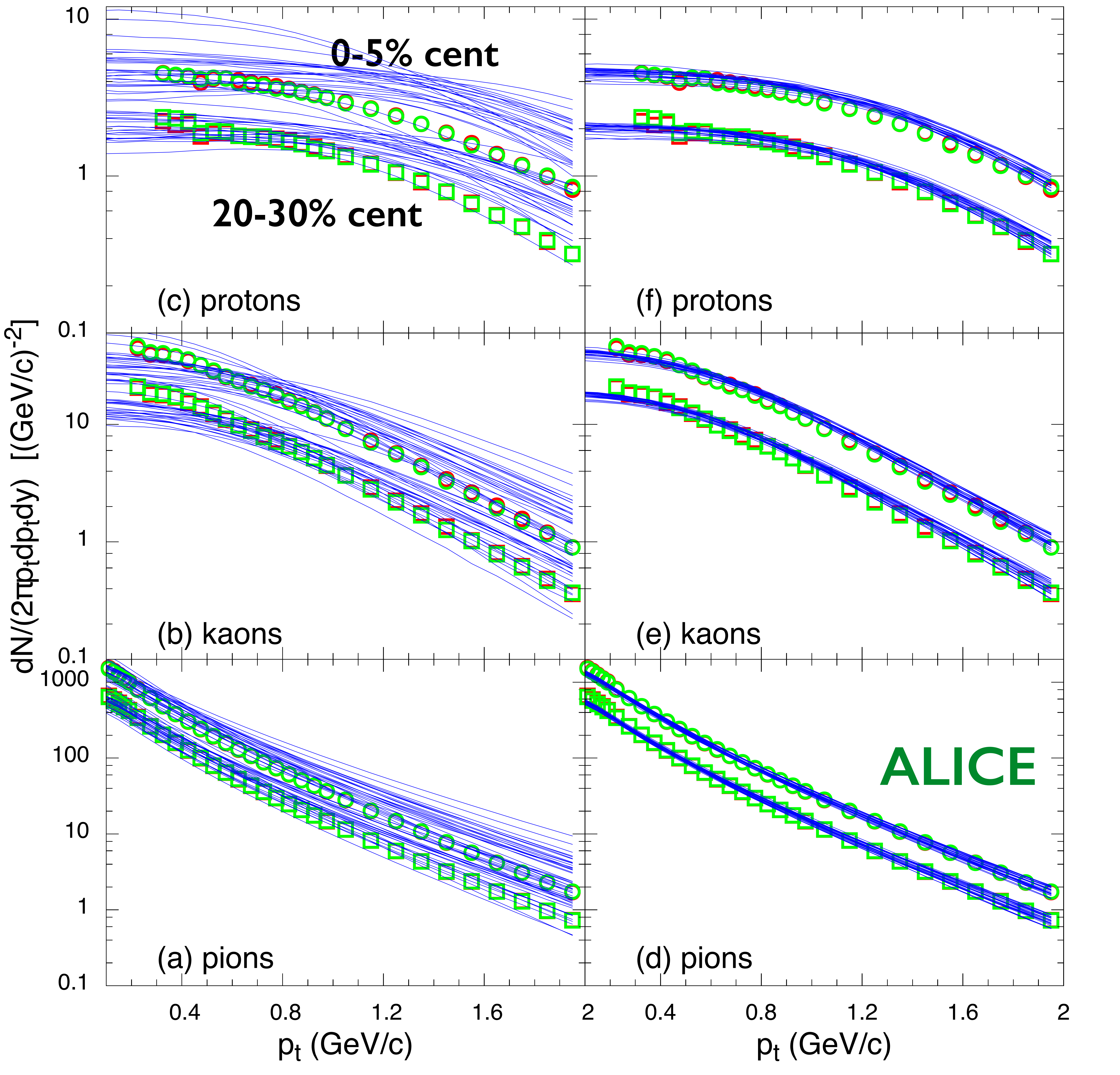

Sample V2 from Prior and Posterior

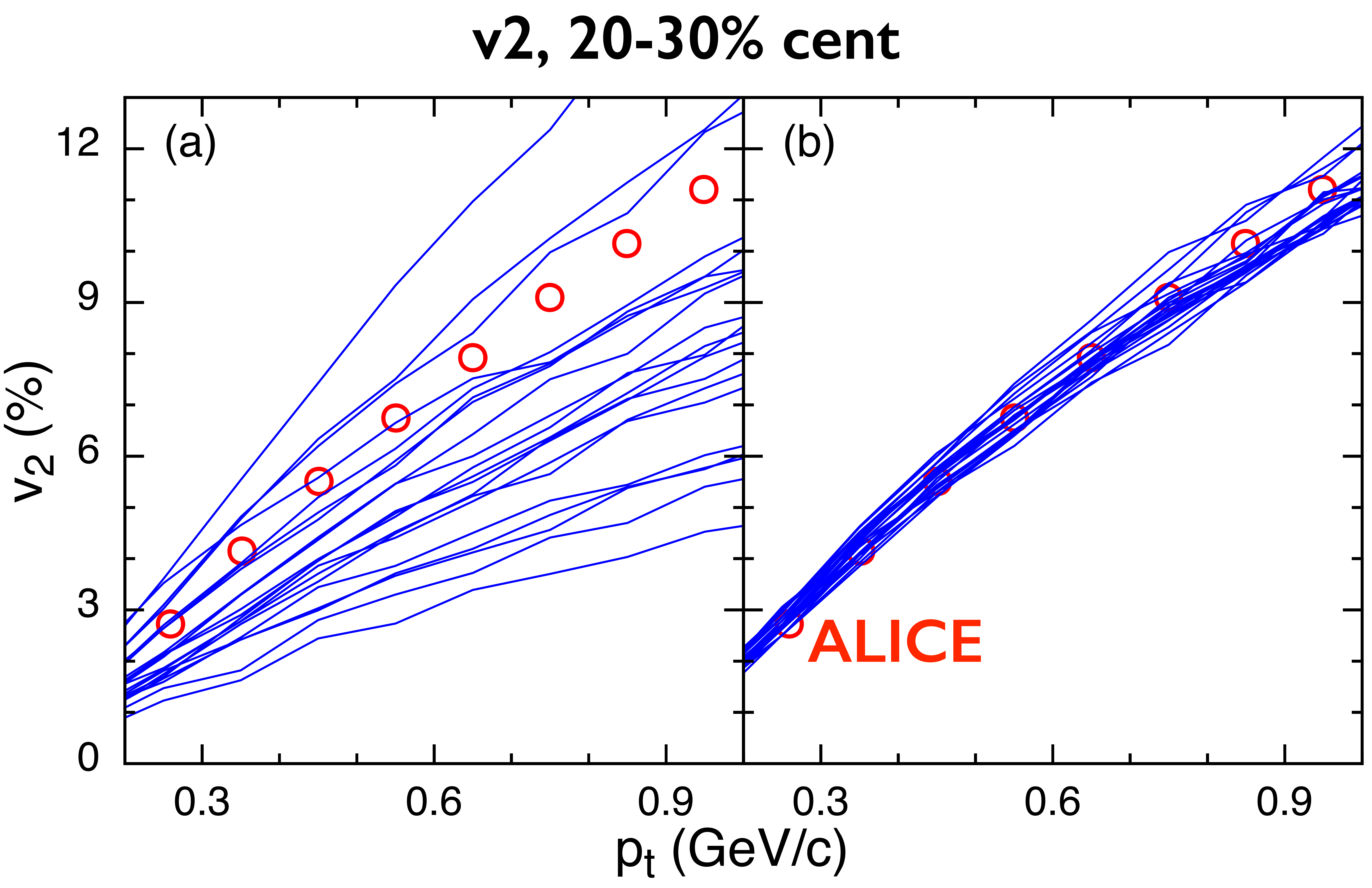

Sample HBT from Prior and Posterior

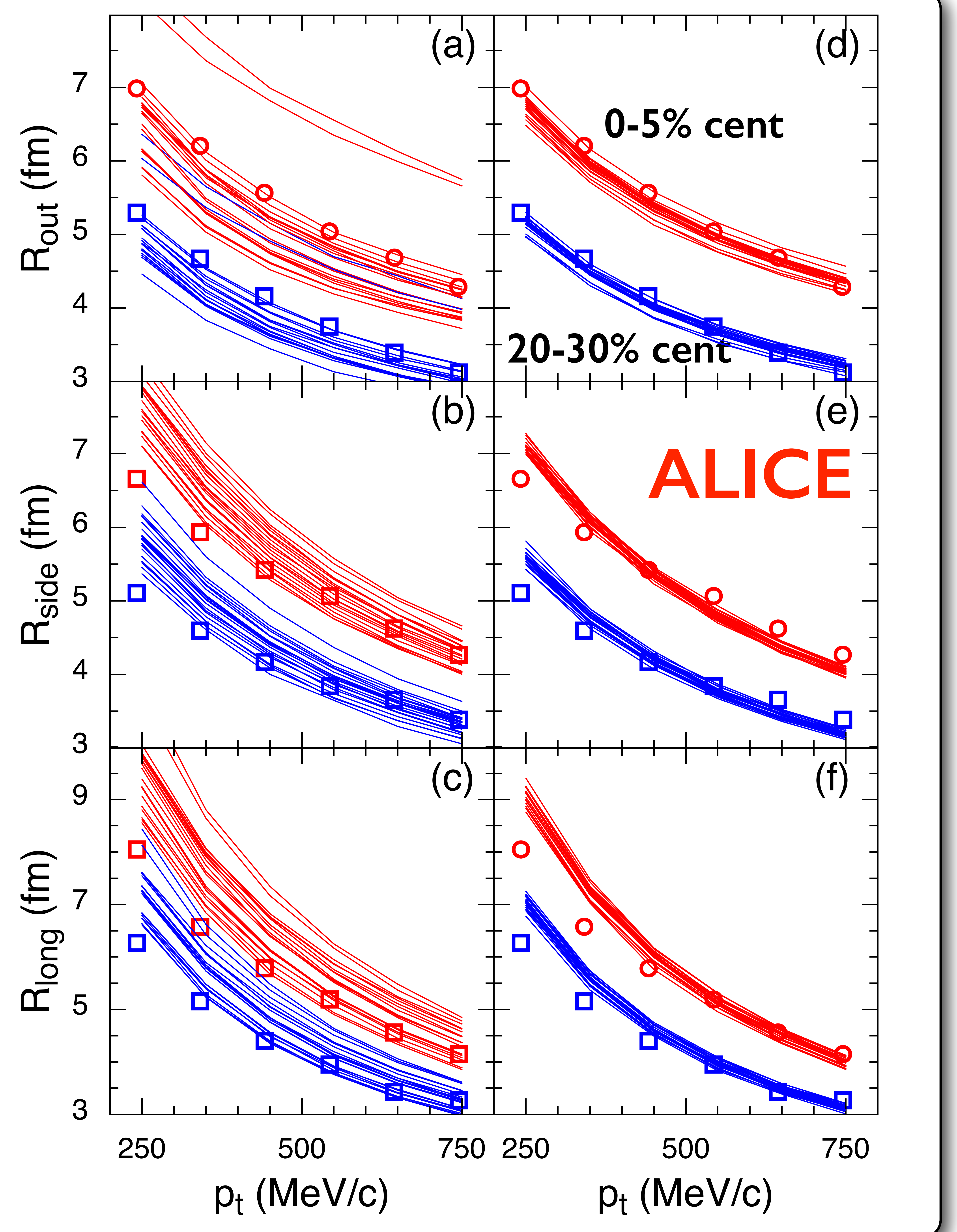

η/s(T)

$$\eta/s = (\eta/s)_0 + \kappa \ln(T/165)$$

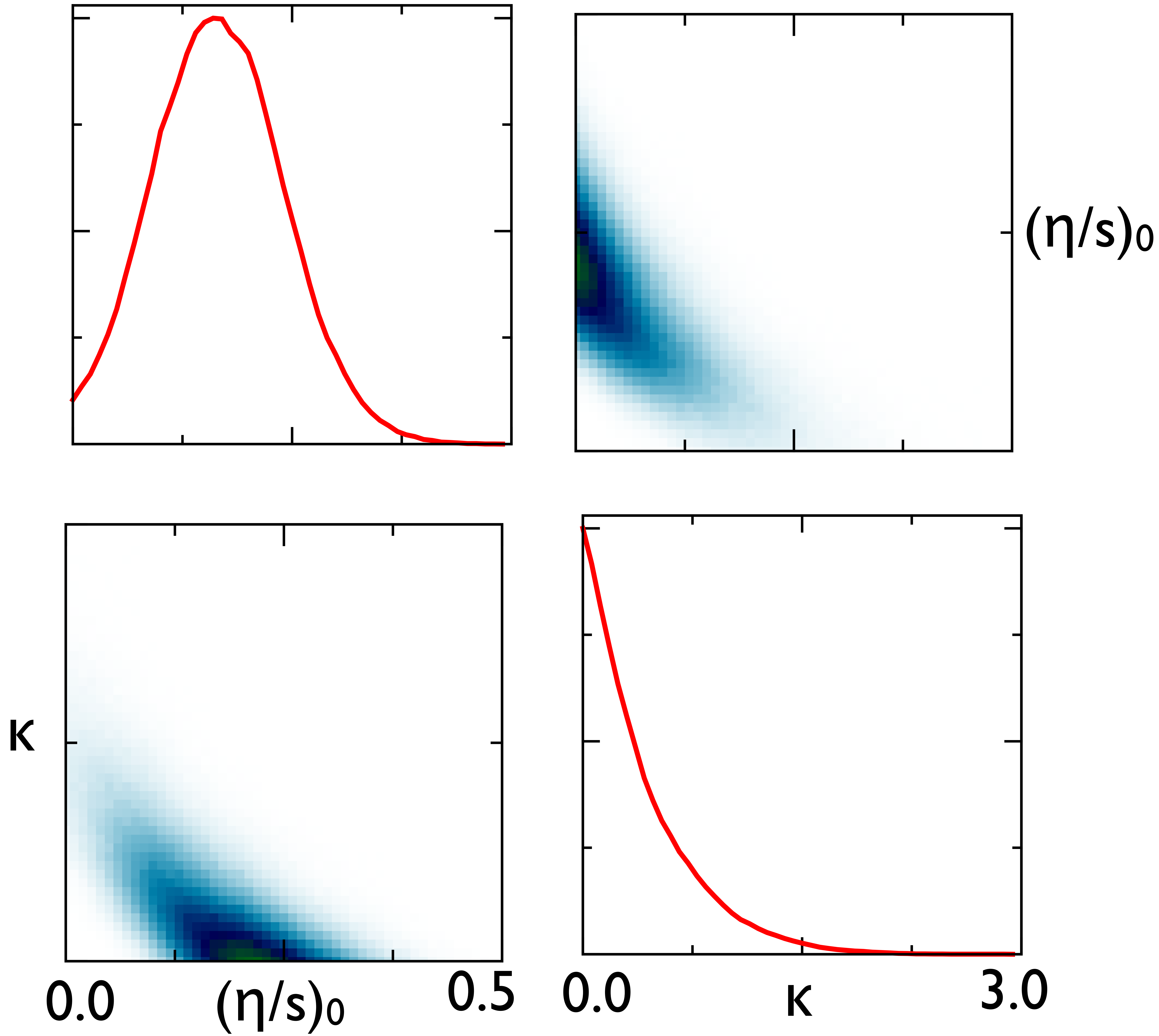

η/s vs saturation picture

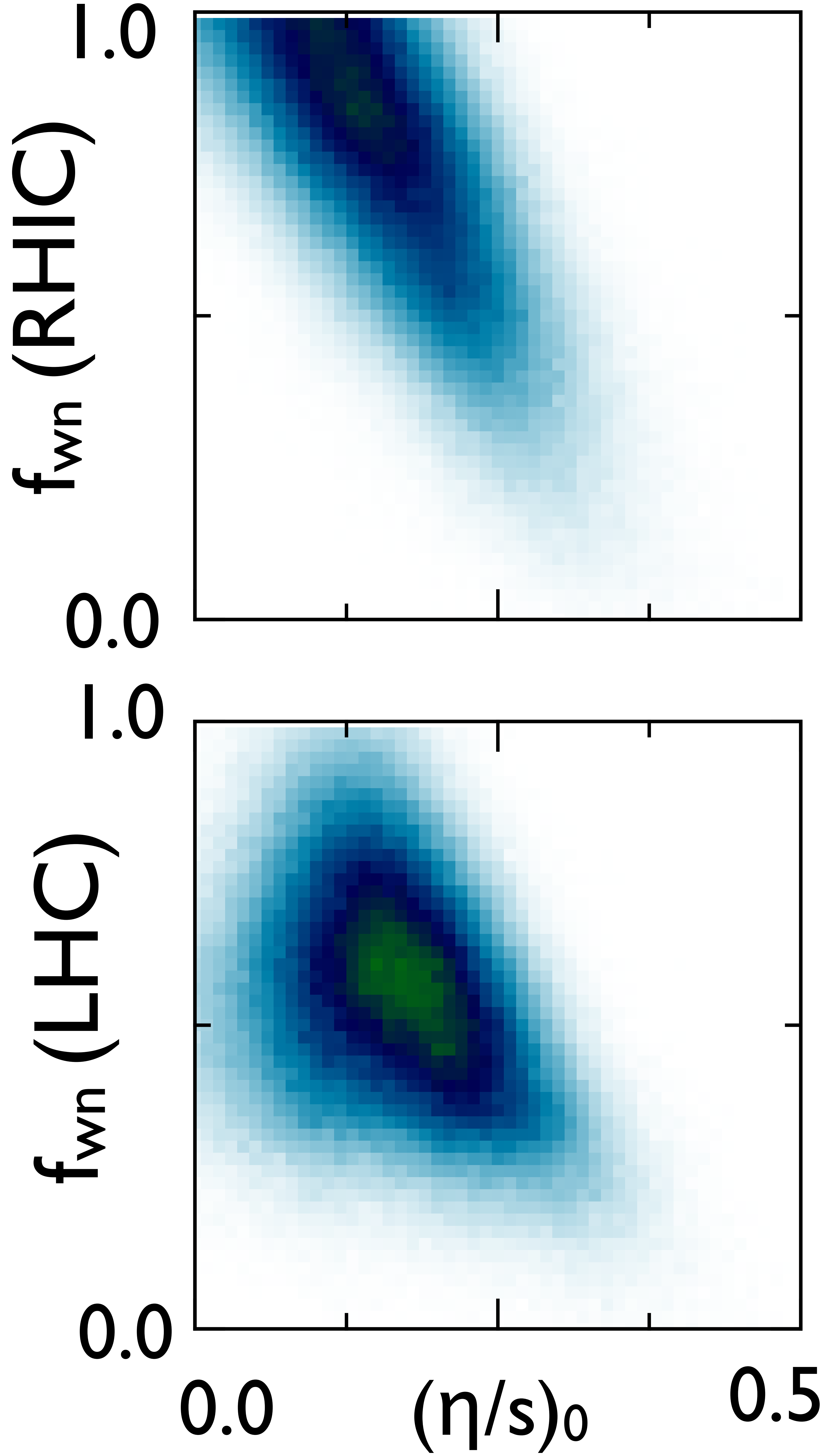

See Drescher, Dumitru, Gombeaud and Ollitrault
PRC 2007

Eq. of State

$$c_s^2(\epsilon) = c_s^2(\epsilon_h) + \left(\frac{1}{3} - c_s^2(\epsilon_h)\right) \frac{X_0 x + x^2}{X_0 x + x^2 + X'^2},$$

$$X_0 = X' R c_s(\epsilon)\sqrt{12},$$

$$x \equiv \ln \epsilon/\epsilon_h$$

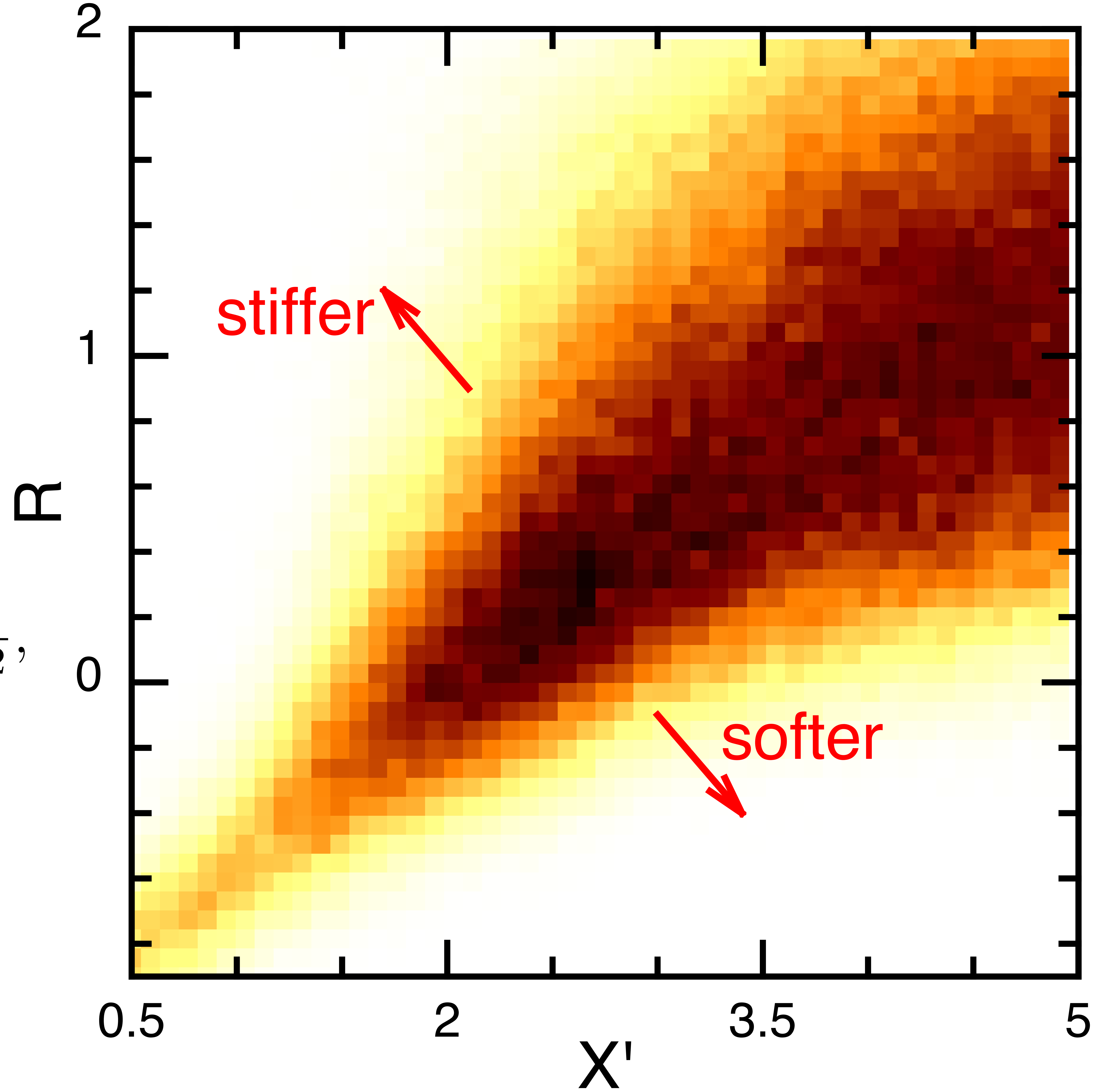


Constraining Eq. of State with RHIC/LHC Data (MADAI Collab.)
Lattice: Hot QCD / BW
upper/lower ranges (arXiv:1407.6387)
UNCONSTRAINED
CONSTRAINED
BY DATA
HADRON GAS
c_s^2 (speed of sound squared)
0.1
0.2
0.3
150
200
250
300
350
T (MeV)

Which observables constrain the EoS?

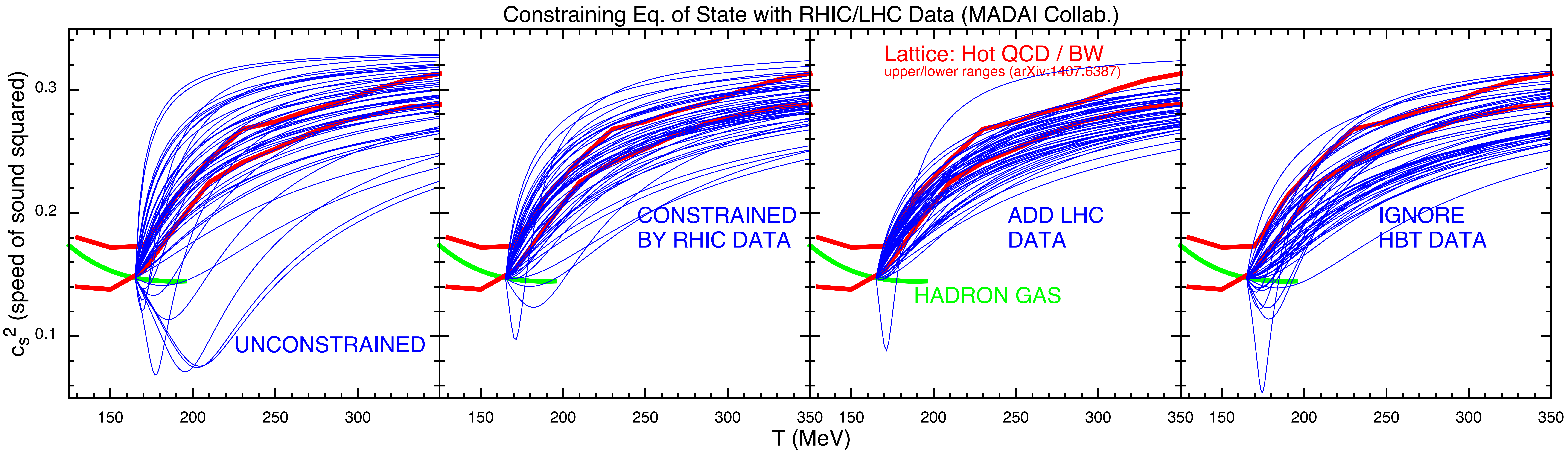

Sensitivity to Uncertainty

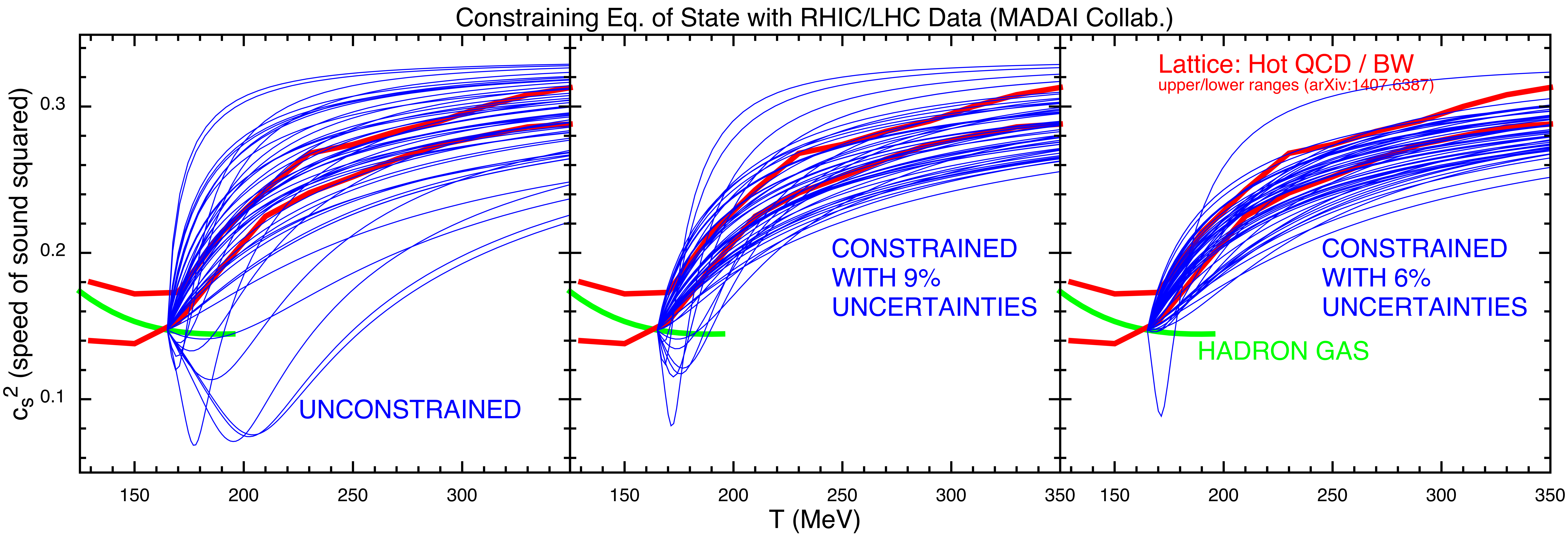

SUMMARY

- Robust
- Emulation works splendidly
- Scales well to more parameters & more data
- Eq. of State and Viscosity can be extracted from RHIC & LHC data
- Other parameters not as well constrained
- Heavy-Ion Physics can be a Quantitative Science!!!!

NEAR FUTURE

- **Improve models (will lead to more parameters)**
  - hadronization uncertainties
  - bulk viscosity
  - more realistic cascade
    Bose enhancement, better cross sections
  - 3D corrections
  - lumpy IC
- **Better statements of uncertainty**
  - Requires cooperation, both experimenters and theorists
- **Extend to different analyses**
  - Initial state studies
  - Jet Physics
  - …

BEAM ENERGY SCAN

- **Improve models (MANY more parameters)**
  - 3D Initial Conditions
    baryon stopping, initial flow and rotation, initial temperatures, corona
  - Paramterize IC
  - Density Dependent EoS
  - Mean-field for hadronic Boltzmann

- **Statistics may require rethinking**
  - $N_{\text{parameters}} \sim 50$

- **Should be able to determine $P(\rho,T)$**

If you're interested…

1. Tools are readily extended
2. Download software and tutorial from http://madai.us
3. Talk to me (prattsc@msu.edu)
   or Evan Sangaline (esangaline@gmail.com)

Made possible by contributions from DOE, NSF, Chris Coleman-Smith, John Novak, Kevin Novak, Evan Sangaline, Paul Sorensen, Joshua Vredevoogd, Hui Wang, Robert Wolpert, and viewers like you.

Additional slide: Charge BFs and charge susceptibilities

S.P., C. Ratti and W.McCormack, arXiv:1409.2164

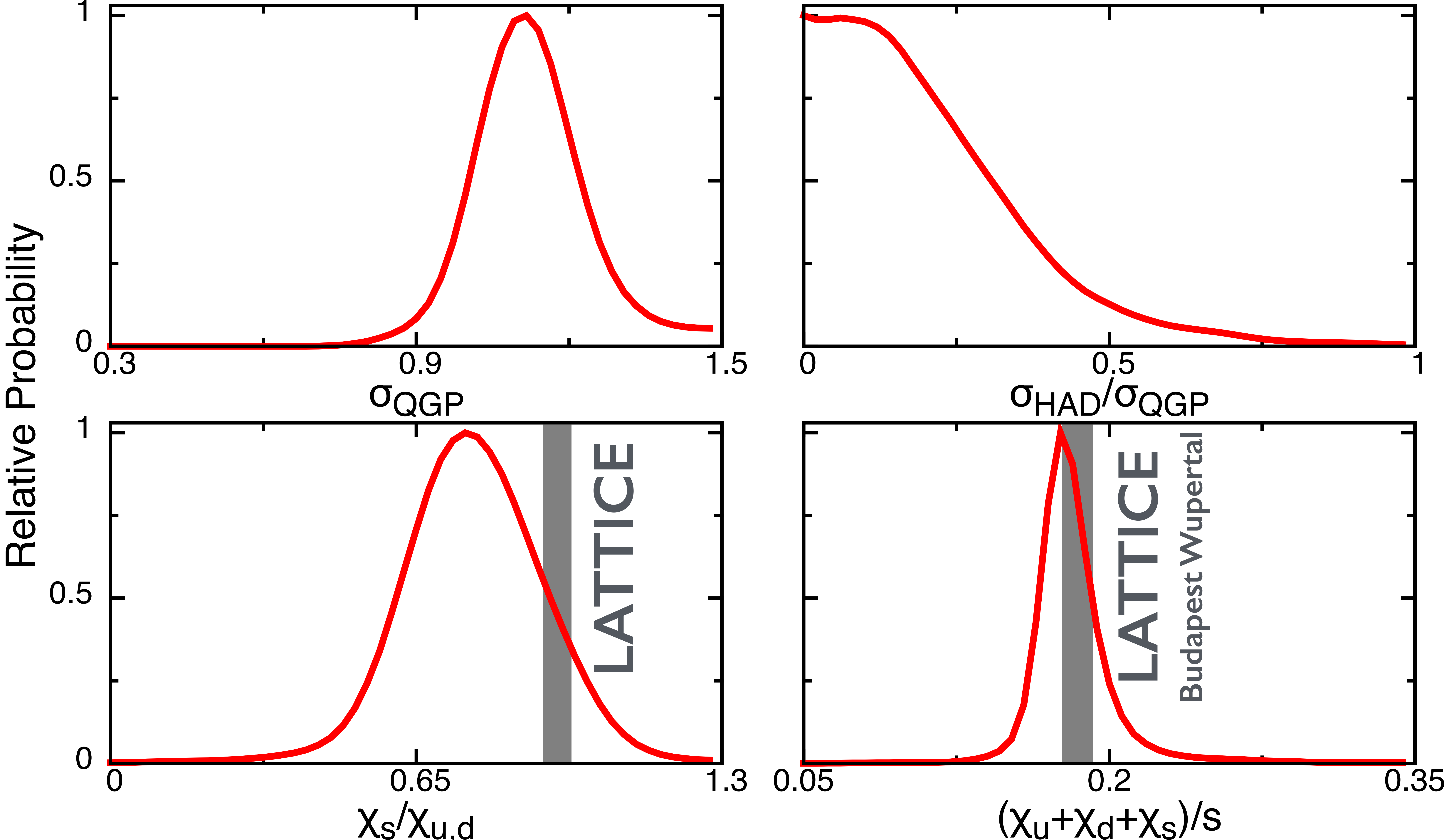

Probability distribution of conserved charges: chemical freezeout and the chiral crossover

Krzysztof Redlich, Uni Wroclaw

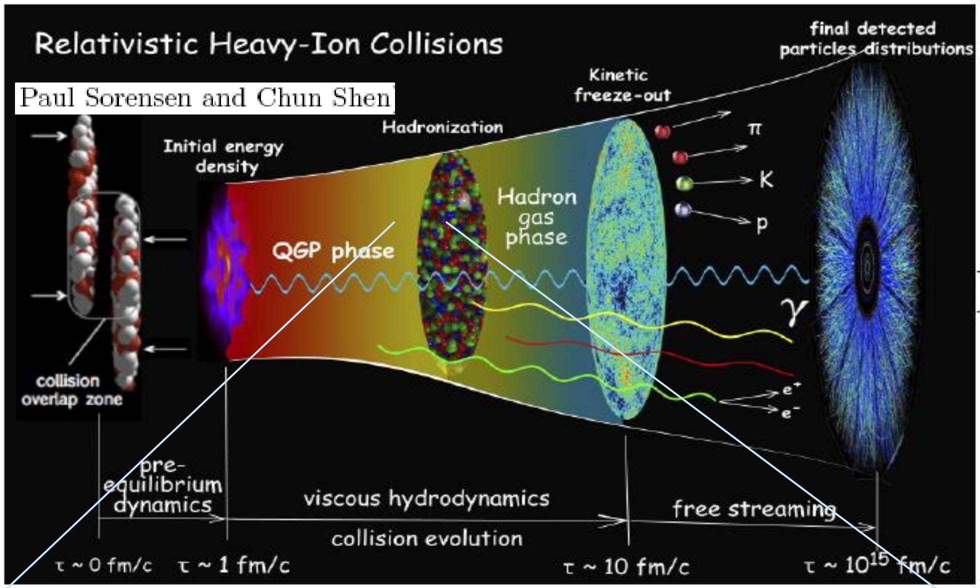

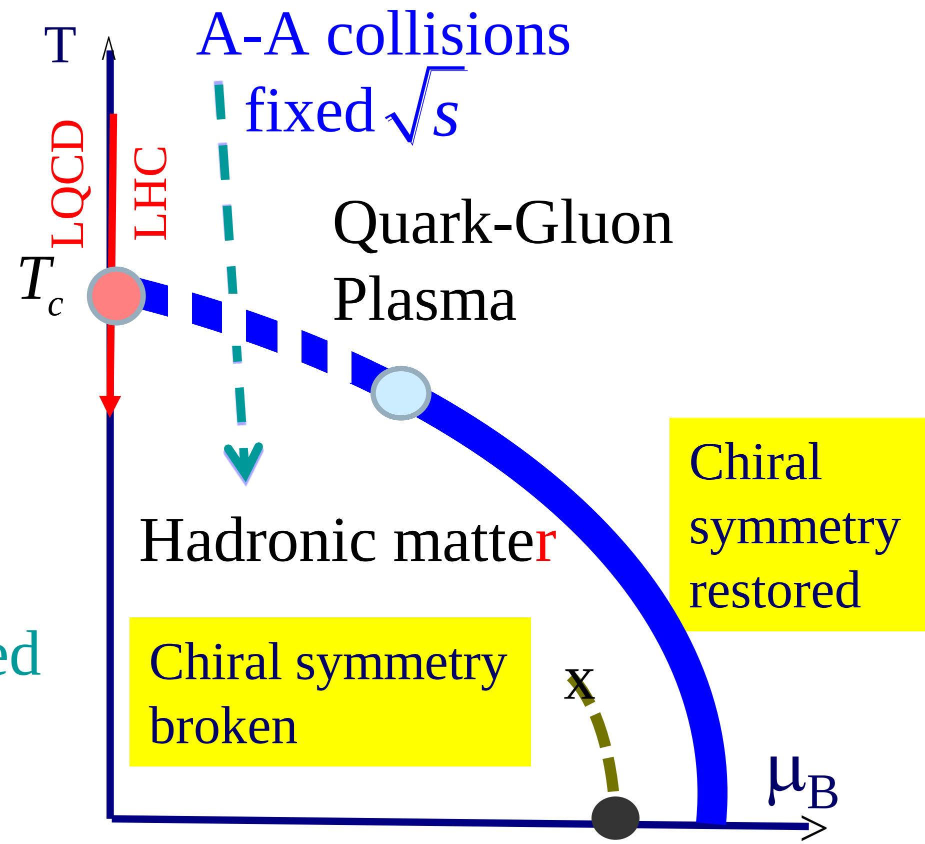

- Fluctuations and correlations of conserved charges at the LHC and LQCD results
  With: P. Braun-Munzinger, A. Kalweit and J. Stachel
- The influence of critical fluctuations on the probability distribution of net baryon number. With B. Friman & K. Morita

1st principle calculations:

$\mu, T << \Lambda_{QCD}$: χ – perturbation theory

$\mu, T >> \Lambda_{QCD}$: pQCD >

$\mu_q < T$: LGT

Excellent data of ALICE Collaboration for particle yields

ALICE Collaboration

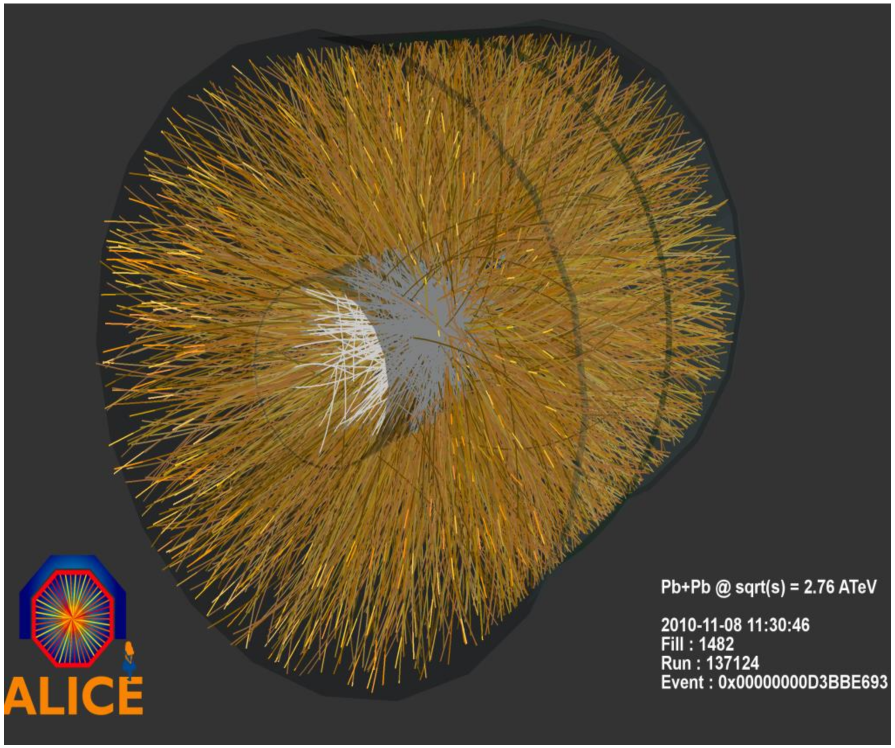

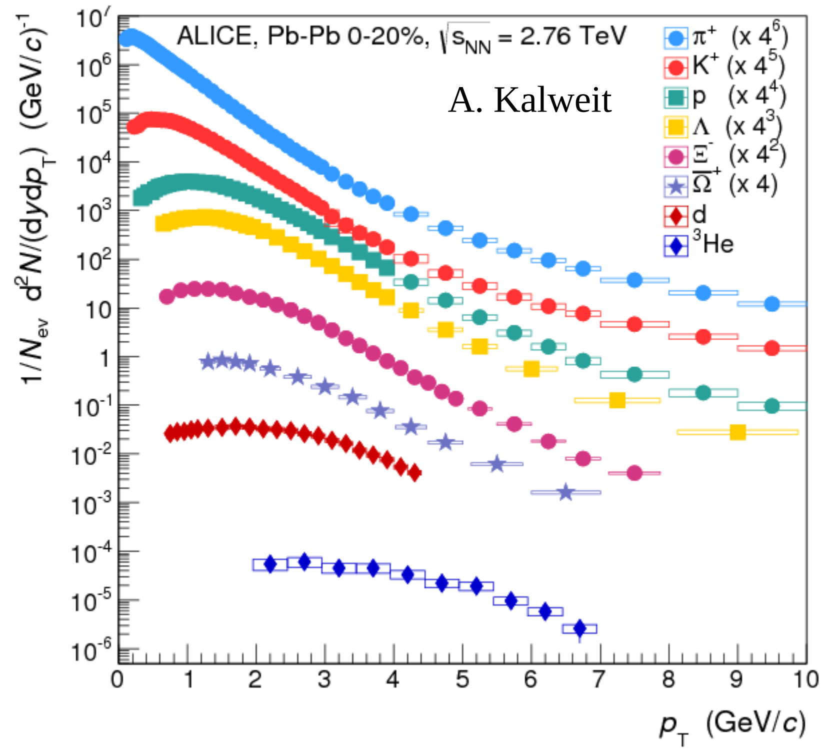

ALICE Time Projection Chamber (TPC), Time of Flight Detector (TOF), High Momentum Particle Identification Detector (HMPID) together with the Transition Radiation Detector (TRD) and the Inner Tracking System (ITS) provide information on the flavour composition of the collision fireball, vector meson resonances, as well as charm and beauty production through the measurement of leptonic observables.

Consider fluctuations and correlations of conserved charges

Excellent probe of:

- QCD criticality

A. Asakawa at. al.
S. Ejiri et al.,…
M. Stephanov et al.,
K. Rajagopal et al.

- freezeout conditions in HIC

F. Karsch &
S. Mukherjee et al.,
P. Braun-Munzinger et al.,,

- They are quantified by susceptibilities:

If $P(T,\mu_B,\mu_Q,\mu_S)$ denotes pressure, then

$$\frac{\chi_N}{T^2} = \frac{\partial^2(P)}{\partial(\mu_N)^2} \qquad \frac{\chi_{NM}}{T^2} = \frac{\partial^2(P)}{\partial\mu_N\partial\mu_M}$$

$$N = N_q - N_{-q},\ N,M = (B,S,Q), \quad \mu = \mu/T, \quad P = P/T^4$$

- Susceptibility is connected with variance

$$\frac{\chi_N}{T^2} = \frac{1}{VT^3}(<N^2> - <N>^2)$$

- If $\mathrm{P}(N)$ probability distribution of N then

$$<N^n> = \sum_N N^n \mathrm{P}(N)$$

Consider special case:

P. Braun-Munzinger,
B. Friman, F. Karsch,
V Skokov &K.R.
Phys .Rev. C84 (2011) 064911
Nucl. Phys. A880 (2012) 48)

$$< N_q > \equiv \bar{N}_q \quad =>$$

- Charge and anti-charge uncorrelated and Poisson distributed, then
- $P(N)$ the Skellam distribution

$$P(N) = \left(\frac{\bar{N}_q}{\bar{N}_{-q}} \right)^{N/2} I_N (2\sqrt{\bar{N}_{-q} \bar{N}_q}) \exp[-(\bar{N}_{-q} + \bar{N}_q)]$$

- Then the susceptibility

$$\frac{\chi_N}{T^2} = \frac{1}{VT^3} (< N_q > + < N_{-q} >)$$

Consider special case: particles carrying $q = \pm 1, \pm 2, \pm 3$

P. Braun-Munzinger,
B. Friman, F. Karsch,
V Skokov &K.R.
Phys .Rev. C84 (2011) 064911
Nucl. Phys. A880 (2012) 48)

- The probability distribution

$$< S_{-q} > \equiv \overline{S}_{-q}$$

$$q = \pm 1, \pm 2, \pm 3$$

$$\begin{aligned} P(S) \;=\; & (\frac{\bar{S}_1}{\bar{S}_{\bar{1}}})^{\frac{S}{2}} \exp[\sum_{n=1}^{3}(\bar{S}_n + \bar{S}_{\bar{n}})] \\ & \sum_{i=-\infty}^{\infty} \sum_{k=-\infty}^{\infty} (\frac{\bar{S}_3}{\bar{S}_{\bar{3}}})^{k/2} I_k(2\sqrt{\bar{S}_3 \bar{S}_{\bar{3}}}) \\ & (\frac{\bar{S}_2}{\bar{S}_{\bar{2}}})^{i/2} I_i(2\sqrt{\bar{S}_2 \bar{S}_{\bar{2}}}) \\ & (\frac{\bar{S}_1}{\bar{S}_{\bar{1}}})^{-i-3k/2} I_{2i+3k-S}(2\sqrt{\bar{S}_1 \bar{S}_{\bar{1}}}) \end{aligned}$$

Fluctuations

$$\frac{\chi_S}{T^2} = \frac{1}{VT^3} \sum_{n=1}^{|q|} n^2 (\langle S_n \rangle + \langle S_{-n} \rangle)$$

Correlations

$$\frac{\chi_{NM}}{T^2} = \frac{1}{VT^3} \sum_{n=-q_N}^{q_N} \sum_{m=-q_M}^{q_M} nm \langle N_{n,m} \rangle$$

$\langle N_{n,m} \rangle$, is the mean number of particles
; carrying charge $N = n$ and $M = m$.

Deconfinement and chiral symmetry restoration in QCD

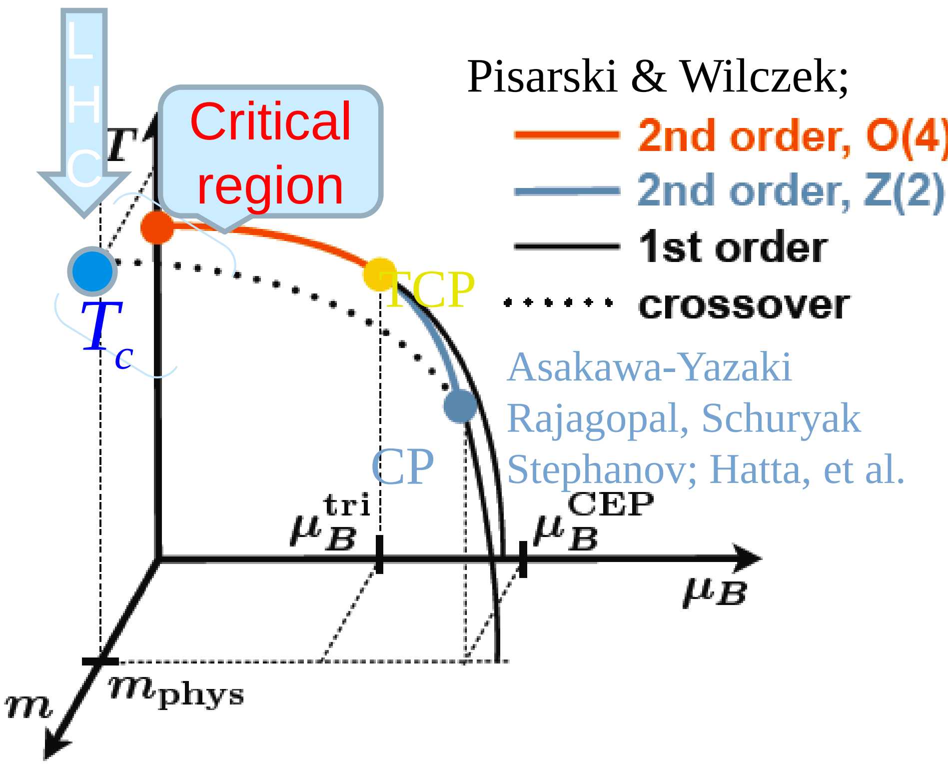

- The QCD chiral transition is crossover Y.Aoki, et al Nature (2006) and appears in the O(4) critical region

  O. Kaczmarek et.al. Phys.Rev. D83, 014504 (2011)

- Chiral transition temperature

  $$T_c = 155(1)(8)\ \text{MeV}$$

  T. Bhattacharya et.al.
  Phys. Rev. Lett. 113, 082001 (2014)

- Deconfinement of quarks sets in at the chiral crossover

  A.Bazavov, Phys.Rev. D85 (2012) 054503

- The shift of T_c with chemical potential

$$\boxed{T_c(\mu_B) = T_c(0)[1 - 0.0066 \cdot (\mu_B / T_c)^2]}$$

Ch. Schmidt Phys.Rev. D83 (2011) 014504

See also:
Y. Aoki, S. Borsanyi, S. Durr, Z. Fodor, S. D. Katz, *et al.*
JHEP, 0906 (2009)

Probing O(4) chiral criticality with charge fluctuations

- Due to expected O(4) scaling in QCD the free energy:

$$\boxed{P = P_R(T, \mu_q, \mu_I) + b^{-1} P_S(b^{(2-\alpha)^{-1}} t(\mu), b^{\beta\delta/\nu} h)}$$

- Generalized susceptibilities of net baryon number

$$c_B^{(n)} = \frac{\partial^n (P/T^4)}{\partial(\mu_B/T)^n} = c_R^{(n)} + c_S^{(n)} \quad \text{with} \quad \begin{aligned} c_s^{(n)}\big|_{\mu=0} &= d\ h^{(2-\alpha-n/2)/\beta\delta}\ f_\pm^{(n)}(z) \\ c_s^{(n)}\big|_{\mu\neq 0} &= d\ h^{(2-\alpha-n)/\beta\delta}\ f_\pm^{(n)}(z) \end{aligned}$$

- At $\mu = 0$ only $c_B^{(n)}$ with $n \geq 6$ receive contribution from $c_S^{(n)}$
- At $\mu \neq 0$ only $c_B^{(n)}$ with $n \geq 3$ receive contribution from $c_S^{(n)}$

- $\boxed{c_B^{n=2} = \chi_B / T^2}$ Generalized susceptibilities of the net baryon number non critical with respect to O(4)

Variance at 200 GeV AA central coll. at RHIC

P. Braun-Munzinger, et al.
Nucl. Phys. A880 (2012) 48)

STAR Collaboration data in central coll. 200 GeV

- Consistent with Skellam distribution

$$\frac{<p>+<\bar{p}>}{\sigma^2} = 1.022 \pm 0.016 \qquad \frac{\chi_1}{\chi_3} = 1.076 \pm 0.035$$

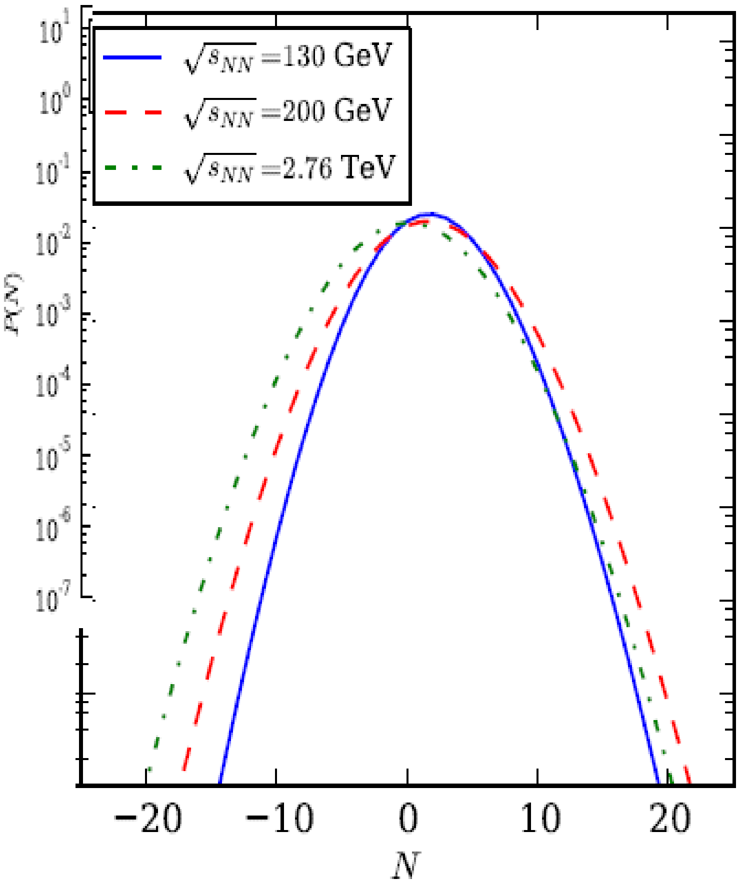

- Consider ratio of cumulants in in the whole momentum range:

$$\frac{\sigma^2}{p-\bar{p}} = 6.18 \pm 0.14 \ \ in \ \ 0.4 < p_t < 0.8 GeV$$

$$\frac{p+\bar{p}}{p-\bar{p}} = 7.67 \pm 1.86 \ \ in \ \ 0.0 < p_t < \infty \ GeV$$

Constructing net charge fluctuations and correlation from ALICE data

- Net baryon number susceptibility

$$\frac{\chi_B}{T^2} \approx \frac{1}{VT^3}\left(\langle p\rangle + \langle N\rangle + \langle \Lambda + \Sigma_0\rangle + \langle \Sigma^+\rangle + \langle \Sigma^-\rangle + \langle \Xi^-\rangle + \langle \Xi^0\rangle + \langle \Omega^-\rangle + \overline{par}\right)$$

- Net strangeness

$$\frac{\chi_S}{T^2} \approx \frac{1}{VT^3}\Big(\langle K^+\rangle + \langle K_S^0\rangle + \langle \Lambda + \Sigma_0\rangle + \langle \Sigma^+\rangle + \langle \Sigma^-\rangle + 4\langle \Xi^-\rangle + 4\langle \Xi^0\rangle + 9\langle \Omega^-\rangle + \overline{par}$$
$$-(\Gamma_{\varphi\to K^+} + \Gamma_{\varphi\to K^-} + \Gamma_{\varphi\to K_S^0} + \Gamma_{\varphi\to K_L^0})\langle \varphi\rangle\Big)$$

- Charge-strangeness correlation

$$\frac{\chi_{QS}}{T^2} \approx \frac{1}{VT^3}\Big(\langle K^+\rangle + 2\langle \Xi^-\rangle + 3\langle \Omega^-\rangle + \overline{par}$$
$$-(\Gamma_{\varphi\to K^+} + \Gamma_{\varphi\to K^-})\langle \varphi\rangle - (\Gamma_{K_0^*\to K^+} + \Gamma_{K_0^*\to K^-})\langle K_0^*\rangle\Big)$$

$\chi_B, \chi_S, \chi_{QS}$ constructed from ALICE particle yields

- use also $\Sigma^0/\Lambda = 0.278$ from pBe at $\sqrt{s} = 25\ GeV$
- Net baryon fluctuations $$\frac{\chi_B}{T^2} \approx \frac{1}{VT^3}(203.7 \pm 11.4)$$
- Net strangeness fluctuations $$\frac{\chi_S}{T^2} \approx \frac{1}{VT^3}(504.2 \pm 16.8)$$
- Charge-Strangeness corr. $$\frac{\chi_{QS}}{T^2} \approx \frac{1}{VT^3}(191 \pm 12)$$
- Ratios is volume independent

$$\boxed{\frac{\chi_B}{\chi_S} = 0.404 \pm 0.026} \quad \text{and} \quad \boxed{\frac{\chi_B}{\chi_{QS}} = 1.066 \pm 0.09}$$

Compare the ratio with LQCD data:

A. Bazavov, H.-T. Ding, P. Hegde, O. Kaczmarek, F. Karsch, E. Laermann, Y. Maezawa and S. Mukherjee

Phys.Rev.Lett. 113 (2014) and HotQCD Coll. A. Bazavov et al. Phys.Rev. D86 (2012) 034509

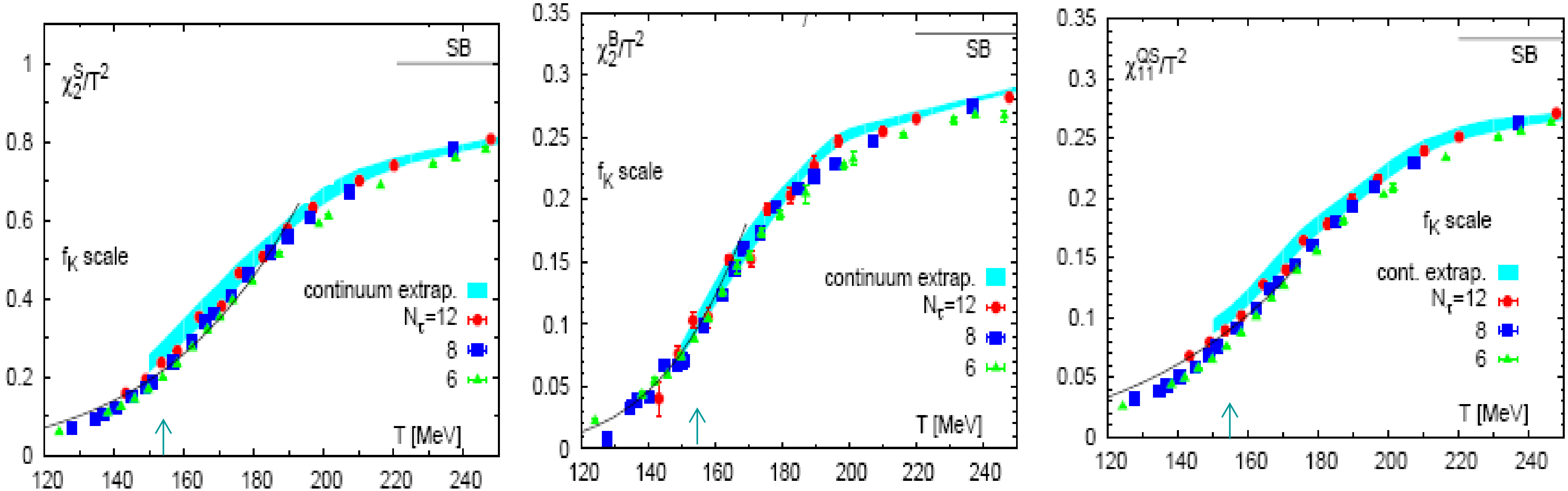

- Is there a temperature where calculated ratios from ALICE data agree with LQCD?

Baryon number, strangeness and Q-S correlations

Compare at the chiral crossover

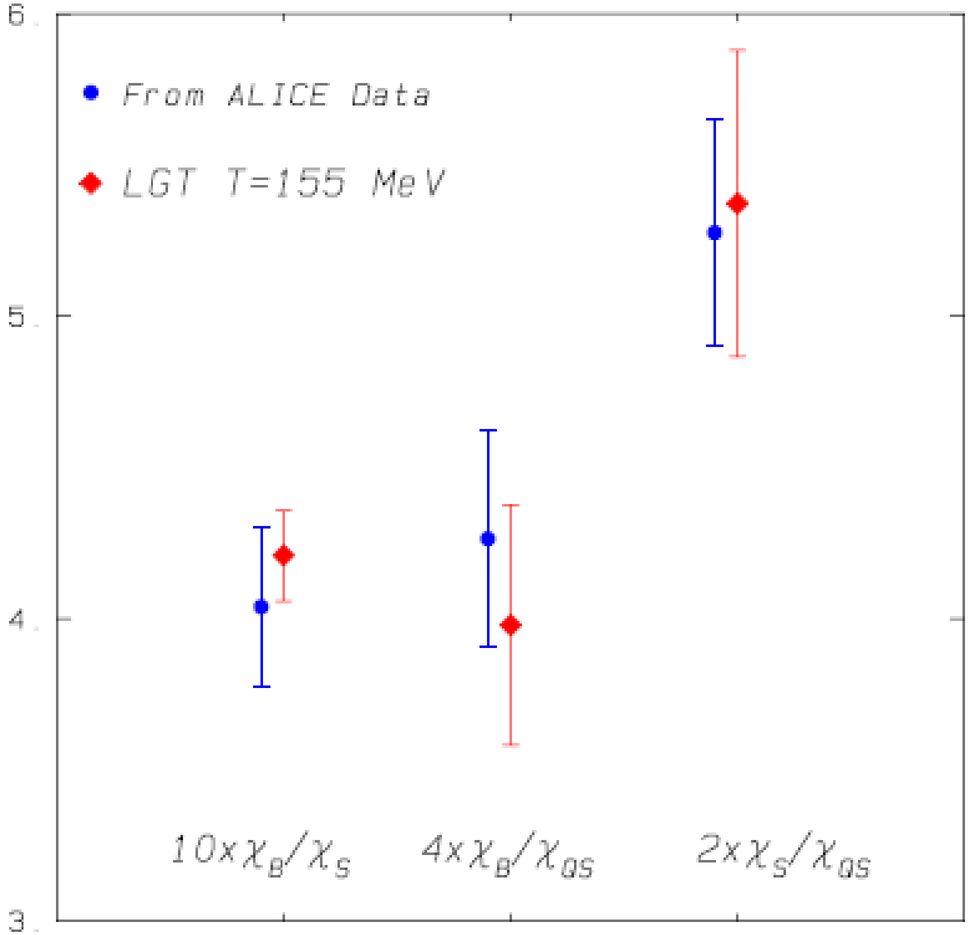

- There is a very good agreement, within systematic uncertainties, between extracted susceptibilities from ALICE data and LQCD at the chiral crossover

- How unique is the determination of the temperature at which such agreement holds?

Consider T-dependent LQCD ratios and compare with ALICE data

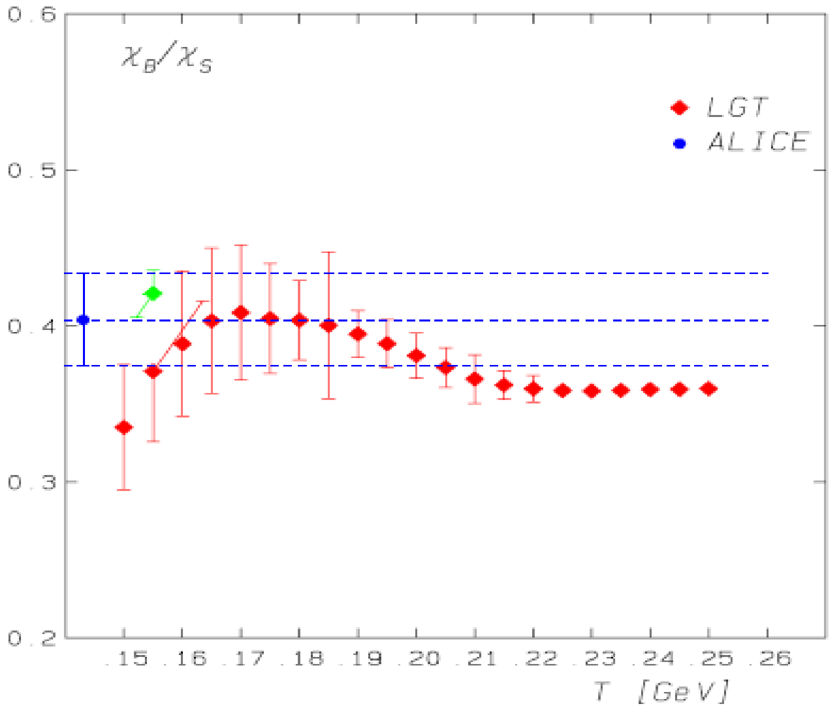

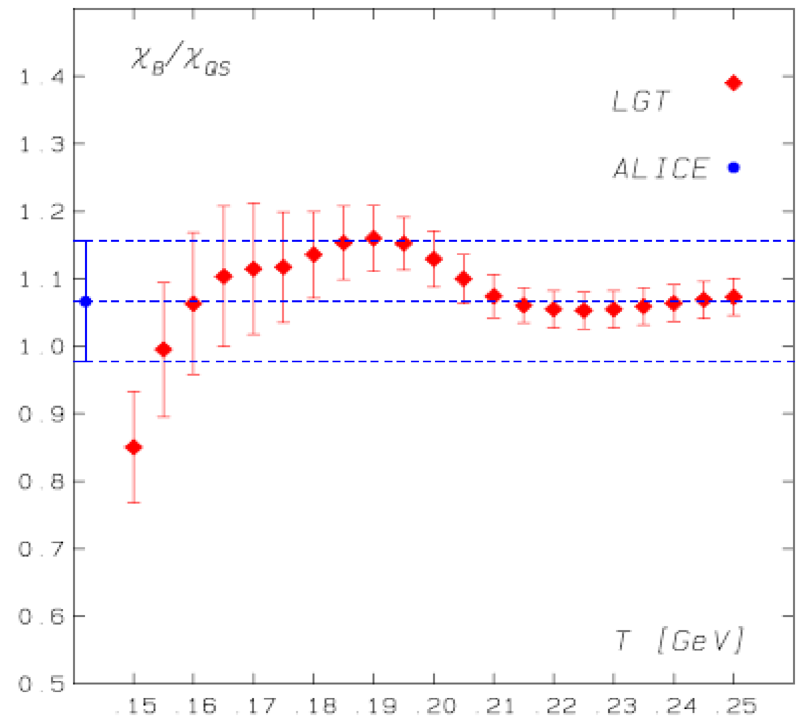

- The LQCD susceptibilities ratios are weakly T-dependent for $T \geq T_c$
- We can reject $T \leq 0.15\ GeV$ for saturation of χ_B, χ_S *and* χ_{QS} at LHC and fixed to be in the range $0.15 < T \leq 0.21\ GeV$, however
- LQCD => for $T > 0.163\ GeV$ thermodynamics cannot be anymore described by the hadronic degrees of freedom

Extract the volume by comparing data with LQCD

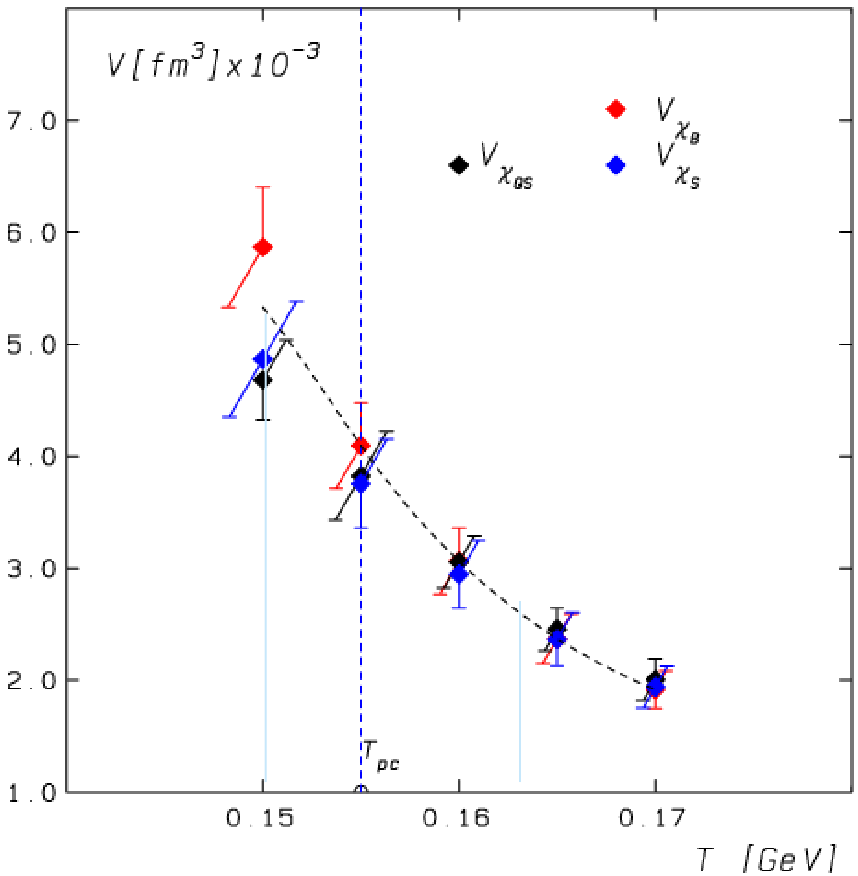

- Since

$$(\chi_N / T^2)_{LQCD} = \frac{(<N^2> - <N>^2)_{LHC}}{V_N T^3}$$

thus

$$V_{\chi_B}(T) = \frac{203.7 \pm 11.4}{T^3 (\chi_B / T^2)_{LQCD}} \qquad V_{\chi_S}(T) = \frac{504.2 \pm 24.2}{T^3 (\chi_B / T^2)_{LQCD}}$$

$$V_{\chi_{QS}}(T) = \frac{191 \pm 12}{T^3 (\chi_B / T^2)_{LQCD}}$$

- All volumes, should be equal at a given temperature if originating from the same source, thus

$$T > 150\ MeV$$

Constraining the volume from HBT and percolation theory

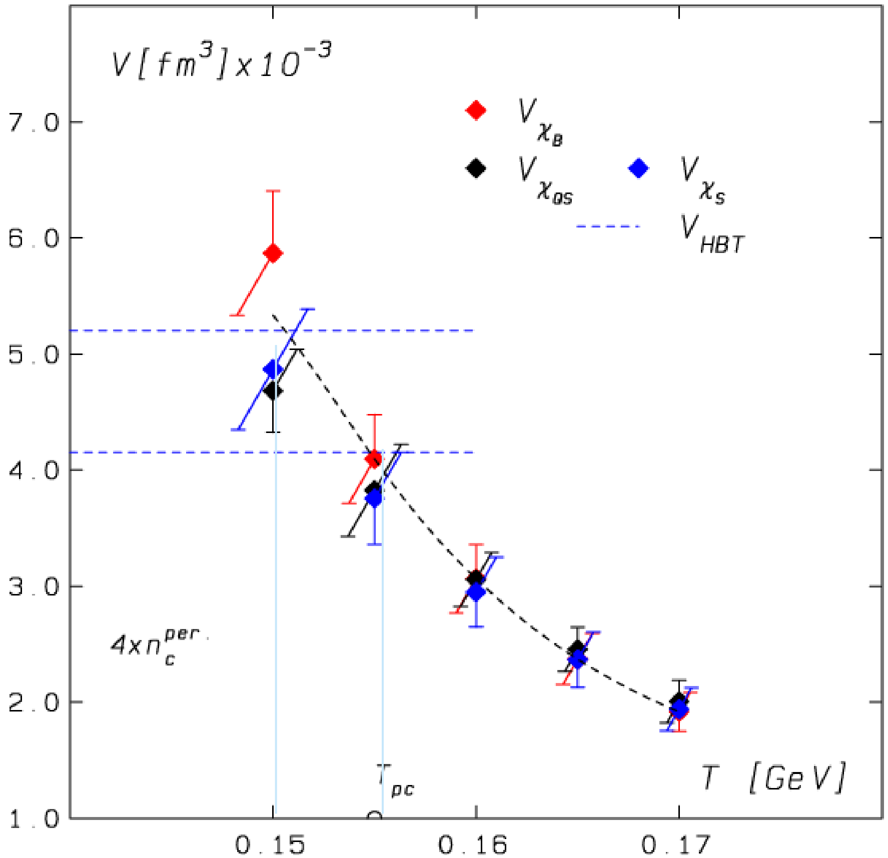

- Some limitation on volume from Hanbury-Brown–Twiss: HBT volume $V_{HBT} = (2\pi)^{3/2} R_l R_o R_s.$

  Take ALICE data from pion interferometry $V_{HBT} = 4800 \pm 640\ fm^{-3}$

If the system would decouple at the chiral crossover, then $V \geq V_{HBT}$

From these results: variance extracted from LHC data and HBT consistent with LQCD for $150 < T \leq 156\ MeV$ and the fireball volume

$$V \approx 4500 \pm 500\ \ fm^3$$

Particle density and percolation theory

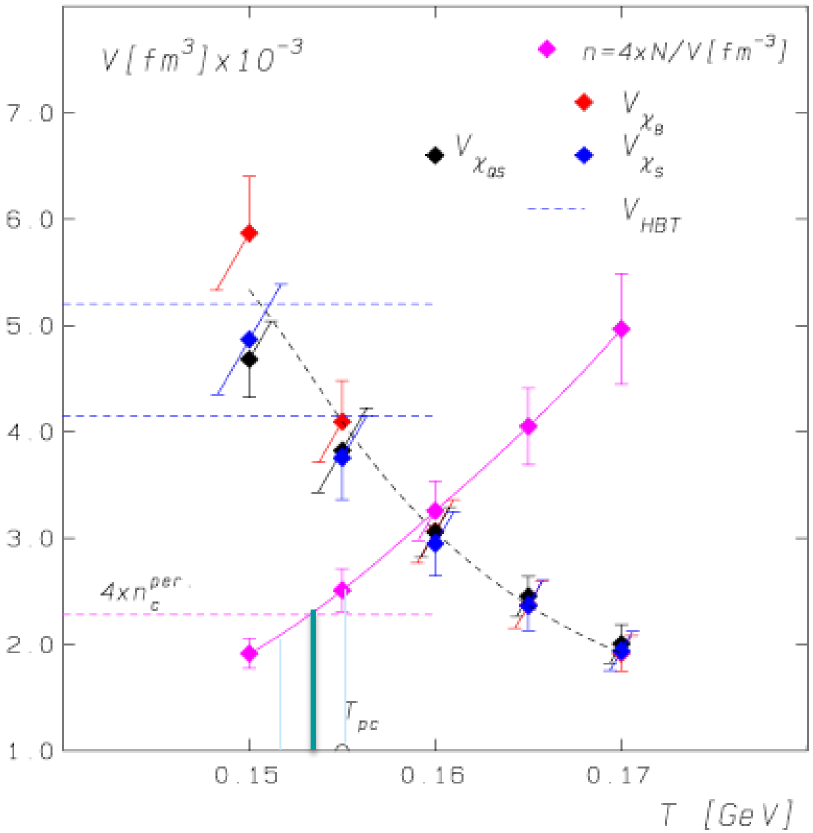

- Density of particles at a given volume $n(T) = \dfrac{N_{total}^{\exp}}{V(T)}$

- Total number of particles in HIC at LHC, ALICE

$$\langle N_t \rangle = 3\langle \pi \rangle + 4\langle p \rangle + 4\langle K \rangle + (2 + 4 \times 0.2175)\langle \Lambda_\Sigma \rangle + 4\langle \bar{\Xi} \rangle + 2\langle \bar{\Omega} \rangle,$$

$$\boxed{\langle N_t \rangle = 2486 \pm 146}$$

- Percolation theory: 3-dim system of objects of volume $V_0 = 4/3\pi R_0^3$

$$n_c = \frac{1.22}{V_0} \quad \text{take} \quad R_0 \approx 0.8\,fm \;\Rightarrow\; n_c \approx 0.57\ [fm^{-3}] \;\Rightarrow\; T_c^p \approx 154\ [MeV]$$

P. Castorina, H. Satz &K.R. Eur.Phys.J. C59 (2009)

Thermal origin of particle yields with respect to HRG

Rolf Hagedorn => the Hadron Resonace Gas (HRG):

"uncorrelated" gas of hadrons and resonances

$$< N_i > = V\,[n_i^{th}(T,\vec{\mu}) + \sum_K \Gamma_{K\to i}\, n_i^{th-Res.}(T,\vec{\mu})]$$

A. Andronic, Peter Braun-Munzinger, & Johanna Stachel, et al.

Particle yields with no resonance decay contributions:

$$\frac{1}{2j+1}\frac{dN}{dy} = V(m/T)^2 K_2(m/T)$$

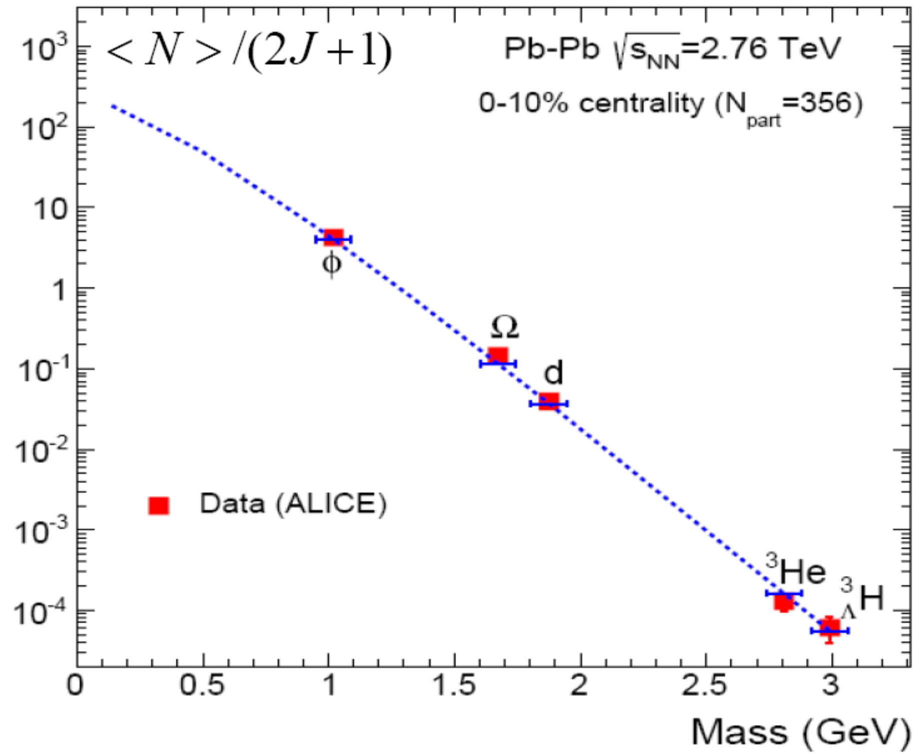

- Measured yields are reproduced with HRG at $T = 156\ \text{MeV}$

What is the influence of O(4) criticality on P(N)?

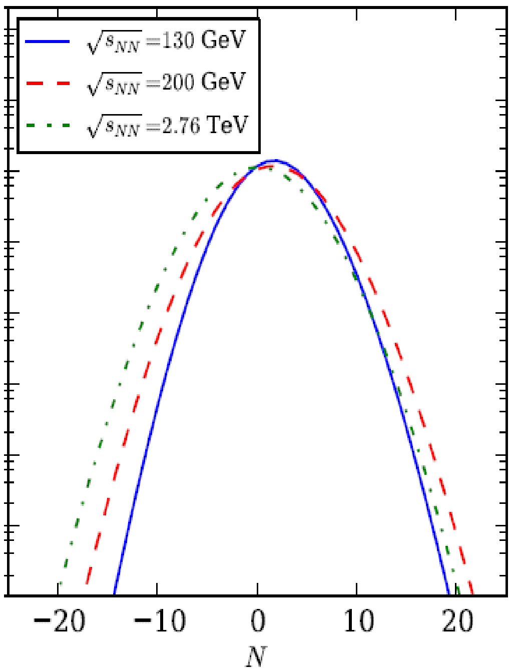

- For the net baryon number use the Skellam distribution (HRG baseline)

$$P(N) = \left(\frac{B}{\bar{B}}\right)^{N/2} I_N(2\sqrt{B\bar{B}})\exp[-(B+\bar{B})]$$

as the reference for the non-critical behavior

- Calculate P(N) in an effective chiral model which exhibits O(4) scaling and compare to the Skellam distribtuion

$$P(N) = \frac{Z_C(N)}{Z_{GC}} e^{\frac{\mu N}{T}}$$

Modelling O(4) transtion: effective Lagrangian and FRG

$$\mathscr{L}_{\mathrm{QM}} = \bar{q}[i\gamma_\mu \partial^\mu - g(\sigma + i\gamma_5 \vec{\tau}\cdot\vec{\pi})]q + \frac{1}{2}(\partial_\mu \sigma)^2 + \frac{1}{2}(\partial_\mu \vec{\pi})^2 - U(\sigma, \vec{\pi})$$

Effective potential is obtained by solving *the exact flow equation* (Wetterich eq.) with the approximations resulting in the O(4) critical exponents

J. Berges, D. U. Jungnickel & C. Wetterich; B .J. Schaefer & J. Wambach; B. Stokic, B. Friman & K.R.

$$\partial_k \Omega_k(\sigma) = \frac{Vk^4}{12\pi^2}\left[\sum_{i=\pi,\sigma} \frac{d_i}{E_{i,k}}[1+2n_B(E_{i,k})] - \frac{2\nu_q}{E_{q,k}}[1-n_F(E^+_{q,k}) - n_F(E^-_{q,k})]\right]$$

$$E_{\pi,k} = \sqrt{k^2 + \Omega'_k}$$

$$E_{\sigma,k} = \sqrt{k^2 + \Omega'_k + 2\rho\Omega''_k}$$

$$E_{q,k} = \sqrt{k^2 + 2g^2\rho}$$

$$\Omega'_k \equiv \frac{\partial \Omega_k}{\partial(\sigma^2/2)}$$

Full propagators with $k < q < \Lambda$

$\Gamma_\Lambda = S_{\text{classical}}$

Integrating from $k=\Lambda$ to $k=0$ gives a full quantum effective potential

Put $\Omega_{k=0}(\sigma_{\min})$ into the integral formula for P(N)

The influence of O(4) criticality on P(N) for $\mu=0$

- Take the ratio of $P^{FRG}(N)$ which contains O(4) dynamics to Skellam distribution with the same Mean and Variance at different T/T_{pc}

K. Morita, B. Friman &K.R. (QM model within renormalization group FRG)

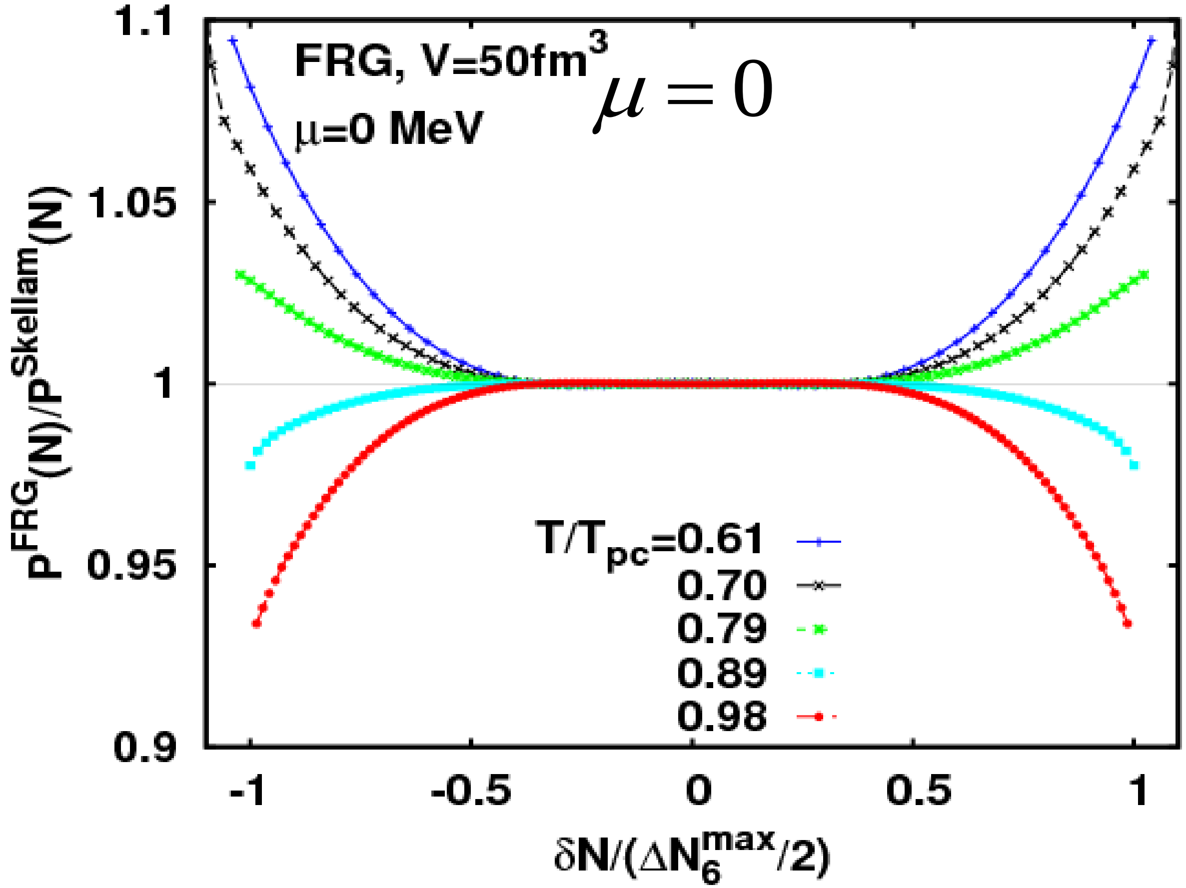

Ratio < 1 at larger |N| if $c_6/c_2 < 1$

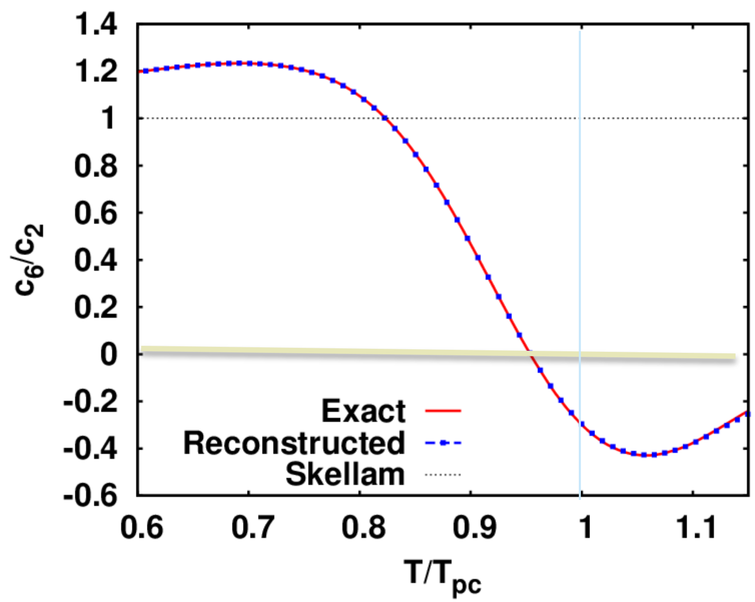

The influence of O(4) criticality on P(N) at $\mu \neq 0$

- Take the ratio of $P^{FRG}(N)$ which contains O(4) dynamics to Skellam distribution with the same Mean and Variance near $T_{pc}(\mu)$

K. Morita, B. Friman et al.

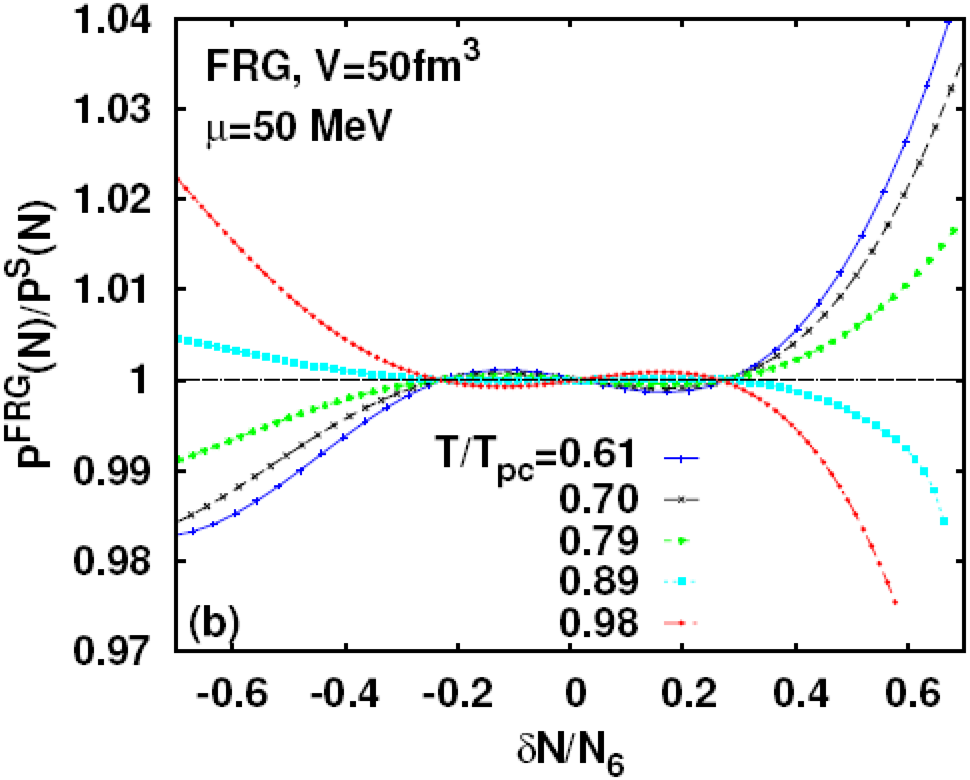

- Asymmetric P(N) $N > < N >$
- Near $T_{pc}(\mu)$ the ratios less than unity for

Probability distribution of net proton number STAR Coll. data at RHIC

Thanks to Nu Xu and Xiofeng Luo

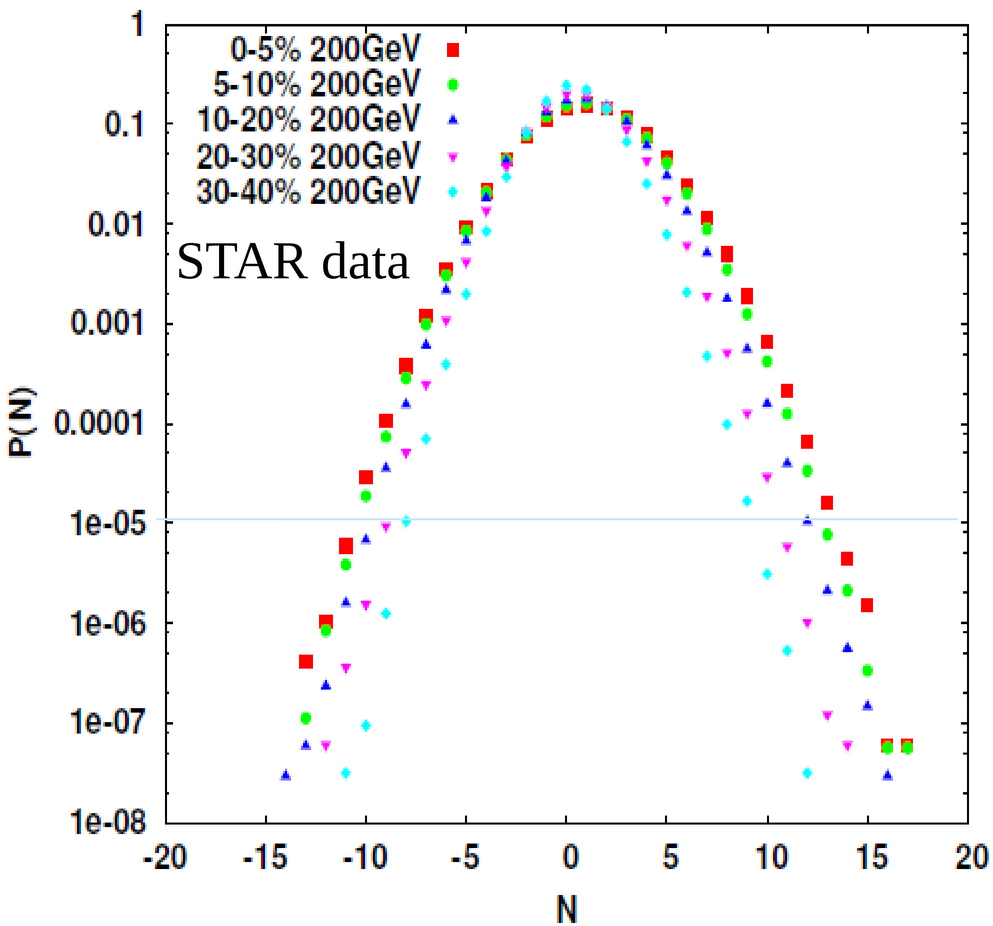

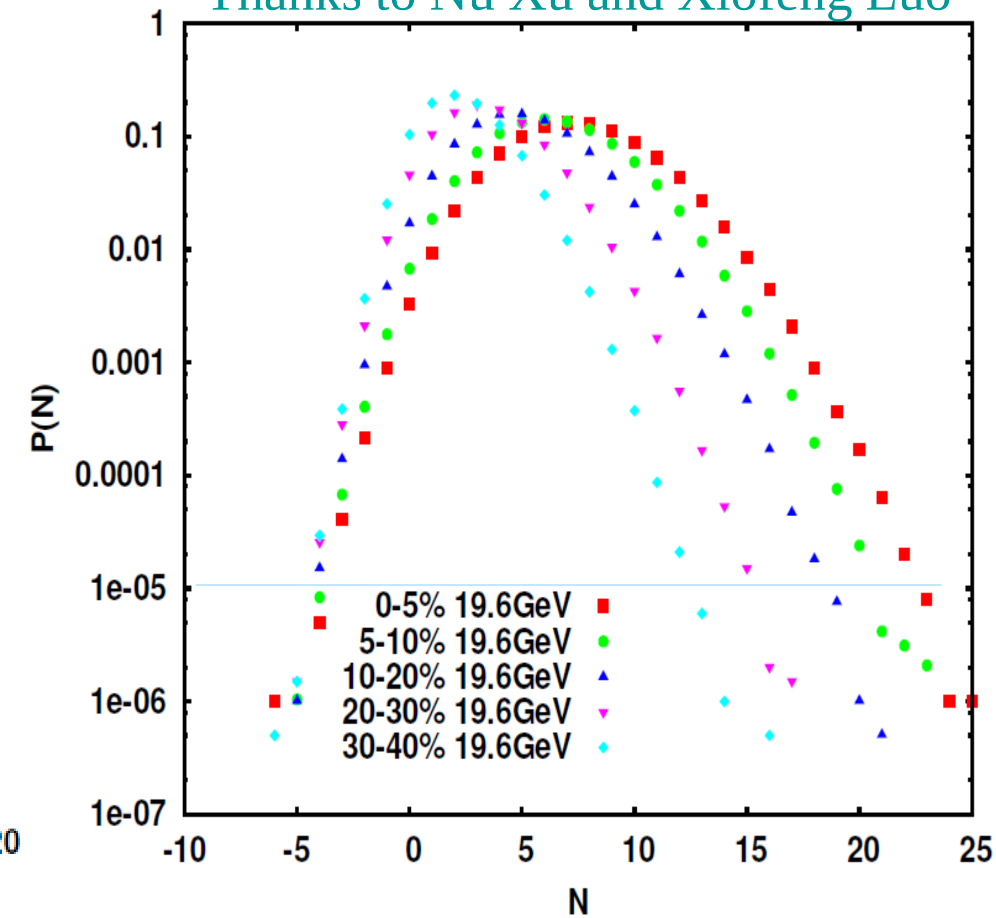

Do we also see the O(4) critical structure in these probability distributions ?
Efficiency uncorrected data!!

The influence of O(4) criticality on P(N) for $\mu \neq 0$

- In central collisions the probability behaves as being influenced by the chiral transition

K. Morita, B. Friman & K.R.

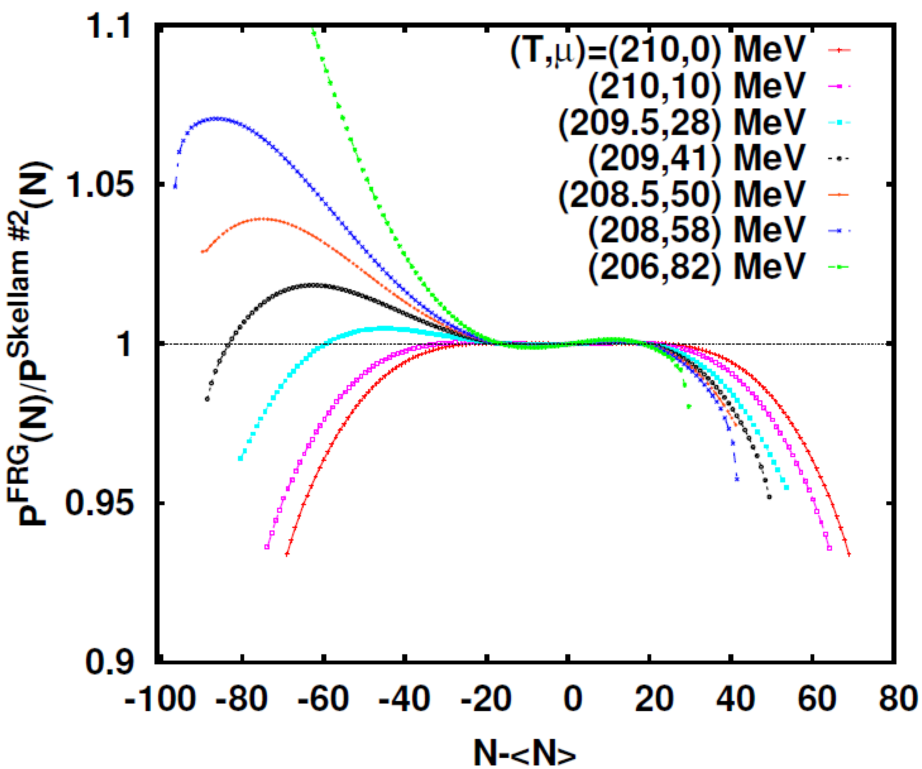

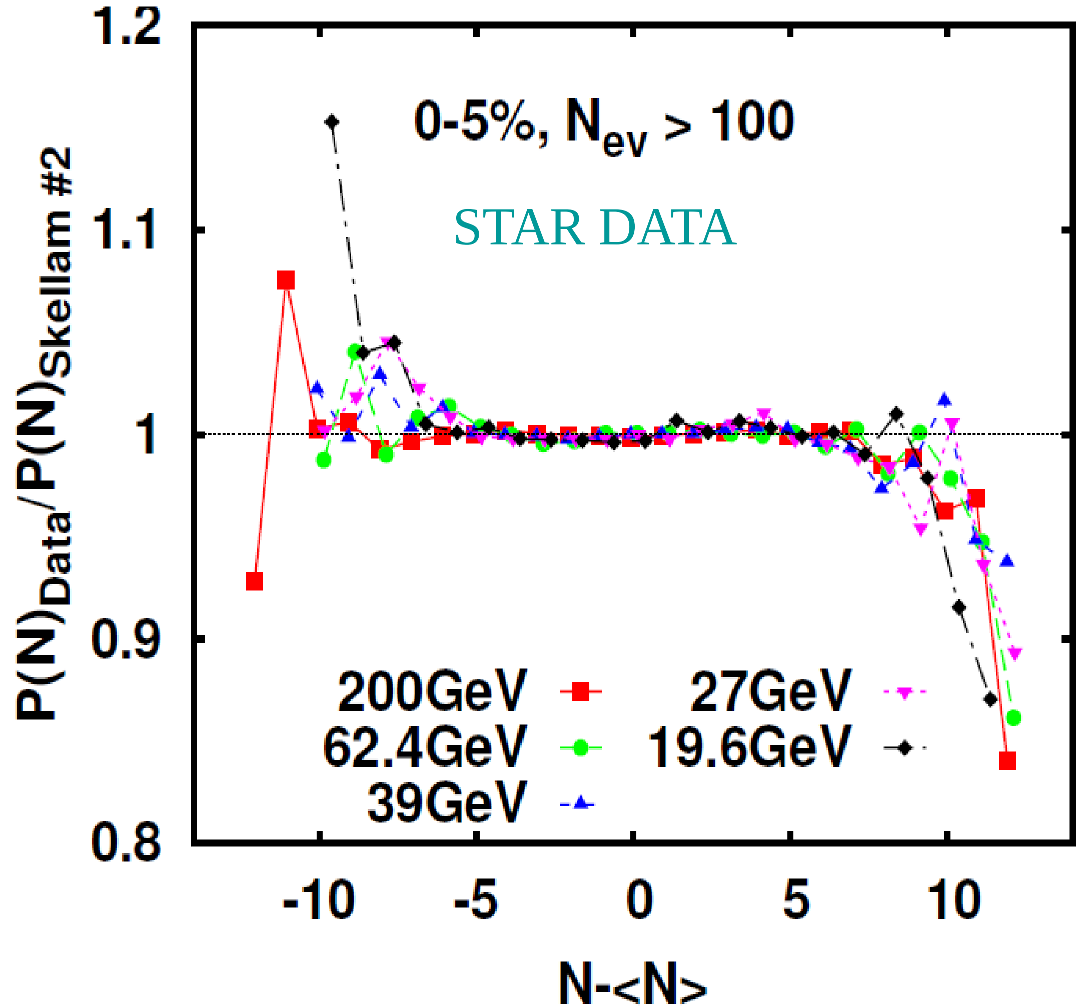

Centrality dependence of probability ratio

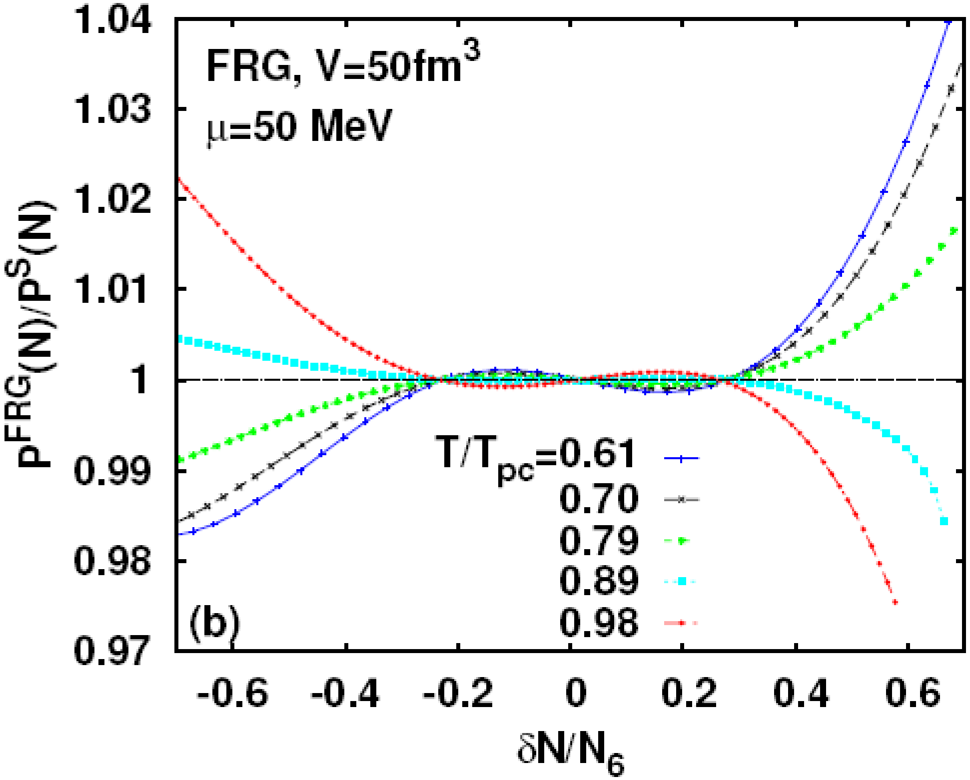

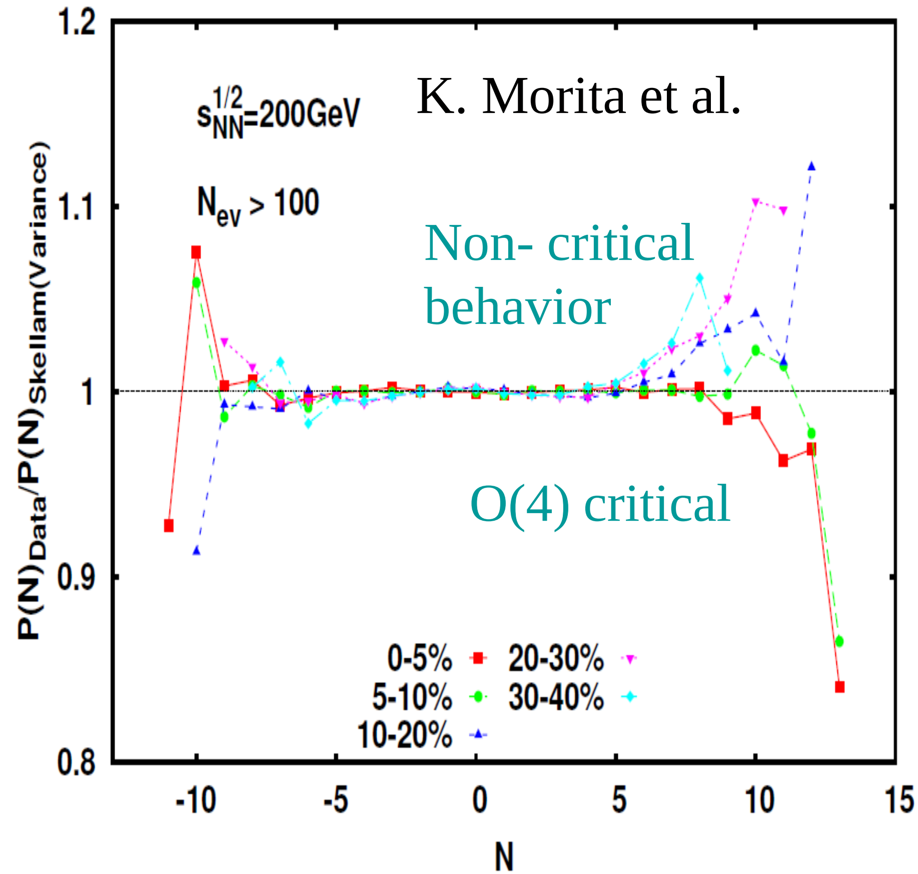

- For less central collisions, the freezeout appears away of the pseudocritical line, resulting in an absence of the O(4) critical structure in the probability ratio.

Conclusions:

From a direct comparison of fluctuations constructed from ALICE data, and LQCD results one concludes that:

- there is thermalization in heavy ion collisions at the LHC and the 2nd order charge fluctuations and correlations are saturated at the chiral crossover temperature

Skellam distribution, and its generalization, is a good approximation of the net charge probability distribution P(N) for small N. The chiral criticality sets in at larger N>3 and implies deviation from Skellam distribution.

Missing resonances in strangeness fluctuations

Pok Man Lo, M. Marczenko et al.

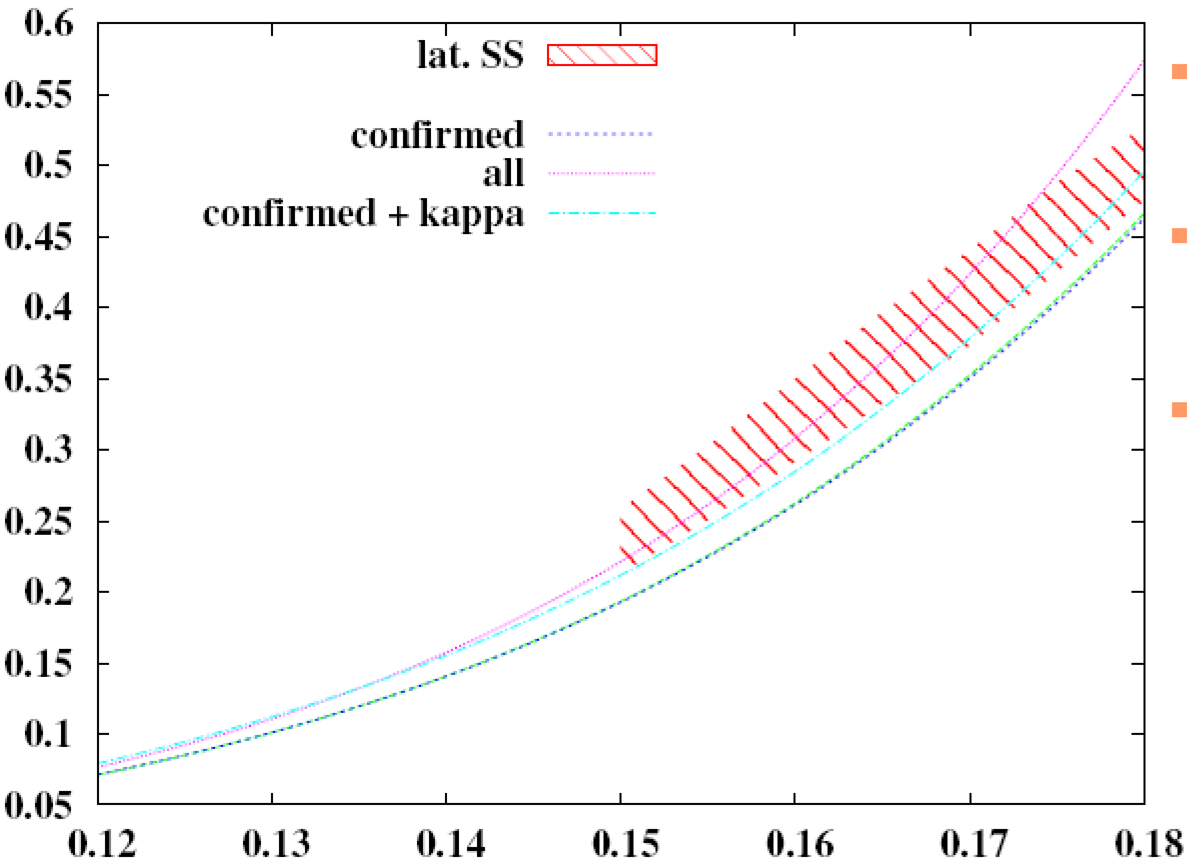

- Known strange hadrons underestimate LGT strangeness fluctuations
- One needs to include states expected in the Quark Model , particularly the low lying strange-hadrons
- The main contribution is due to expected “kappa” K*(800) strange 0^- meson in addition to already known 1^- state

K*0(800) MASS 682±29 MeV

K*0(800) WIDTH 547±24 MeV

Ratios of cumulants at finite density in PQM model with FRG

B. Friman, F. Karsch, V. Skokov &K.R.
Eur.Phys.J. C71 (2011) 1694

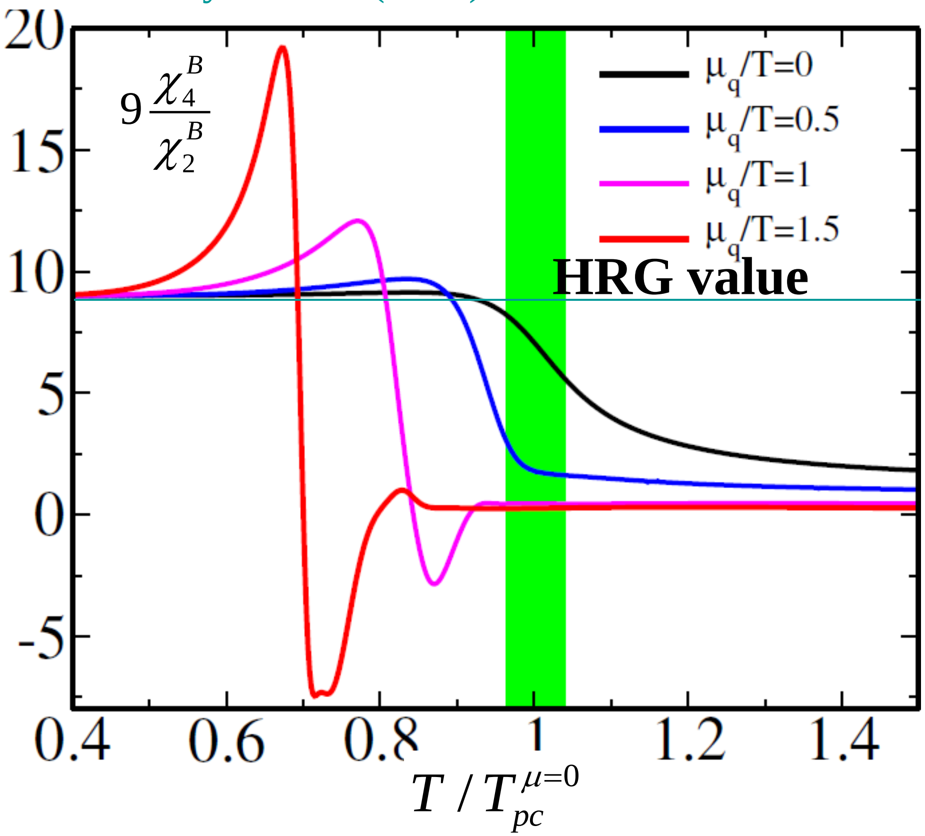

B. Friman, V. Skokov &K.R.
Phys.Rev. C83 (2011) 054904

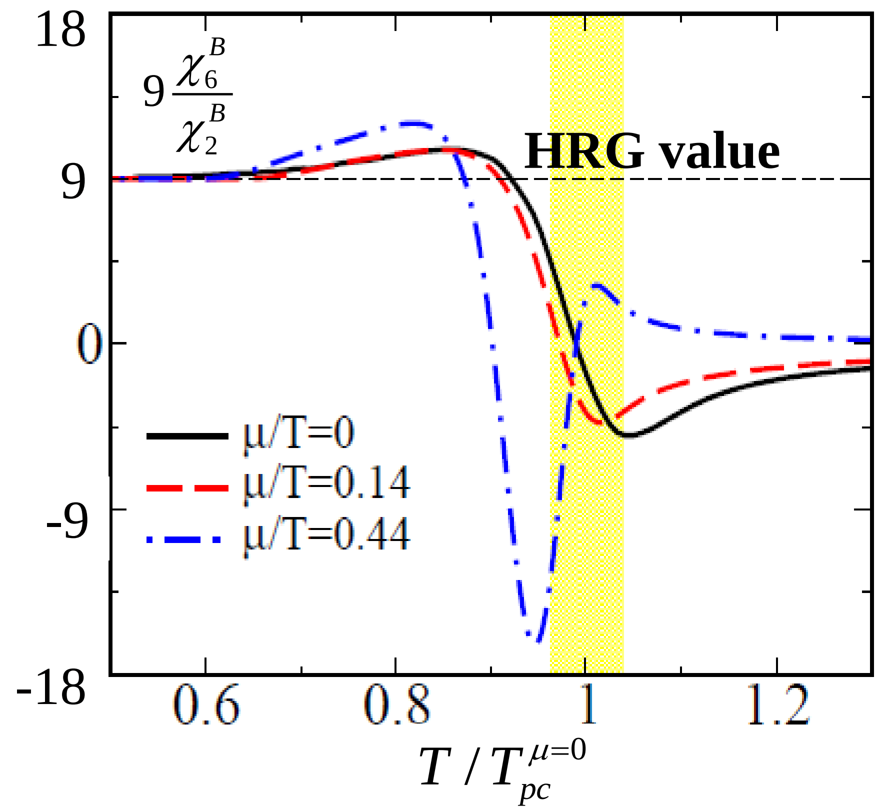

Deviations from low -T HRG values are increasing with μ/T **and the cumulant order . Negative fluctuations near the chiral crossover.**

Excellent description of the QCD Equation of States by Hadron Resonance Gas

A. Bazavov et al. HotQCD Coll. July 2014

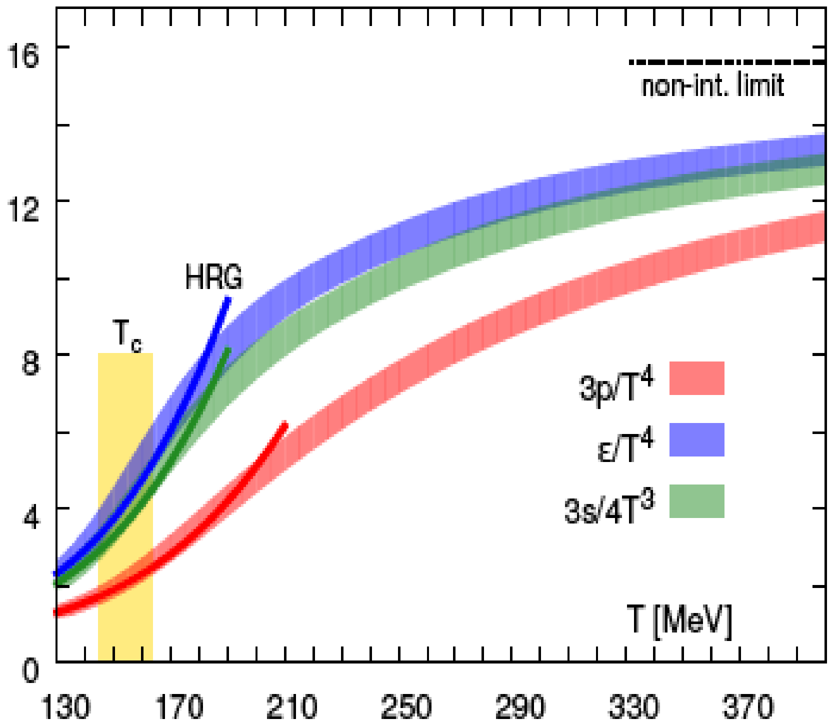

F. Karsch et al. HotQCD Coll.

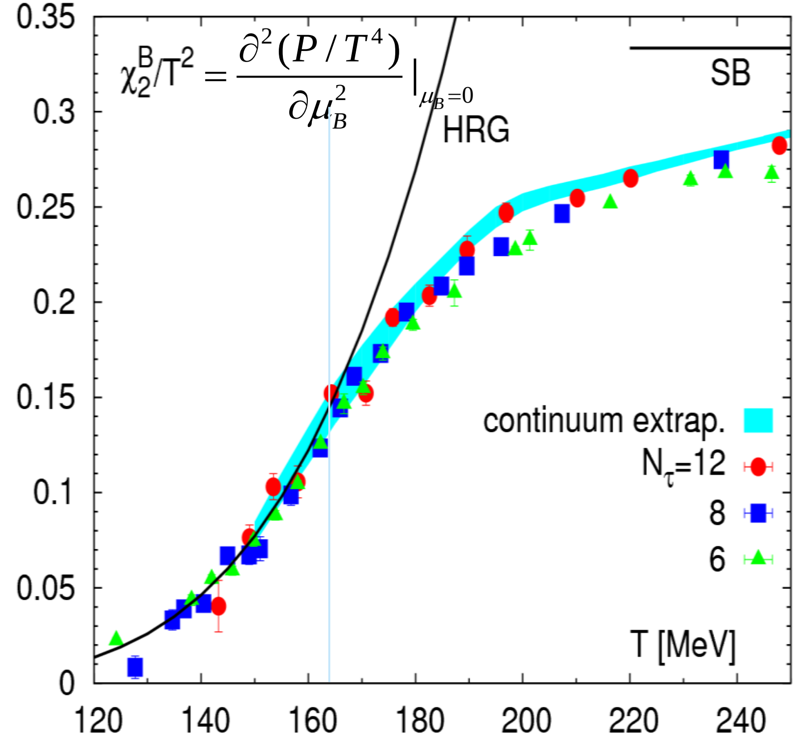

- "Uncorrelated" Hadron Gas provides an excellent description of the QCD equation of states in confined phase
- "Uncorrelated" Hadron Gas provides also an excellent description of net baryon number fluctuations

MUSIC with diffusion

Chun Shen
McGill University

In collaboration with Gabriel Denicol, Akihiko Monnai, Bjoern Schenke, Sangyong Jeon, and Charles Gale

Little Bang

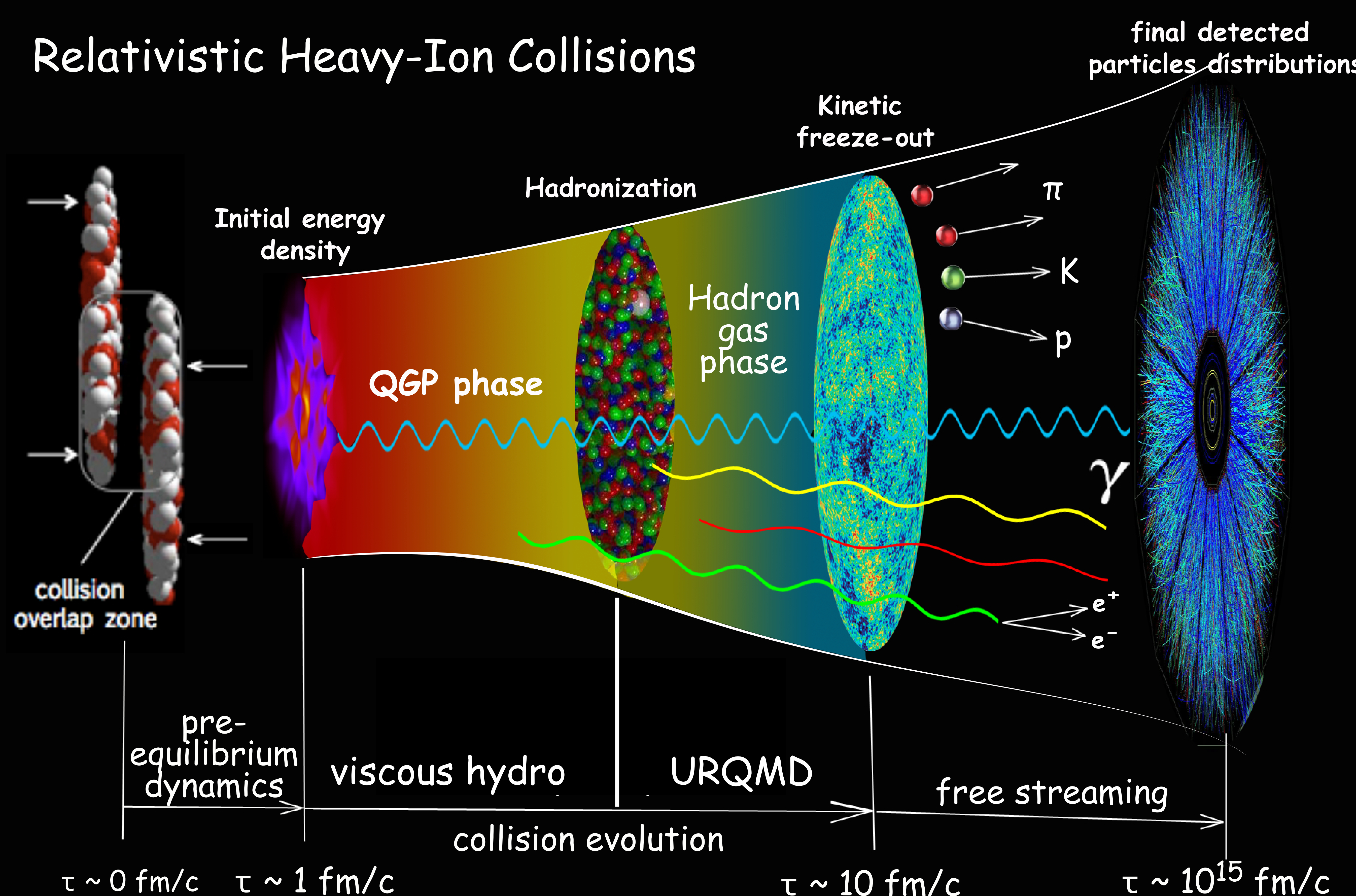
Relativistic Heavy-Ion Collisions
final detected particles distributions
Kinetic freeze-out
Hadronization
Initial energy density
Hadron gas phase
QGP phase
π
K
p
γ
e+
e−
collision overlap zone
pre-equilibrium dynamics
viscous hydro
URQMD
free streaming
collision evolution
τ ~ 0 fm/c
τ ~ 1 fm/c
τ ~ 10 fm/c
τ ~ 10^15 fm/c

Exploring the phase of QCD

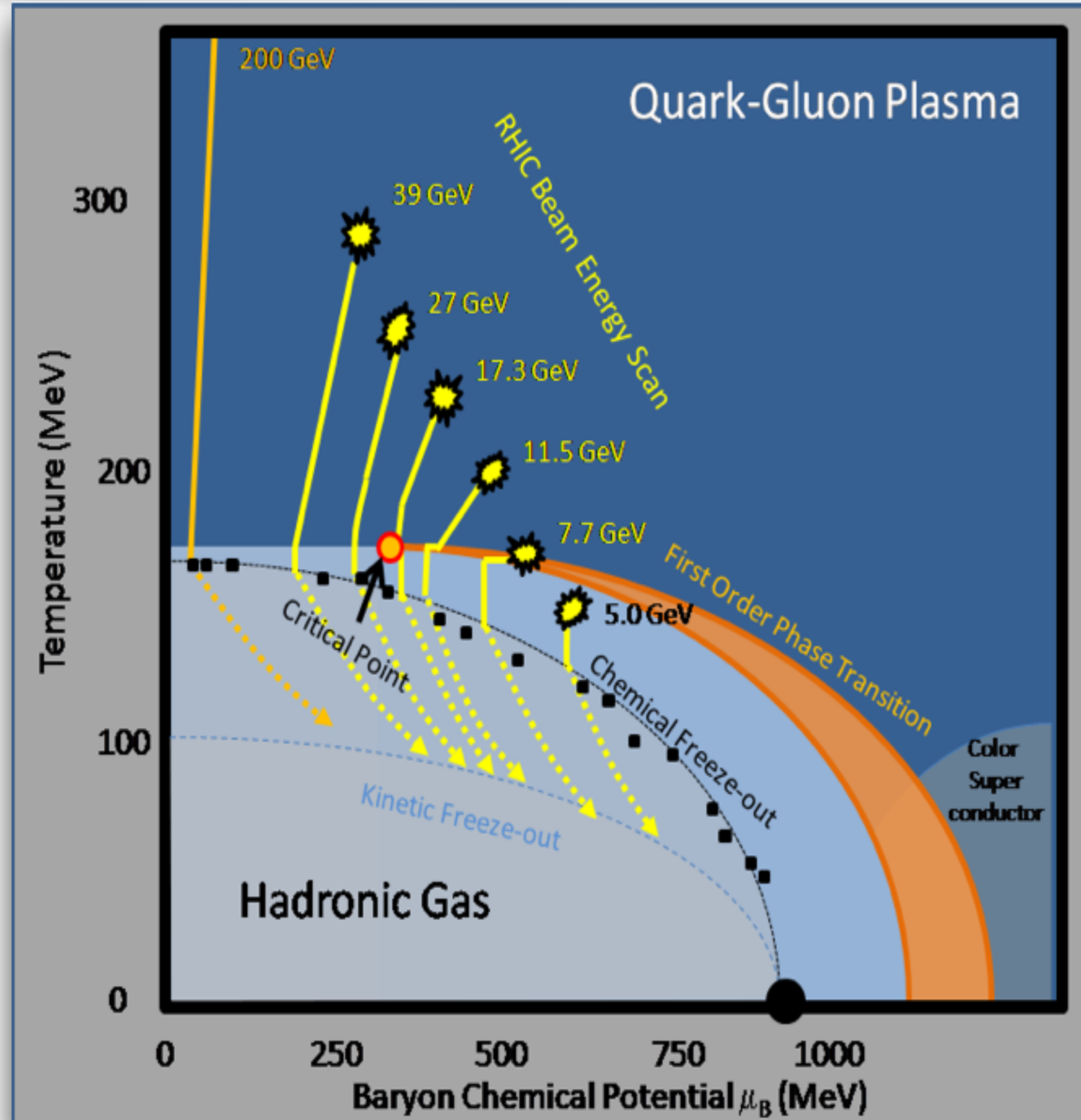

Exploring the phase of QCD

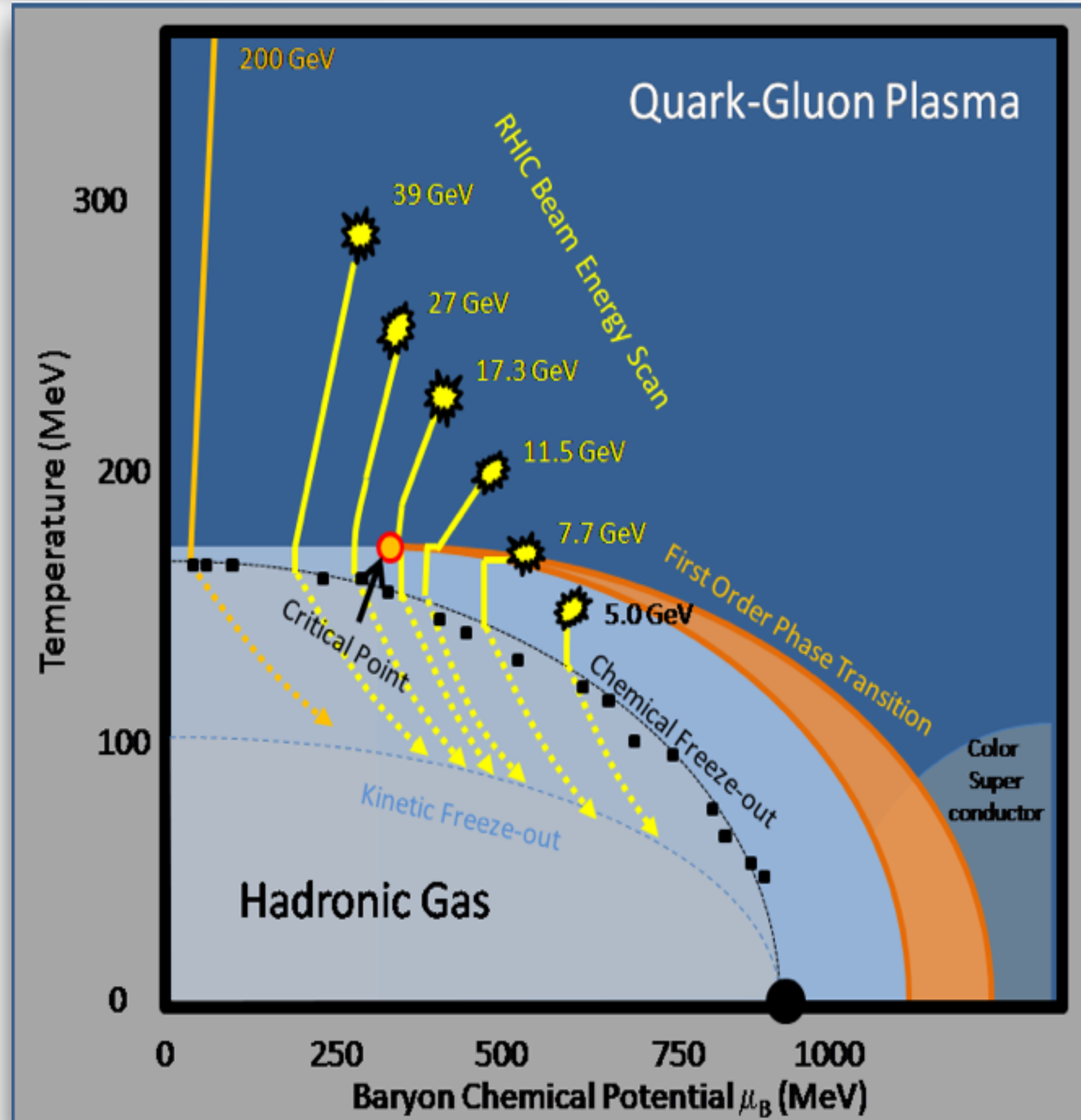

- Event-by-event fluctuating initial conditions
- (3+1)-d dissipative hydrodynamic modelling of the QGP
- Microscopic description for hadronic phase

Exploring the phase of QCD

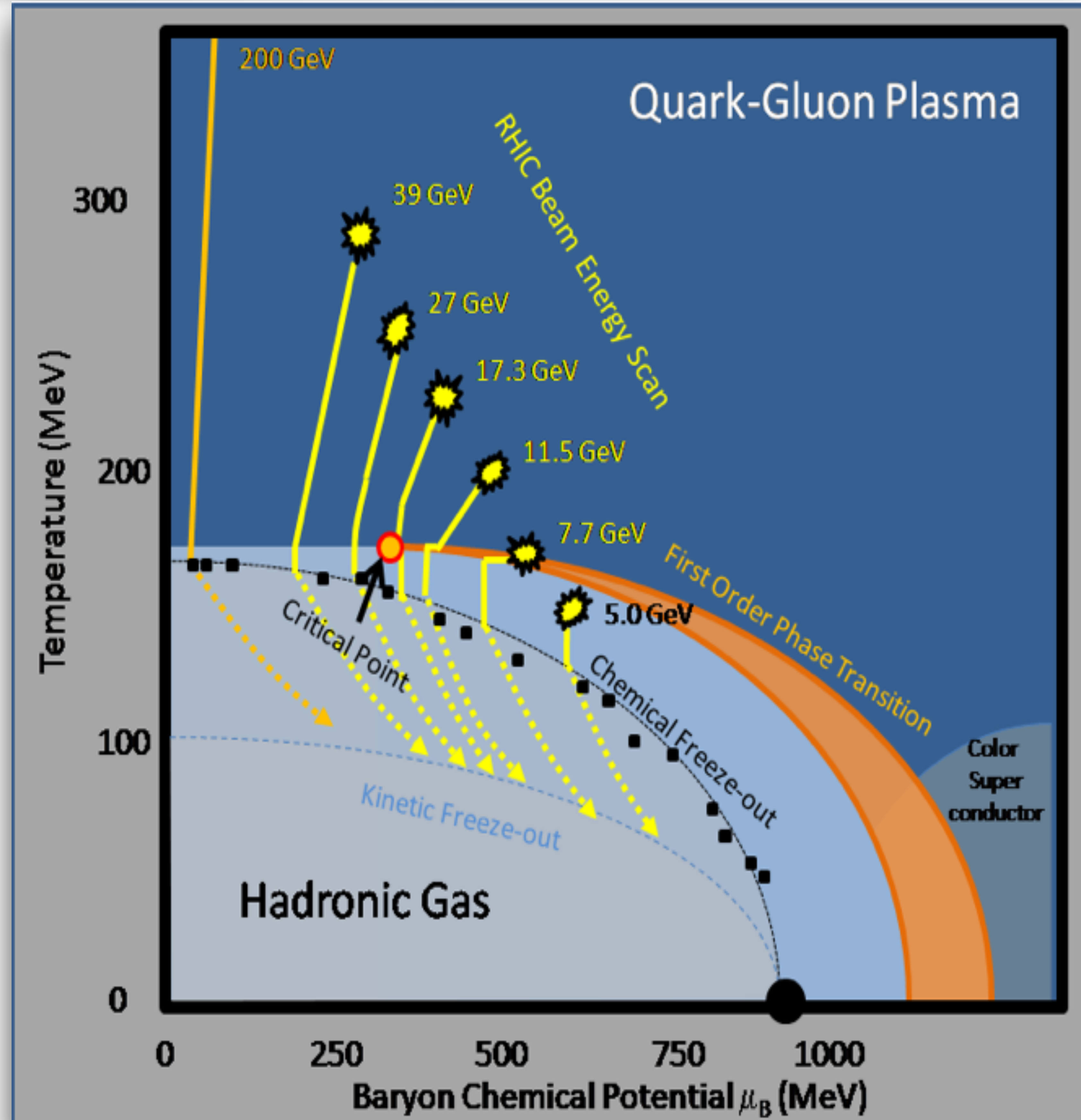

- Event-by-event fluctuating initial conditions
  (AMPT, UrQMD, MCGlb*, ...)
- (3+1)-d dissipative hydrodynamic modelling of the QGP
  MUSIC
- Microscopic description for hadronic phase
  UrQMD

Exploring the phase of QCD

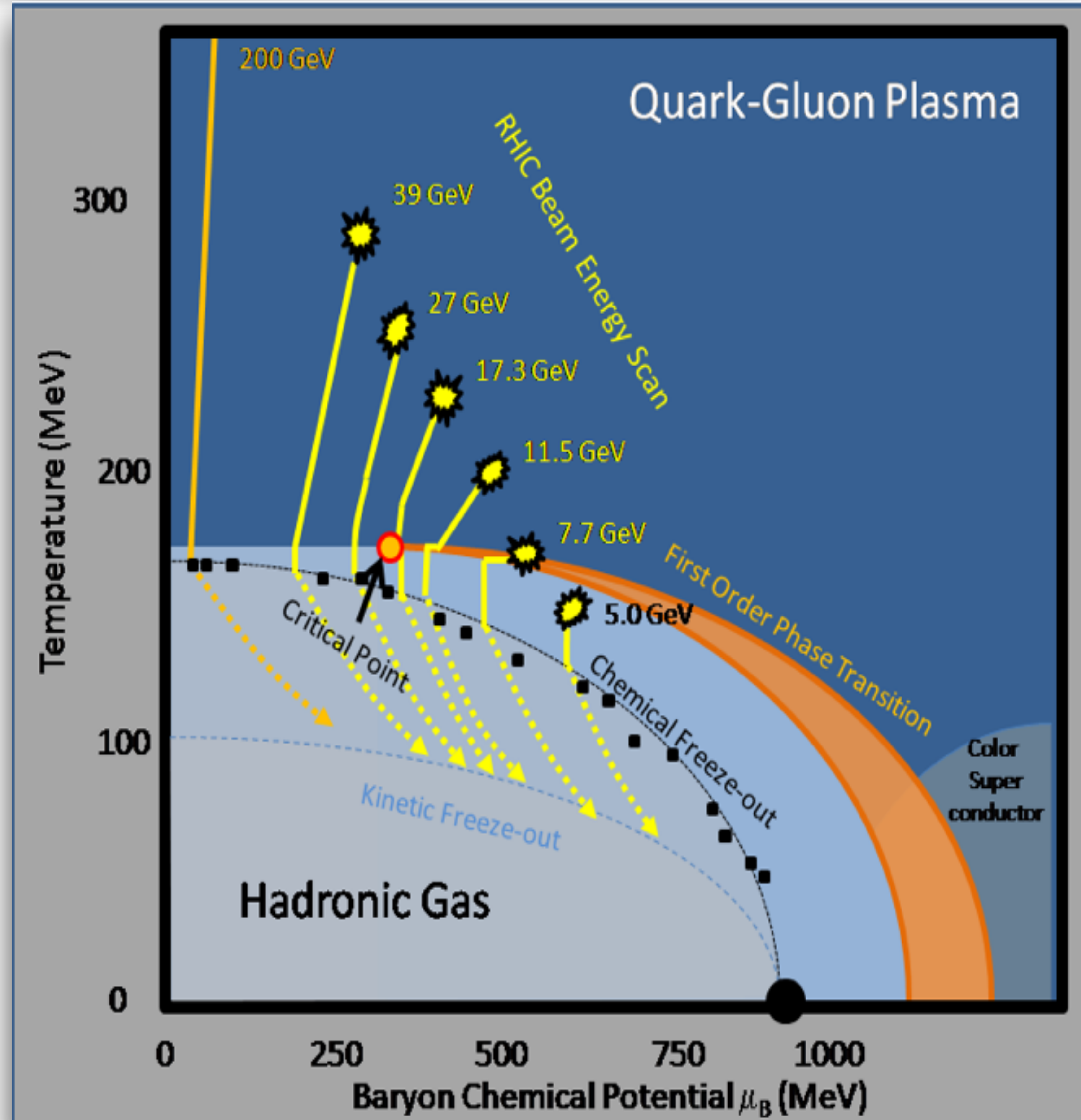

- Event-by-event fluctuating initial conditions

  (AMPT, UrQMD, MCGlb*, ...)

- (3+1)-d dissipative hydrodynamic modelling of the QGP

  MUSIC

- Microscopic description for hadronic phase

  UrQMD

Exploring the phase of QCD

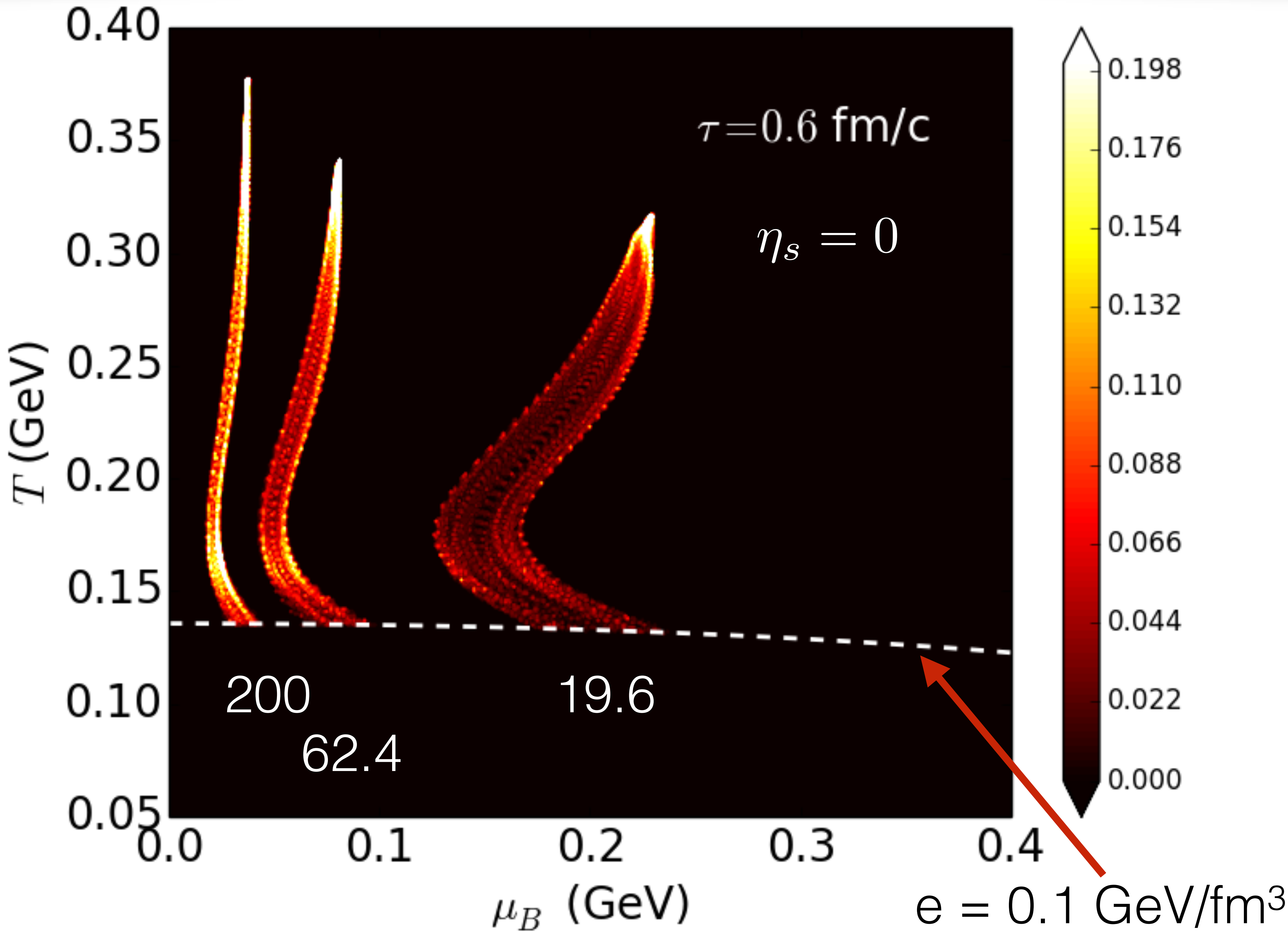

Exploring the phase of QCD

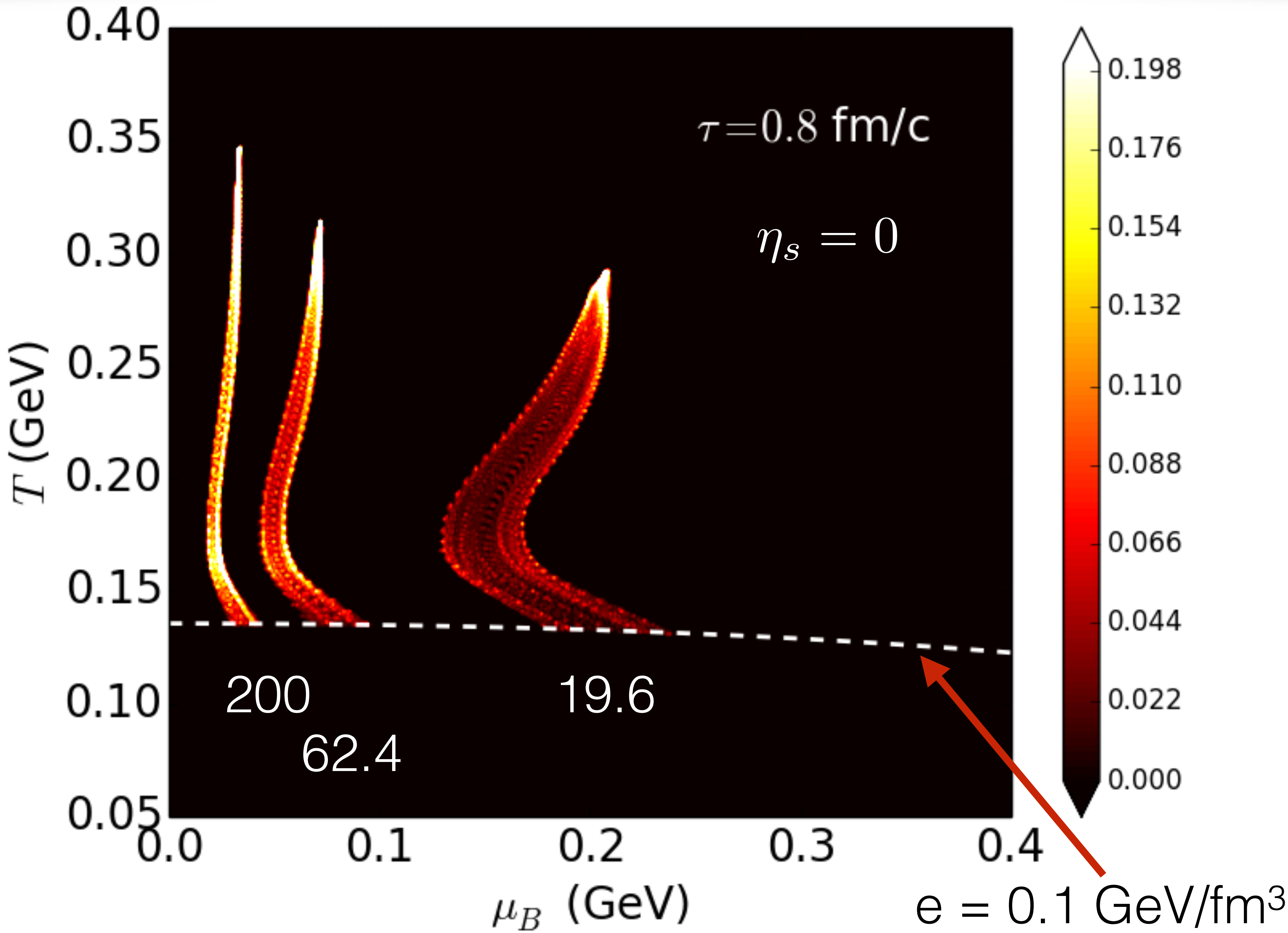

Exploring the phase of QCD

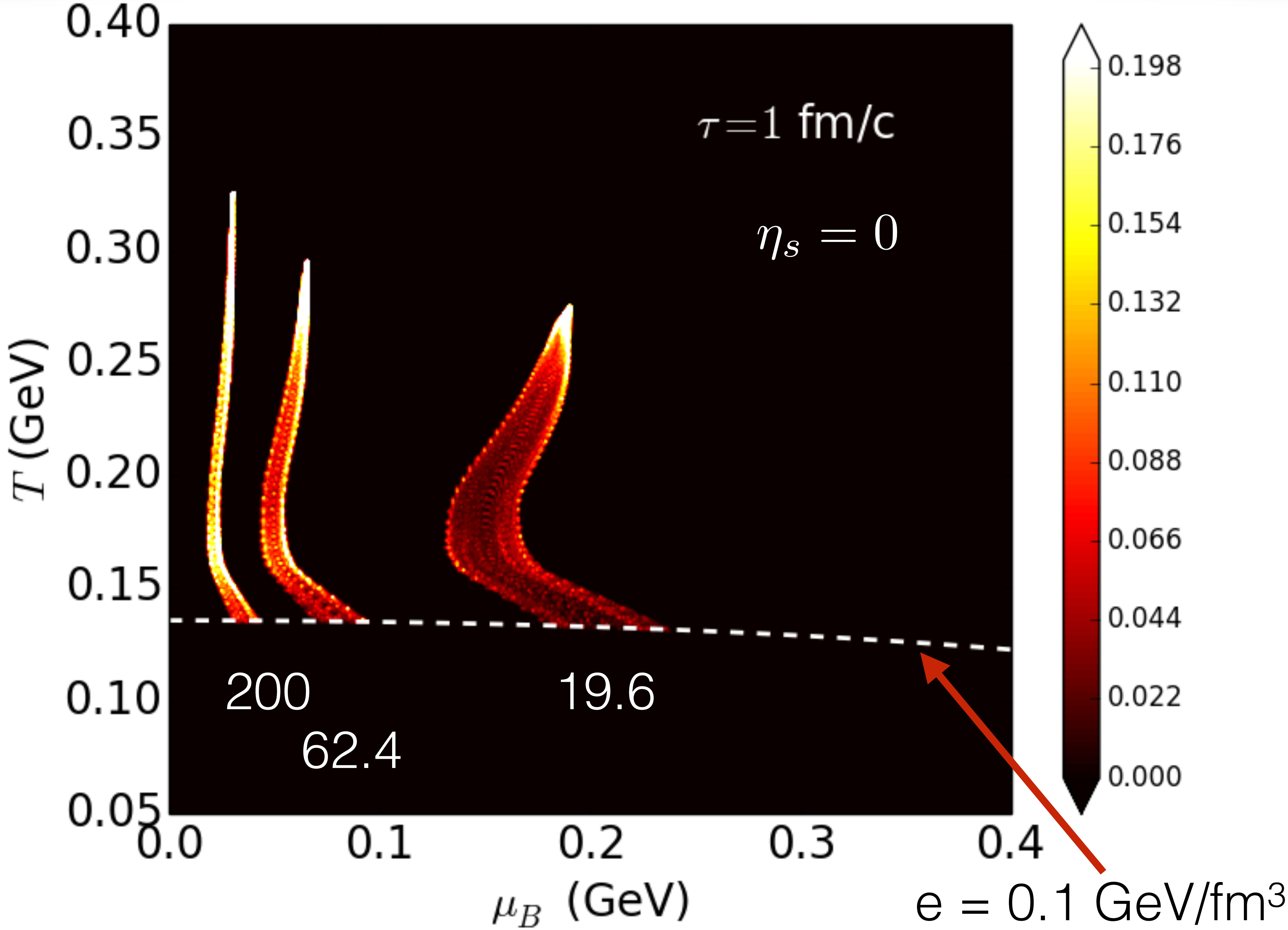

Exploring the phase of QCD

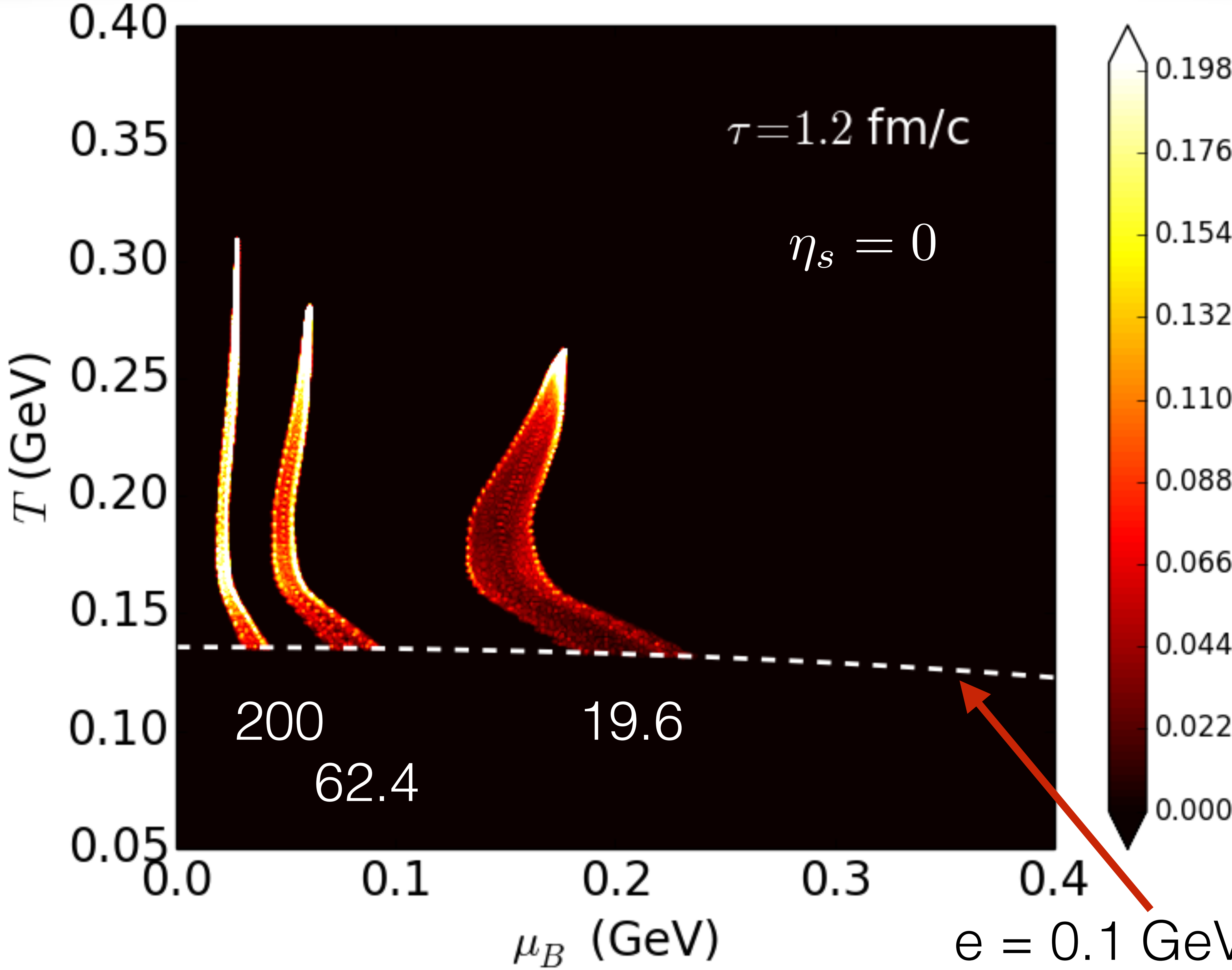

e = 0.1 GeV/fm^3

Exploring the phase of QCD

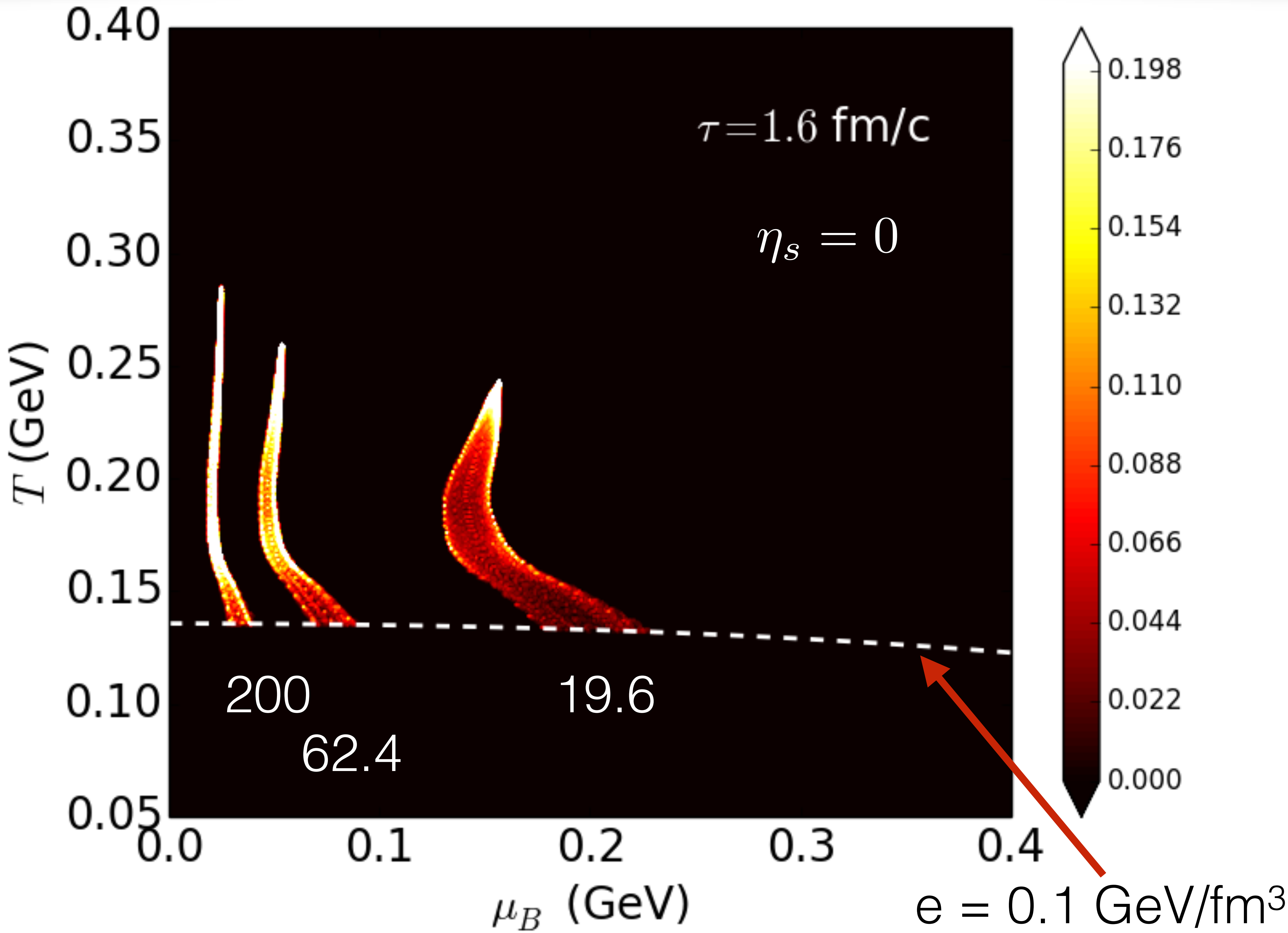

Exploring the phase of QCD

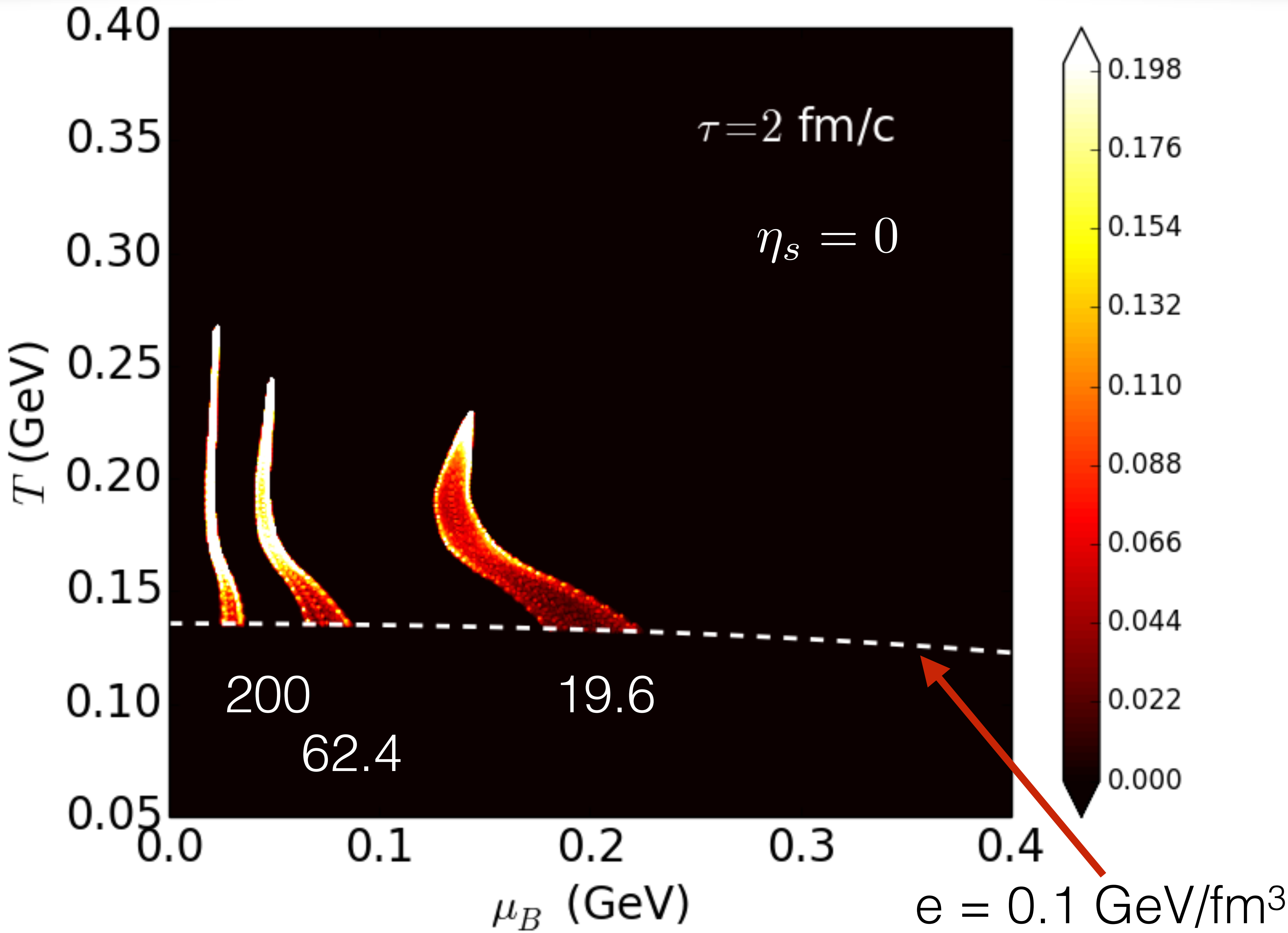

Exploring the phase of QCD

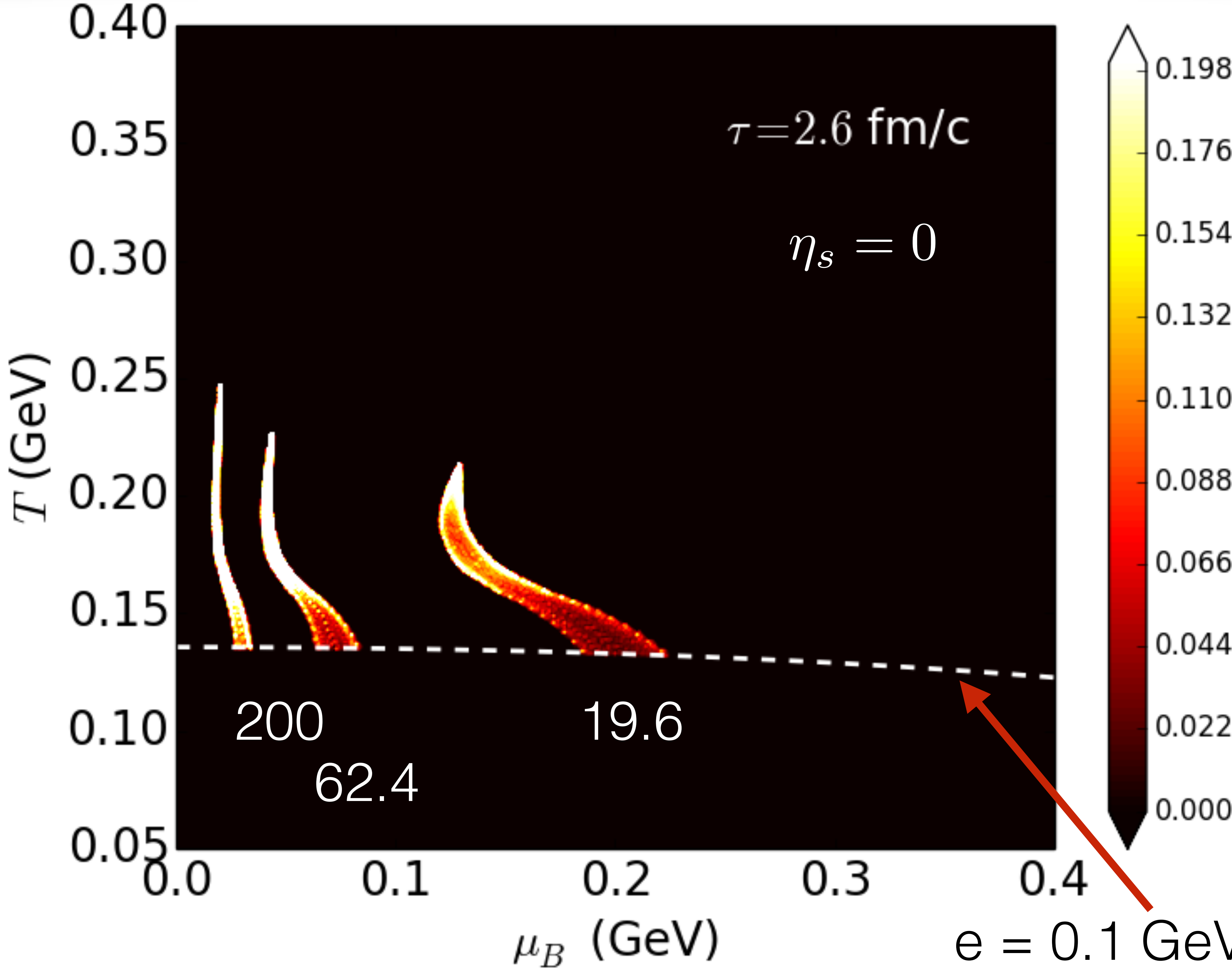

e = 0.1 GeV/fm^3

Exploring the phase of QCD

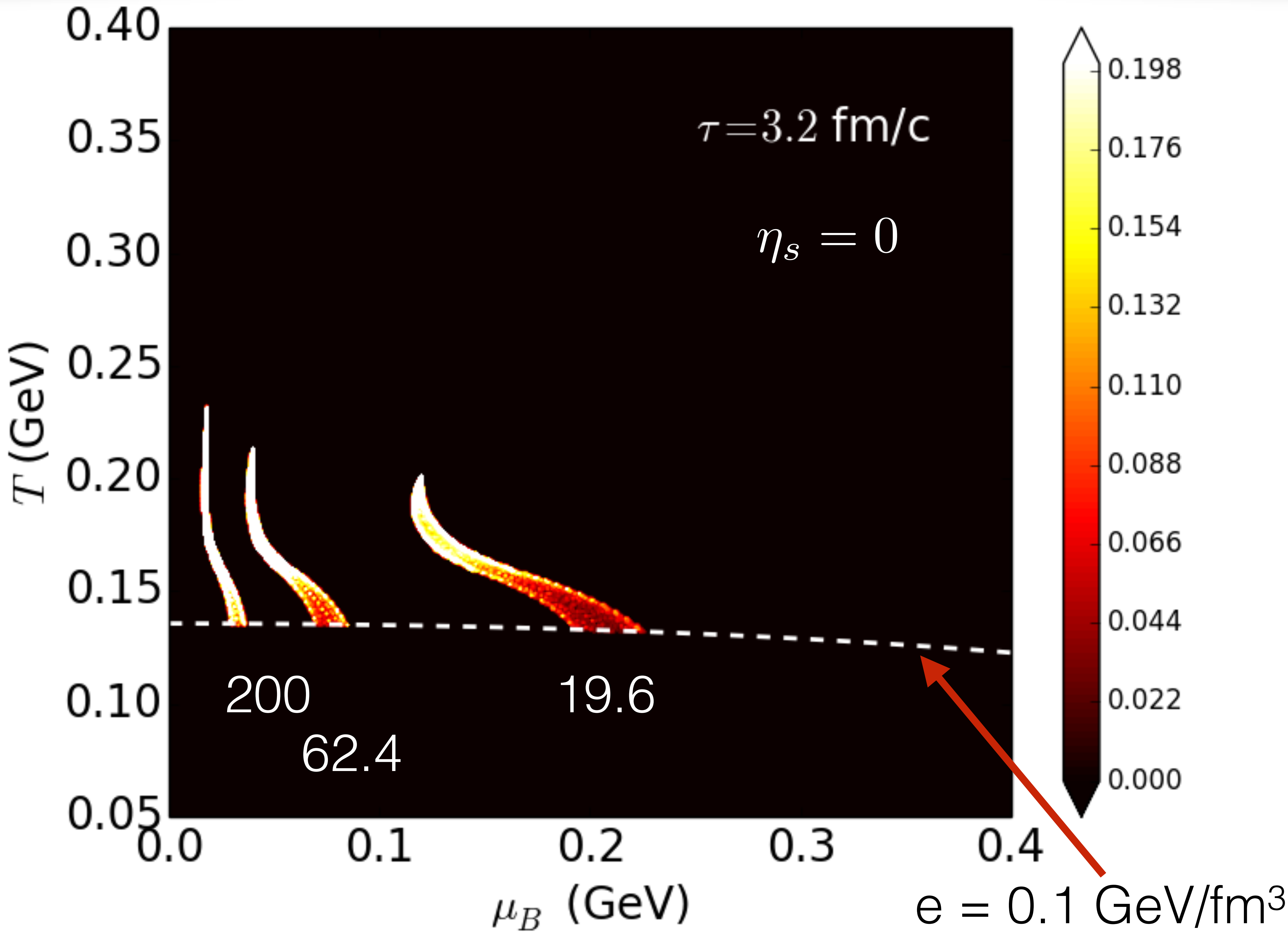

Exploring the phase of QCD

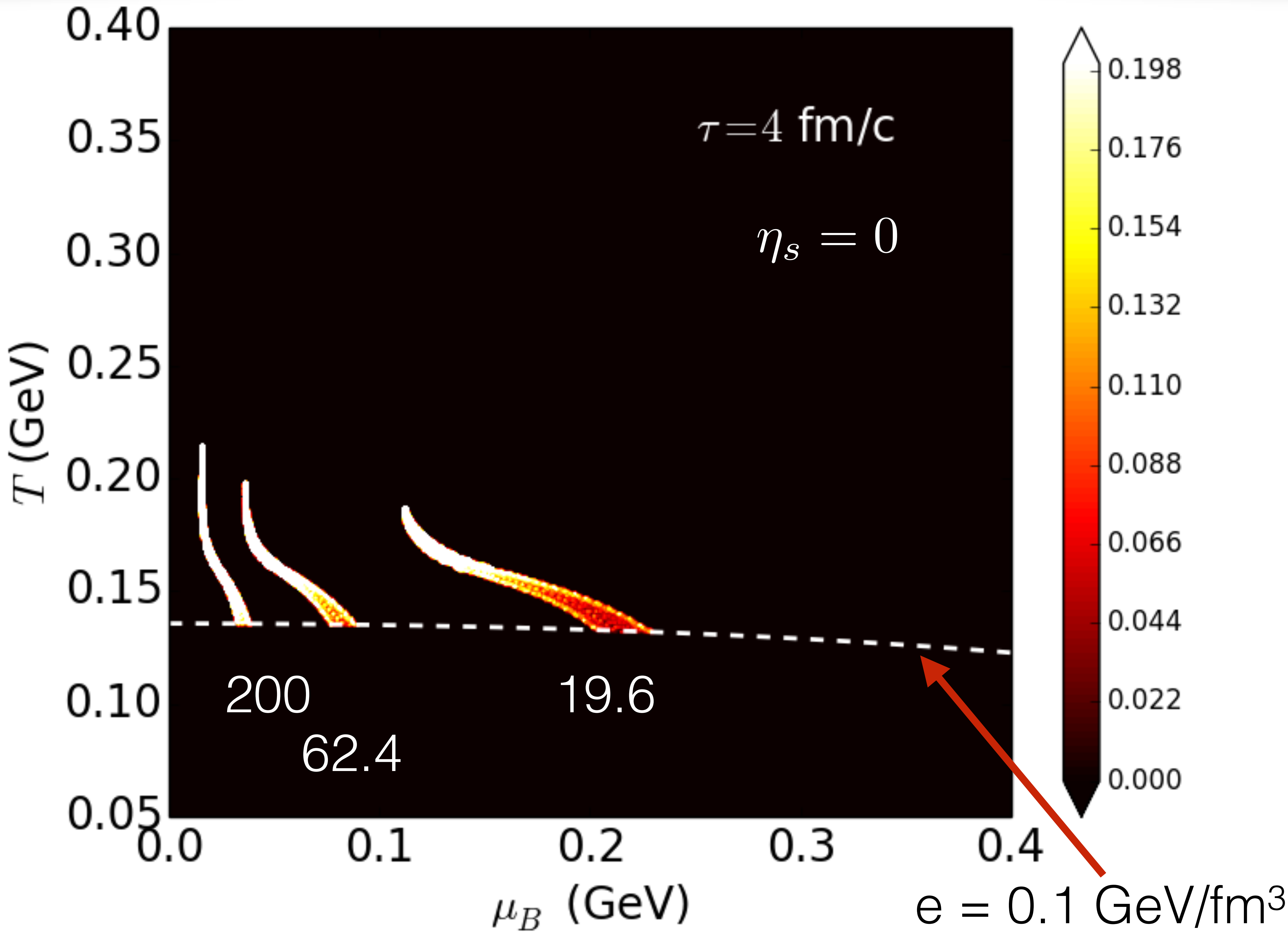

Exploring the phase of QCD

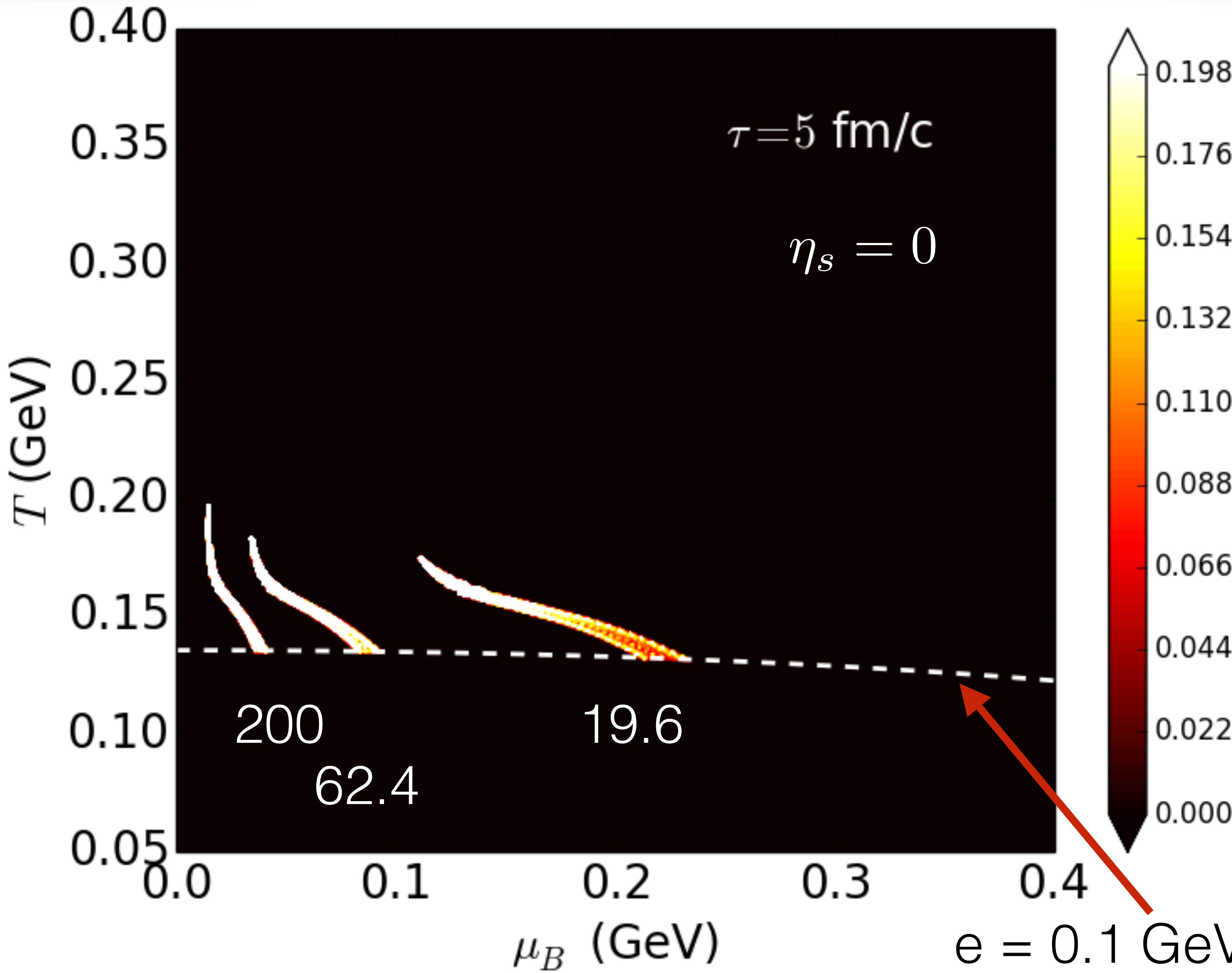

e = 0.1 GeV/fm^3

Exploring the phase of QCD

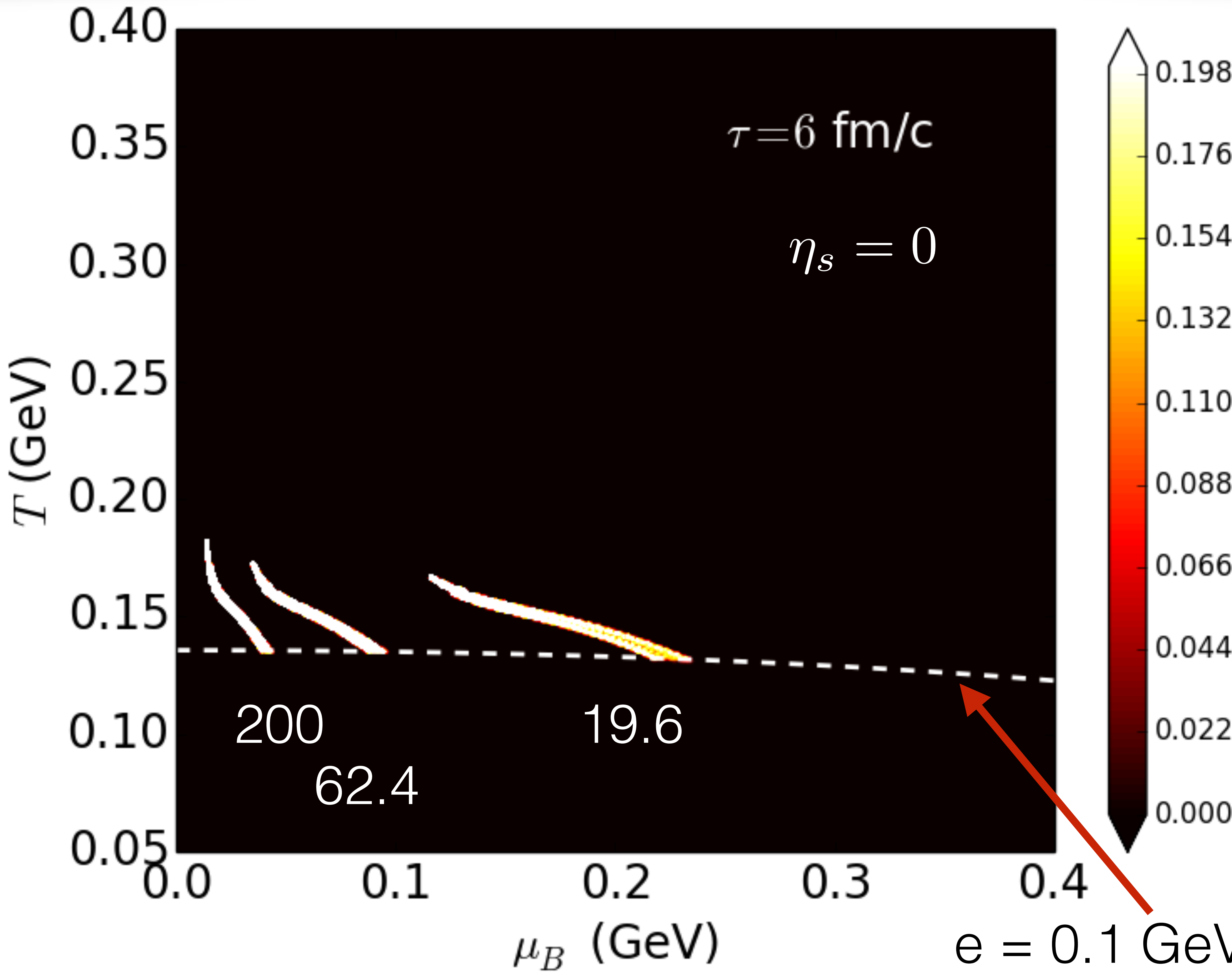

e = 0.1 GeV/fm^3

Exploring the phase of QCD

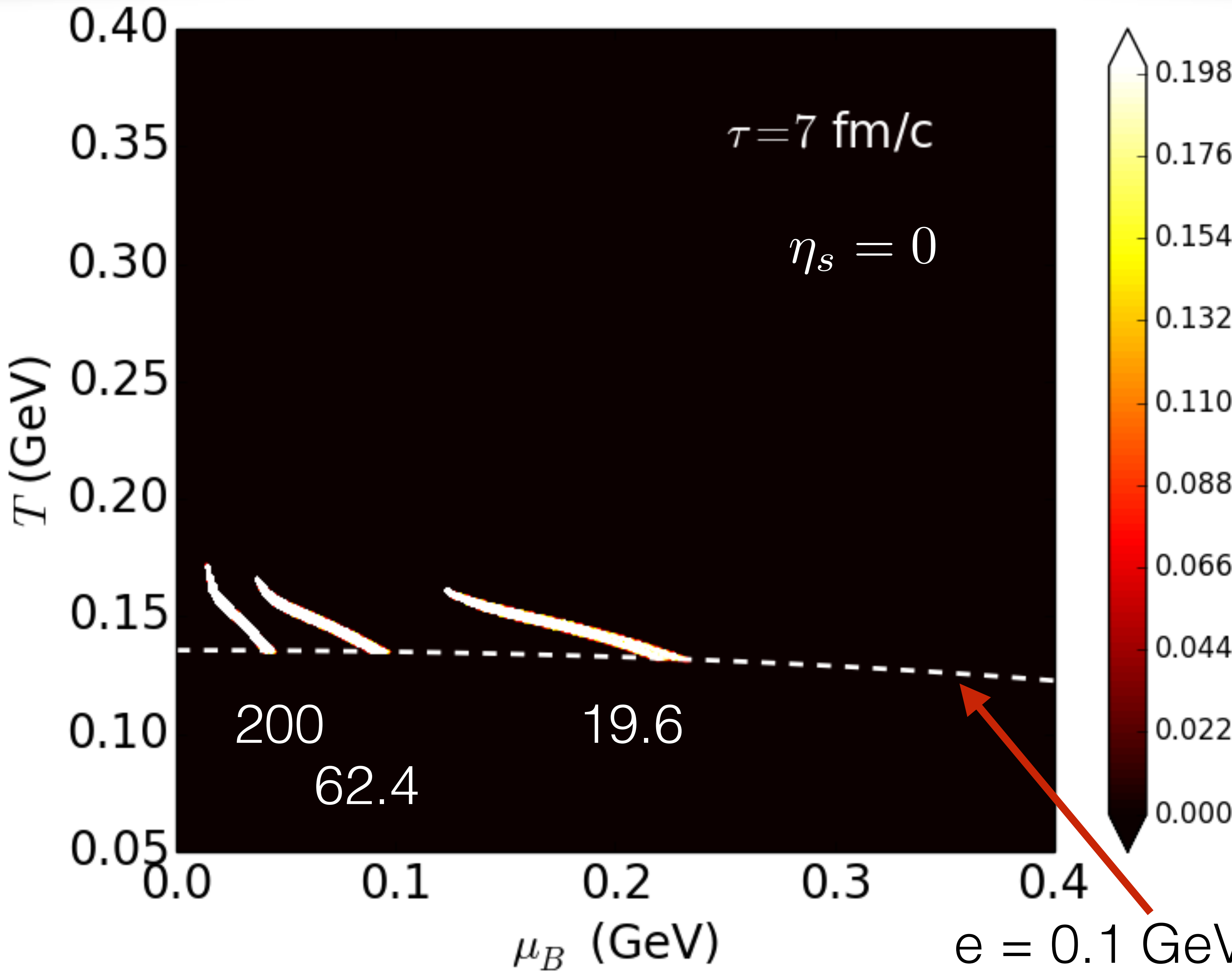

e = 0.1 GeV/fm^3

Exploring the phase of QCD

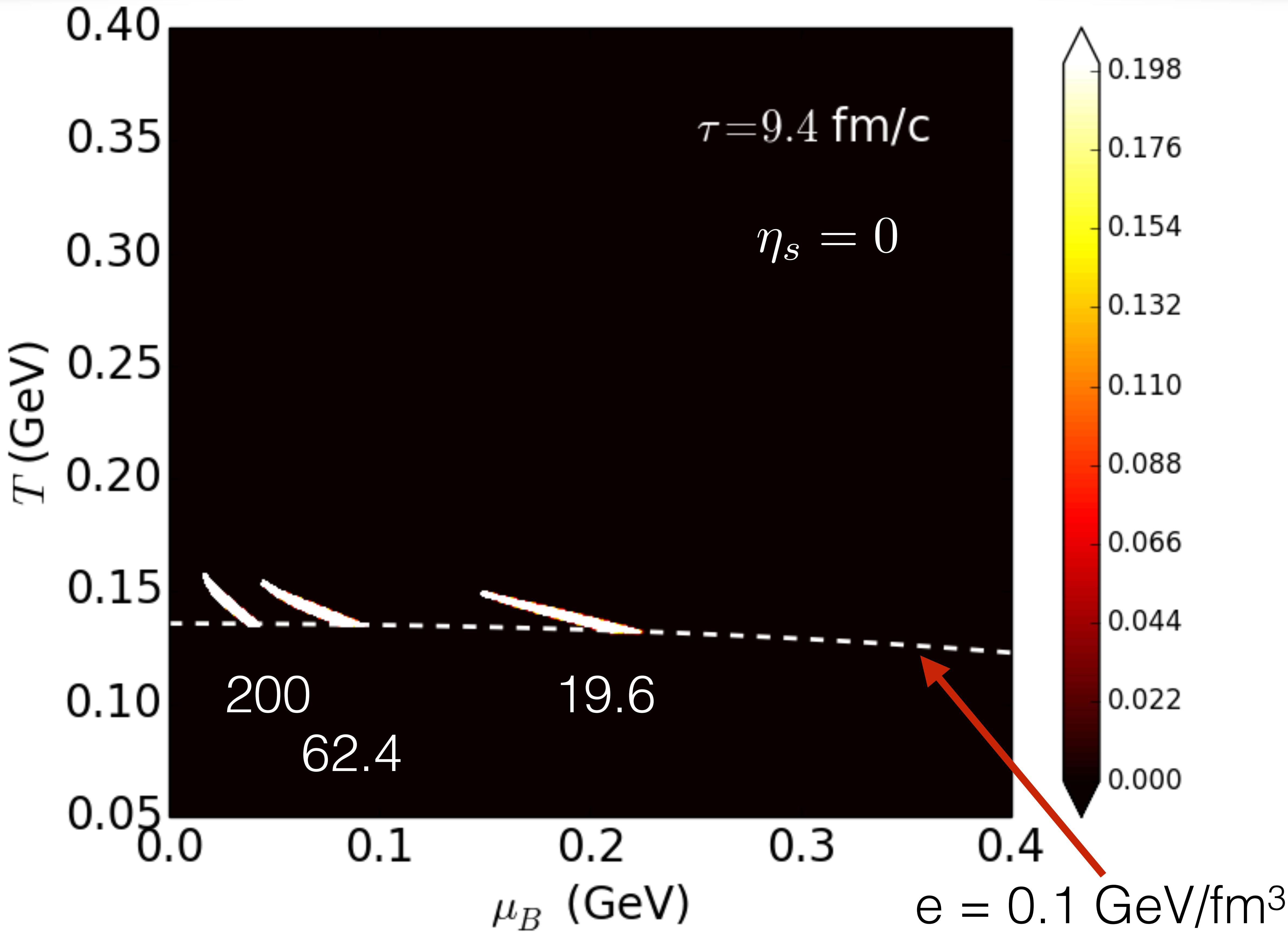

Exploring the phase of QCD

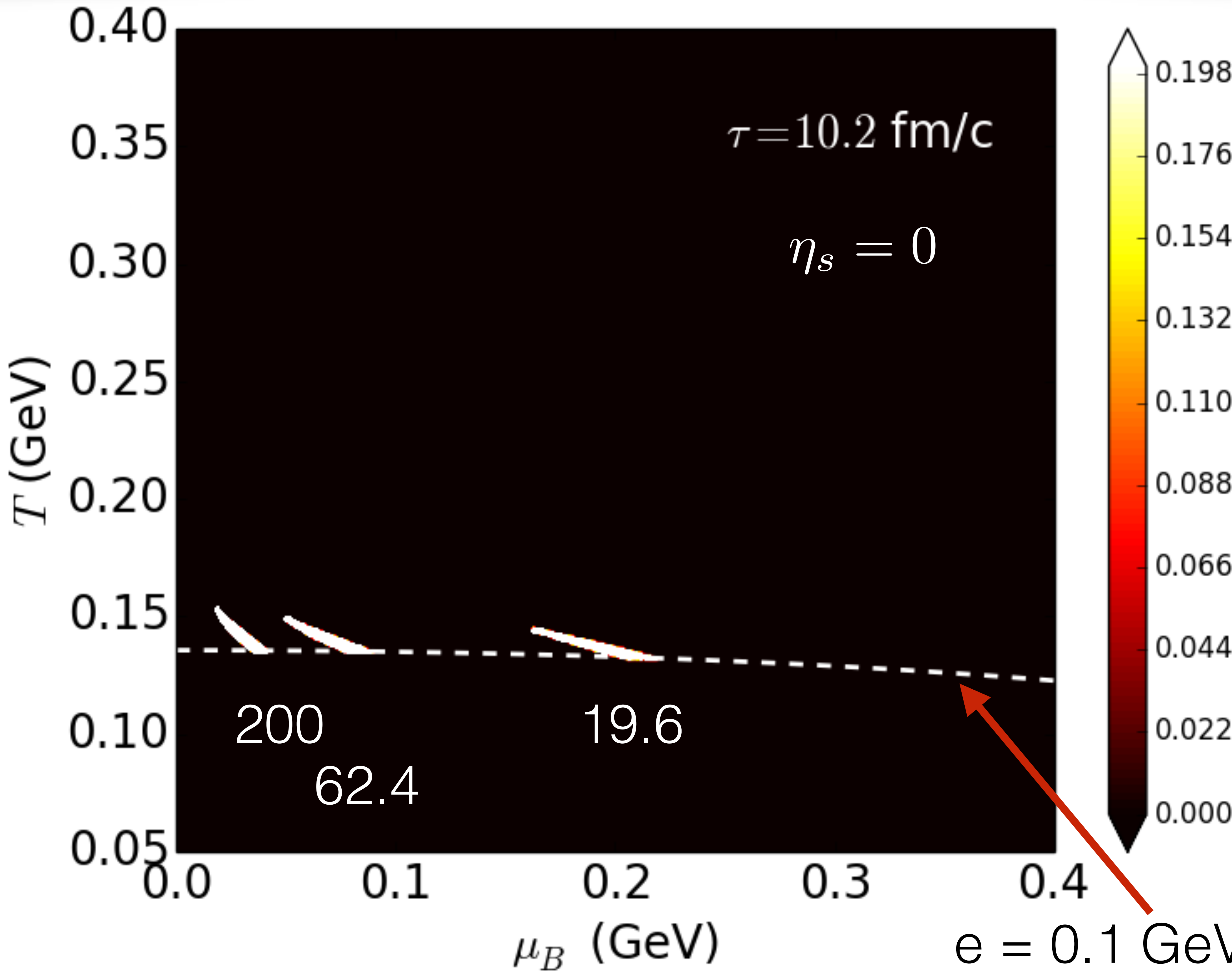

e = 0.1 GeV/fm^3

Exploring the phase of QCD

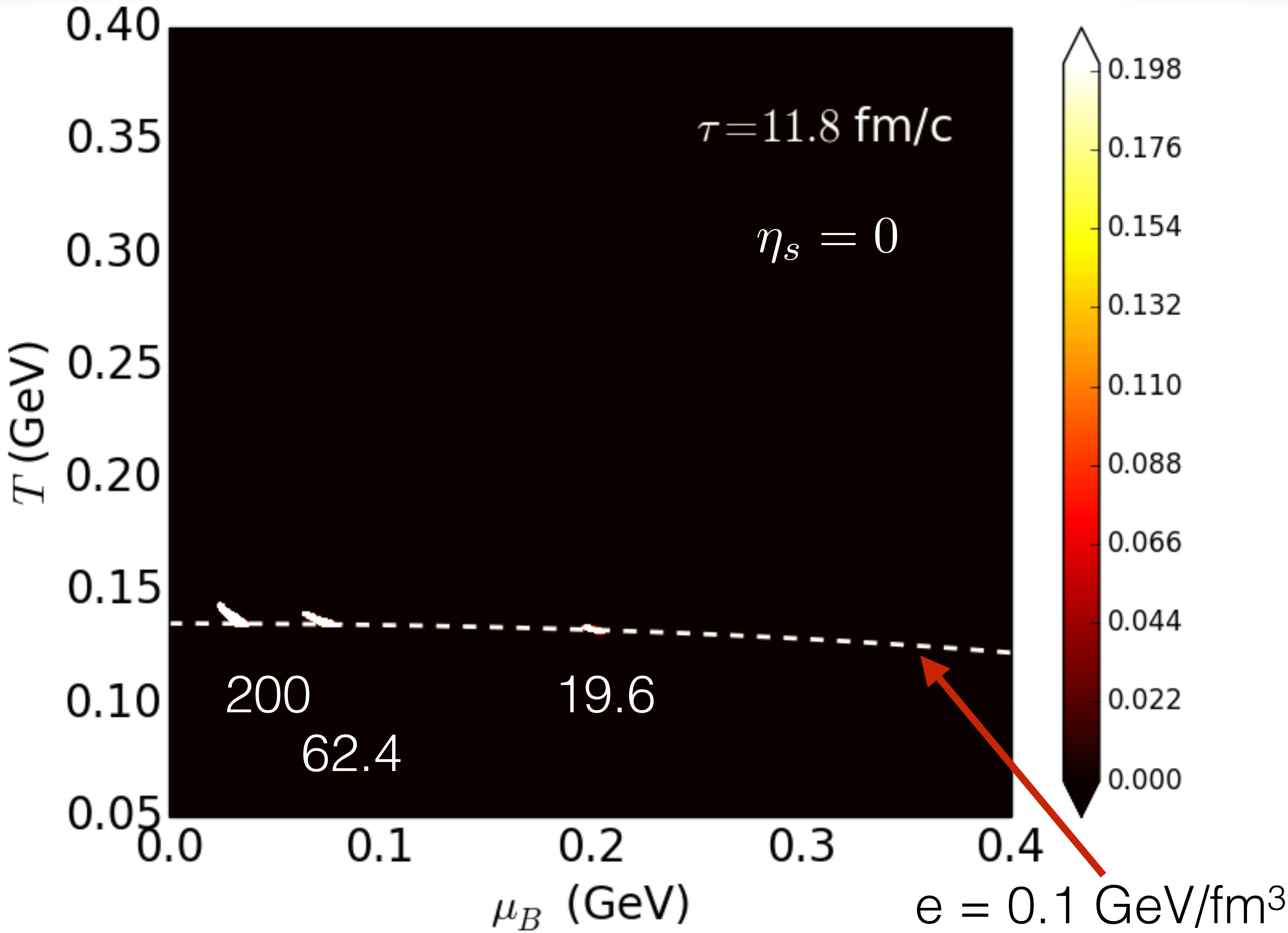

Exploring the phase of QCD

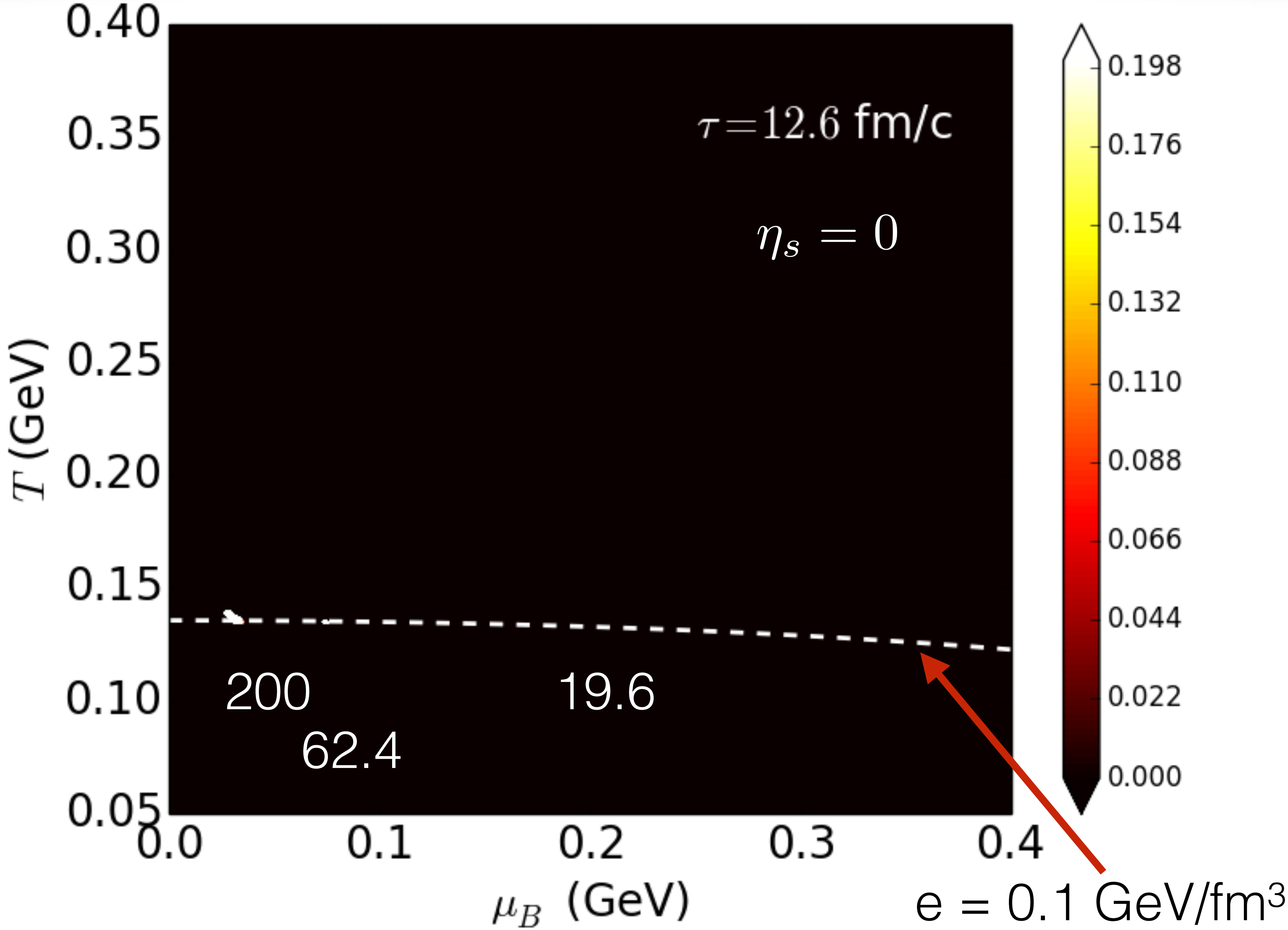

Exploring the phase of QCD

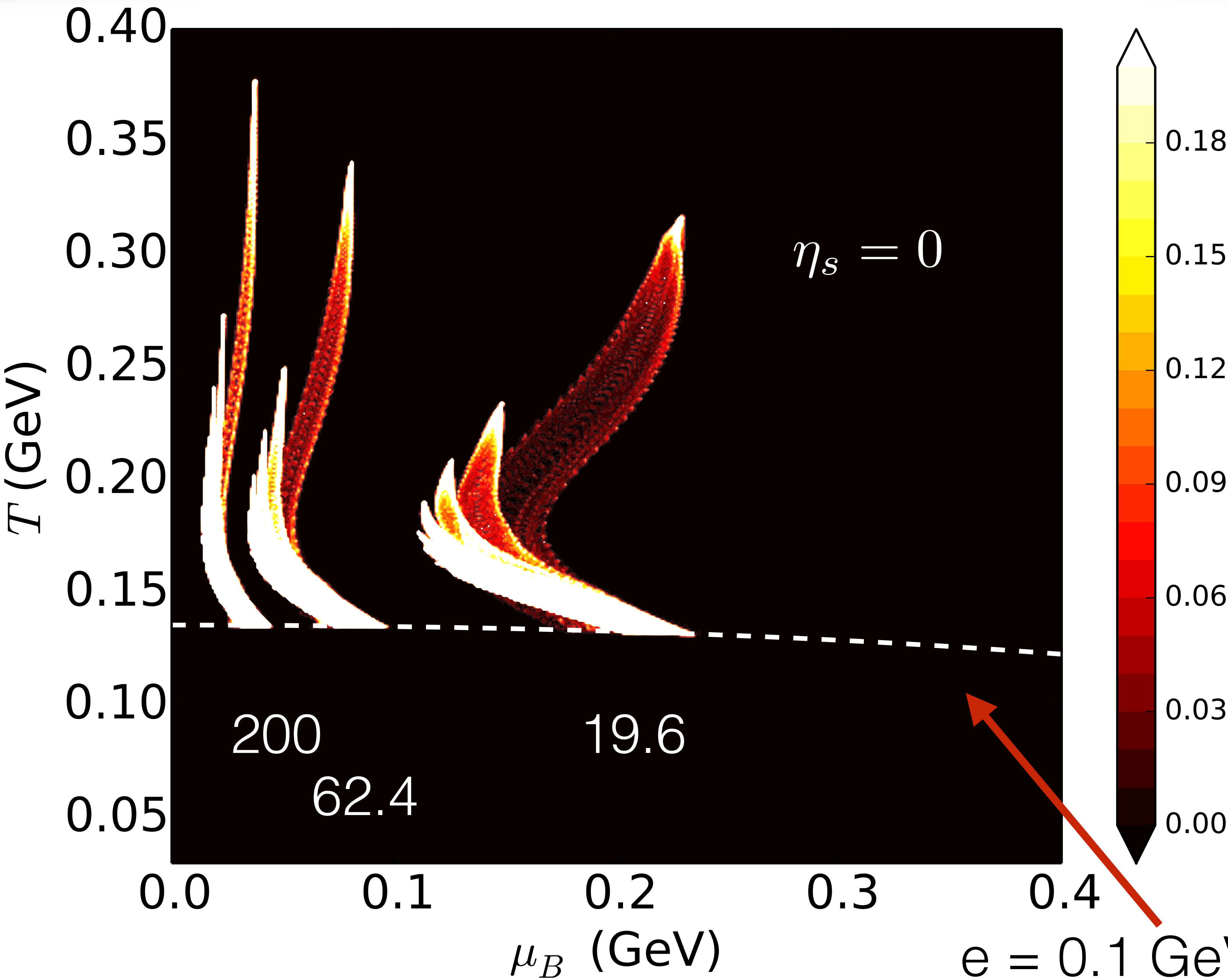

e = 0.1 GeV/fm^3

Initialize MUSIC with net baryon density

Since baryon number is conserved,

$$\int \tau_0 d\eta_s \int d^2\mathbf{x}_\perp \rho_B(\mathbf{x}_\perp, \eta_s) = N_{\mathrm{part}}.$$

For Glauber initial conditions, we assume

$$\rho_B(\mathbf{x}_\perp, \eta_s) = f(\eta_s)\tilde{\rho}_B(\mathbf{x}_\perp).$$

$$\int \tau_0 d\eta_s f(\eta_s) = 1.$$

$$\begin{aligned}\tilde{\rho}_B(\mathbf{x}_\perp) &= n_{\mathrm{part}}(\mathbf{x}_\perp) \\ &\equiv T_A(\mathbf{x}_\perp) + T_B(\mathbf{x}_\perp),\end{aligned}$$

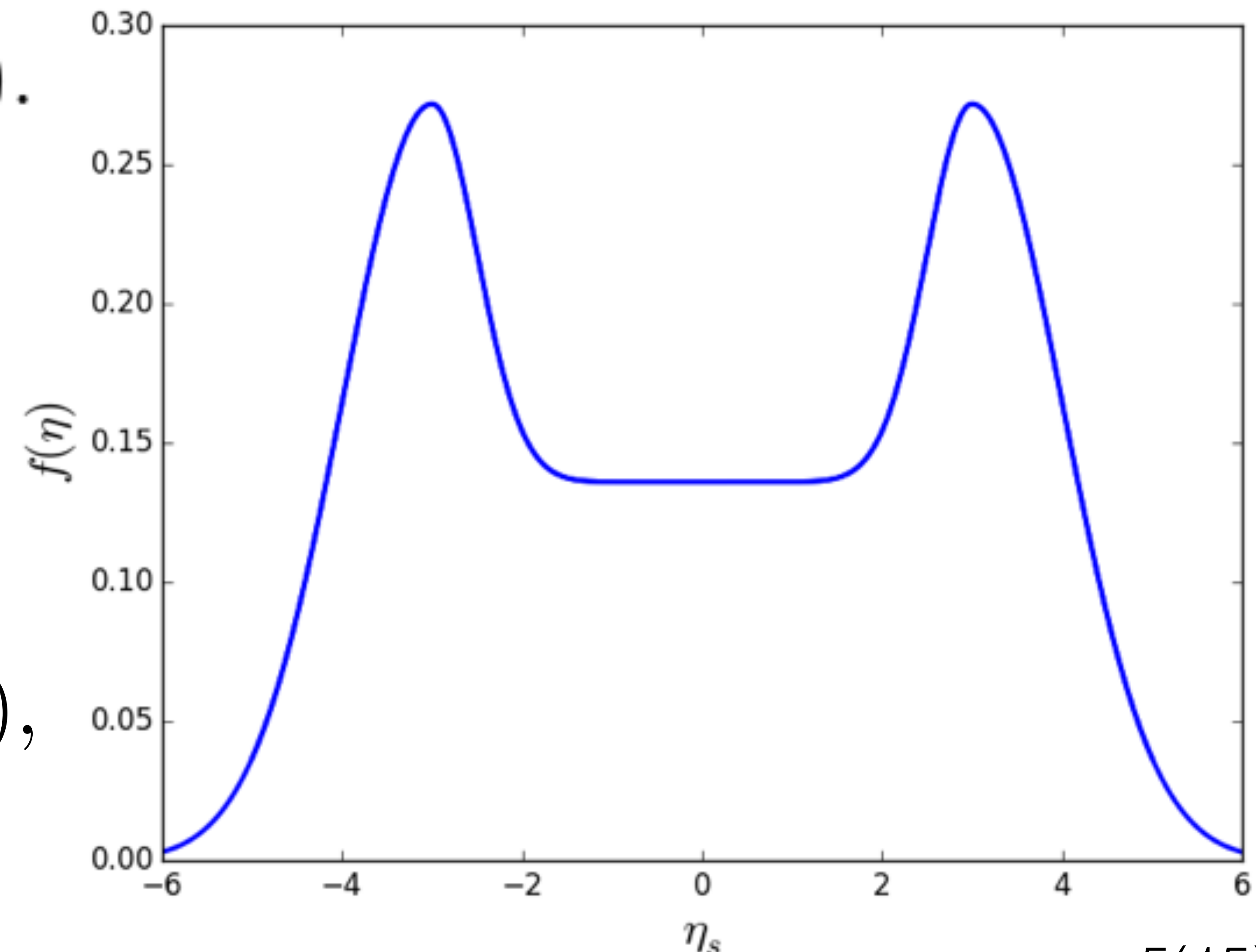

Initialize MUSIC with net baryon density

Since baryon number is conserved,

$$\int \tau_0 d\eta_s \int d^2\mathbf{x}_\perp \rho_B(\mathbf{x}_\perp, \eta_s) = N_{\mathrm{part}}.$$

For Glauber initial conditions, we assume

$$\rho_B(\mathbf{x}_\perp, \eta_s) = f(\eta_s)\tilde{\rho}_B(\mathbf{x}_\perp).$$

$$\int \tau_0 d\eta_s f(\eta_s) = 1.$$

$$\tilde{\rho}_B(\mathbf{x}_\perp) = n_{\mathrm{part}}(\mathbf{x}_\perp)$$
$$\equiv T_A(\mathbf{x}_\perp) + T_B(\mathbf{x}_\perp),$$

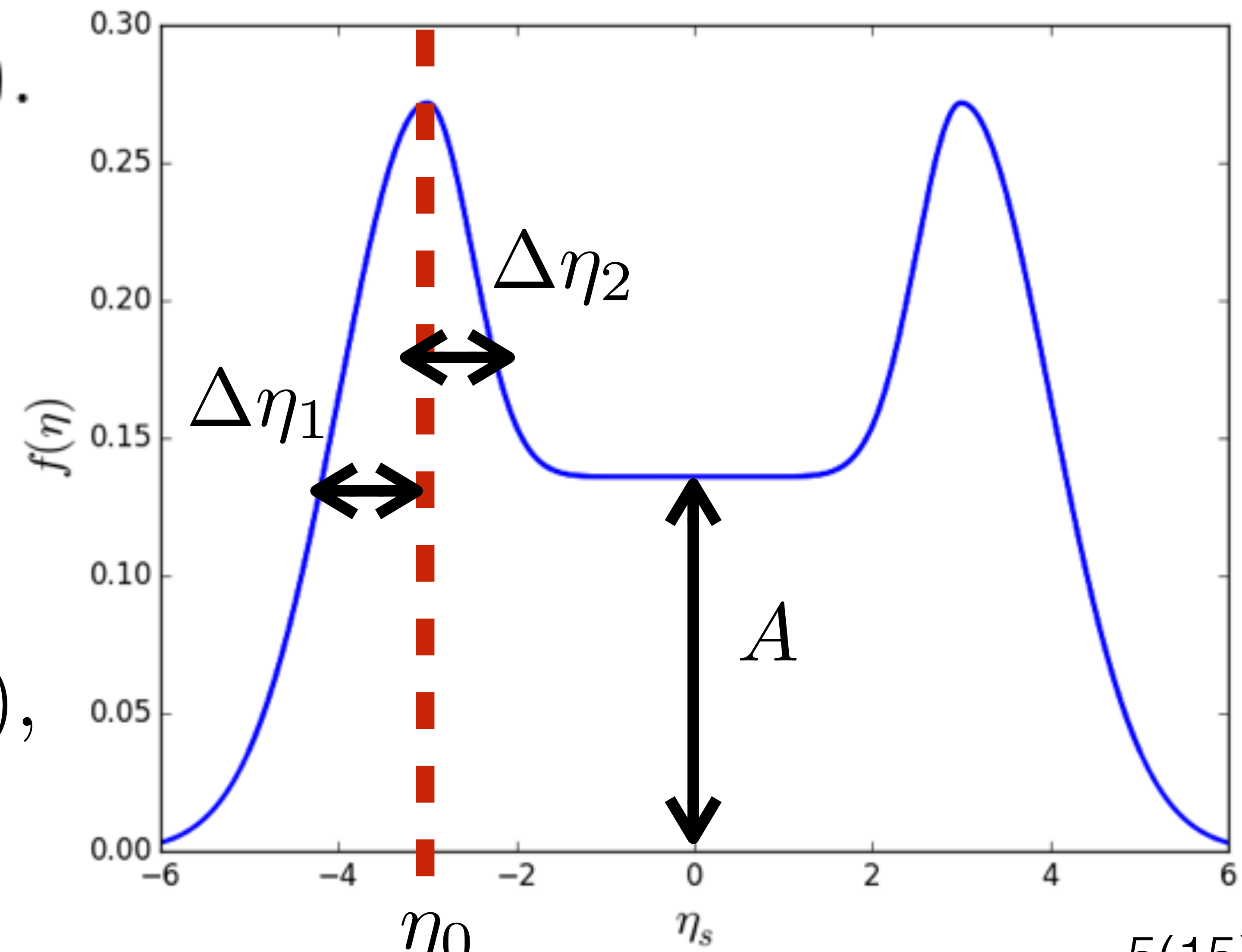

Dissipative hydrodynamics

Energy momentum tensor

$$T^{\mu\nu} = e u^\mu u^\nu - (P + \Pi)\Delta^{\mu\nu} + \pi^{\mu\nu}$$

$$d_\mu T^{\mu\nu} = T^{\mu\nu}{}_{;\mu} = 0$$

$$\Delta^{\mu\nu} = g^{\mu\nu} - u^\mu u^\nu$$

Conserved currents

$$J^\mu = n u^\mu + q^\mu$$

$$d_\mu J^\mu = 0$$

$$D = u^\mu d_\mu$$
$$\nabla^\mu = \Delta^{\mu\nu} d_\nu$$
$$\theta = d_\mu u^\mu$$

Dissipative part:

$$\Delta^{\mu\alpha}\Delta^{\nu\beta} D\pi_{\alpha\beta} = -\frac{1}{\tau_\pi}(\pi^{\mu\nu} - 2\eta\sigma^{\mu\nu}) - \frac{4}{3}\pi^{\mu\nu}\theta$$

$$\Delta^{\mu\nu} D q_\nu = -\frac{1}{\tau_q}\left(q^\mu - \kappa\nabla^\mu\frac{\mu_B}{T}\right) - q^\mu\theta - \frac{3}{5}\sigma^{\mu\nu}q_\nu$$

$$\frac{\eta T}{e + \mathcal{P}} = 0.08 \qquad \kappa = 0.2\frac{n_B}{\rho_B} \qquad \tau_q = \frac{0.2}{T}$$

Code Check

1+1D cross check:

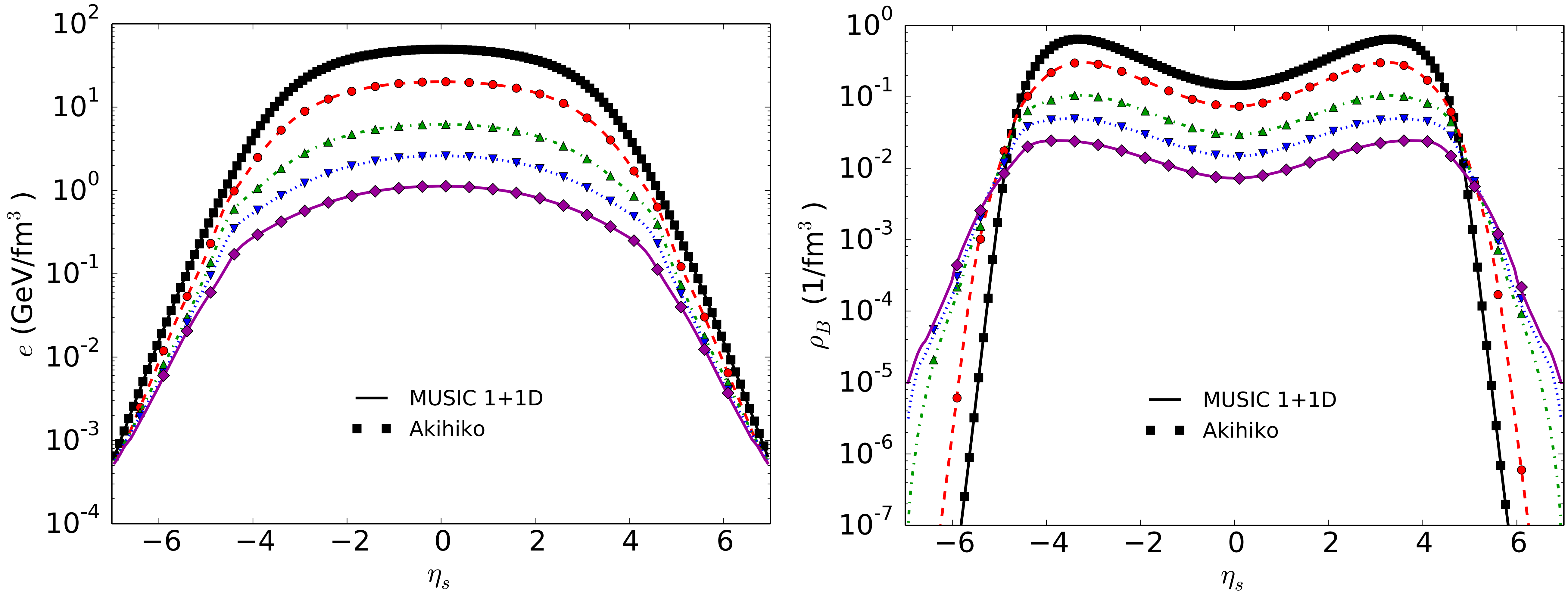

MUSIC results agree very well with Akihiko's results

Code Check

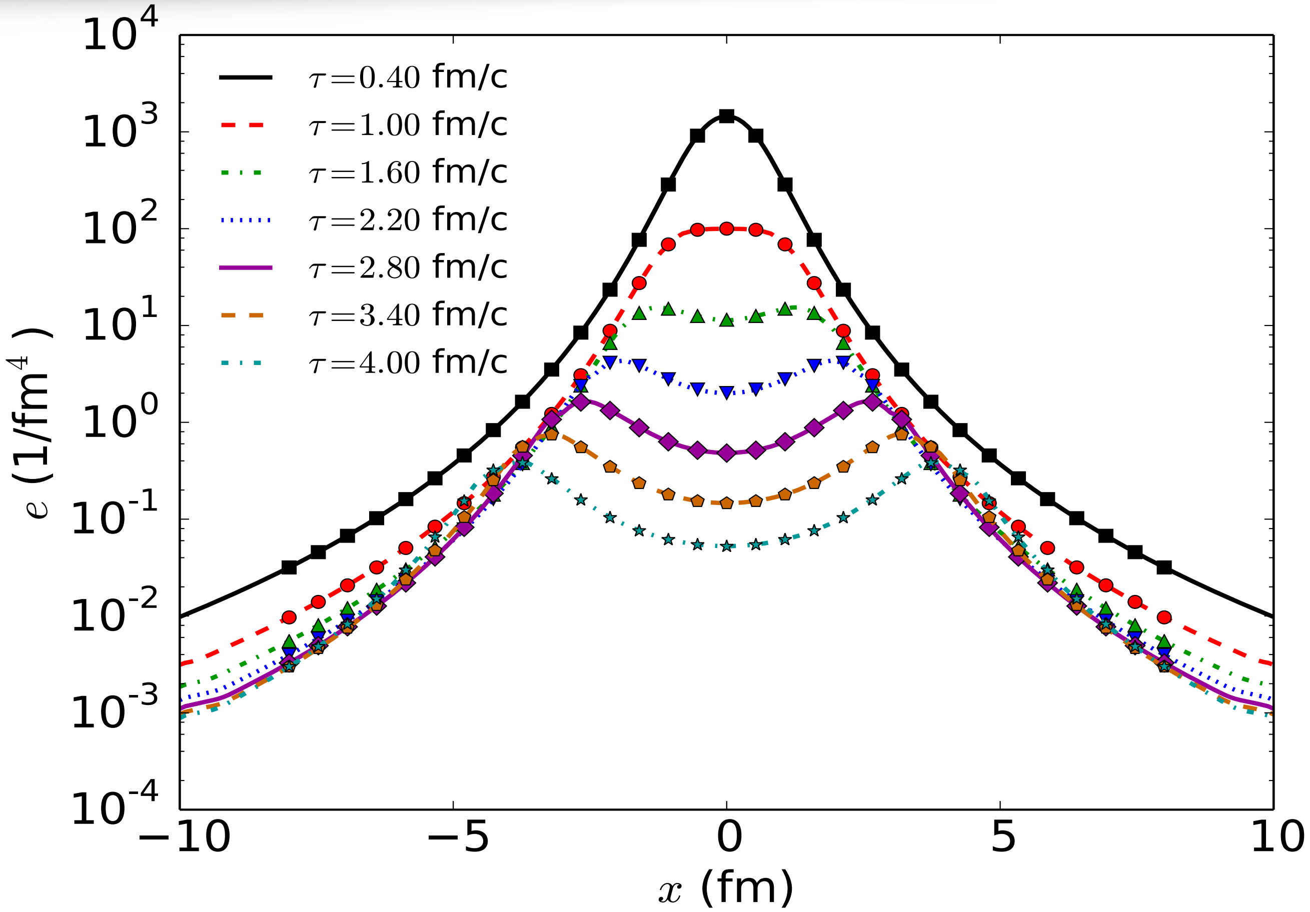

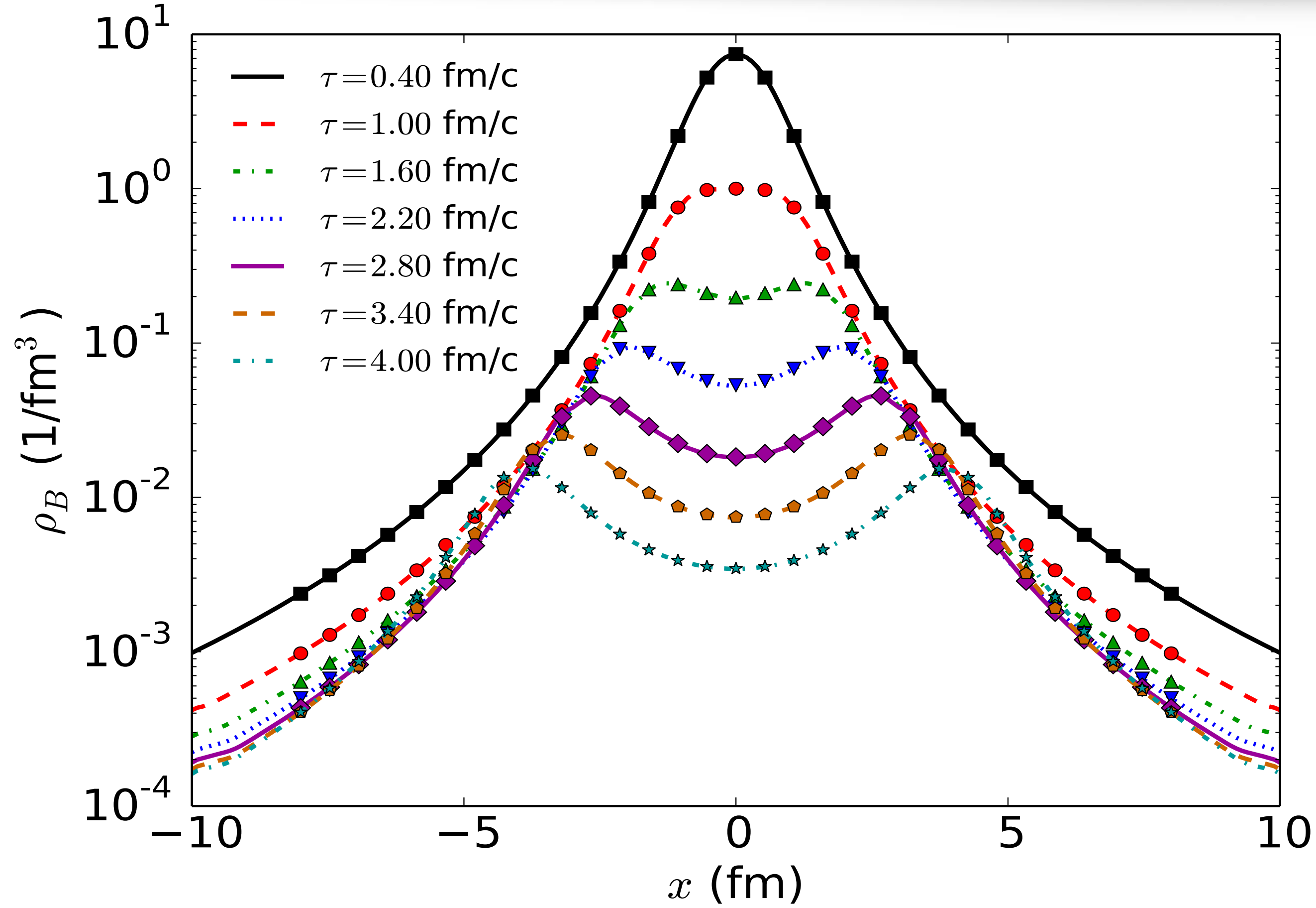

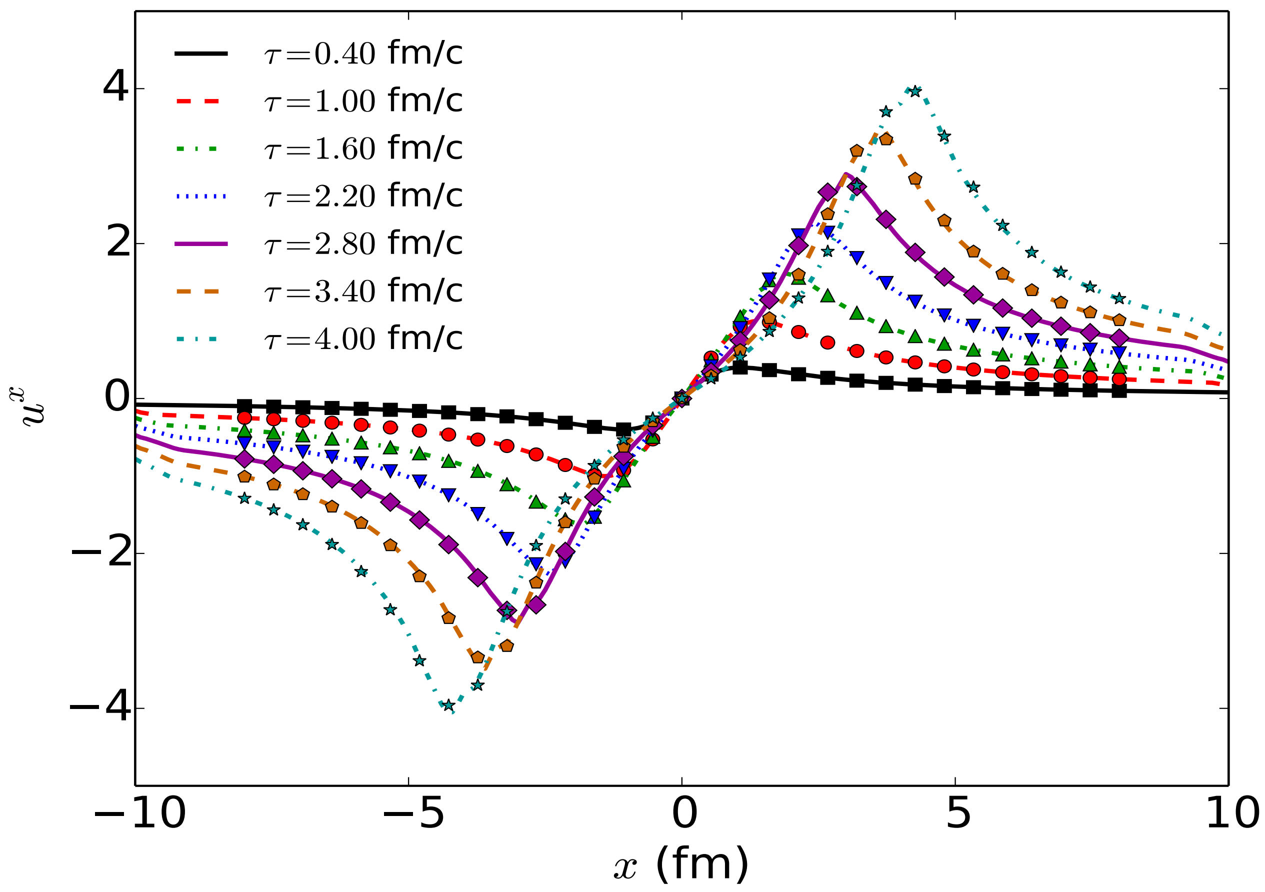

- MUSIC with baryon propagation passed ideal Gubser flow test for the transverse dynamics

Cooper-Frye freeze-out

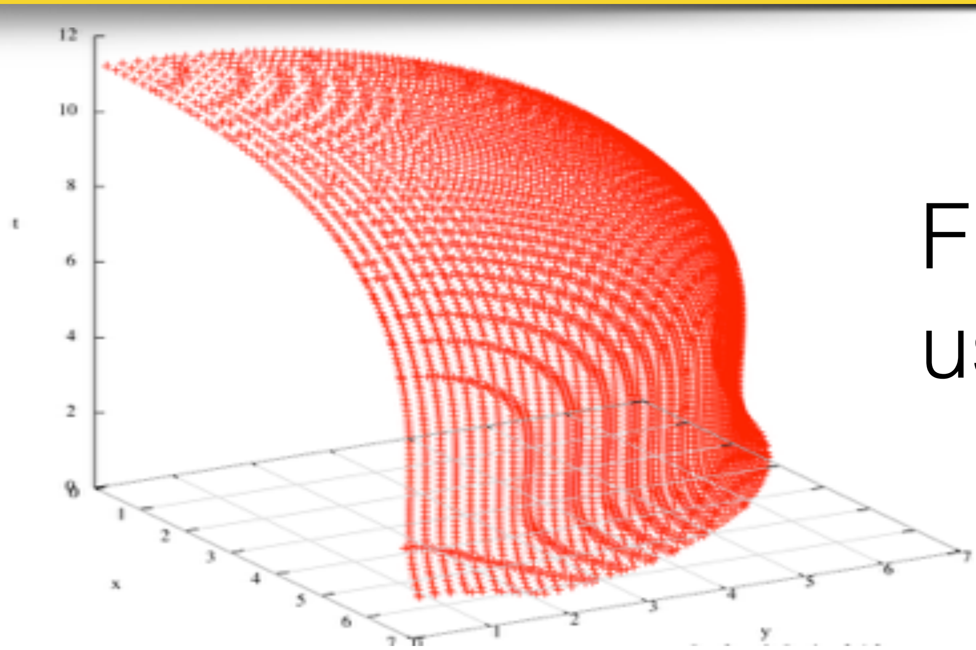

Freeze-out hyper surface is determined using **Cornelius** freeze-out algorithm

P. Huovinen and H. Petersen, Eur. Phys. J. A **48**, 171 (2012)

$$E\frac{dN_i}{d^3p} = \frac{g_i}{(2\pi)^3}\int p^\mu d^3\sigma_\mu(x)(f_0(x,p) + \delta f(x,p))$$

$$f_0^i(x,p) = \frac{1}{e^{(E-b_i\mu_B(x))/T(x)} \pm 1}$$

Using relaxation time approximation,

$$\delta f_0^i(x,p) = f_0^i(x,p)(1 \pm f_0^i(x,p))\left(\frac{n_B}{e+\mathcal{P}} - \frac{b_i}{E}\right)\frac{p\cdot q}{\hat{\kappa}}$$

$$\hat{\kappa} = \kappa/\tau_q$$

$\hat{\kappa}(T,\mu_B)$ is calculated using hadron resonance gas model

Cooper-Frye freeze-out

$$E\frac{dN_i}{d^3p} = \frac{g_i}{(2\pi)^3}\int p^\mu d^3\sigma_\mu(x)\left(f_0(x,p) + \delta f(x,p)\right)$$

$$f_0^i(x,p) = \frac{1}{e^{(E-b_i\mu_B(x))/T(x)} \pm 1}$$

$$\delta f_0^i(x,p) = f_0^i(x,p)(1 \pm f_0^i(x,p))\left(\frac{n_B}{e+\mathcal{P}} - \frac{b_i}{E}\right)\frac{p\cdot q}{\hat{\kappa}}$$

$$N^B - N^{\bar{B}} = \int d^3\sigma_\mu \sum \frac{g_i}{(2\pi)^3}\int_p p^\mu \left[\left(f_0^B(x,p) - f_0^{\bar{B}}(x,p)\right) + \left(\delta f^B(x,p) - \delta f^{\bar{B}}(x,p)\right)\right]$$

$$= \int d^3\sigma_\mu (n_B u^\mu + q^\mu)$$

$$\partial_\mu(n_B u^\mu + q^\mu) = 0$$

$\Rightarrow$ $N^B - N^{\bar{B}}$ is conserved

- With diffusion, δf is essential to ensure net baryon number conservation

Results

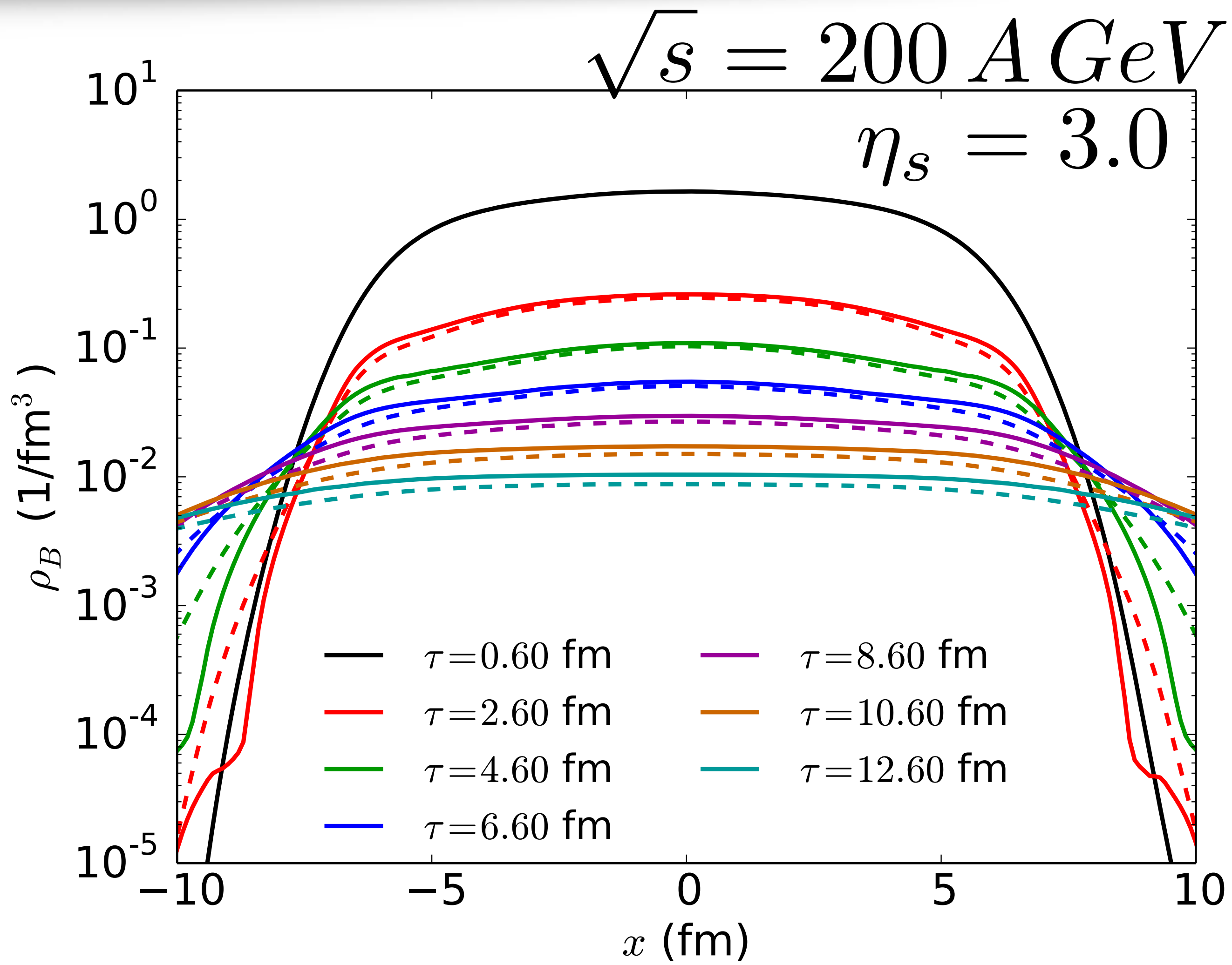

solid: with diffusion dashed: no diffusion

- With diffusion, ρ_B is larger in the center of the transverse plane

Results

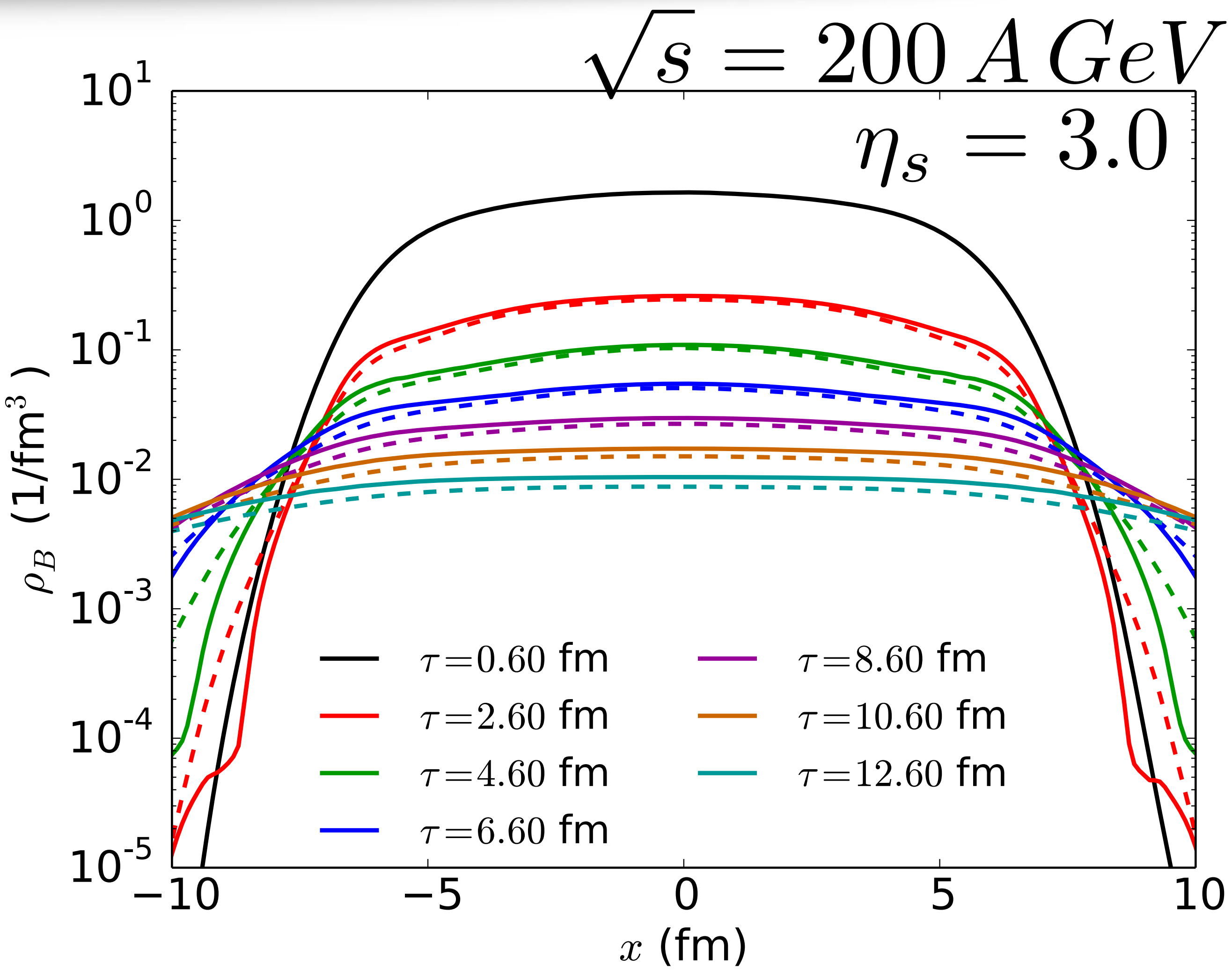

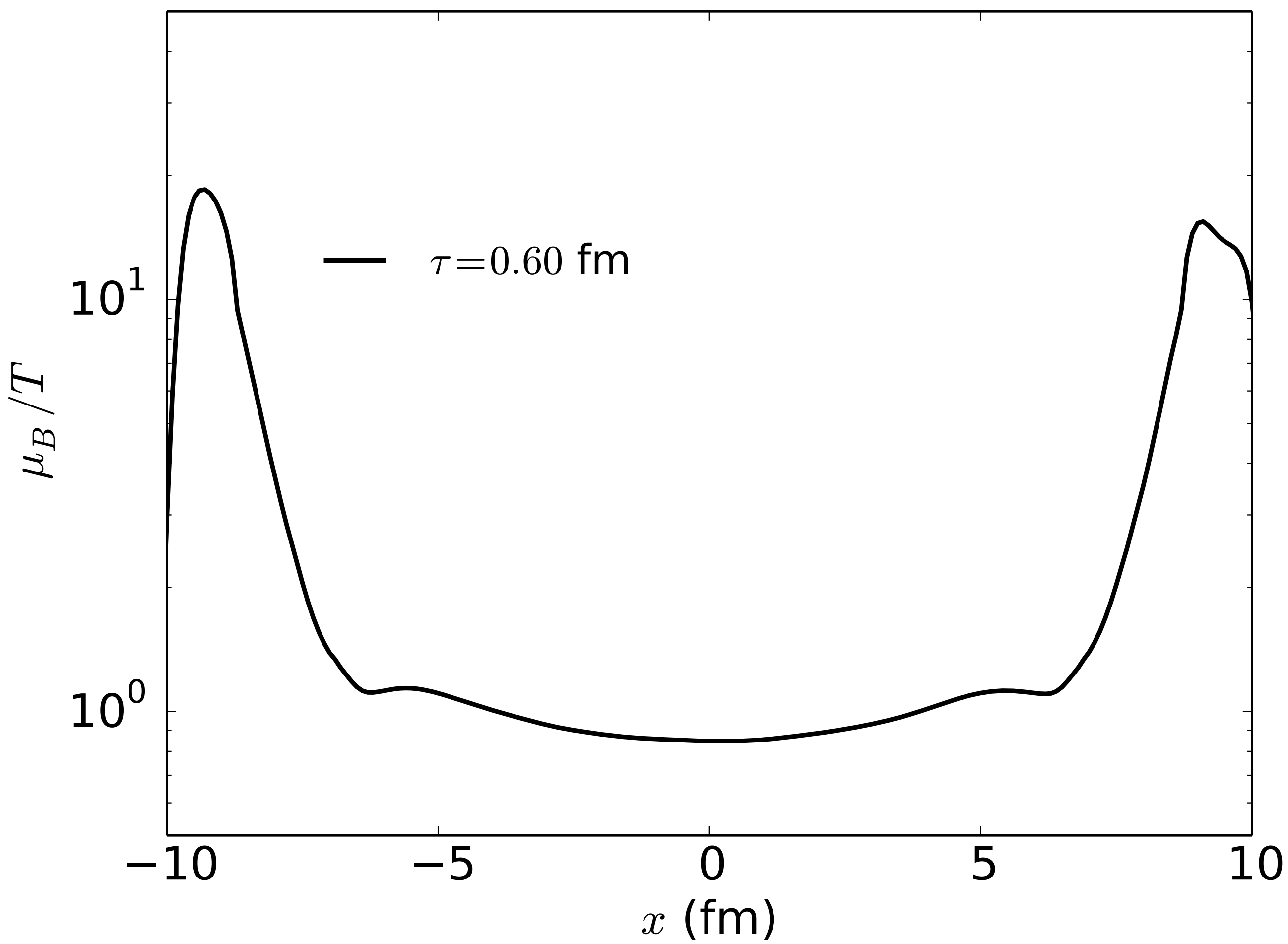

solid: with diffusion dashed: no diffusion

- With diffusion, ρ_B is larger in the center of the transverse plane
- The dynamics of ρ_B is driven by the evolution of u^μ and $\nabla^\mu \frac{\mu_B}{T}$

Results

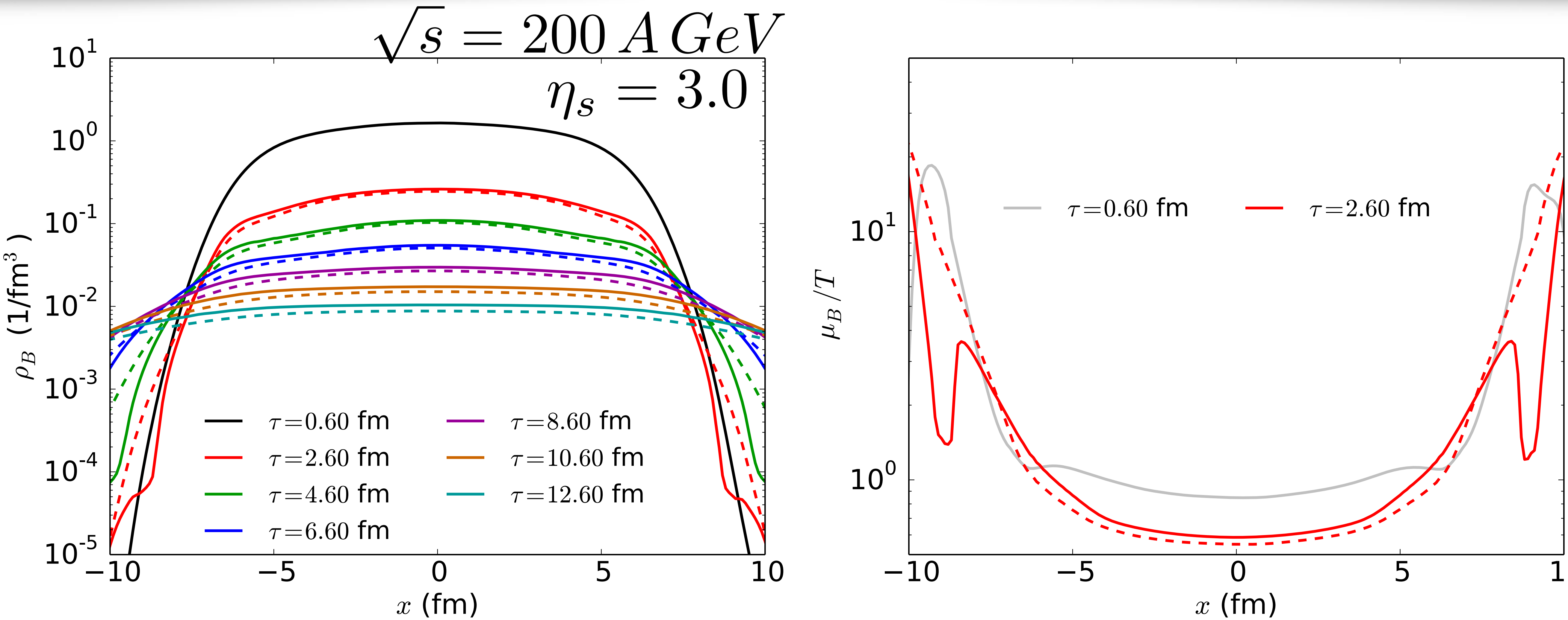

solid: with diffusion dashed: no diffusion

- With diffusion, ρ_B is larger in the center of the transverse plane
- The dynamics of ρ_B is driven by the evolution of u^μ and $\nabla^\mu \frac{\mu_B}{T}$

Results

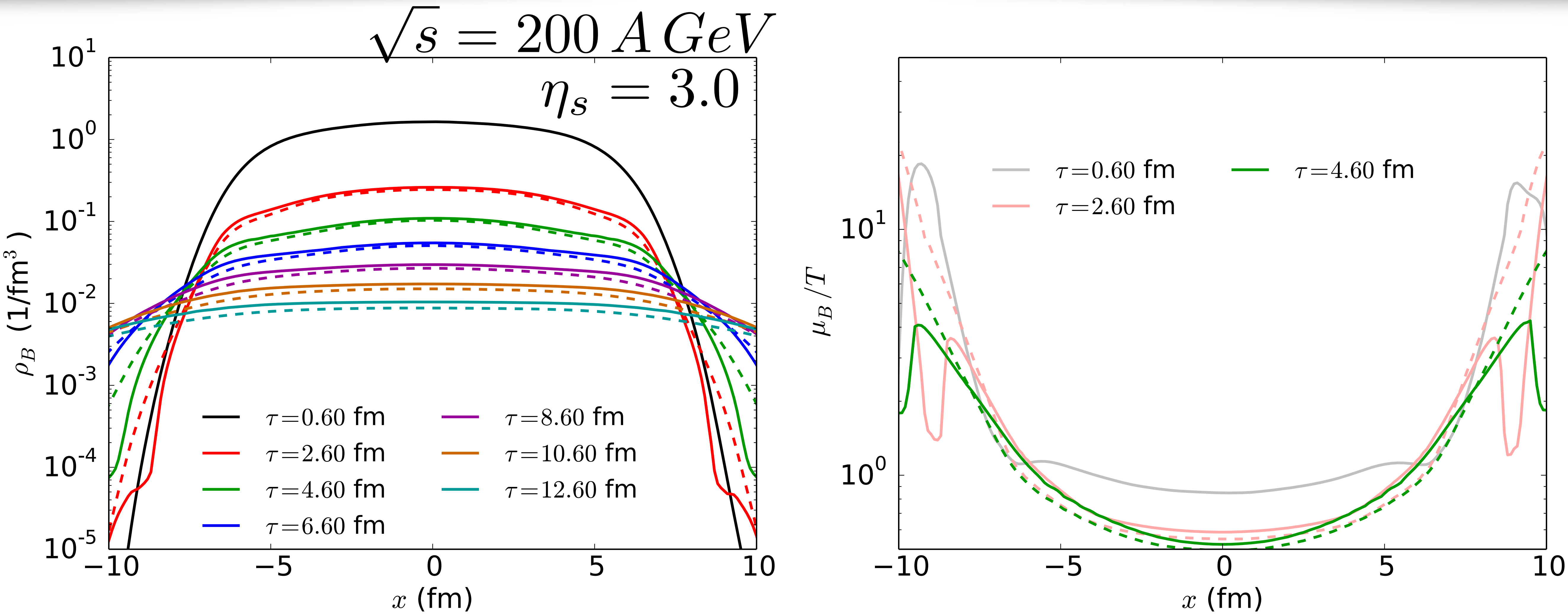

solid: with diffusion dashed: no diffusion

- With diffusion, ρ_B is larger in the center of the transverse plane
- The dynamics of ρ_B is driven by the evolution of u^μ and $\nabla^\mu \frac{\mu_B}{T}$

Results

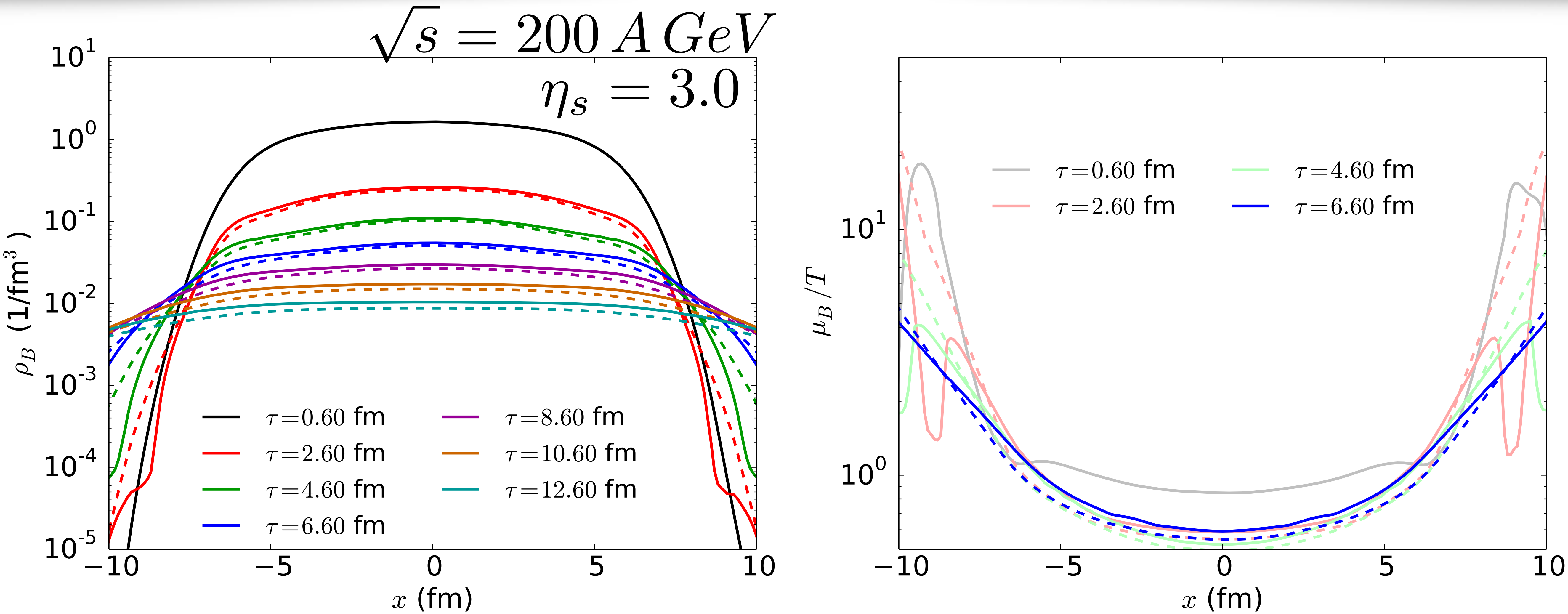

solid: with diffusion dashed: no diffusion

- With diffusion, ρ_B is larger in the center of the transverse plane
- The dynamics of ρ_B is driven by the evolution of u^μ and $\nabla^\mu \frac{\mu_B}{T}$

Results

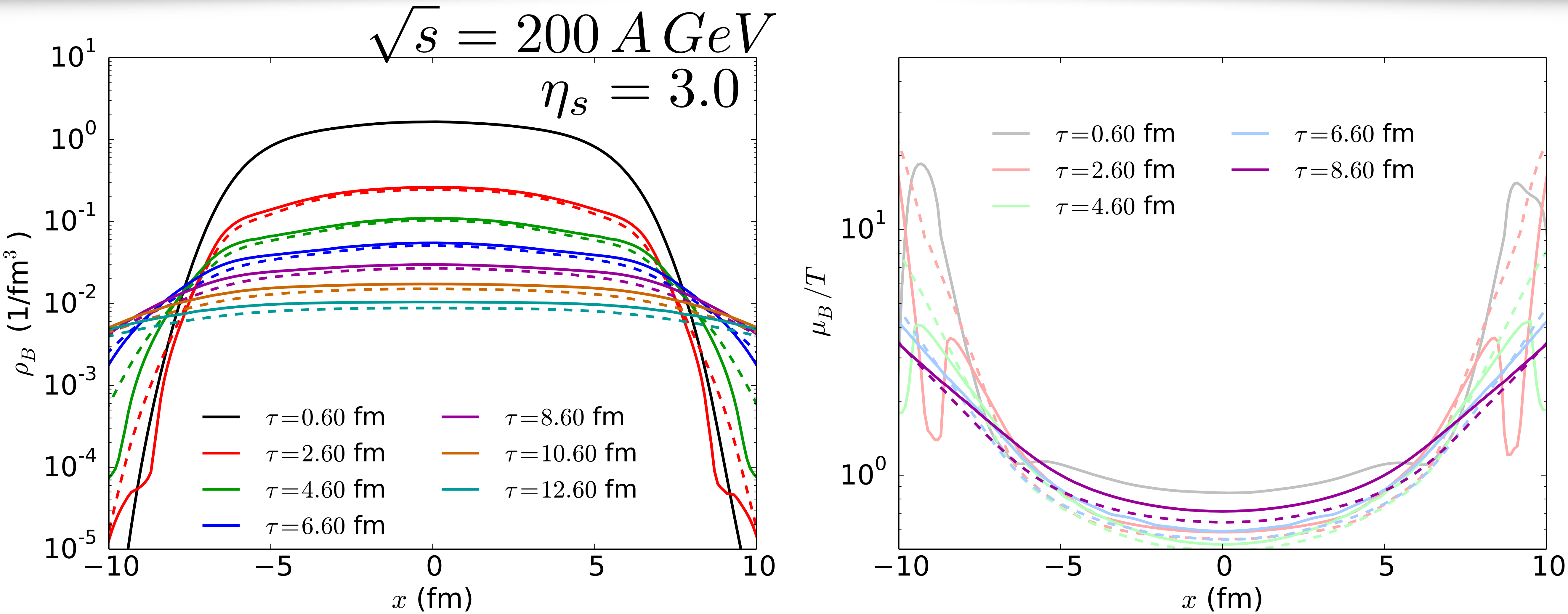

solid: with diffusion dashed: no diffusion

- With diffusion, ρ_B is larger in the center of the transverse plane
- The dynamics of ρ_B is driven by the evolution of u^μ and $\nabla^\mu \frac{\mu_B}{T}$

Results

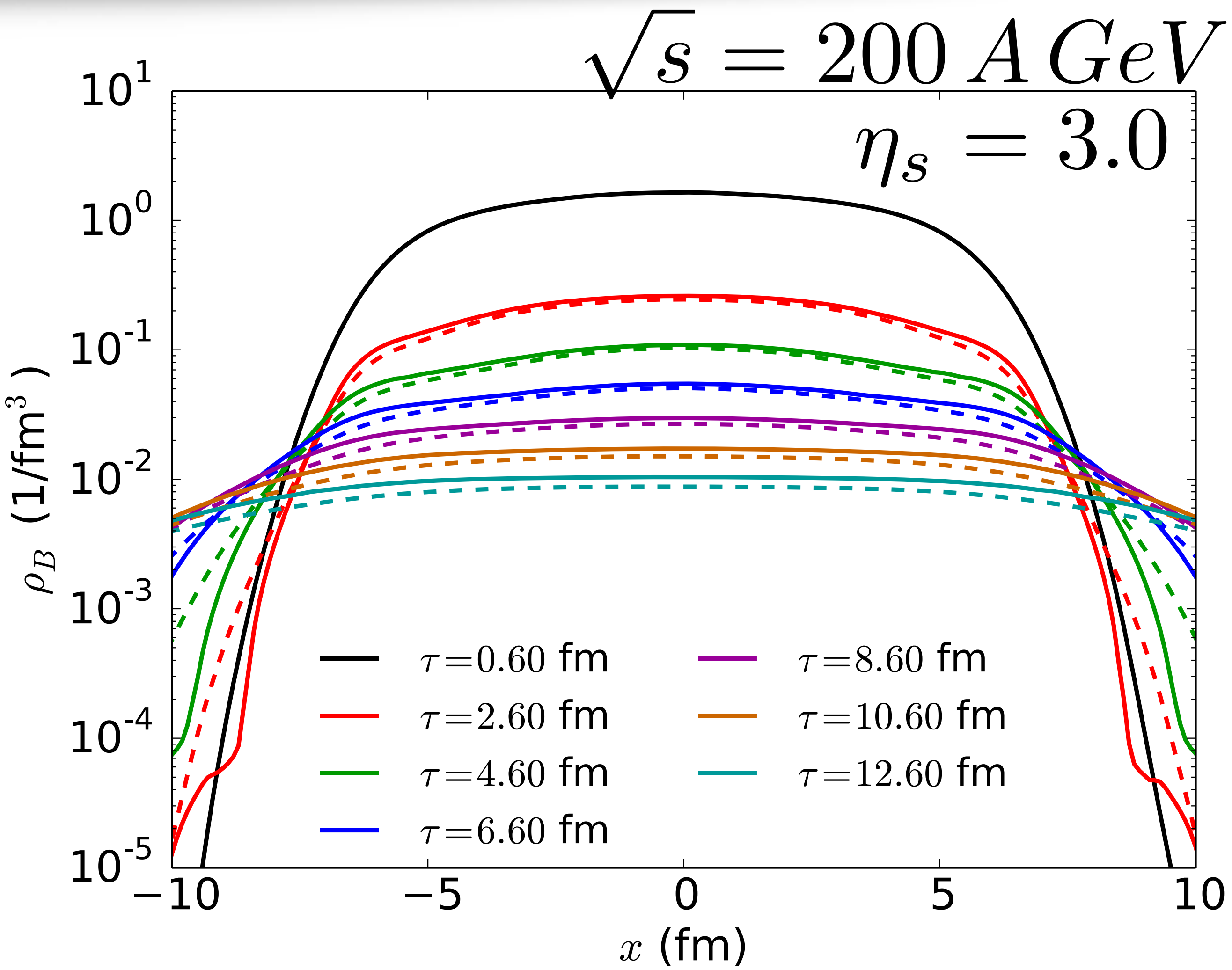

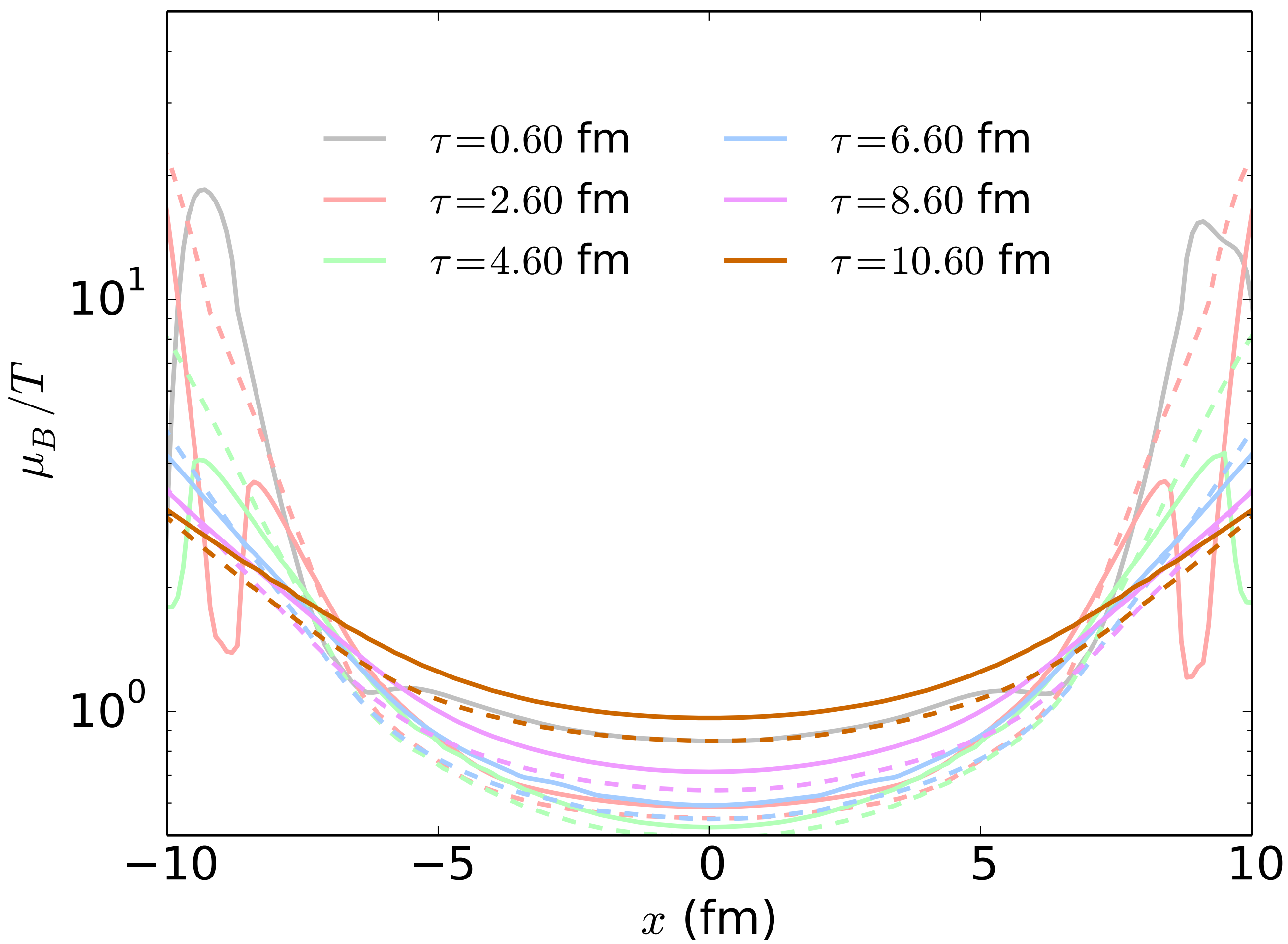

solid: with diffusion dashed: no diffusion

- With diffusion, ρ_B is larger in the center of the transverse plane
- The dynamics of ρ_B is driven by the evolution of u^μ and $\nabla^\mu \frac{\mu_B}{T}$

Results

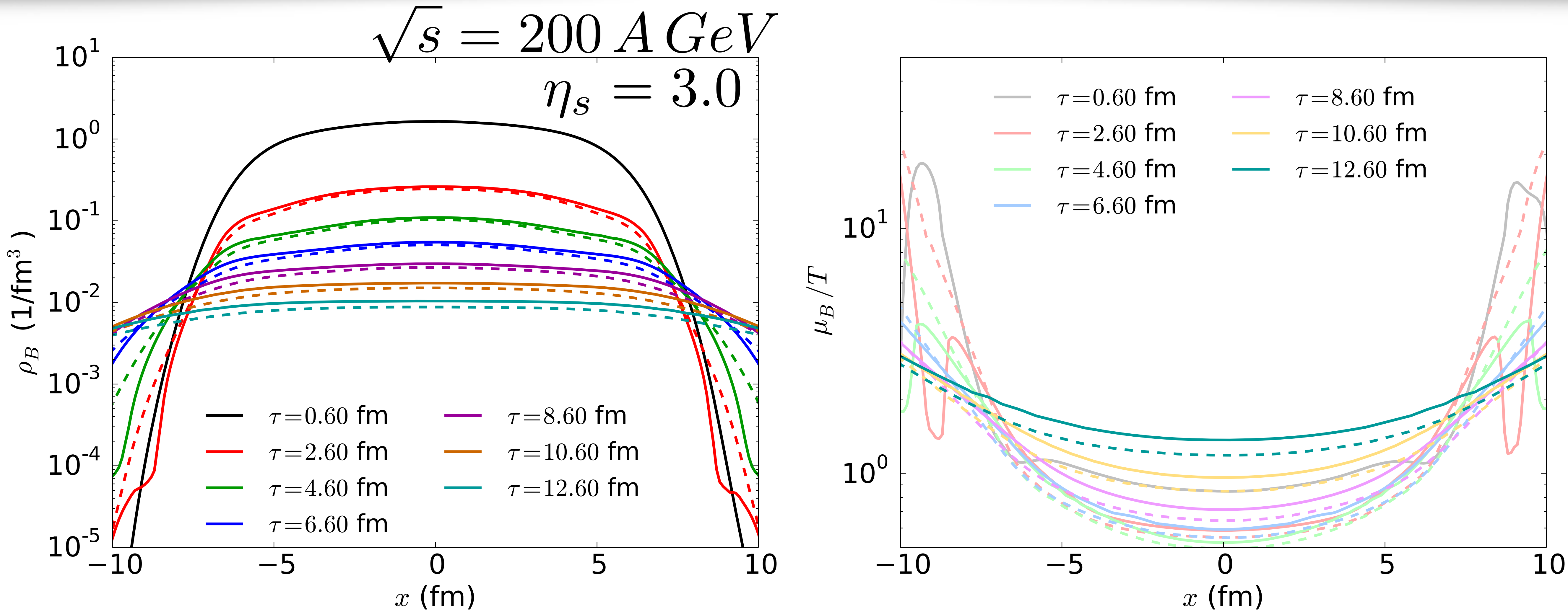

solid: with diffusion dashed: no diffusion

- With diffusion, ρ_B is larger in the center of the transverse plane
- The dynamics of ρ_B is driven by the evolution of u^μ and $\nabla^\mu \frac{\mu_B}{T}$

Results

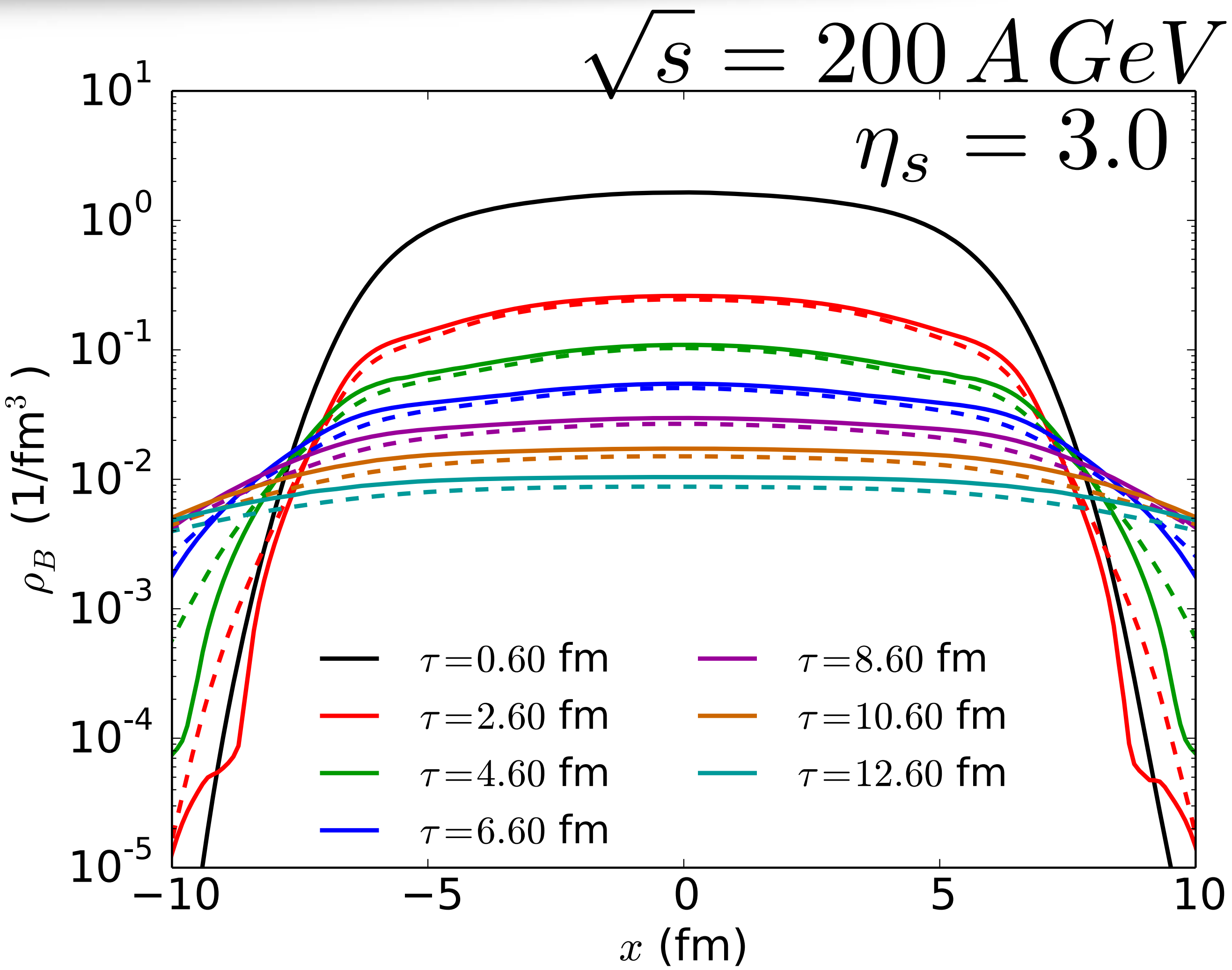

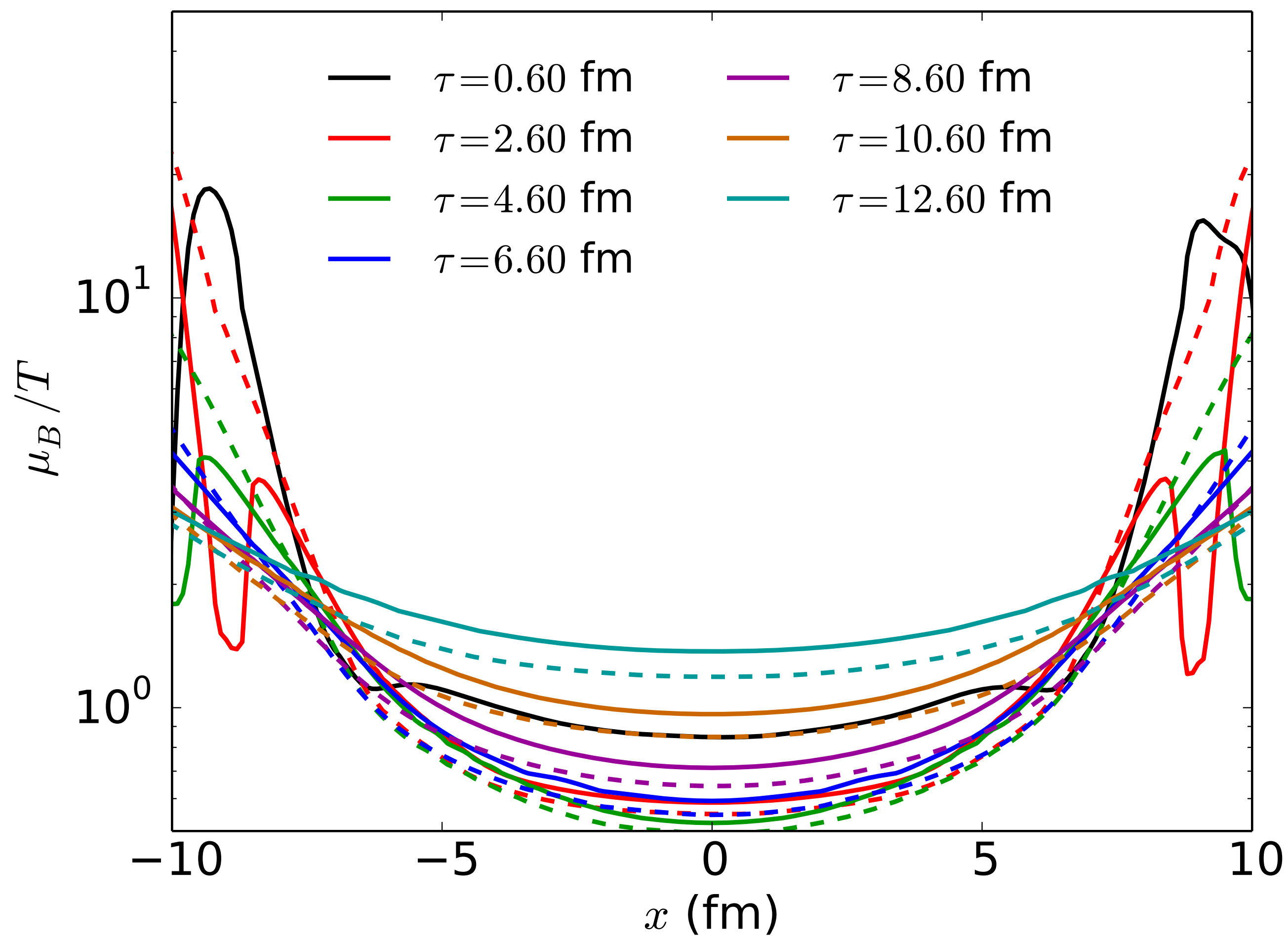

solid: with diffusion dashed: no diffusion

- With diffusion, ρ_B is larger in the center of the transverse plane
- The dynamics of ρ_B is driven by the evolution of u^μ and $\nabla^\mu \frac{\mu_B}{T}$

Results

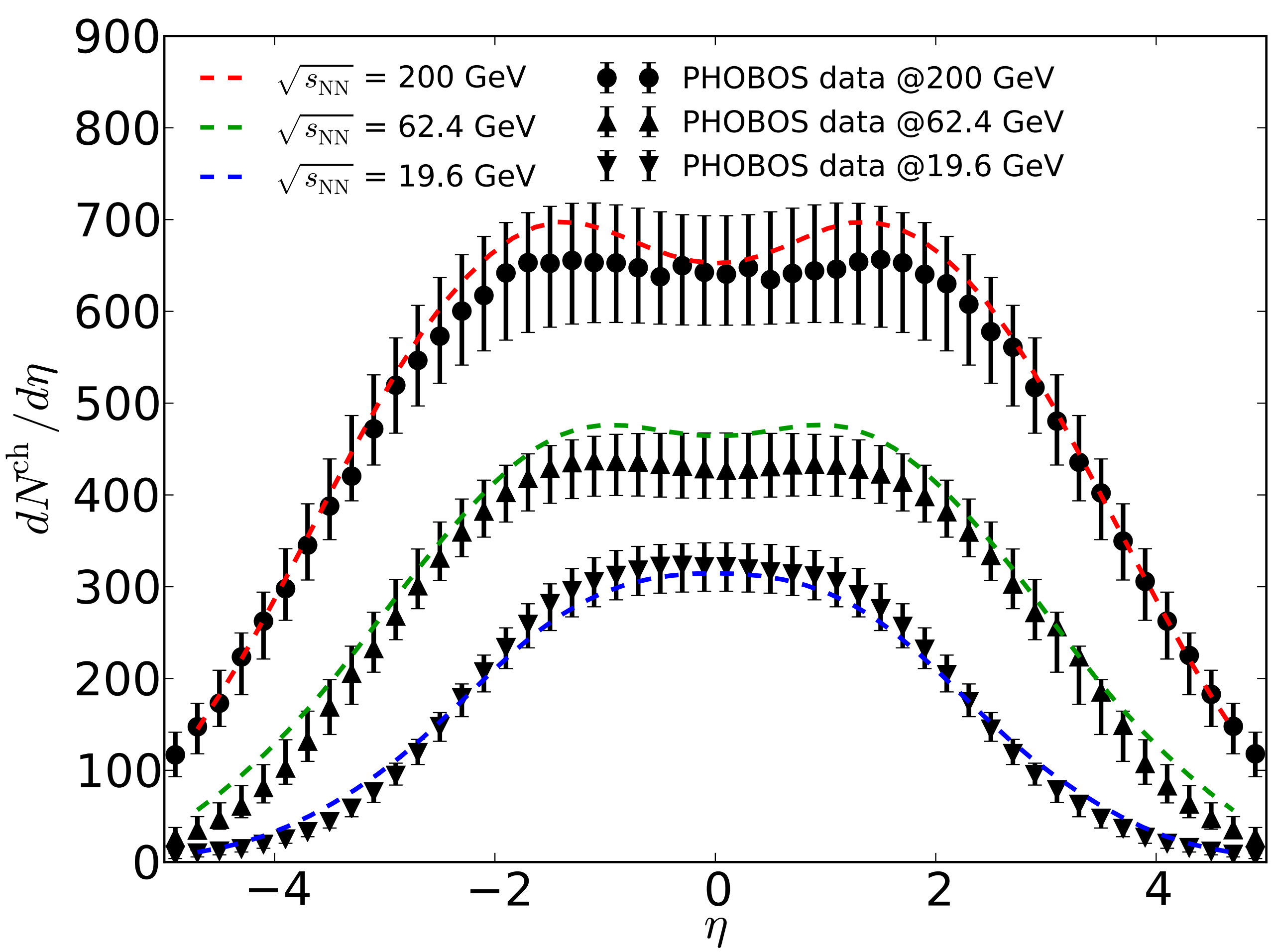

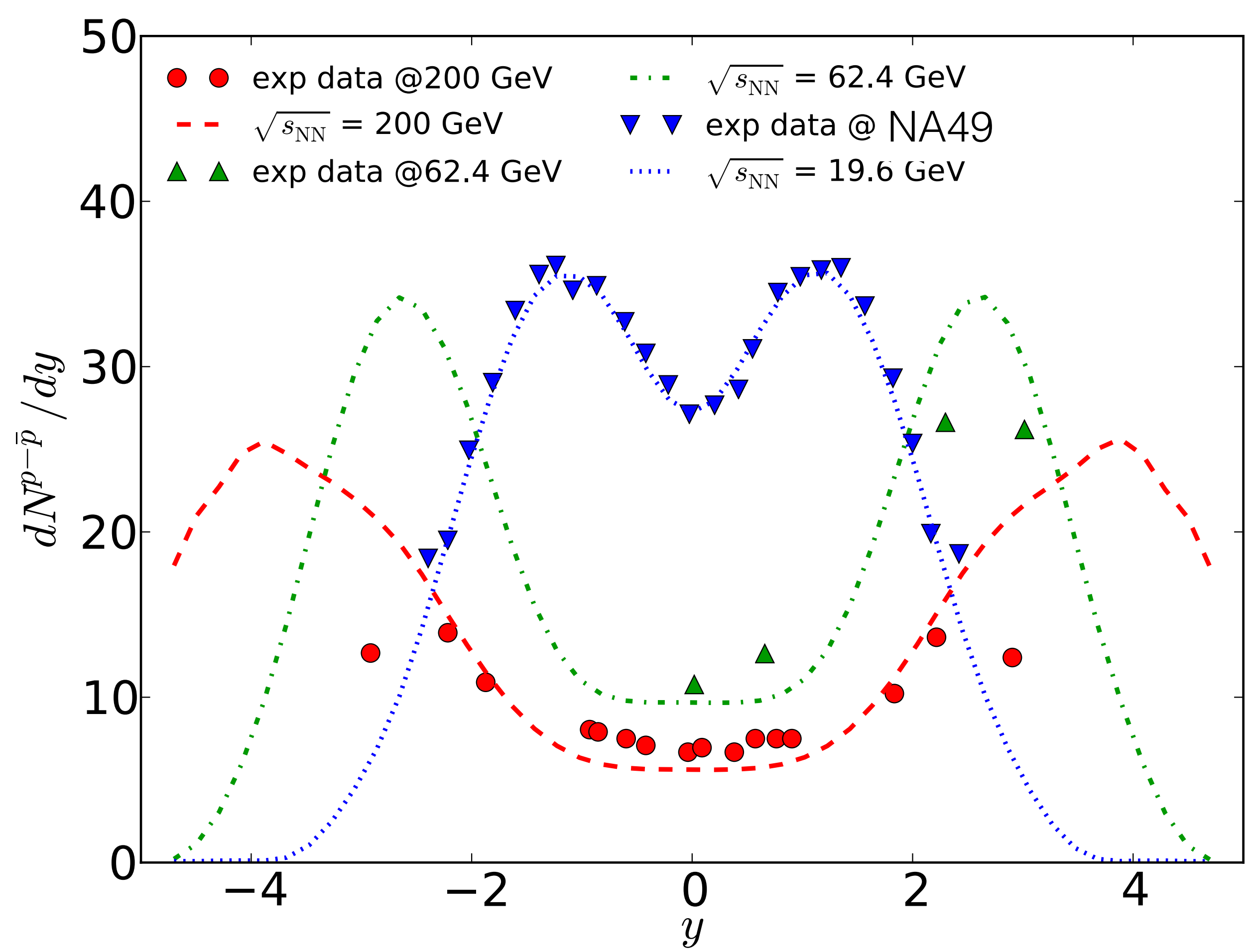

- The initial envelope functions in η_s are tuned to reproduce experimental $dN^{\mathrm{ch}}/d\eta$ and $dN^{p-\bar{p}}/dy$

Results

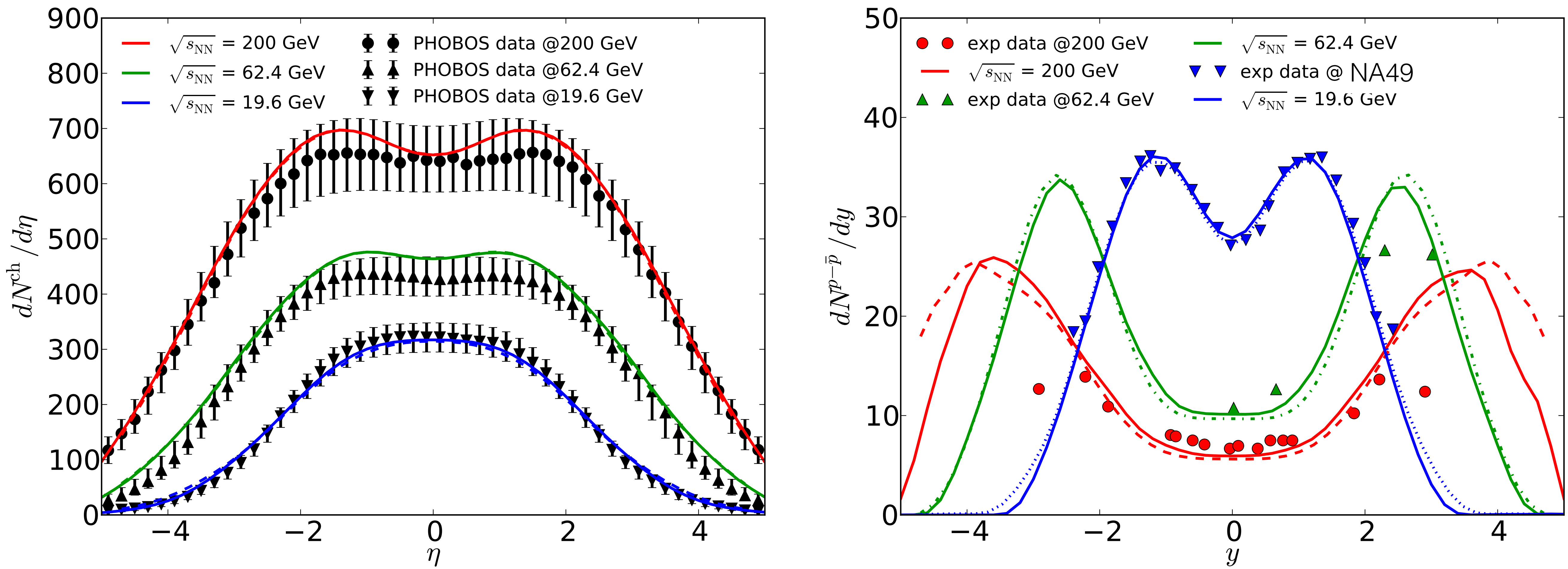

- The initial envelope functions in η_s are tuned to reproduce experimental $dN^{\mathrm{ch}}/d\eta$ and $dN^{p-\bar{p}}/dy$

- Baryon diffusion slightly increases $dN^{p-\bar{p}}/dy$ at mid-rapidity and narrows the tail in its distribution.

Results

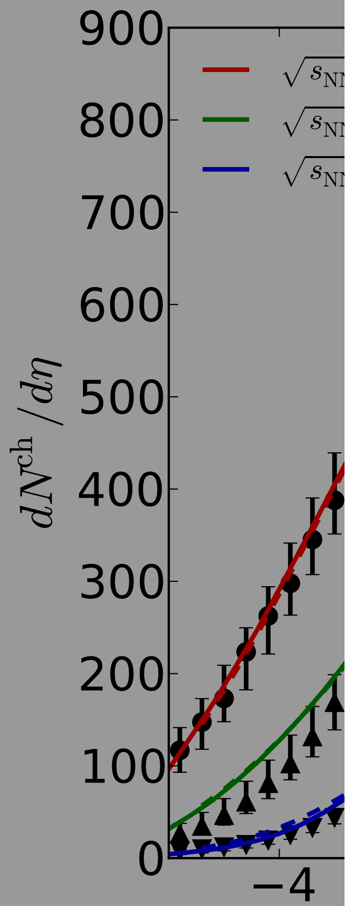

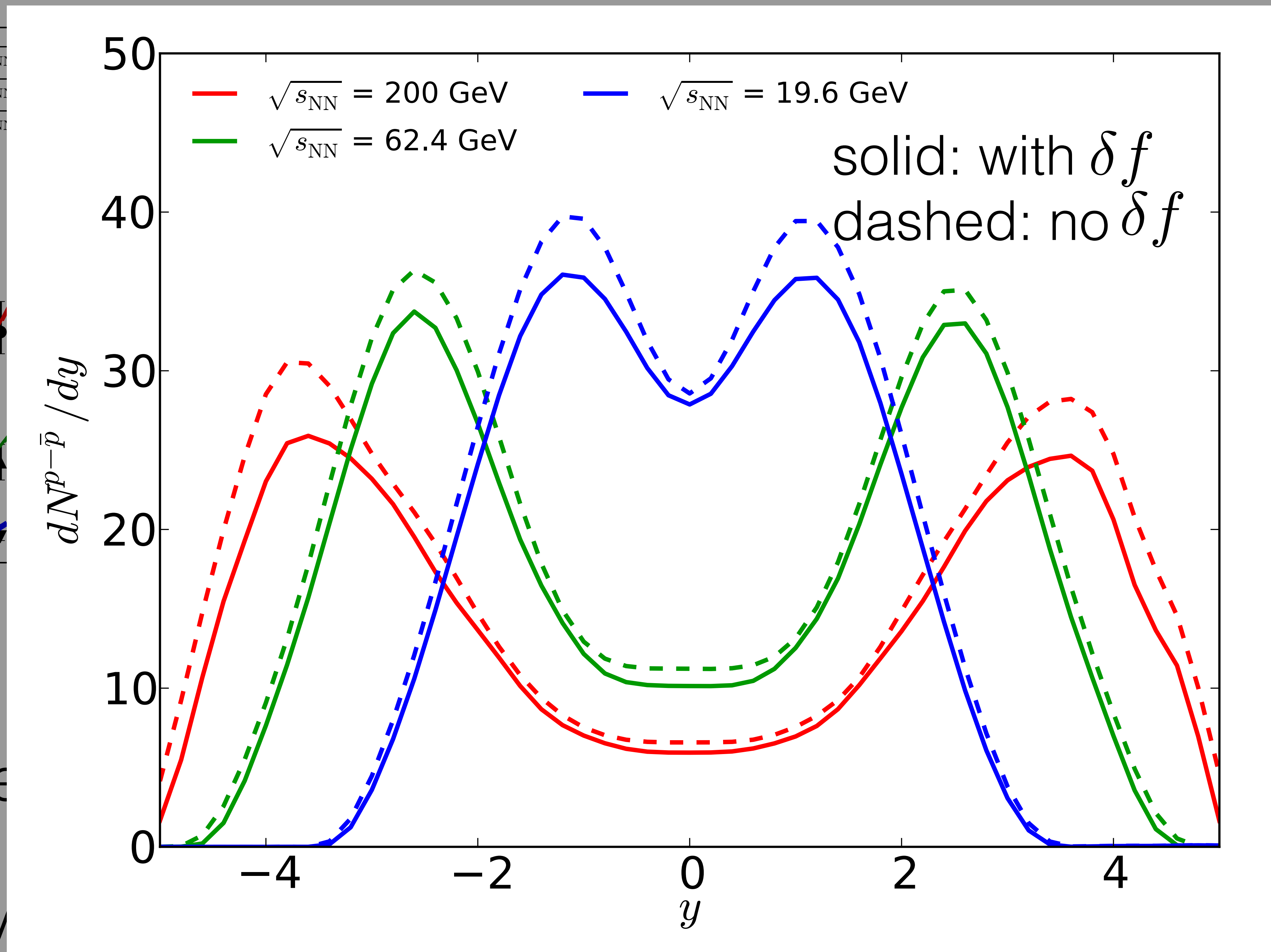

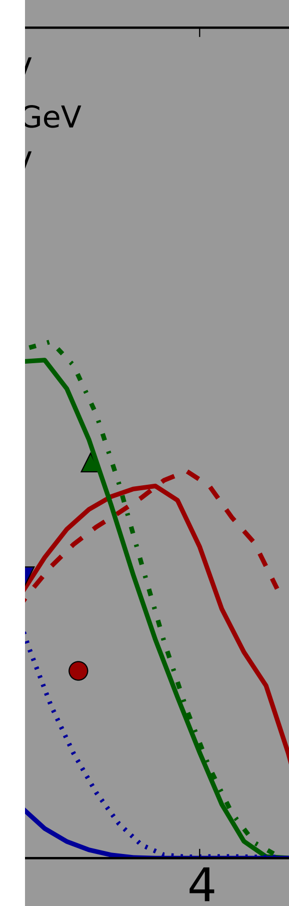

- The ... roduce expe...
- Bary... d-rapidity and narrows the tail in its distribution.

Light meson spectra and v_2

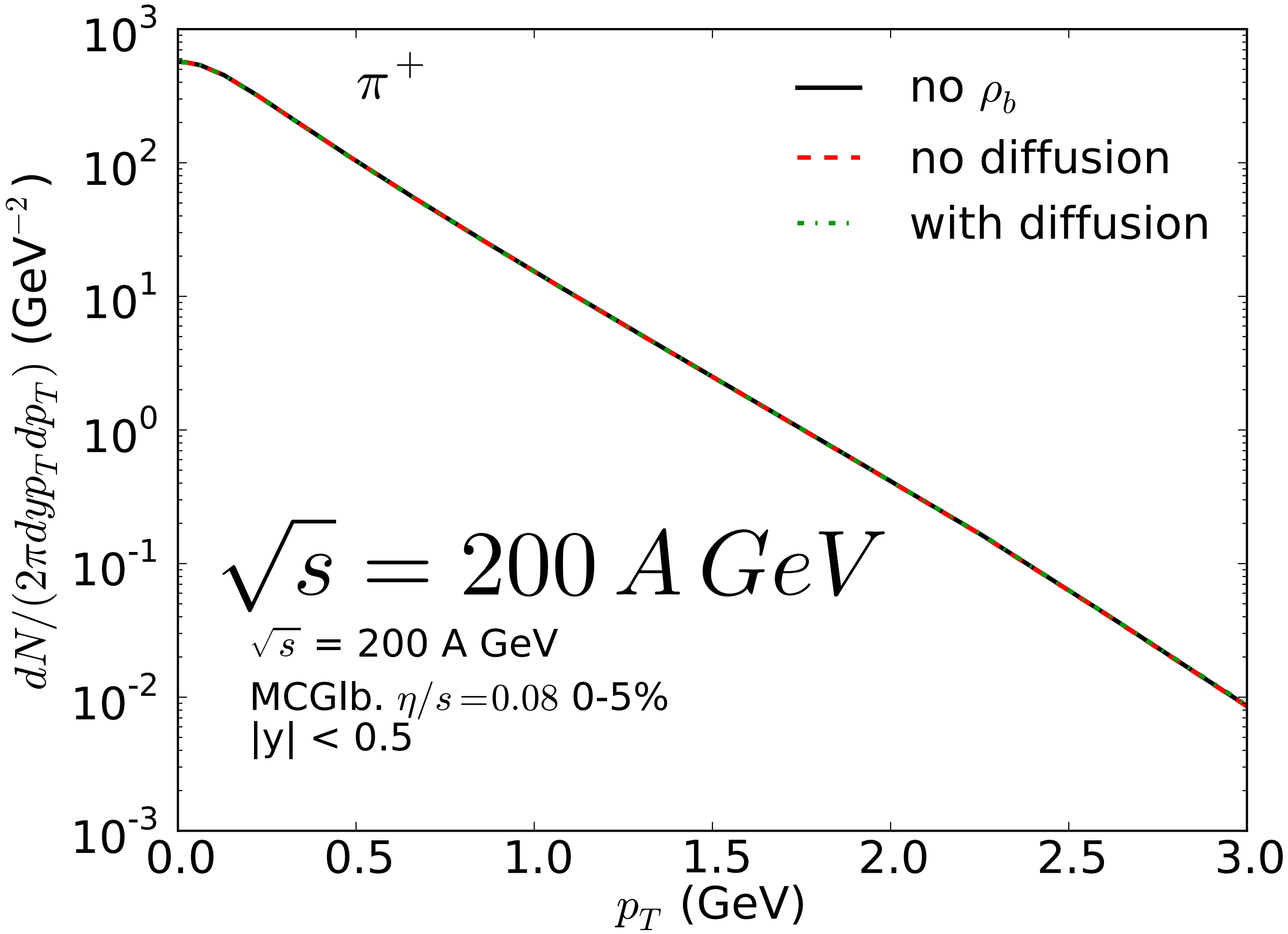

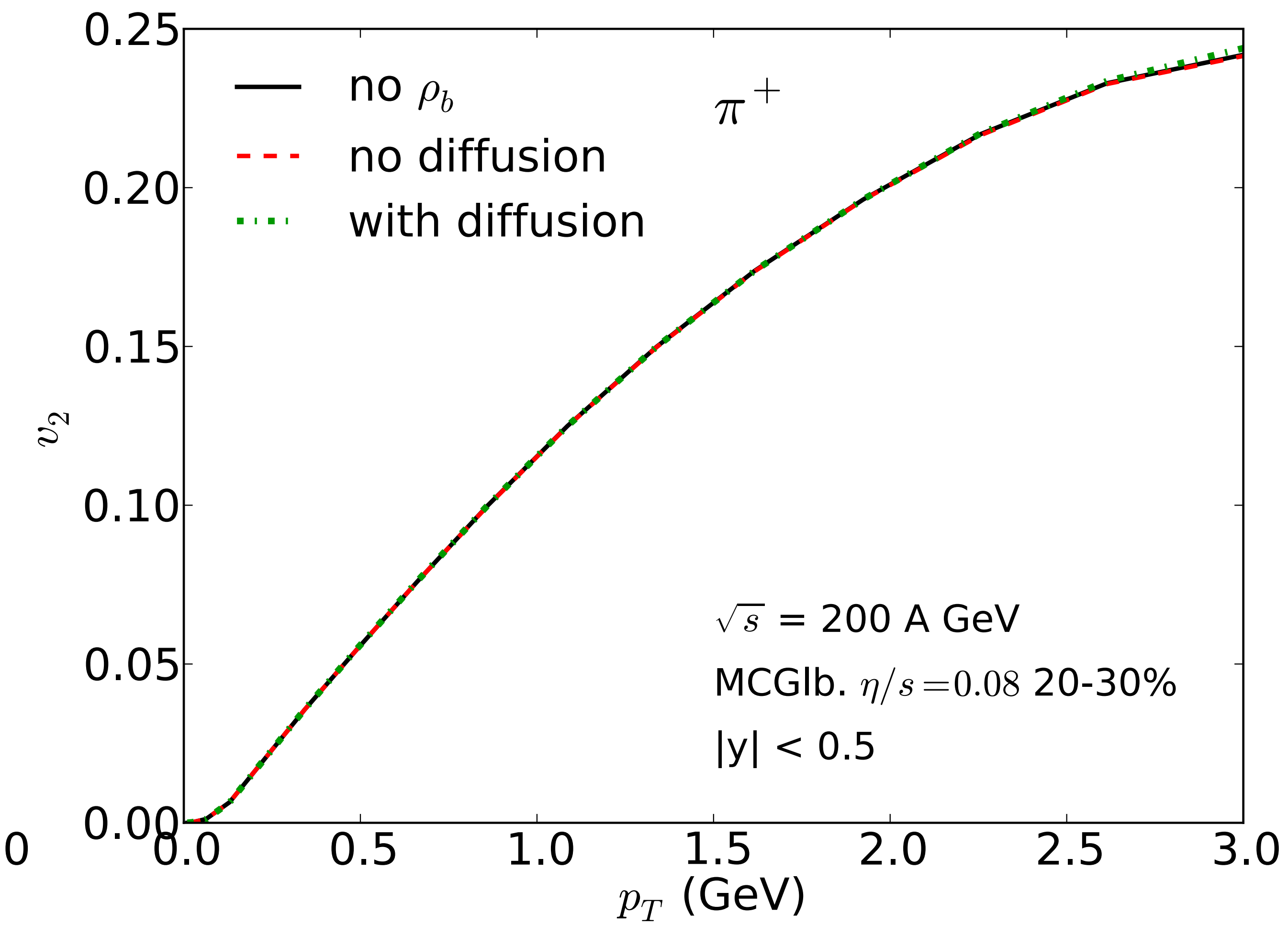

- At top RHIC energy, finite ρ_b and diffusion have little effects on pion spectra and v_2 at mid-rapidity

Light meson spectra and v_2

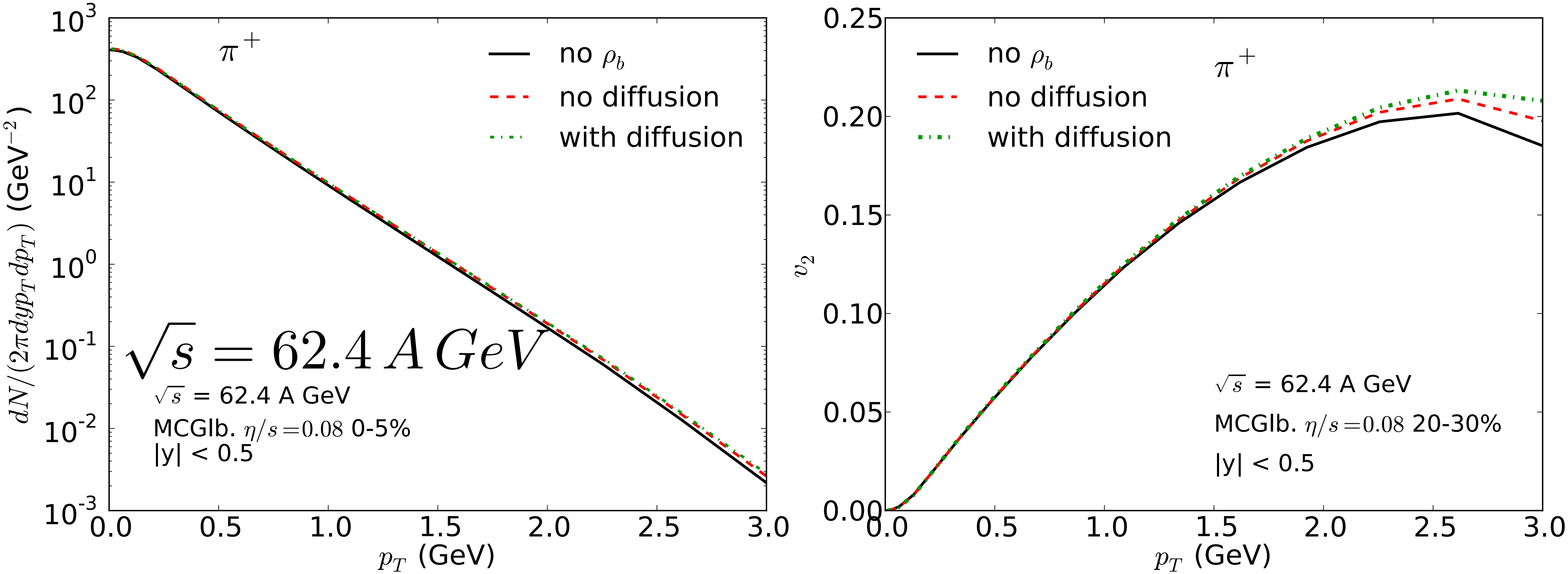

- At top RHIC energy, finite ρ_b and diffusion have little effects on pion spectra and v_2 at mid-rapidity

Light meson spectra and v_2

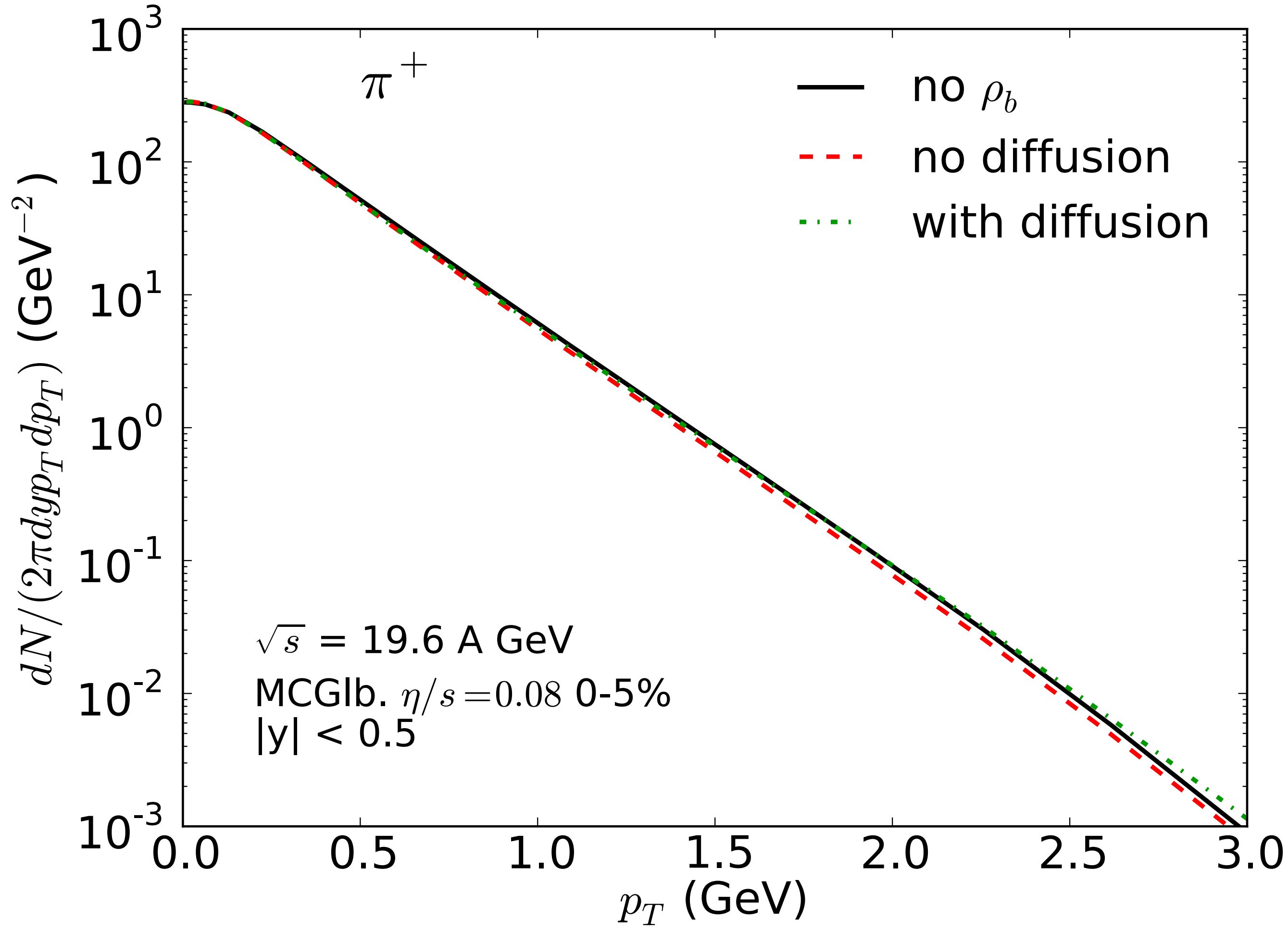

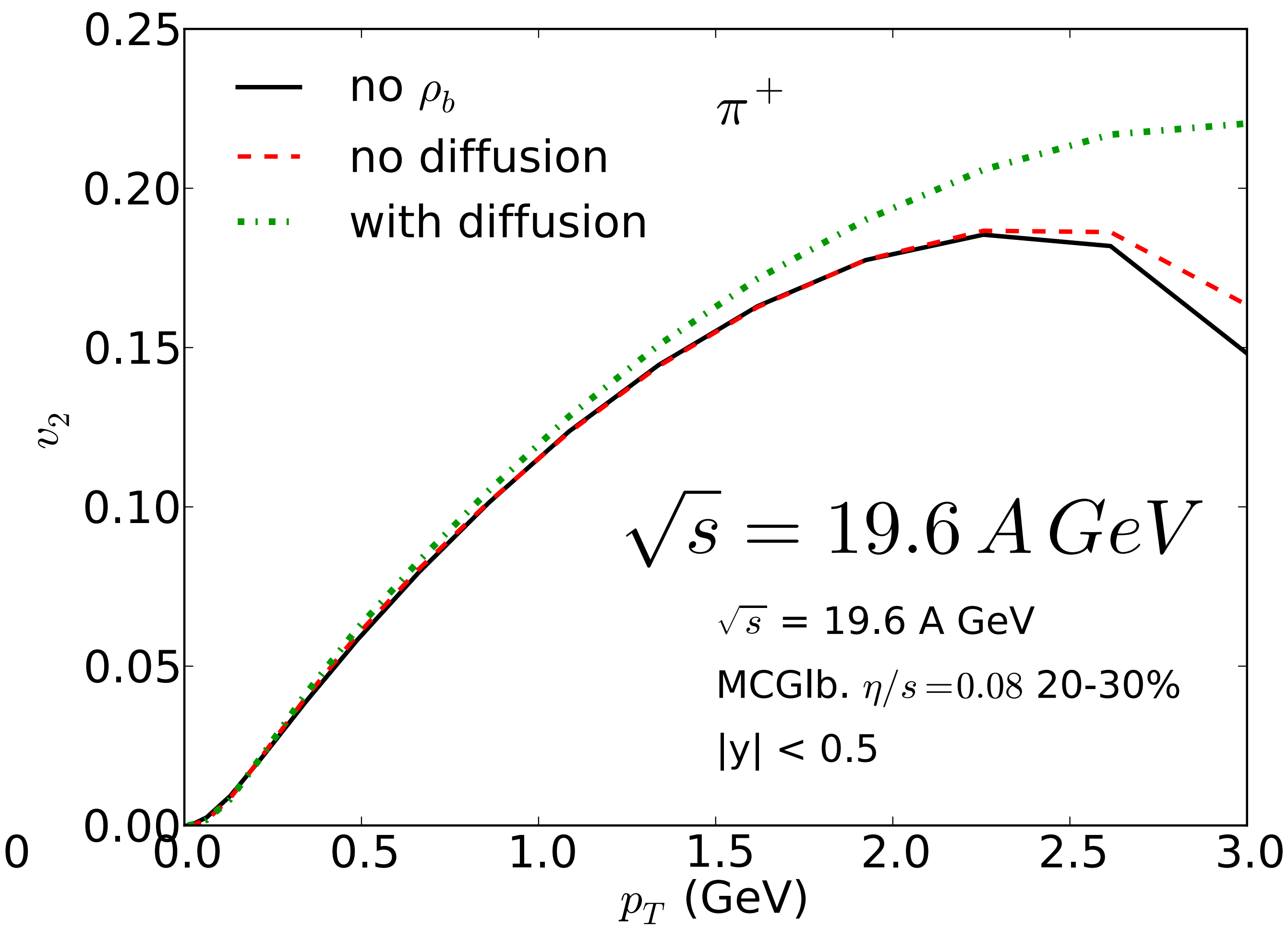

- At top RHIC energy, finite ρ_b and diffusion have little effects on pion spectra and v_2 at mid-rapidity
- The effects increase as collision energy goes down.

Light meson spectra and v_2

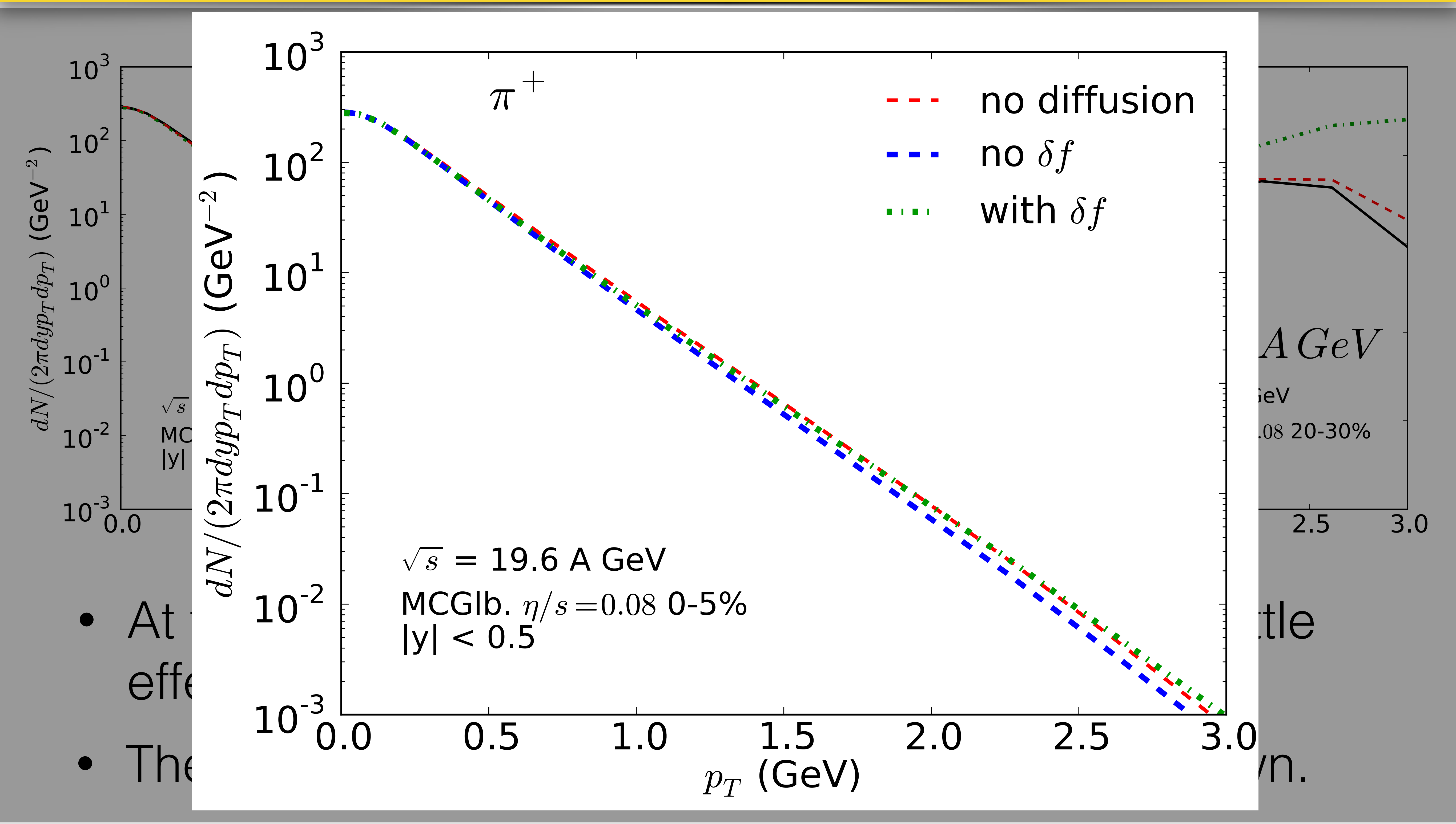

- Baryon diffusion reduces radial flow; δf makes the pion spectra flatter

Light meson spectra and v_2

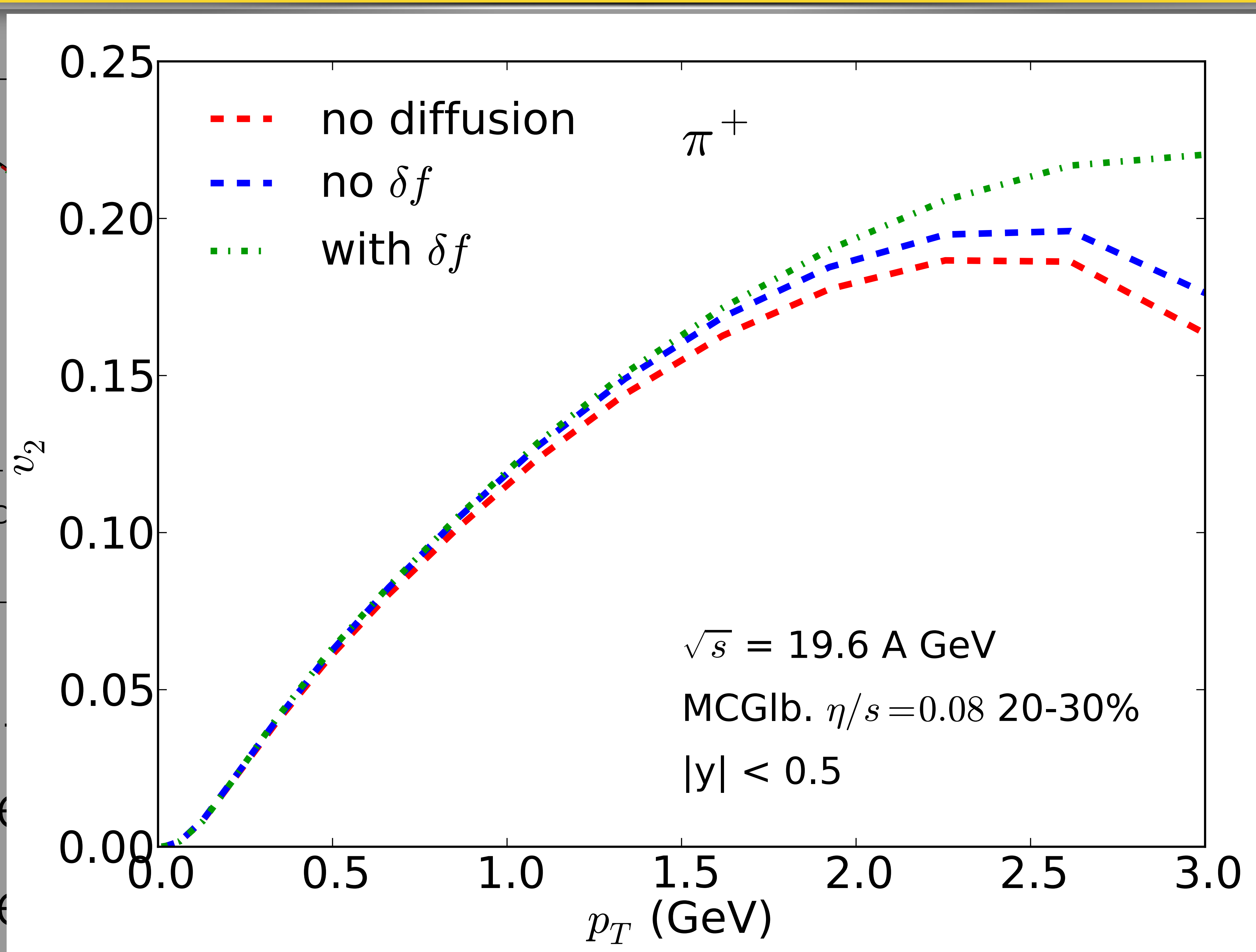

- At ttle
effe
- The wn.

- Baryon diffusion increases pion $v_2(p_T)$; δf increases pion v_2 at high p_T

proton vs anti-proton spectra and v_2

Solid: with diffusion; Dashed: no diffusion; Dash-dotted: no ρ_B

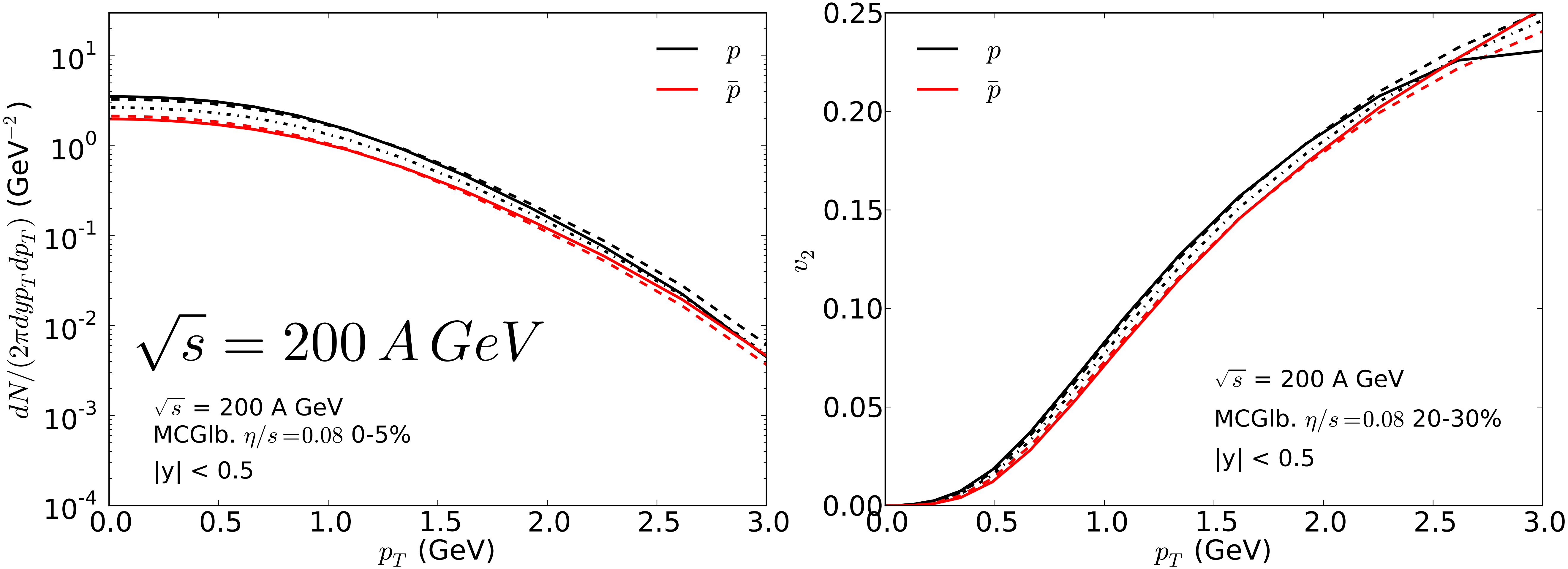

- Baryon diffusion has small effects on proton, antiproton spectra and v_2 at top RHIC energy

proton vs anti-proton spectra and v_2

Solid: with diffusion; Dashed: no diffusion; Dash-dotted: no ρ_B

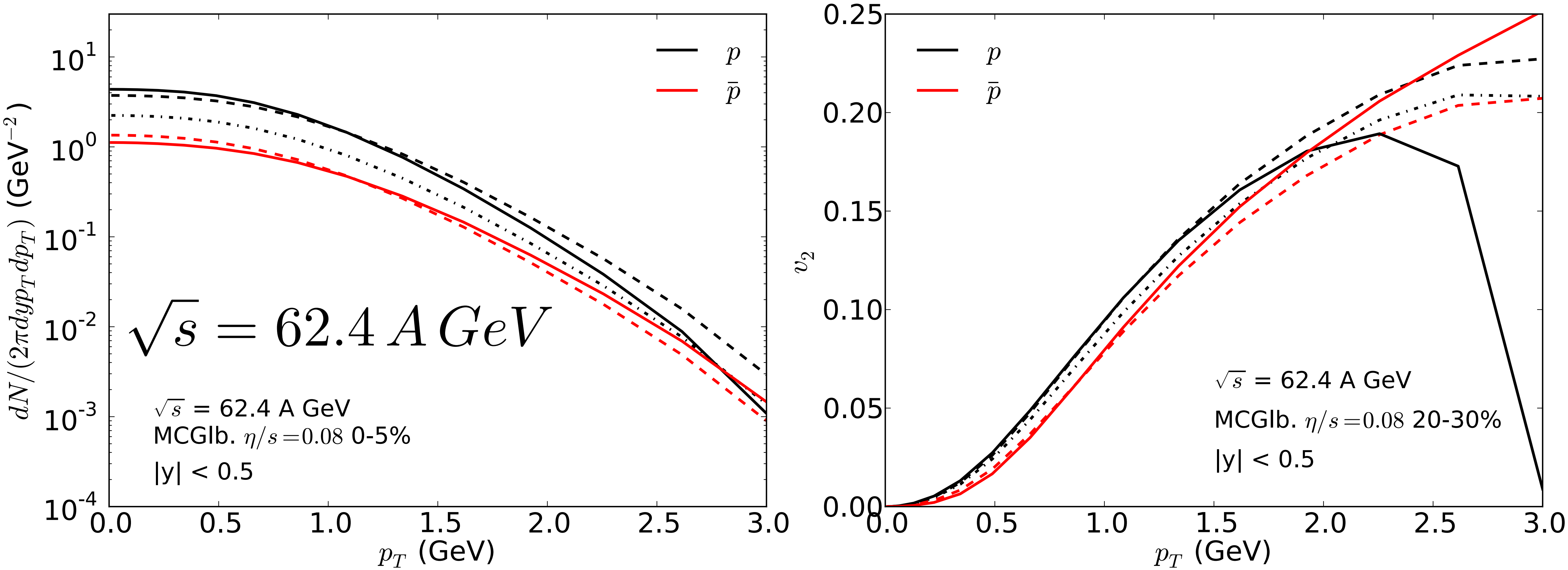

- Baryon diffusion has small effects on proton, antiproton spectra and v_2 at top RHIC energy

proton vs anti-proton spectra and v_2

Solid: with diffusion; Dashed: no diffusion; Dash-dotted: no ρ_B

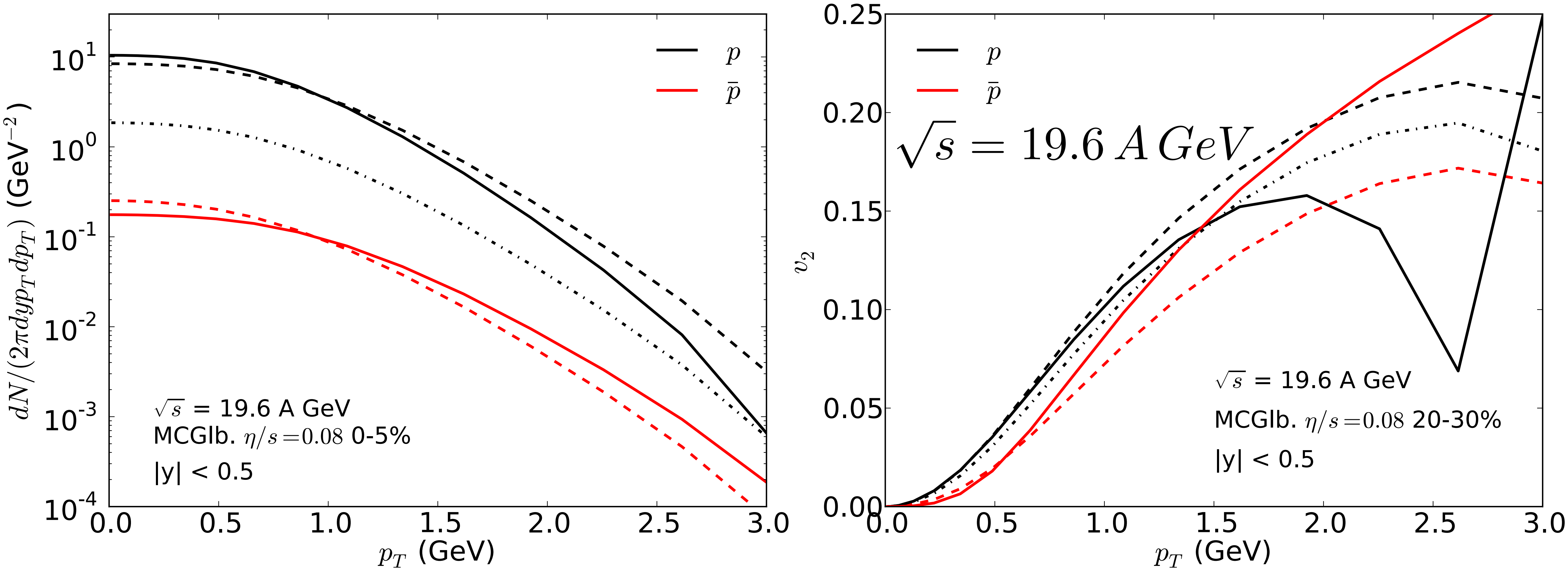

- Baryon diffusion slightly increases $N^p - N^{\bar{p}}$; but it reduces the difference in v_2 between proton and antiproton

proton vs anti-proton spectra and v_2

Solid: with δf ; Dash-dotted: no δf ; Dashed no diffusion

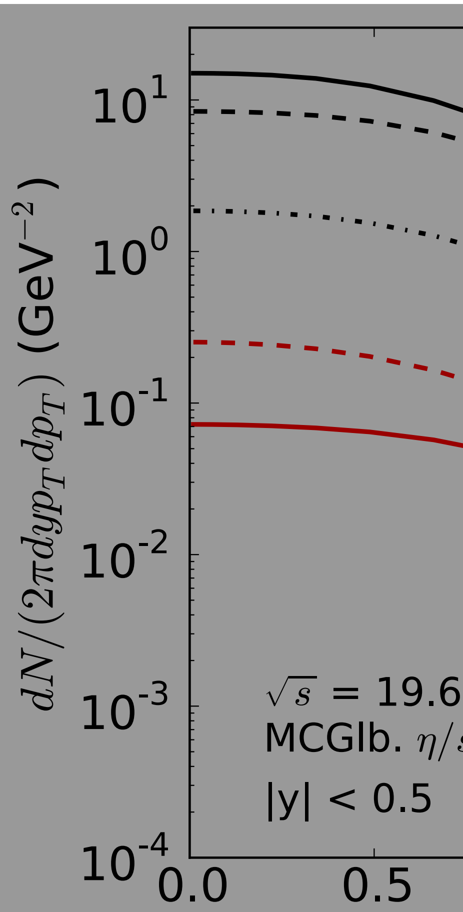

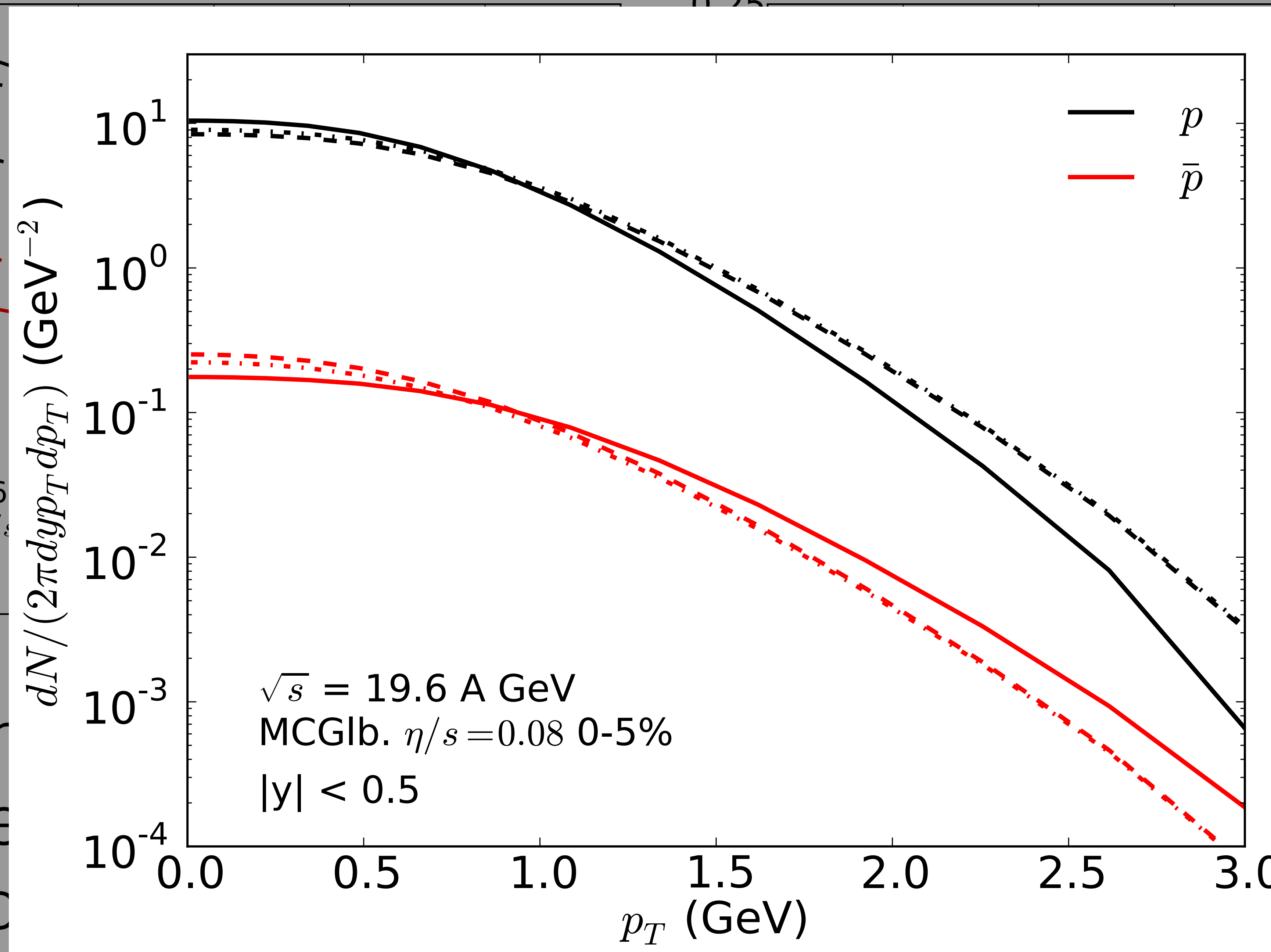

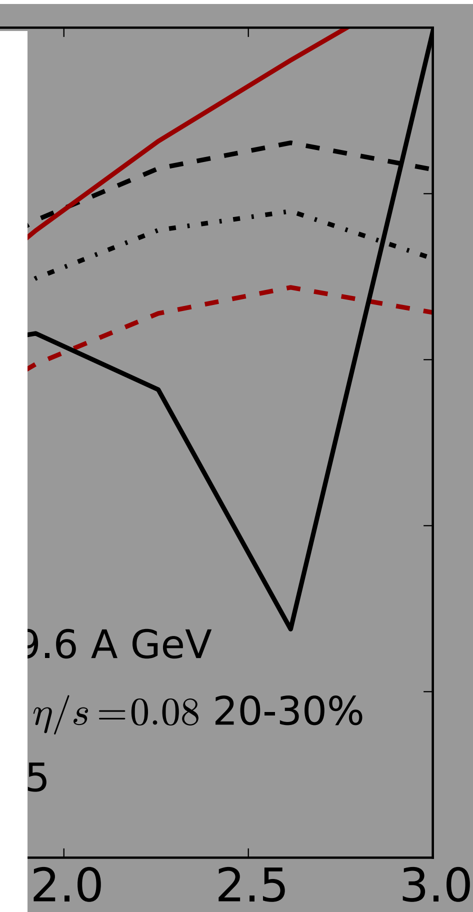

- Baryon ... t it reduce ... d antipro

- Opposite δf corrections to protons and anti-protons

proton vs anti-proton spectra and v_2

Solid: with δf ; Dash-dotted: no δf ; Dashed no diffusion

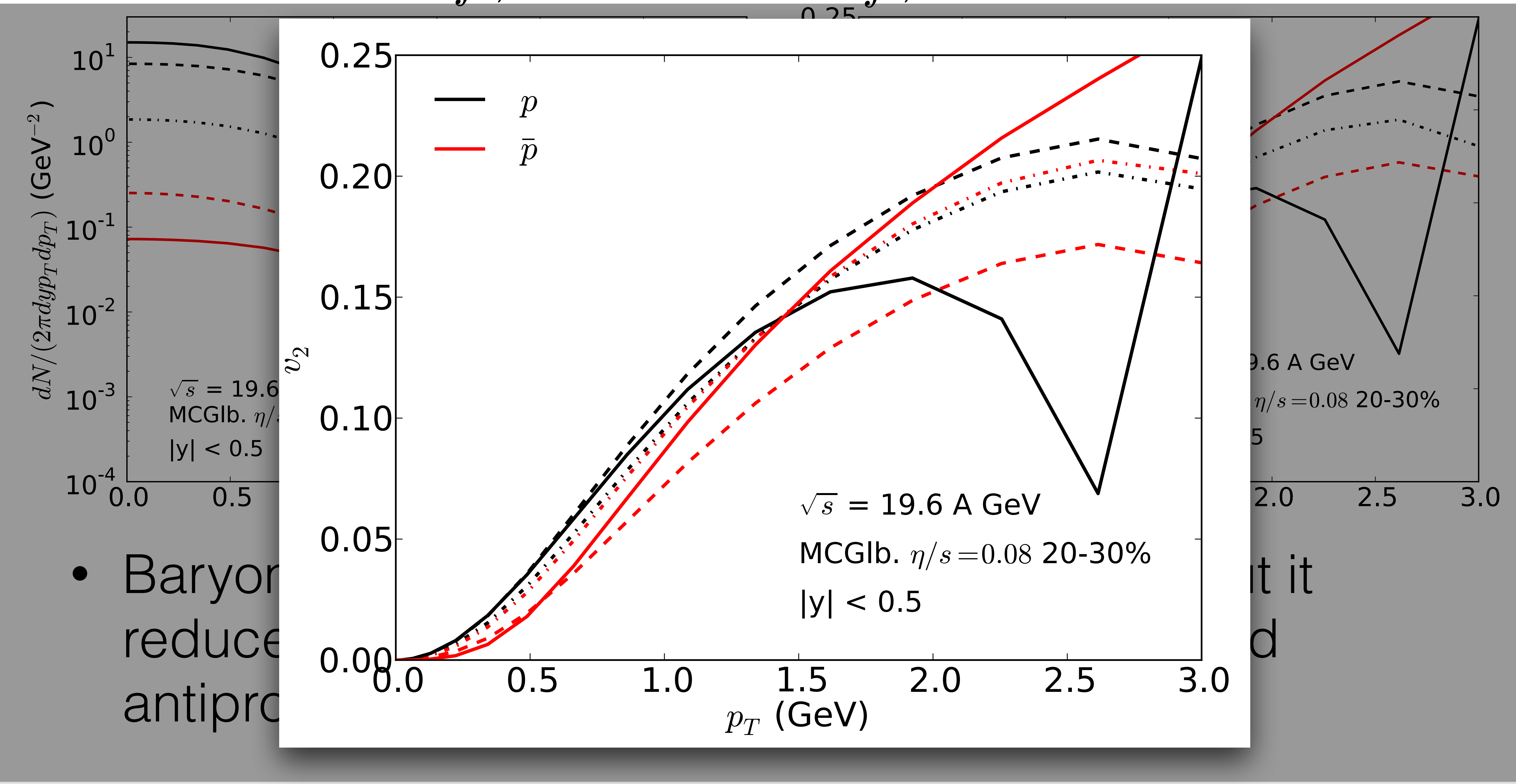

- Baryon diffusion reduces v_2 asymmetry between protons and anti-protons; δf corrections increase the difference

Conclusion

- We present preliminary **(3+1)-d** viscous hydrodynamic simulations including **net baryon diffusion** for the RHIC BES program
- Out-of-equilibrium δf corrections from baryon diffusion is essential to ensure net baryon number conservation
- Baryons and anti-baryons receive large opposite corrections from baryon diffusion δf
- Baryons diffusion reduce the proton antiproton v_2 asymmetry at the low collision energies
- Evolving more conserved currents, including initial state fluctuations, and coupling to UrQMD will come soon

back up

Stabilizing MUSIC with diffusion

We implement quest_revert for q^μ to stabilize the hydro evolution with diffusion,

$$u^\mu q_\mu = 0 \longrightarrow q^0 = \frac{u^i q^i}{u^0}$$

The size of q^μ

$$\xi_q \equiv \frac{\sqrt{-q^\mu q_\mu}}{|\rho_B|} \frac{1}{\mathrm{prefactor} \times \tanh(e/e_{\mathrm{dec}})}$$

$$\mathrm{prefactor} = 300$$

If $\xi_q > \xi_q^{\max}$

$$\xi_q^{\max} = 0.1$$

$$\tilde{q}^\mu = \frac{\xi_q^{\max}}{\xi_q} q^\mu$$

Stabilizing MUSIC with diffusion

We implement quest_revert for q^μ to stabilize the hydro evolution with diffusion,

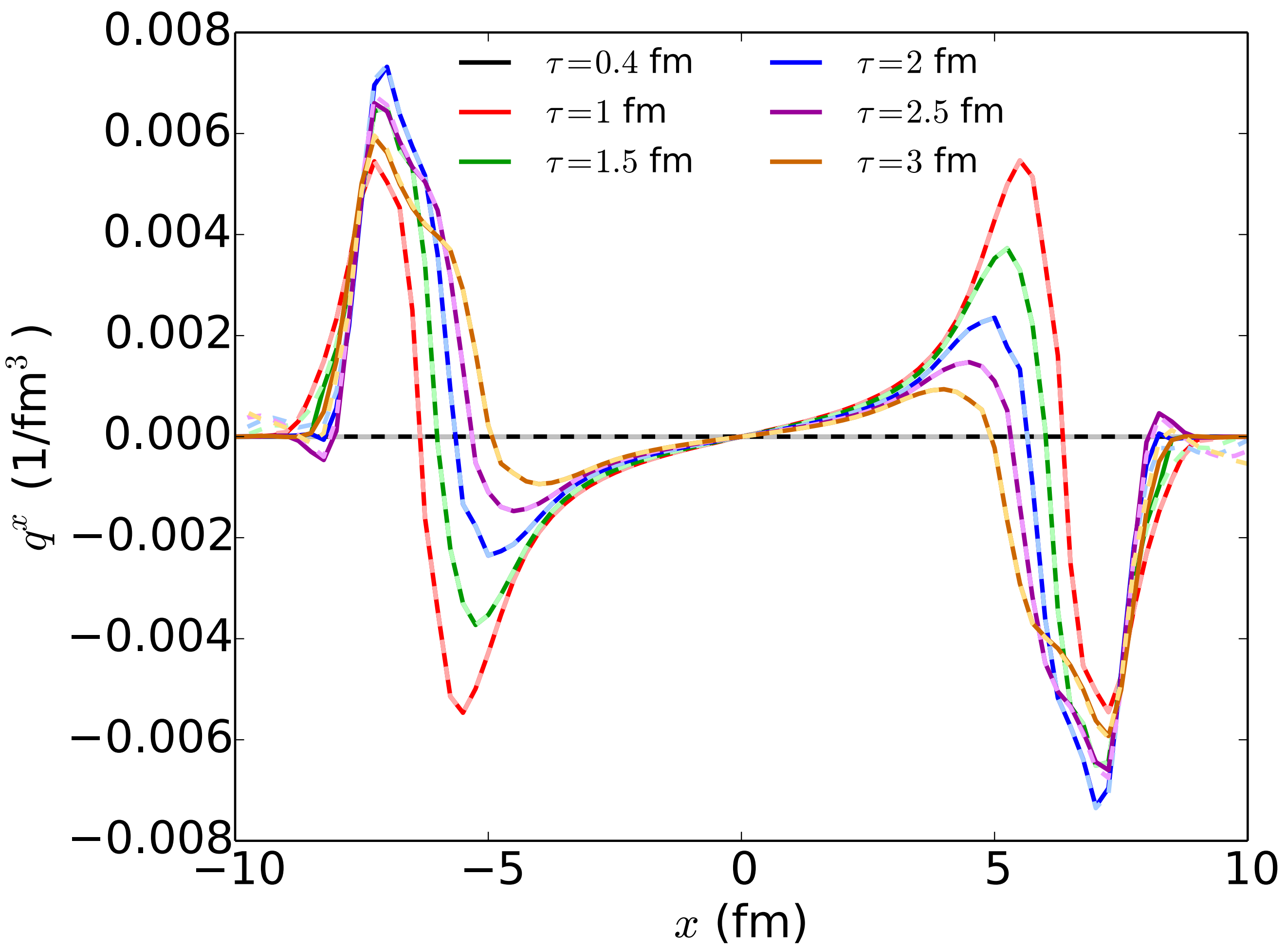

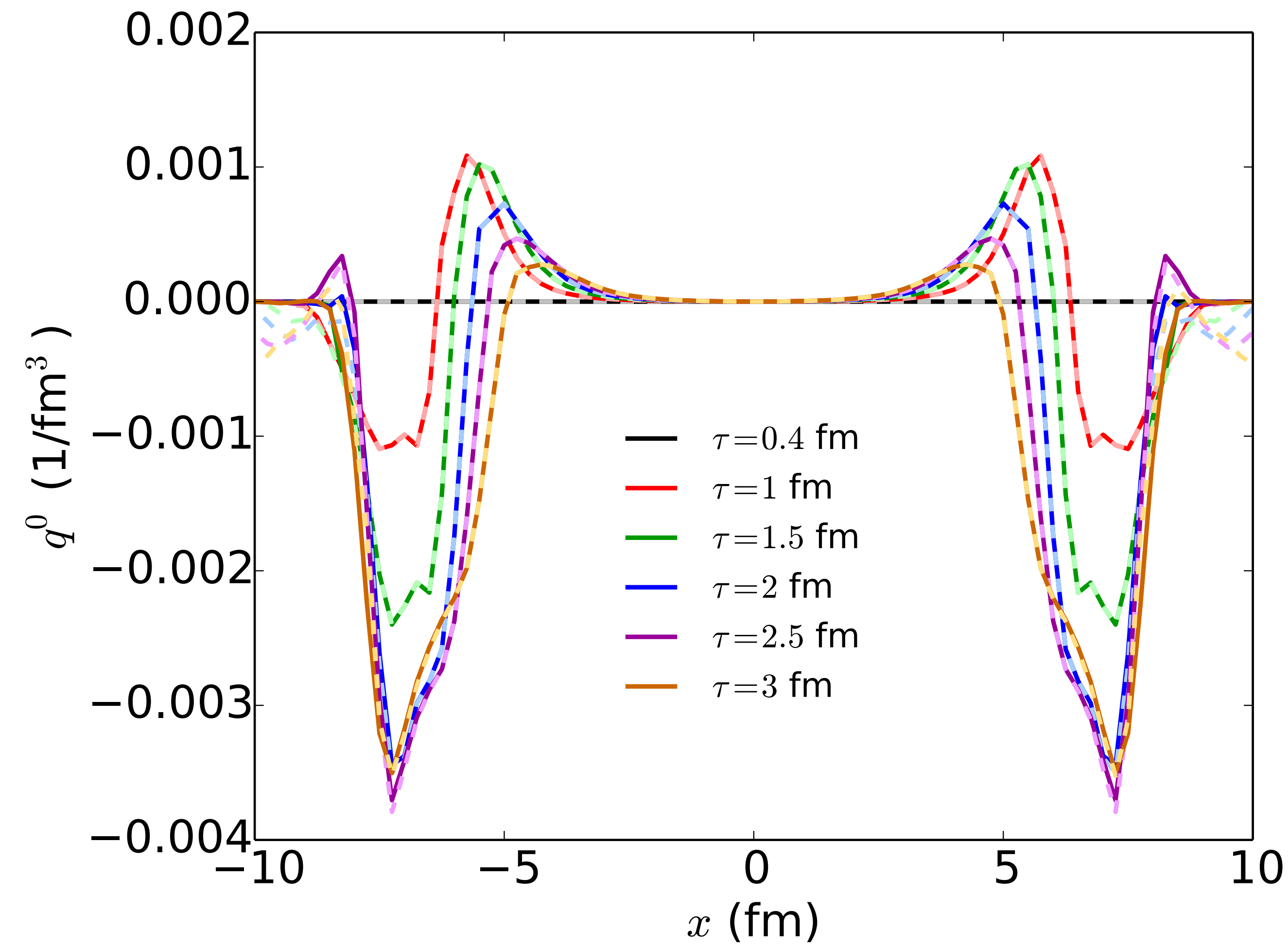

most of the modifications are at the edges of the fireball

Experimental Overview of Baryon Transport

Flemming Videbæk

BNL

RBRC
RIKEN BNL Research Center

BROOKHAVEN NATIONAL LABORATORY

Office of Science
U.S. DEPARTMENT OF ENERGY

Overview

- Introduction
- pp
- pA
- Heavy Ion baryon transport
- A few model comparisons
- Summary

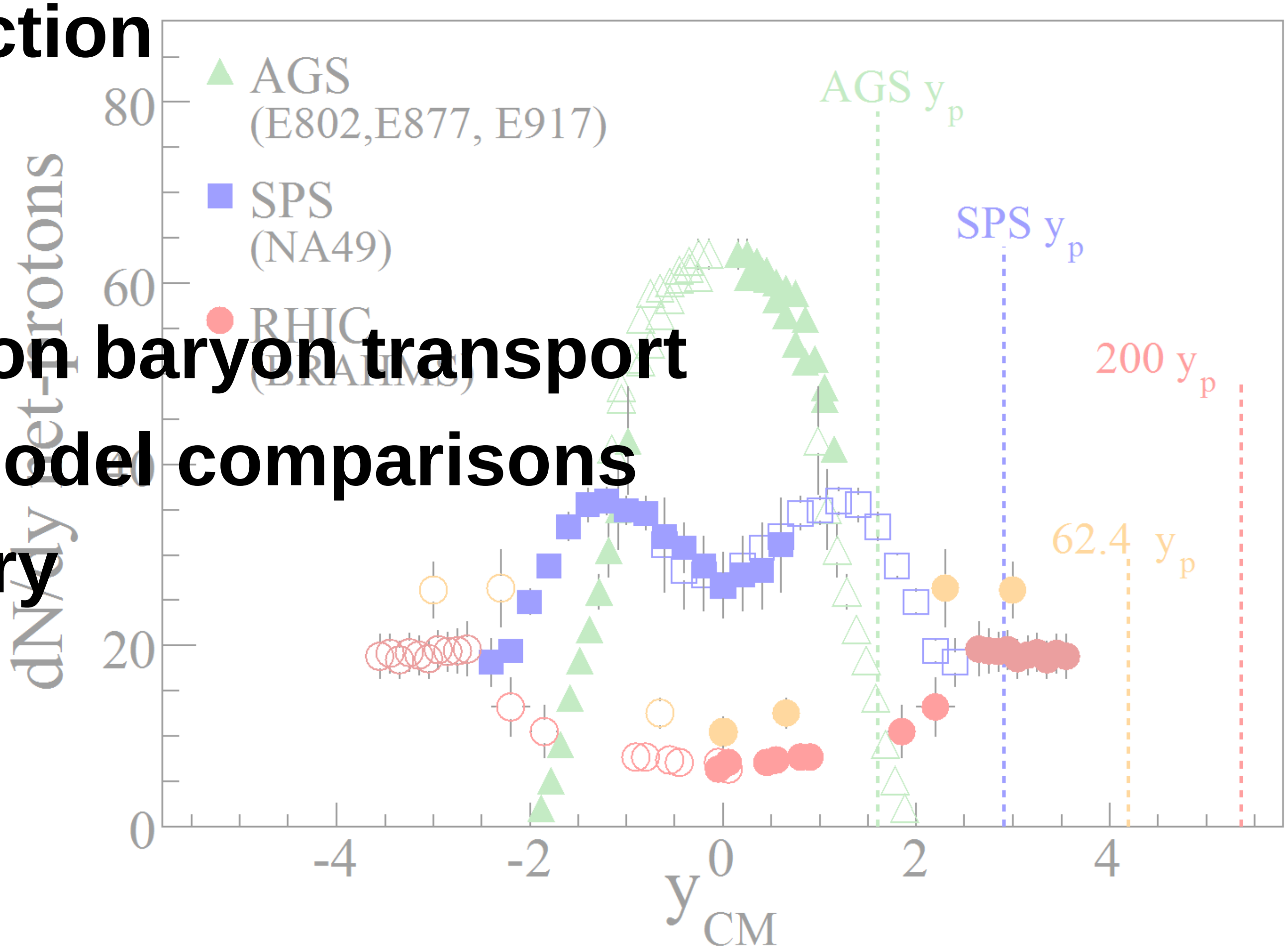

Introduction

- Interest since 80’s when HI and QGP was first considered
- Seminal paper by Busza & Goldhaber, with expectation based on data from pp, pA
- Net-baryon vs. net-protons
- What have we learned from 30 more years experience
- The importance of transport/stopping at BES energies

Early Considerations

Low energy pp data shows that dn/dx_F is ~ constants i.e. $dn/dy \sim \exp(-\Delta y)$

$x_F = pz/(\mathrm{sqrt}(s)/2)$

Reviewed pp and pA data

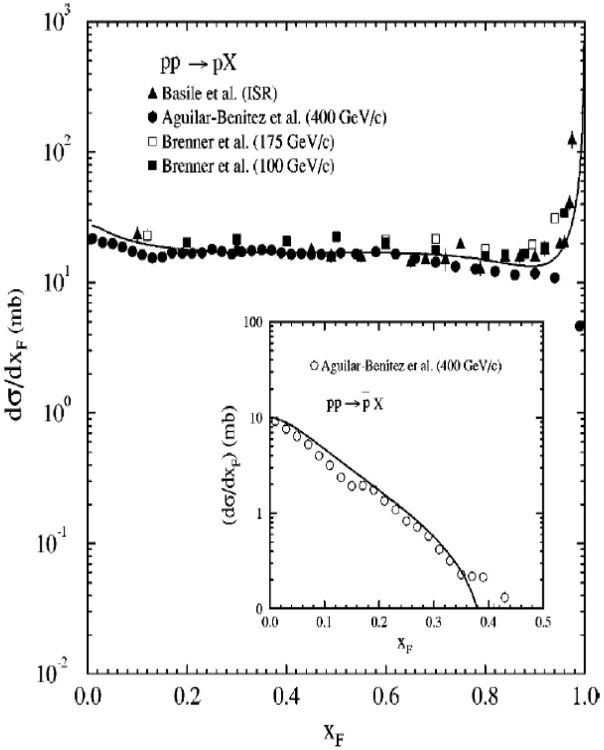

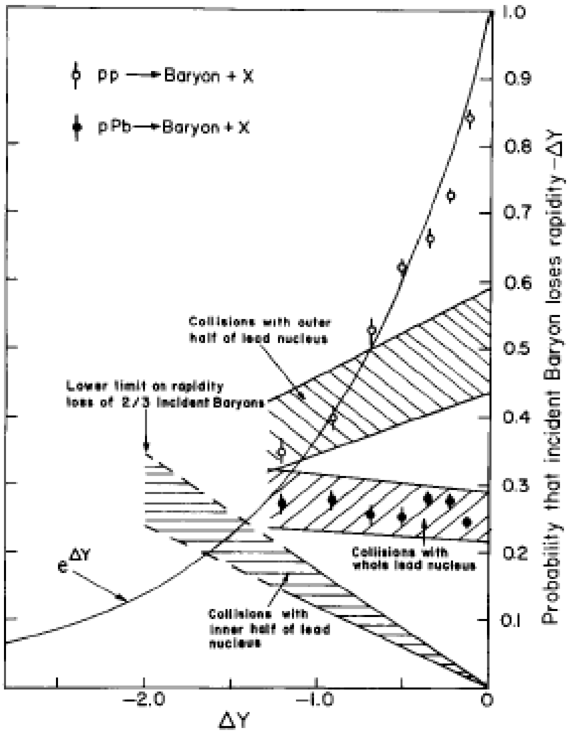

dy ~0.9 for pp; dy~2.3 in central pPb

Busza and Goldhaber
Phys Lett 139B,233(1983)

pp / pA overview

- NA49 data –at 17.3 GeV
- BRAHMS data from 62, 200 GeV
- Net Baryon is hard to measure. Most times net-proton is used as a proxy. Depending on observable this can dilute observations and interpretation
- Net-Baryons have been evaluated taking into account measured neutrons, and heavier hyperons.

NA49 pp 158 GeV

NA49 Eur.Phys.J.C65,9 (2010)

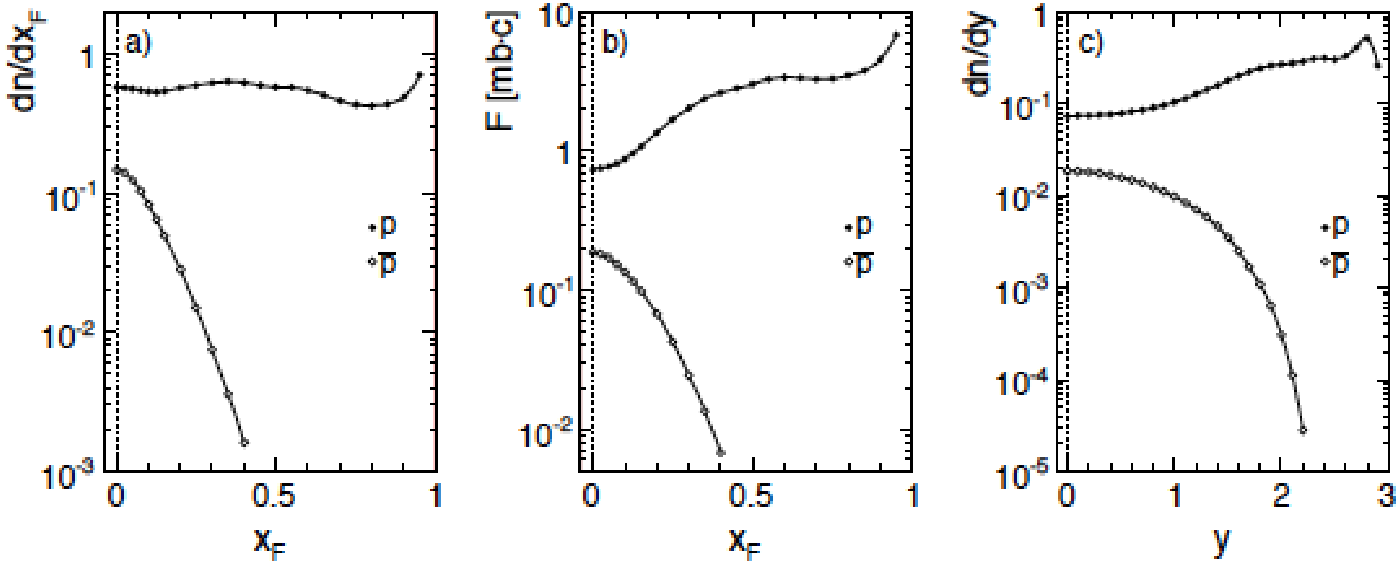

NA49 measured extensive pp, πP reactions.

dn/dx_F ~ constant

Neutrons like p apart from diffractive region

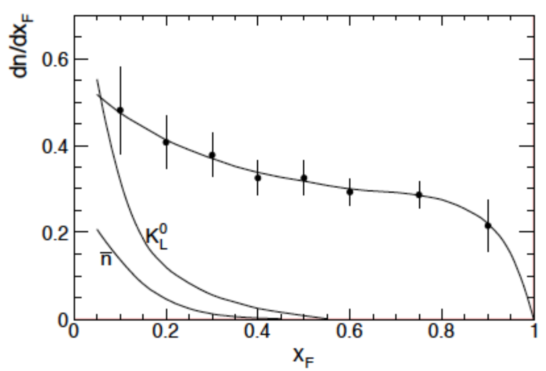

Net-proton in pp is a reference

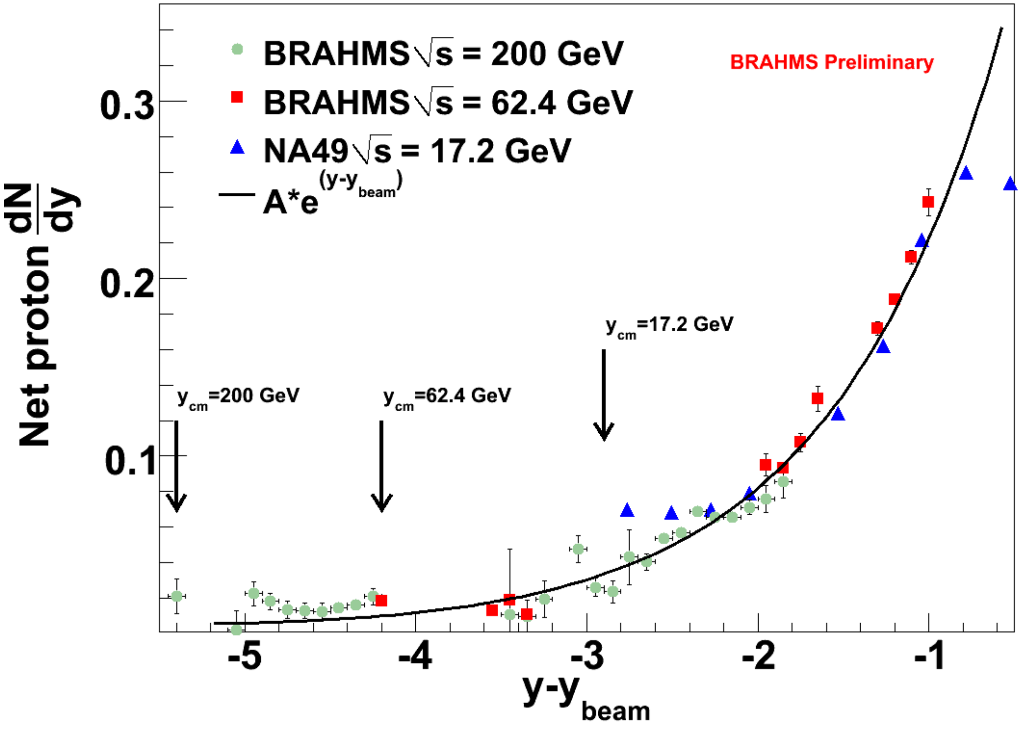

The pp Net-p distributions at 62 and 200 GeV exhibits same behavior as the low energy data. Leaves little room for new mechanisms in p+p stopping

pA

- To look better at projectile vs. target contribution NA49 compare πp,πA with pp and pA.
- Strong increase of transported protons with centrality at y~0
- These detailed measurement in essence confirmed the early work by Busza

Net baryon distribution
Projectile component

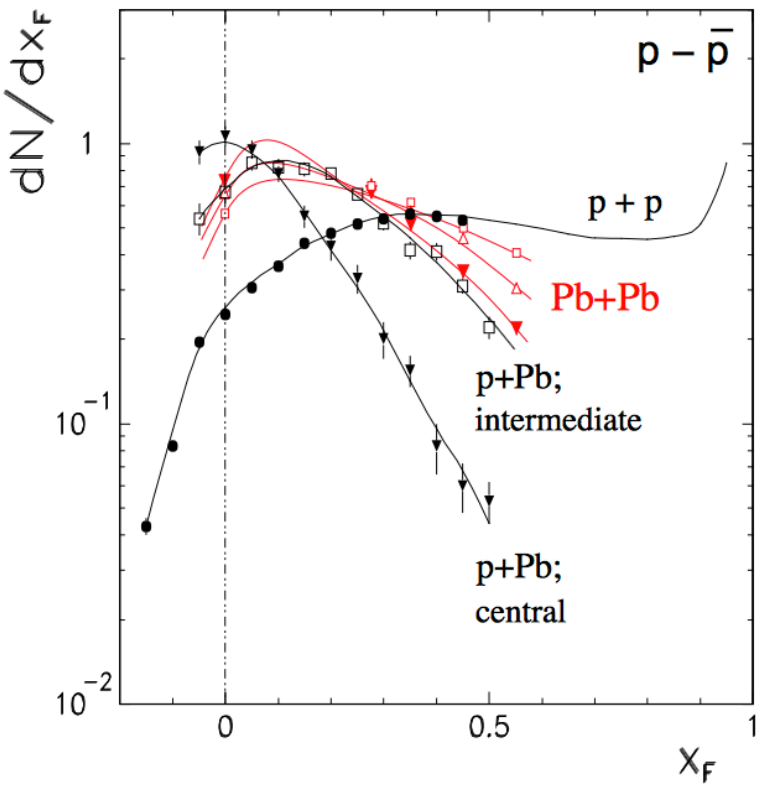

A.Rybick, SQM 2003 (NA49)

Very high energy

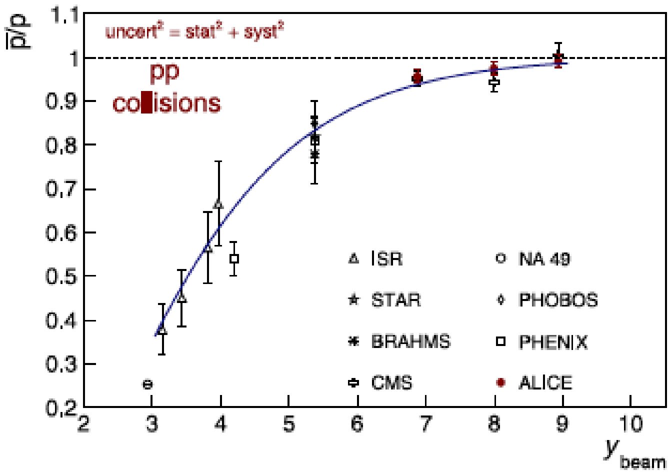

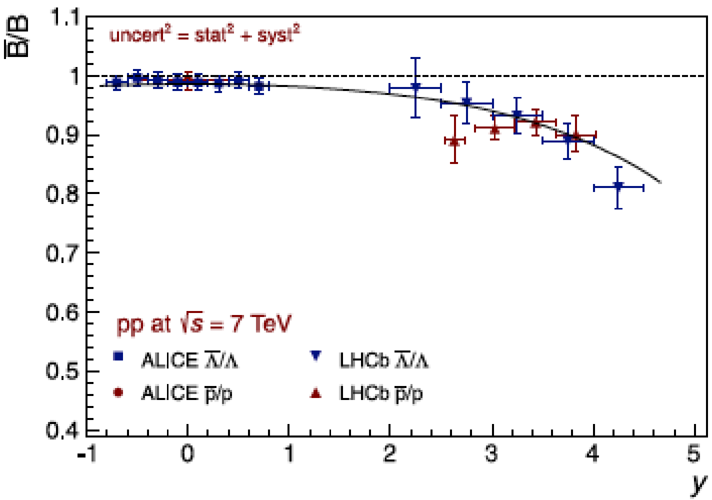

- Pbar/p as a proxy for baryon stopping
- All mid rapidity from seaquark or gluons. Almost no contribution from transported baryons.

ALICE
Eur. Phys. J. C (2013) 73:2496

Data can be described by exchanges with the Regge-trajectories intercept of Aj ~ 0.5. Implies any transport not suppressed at large delta y is disfavoured.

What is learned about mechanism

Long history on ideas

- 1980 Valence quark recombination $\langle x_F \rangle \sim 0.5$
- Valence q-qq breaking $\langle x_F \rangle \sim 1/3$ (in many models)
- Valence quark fragmentation, CGC
- Baryon Junction

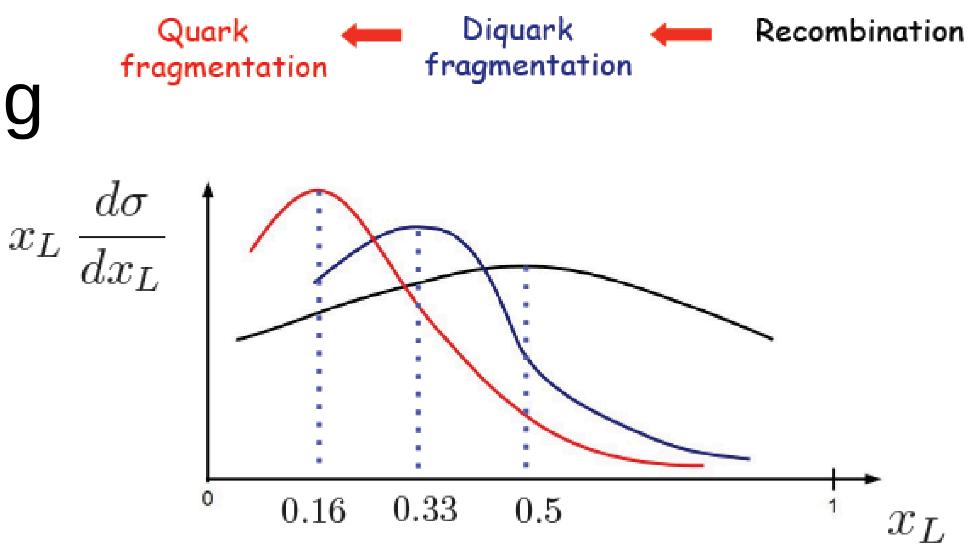

FS Navarra, WND 2015

Heavy Ion

- Overview of data energy and centrality dependence
- Net-p to net B
  - AGS 917
  - AGS E866
  - SPS
  - RHIC
  - LHC
- Where do distinction between transported proton and net-p cease to be relevant?
- Where is absorption relevant for quantities?
- Net proton, net-B variables
  - Directed flow, v2 particle anti particles
  - Kurtosis..

Data Sample Considered

Experiment	Ek	Sqrt(s)	Ybeam	Specie	pp
917	6	3.84	1.34	AuAu	
	8	4.30	1.47		
917,E866	10.8	4.70	1.57		
NA49	20-80	6.40-12.4	1.90-2.57	PbPb	
NA49	158	17.3	2.91	PbPb	Pp, pPb
BRAHMS		62.5	4.5	AuAu	Pp
		200	5.4	AuAu	pp
ALICE,LHCb		7,600			pp

AGS energies

E917 measured at 8-11 GeV.A

Increased stopping with centrality, but not complete

Small rapidity losses ~0.6-0.9

Limited phase space

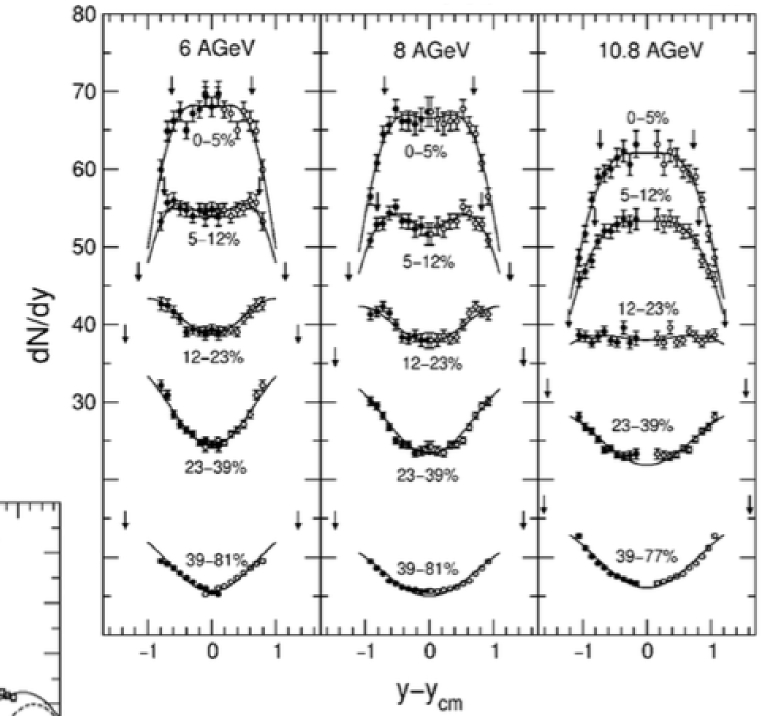

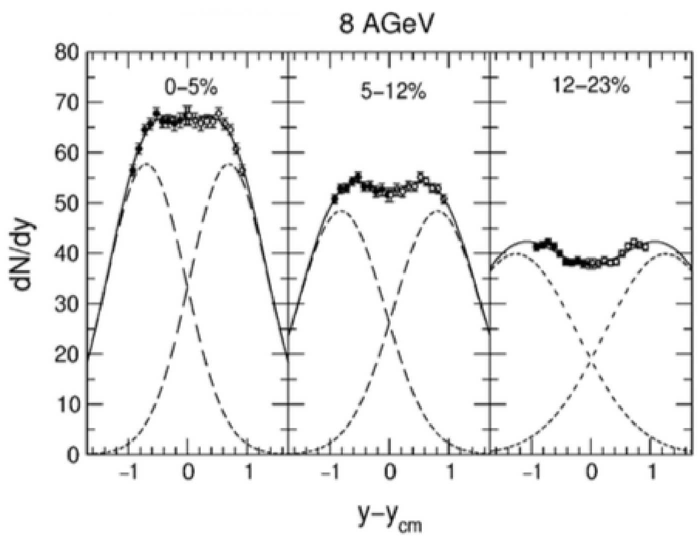

Baryon Transport: rapidity loss, energy available from the collision?

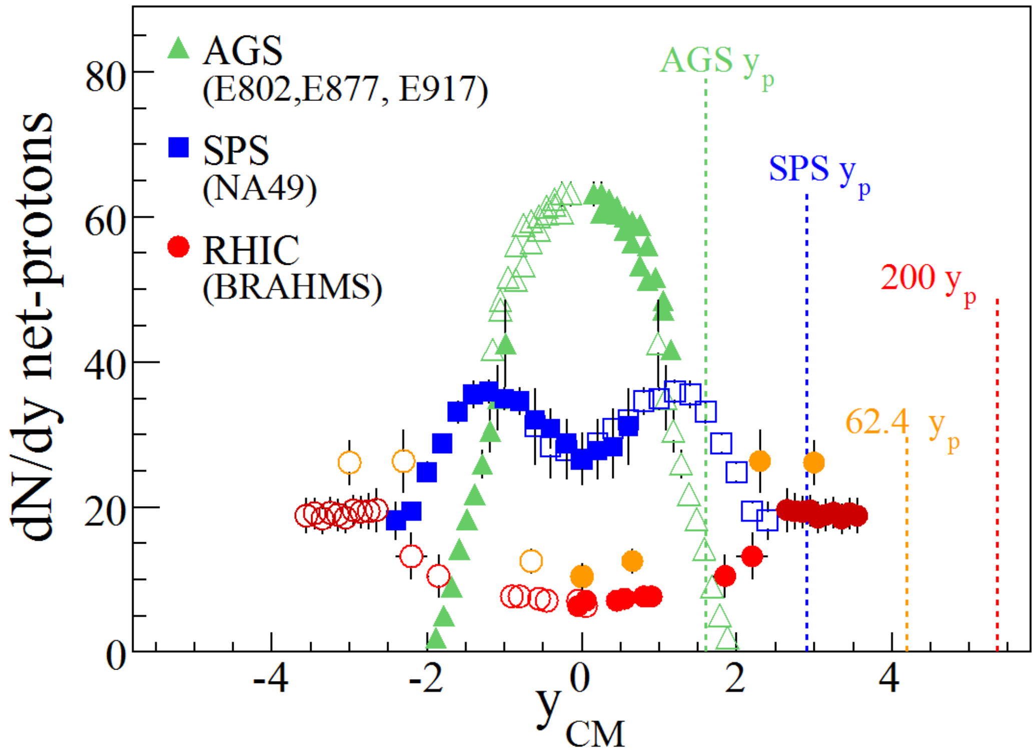

Central collisions Au,
Data from 62 GeV BRAHMS Phys.Lett.B677,677(2009)
High rapidity 200 GeV data

Quantifying rapidity Loss

$$\delta y = y_b - \frac{2}{N_{part}} \int_0^{y_b} y \cdot dN/dy \cdot dy$$

- Conversion to net-Baryon and accounting for un-measured region results in dy = 2.1 at 200 GeV , and 2.0 at 62.4 GeV
- The corresponding energy available for particle production and transverse longitudinal expansion is 72 and 22 GeV per participant nucleon.

Average Rapidity loss

- The average rapidity loss from the 62 GeV data together with previous measurements from AGS,SPS and BRAHMS at 200 GeV
- Slowly increasing or flat trend above SPS energies.

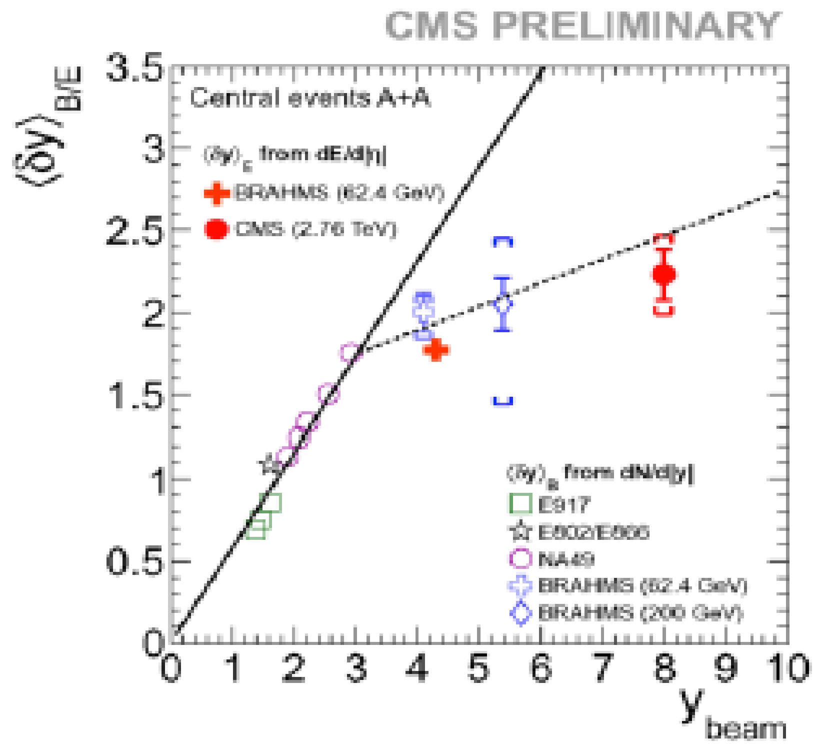

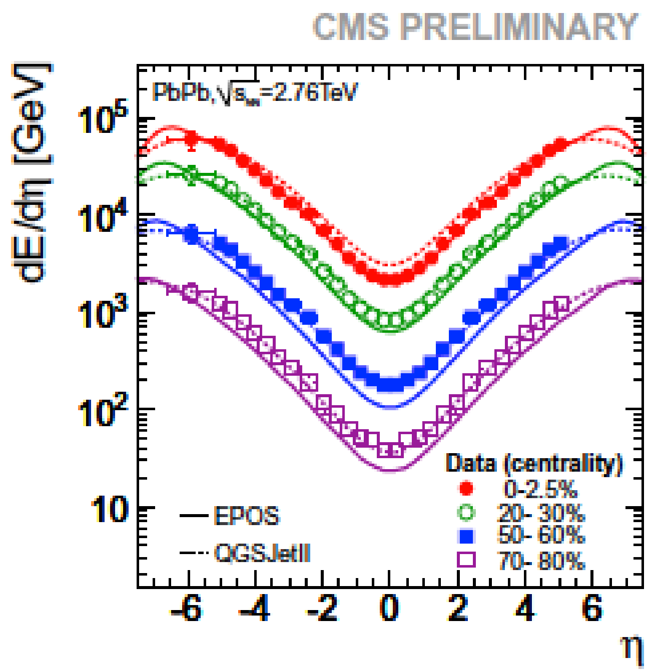

787c–790c

Target/Projectile Baryons

Just like in pA it is of interest to understand the contribution from projectile alone near mid-rapidity.

BRAHMS developed a de-composition that shows a quite general stopping, transport behavior for net-protons.

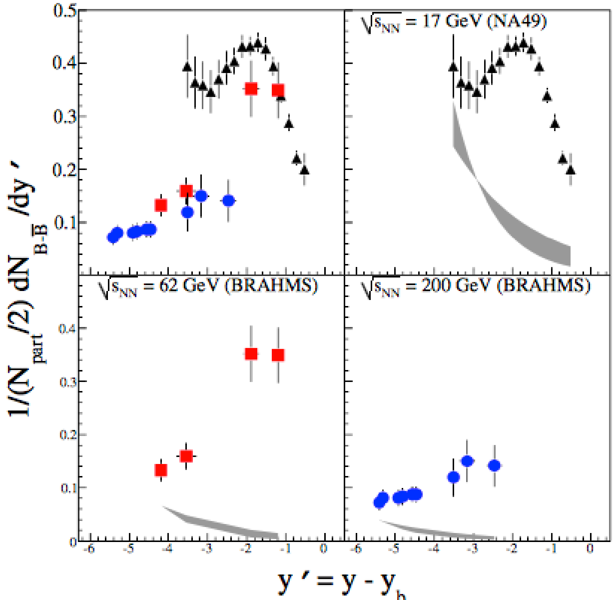

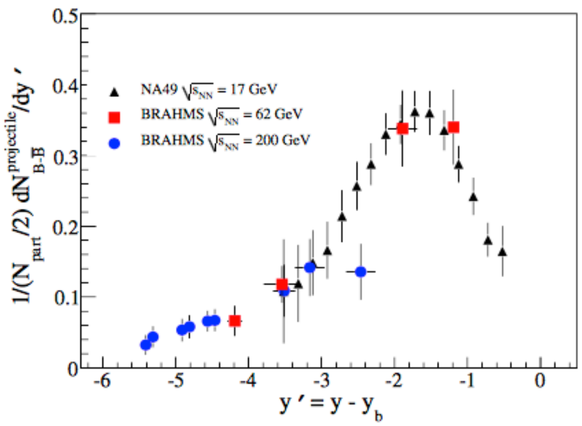

Centrality dependence

- Compare pp and AuAu centrality dependence
- Yield normalized to $N_{part}/2$
- Central collisions exhibits large transport of baryon to mid-rapidity number and energy toward y~0

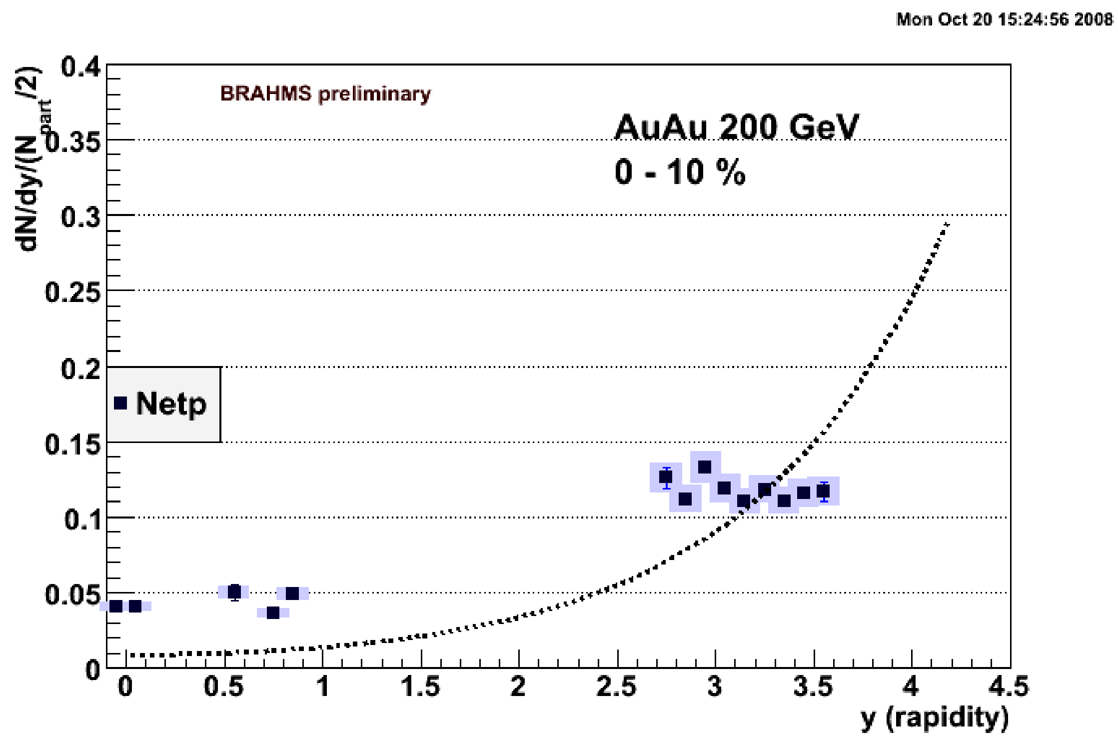

Centrality dependence NA49

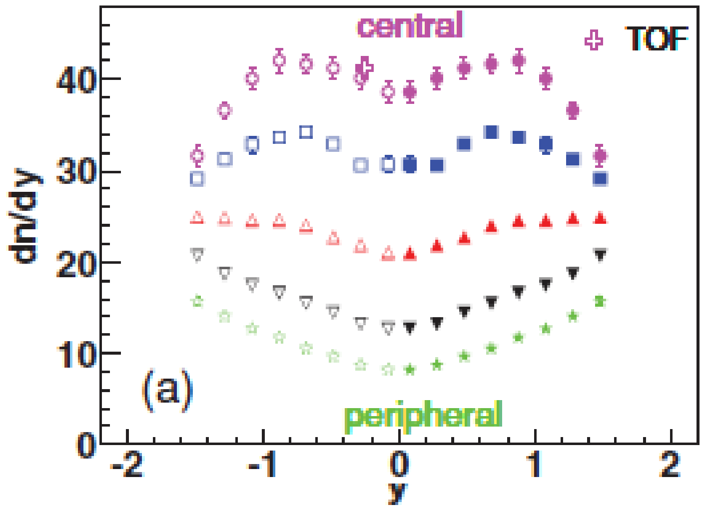

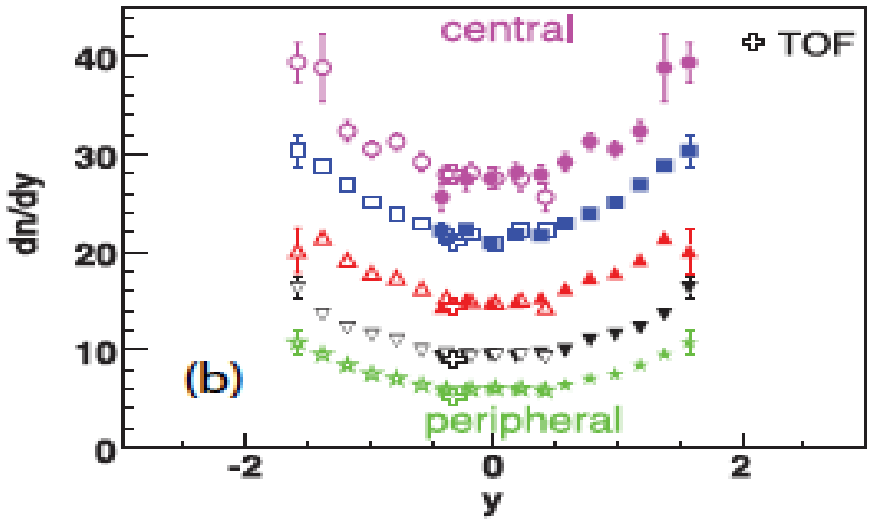

NA49 show similar centrality dependence at 40 and 158 GeV (8.8 and 17.3)

BES observables

- At BES energies several observables are studied for net-protons as underlying variable.
- At these energies produced protons/anti-protons becomes important. Anti-protons are used as proxy for produced protons
- Need to understand how scattering and annihilation may change observables

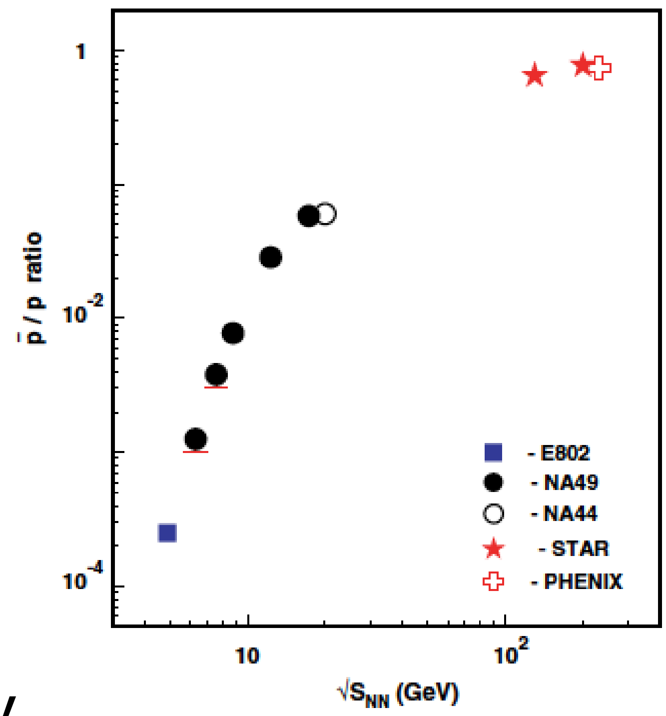

P, pbar vs. centrality

- At high energy both p, pbar grows with centrality, whereas at lower energy (here 17.3) protons rise while p-bar falls

NA49 17.3 GeV

PHENIX

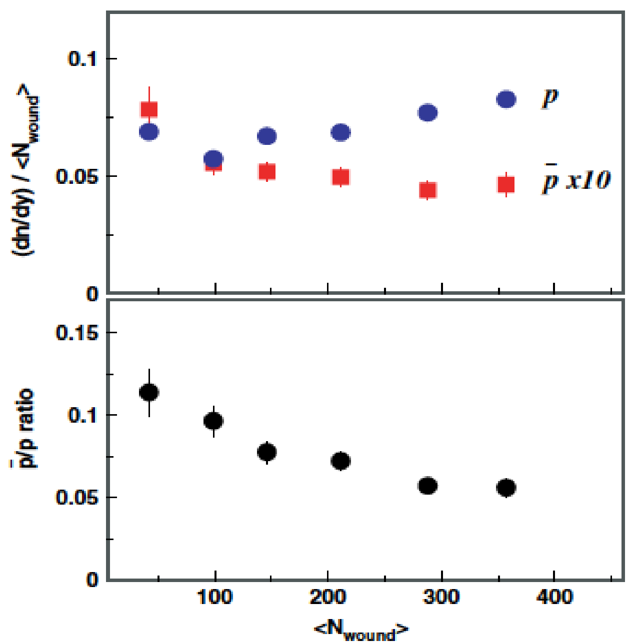

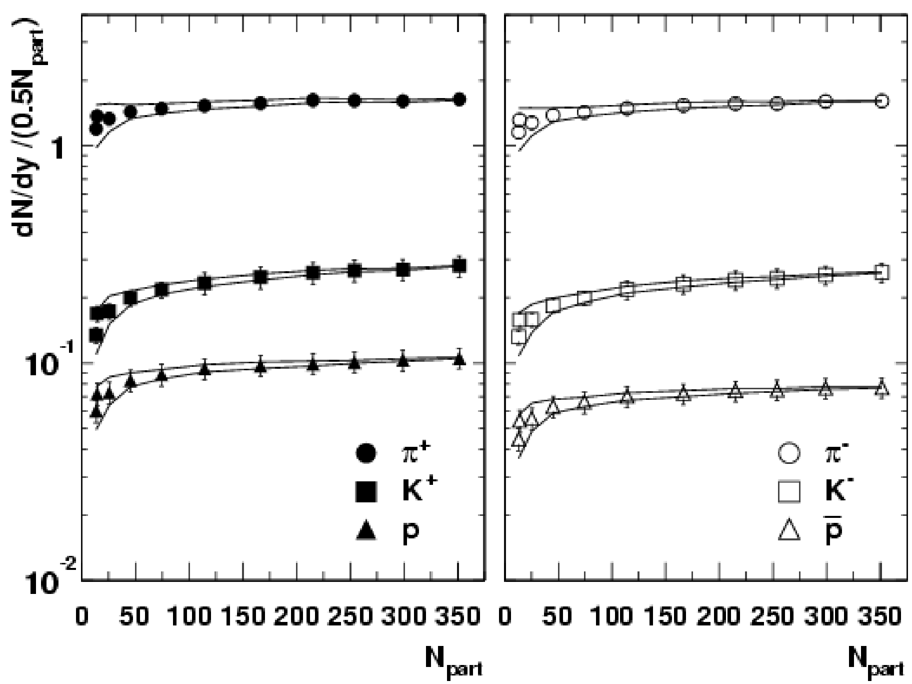

Annihilation

- At low energies annihilation is likely quite important.
- This process could change the kinematics for observed p-bars
- It does of course not change the net-baryon numbers
- Are effects observed in inclusive spectra ?
- No definitive answer from experiment

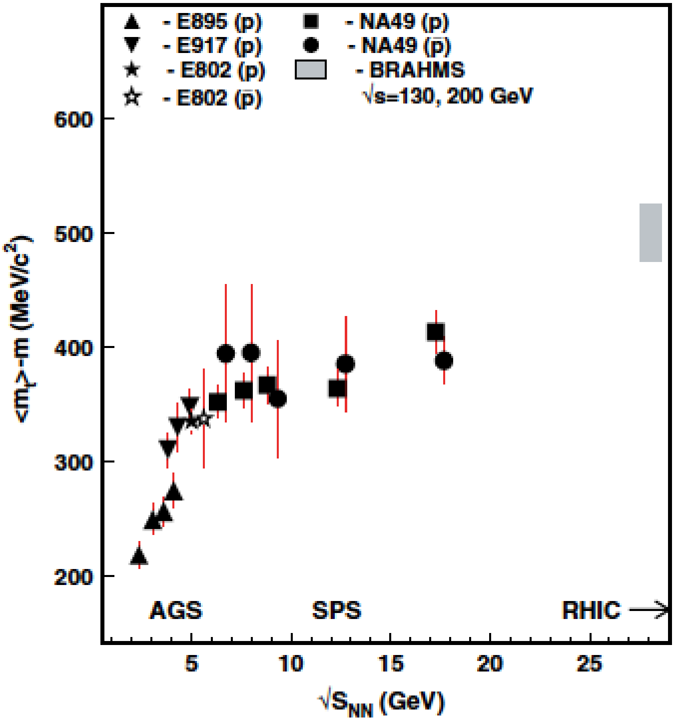

Directed flow

- Protons and anti-protons different trend
- Quantity for net-p extracted under assumption that p-bar is a proxy for the produced protons.
- In addition the pbar/p ratio changes fairy quickly vs. rapidity (e.g. at 17.3 by factor 2 over one unit of rapidity

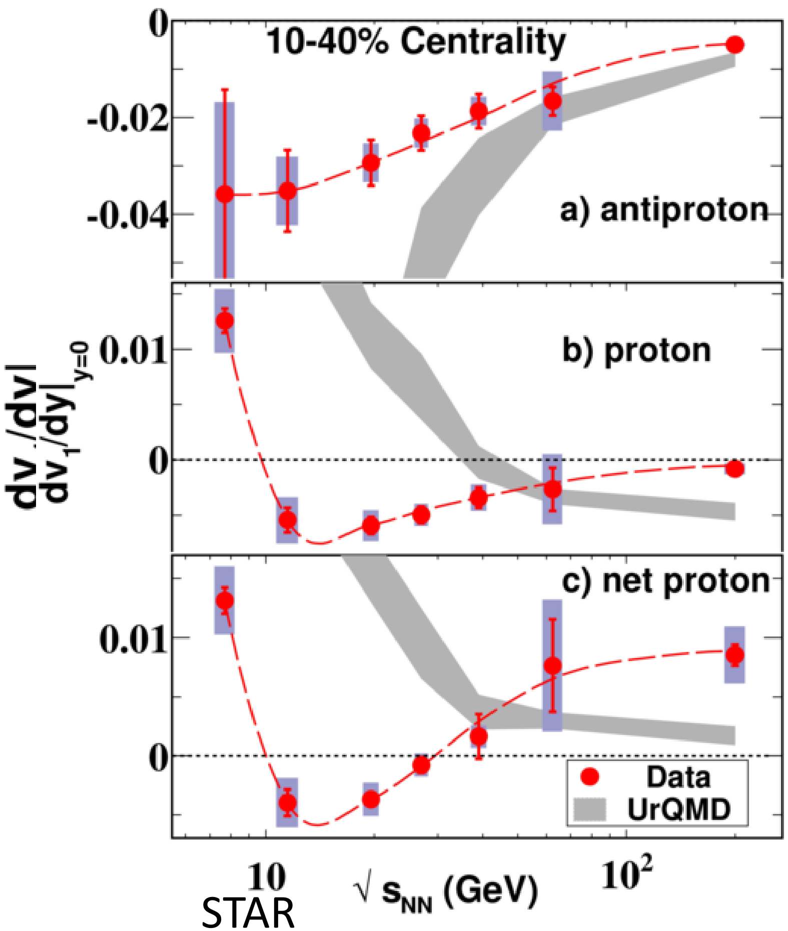

STAR

Phys. Rev. Lett. **108** (2012) 202301

Flow particle vs. anti-particle

- Clear energy dependence is if found for flow difference of particle vs. anti-particle flow
- It has been argued this could be due to transport of baryons (valence quarks) with different underlying basic properties. (Dunlop et.al PRC84,044914(2011)

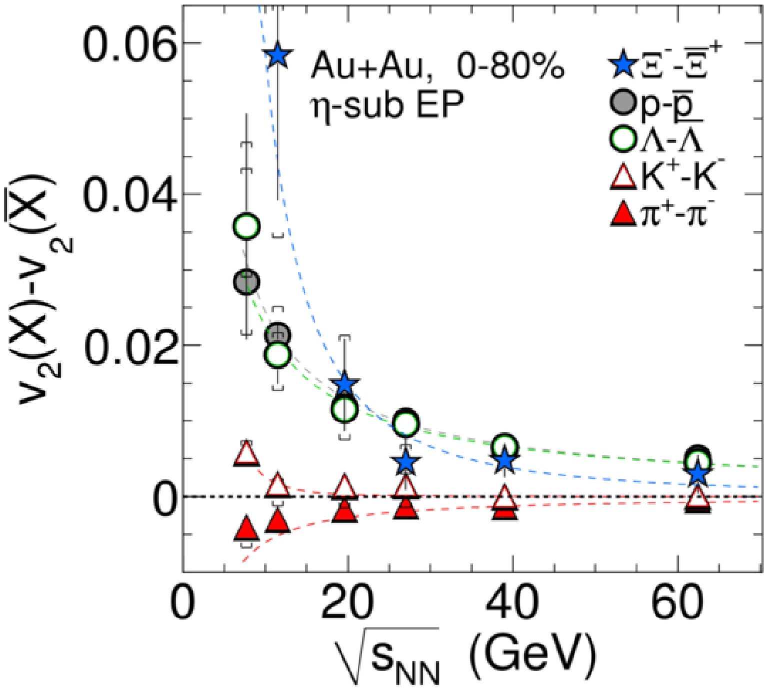

STAR PRL110,142319(2013)

pp Models

- BRAHMS (not published) pp data compared to Pythia and EPOS 1.99/
- The PYTHIA is poor descritiption of net-protons, similar to most other models (QGSM, HSD, ..)
- EPOS has a proper description of dn/dy and thus dn/dx_F flat
- Most other models do not have this feature

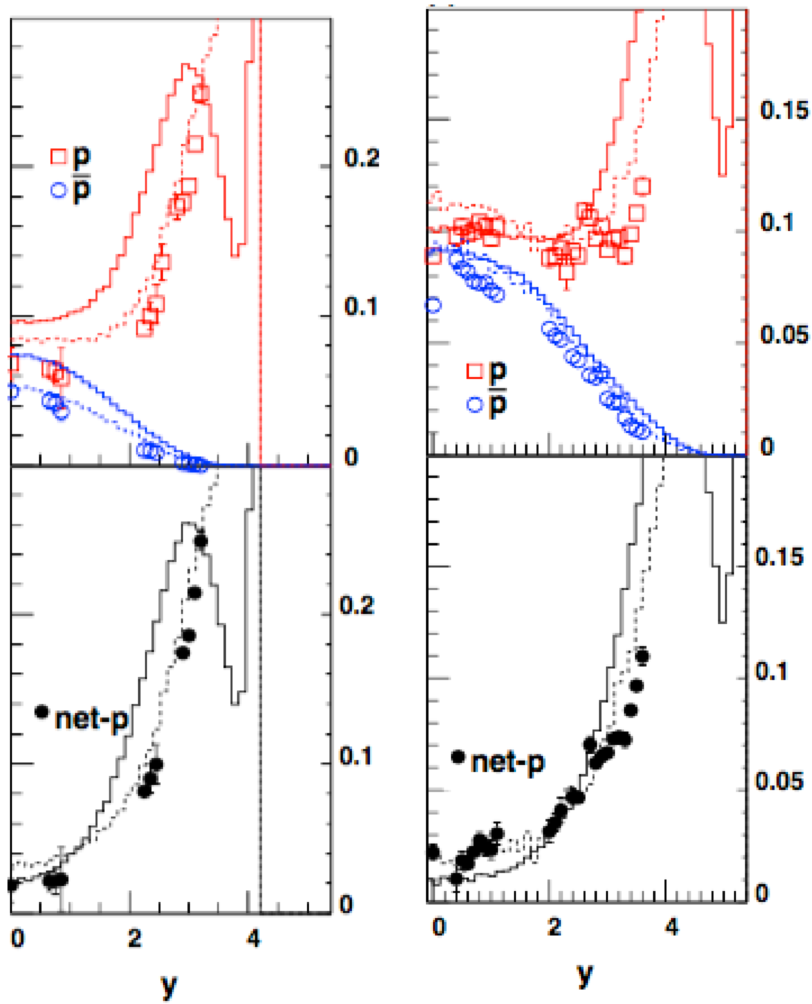

Model Comparisons

A number of comparisons of other observables in the parallel talks and poster; Only example in this talk: net-p

Event generators /transports model have varying success in describing the features of the HI reaction dynamics.

Looks ok, but neither describes the pp

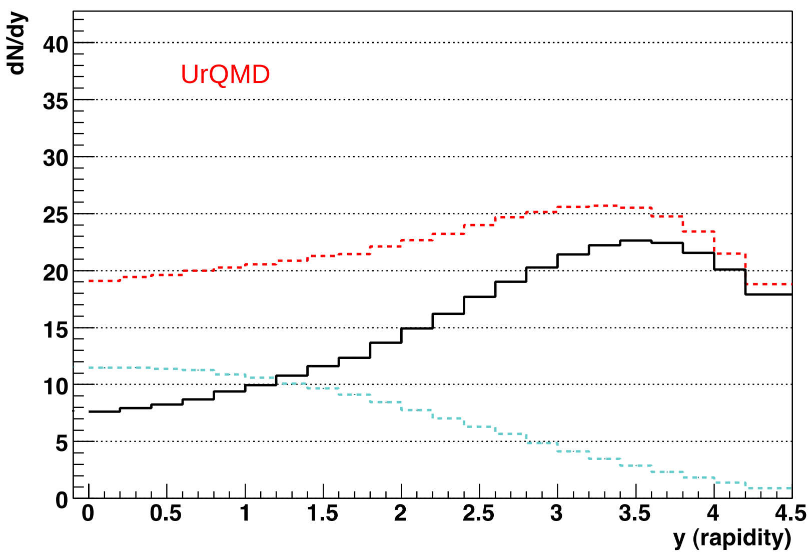

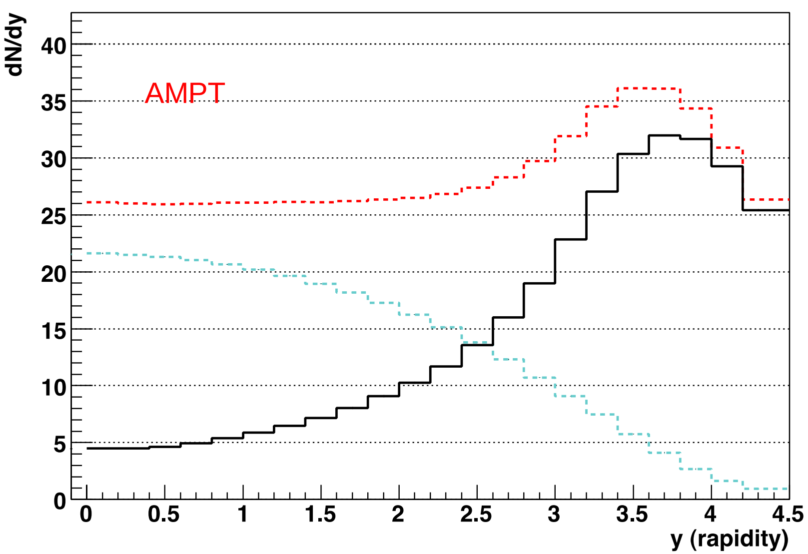

Summary and questions

- Extensive body of proton and p-bar distributions exists in pp ,pA, and AA for a wide range of energies.
- Touches on Baryon transport and stopping.
- Illustrates what could be important
- Disentangling baryon transport from mid-rapidity production gets increasingly difficult at lower energies in part because of absorption effects.
- Will have to rely on modeling to large extend
- In view of current pp data many models do not describe baryon transport in pp. Description of AA might be coincidental.

BACKUP

Ideas

- Effect of Baryons, particular in regard to BES
- Summarize knowledge on spectra p-bar/p
- When will absorption be important?
- Do we see differences in spectra between net-p and produced – RHIC, lower energy?
- What do we see at LHC p-bar/p in pp, AA
- Any sign of non-standard stopping in pp
- Make some preliminary AA data from BRAHMS (Knowville)
- V1-directed flow – refer to Jamie et al speculation on

References

- http://journals.aps.org/prc/abstract/10.1103/PhysRevC.83.014901 NA49, 40 and 158GeV

NA49 newer vs. older data)

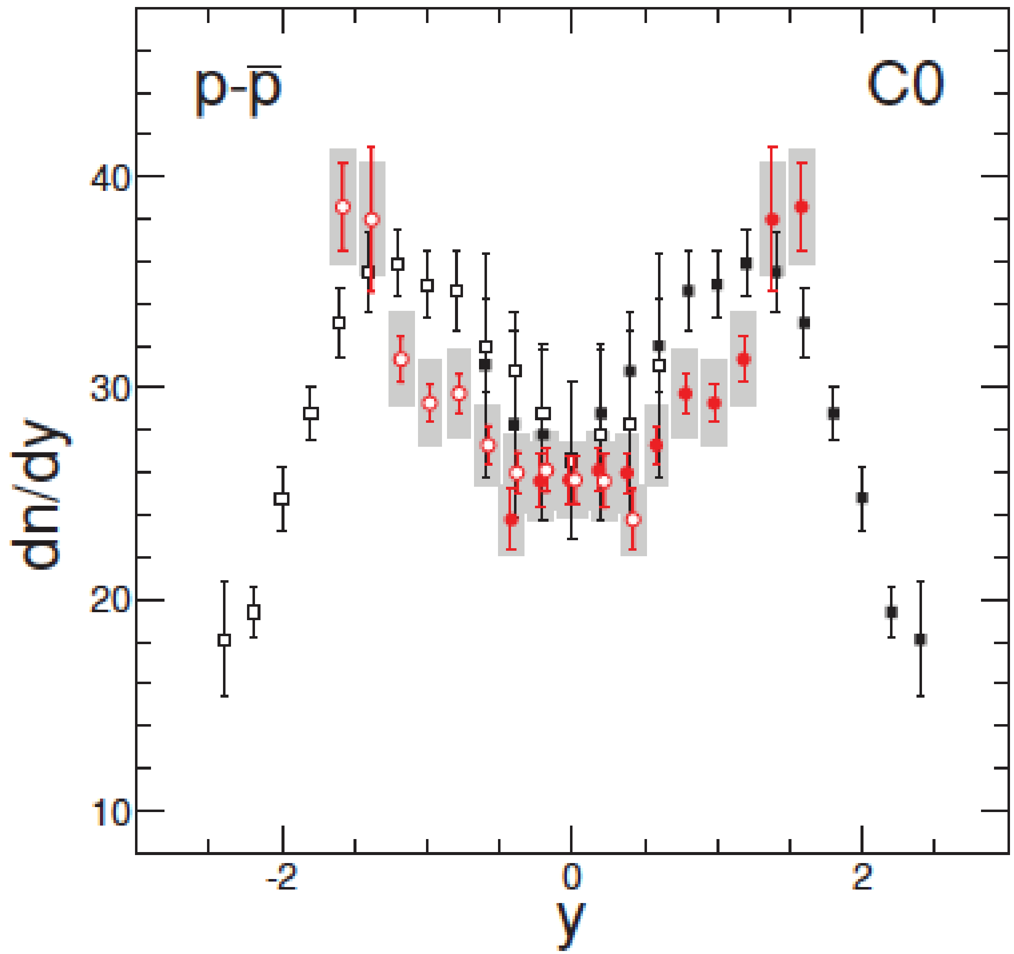

•

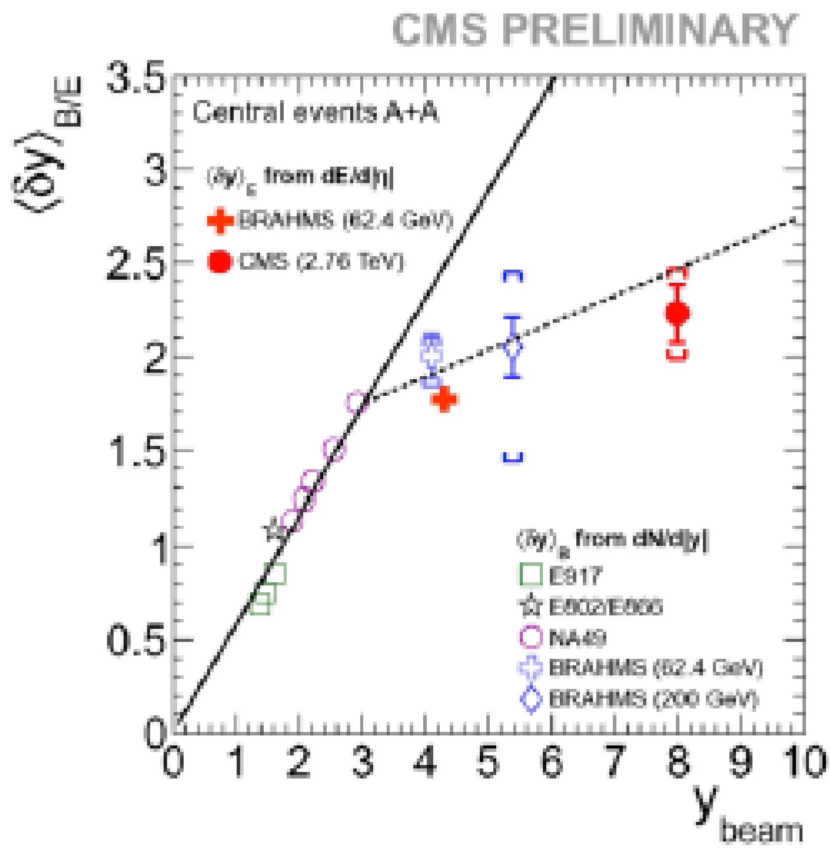

CMS PRELIMINARY
Central events A+A
$\langle \delta y \rangle_E$ from dE/d|η|
BRAHMS (62.4 GeV)
CMS (2.76 TeV)
$\langle \delta y \rangle_B$ from dN/d|y|
E917
E802/E866
NA49
BRAHMS (62.4 GeV)
BRAHMS (200 GeV)
$\langle \delta y \rangle_{B/E}$
y_{beam}

A few words on models

- Not a review of models

Curses and Blessings out of the critical slowing down: the evolution of cumulants in QCD critical regime

Yi Yin

BROOKHAVEN NATIONAL LABORATORY Nuclear Theory Group

Based on: S. Mukherjee, R. Venugopalan and YY, to appear.

Theory and Modeling for the Beam Energy Scan
RBRC-BNL, Feb. 26-27th

Memory effects from Prof. Stephanov

- Thanks for your supervising, collaboration and conversation.

- Such memory will never be washed out.

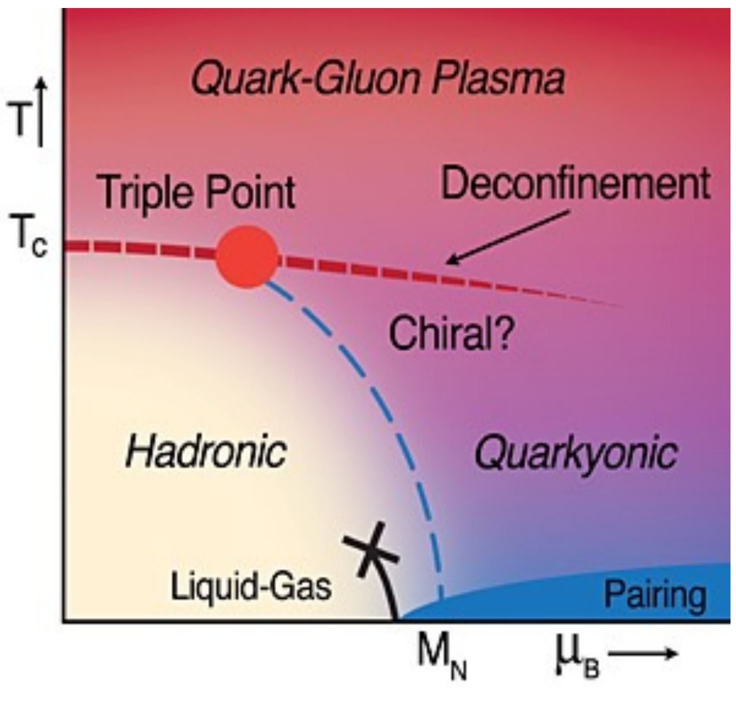

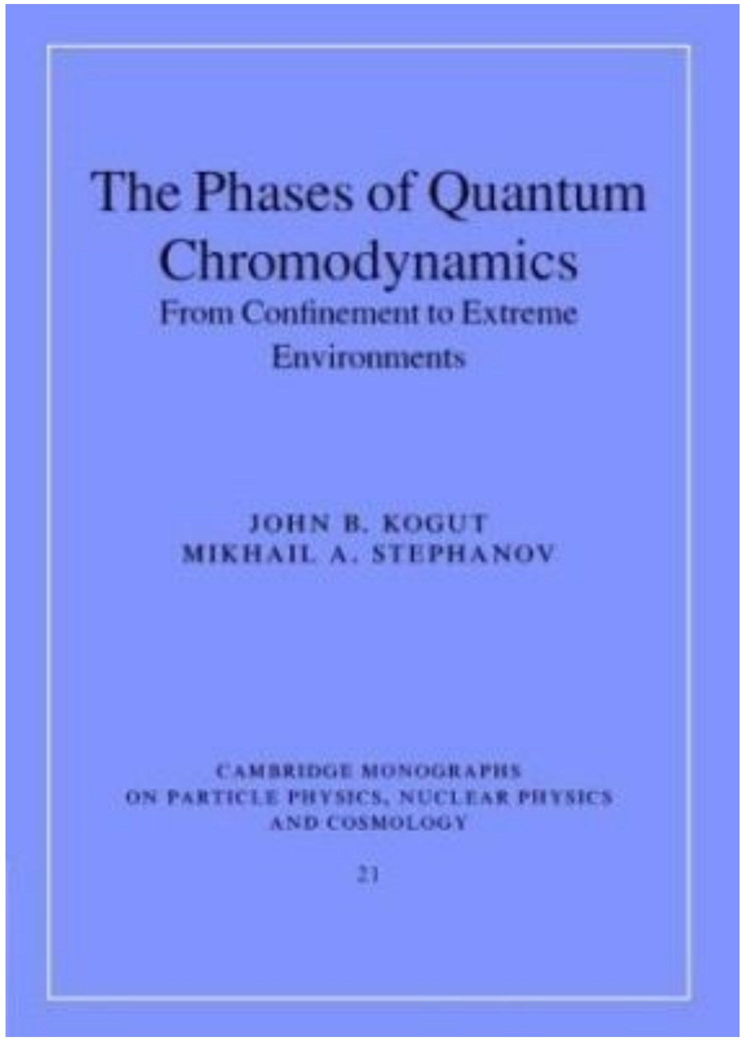

Motivations

- Why cumulants: cumulants, in particular non-Gaussian cumulants are important observables for search for QCD critical point.

- Why real time evolution: fireball only spends a finite time in critical regime, soft-mode in responsible for critical fluctuations is not in equilibrium with the medium.

- Why evolution of the skewness and kurtosis: the sign of them are indefinite. Even a qualitative understanding of their beam energy dependence requires taking memory effects into consideration.

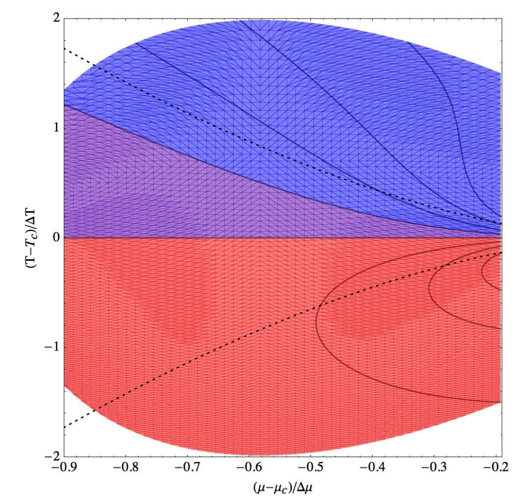

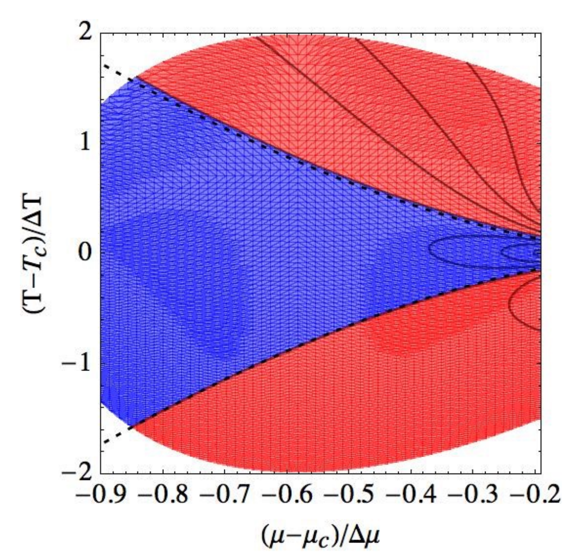

This talk

- Purpose: understand how memory effects would affect the evolution of cumulants, in particular the non-Gaussian ones. Understand the implication of such memory effects for detecting QCD critical point.

- We will focus on the evolution of cumulants(the mean, variance, skewness and kurtosis) of sigma-field in critical regime.

- We will restrict ourselves to the cross-over side of the critical regime but will take universal non equilibrium dynamics into account.

Outline

- Part I: The evolution equations for cumulants.

- Part II: Evolution of cumulants in QCD critical regime.

- Part III: Implications on search for QCD critical point.

Part I: The evolution equations for cumulants.

Moments(cumulants) of σ-field

- We consider zero moment mode of order parameter field σ-field: $\sigma \equiv \frac{1}{V}\int d^3x\, \sigma(\mathbf{x})$.

- Given the probability distribution $P(\sigma;\tau)$, we have (time-dependent) moments

$$\bar{\sigma}(\tau) \equiv \langle \sigma \rangle\,, \qquad \kappa_2(\tau) \equiv \langle (\delta\sigma(\tau))^2 \rangle\,, \qquad \kappa_3(\tau) \equiv \langle (\delta\sigma(\tau))^3 \rangle\,,$$

$$\kappa_4(\tau) \equiv \langle (\delta\sigma(\tau))^4 \rangle - 3\kappa_2^2(\tau) \qquad \delta\sigma \equiv \sigma - \bar{\sigma}(\tau)\,.$$

- We define Skewness and Kurtosis which are independent of the normalization of σ-field(but depends on the volume of the system):

$$S(\text{Skewness}) \equiv \frac{\kappa_3}{\kappa_2^{3/2}}\,, \qquad K(\text{Kurtosis}) \equiv \frac{\kappa_4}{\kappa_2^2}\,.$$

Fluctuations in Equilibrium in 3d Ising Model universality class

- Equilibrium distribution $P_0(\sigma) \sim \exp\left(-V\Omega_0(\sigma)/T\right)$ with the free-energy(density)($m_\sigma^{-1} \equiv \xi_{\rm eq}$)

$$\Omega_0(\sigma) = \frac{1}{2}m_\sigma^2\left(\sigma - \sigma_0\right)^2 + \frac{\lambda_3}{3}\left(\sigma - \sigma_0\right)^3 + \frac{\lambda_4}{4}\left(\sigma - \sigma_0\right)^4 ,$$

- Universality scaling($V_4 \equiv V/T$):

$$\sigma_0 \sim \tilde{\sigma}_0 T(T\xi)^{-1/2}, \qquad \lambda_3 \sim \tilde{\lambda}_3(T\xi)^{-3/2}, \qquad \lambda_4 \sim \tilde{\lambda}_4(T\xi)^{-1}.$$

- The equilibrium moments are given by:

$$\kappa_2^{\rm eq} = \frac{\xi_{\rm eq}^2}{V_4}\left[1 + \mathcal{O}(\epsilon^2)\right] , \qquad \kappa_3^{\rm eq} = -\frac{2\xi_{\rm eq}^6}{V_4^2}\lambda_3 , \qquad \kappa_4^{\rm eq} = \frac{6\xi_{\rm eq}^8}{V_4^3}\left[2(\lambda_3\xi)^2 - \lambda_4\right] ,$$

- It is convenient to rescale the quantity by the width of the equilibrium distribution, we observe hierarchy ϵ for different cumulants.

$$b \equiv \sqrt{\frac{1}{V_4 m_\sigma^2}},$$

- For rescaled moments, $\tilde{\kappa}_n \equiv \kappa_n/b^n , \qquad n = 2, 3, 4, \ldots ,$

$$\tilde{\kappa}_2^{\rm eq} = 1 + \mathcal{O}(\epsilon^2) , \qquad \tilde{\kappa}_3^{\rm eq} = -2\tilde{\lambda}_3\epsilon , \qquad \tilde{\kappa}_4^{\rm eq} = 6\left[2(\tilde{\lambda}_3)^2 - \tilde{\lambda}_4\right]\epsilon^2 , \qquad \epsilon \equiv \sqrt{\frac{\xi_{\rm eq}^3}{V}} .$$

The evolution of non-equilibrium $P(\sigma;\tau)$

- Fokker-Planck equation descrbies the relaxation of non-equilibrium distribution $P(\sigma,\tau)$ towards the equilibrium distribution(Hohenberg-Halperin, 1977),

$$\partial_\tau P(\sigma;\tau) = \frac{1}{m_\sigma^2 \tau_{\text{eff}}} \left\{ \partial_\sigma \left[\partial_\sigma \Omega_0(\sigma) + V_4^{-1} \partial_\sigma \right] P(\tilde{\sigma};\tau) \right\}, \qquad \tau_{\text{eff}} \sim \xi^z$$

- The information on the evolution of all cumulants are encoded in Fokker-Planck equation. However, it not easy to gain intuition on how non-Gaussian cumulants evolves by solving it numerically.

- Can one find a a set of equation which directly describe the evolution of cumulants we are interested in$(\bar{\sigma}, \kappa_2, \kappa_3, \kappa_4)$?

A set of equation of cumulants evolution

- We derive, to leading order in $\epsilon = \sqrt{\xi^3/V}$($\xi$ is larger than microscopic scale but smaller than the size of the system), a set of equation from Fokker-Planck equation for $\bar{\sigma}, \kappa_2, \kappa_3, \kappa_4$(S. Mukherjee, R. Venugopalan and YY, to appear.):

$$b^{-1}\partial_\tau \bar{\sigma}(\tau) = -\tau_{\text{eff}}^{-1}\left[(\frac{\bar{\sigma}-\sigma_0}{b}) F_1(\bar{\sigma}) \right] [1+\mathcal{O}(\epsilon)] \ ,$$

$$b^{-2}\partial_\tau \kappa_2(\tau) = -2\tau_{\text{eff}}^{-1} \left[F_2(\bar{\sigma})\tilde{\kappa}_2 - 1 \right] [1+\mathcal{O}(\epsilon)] \ ,$$

$$b^{-3}\partial_\tau \kappa_3(\tau) = -3\tau_{\text{eff}}^{-1} \left[F_2(\bar{\sigma})\tilde{\kappa}_3(\tau) + \epsilon F_3(\bar{\sigma}) \left(\tilde{\kappa}_2(\tau)\right)^2 \right] [1+\mathcal{O}(\epsilon)] \ ,$$

$$b^{-4}\partial_\tau \kappa_4(\tau) = -4\tau_{\text{eff}}^{-1} \left[F_2(\bar{\sigma})\tilde{\kappa}_4(\tau) + 3\epsilon F_3(\bar{\sigma}) \left(\tilde{\kappa}_2(\tau)\tilde{\kappa}_3(\tau)\right) + \epsilon^2 F_4 \left(\tilde{\kappa}_2\right)^2 \right] [1+\mathcal{O}(\epsilon)] \ .$$

  $F_n(\bar{\sigma}), n = 1,2,3,4$ are polynomials of $\bar{\sigma}$ and only depends on the equilibrium properties of the system.

- Derivation is straightforward by substituting σ^n into Fokker-Planck equation and integrate over σ.

The Gaussian limit

- If the equilibrium distribtuion is Gaussian: $\tilde{\Omega}_0(\sigma) = \frac{1}{2}\left(\tilde{\sigma} - \tilde{\sigma}_0\right)^2, (\kappa_2^{\mathrm{eq}}(\tau) = b^2(\tau)\,, \kappa_3^{\mathrm{eq}} = \kappa_4^{\mathrm{eq}} = 0)$, the evolution among cumulants decouple:

$$\partial_\tau \bar{\sigma} = -\tau_{\mathrm{eff}}^{-1}\left[\bar{\sigma}(\tau) - \sigma_0(\tau)\right]\,, \qquad \partial_\tau \kappa_2(\tau) = -2\tau_{\mathrm{eff}}^{-1}\left[\kappa_2(\tau) - k_2^0(\tau)\right]\,,$$

$$\partial_\tau \kappa_3(\tau) = -3\tau_{\mathrm{eff}}^{-1}\kappa_3(\tau)\,, \qquad \partial_\tau \kappa_4(\tau) = -4\tau_{\mathrm{eff}}^{-1}\kappa_4(\tau)\,.$$

- Simple relaxation equaiton, any non-Gaussian cumulants will be damped.
- If one defines non-equilibrium correlation length $\xi(\tau) \equiv \sqrt{V_4\kappa_2(\tau)}$. In the near equilibrium limit, it can be matched to equation used by Berdnikov-Rajagopal:

$$\partial_\tau\left[\xi^{-1}(\tau)\right] = -\tau_{\mathrm{eff}}^{-1}\left[\xi^{-1}(\tau) - \xi_{\mathrm{eq}}^{-1}(\tau)\right]\,.$$

Near equilibrium limit

- If $\sigma \to \sigma_0$ and the deviation from equilibrium of cumulants is small $\delta\tilde{\kappa}_n \equiv \tilde{\kappa}_n - \tilde{\kappa}_n^{\text{eq}}$

$$\partial_\tau \bar{\sigma}(\tau) = -\tau_{\text{eff}}^{-1}\left(\bar{\sigma} - \sigma_0\right), \qquad b^{-1}\partial_\tau \kappa_2(\tau) = -2\tau_{\text{eff}}^{-1}\delta\tilde{\kappa}_2(\tau),$$

$$b^{-3}\partial_\tau \kappa_3(\tau) = -3\tau_{\text{eff}}^{-1}\left[\delta\tilde{\kappa}_3(\tau) + 4\epsilon\tilde{\lambda}_3\delta\tilde{\kappa}_2(\tau)\right],$$

$$b^{-4}\partial_\tau \kappa_4(\tau) = -4\tau_{\text{eff}}^{-1}\{\delta\tilde{\kappa}_4(\tau) + 6\epsilon\tilde{\lambda}_3\delta\tilde{\kappa}_3 - 12\epsilon^2\left[(\tilde{\lambda}_3)^2 - \tilde{\lambda}_4\right]\delta\tilde{\kappa}_2\}.$$

- Coupled evolution. Lower moments will be relaxed back to the equilibrium first.

Summary of Part I:

- We have derived a set of equations for the evolution of cumulants.

- The evolution of non-Gaussian cumulants are coupled to the Gaussian cumulant and the mean.

- We now apply it to the QCD critical regime.

Phenomenological inputs

- We will apply our equations to study the evolution of cumulants in QCD critical regime. We therefore need phenomenological inputs.
- We define the scaling regime with the criterion: $\xi_{min} < \xi_{\rm eq} < \xi_{\rm max}$ and to be specific, we will take $\xi_{\rm max}/\xi_{\rm min} = 3$ below.
- The equilibrium distribution is known in Ising variables r, h. We need to map them to QCD variables T, μ_B.(Non-universal, major uncertainty). We use linear mapping with $\Delta T, \Delta\mu$ the width of critical regime in QCD phase diagram.

$$\frac{T - T_c}{\Delta T} = -\frac{h}{\Delta h}, \qquad \frac{\mu - \mu_c}{\Delta\mu} = -\frac{r}{\Delta r}.$$

- Parametrization of $\tau_{\rm eff}$ on $\xi_{\rm eq}$ is universal:$\tau_{\rm rel}$ the relaxation time at $\xi = \xi_{\rm min}$.

$$\tau_{\rm eff} = \tau_{\rm rel}\left(\frac{\xi}{\xi_{\rm min}}\right)^z .$$

and we use Model H, $z = 3$.

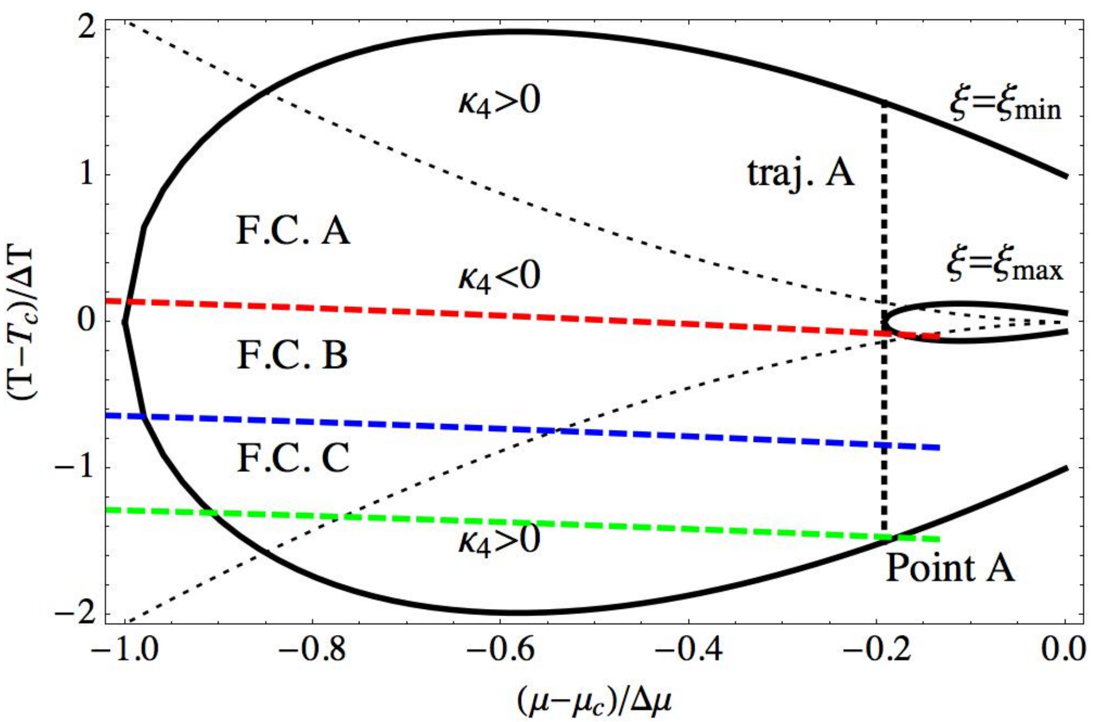

Trajectory

- We will assume for each trajectory, the μ_B of the fireball is constant. It would then be corresponding to a vertical line in the critical regime due to our mapping relation.
- Along each trajectory, we parametrize the evolution of volume and temperature by expansion rate $n_V = 3$ and speed of sound c_s^2:

$$\frac{V(\tau)}{V_I} = \left(\frac{\tau}{\tau_I}\right)^{n_V}, \qquad \frac{T(\tau)}{T_I} = \left(\frac{\tau}{\tau_I}\right)^{-n_V c_s^2},$$

where V_I, T_I are volume and temperature of the system at τ_I, the time when the trajectory hits the boundary of critical regime.

- Initial condition: we will assume $\bar{\sigma}, \kappa_2, \kappa_3, \kappa_4$ equal to their equilibrium value at $\tau = \tau_I(\tau_{\text{eff}}$ is small).

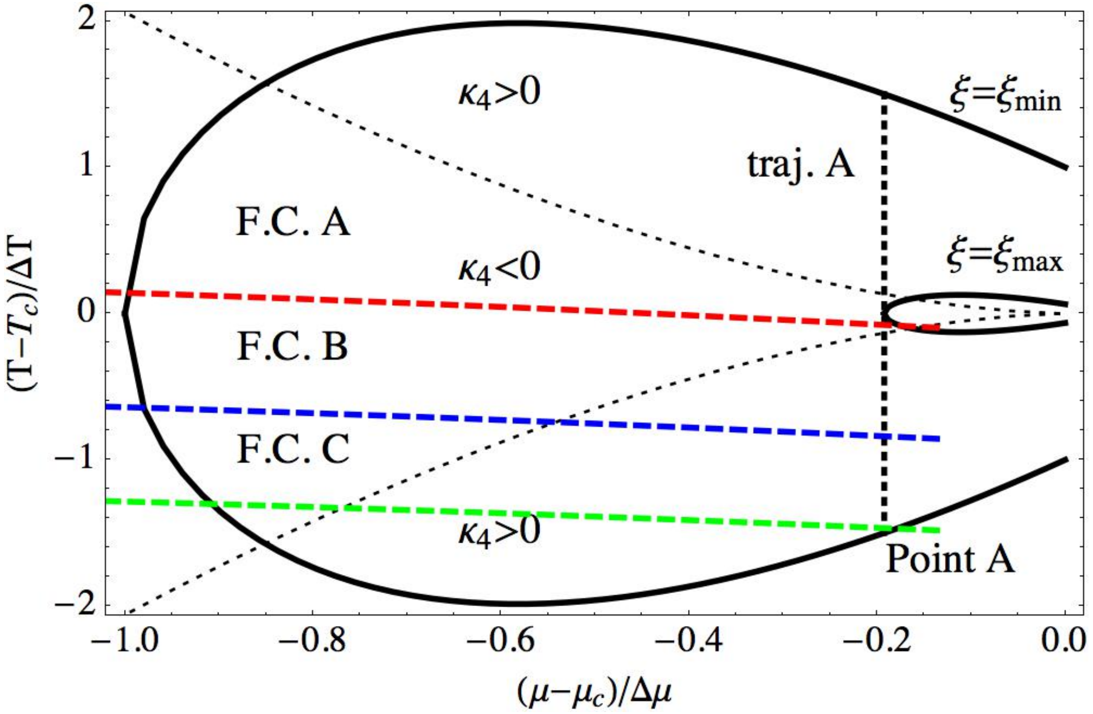

Part II: Evolution of cumulants in QCD critical regime.

The evolutions

- Only one free parameter: $\tau_{\mathrm{rel}}/\tau_I$

- We have solved evolution equations along trajectories passing through the critical regime.

- We label the trajectory crossing the critical regime by the corresponding temperature and will present the non-equilibrium value with different choices of relaxation time.

- We rescale our results by the corresponding equilibrium value at point A.

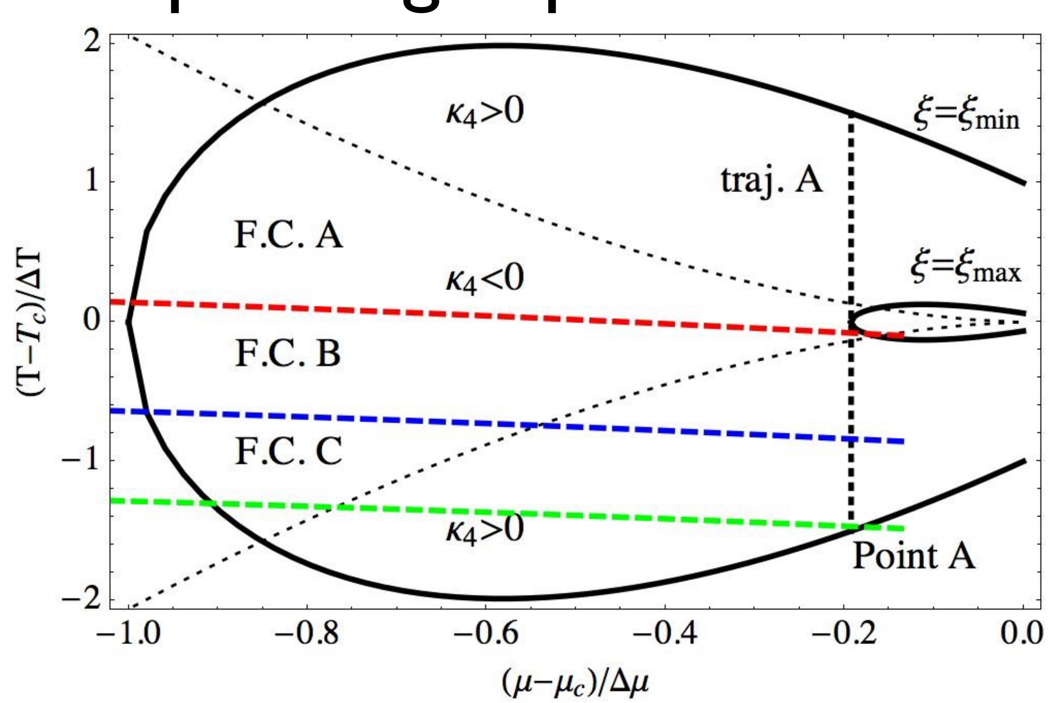

Evolution of magnetization $\bar{\sigma}$

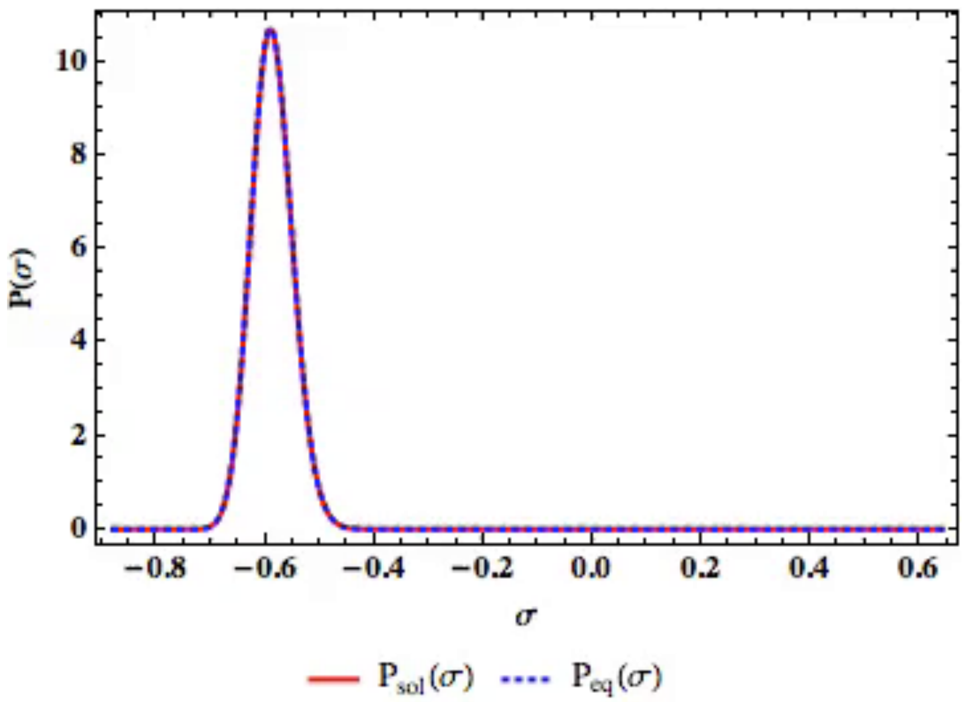

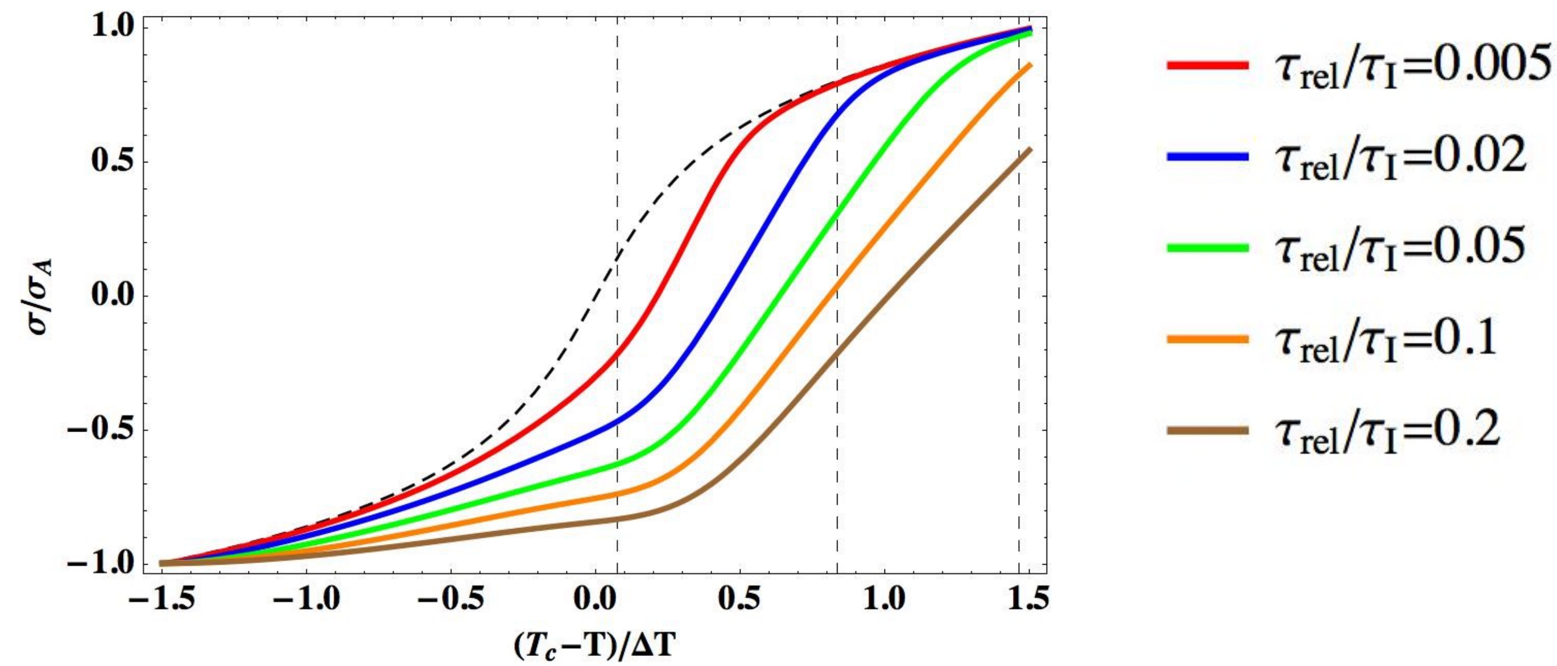

- $\bar{\sigma}$ tend to approach its equilibrium value but still fall behind

- As expected, the slowing down is most visible around Tc where the equilibrium correlation becomes large.

Evolution of Gaussian moment

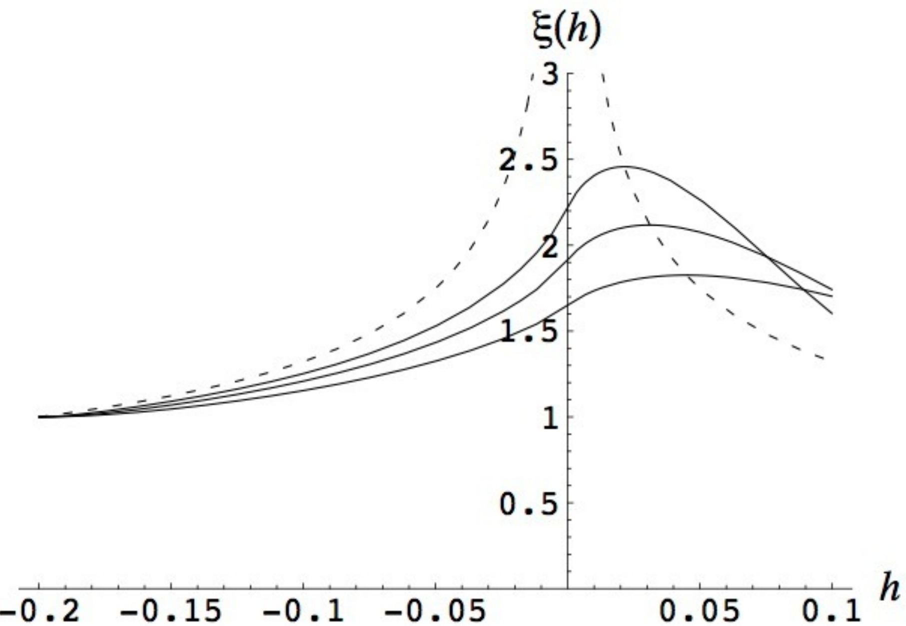

Berdnikov-Rajagopal, 2000

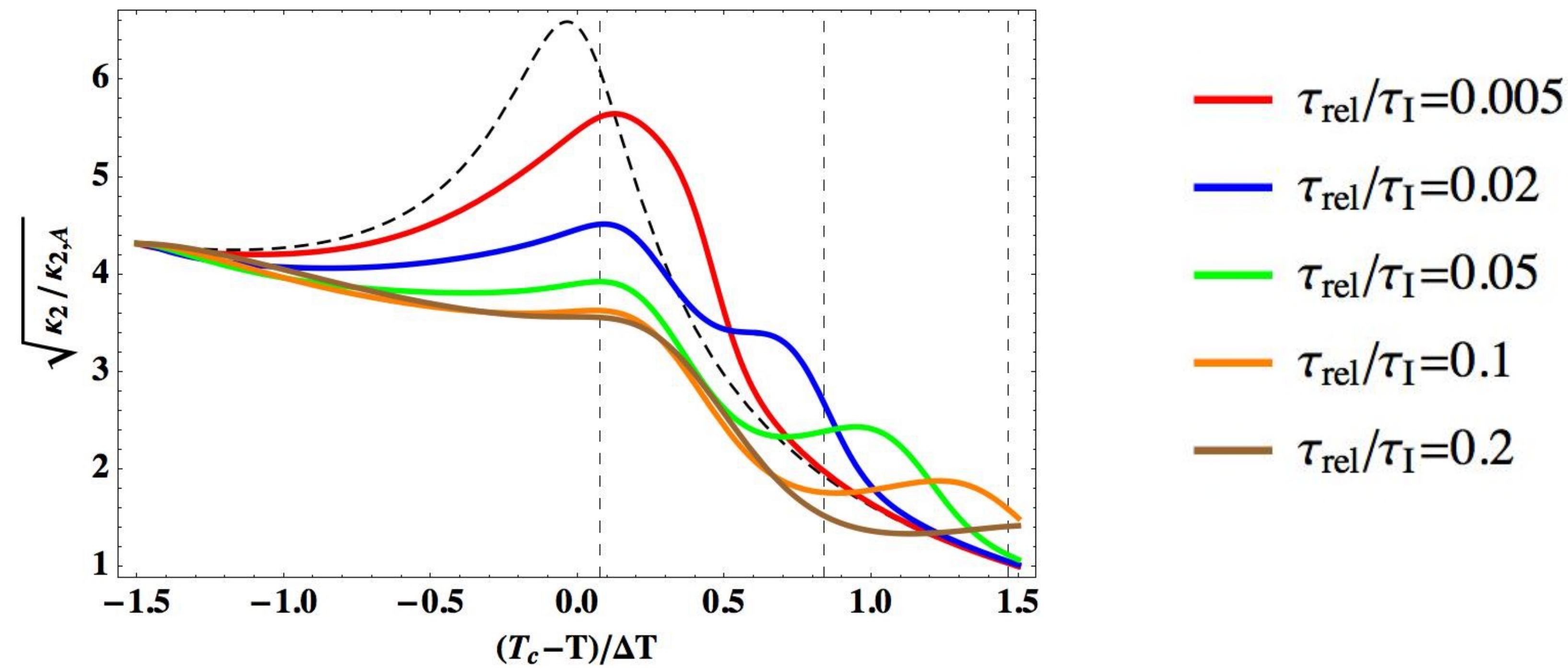

Evolution of variance along a representative trajectory

- The effects of critical slowing down would delay the growth of non-equilibrium length.

- On the other hand, memory effect also protects the memory of the system in critical regime from being completely washed out.
  - Similar to previous results.

Skewness and Kurtosis

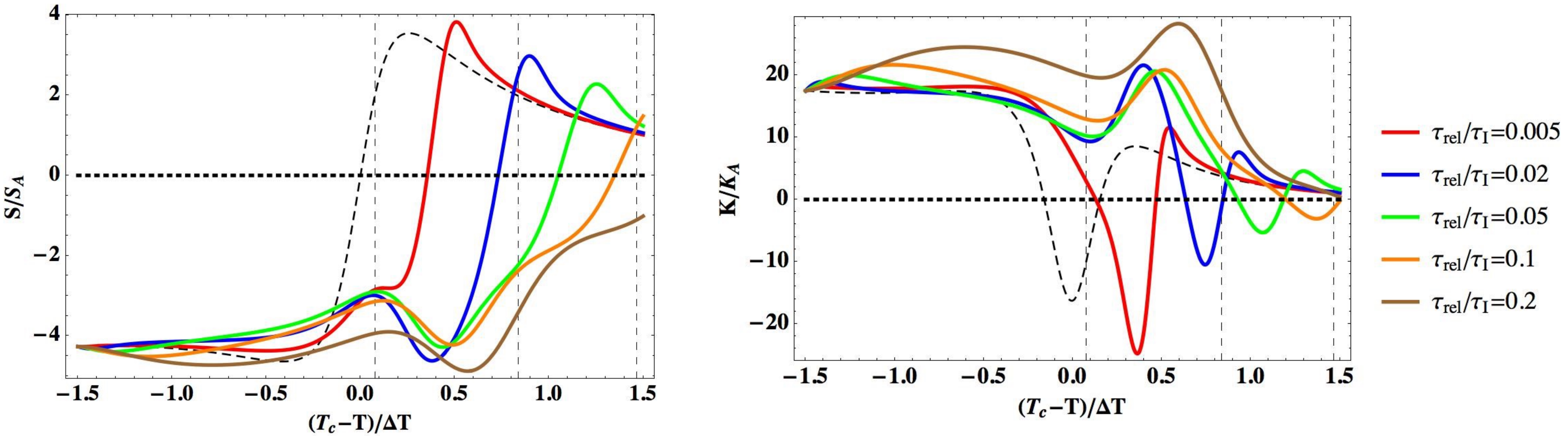

Evolution of skewness and kurtosis along a representative trajectory

- The evolution of higher cumulants might not follow the equilibrium moments (low moments will affect the evolution of the higher one).
- Depending on the temperature at which you take the snapshot, the non-equilibrium value can be substantially different(including sign) from the equilibrium one.
- Evolution of higher cumulants has a richer pattern(the evolution equations are coupled.)

Quick Synopsis

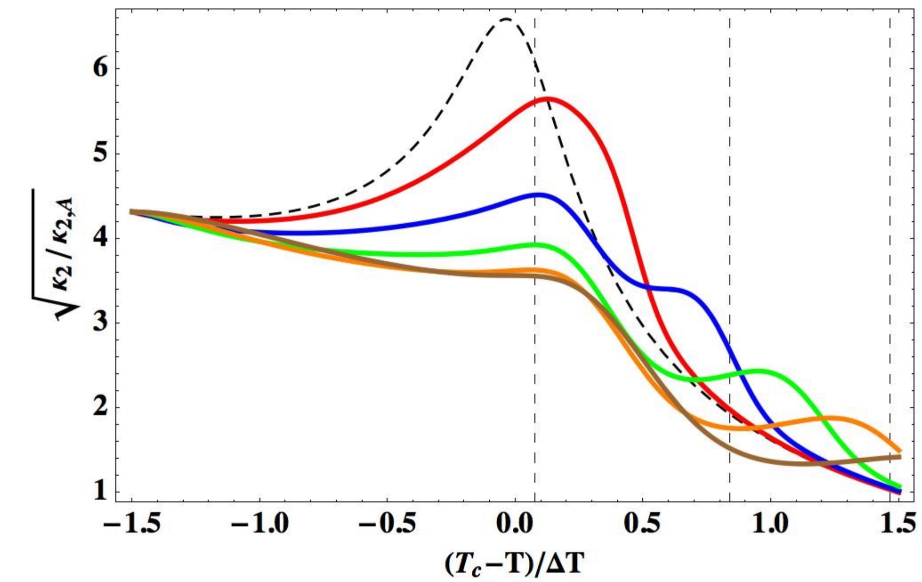

- Memory effects are important.

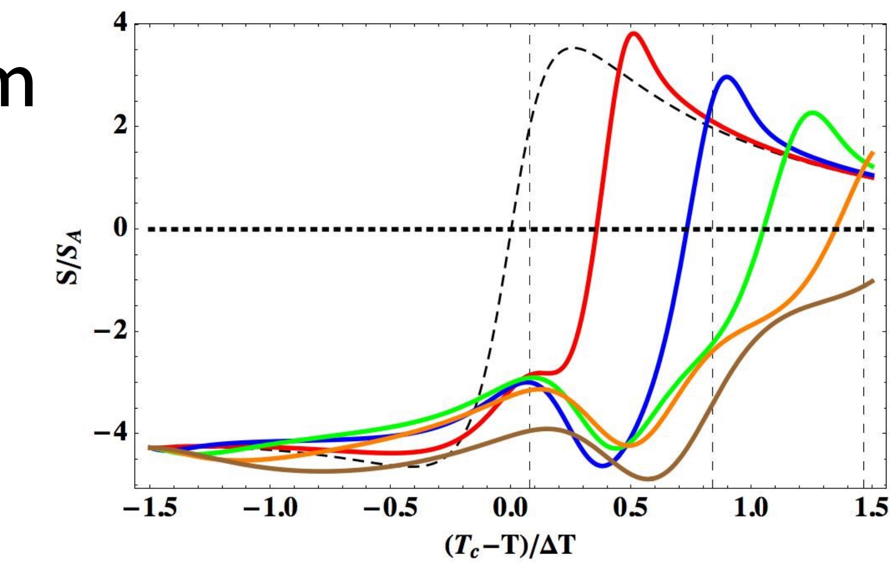

- Gaussian cumulants approach equilibrium first, then higher cumulants.

- The tails of evolutions for different relaxation times exhibit possible self-similarity behavior(finite time scaling?).

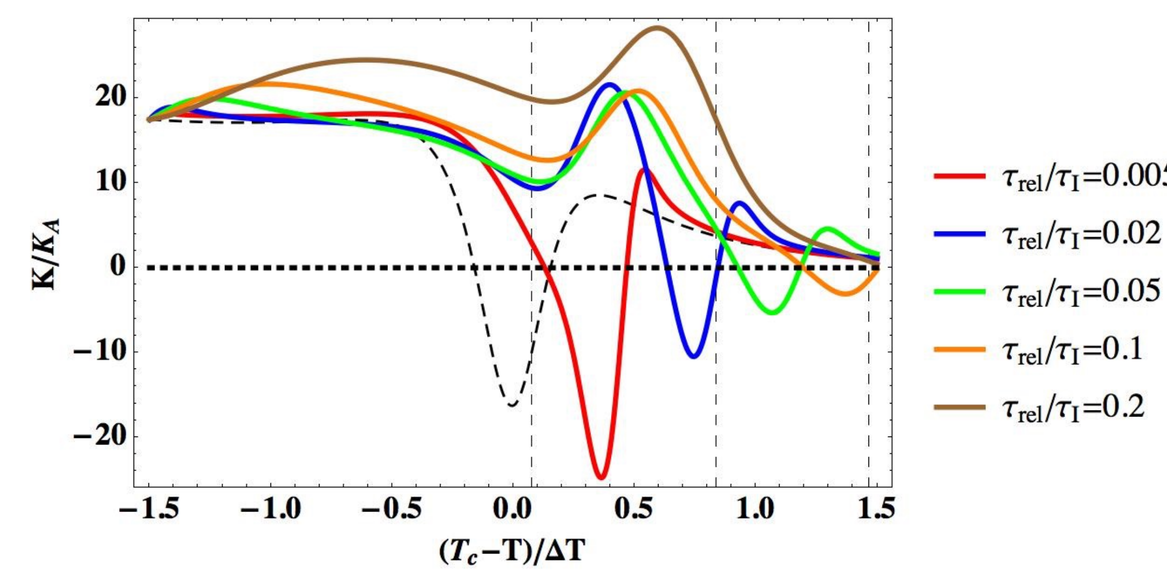

Part III: Implications of results for the search for QCD critical point

Mimicking Beam Energy Scan

- To mimic the beam energy scan, we also solved the evolution equations for all constant μ trajectories. We therefore obtain non-equilibrium at each point in the critical regime.
- We now examine the memory effects on BES scan.
- We will concentrate on the Skewness and Kurtosis and will start with their most prominent feature: sign.

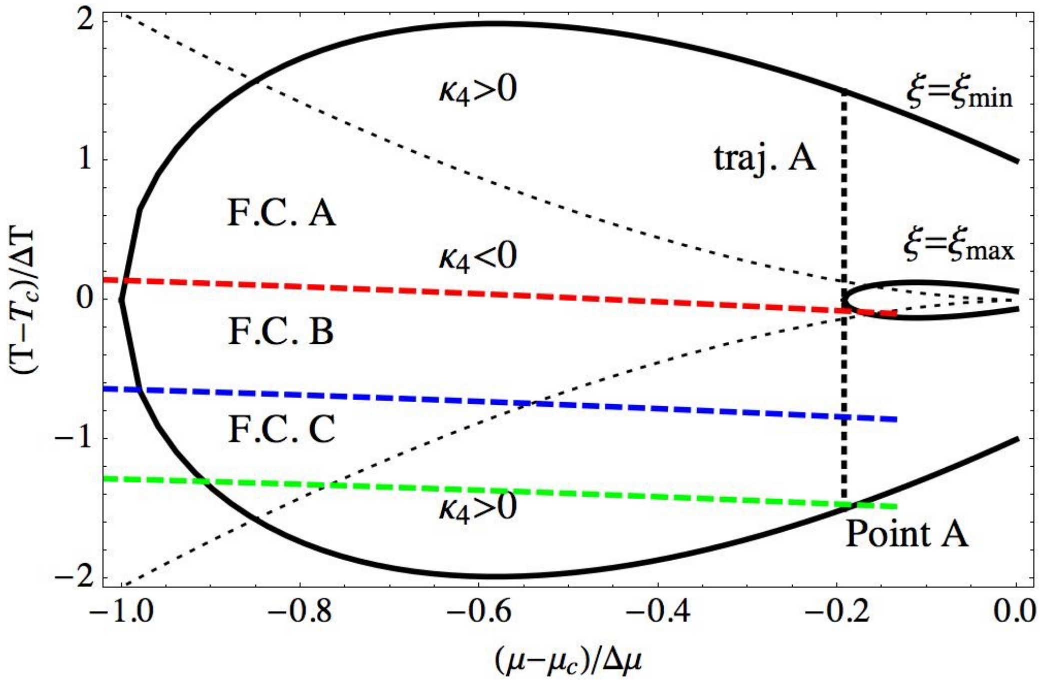

(Sign of)Equilibrium Skewness and Kurtosis

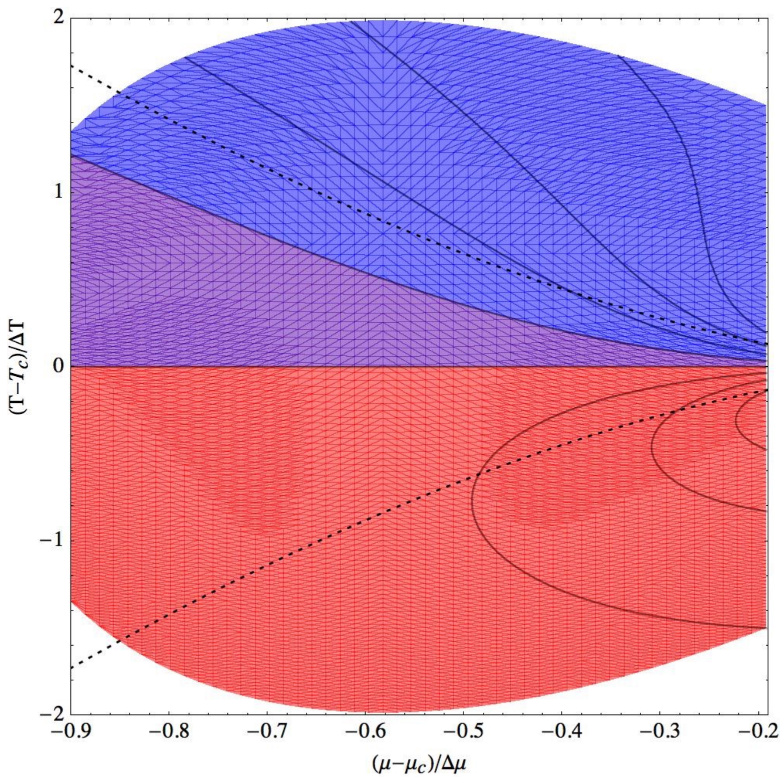

Skewness

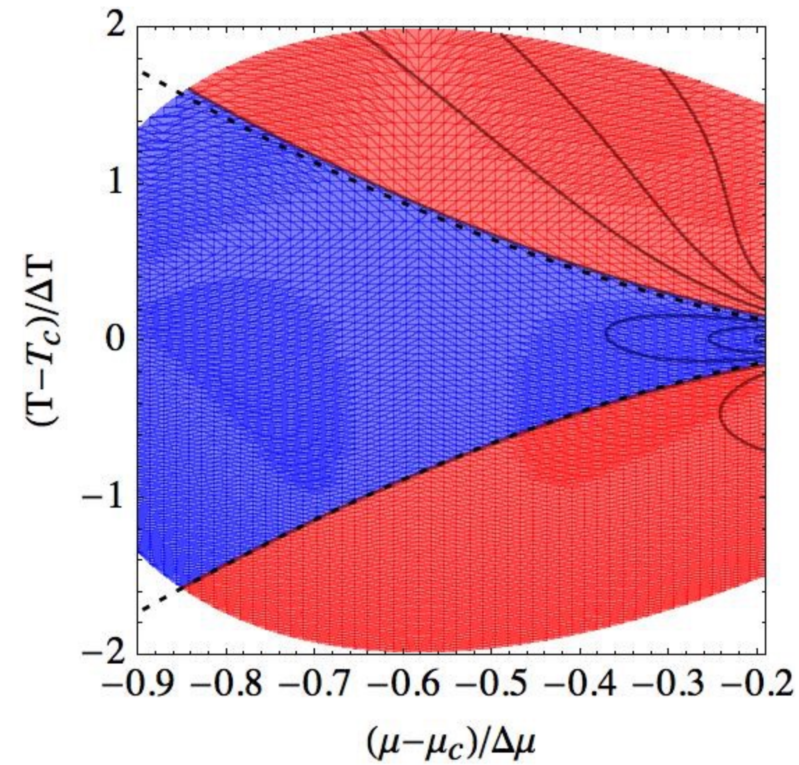

Kurtosis

Red >0

Blue<0

- Following the argument by Stephanov(Phys.Rev.Lett. 102 (2009) 032301), we assume the sign of skewness is positive below cross-over line.

- How would non-equilibrium effects change the above picture?

Deformation effects: Skewness

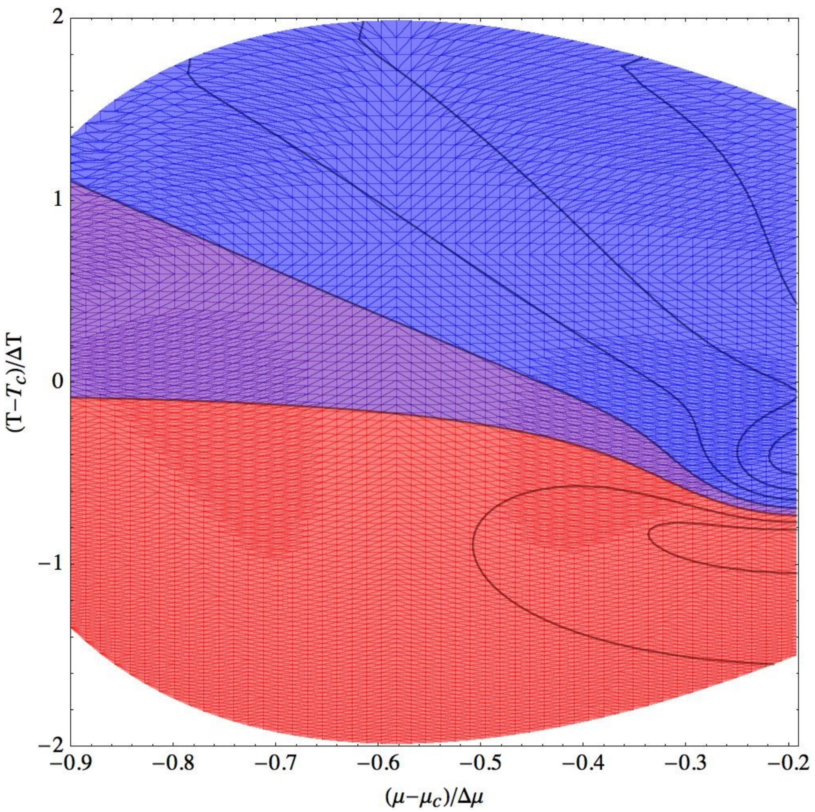

$\tau_{\rm rel}/\tau_I = 0.02$

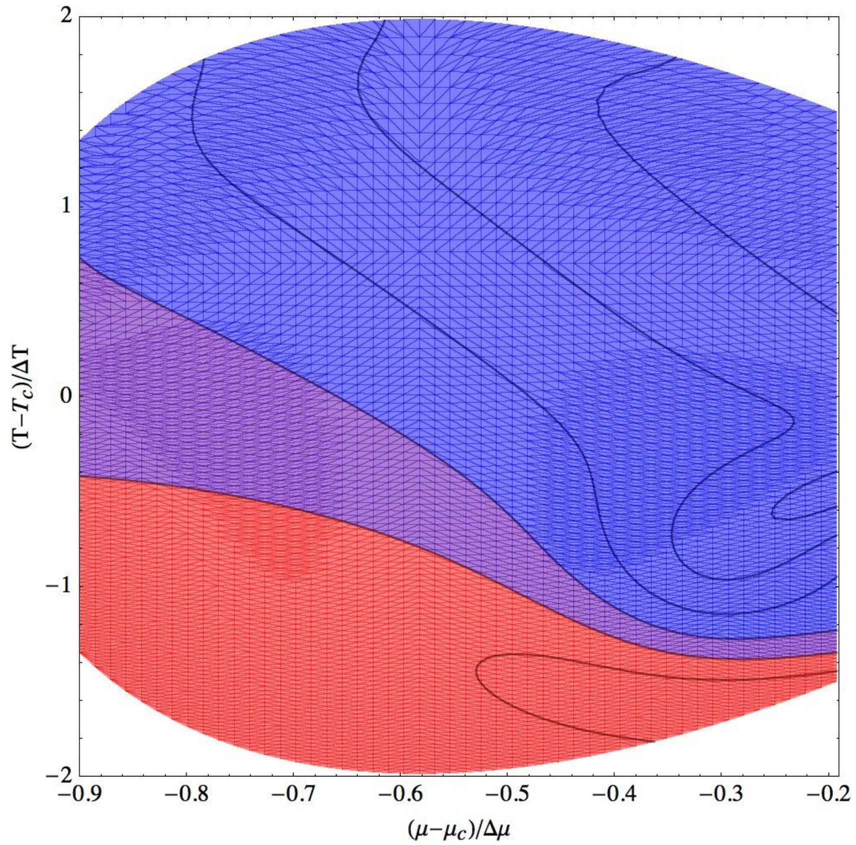

$\tau_{\rm rel}/\tau_I = 0.2$

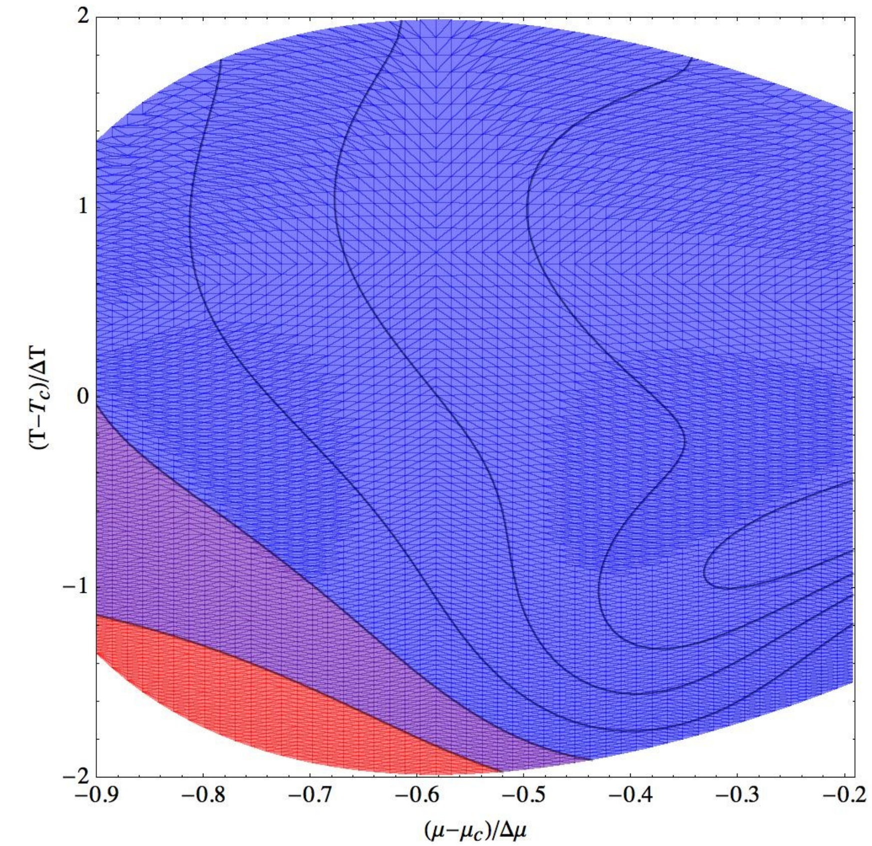

$\tau_{\rm rel}/\tau_I = 0.5$

Non-equilibrium skewness in critical regime

- Non-equilibrium effects deforms the regime that skewness is positive(negative).
- Non-equilibrium skewness carries the memory from deconfined phase(negative sign).

Deformation effects: Kurtosis

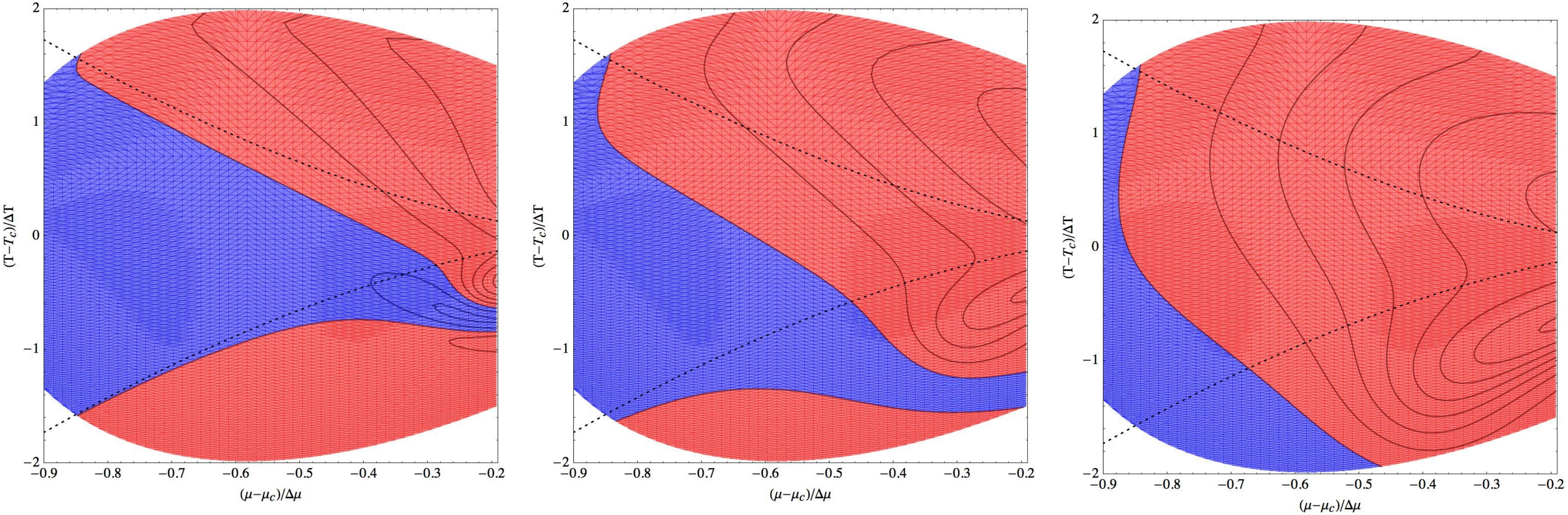

$\tau_{\rm rel}/\tau_I = 0.02$ $\tau_{\rm rel}/\tau_I = 0.2$ $\tau_{\rm rel}/\tau_I = 0.5$

Non-equilibrium kurtosis in critical regime

- Similar for kurtosis. The boundary that kurtosis will change sign also deform.

Skewness and Kurtosis on freeze-out curves

- We now present non-equilibrium results on the freeze-out curves.
- The relative position between the freeze-out curves and critical regime depends on the location of critical as well as the width of the critical regime.

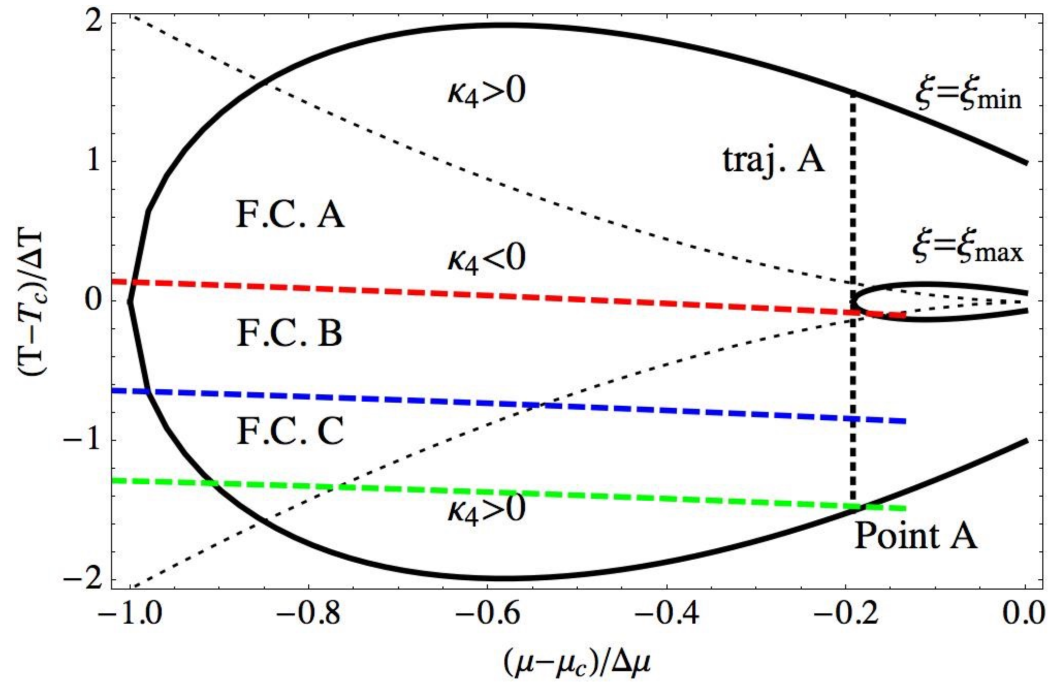

We fix $\mu_c = 300$ MeV, $\Delta\mu = 100$ MeV, $\Delta T/T_c = 1/8$ but take $T_c = 160, 175, 190$ MeV to consider three different relative positions of freeze-out curves. We will convert μ into $\sqrt{s}$ dependence as well.

- Disclaimer: This is neither a prediction nor a fitting. The purpose is to illustrate memory effects.

Skewness on freeze-out curves

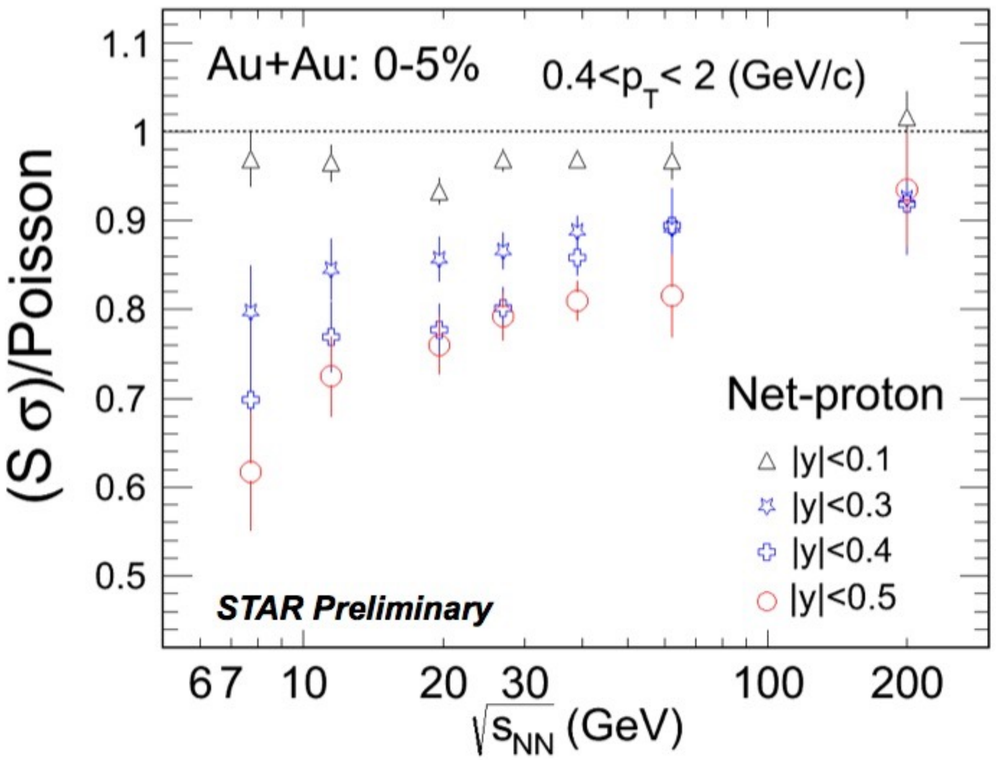

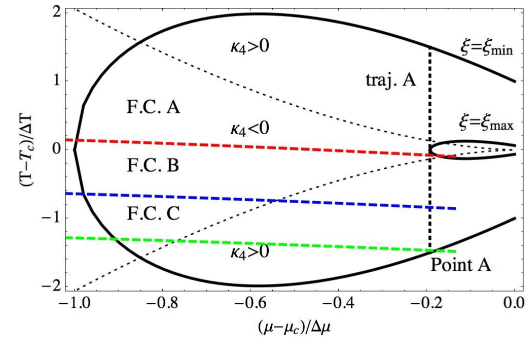

Skewness on f. curves for three different positions of f.curves.

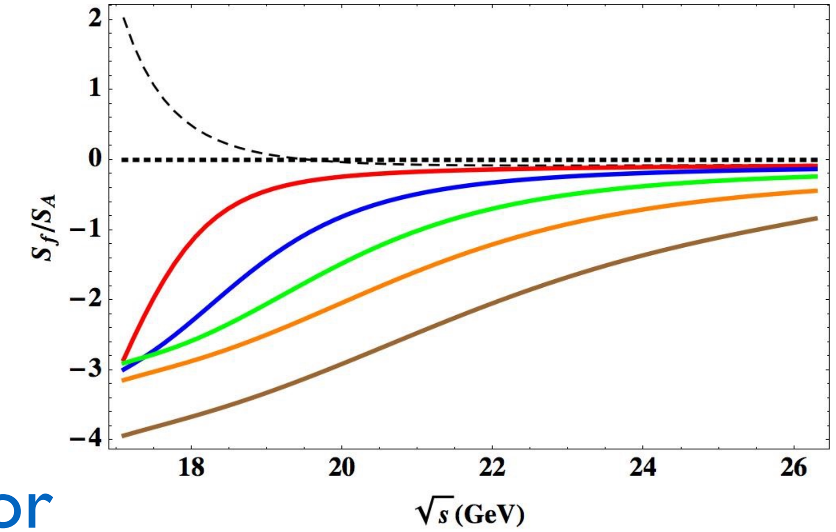

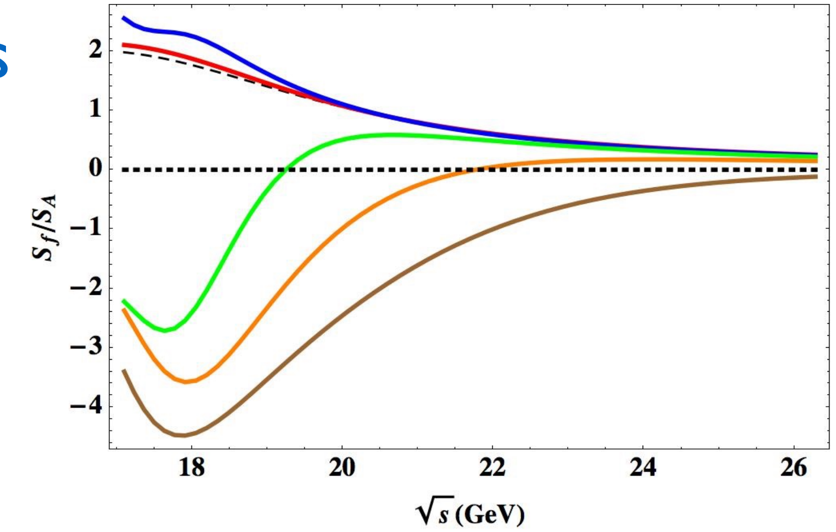

- The behavior of non-equilibrium skewness can be non-monotonous even if the equilibrium skewness is monotonous.

- The sign of non-equilibrium skewness can be opposite to the equilibrium skewness.

- Negative contribution to skewness: memory effects?

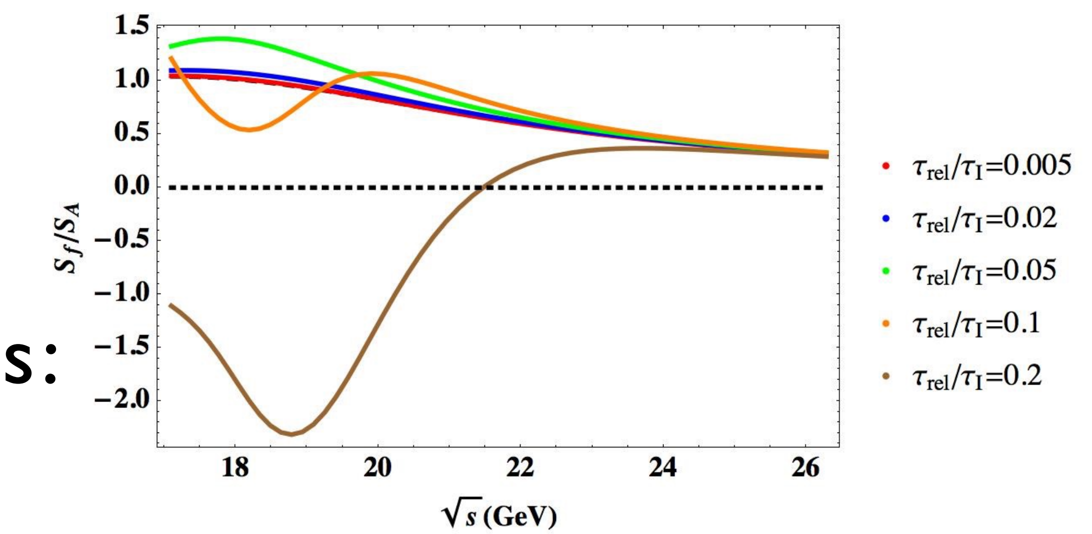

Non-equilibrium Kurtosis(of sigma field) on freeze-out curves

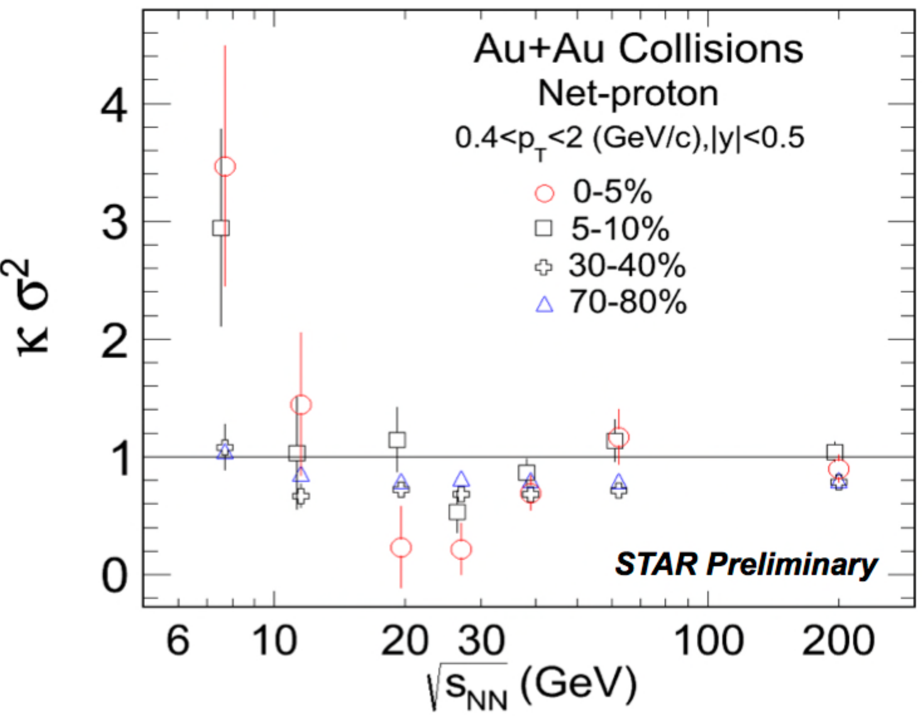

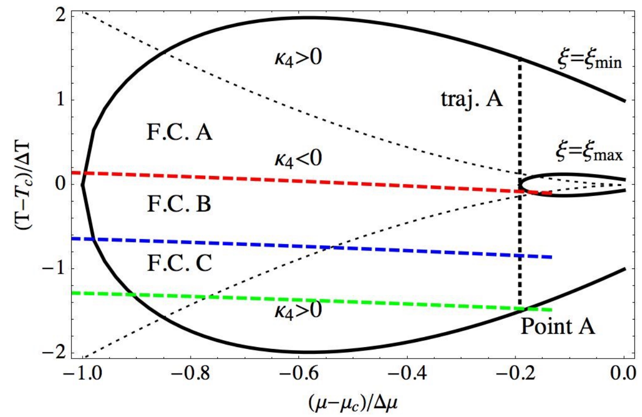

Kurtosis on f. curves for three different positions of f.curves.

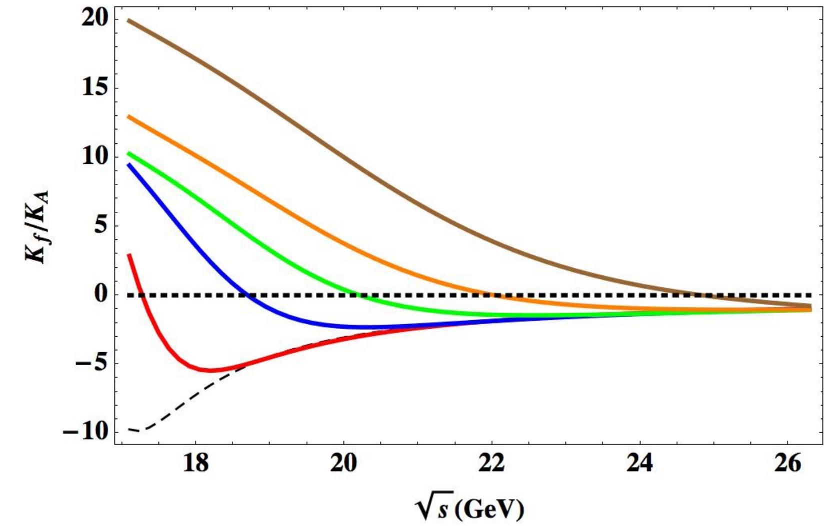

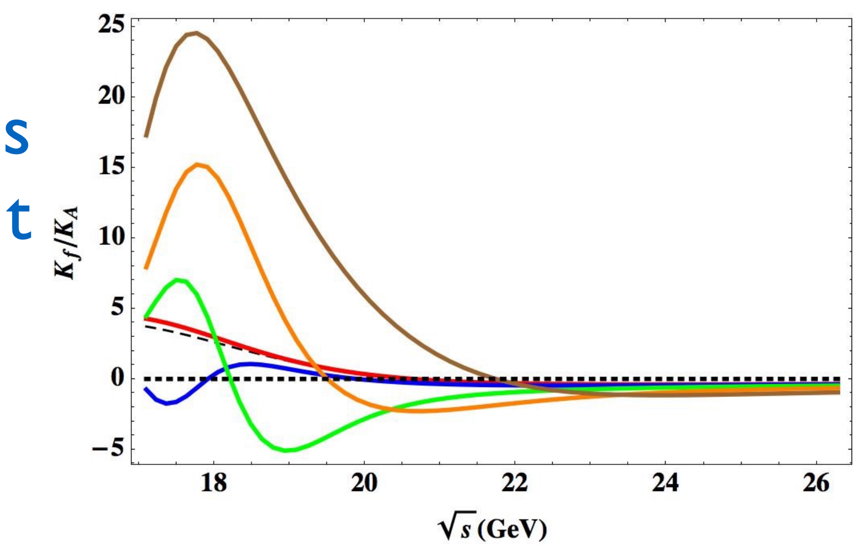

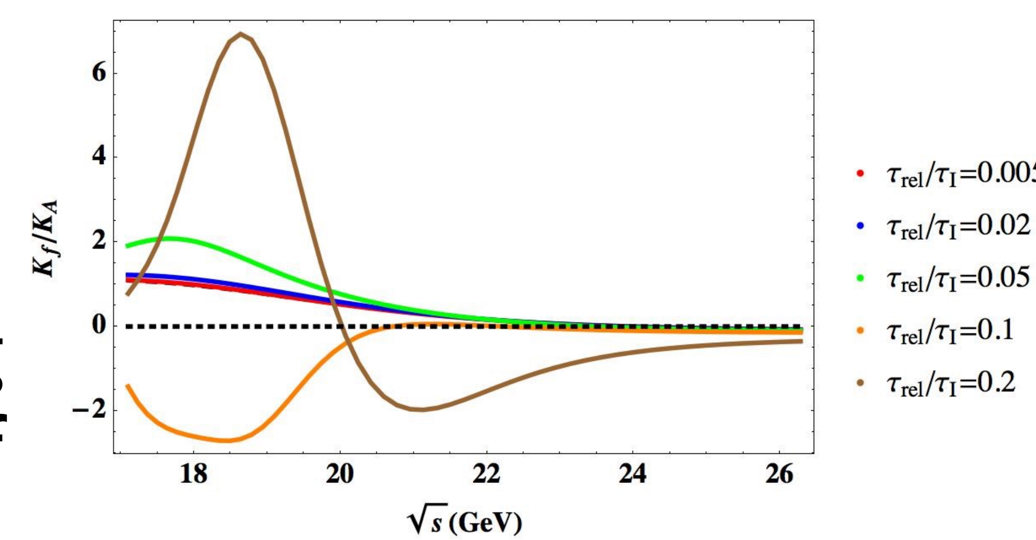

- The flipping of sign of kurtosis is still robust!
- The location that the sign changes depends on non-equilibrium effects.
- The trends in data can be captured by tuning relaxation time and the relative position of freeze-out curve.

Summary I

- We have developed a set of equations to describe the evolution of cumulants in heavy-ion collisions.
- We illustrate possible complications the would occur in a more comprehensive simulation(mapping between Ising model and QCD, relative position of freeze-out curve, relaxation time etc)
- Regarding the data: keeping non-equilibrium effects in mind are important(such as deformation of the boundary that sign of higher cumulants will change).

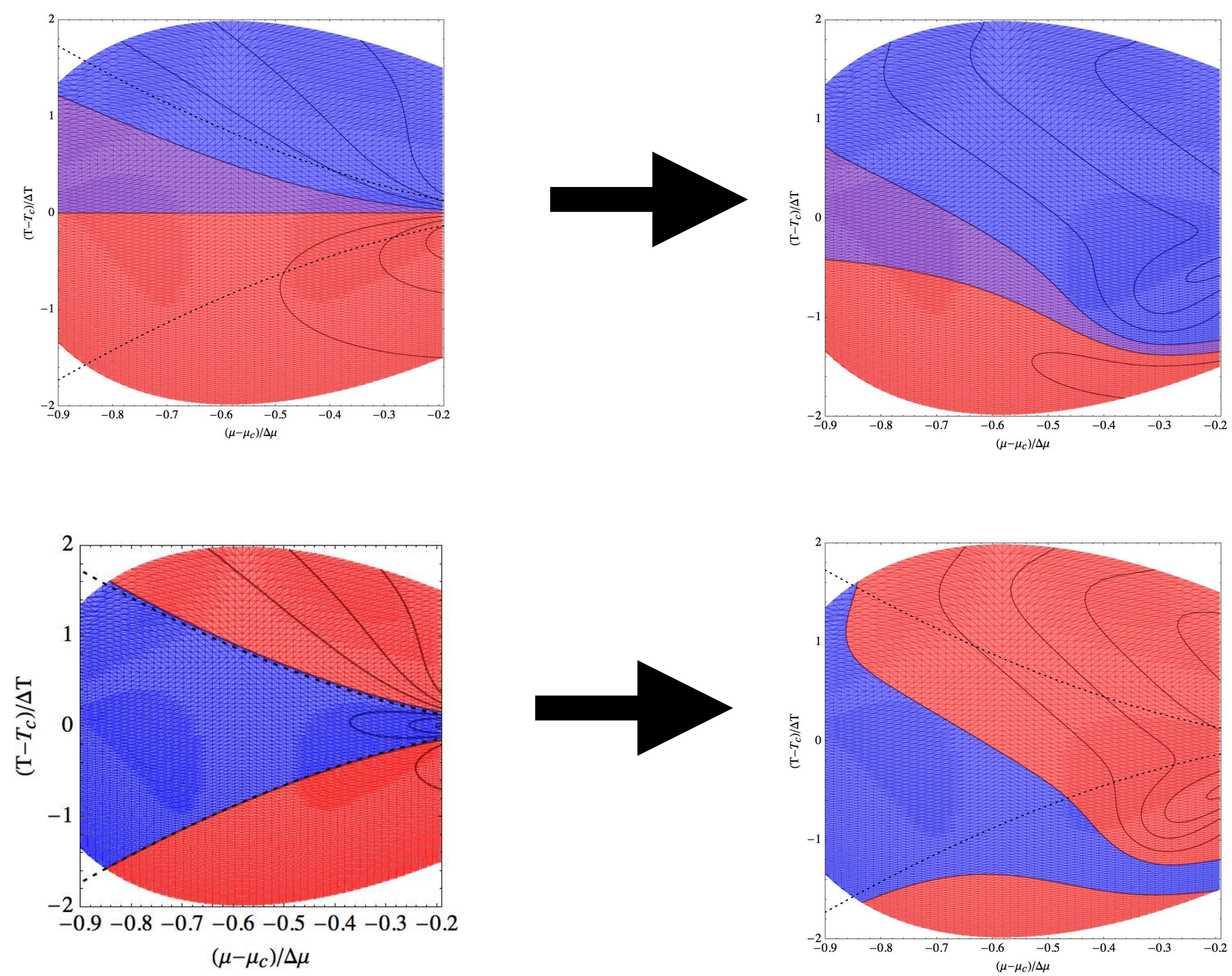

Summary II

- Even in this simple model, results are sensitive to the choice of parameters(relaxation time, relative position of freeze-out curves).
- The parameter space might be constrained by considering correlations among cumulants, finite time scaling among different centrality bins.

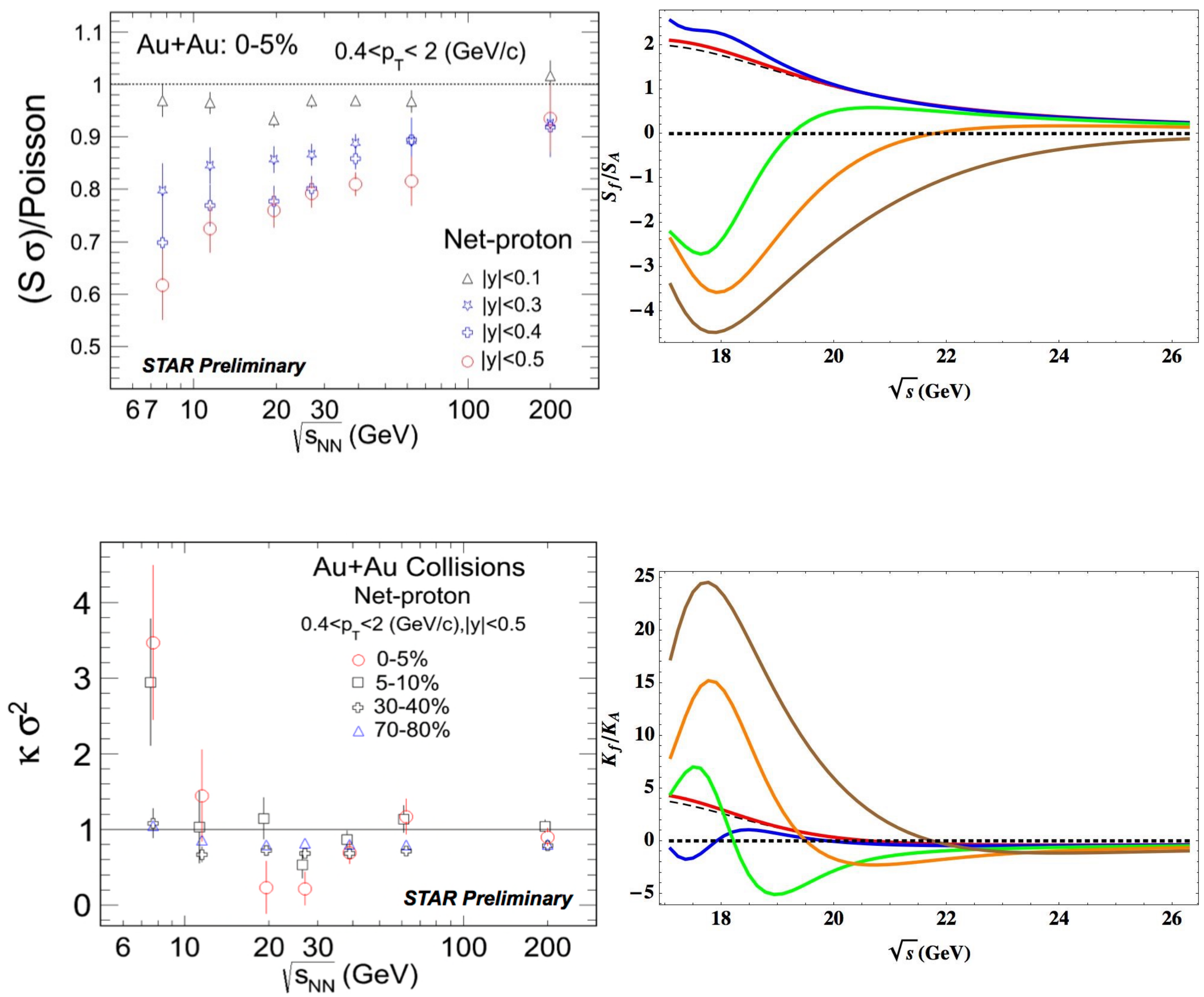

- Possibility to reveal dynamical critical properties of QCD in critical regime(similar story at RHIC top energy, not just thermodynamic, also hydrodynamics.)

Back-up Slides

RBRC Workshop:
THEORY AND MODELING FOR THE BEAM ENERGY SCAN:
From Exploration to Discovery

February 26-27, 2015
Physics Department, Bldg. 510, Large Seminar Room

~ ~ ~ ~ ~ ~ ~

Thursday, February 26

08:30 – 09:00 **REGISTRATION**

Chair: Paul Sorensen
09:00 – 09:40 William Llope .... Experimental overview of RHIC BES
09:40 – 10:20 Frithjof Karsch .... Lattice QCD and search for the critical point

10:20 – 10:50 **COFFEE BREAK**

Chair: Michael Lisa
10:50 – 11:30 Flemming Videbaek . Experimental overview of baryon transport in heavy ion collisions
11:30 – 12:10 Roy Lacey .... Finite size scaling of HBT

12:10 – 13:30 **LUNCH BREAK**

Chair: Hannah Petersen
13:30 – 14:10 Krzysztof Redlich ...... Influence of criticality on the probability distribution of conserved charges
14:10 – 14:50 Scott Pratt .... Toward quantitative and rigorous conclusions from heavy ion collisions
14:50 – 15:30 Yuji Hirono .... Dynamical modeling of the chiral magnetic effect in heavy-ion collisions

15:30 – 16:00 **COFFEE BREAK**

16:00 – 16:40 Iurii Karpenko........... Viscous hydrodynamics at high baryon densities
16:40 – 17:20 Marlene Nahrgang ... Fluctuations and fluid dynamics at the QCD phase transition

Chair: Swagato Mukherjee
17:20 – 18:30 Discussion .... Theory topical collaboration on BES

Back to Contents

Friday, February 27

Chair: Misha Stephanov

09:00 –0 9:40 Xiaofeng Luo .... New analysis of net-proton fluctuations in BES I
09:40 – 10:20 Dan Cebra .... New results on proton spectra in BES I

10:20 – 10:50 **COFFEE BREAK**

10:50 – 11:25 Akihiko Monnai .... Baryon diffusion in heavy-ion collisions
11:25 – 12:00 Chun Shen .... MUSIC with diffusion, recent developments for BES program
12:00 – 12:35 Yi Yin......................... Real time evolution of cumulants in QCD critical regime

12:35 – 14:00 **LUNCH BREAK**

Chair: Krishna Rajagopal

14:00 – 15:30 Discussion .... Theory topical collaboration on BES

15:30 – 16:00 **COFFEE BREAK**

16:00 – 17:00 Discussion .... Theory topical collaboration on BES

Back to Contents

Theory and Modeling for the Beam Energy Scan: From Exploration to Discovery

February 26-27, 2015

Participants

Name	Affiliation	e-Mail Address
Jussi Auvinen	Duke University	jaa49@phy.duke.edu
Daniel Cebra	University of California-Davis	cebra@physics.ucdavis.edu
Yuji Hirono	Stony Brook University	yuji.hirono@stonybrook.edu
Huan Huang	University of California Los Angeles	huang@physics.ucla.edu
Shengli Huang	Vanderbilt University	shengli.huang@vanderbilt.edu
Iurii Karpenko	Frankfurt Institute for Advanced Studies	karpenko@fias.uni-frankfurt.de
Frithjof Karsch	Brookhaven National Laboratory	karsch@bnl.gov
Declan Keane	Kent State University	keane@kent.edu
Dmitri Kharzeev	Brookhaven National Laboratory	kharzeev@bnl.gov
Volker Koch	Lawrence Berkeley National Laboratory	vkoch@lbl.gov
Roy Lacey	Stony Brook University	Roy.Lacey@Stonybrook.edu
Jinfeng Liao	Indiana Univ & RIKEN BNL Research Center	liaoji@indiana.edu
Shu Lin	RIKEN BNL Research Center	slin@bnl.gov
Michael Lisa	Ohio State University	lisa.1@osu.edu
William Llope	Wayne State University	wjllope@wayne.edu
Xiaofeng Luo	Central China Normal University	xfluo@mail.ccnu.edu.cn
Jeffery Mitchell	Brookhaven National Laboratory	mitchell@bnl.gov
Akihiko Monnai	RIKEN BNL Research Center	amonnai@riken.jp
David Morrison	Brookhaven National Laboratory	morrison@bnl.gov
Swagato Mukherjee	Brookhaven National Laboratory	swagato@bnl.gov
Marlene Nahrgang	Duke University	marlene.nahrgang@phy.duke.edu
Grazyna Odyniec	Lawrence Berkeley National Laboratory	G_Odyniec@lbl.gov
Vitaly Okorokov	National Research Nuclear University "MEPhI"	okorokov@bnl.gov
Robert Pak	Brookhaven National Laboratory	pak@bnl.gov
Scott Pratt	Michigan State University	prattsc@msu.edu
Krishna Rajagopal	Massachusetts Institute of Technology	krishna@mit.edu
Krzysztof Redlich	University of Wroclaw	redlich@ift.uni.wroc.pl
Daisuke Satow	ECT*	daisuke.sato0323@gmail.com
Thomas Schaefer	North Carolina State University	thomas_schaefer@ncsu.edu
Soeren Schlichting	Brookhaven National Laboratory	soeren@kaiden.de
Prashanth Shanmuganathan	Kent State University	sprashan@kent.edu
Sayantan Sharma	Brookhaven National Laboratory	sayantans@bnl.gov
Chun Shen	McGill University	chunshen@physics.mcgill.ca
Paul Sorensen	Brookhaven National Laboratory	prsorensen@bnl.gov
Peter Steinberg	Brookhaven National Laboratory	peter.steinberg@bnl.gov
Mikhail Stephanov	University of Illinois	misha@uic.edu
Raju Venugopalan	Brookhaven National Laboratory	rajuv@mac.com
Flemming Videbaek	Brookhaven National Laboratory	videbaek@bnl.gov
Gary Westfall	Michigan State University	westfall@nscl.msu.edu
Nu Xu	Lawrence Berkeley National Laboratory	nxu@lbl.gov
Zhangbu Xu	Brookhaven National Laboratory	xzb@bnl.gov
Yi Yin	Brookhaven National Laboratory	phyyin@gmail.com

Back to Contents

RIKEN BNL Research Center Proceedings

Volume 120 – Multi-Hadron and Nonlocal Matrix Elements in Lattice QCD, February 5-6, 2015 – BNL-107603-2015
Volume 119 – Thermal Photons and Dileptons in Heavy-Ion Collisions, August 20-22, 2014 – BNL-106066-2014
Volume 118 – The Approach to Equilibrium in Strongly Interacting Matter, April 2-4, 2014 – BNL-104423-2014
Volume 117 – Lattice Meets Experiment 2013: Beyond the Standard Model, December 5-6, 2013 – BNL-103493-2013
Volume 116 – RBRC Scientific Review Committee Meeting, October 31 - November 1, 2013 – BNL-102596-2013
Volume 115 – Jet Quenching at RHIC vs LHC in Light of Recent dAu vs pPb Controls, April 15-17, 2013 – BNL-100766-2013
Volume 114 – The Physics of p↑+A Collisions at RHIC, January 7-9, 2013 – BNL-99107-2013
Volume 113 – Thermal Radiation Workshop, December 5-7, 2012 – BNL-99088-2013
Volume 112 – RBRC Scientific Review Committee Meeting, November 6-8, 2012 – BNL-99621-2013
Volume 111 – Forward Physics at RHIC, July 30-Aug 1, 2012 – BNL-98400-2012
Volume 110 – P- and CP-odd Effects in Hot and Dense Matter, June 25-27, 2012 – BNL-98398-2012
Volume 109 – New Horizons for Lattice Computations with Chiral Fermions, May 14-18, 2012 – BNL-98392-2012
Volume 108 – Hyperon-Hyperon Interactions and Searches for Exotic Di-Hyperons in Nuclear Collisions, February 29 – March 2, 2012 – BNL-97035-2012
Volume 107 – Future Directions in High Energy QCD, October 20-22, 2011 – BNL-98119-2011
Volume 106 – Fluctuations, Correlations and RHIC Low Energy Runs, October 3-5, 2011 – BNL-96514-2011
Volume 105 – Opportunities for Polarized He-3 in RHIC and EIC, September 28-30, 2011 – BNL-96418-2011
Volume 104 – Brookhaven Summer Program on Quarkonium Production in Elementary and Heavy Ion Collisions, June 6-18, 2011 – BNL-96171-2011
Volume 103 – Opportunities for Drell-Yan Physics at RHIC, May 11-13, 2011 – BNL-95236-2011
Volume 102 – Initial State Fluctuations and Final-State Particle Correlations, February 2-4, 2011 – BNL-94704-2011
Volume 101 – RBRC Scientific Review Committee Meeting, October 27-29, 2010 – BNL-94589-2011
Volume 100 – Summer Program on Nucleon Spin Physics, July 14-27, 2010 – BNL-96163-2011
Volume 99 – The Physics of W and Z Bosons, June 24-25, 2010 – BNL-94287-2010
Volume 98 – Saturation, the Color Glass Condensate and the Glasma: What Have We Learned from RHIC? – May 10-12, 2010 – BNL-94271-2010
Volume 97 – RBRC Scientific Review Committee Meeting, October 21-22, 2009 – BNL-90674-2009
Volume 96 – P- and CP-Odd Effects in Hot and Dense Matter, April 26-30, 2010 – BNL-94237-2010
Volume 95 – Progress in High-pT Physics at RHIC, March 17-19, 2010 – BNL-94214-2010
Volume 94 – Summer Program on Nucleon Spin Physics at LBL, June 1-12, 2009
Volume 93 – PHENIX Spinfest School 2009 at BNL - July 1-31, 2009 – BNL-90343-2009
Link: PHENIXSpinfestSchool2009@BNL
Volume 92 – PKU-RBRC Workshop on Transverse Spin Physics, June 30 - July 4, 2008, Beijing, China – BNL-81685-2008
Volume 91 – RBRC Scientific Review Committee Meeting, November 17-18, 2008 – BNL-81556-2008
Volume 90 – PHENIX Spinfest School 2008 at BNL, August 4-8, 2008 – BNL-81478-2008
Volume 89 – Understanding QGP through Spectral Functions and Euclidean Correlators, April 23-25, 2008 – BNL-81318-2008
Volume 88 – Hydrodynamics in Heavy Ion Collisions and QCD Equation of State, April 21-22, 2008 – BNL-81307-2008
Volume 87 – RBRC Scientific Review Committee Meeting, November 5-6, 2007 – BNL-79570-2007
Volume 86 – Global Analysis of Polarized Parton Distributions in the RHIC Era, October 8, 2007 – BNL-79457-2007
Volume 85 – Parity-Violating Spin Asymmetries at RHIC-BNL, April 26-27, 2007 – BNL-79146-2007
Volume 84 – Domain Wall Fermions at Ten Years, March 15-17, 2007 – BNL 77857-2007

Back to Contents

Volume 83 – QCD in Extreme Conditions, July 31 - August 2, 2006 – BNL-76933-2006
Volume 82 – RHIC Physics in the Context of the Standard Model, June 18-23, 2006 – BNL-76863-2006
Volume 81 – Parton Orbital Angular Momentum (Joint RBRC/University of New Mexico Workshop) February 24-26, 2006 – BNL-75937-2006
Volume 80 – Can We Discover the QCD Critical Point at RHIC?, March 9-10, 2006 – BNL-75692-2006
Volume 79 – Strangeness in Collisions, February 16-17, 2006 – BNL-79763-2008
Volume 78 – Heavy Flavor Productions and Hot/Dense Quark Matter, December 12-14, 2005 – BNL-76915-2006
Volume 77 – RBRC Scientific Review Committee Meeting, October 10-12, 2005 – BNL-52649-2005
Volume 76 – Odderon Searches at RHIC, September 27-29, 2005 – BNL-75092-2005
Volume 75 – Single Spin Asymmetries, June 1-3, 2005 – BNL-74717-2005
Volume 74 – RBRC QCDOC Computer Dedication and Symposium on RBRC QCDOC, May 26, 2005 – BNL-74813-2005
Volume 73 – Jet Correlations at RHIC, March 10-11, 2005 – BNL-73910-2005
Volume 72 – RHIC Spin Collaboration Meetings XXXI, XXXII, XXXIII – BNL-73866-2005
Volume 71 – Classical and Quantum Aspects of the Color Glass Condensate – BNL-73793-2005
Volume 70 – Strongly Coupled Plasmas: Electromagnetic, Nuclear & Atomic – BNL-73867-2005
Volume 69 – RBRC Scientific Review Committee Meeting, November 16-17, 2004 – BNL-73546-2004
Volume 68 – Workshop on the Physics Programme of the RBRC and UKQCD QCDOC Machines – BNL-73604-2004
Volume 67 – High Performance Computing with BlueGene/L and QCDOC Architectures, October 27-28, 2004
Volume 66 – RHIC Spin Collaboration Meeting XXIX, Torino Italy – BNL-73534-2004
Volume 65 – RHIC Spin Collaboration Meetings XXVII, XXVIII, XXX – BNL-73506-2004
Volume 64 – Theory Summer Program on RHIC Physics – BNL-73263-2004
Volume 63 – RHIC Spin Collaboration Meetings XXIV, XXV, XXVI – BNL-72397-2004
Volume 62 – New Discoveries at RHIC, May 14-15, 2004 – BNL-72391-2004
Volume 61 – RIKEN-TODAI Mini Workshop on "Topics in Hadron Physics at RHIC", March 23-24, 2004 – BNL-72336-2004
Volume 60 – Lattice QCD at Finite Temperature and Density – BNL-72083-2004
Volume 59 – RHIC Spin Collaboration Meetings XXI, XXII, XXIII – BNL-72382-2004
Volume 58 – RHIC Spin Collaboration Meeting XX – BNL-71900-2004
Volume 57 – High pt Physics at RHIC, December 2-6, 2003 – BNL-72069-2004
Volume 56 – RBRC Scientific Review Committee Meeting, November 20-21, 2003 – BNL-71899-2003
Volume 55 – Collective Flow and QGP Properties – BNL-71898-2003
Volume 54 – RHIC Spin Collaboration Meetings XVII, XVIII, XIX – BNL-71751-2003
Volume 53 – Theory Studies for Polarized pp Scattering – BNL-71747-2003
Volume 52 – RIKEN School on QCD "Topics on the Proton" – BNL-71694-2003
Volume 51 – RHIC Spin Collaboration Meetings XV, XVI – BNL-71539-2003
Volume 50 – High Performance Computing with QCDOC and BlueGene – BNL-71147-2003
Volume 49 – RBRC Scientific Review Committee Meeting, November 21-22, 2002 – BNL-52679
Volume 48 – RHIC Spin Collaboration Meeting XIV – BNL-71300-2003
Volume 47 – RHIC Spin Collaboration Meetings XII, XIII – BNL-71118-2003
Volume 46 – Large-Scale Computations in Nuclear Physics using the QCDOC – BNL-52678
Volume 45 – Summer Program: Current and Future Directions at RHIC – BNL-71035
Volume 44 – RHIC Spin Collaboration Meetings VIII, IX, X, XI – BNL-71117-2003
Volume 43 – RIKEN Winter School – Quark-Gluon Structure of the Nucleon and QCD – BNL-52672
Volume 42 – Baryon Dynamics at RHIC – BNL-52669
Volume 41 – Hadron Structure from Lattice QCD – BNL-52674

Back to Contents

Volume 40 – Theory Studies for RHIC-Spin – BNL-52662
Volume 39 – RHIC Spin Collaboration Meeting VII – BNL-52659
Volume 38 – RBRC Scientific Review Committee Meeting, November 29-30, 2001 – BNL-52649
Volume 37 – RHIC Spin Collaboration Meeting VI (Part 2) – BNL-52660
Volume 36 – RHIC Spin Collaboration Meeting VI – BNL-52642
Volume 35 – RIKEN Winter School – Quarks, Hadrons and Nuclei – QCD Hard Processes and the Nucleon Spin – BNL-52643
Volume 34 – High Energy QCD: Beyond the Pomeron – BNL-52641
Volume 33 – Spin Physics at RHIC in Year-1 and Beyond – BNL-52635
Volume 32 – RHIC Spin Physics V – BNL-52628
Volume 31 – RHIC Spin Physics III & IV Polarized Partons at High Q^2 Region – BNL-52617
Volume 30 – RBRC Scientific Review Committee Meeting, September 28-29, 2000 – BNL-52603
Volume 29 – Future Transversity Measurements – BNL-52612
Volume 28 – Equilibrium & Non-Equilibrium Aspects of Hot, Dense QCD – BNL-52613
Volume 27 – Predictions and Uncertainties for RHIC Spin Physics & Event Generator for RHIC Spin Physics III – Towards Precision Spin Physics at RHIC – BNL-52596
Volume 26 – Circum-Pan-Pacific RIKEN Symposium on High Energy Spin Physics – BNL-52588
Volume 25 – RHIC Spin – BNL-52581
Volume 24 – Physics Society of Japan Biannual Meeting Symposium on QCD Physics at RIKEN BNL Research Center – BNL-52578
Volume 23 – Coulomb and Pion-Asymmetry Polarimetry and Hadronic Spin Dependence at RHIC Energies – BNL-52589
Volume 22 – OSCAR II: Predictions for RHIC – BNL-52591
Volume 21 – RBRC Scientific Review Committee Meeting, May 27-28, 1999 – BNL-52568
Volume 20 – Gauge-Invariant Variables in Gauge Theories – BNL-52590
Volume 19 – Numerical Algorithms at Non-Zero Chemical Potential – BNL-52573
Volume 18 – Event Generator for RHIC Spin Physics – BNL-52571
Volume 17 – Hard Parton Physics in High-Energy Nuclear Collisions – BNL-52574
Volume 16 – RIKEN Winter School - Structure of Hadrons - Introduction to QCD Hard Processes – BNL-52569
Volume 15 – QCD Phase Transitions – BNL-52561
Volume 14 – Quantum Fields In and Out of Equilibrium – BNL-52560
Volume 13 – Physics of the 1 Teraflop RIKEN-BNL-Columbia QCD Project First Anniversary Celebration – BNL-66299
Volume 12 – Quarkonium Production in Relativistic Nuclear Collisions – BNL-52559
Volume 11 – Event Generator for RHIC Spin Physics – BNL-66116
Volume 10 – Physics of Polarimetry at RHIC – BNL-65926
Volume 9 – High Density Matter in AGS, SPS and RHIC Collisions – BNL-65762
Volume 8 – Fermion Frontiers in Vector Lattice Gauge Theories – BNL-65634
Volume 7 – RHIC Spin Physics – BNL-65615
Volume 6 – Quarks and Gluons in the Nucleon – BNL-65234
Volume 5 – Color Superconductivity, Instantons and Parity (Non?)-Conservation at High Baryon Density – BNL-65105
Volume 4 – Inauguration Ceremony and Non-Equilibrium Many Body Dynamics – BNL-64912
Volume 3 – Hadron Spin-Flip at RHIC Energies – BNL-64724
Volume 2 – Perturbative QCD as a Probe of Hadron Structure – BNL-64723
Volume 1 – Open Standards for Cascade Models for RHIC – BNL-64722

Back to Contents

Li Keran

Nuclei as heavy as bulls
Through collision
Generate new states of matter.
T.D. Lee

Organizers
Michael Lisa (Ohio State University)
Swagato Mukherjee (Brookhaven National Laboratory)
Hannah Petersen (Frankfurt Institute for Advanced Studies)
Misha Stephanov (University of Illinois)
Paul Sorenson (Brookhaven National Laboratory)

RIKEN BNL Research Center
Bldg. 510A, Brookhaven National Laboratory
Upton, NY 11973-5000, USA

February 2015